Vision

PSYC 5665 - Prosem

Lew Harvey

28 October 2020

Main Points

- “Light” is energy
- “Light” is an experience
- The core of vision science is to understand the relationship between these two domains.

Levels of Understanding

- Molecular
- Cellular
- Systems
- Behavioral
- We want it all!

Light as Energy

Light as Energy

- Quanta
- Only one property
  - Energy (E)
  - Frequency (nu)
  - Wavelength (lambda)
- Light has no color

$$E = h \cdot \nu$$ Planck-Einstein

$$c = \lambda \cdot \nu$$

$$E = \frac{c \cdot h}{\lambda}$$

Black Body Radiator

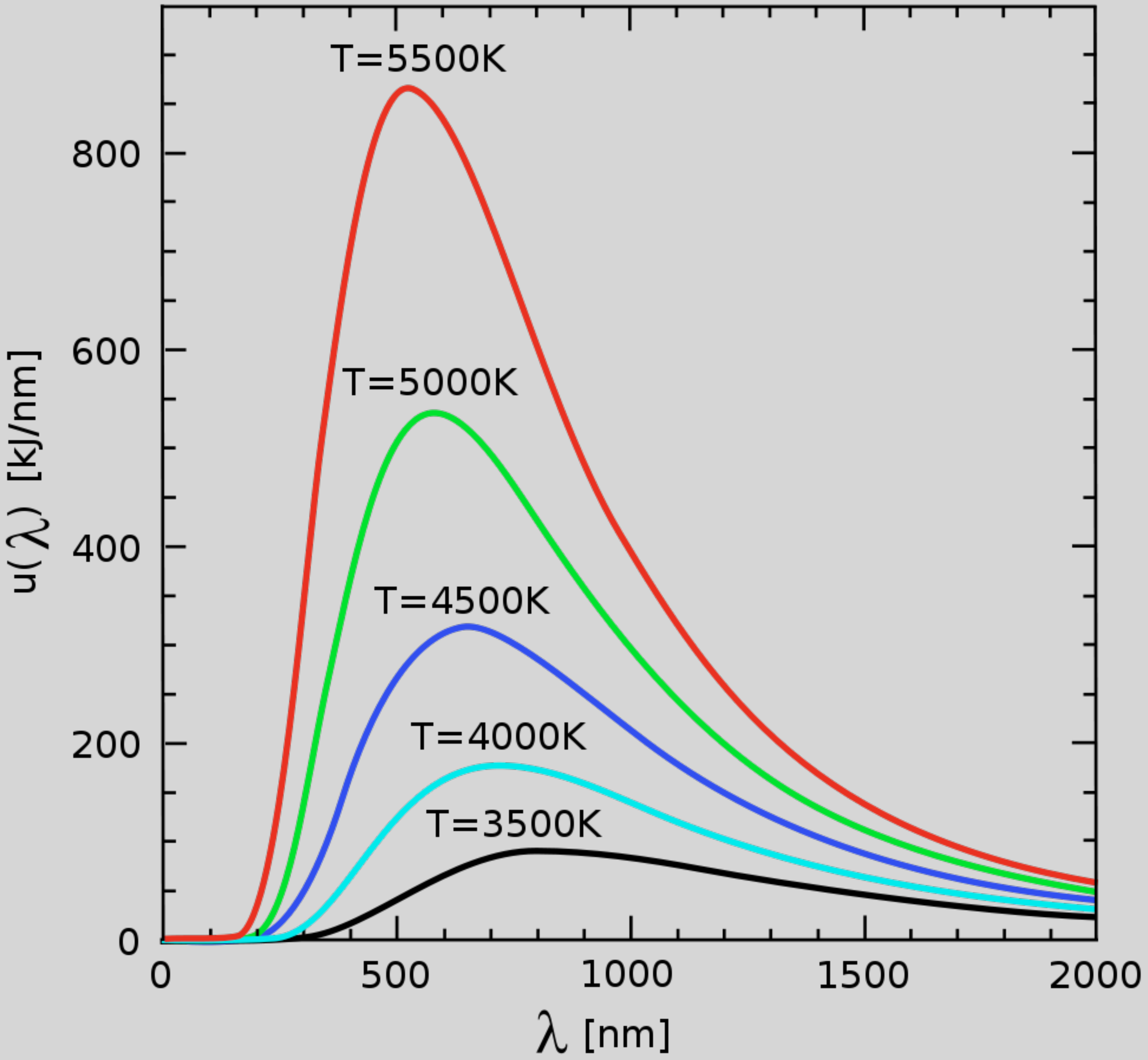

Black Body Radiator

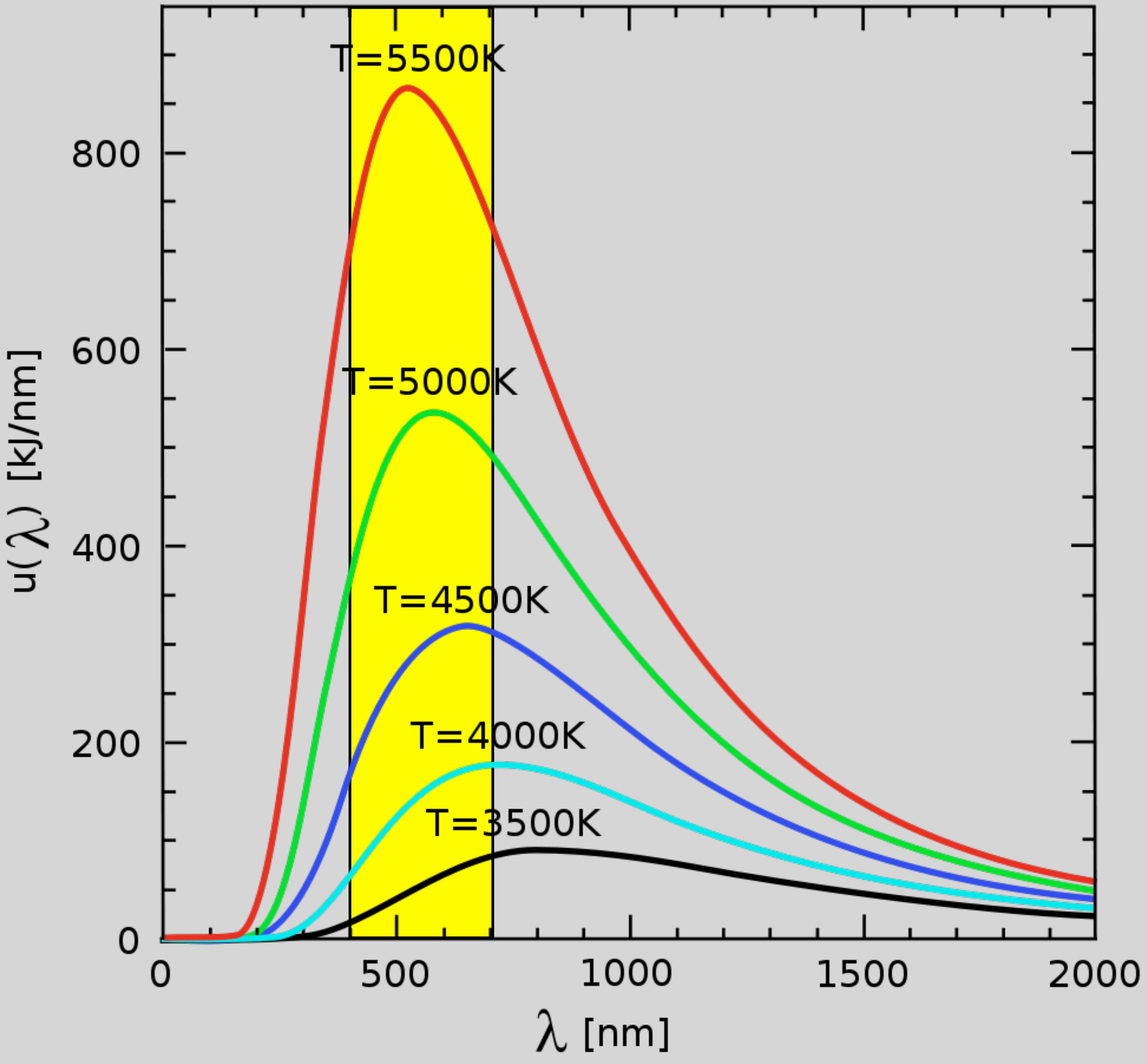

Light Energy Interacts with Matter

- Reflected
- Transmitted
- Absorbed

Visible Spectra

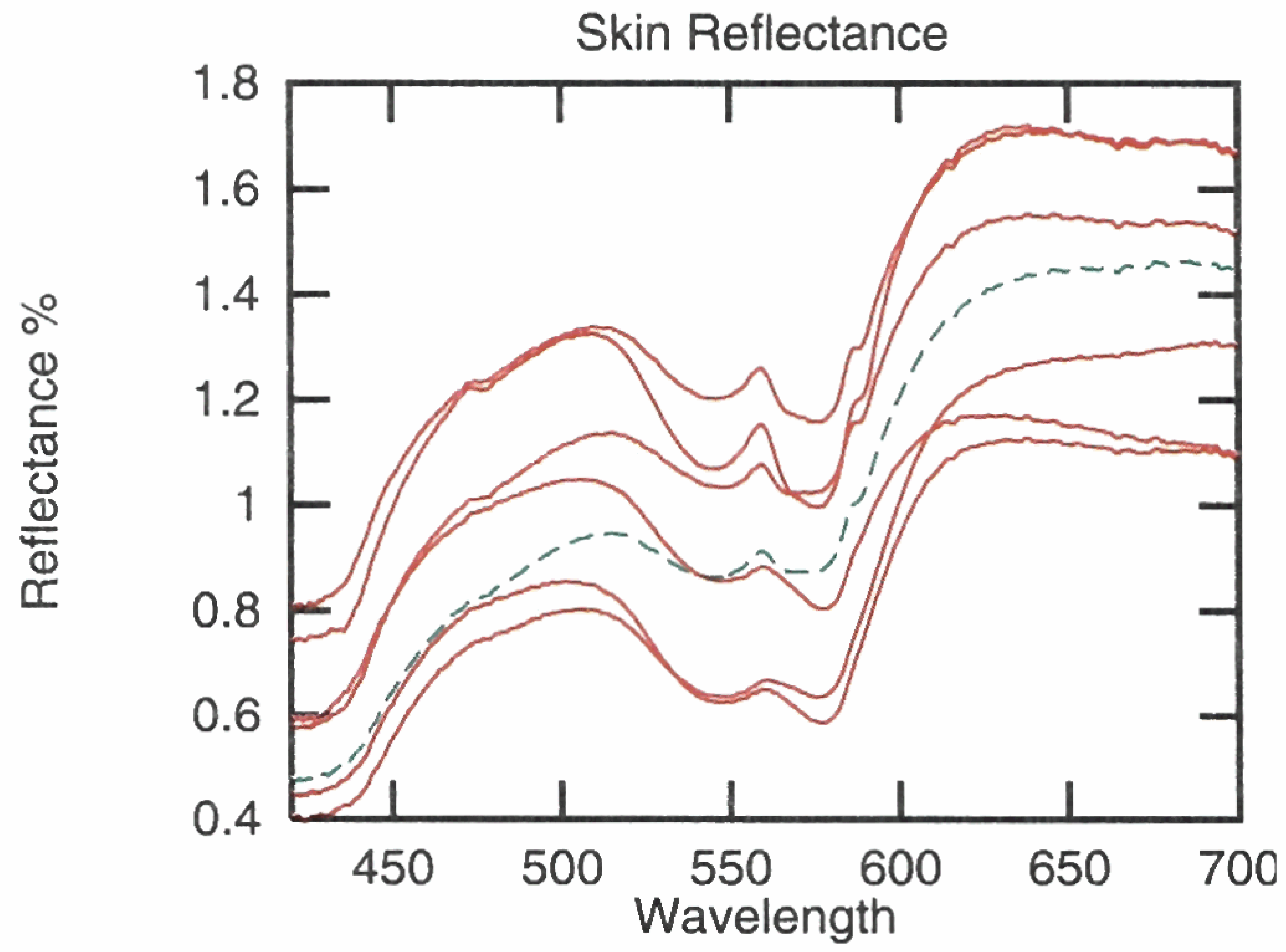

Fig. 4. Spectra of the back of the hand.

How The Eye Works

- Optical instrument
  - Cornea and lens
- Neural information processor
  - Retina – a complex network of neurons

Optics of the Eye:
René Descartes (1596–1650)

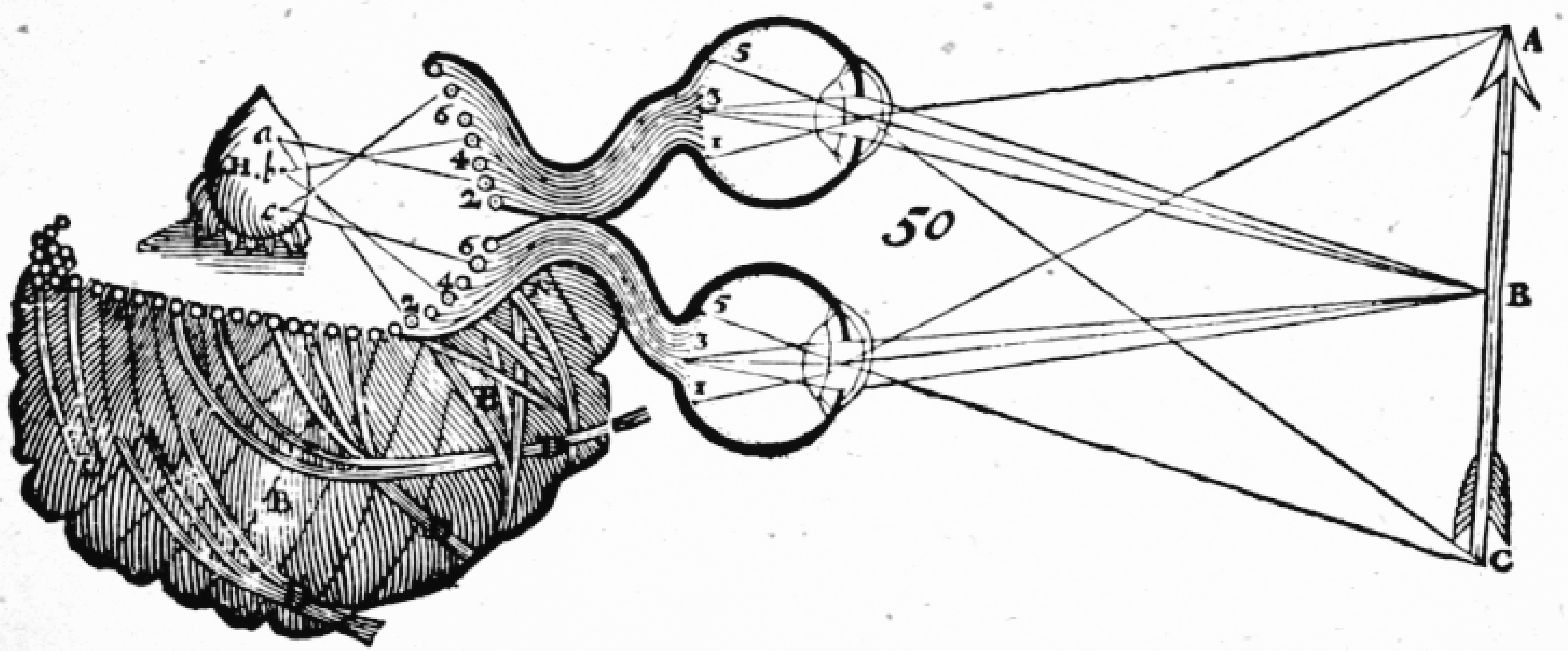

FIGURE 1 Descartes' diagram of the formation of images on the retinae of the eyes and the paths of transmission in the visual nervous system.

The Visual System

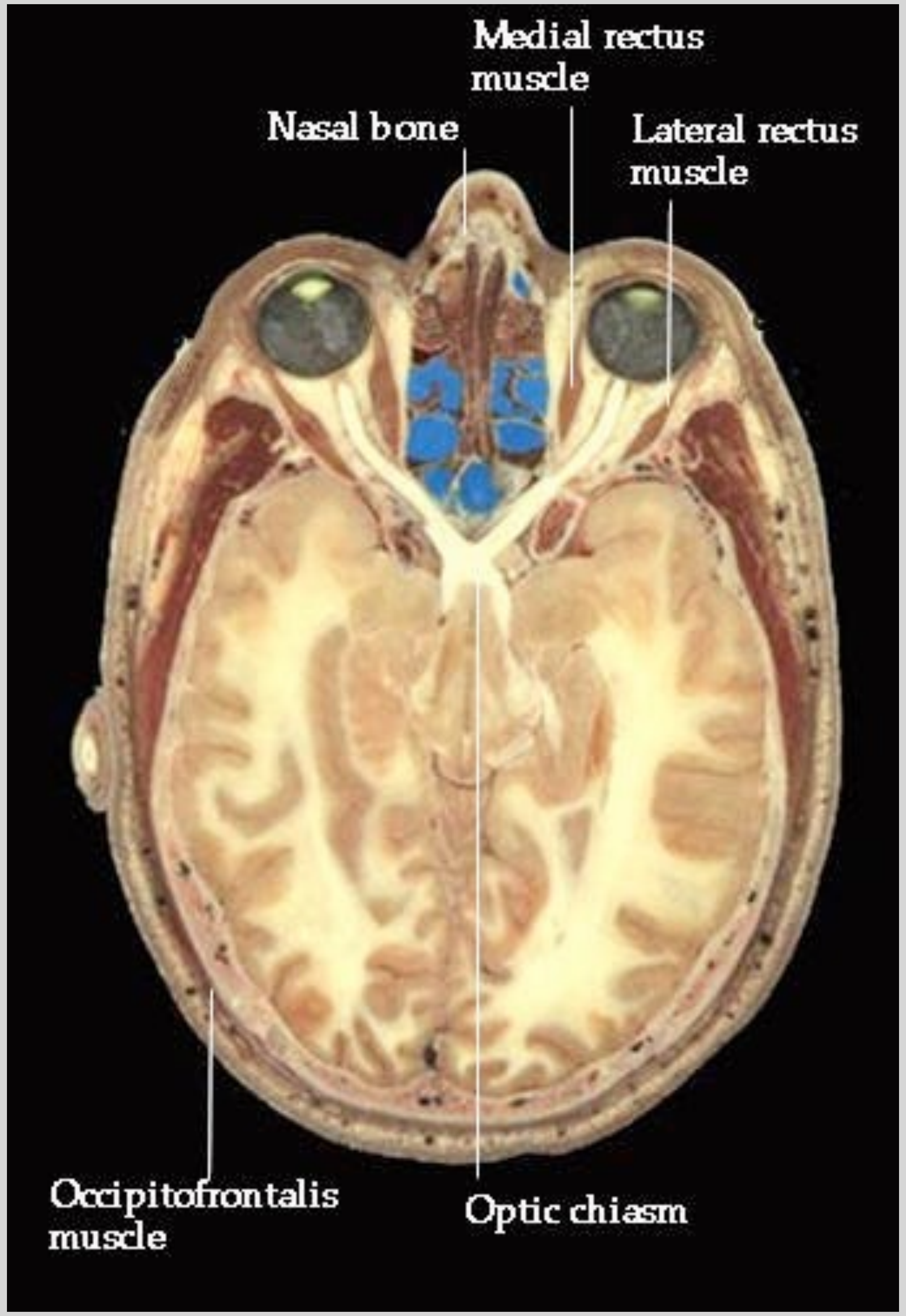

The Eyes in the Head

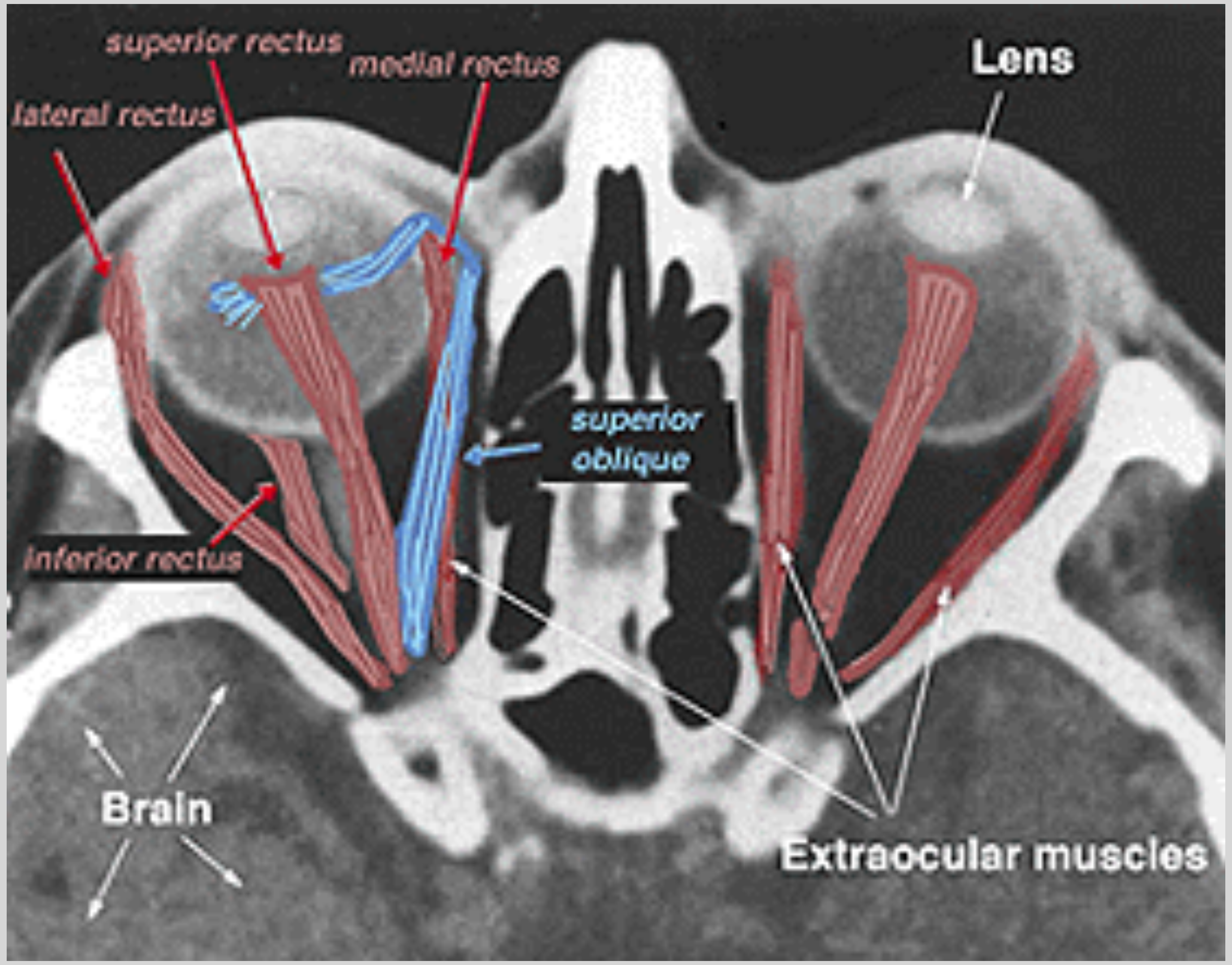

The Normal Eye

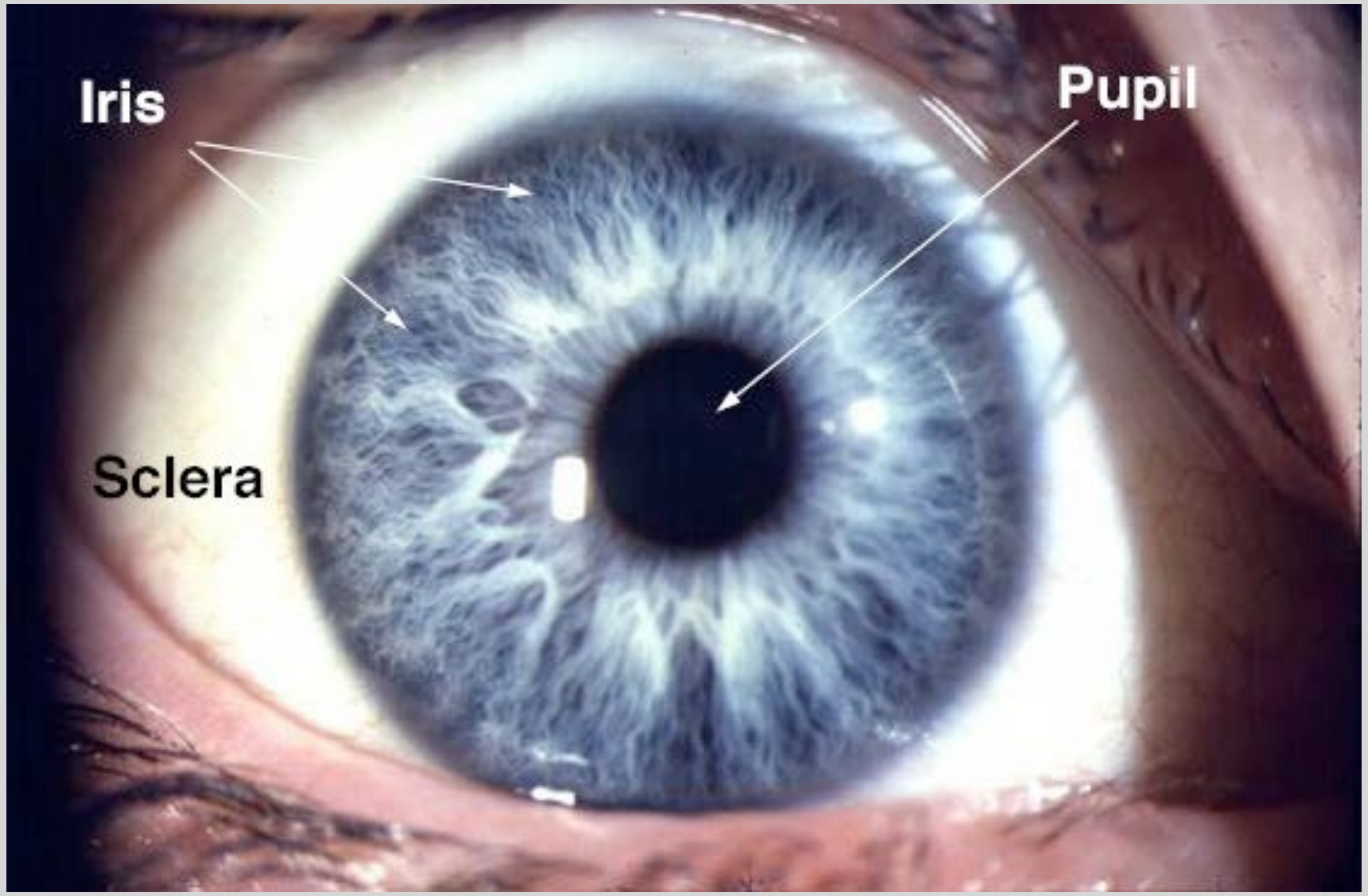

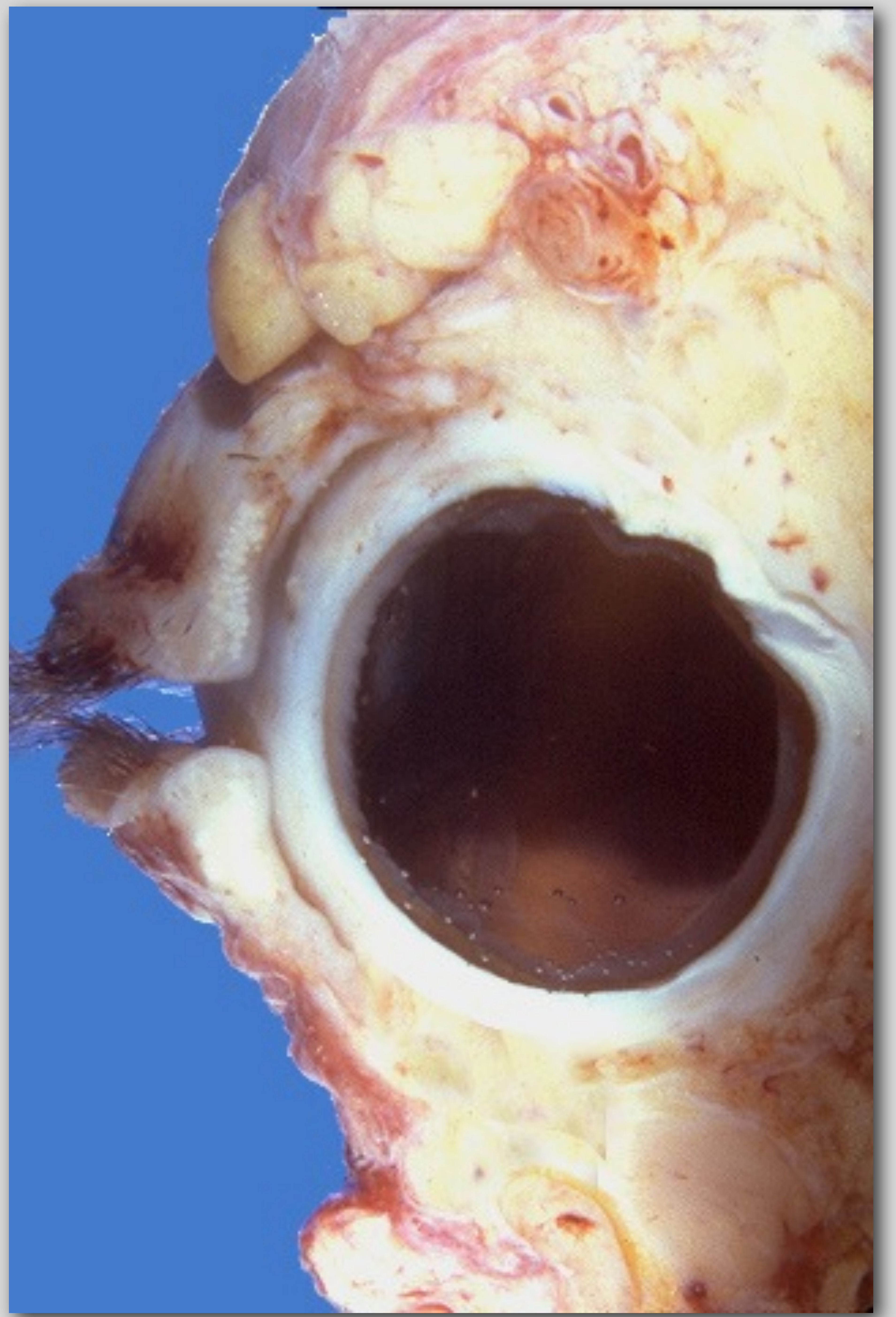

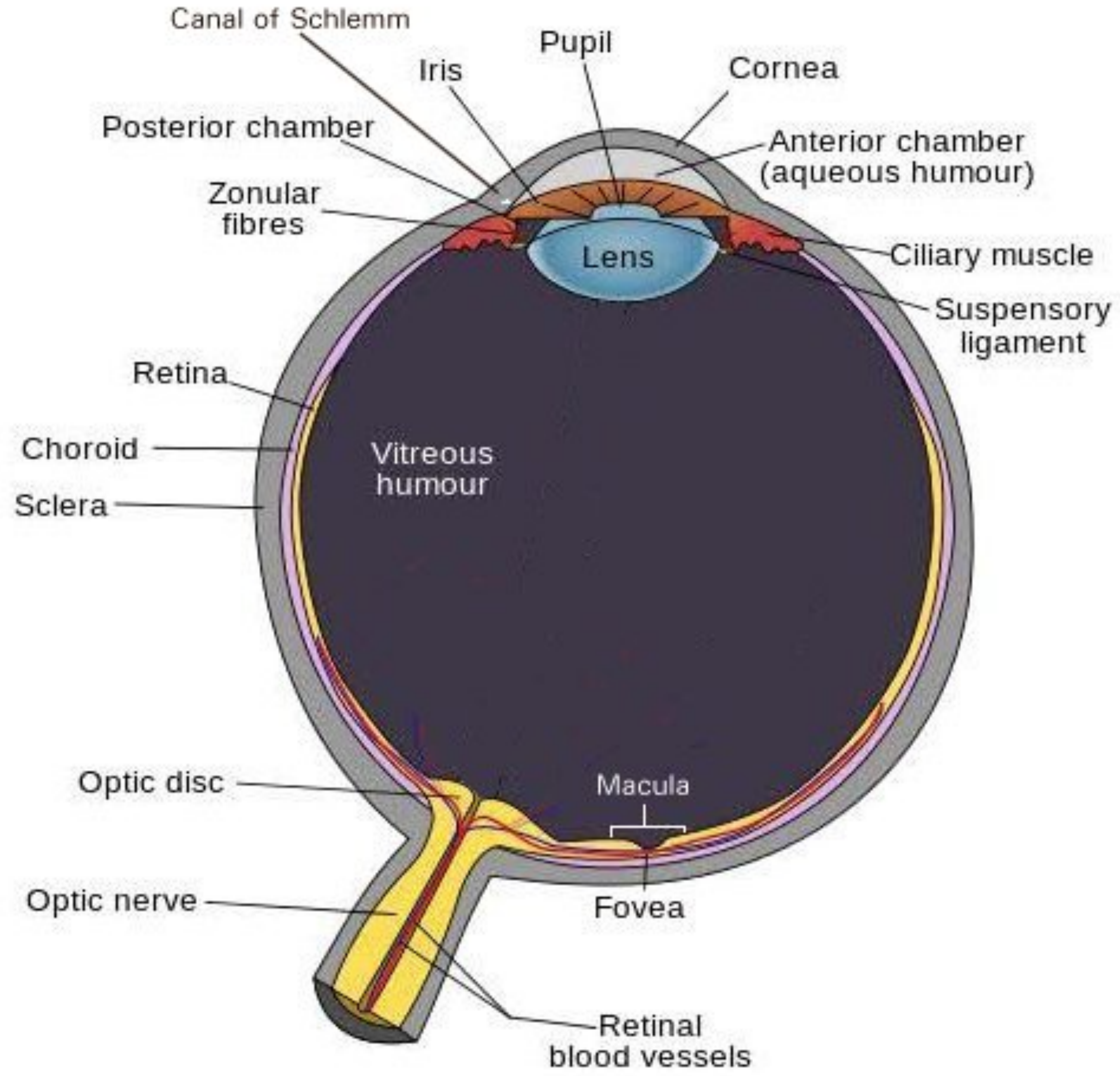
Canal of Schlemm
Pupil
Iris
Cornea
Posterior chamber
Anterior chamber
(aqueous humour)
Zonular
fibres
Lens
Ciliary muscle
Suspensory
ligament
Retina
Choroid
Vitreous
humour
Sclera
Optic disc
Macula
Optic nerve
Fovea
Retinal
blood vessels

Optics of the Eye

- Focal Length of a lens
- Optical Power in dioptres
- Relative Optical Power in dioptres
- Far Point, Near Point, Resting Point

Problems with the Optics

- Where is the far point?
  - At optical infinity (Emmetropia)
  - Closer than infinity (Myopia)
  - Farther than infinity (Hyperopia)
- Cataract
- Astigmatism
- Resting Point

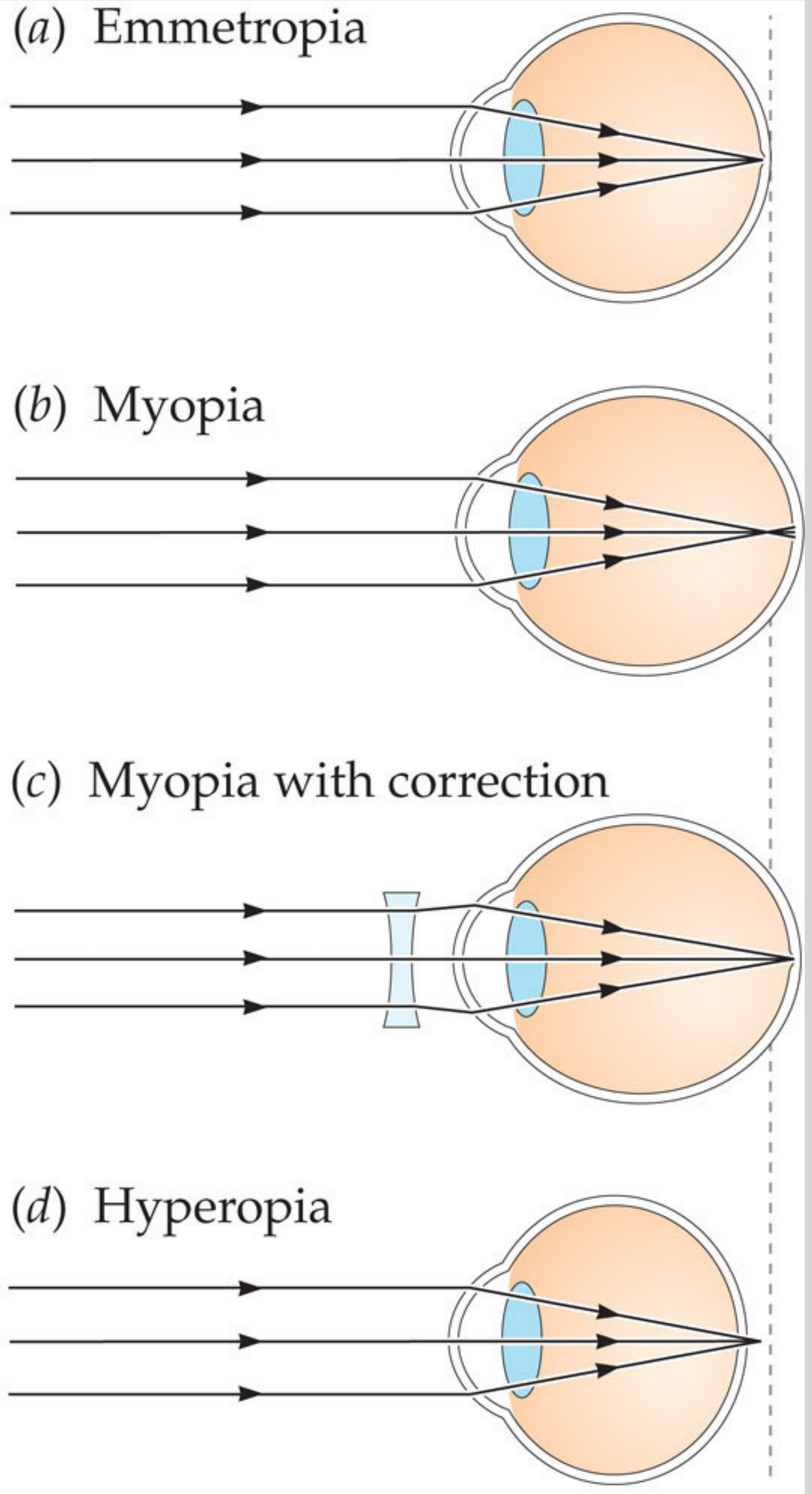

SENSATION & PERCEPTION 4e, Figure 2.3

The normal appearance of the crystalline lens at the bottom and the anterior chamber of the eye above this is shown here. The lens becomes progressively less elastic and distensible with age. This is known as presbyopia because there is diminution of the power of accommodation with greater difficulty focusing at close distances. Hence, the need for bifocals starting in their 40's for many people.

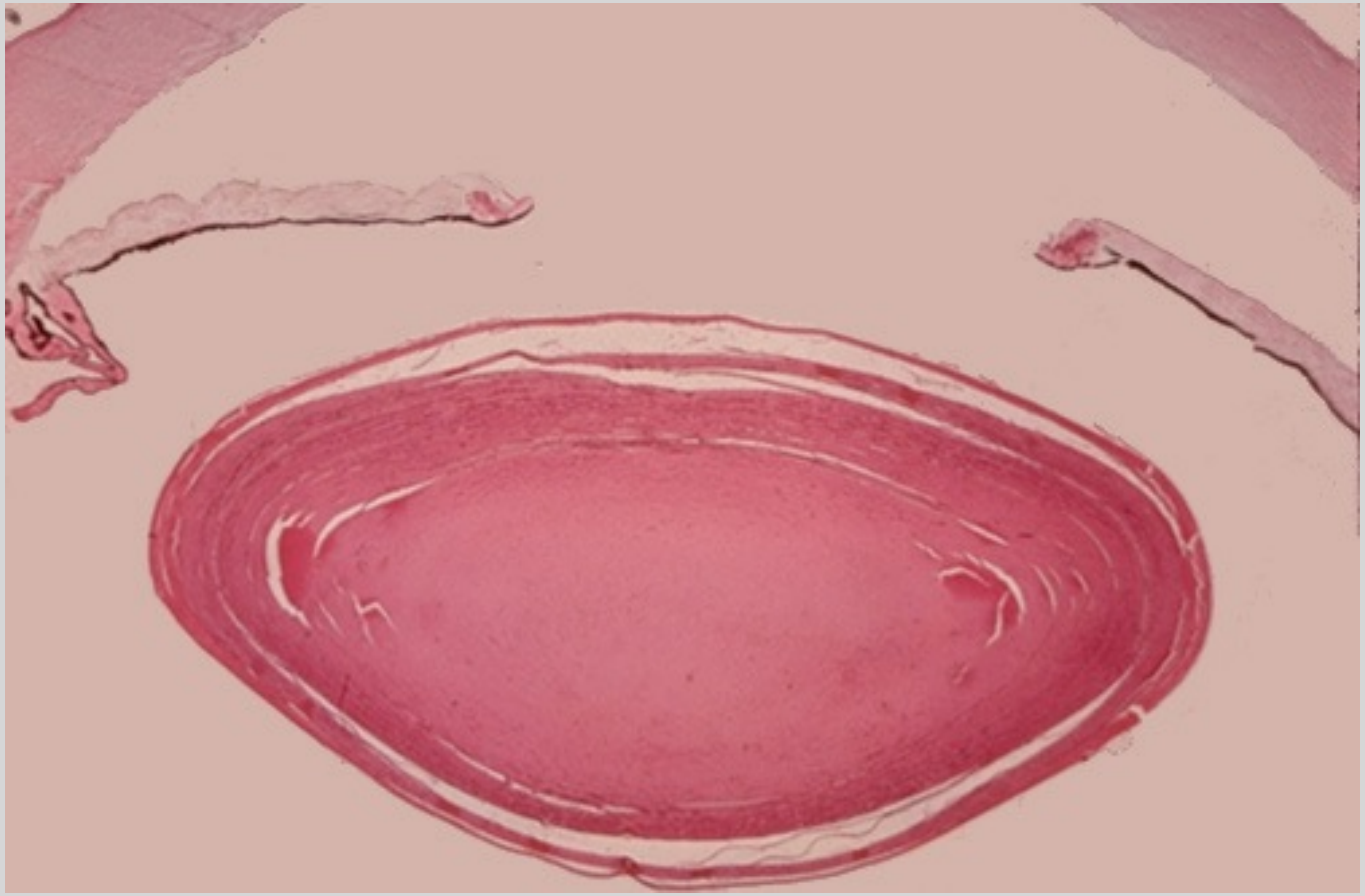

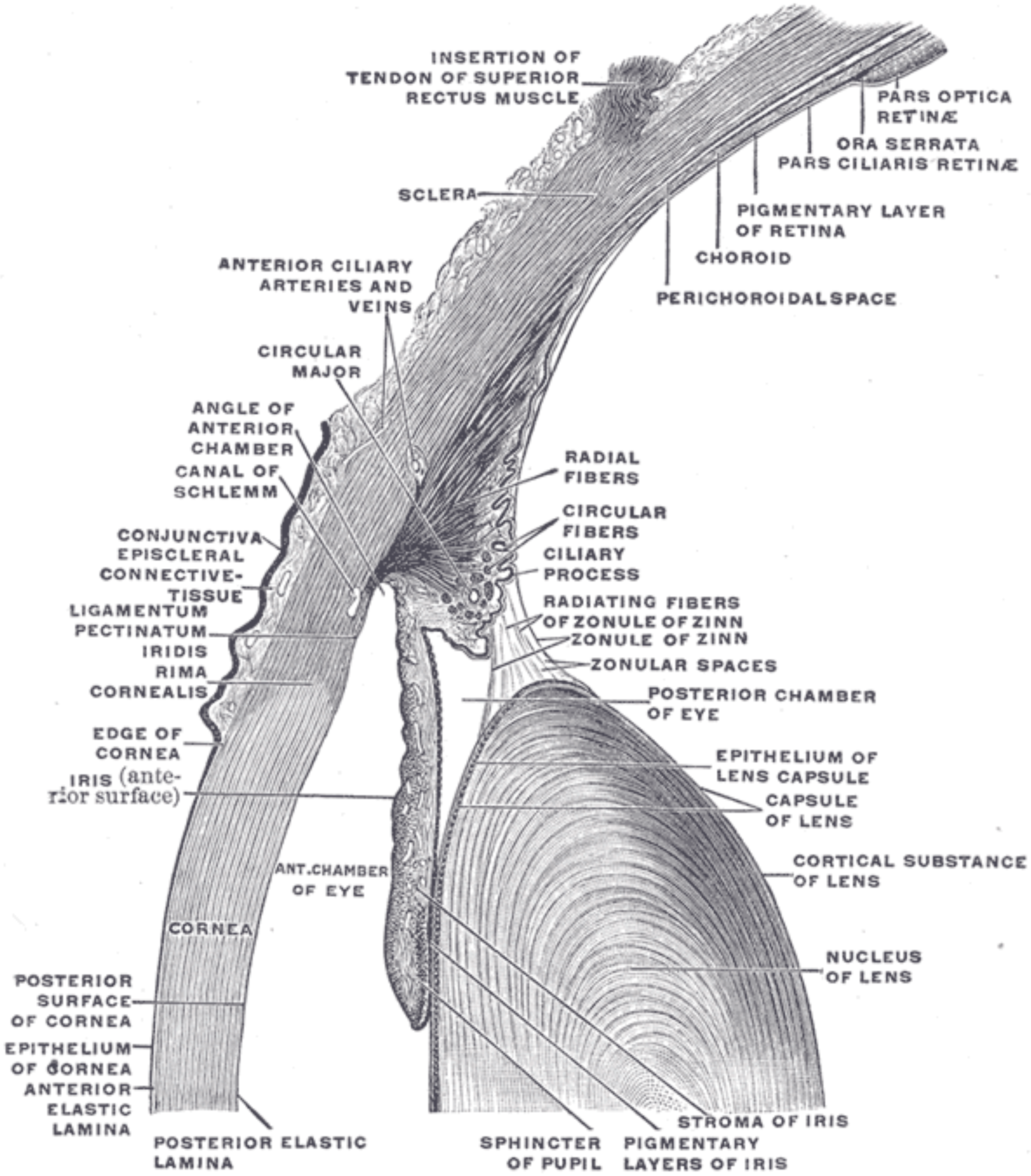
INSERTION OF
TENDON OF SUPERIOR
RECTUS MUSCLE
PARS OPTICA
RETINÆ
ORA SERRATA
PARS CILIARIS RETINÆ
SCLERA
PIGMENTARY LAYER
OF RETINA
CHOROID
PERICHOROIDAL SPACE
ANTERIOR CILIARY
ARTERIES AND
VEINS
CIRCULAR
MAJOR
ANGLE OF
ANTERIOR
CHAMBER
CANAL OF
SCHLEMM
RADIAL
FIBERS
CIRCULAR
FIBERS
CONJUNCTIVA
EPISCLERAL
CONNECTIVE-
TISSUE
CILIARY
PROCESS
LIGAMENTUM
PECTINATUM
IRIDIS
RADIATING FIBERS
OF ZONULE OF ZINN
ZONULE OF ZINN
ZONULAR SPACES
RIMA
CORNEALIS
POSTERIOR CHAMBER
OF EYE
EDGE OF
CORNEA
EPITHELIUM OF
LENS CAPSULE
IRIS (ante-
rior surface)
CAPSULE
OF LENS
ANT. CHAMBER
OF EYE
CORTICAL SUBSTANCE
OF LENS
CORNEA
NUCLEUS
OF LENS
POSTERIOR
SURFACE
OF CORNEA
EPITHELIUM
OF CORNEA
ANTERIOR
ELASTIC
LAMINA
POSTERIOR ELASTIC
LAMINA
SPHINCTER
OF PUPIL
STROMA OF IRIS
PIGMENTARY
LAYERS OF IRIS

Loss of Accommodation Power: Presbyopia

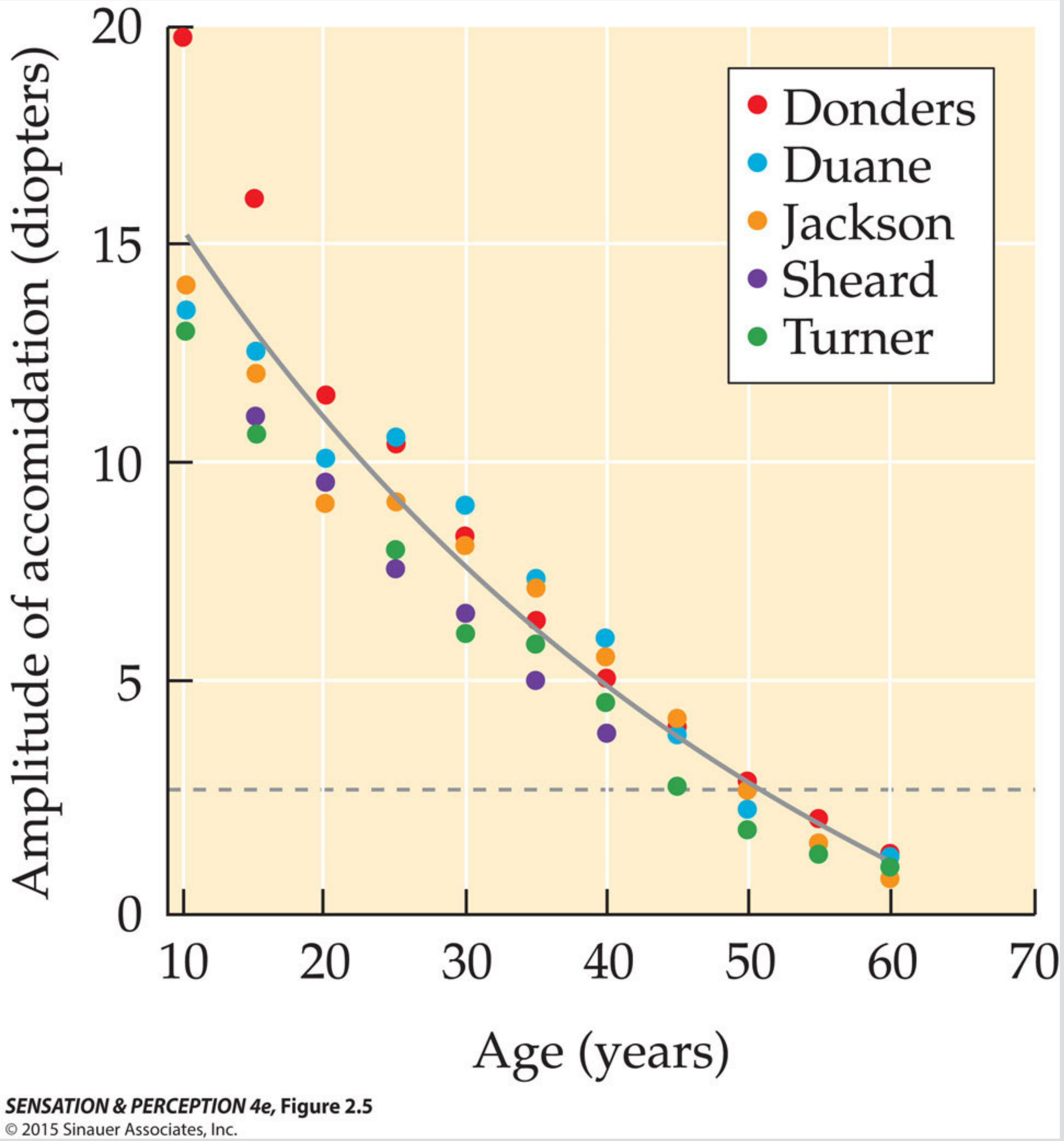

Franciscus Cornelis Donders
1818-1889

Cataracts

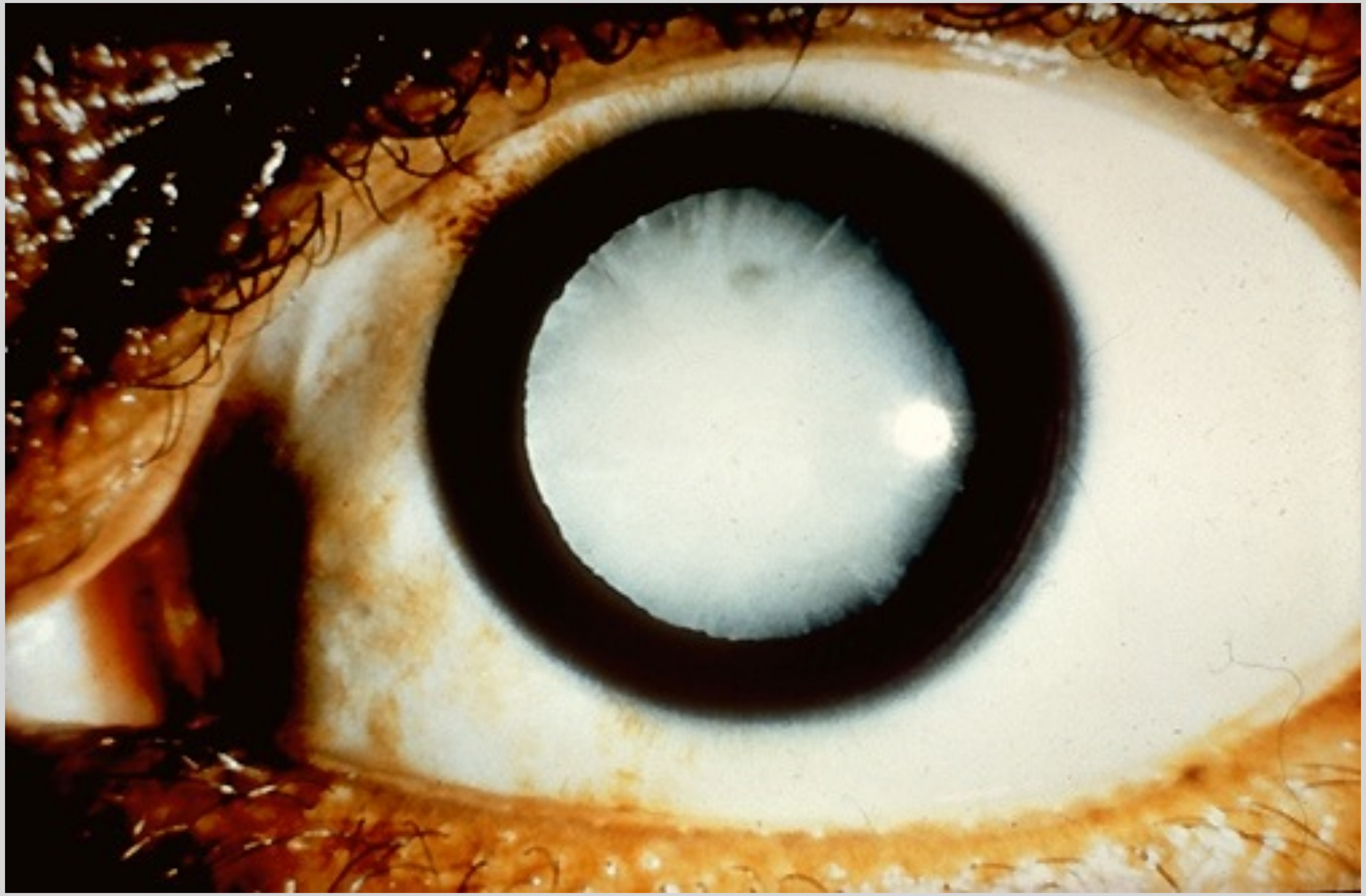

This is a cataract. A cataract results from opacification of the crystalline lens. This opacification results from a series of events starting in the lens cortex with rarefaction, then liquefecation, of cortical cells. This leads to fragmentation of lens fibers and extracellular globule formation. In the lens nucleus there is a progressive increase in the amount of insoluble proteins which leads to hardening (sclerosis) and brownish discoloration (brunescence).

Cataracts

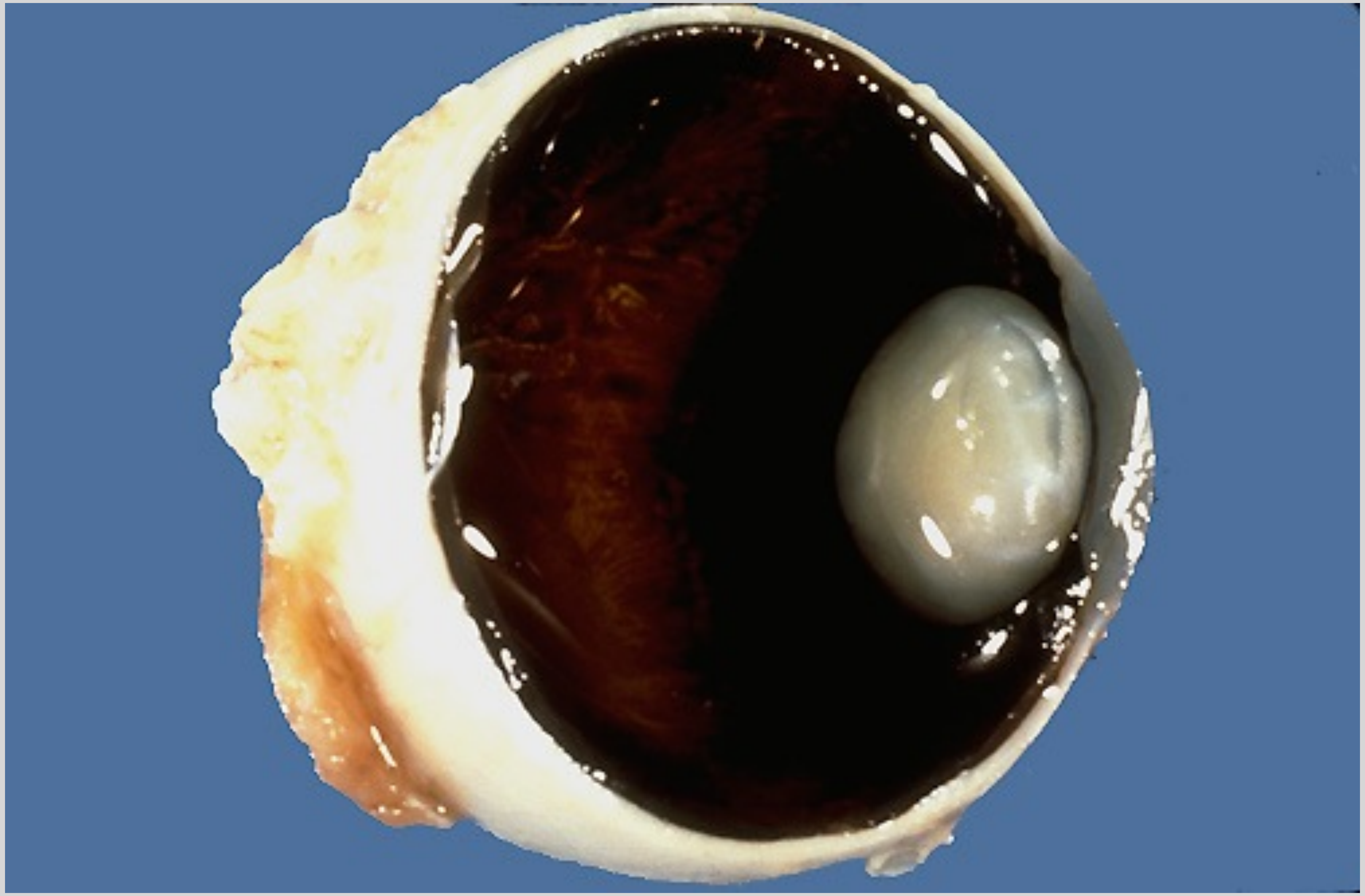

On cross-section of the eyeball can be seen a lens at the right which contains a cataract. Cataracts are more common in the elderly and in persons with diabetes mellitus. Such cataracts can be removed and replaced by a lens implant.

Astigmatism

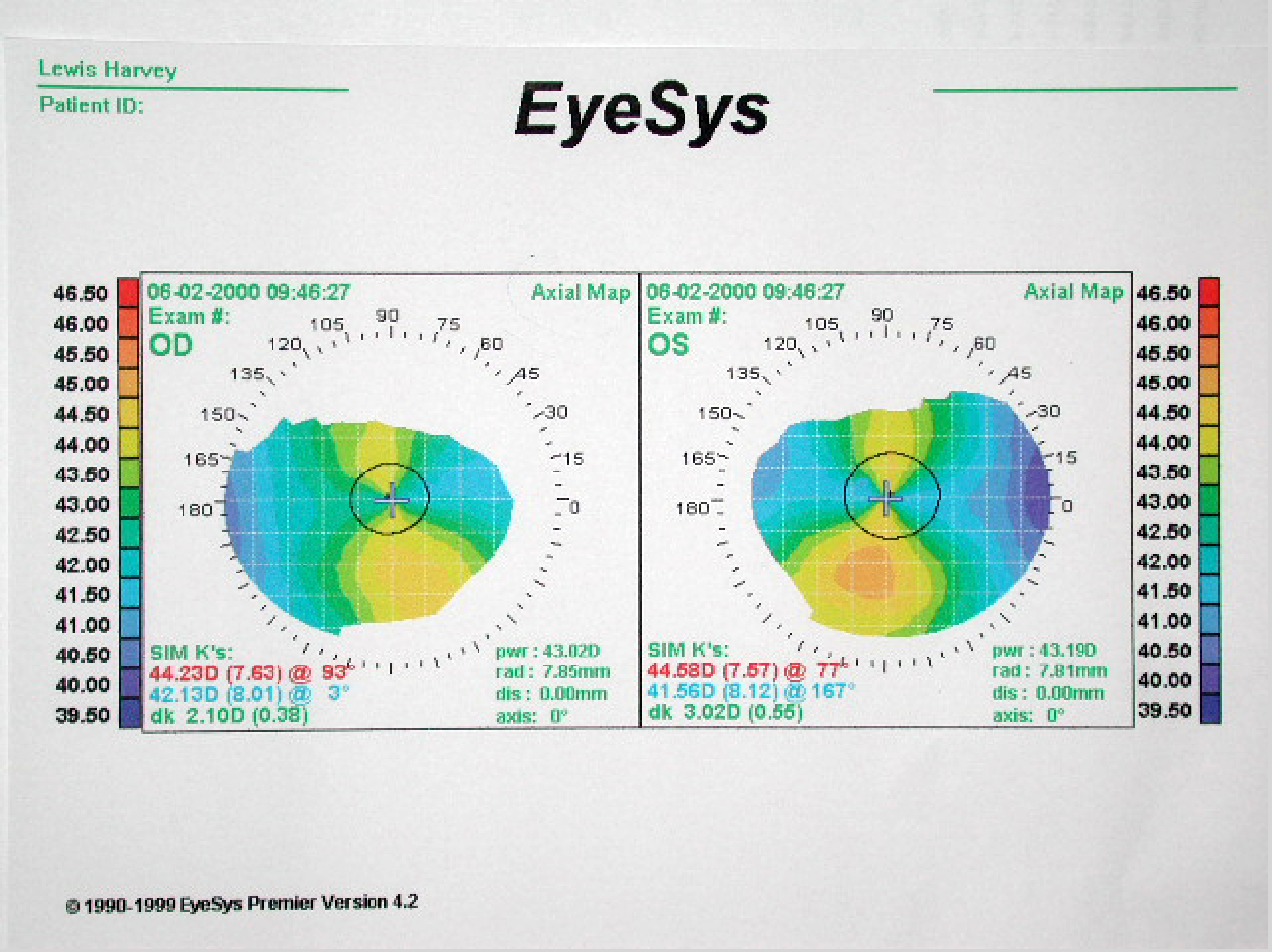

Astigmatism

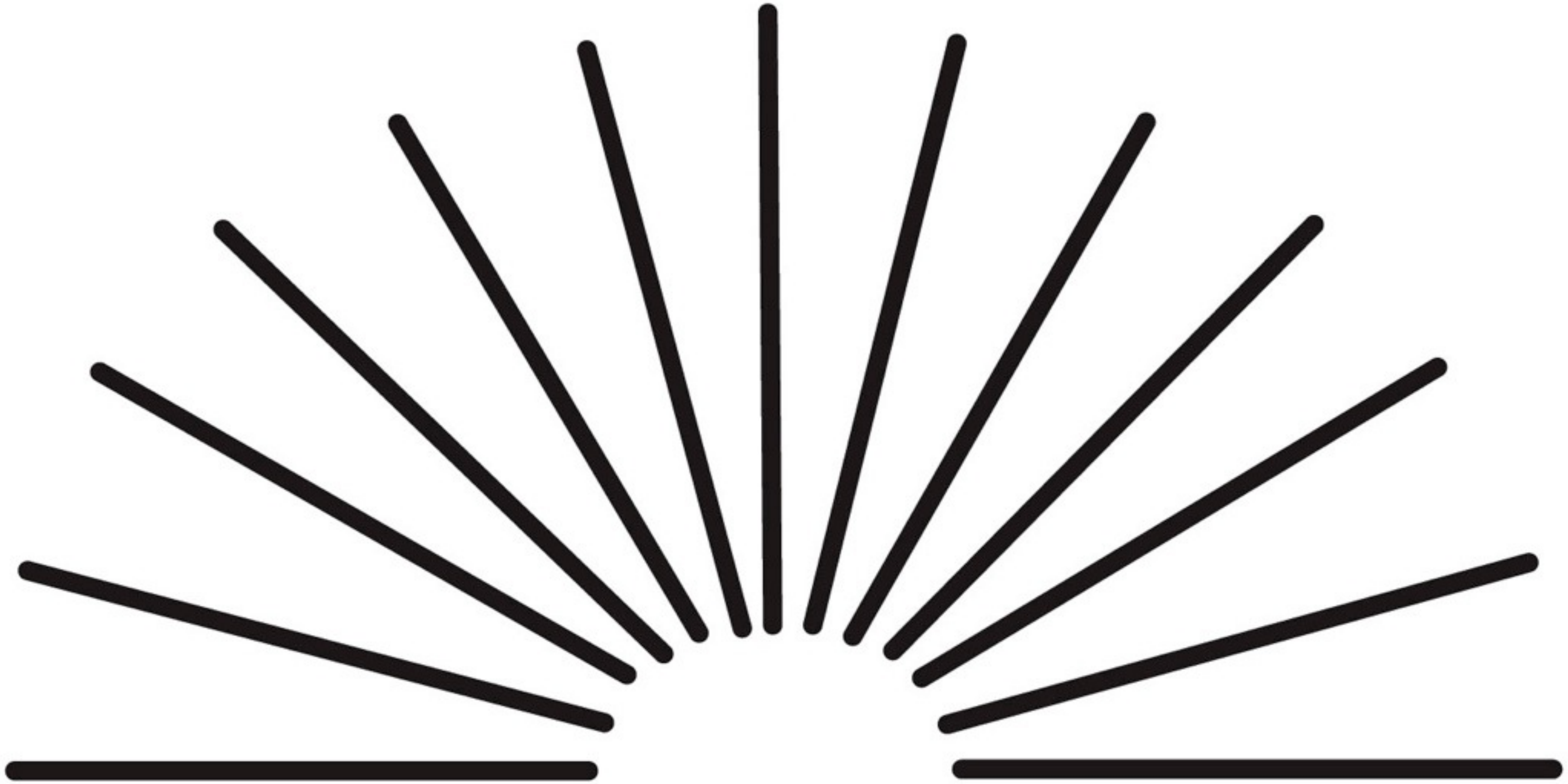

SENSATION & PERCEPTION 2e, Figure 2.4

Resting Point

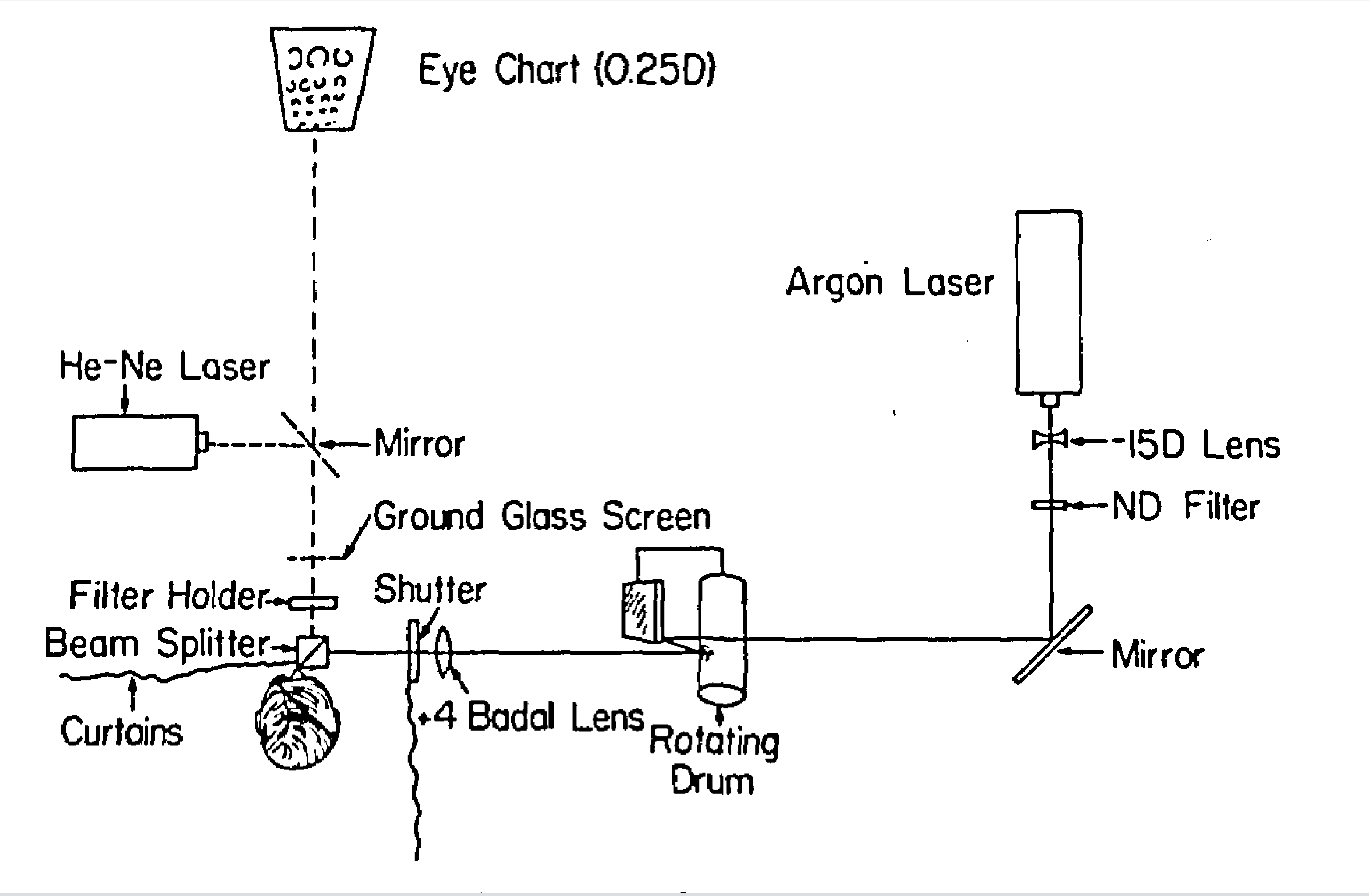

Leibowitz, H. W., & Owens, D. A. (1975). Night myopia and the intermediate dark focus of accommodation. Journal of the Optical Society of America, 65(10), 1121–1128.

Resting Focus of the Eye

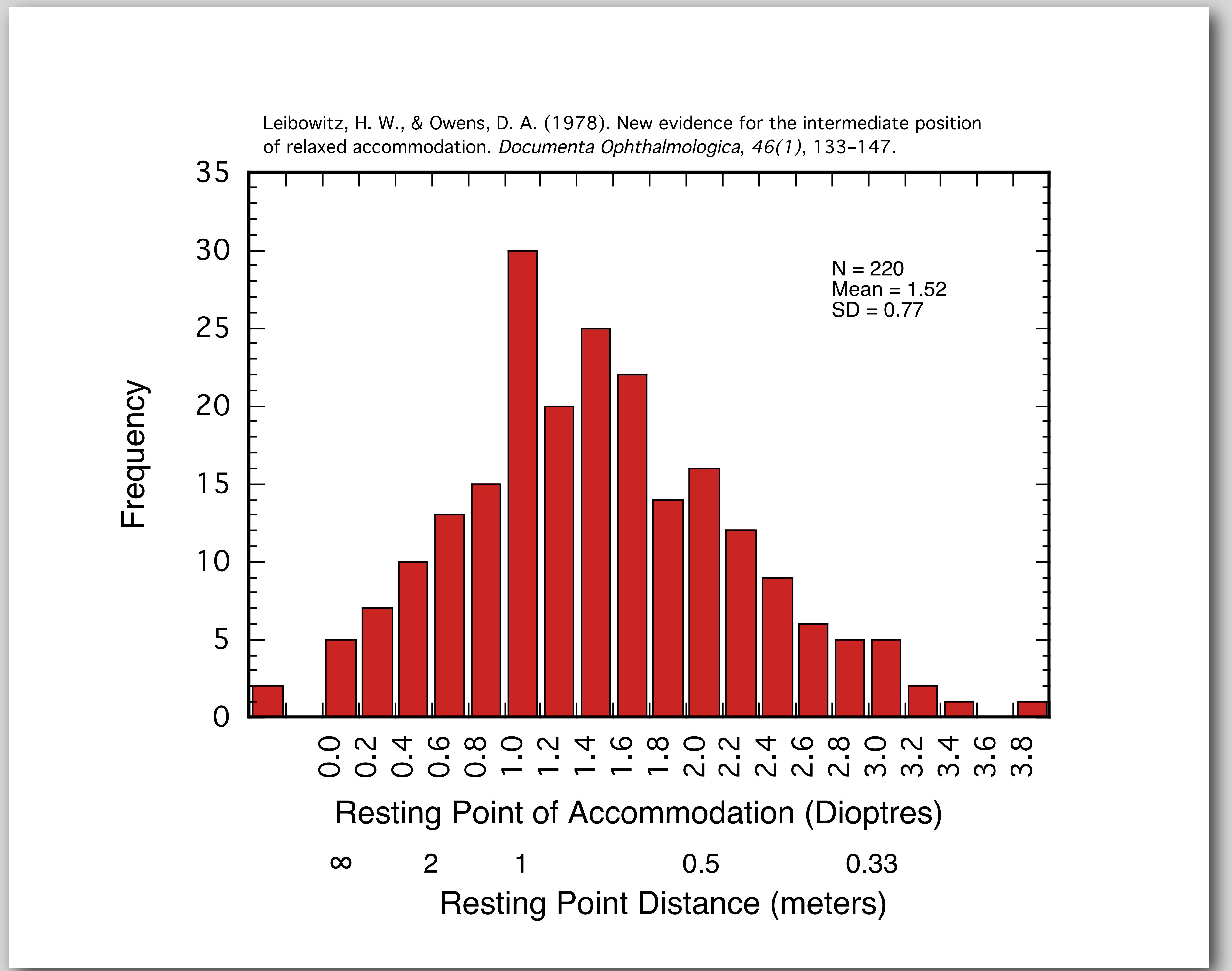

The Normal Retina

Three Layers, Five Cells

- Photoreceptors
- Bipolar Cells
- Retinal Ganglion Cells
- Horizontal Cells
- Amacrine Cells

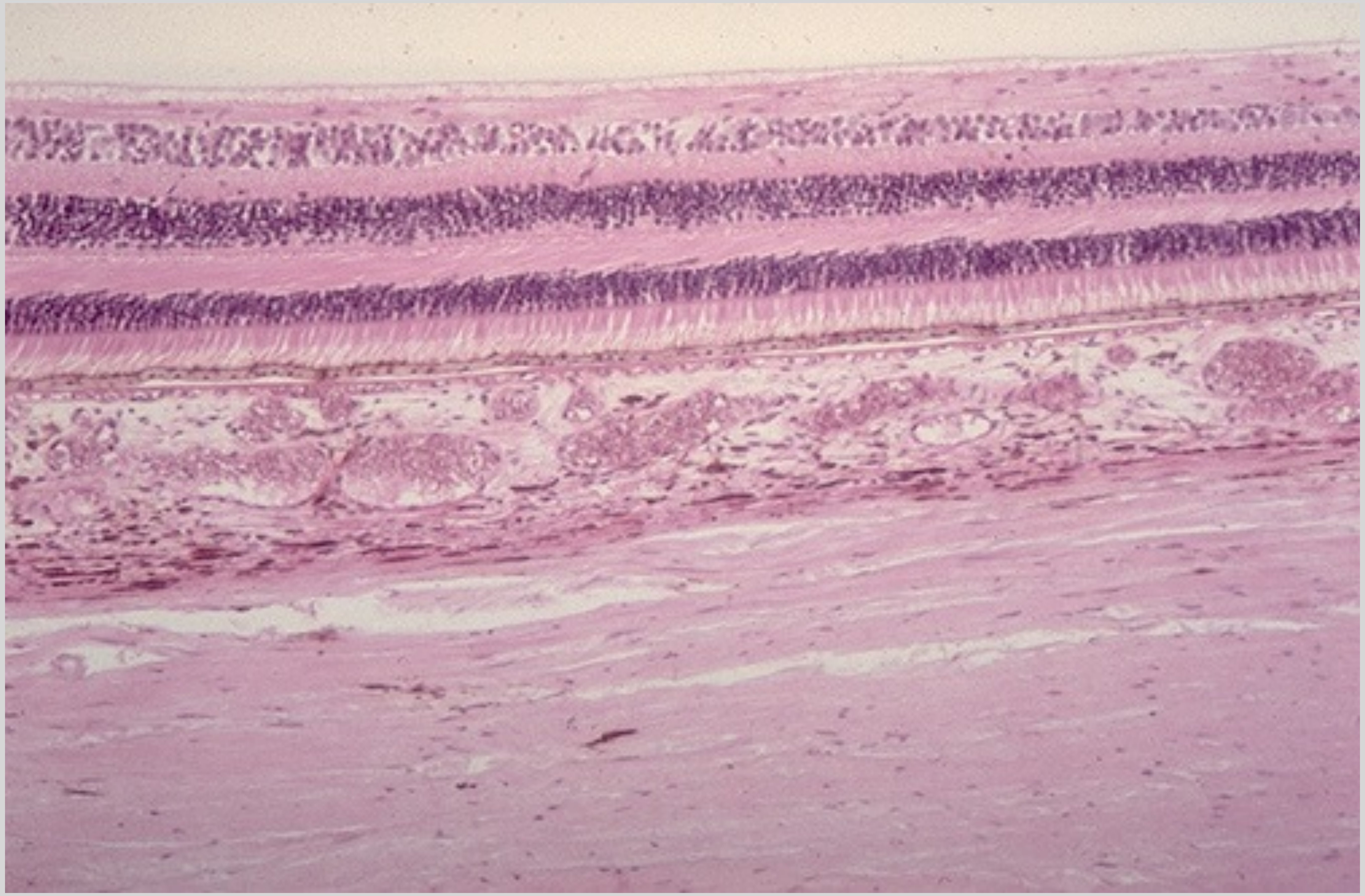

The normal histologic appearance of the retina shows many layers. The lowest layer just above the connective tissue is the layer of rods and cones. Above this are layers of external and internal plexiform and nuclear lamina. The nerve fibers are at the top and collect together to enter the optic nerve at the optic disk.

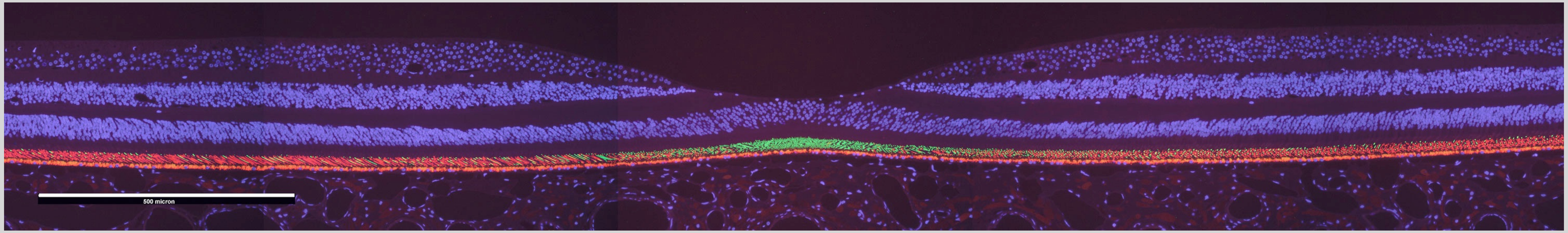

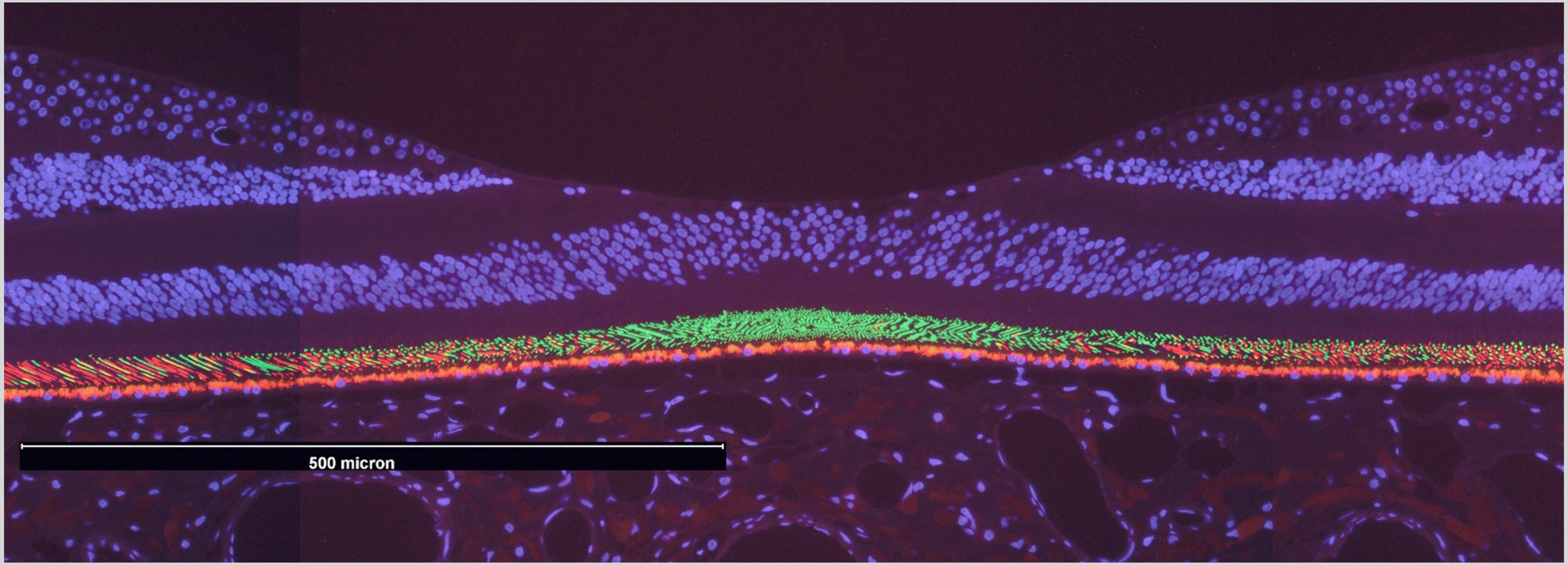

Courtesy of Max Snodderly, University of Texas Austin

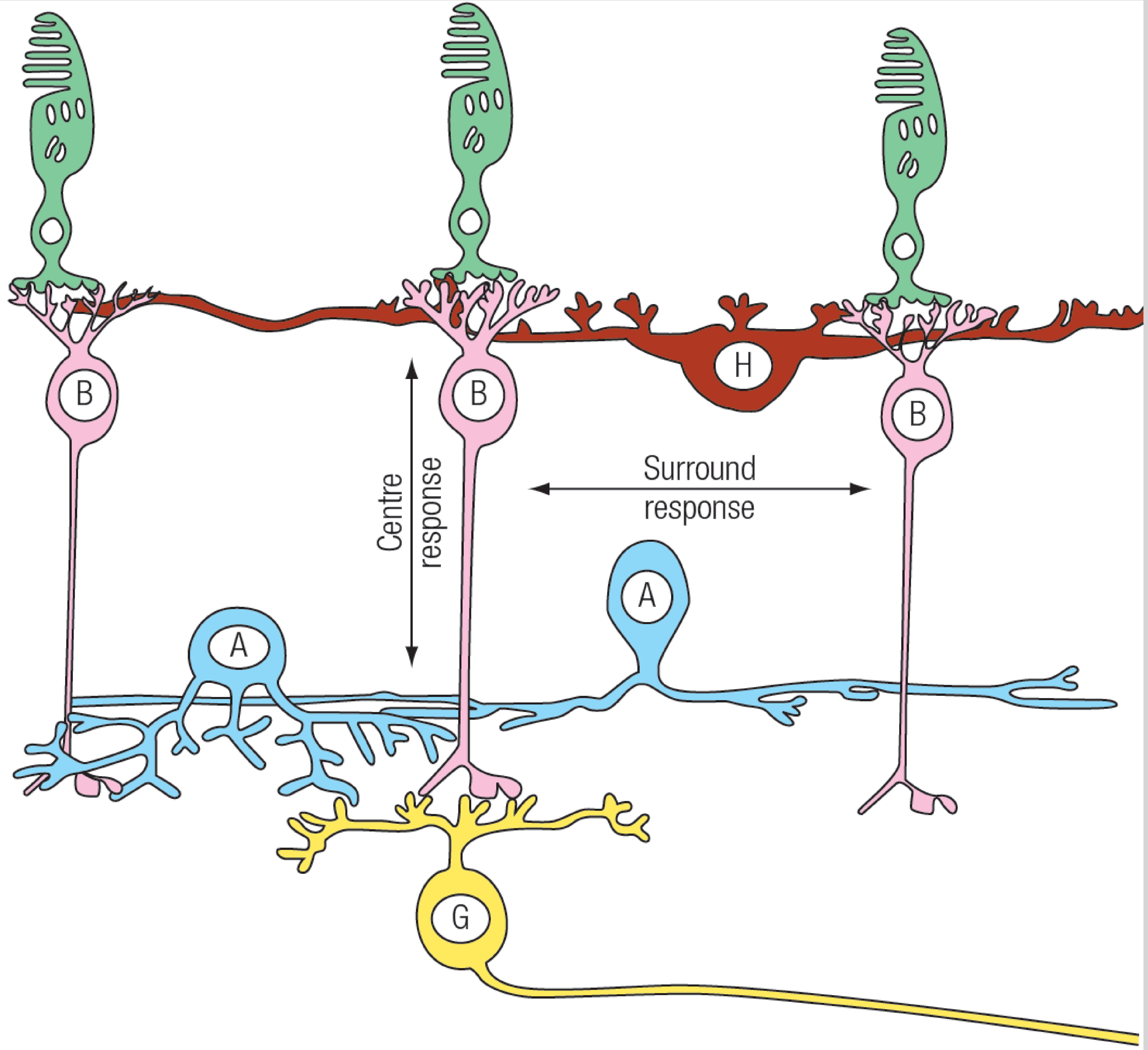
B
B
B
H
Centre response
Surround response
A
A
G

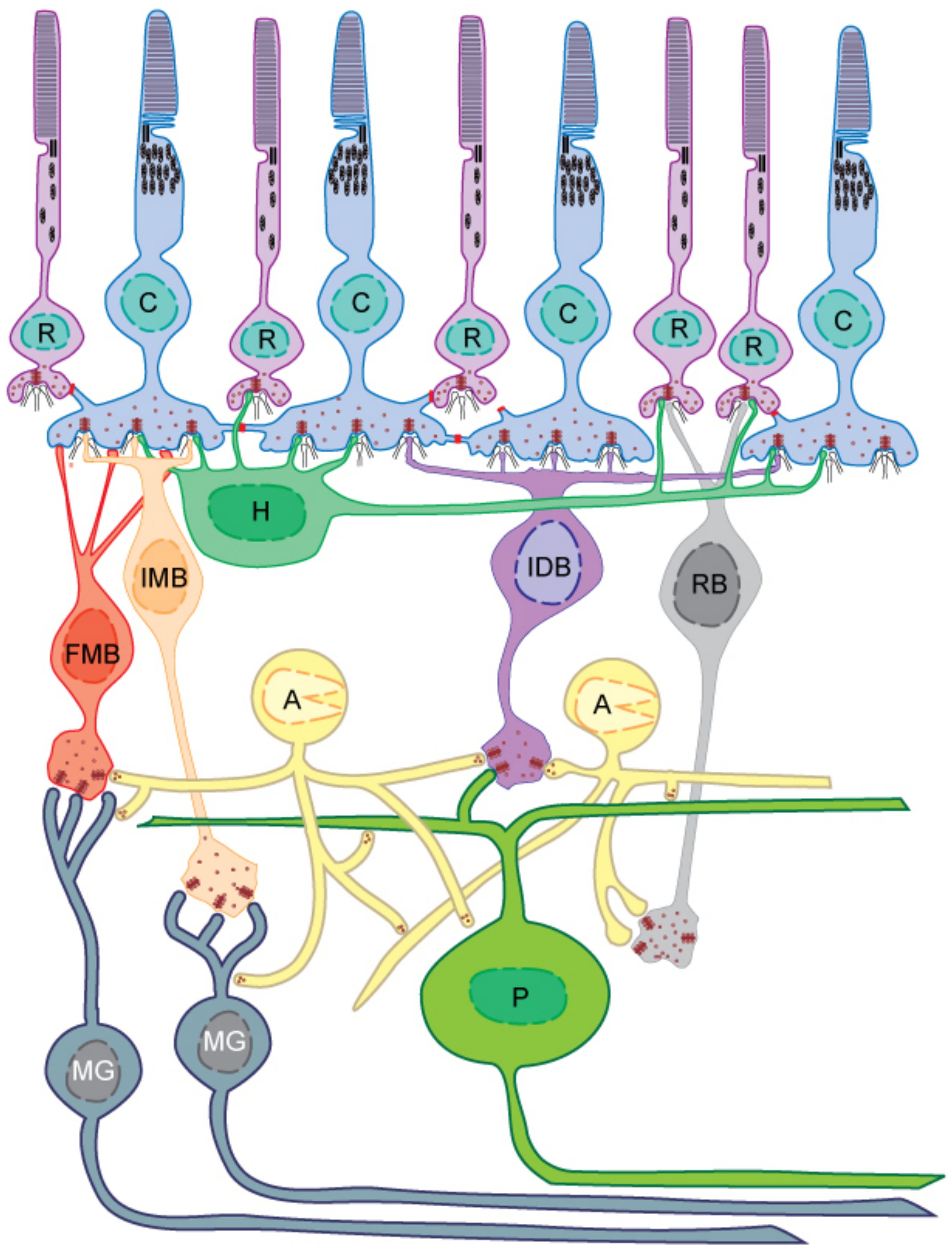

FIGURE 26.2 Summary diagram of the cell types and connections in the primate retina. R, rod; C, cone; H, horizontal cell; FMB, flat midget bipolar; IMB, invaginating midget bipolar; IDB, invaginating diffuse bipolar; RB, rod bipolar; A, amacrine cell; P, parasol cell (also confusingly called an M cell because of its thalamic targets, see text for details); MG, midget ganglion cell (also confusingly called a P cell). *Adapted from Dowling (1997).*

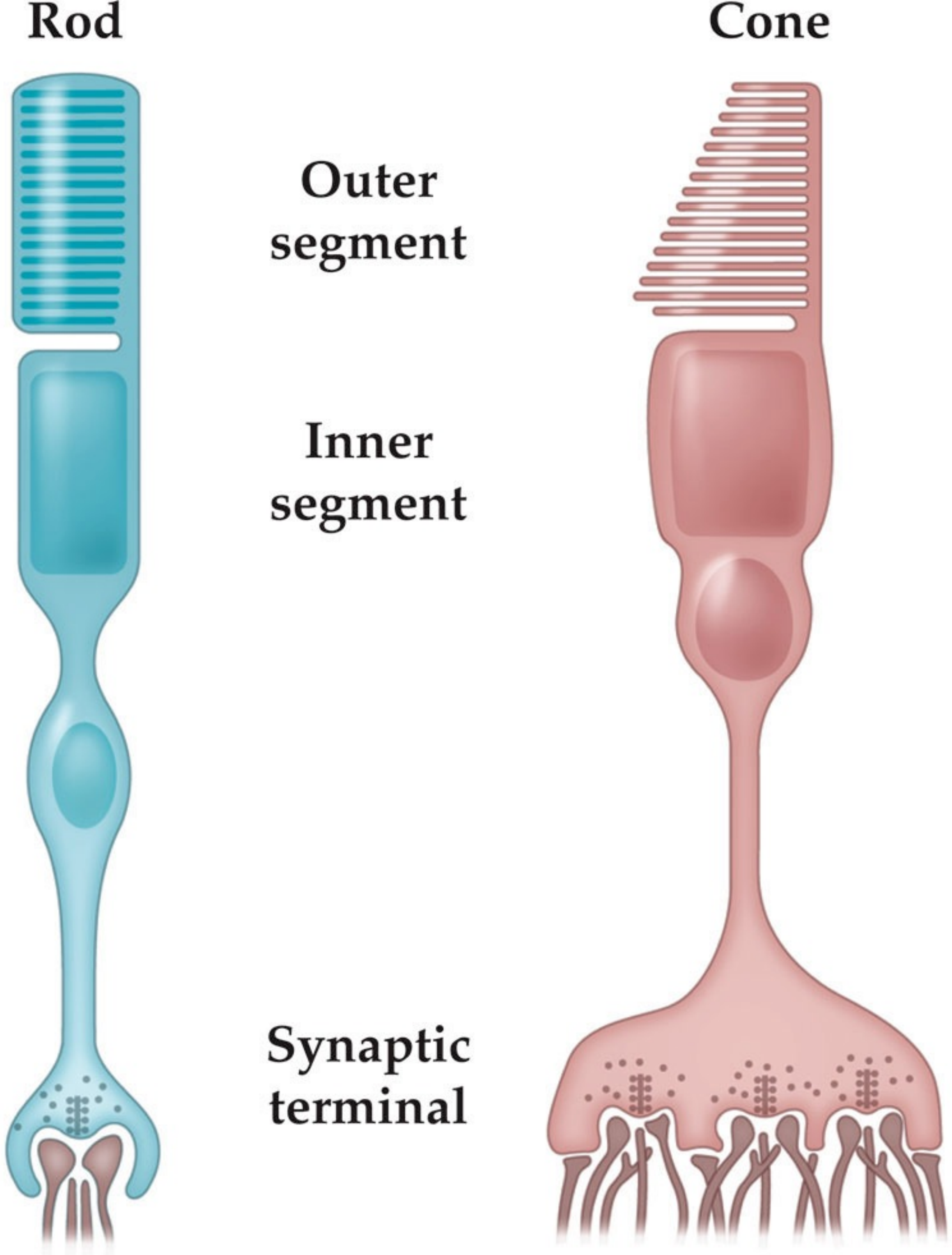

SENSATION & PERCEPTION 3e, **Figure 2.8**

Østerberg (1935)

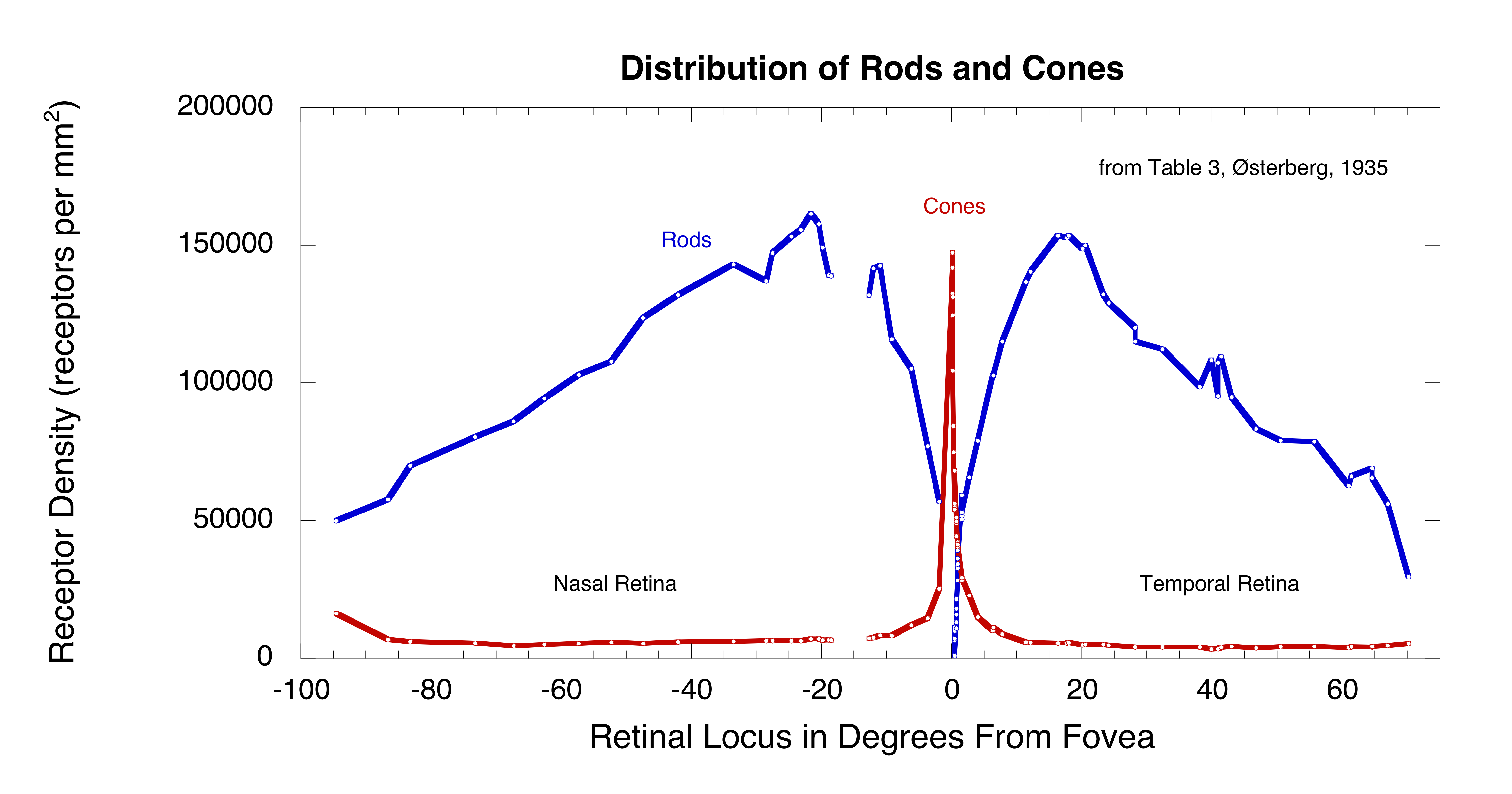

Foveal Mosaic

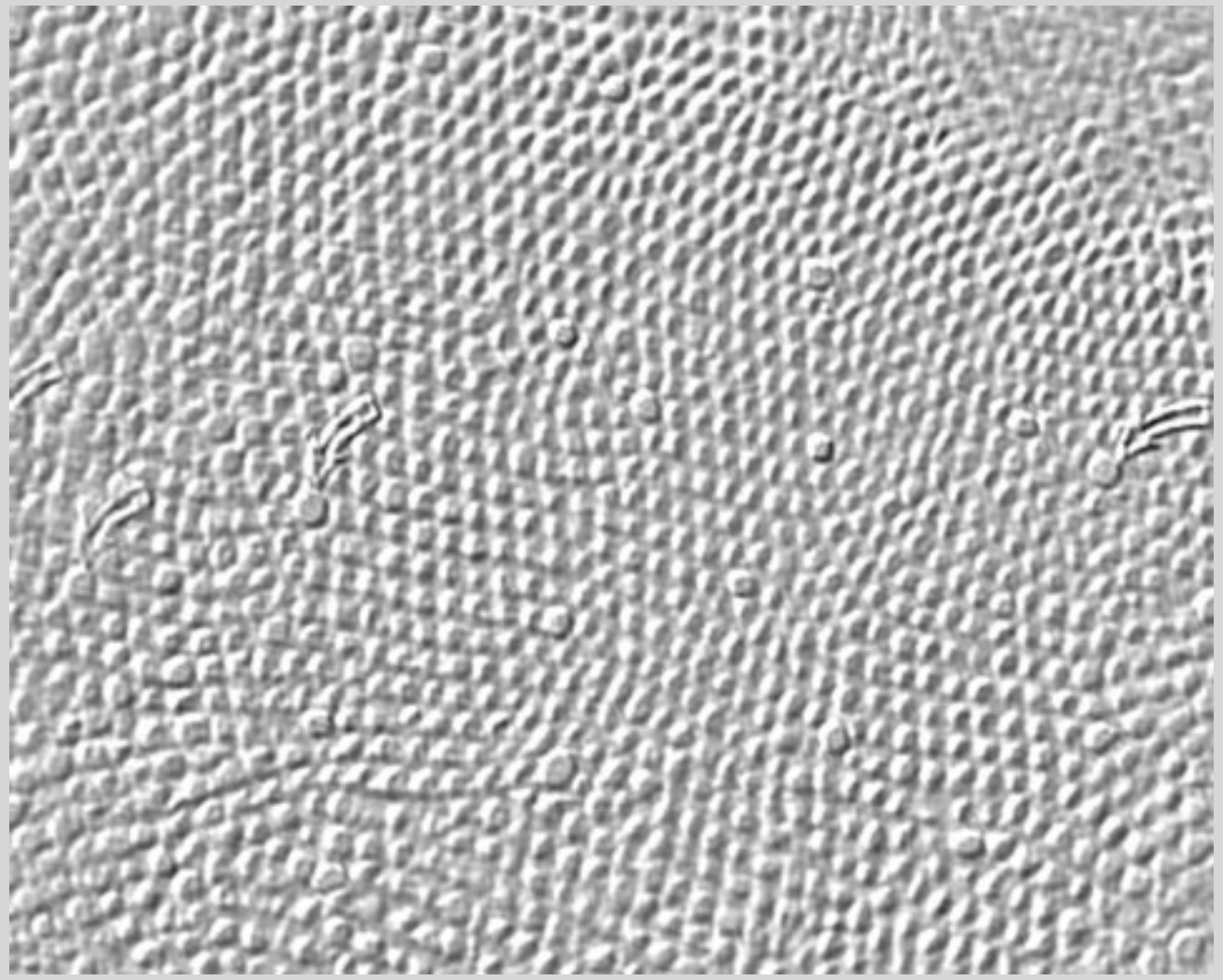

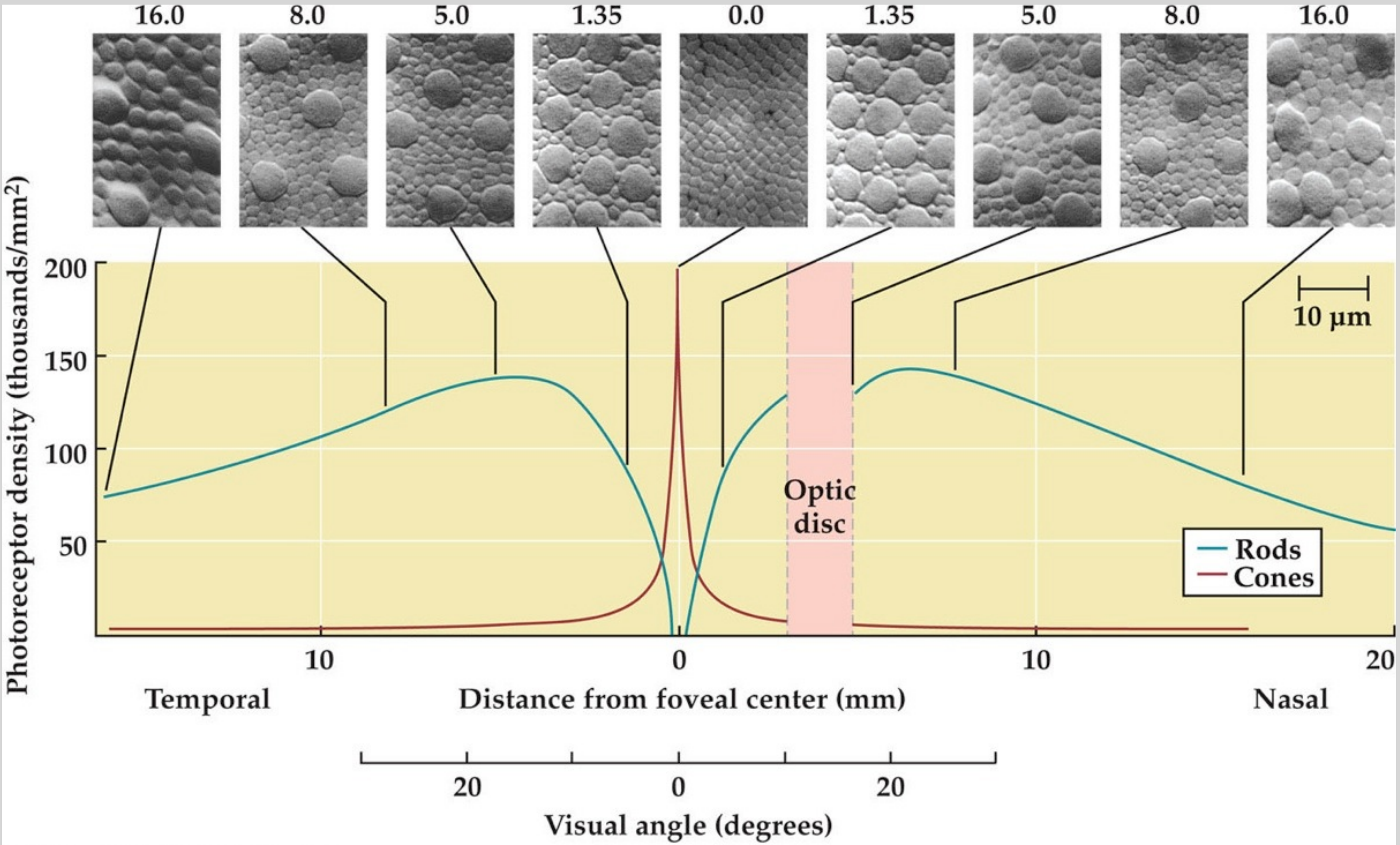

SENSATION & PERCEPTION 3e, **Figure 2.9**

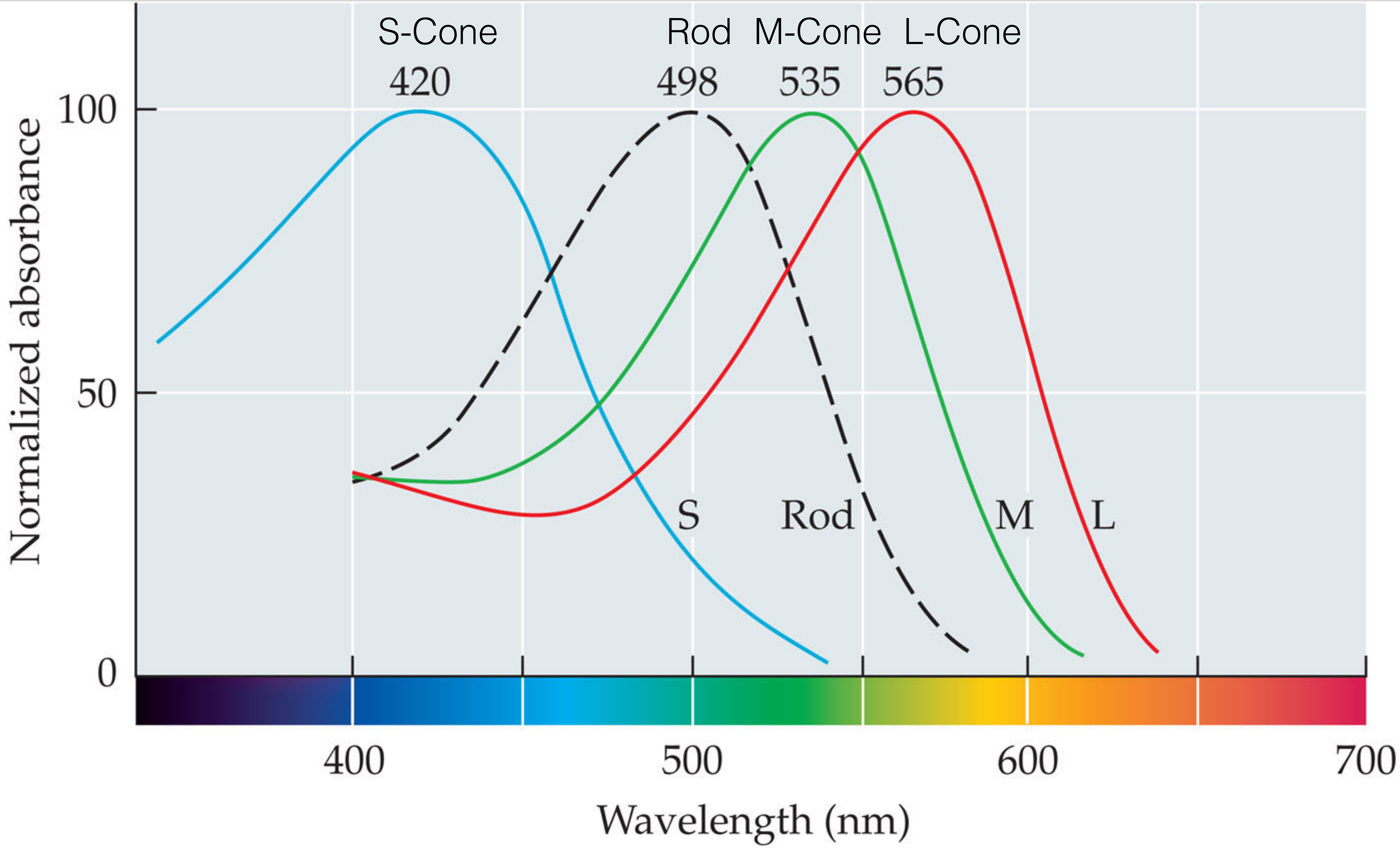

***SENSATION & PERCEPTION 4e,* Figure 5.1**

Photopic vs. Scotopic Vision

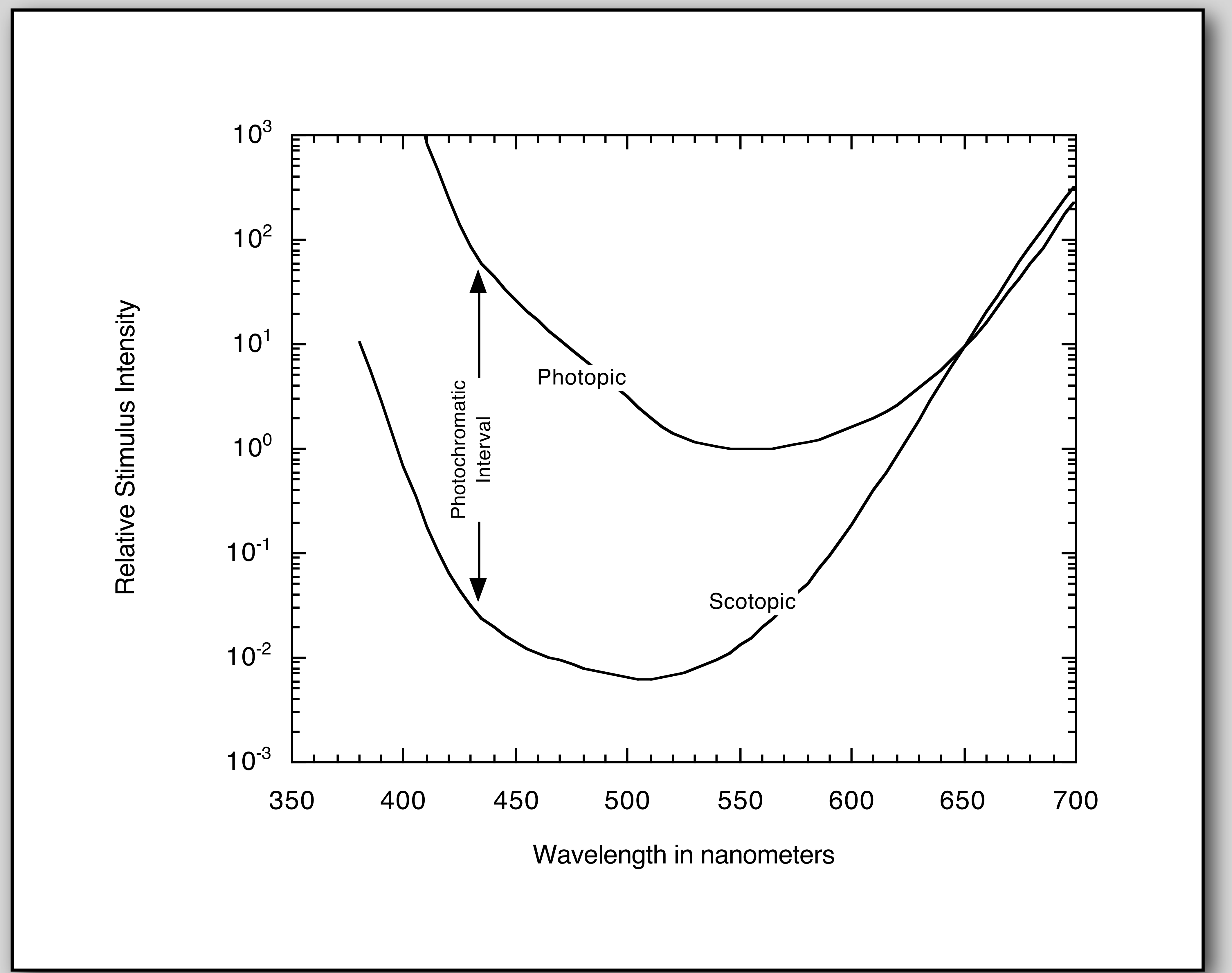

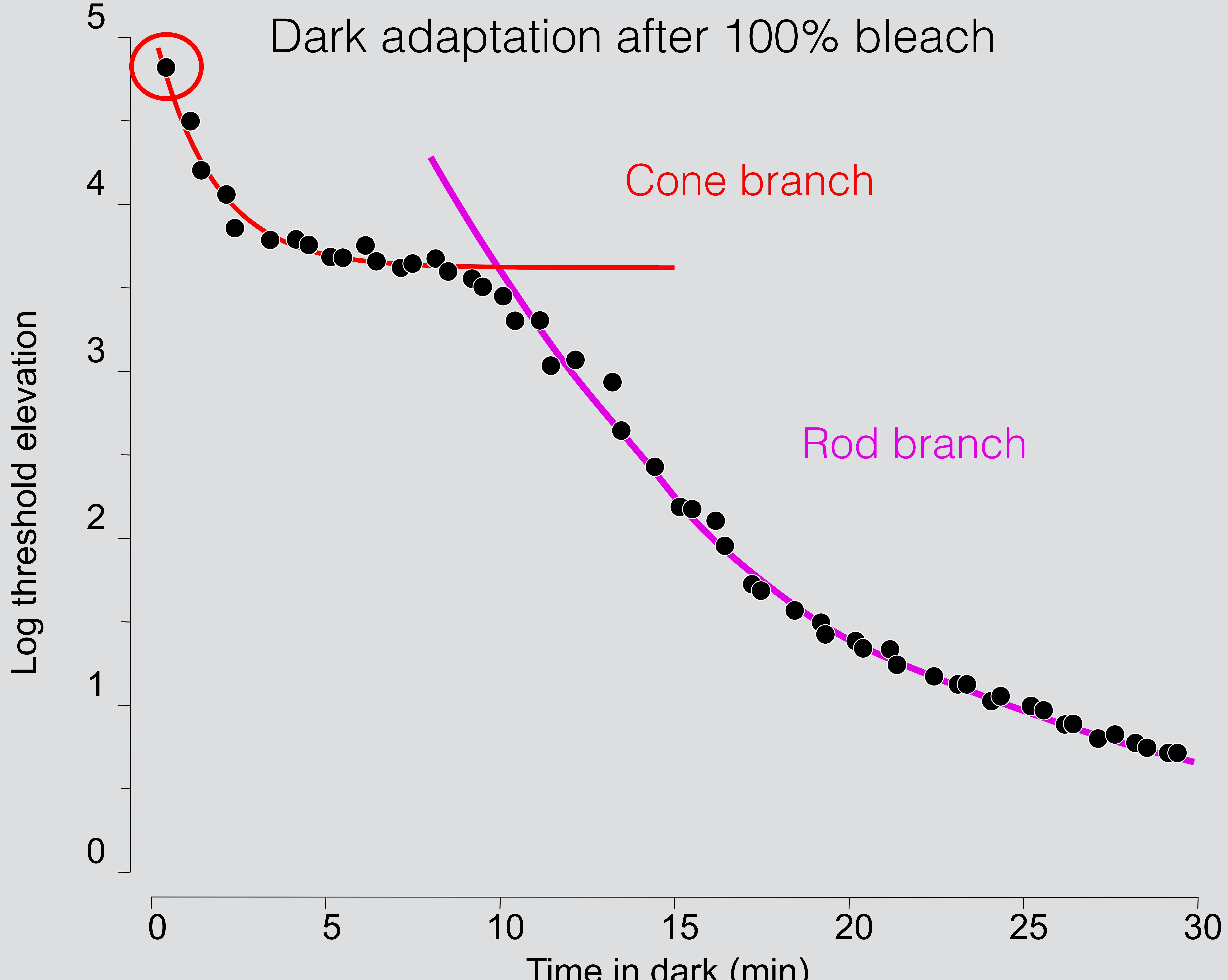

Lamb, T. D. & Pugh, E. N., Jr. (2006). Proctor Lecture, ARVO

Liang, Williams, & Miller (1997)

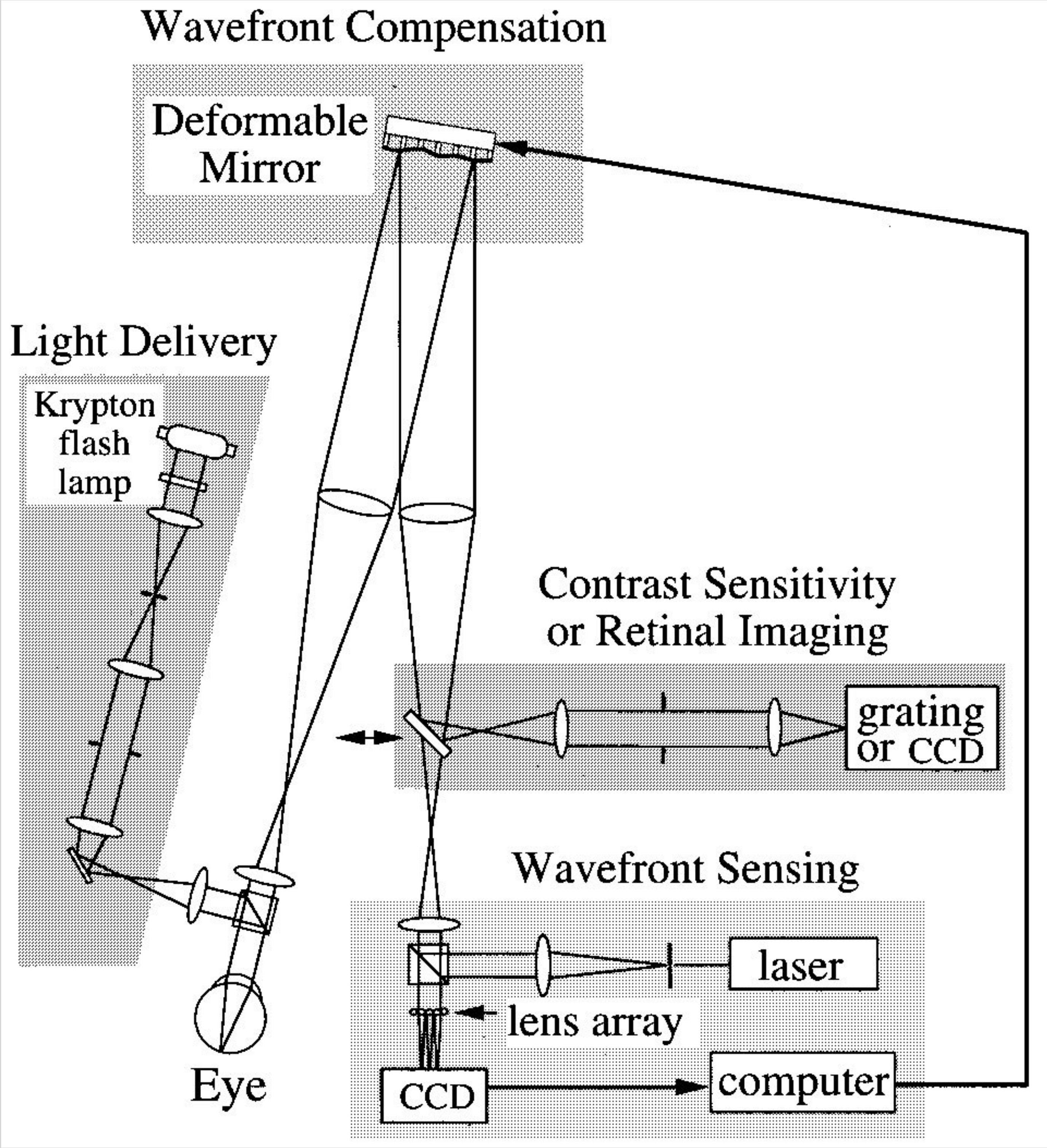

Liang, J., Williams, D. R., & Miller, D. T. (1997). Supernormal vision and high-resolution retinal imaging through adaptive optics. *Journal of the Optical Society of America A, 14*(11), 2884-2892. doi:10.1364/JOSAA.14.002884

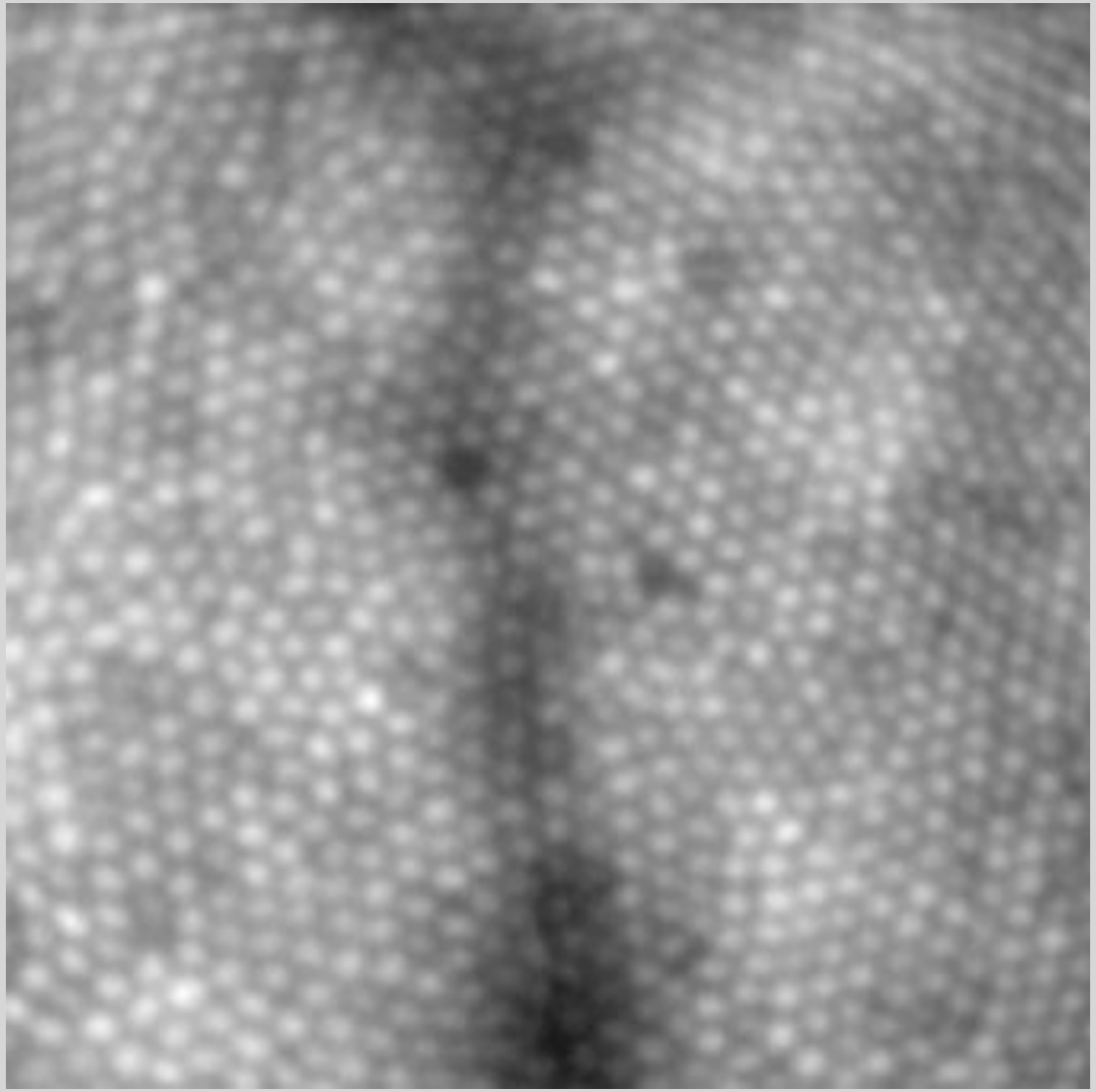

AN 1 deg nasal

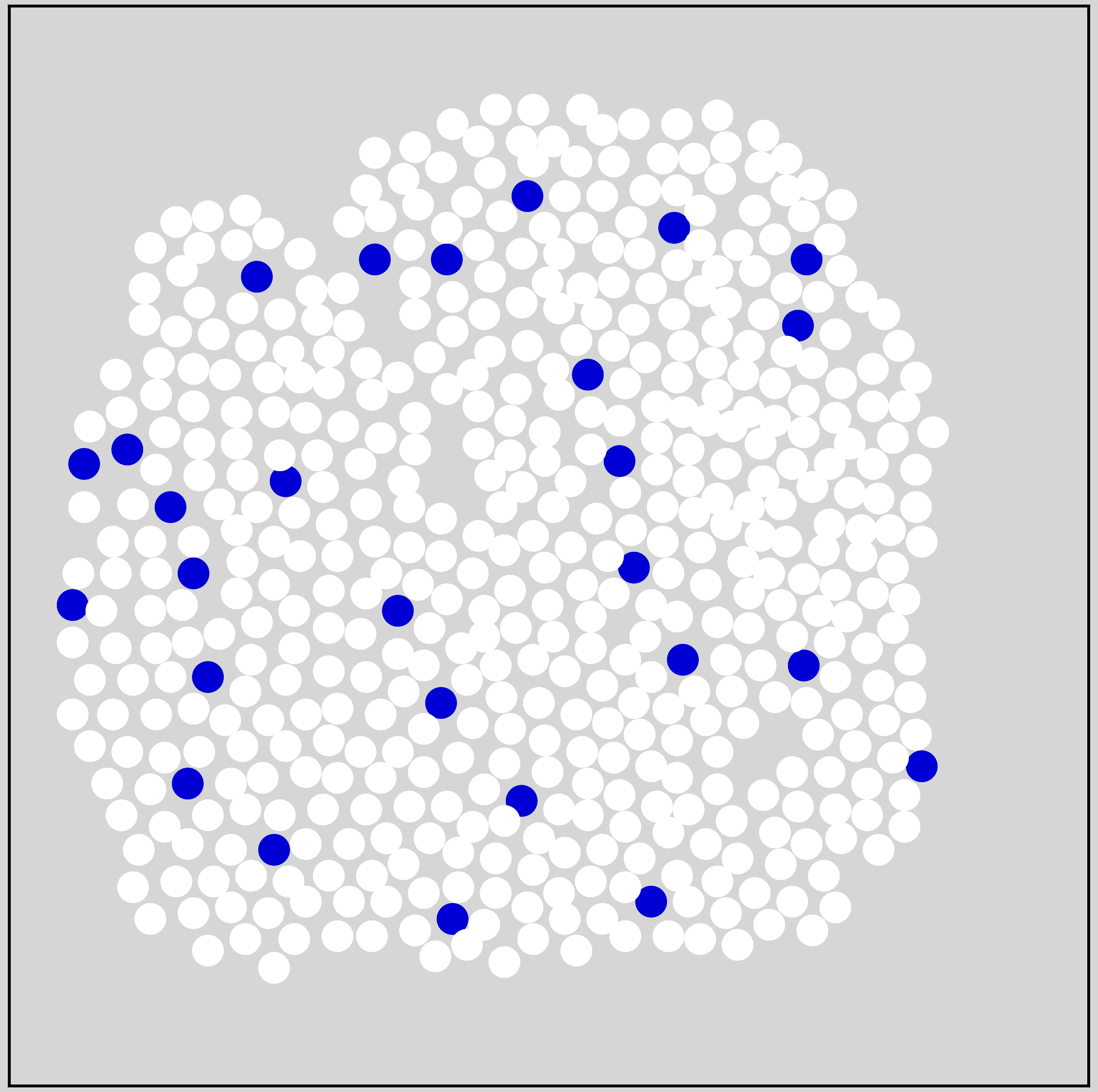

AN 1 deg nasal

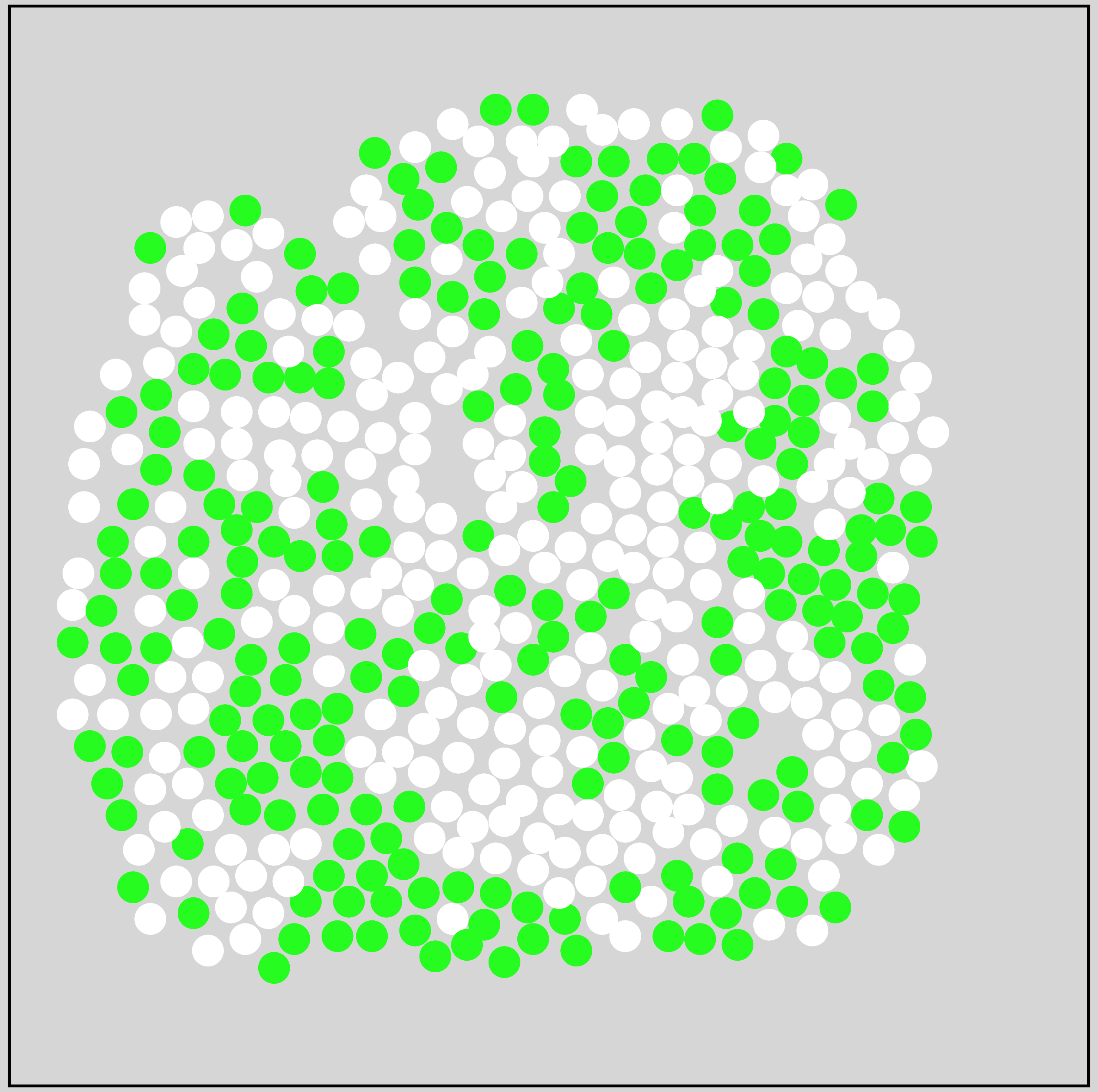

AN 1 deg nasal

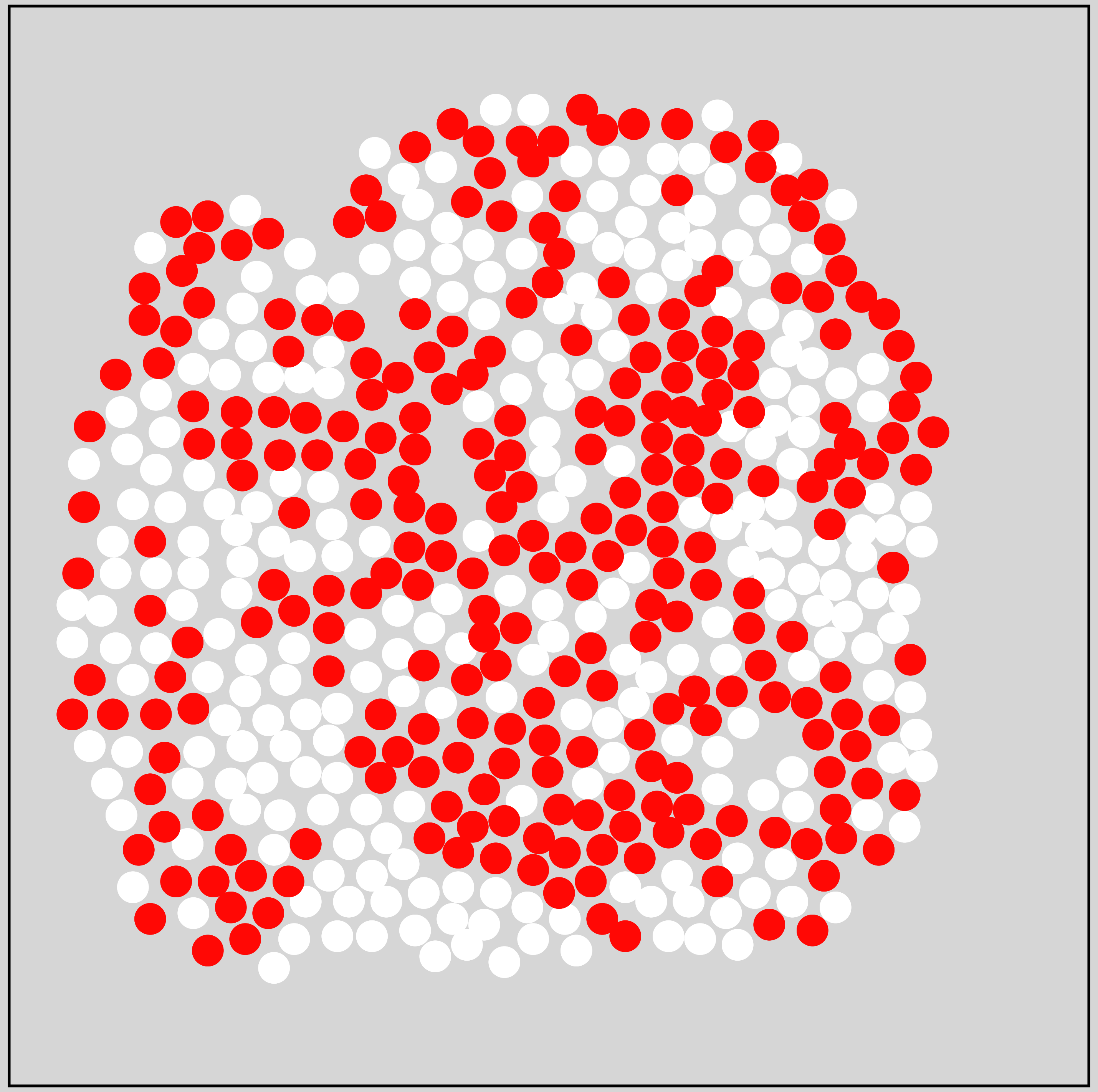

AN 1 deg nasal

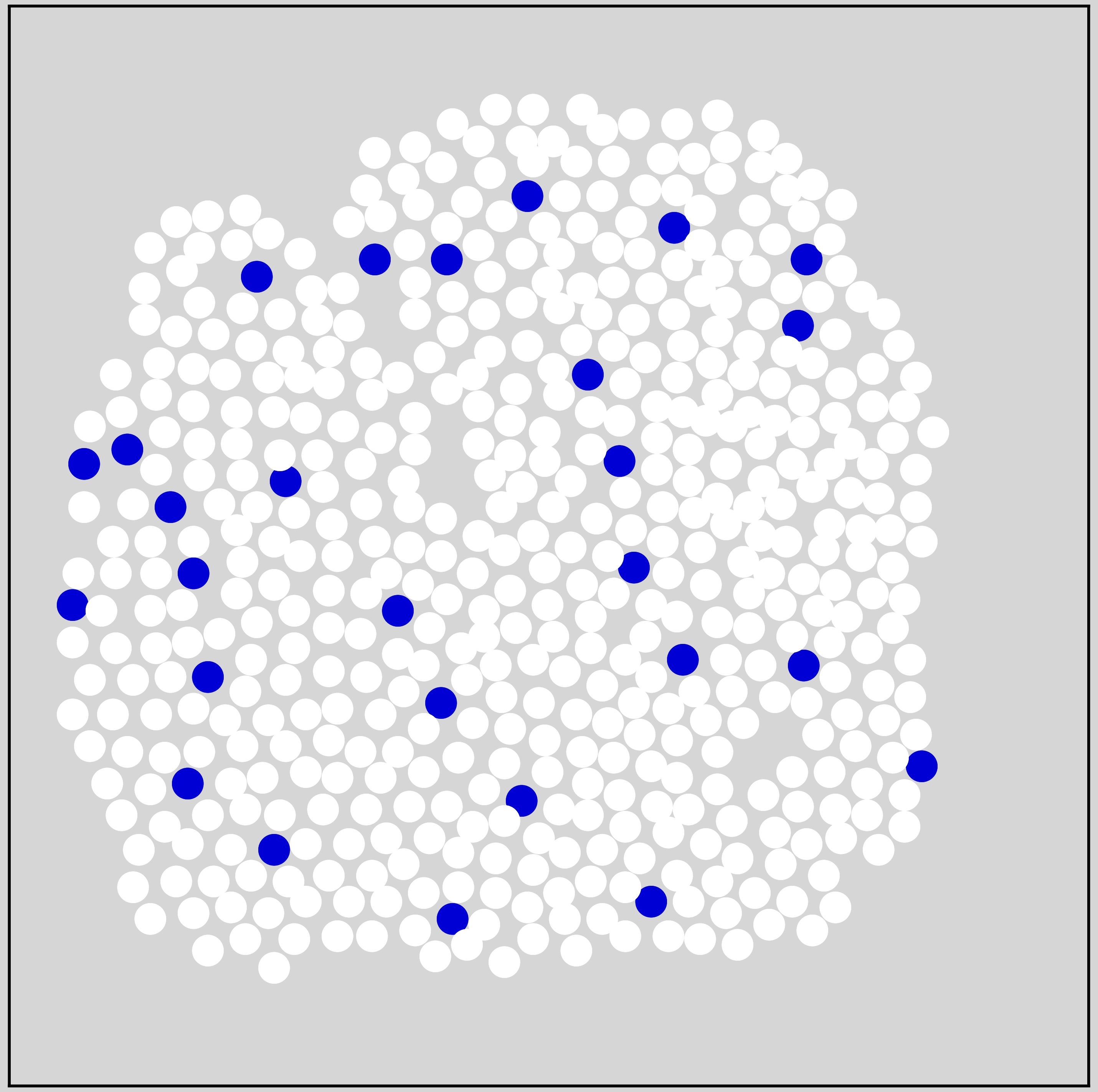

AN 1 deg nasal

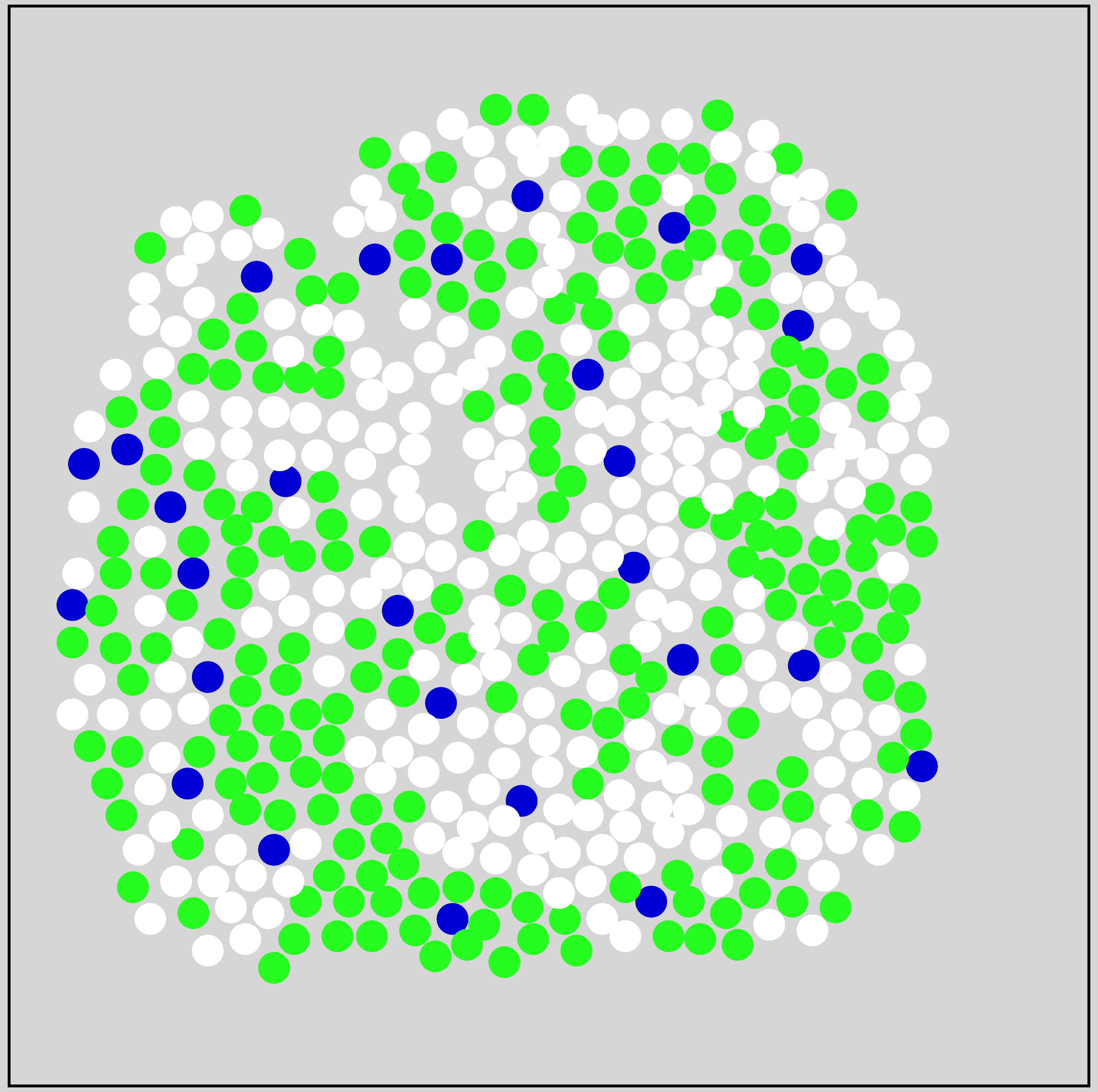

AN 1 deg nasal

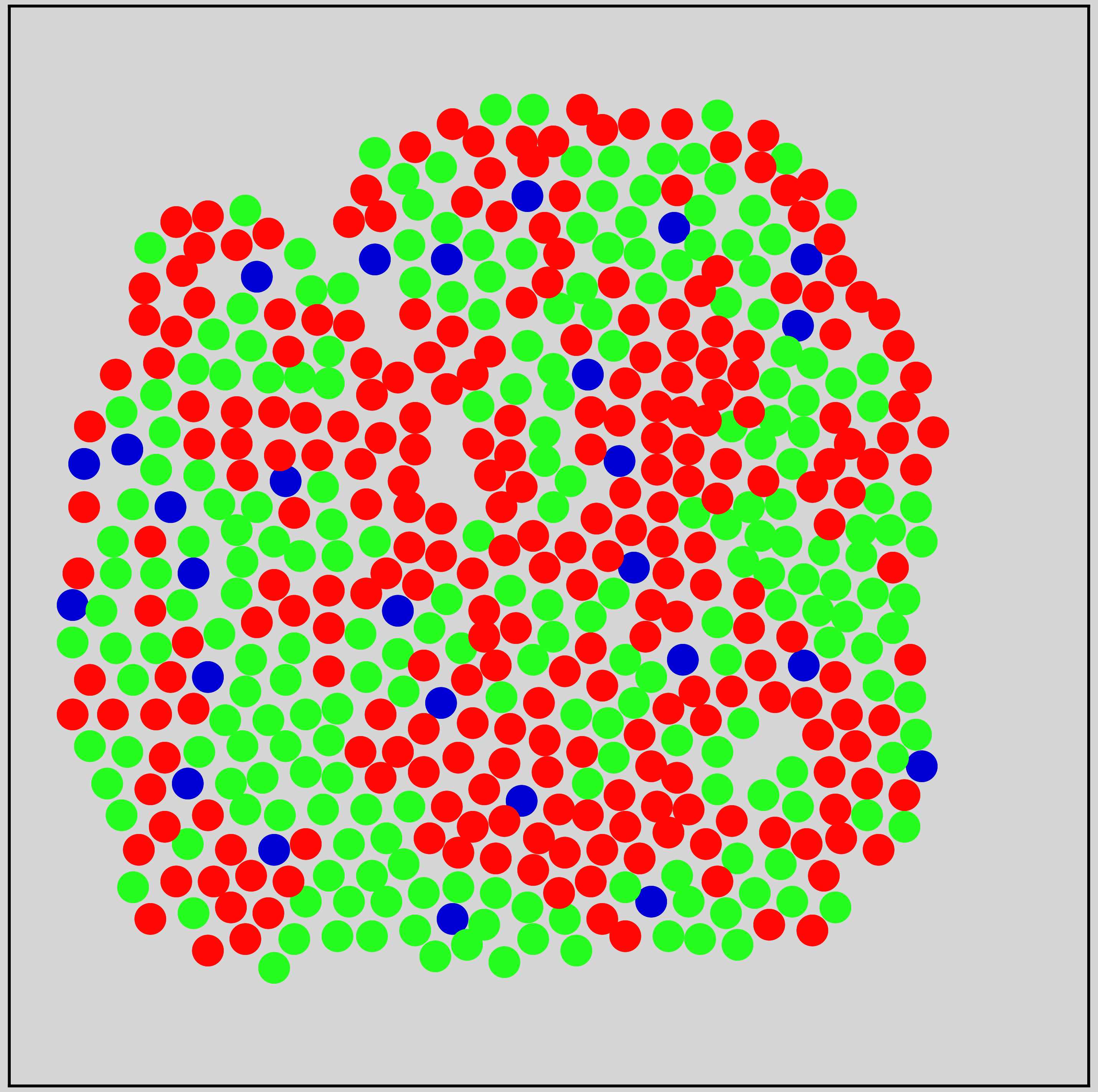

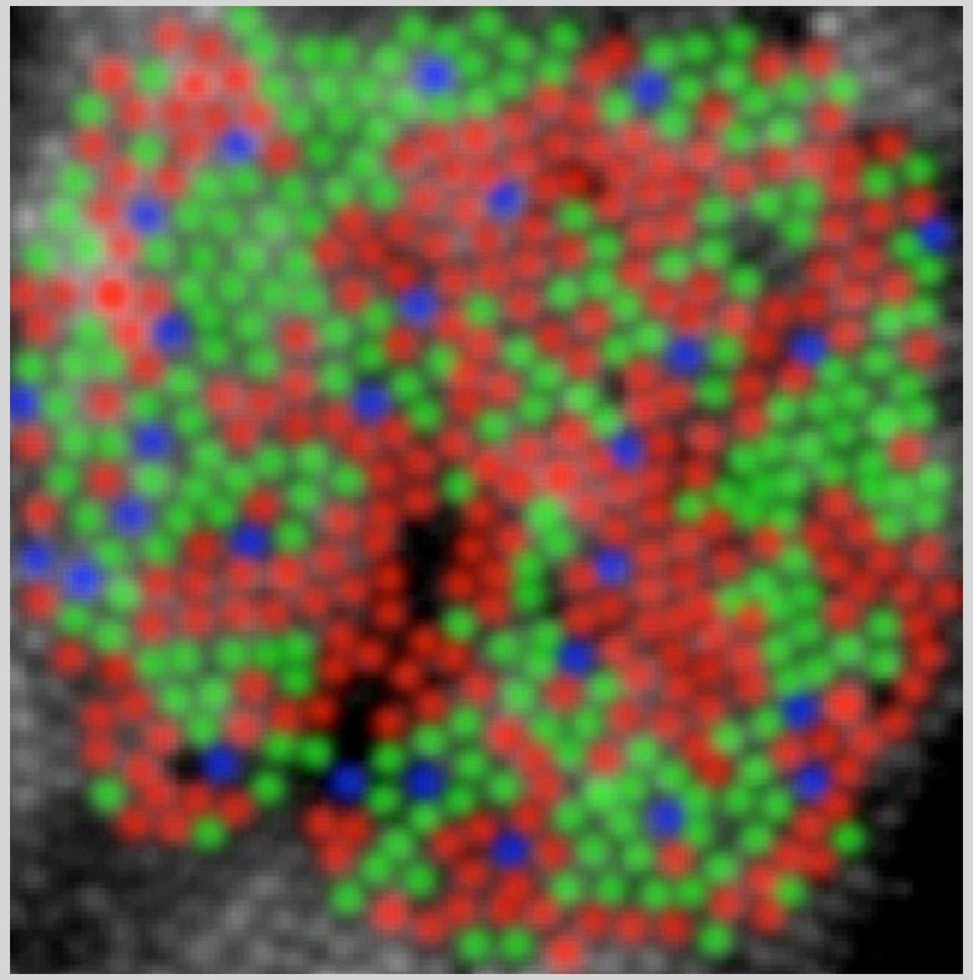

AN
Nasal

JW
Nasal

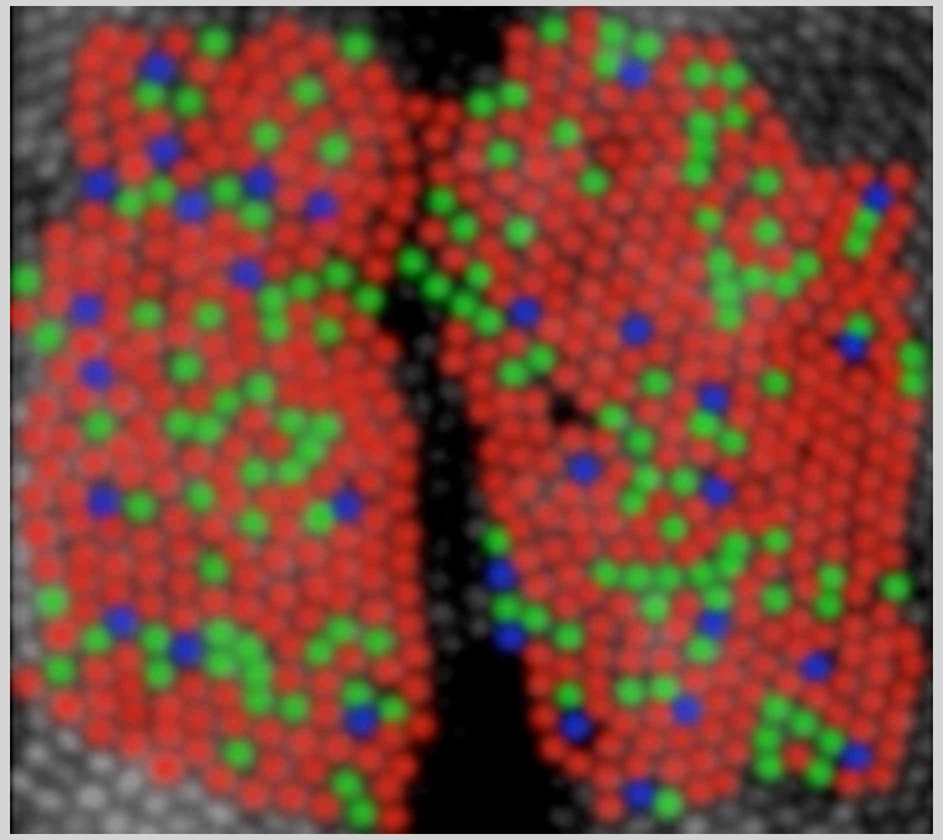

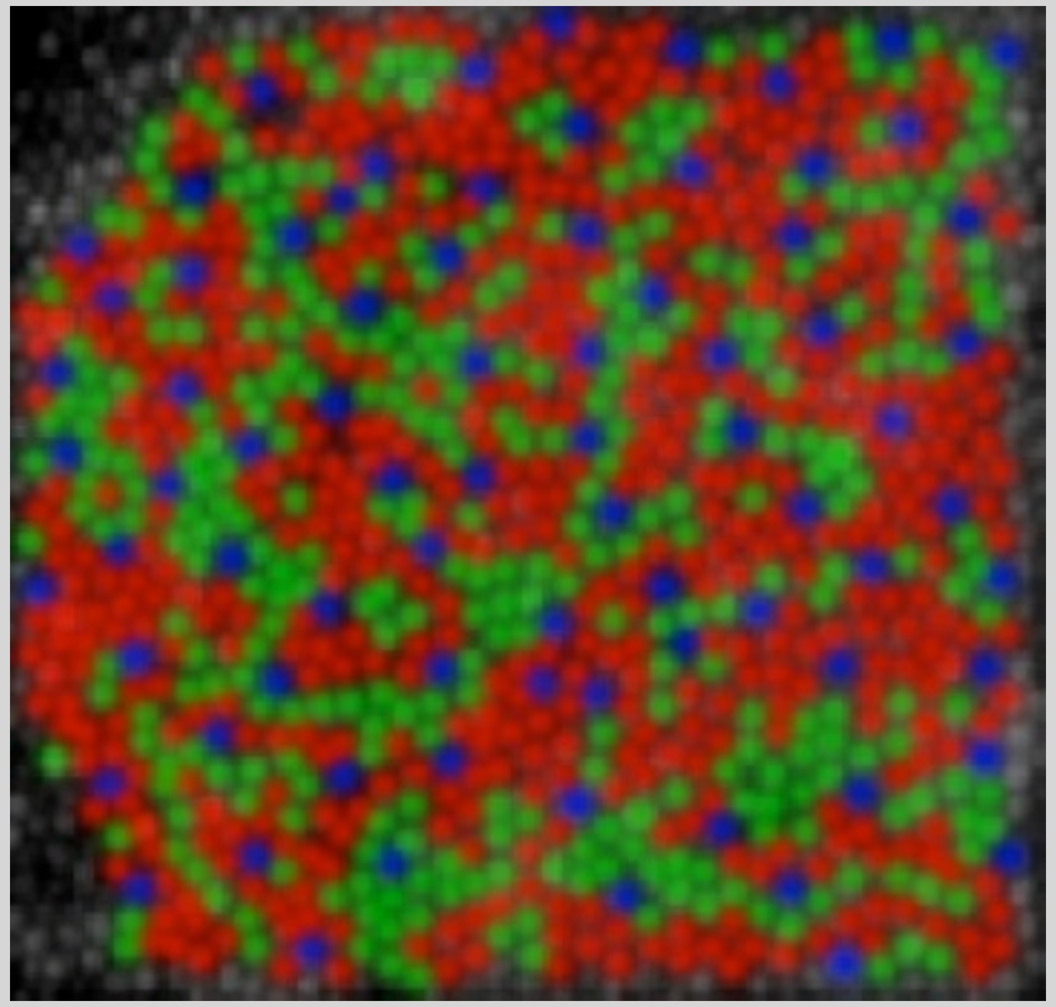

Monkey
Nasal

JW
Temporal

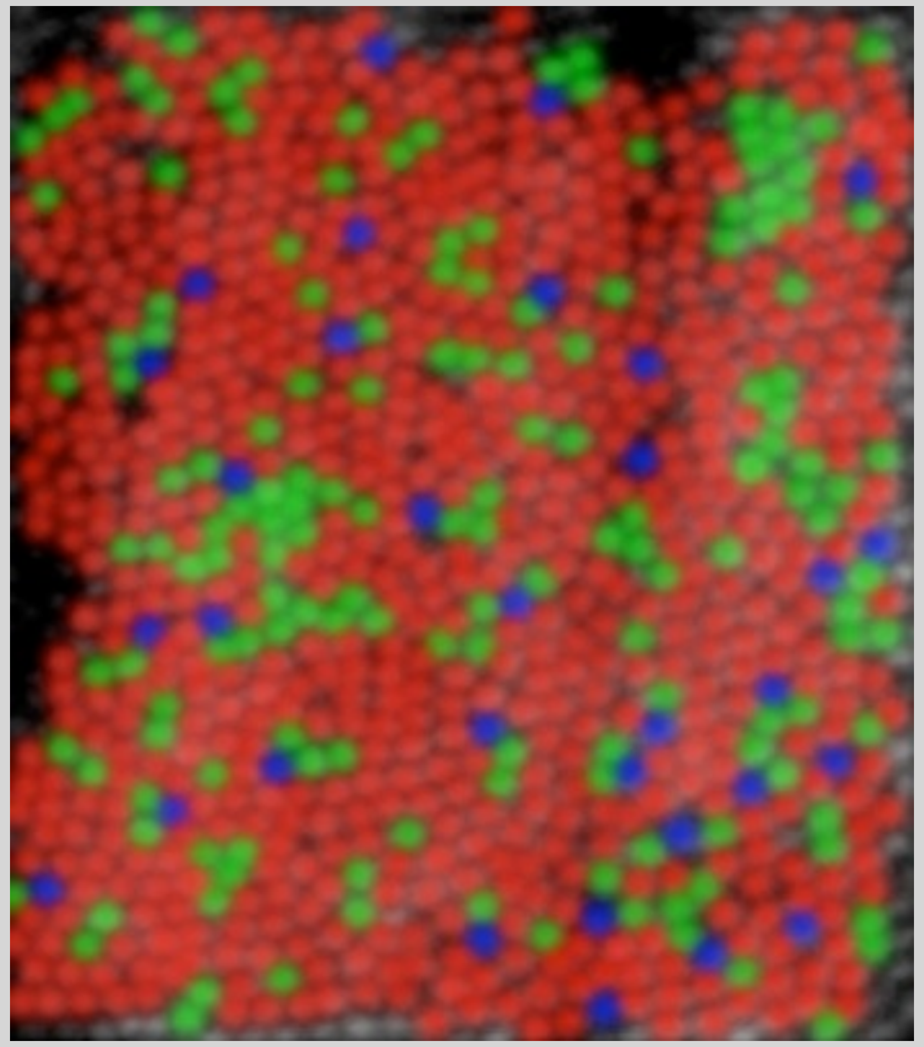

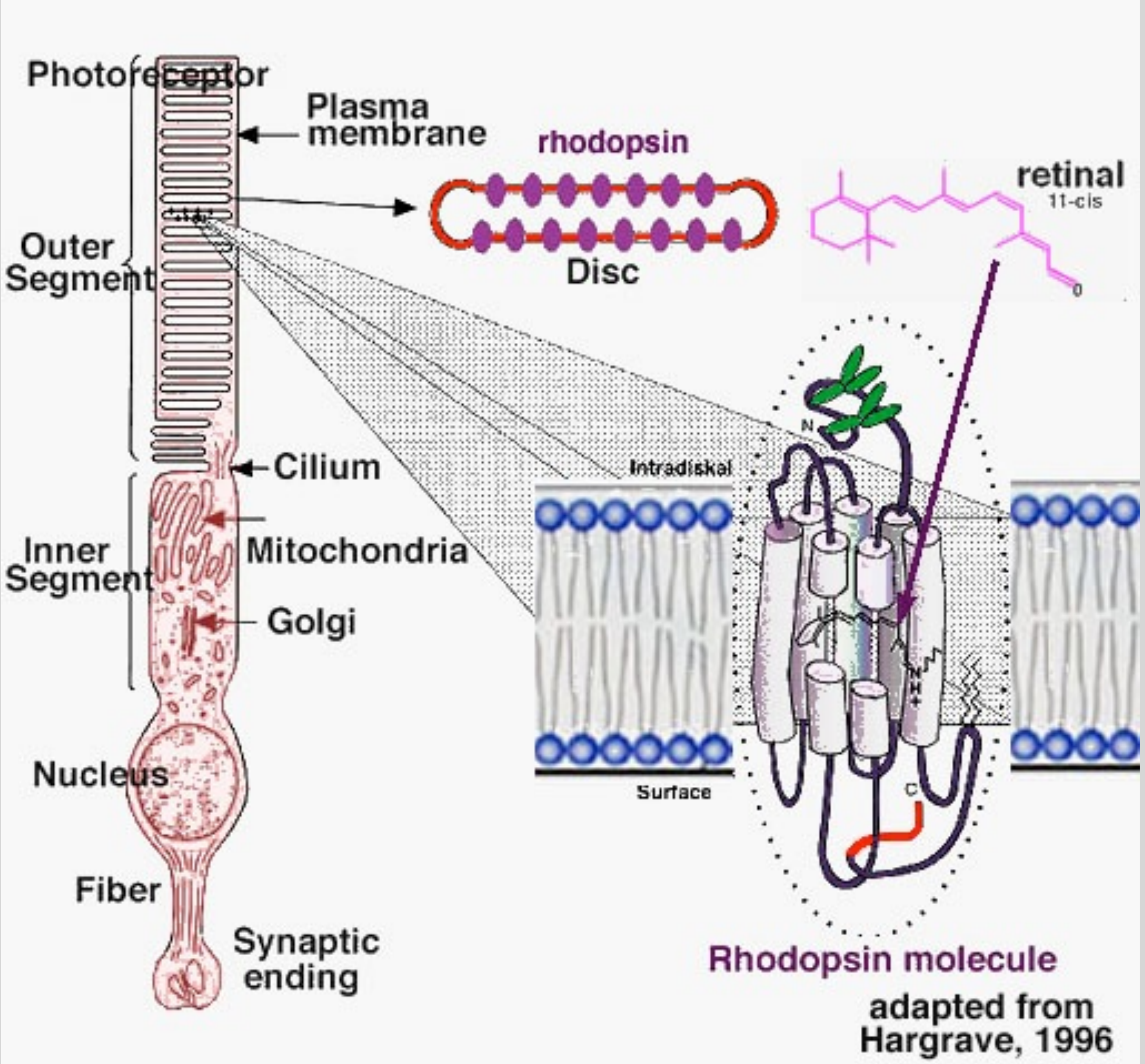

Photoreceptor
Plasma membrane
rhodopsin
retinal
11-cis
Disc
Outer Segment
Cilium
Intradiskal
Inner Segment
Mitochondria
Golgi
Surface
Nucleus
Fiber
Synaptic ending
Rhodopsin molecule
adapted from Hargrave, 1996

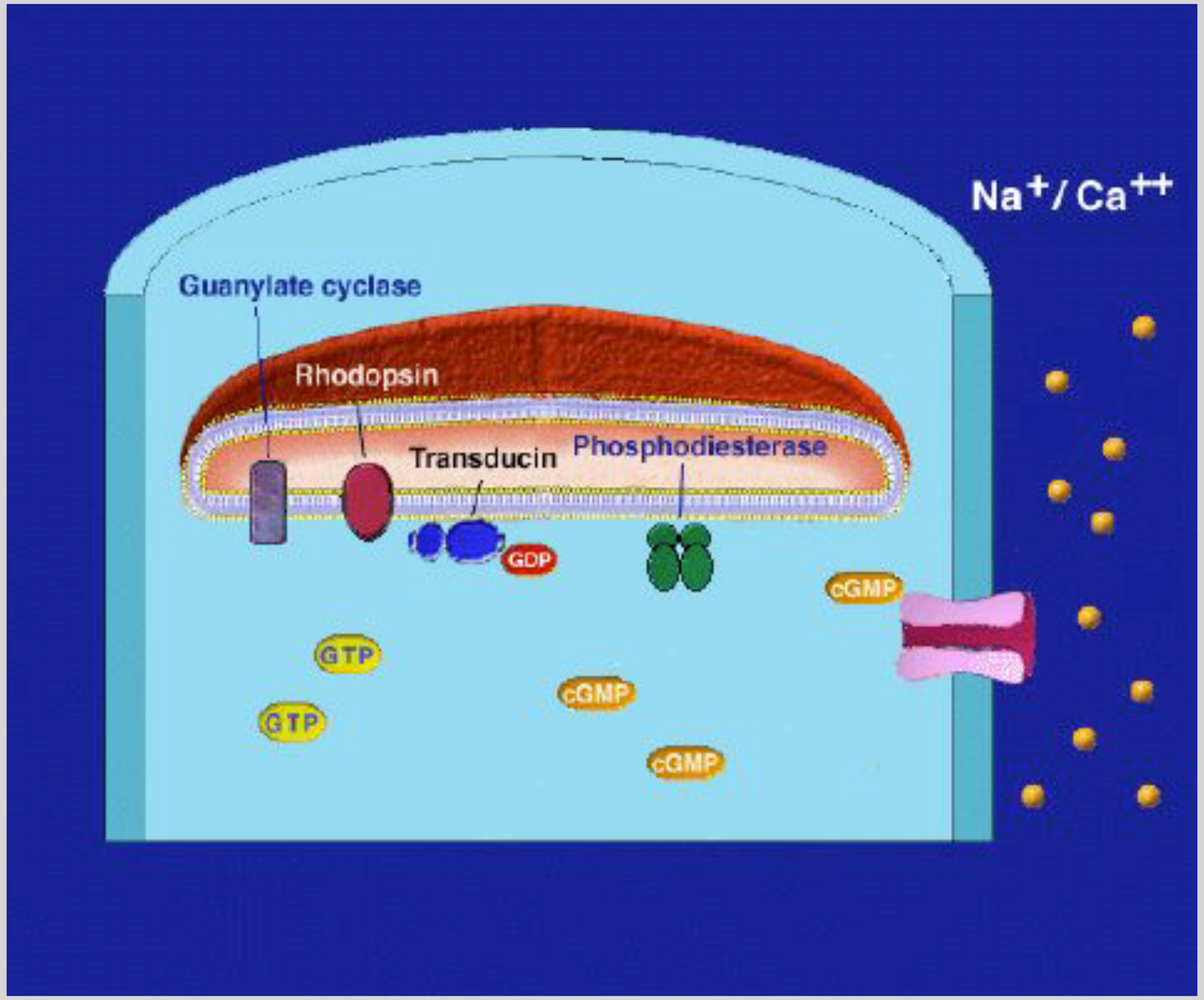
Na+/Ca++
Guanylate cyclase
Rhodopsin
Transducin
Phosphodiesterase
GDP
cGMP
GTP
GTP
cGMP
cGMP

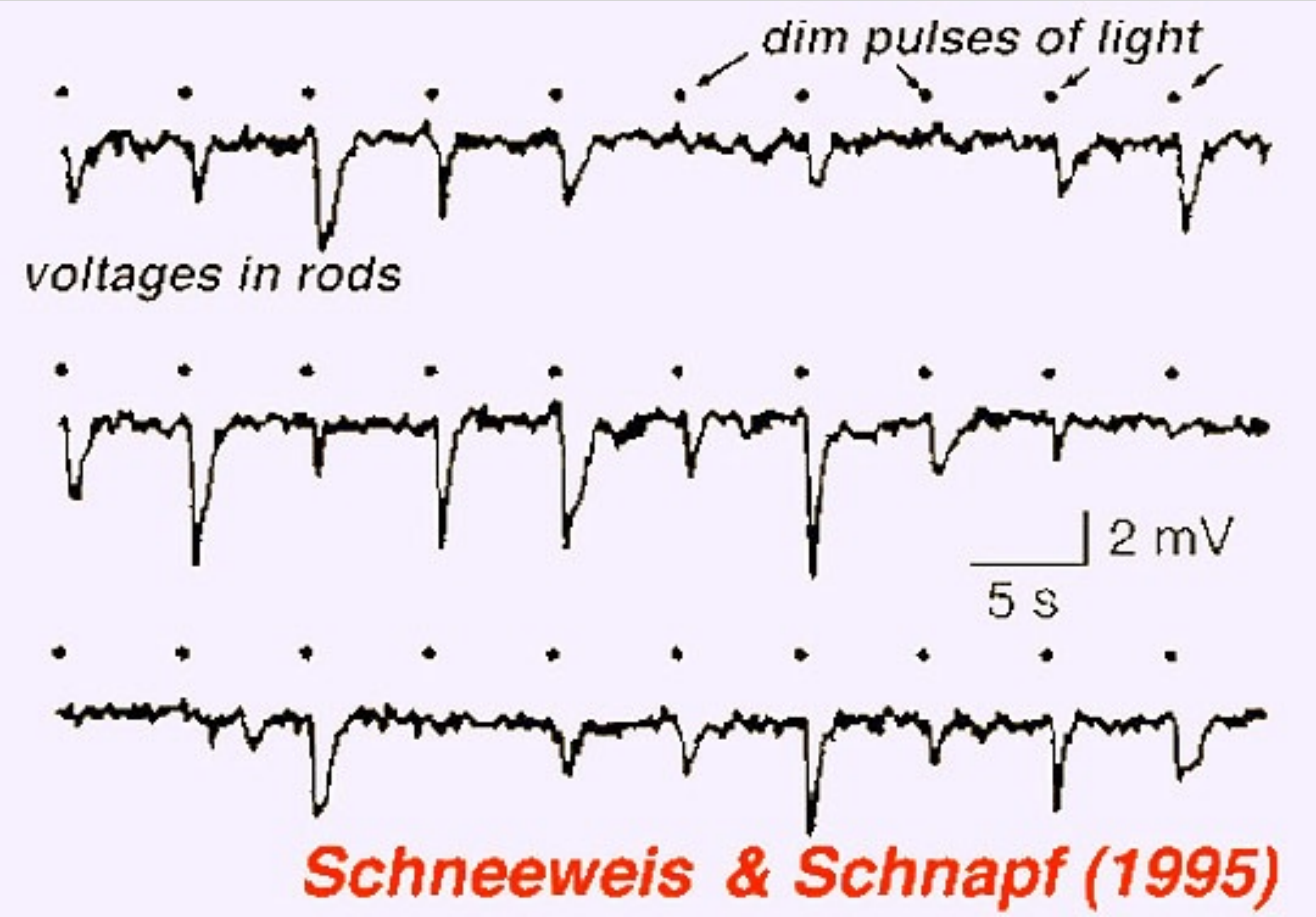
dim pulses of light
voltages in rods
2 mV
5 s
Schneeweis & Schnapf (1995)

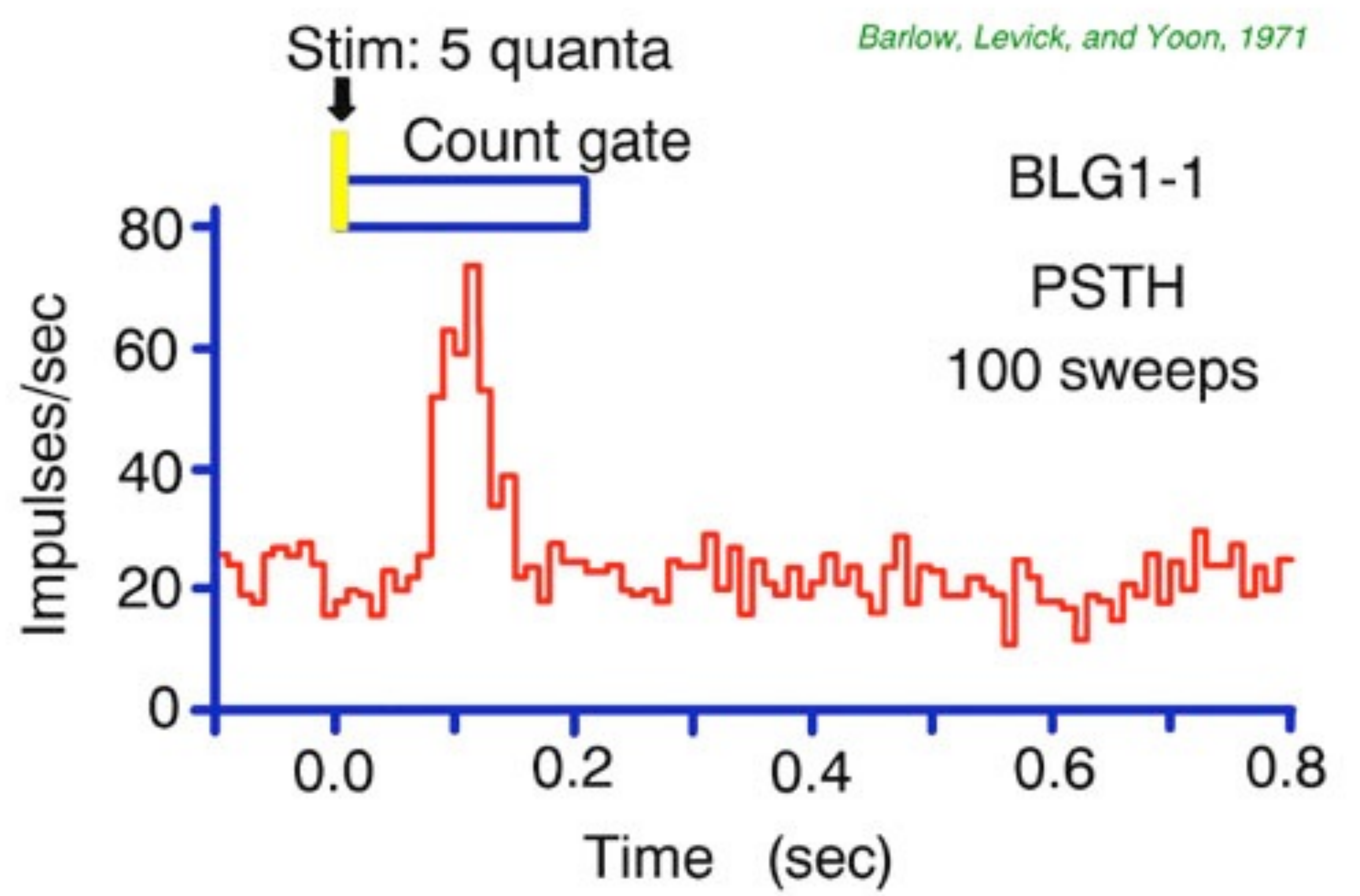
Stim: 5 quanta
Count gate
Barlow, Levick, and Yoon, 1971
BLG1-1
PSTH
100 sweeps
Impulses/sec
80
60
40
20
0
0.0
0.2
0.4
0.6
0.8
Time (sec)

Principle of Univariance

- A receptor signals the number of quanta (or the rate) absorbed. It can not signal the wavelength of the quanta.
- All wavelengths cause the same voltage change when they are absorbed
- 700 microvolts per quantum for rods
- 25 or smaller microvolts per quantum for cones

What Can We Do with Psychometric Functions?

- Answer questions about sensory processes
- What is the minimum amount of energy needed for “seeing?”
- Hecht, Shlaer, & Pirenne (1942)

Hecht, S., Shlaer, S., & Pirenne, M. H. (1942). Energy, quanta, and vision. *Journal of General Physiology, 25*(6), 819840.

Psychometric Function

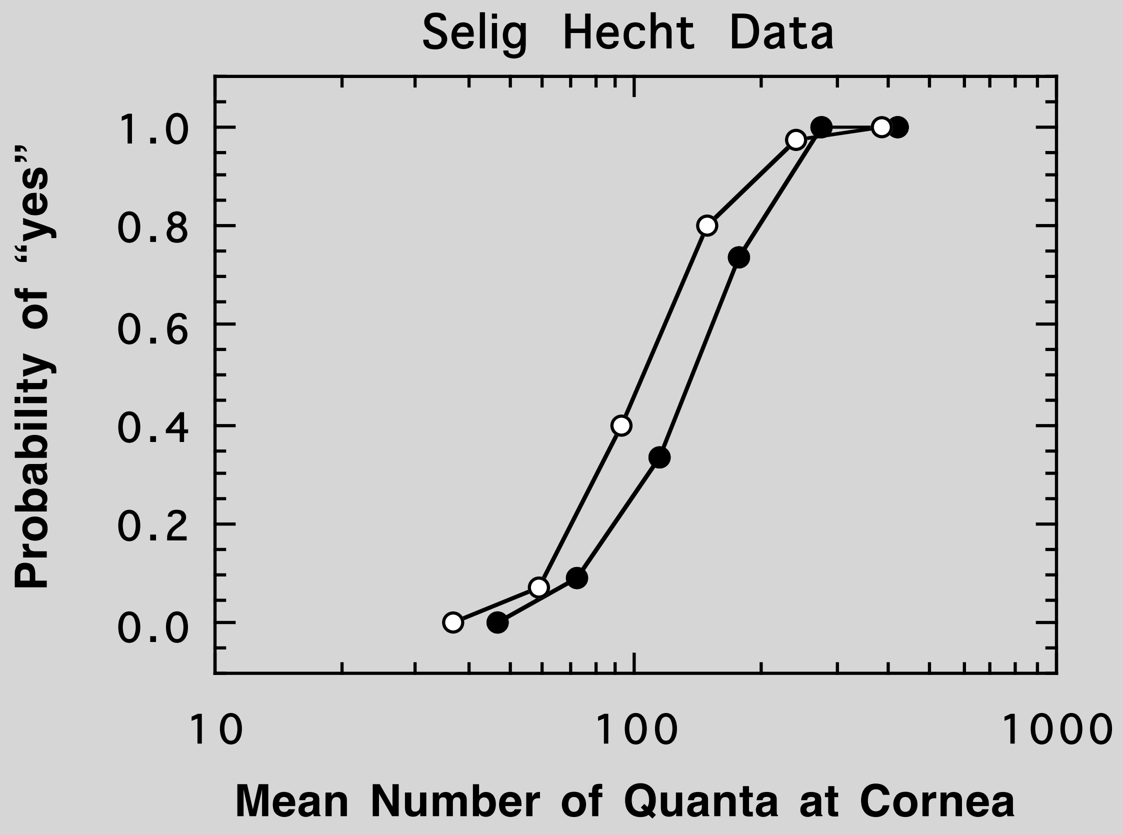

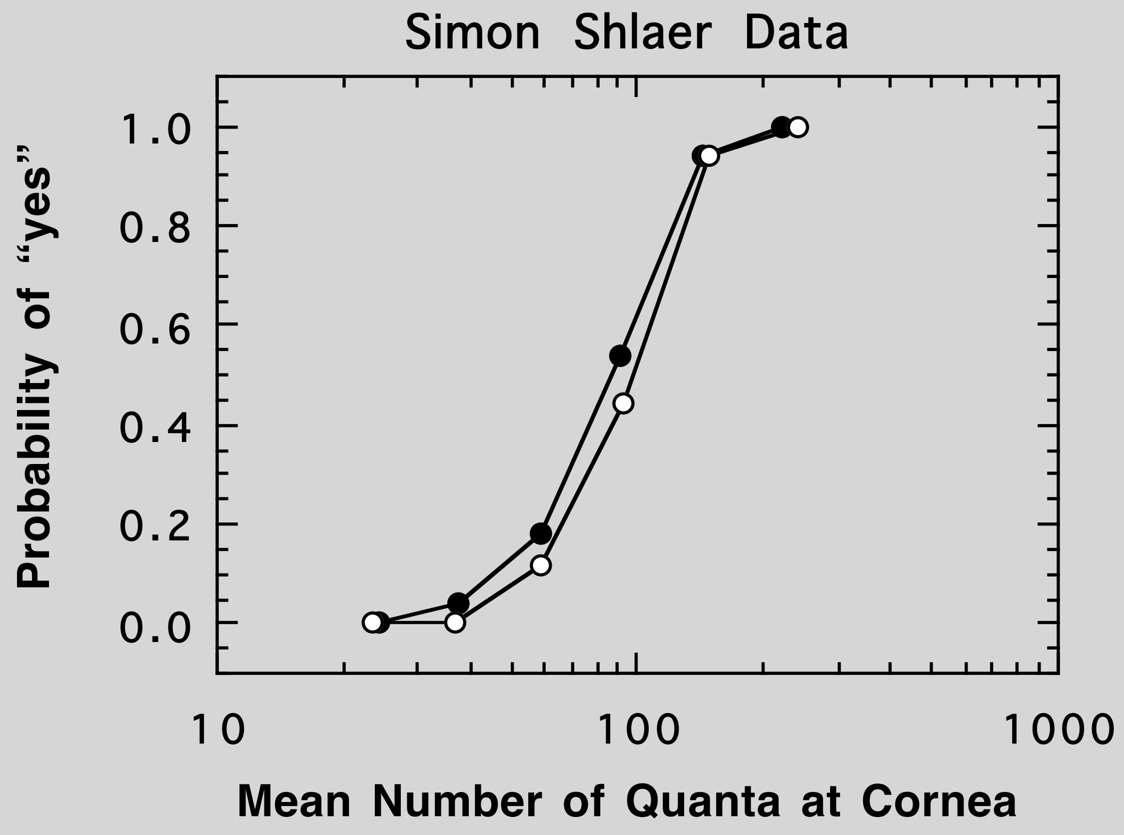

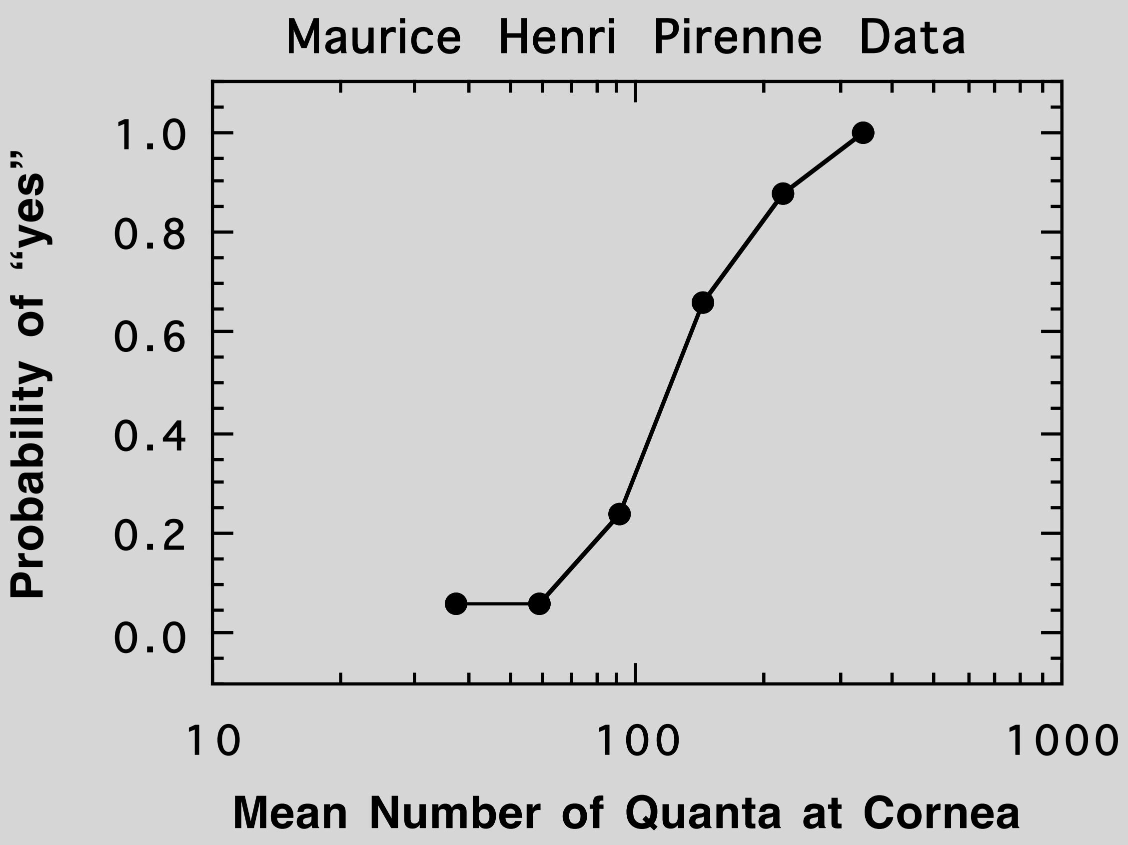

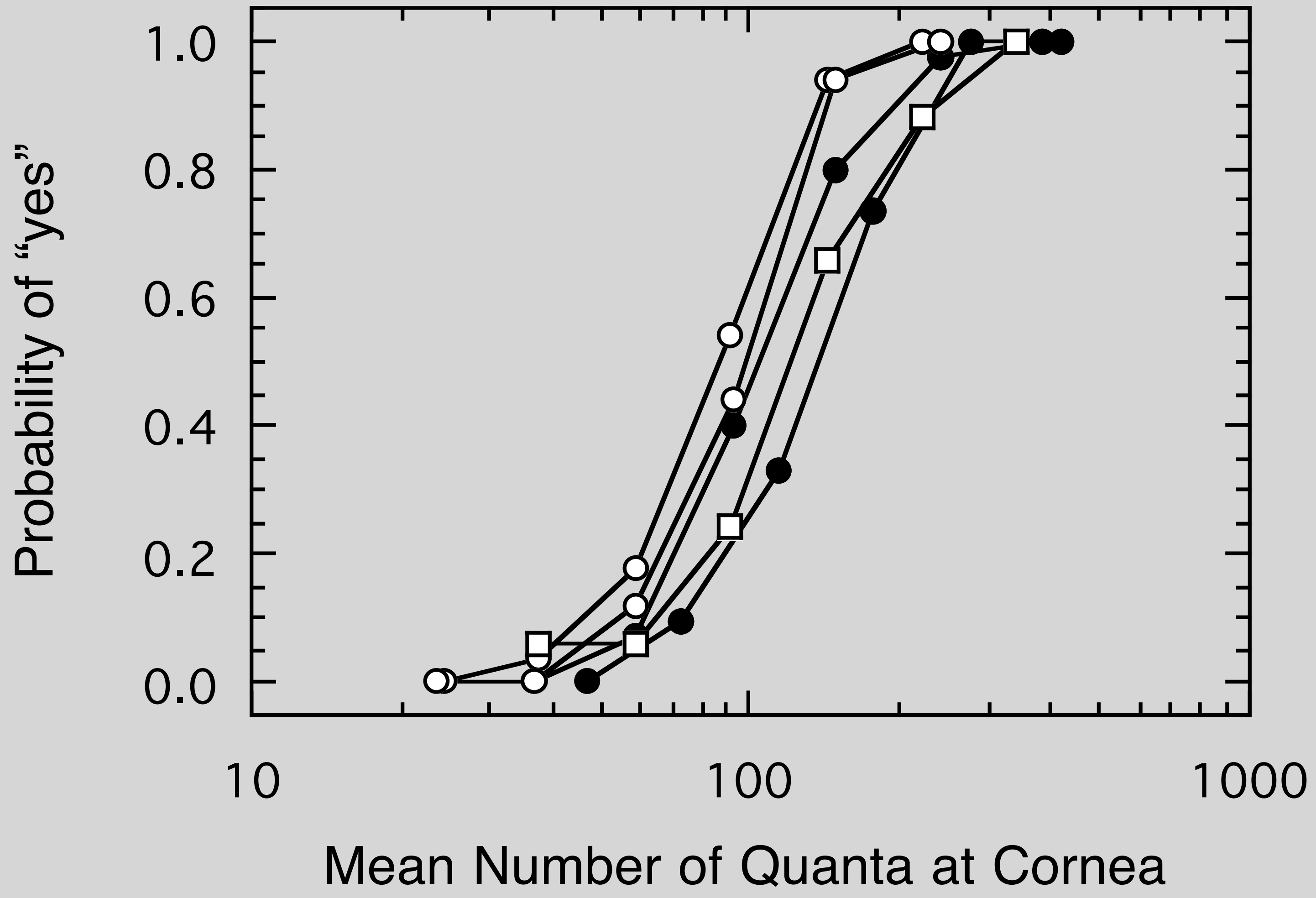

Hecht, S., Shlaer, S., & Pirenne, M. H. (1942). Energy, quanta, and vision. *Journal of General Physiology, 25*(6), 819840.

Poisson Probability Distribution

$$p(n : \lambda) = \frac{\lambda^n e^{-\lambda}}{n!}$$

$$\lambda > 0, \quad n = 0,1,2,3\ldots$$

$$\text{Mean} = \mu = \lambda$$

$$\text{Variance} = \sigma^2 = \lambda$$

$$\text{Standard Deviation} = \sigma = \sqrt{\lambda}$$

Poisson Process

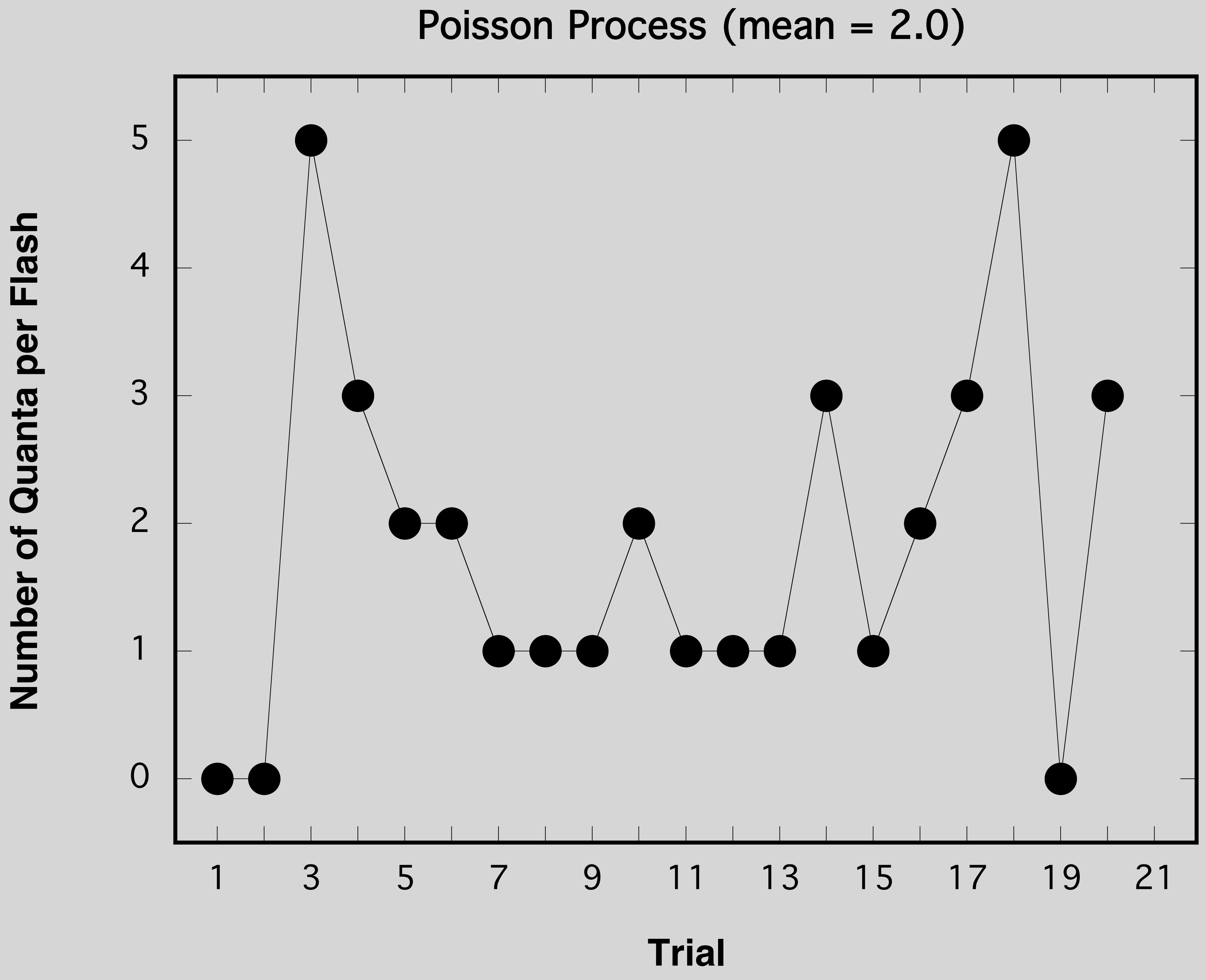

Poisson Process

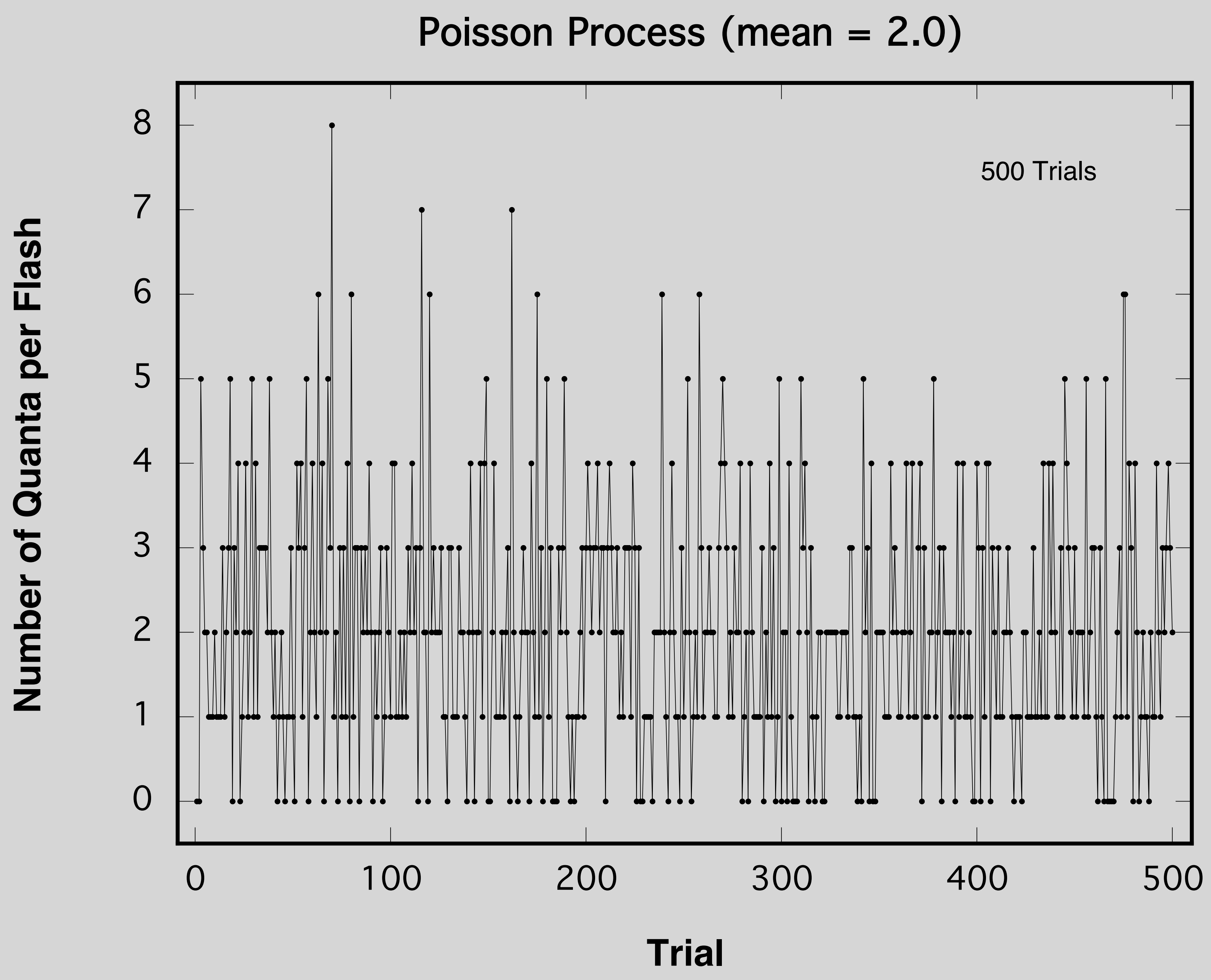

Observed Frequencies

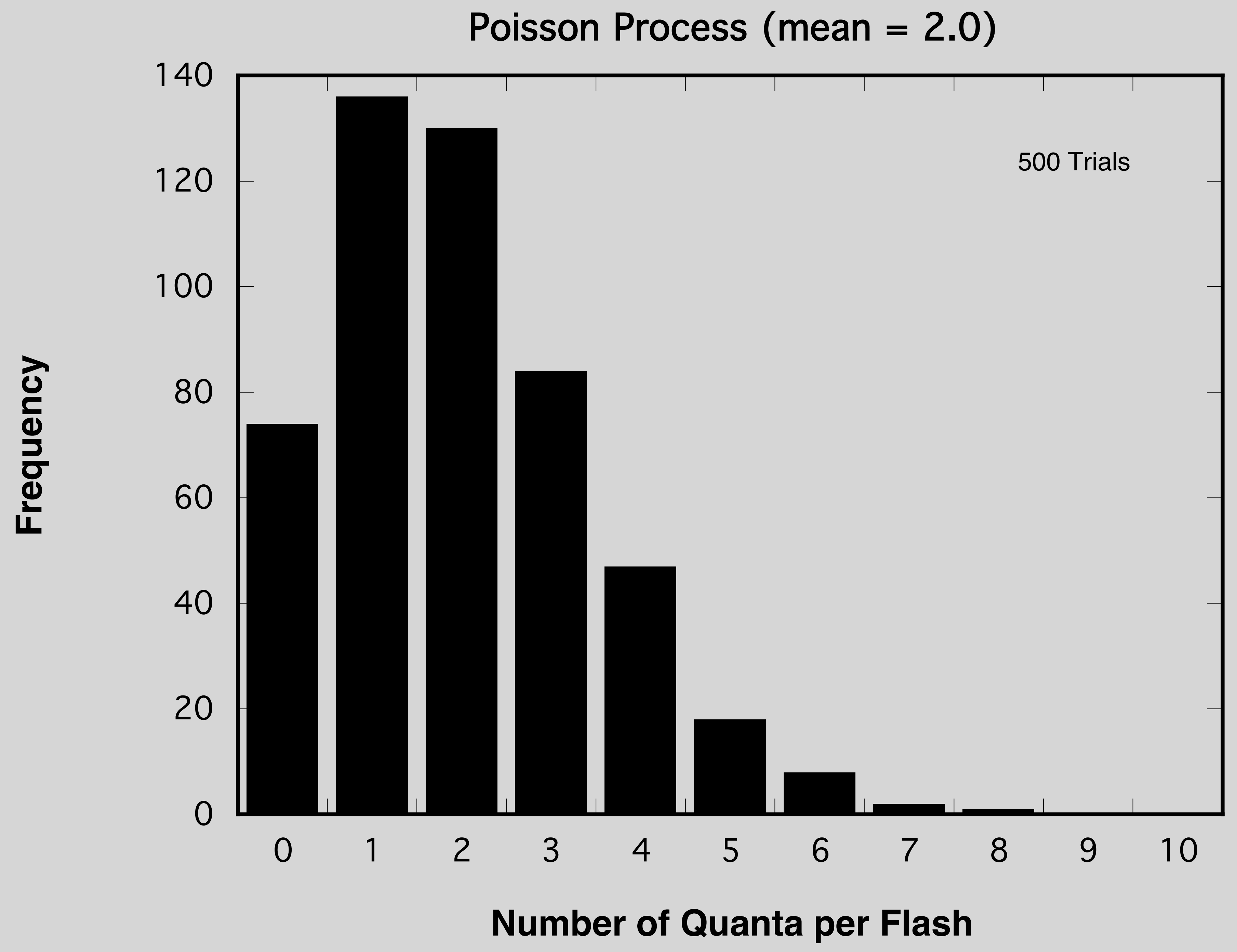

Observed Probabilities

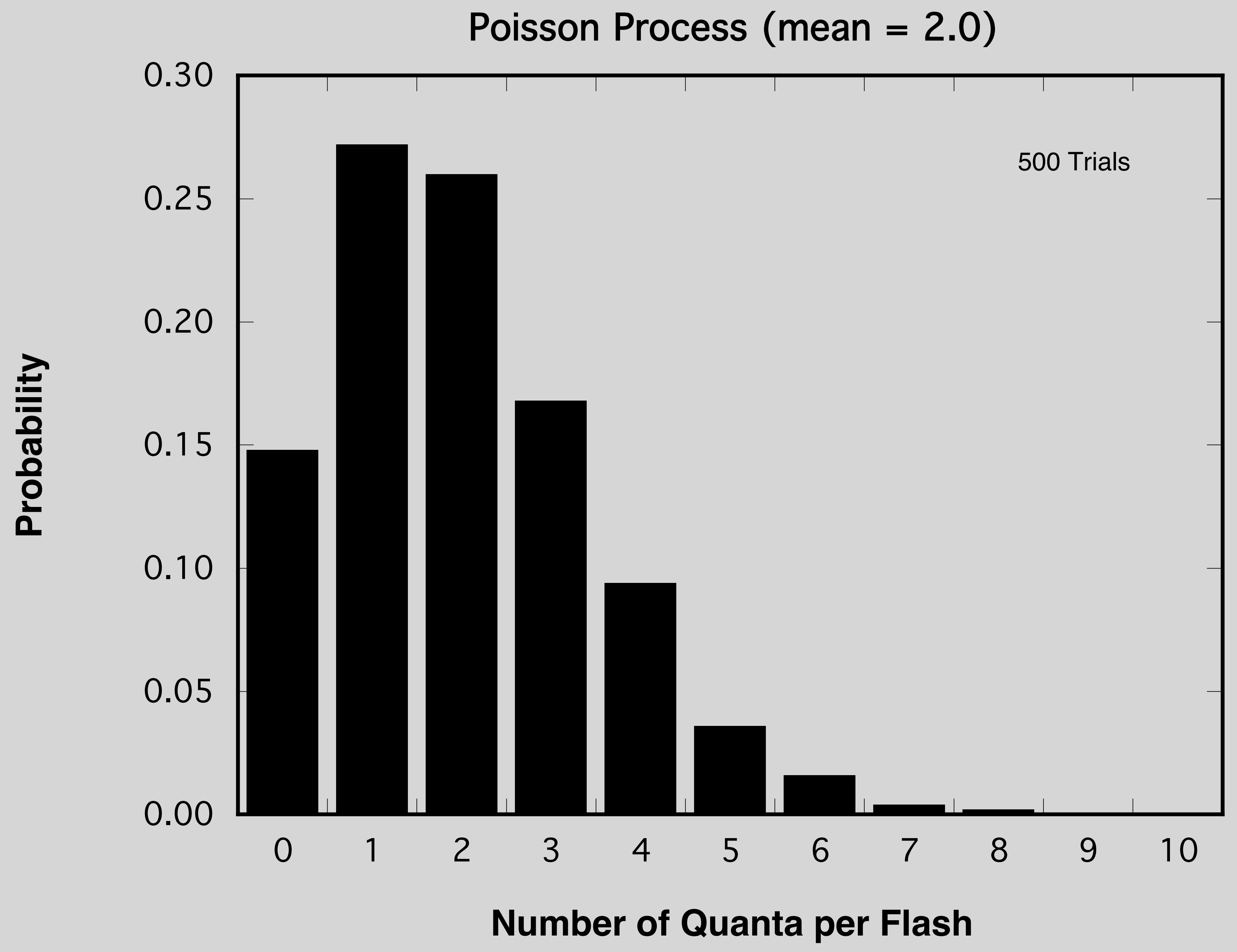

Theoretical Poisson Distribution

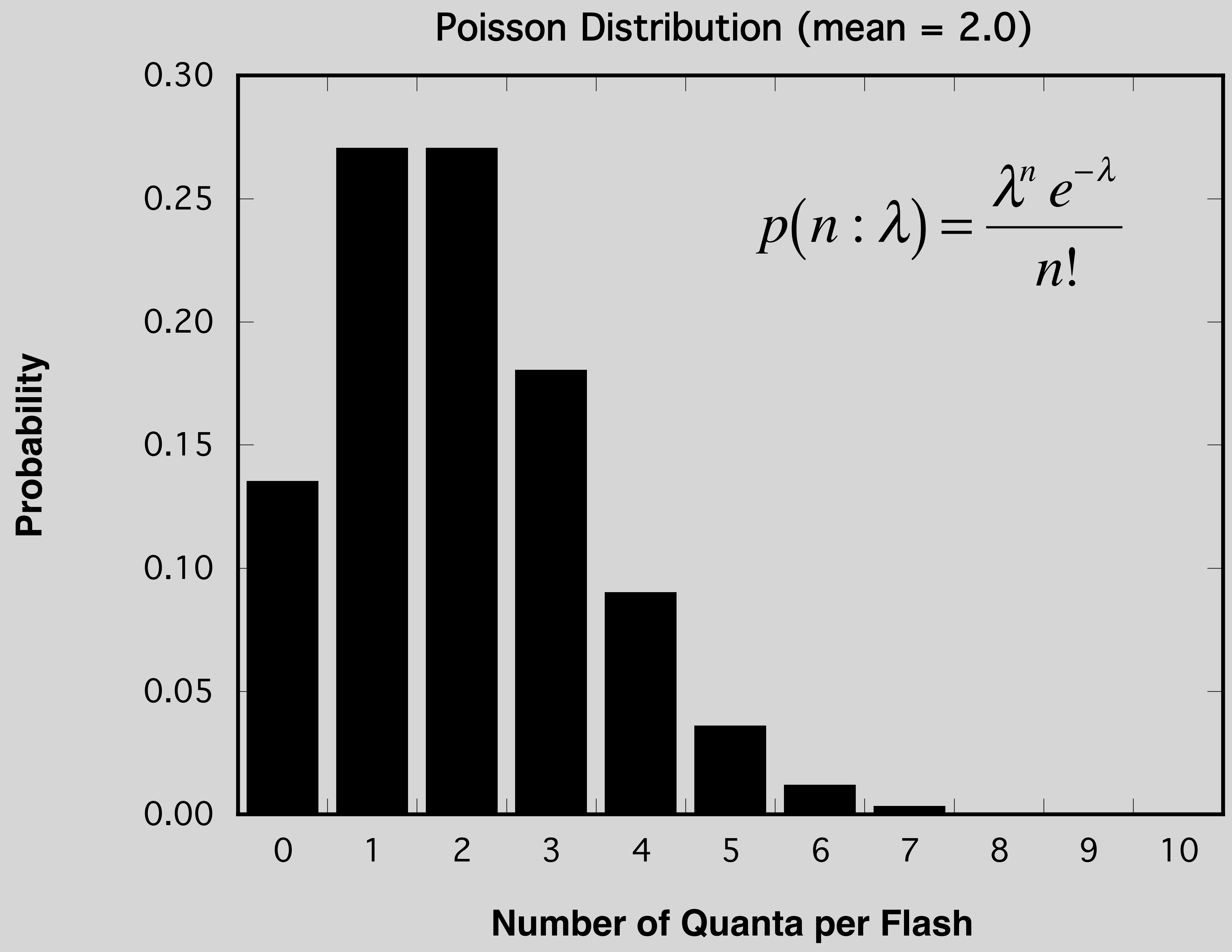

Poisson Probability Distributions

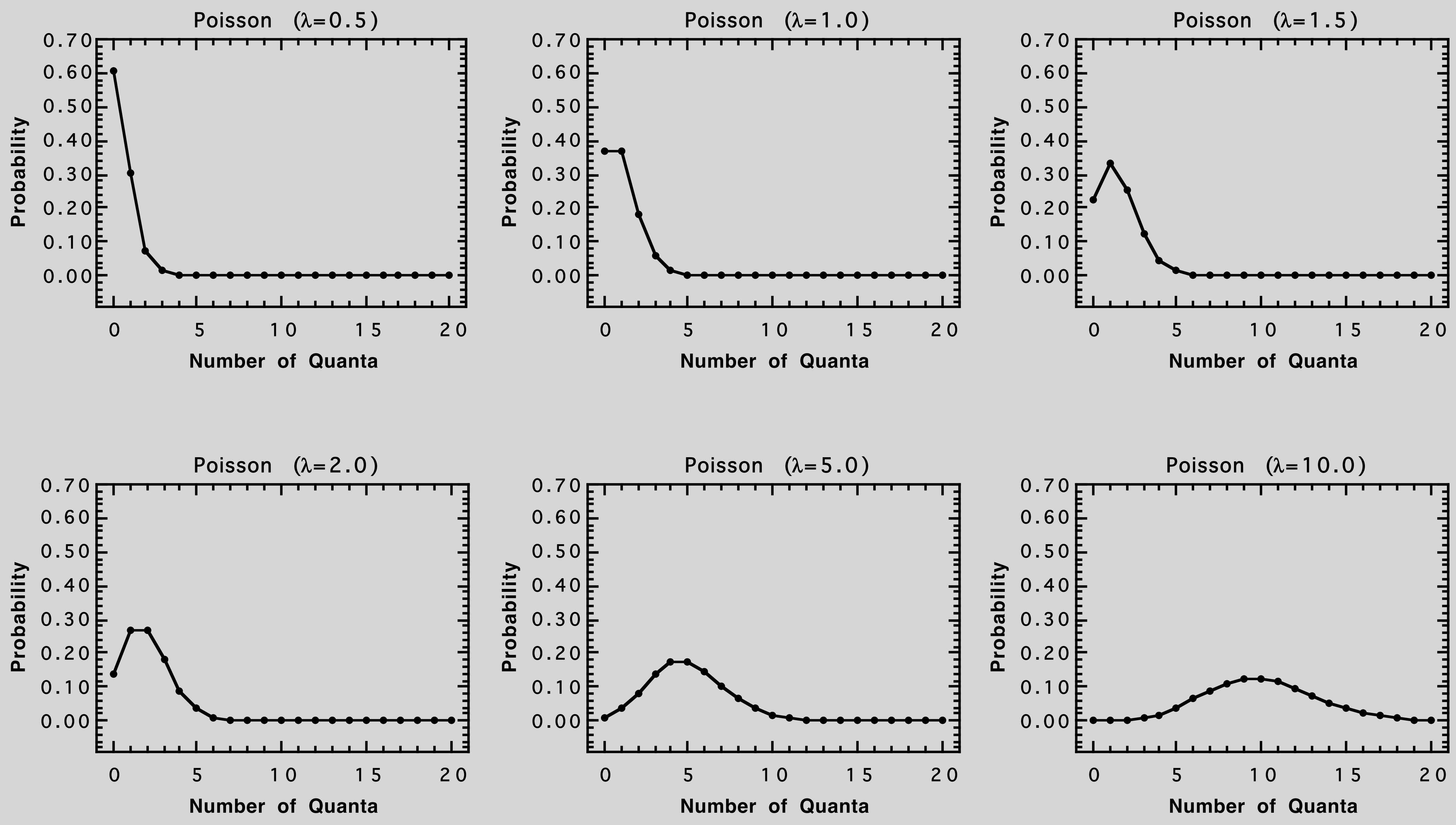

Poisson Psychometric Functions

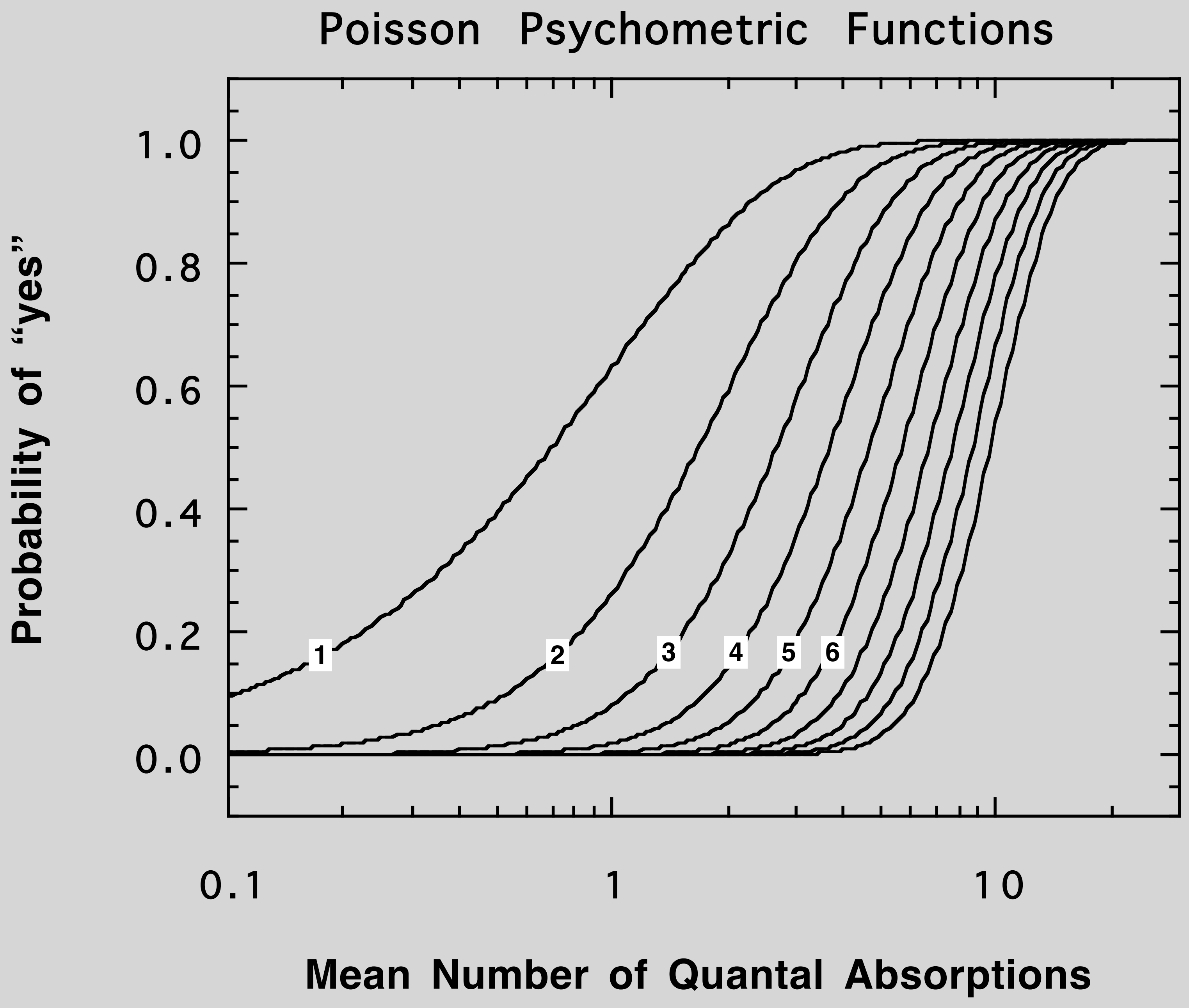

Theory vs. Data

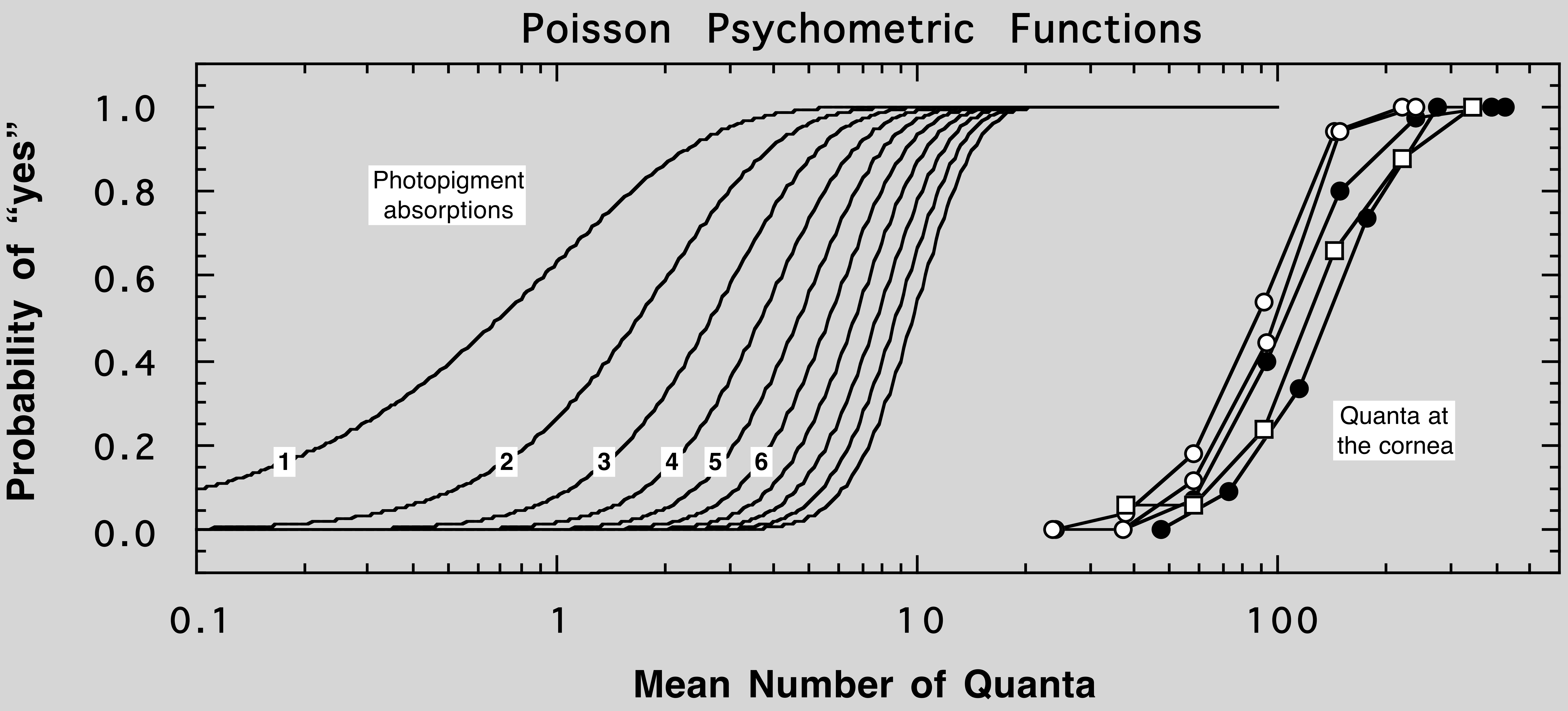

Hecht, S., Shlaer, S., & Pirenne, M. H. (1942). Energy, quanta, and vision. *Journal of General Physiology, 25*(6), 819840.

Fit of Data to Theory

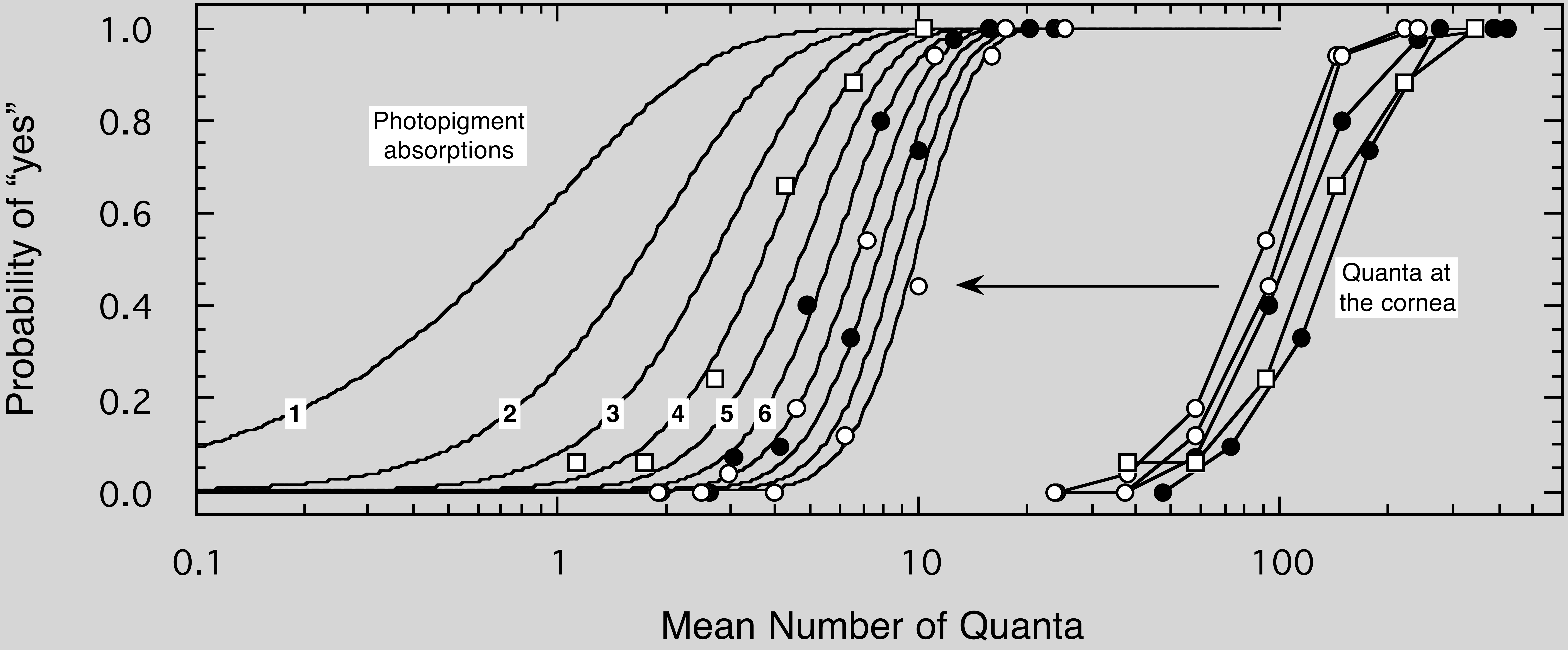

Hecht, S., Shlaer, S., & Pirenne, M. H. (1942). Energy, quanta, and vision. *Journal of General Physiology, 25*(6), 819840.

Fits of Models

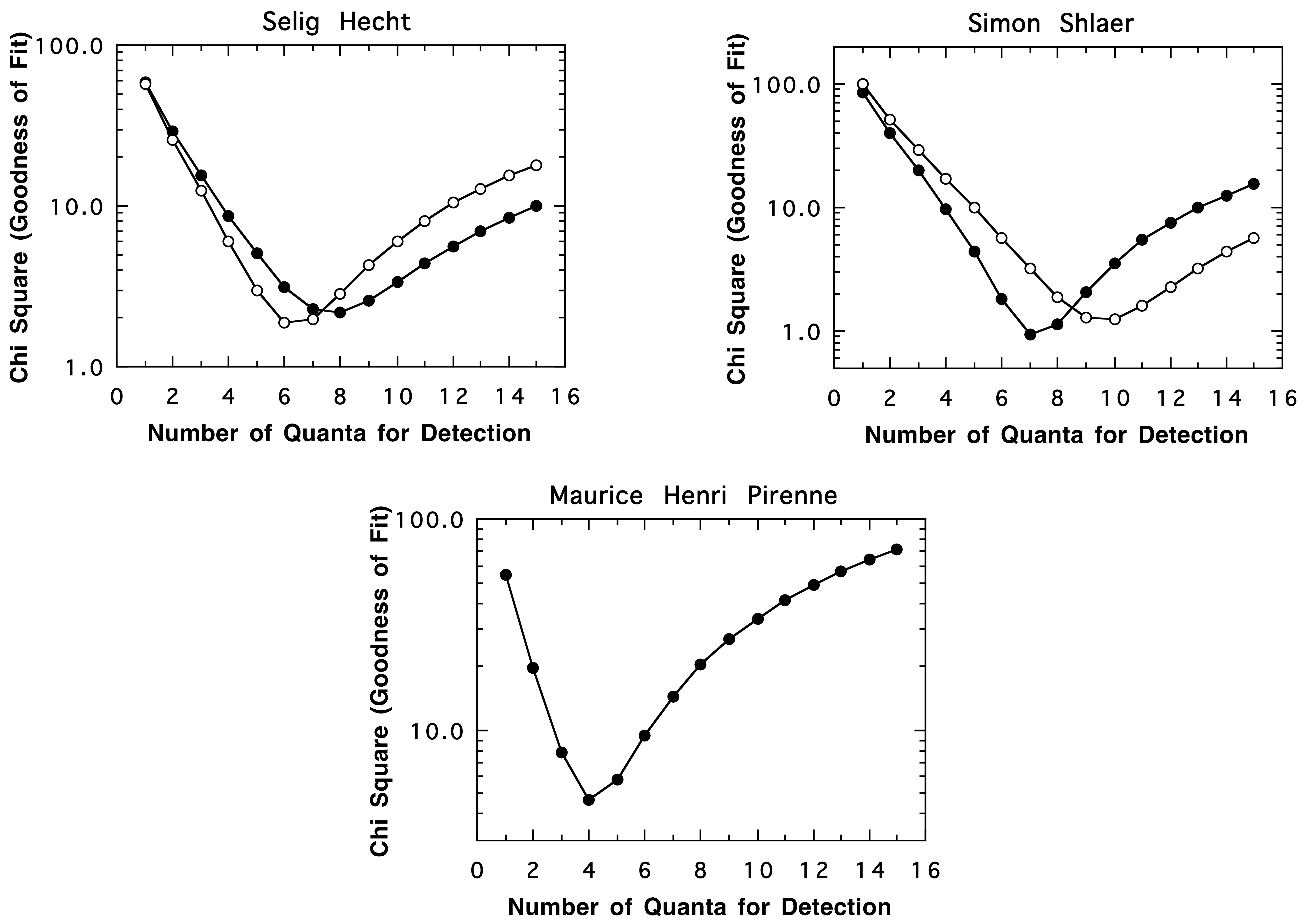

Data from Table V

	SH1	SH2	SS1	SS2	MPH
No. Quanta	8	6	7	10	4
Chi-Square	2.1862	1.8612	0.9524	1.2316	4.6696
DF	4	4	4	4	4
Probability	0.7016	0.7613	0.9169	0.9729	0.3229
Alpha	1.2475	1.2813	1.1058	0.9285	1.5253
Quantum Eff	0.0566	0.0523	0.0784	0.1179	0.0298

Conclusions

- You need 4-10 photons to be absorbed by receptors to “see”
- Quantum efficiency is between 5 and 10 percent

Main Points

- Duplex Retina
- 1 Type of Rod Receptor - Scotopic Vision
- 3 Types of Cone Receptors (S, M, L) - Photopic Vision
- Receptors can only signal rate of quantal absorption

Receptive Fields

Haldan Keffer Hartline
22 December 1903 – 17 March 1983

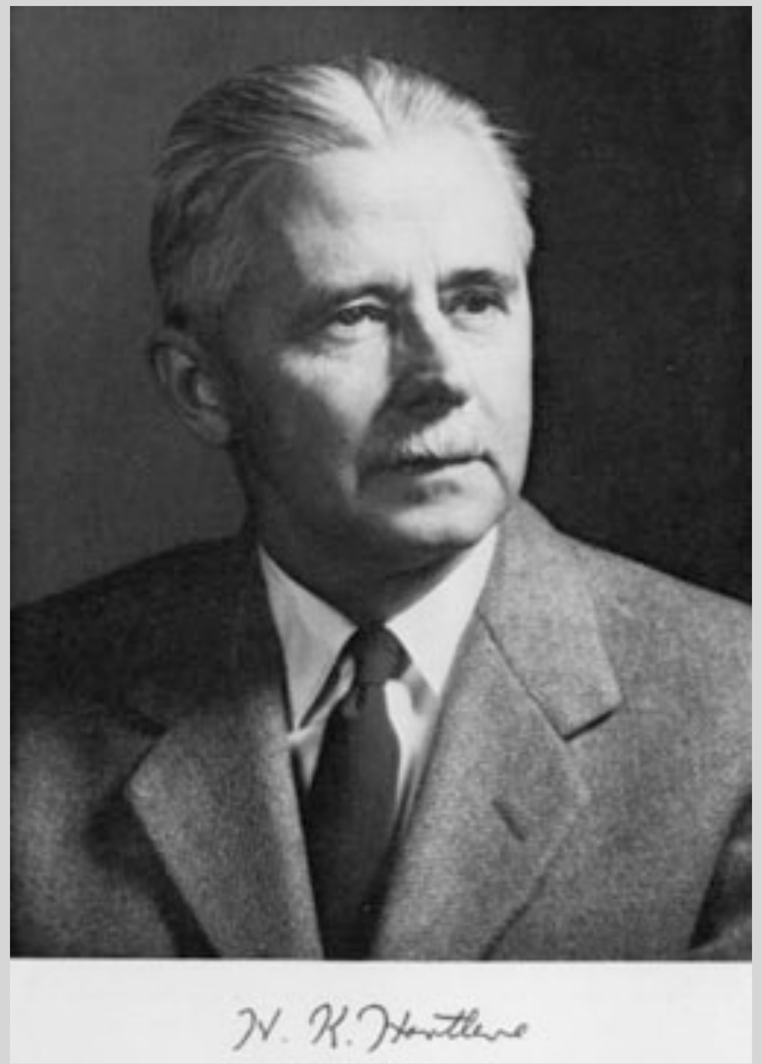

Nobel Laureate in Medicine
1967

"Spatial effects. No description of the optic responses in single fibers would be complete without a description of the region of the retina which must be illuminated in order to obtain a response in any given fiber. This region will be termed the receptive field of the fiber."

Hartline, H. K. (1938). The response of single optic nerve fibers of the vertebrate eye to illumination of the retina. *American Journal of Physiology, 121*(2), 400–415.

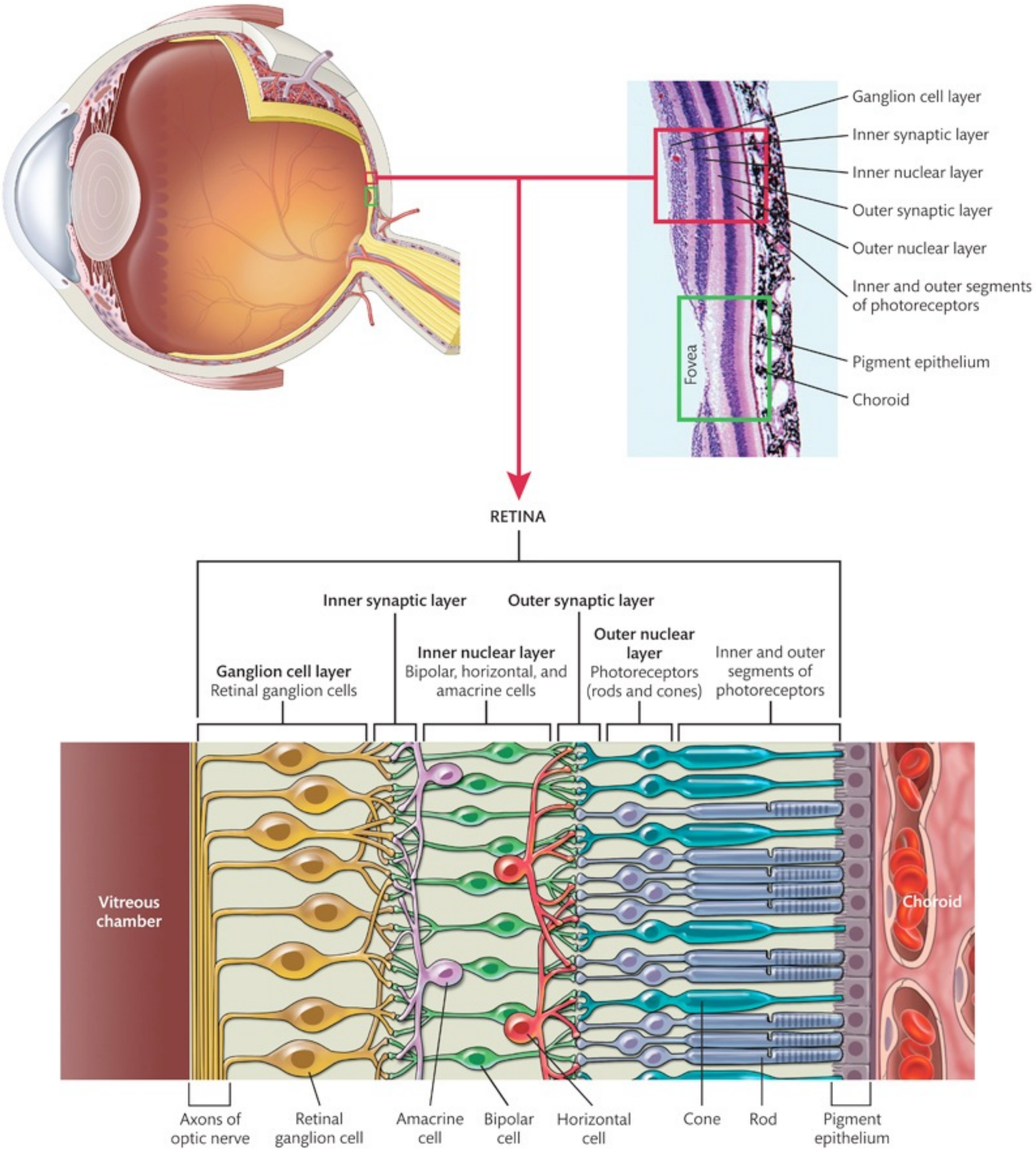

Ganglion cell layer
Inner synaptic layer
Inner nuclear layer
Outer synaptic layer
Outer nuclear layer
Inner and outer segments of photoreceptors
Pigment epithelium
Choroid
Fovea
RETINA
Inner synaptic layer
Outer synaptic layer
Ganglion cell layer
Retinal ganglion cells
Inner nuclear layer
Bipolar, horizontal, and amacrine cells
Outer nuclear layer
Photoreceptors (rods and cones)
Inner and outer segments of photoreceptors
Vitreous chamber
Choroid
Axons of optic nerve
Retinal ganglion cell
Amacrine cell
Bipolar cell
Horizontal cell
Cone
Rod
Pigment epithelium

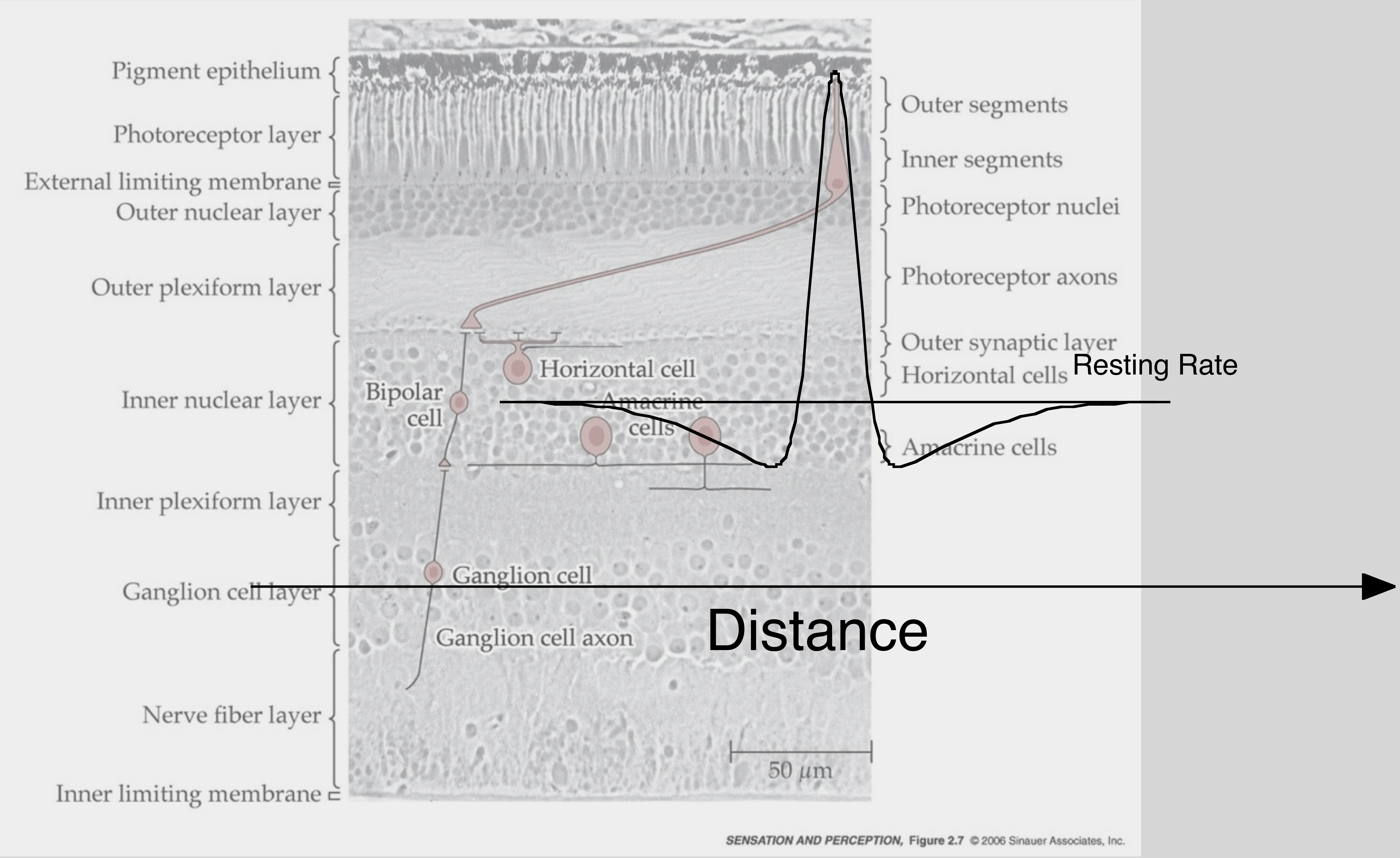
Pigment epithelium
Photoreceptor layer
External limiting membrane
Outer nuclear layer
Outer plexiform layer
Inner nuclear layer
Inner plexiform layer
Ganglion cell layer
Nerve fiber layer
Inner limiting membrane
Outer segments
Inner segments
Photoreceptor nuclei
Photoreceptor axons
Outer synaptic layer
Horizontal cells
Amacrine cells
Horizontal cell
Bipolar cell
Amacrine cells
Ganglion cell
Ganglion cell axon
50 μm
Resting Rate
Distance
SENSATION AND PERCEPTION, Figure 2.7 © 2006 Sinauer Associates, Inc.

Ganglion Cell Receptive Fields

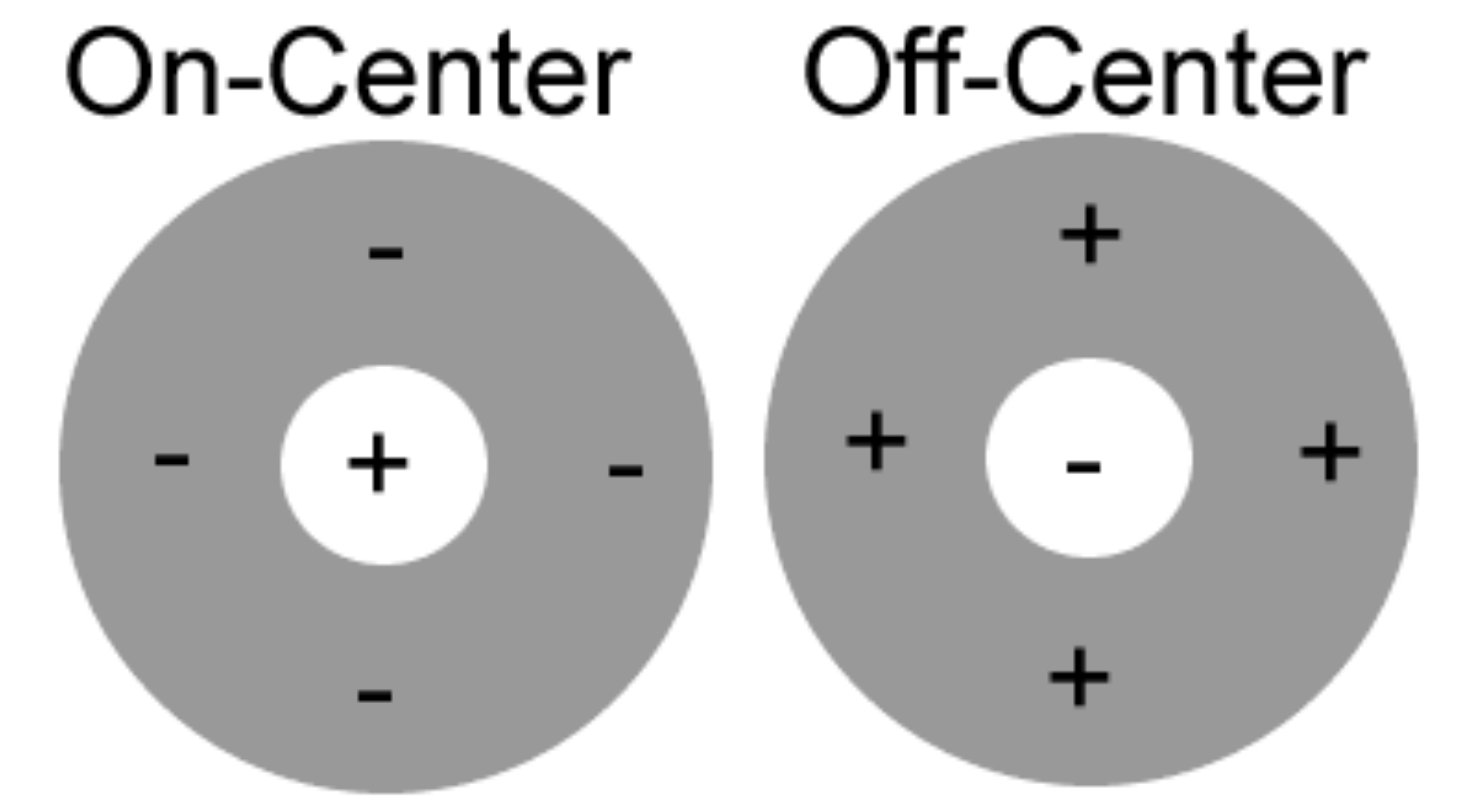

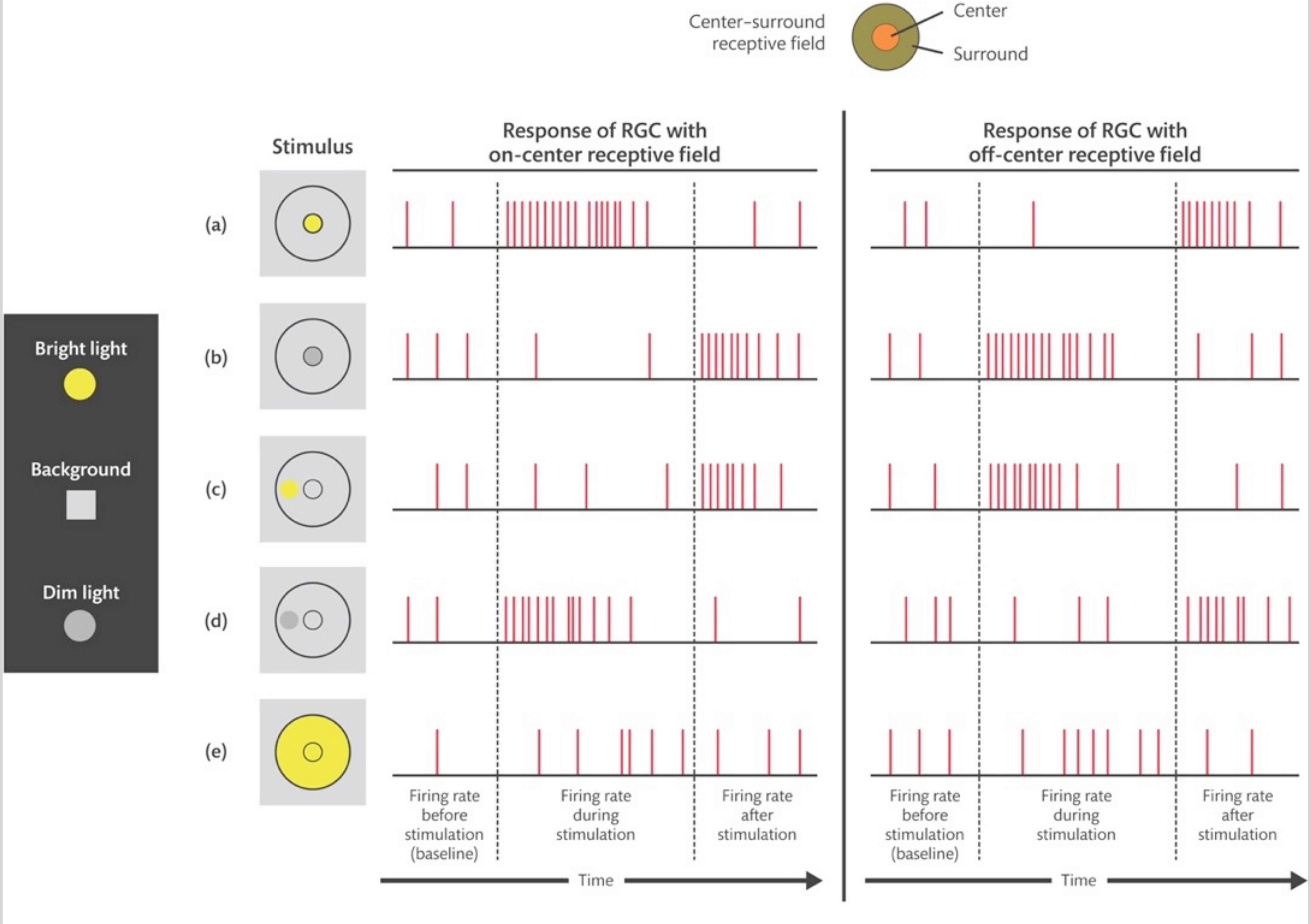

Center-surround receptive field
Center
Surround
Stimulus
Response of RGC with on-center receptive field
Response of RGC with off-center receptive field
Bright light
Background
Dim light
(a)
(b)
(c)
(d)
(e)
Firing rate before stimulation (baseline)
Firing rate during stimulation
Firing rate after stimulation
Firing rate before stimulation (baseline)
Firing rate during stimulation
Firing rate after stimulation
Time
Time

On-Center, Off-Surround Ganglion Cell Receptive FieldResponse Surface

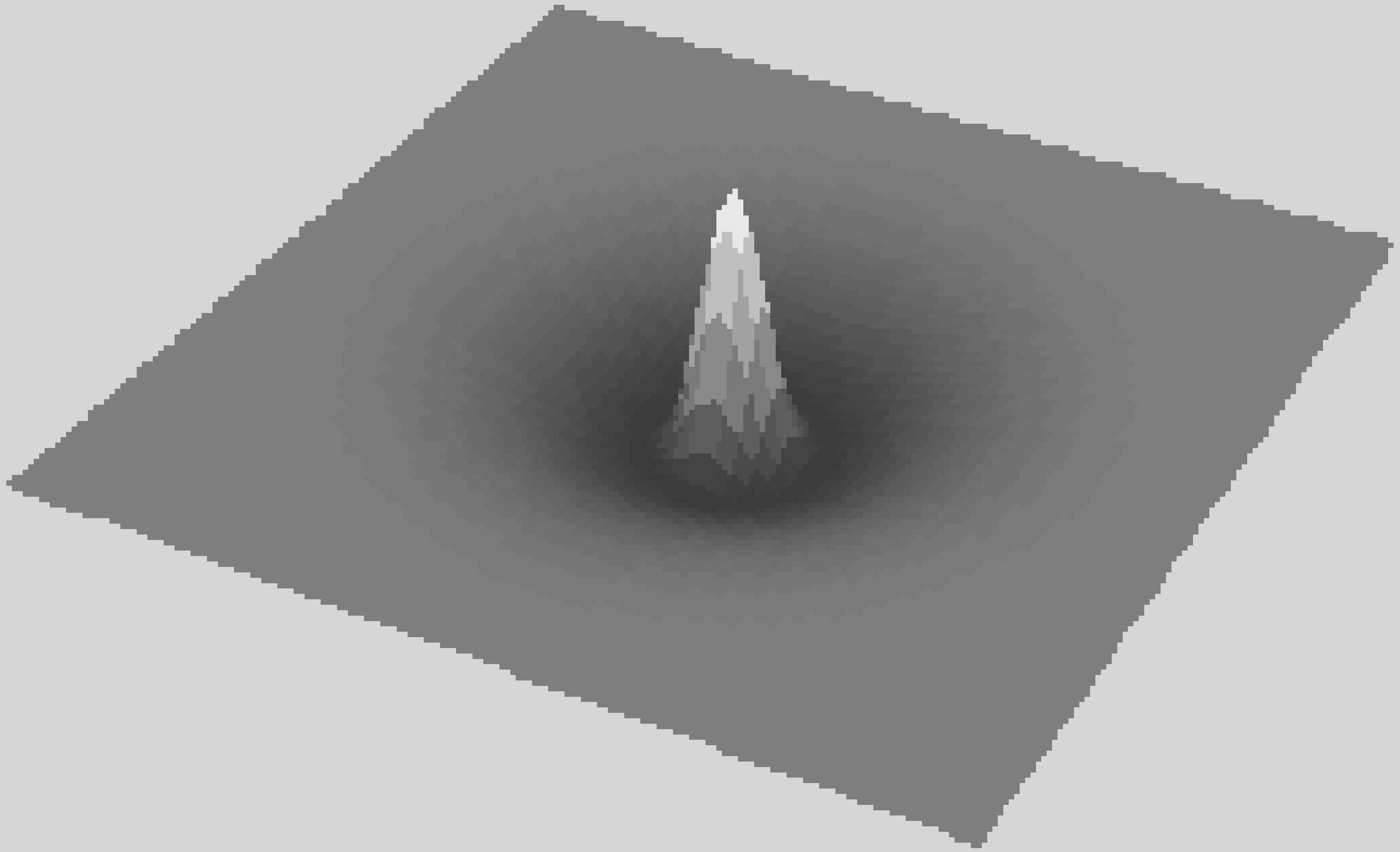

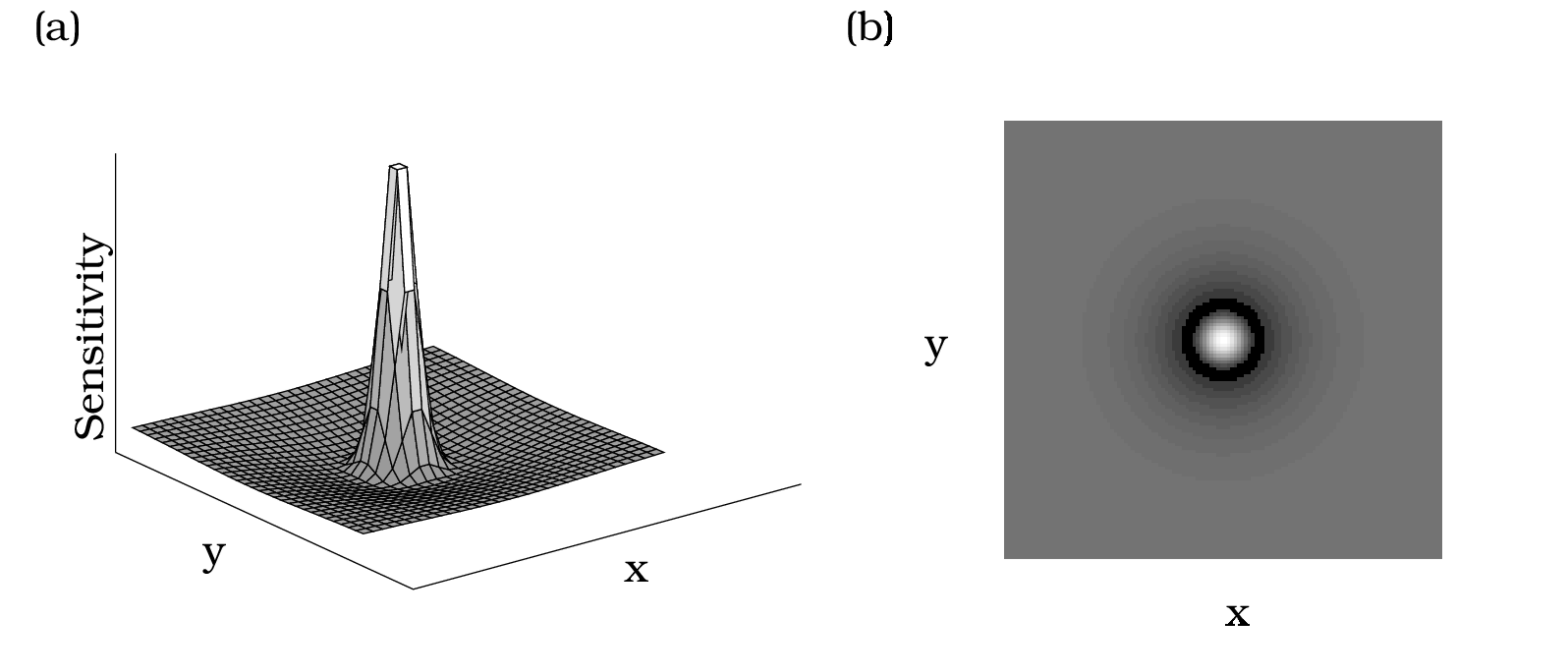
(a)
Sensitivity
y
x
(b)
y
x

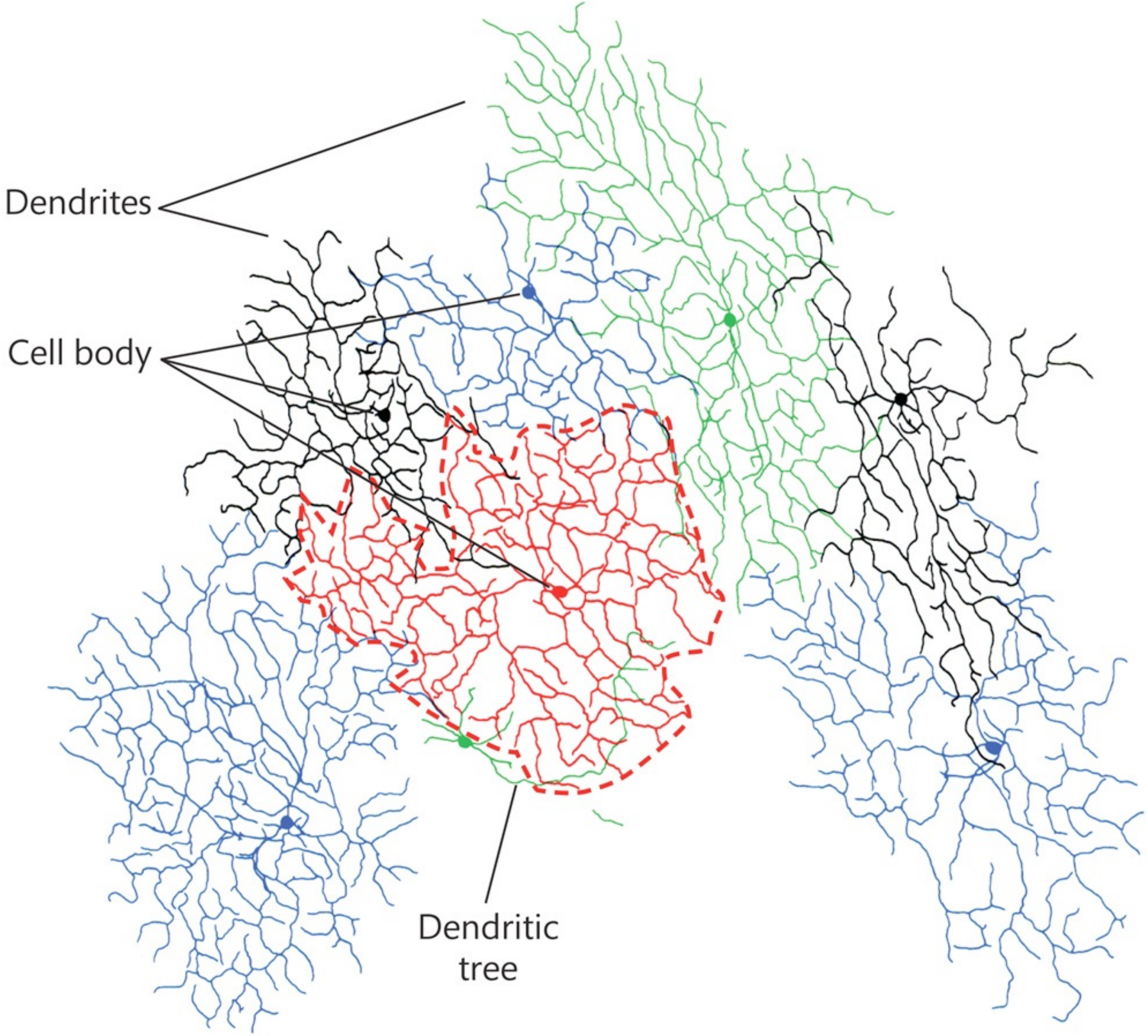
Dendrites
Cell body
Dendritic
tree

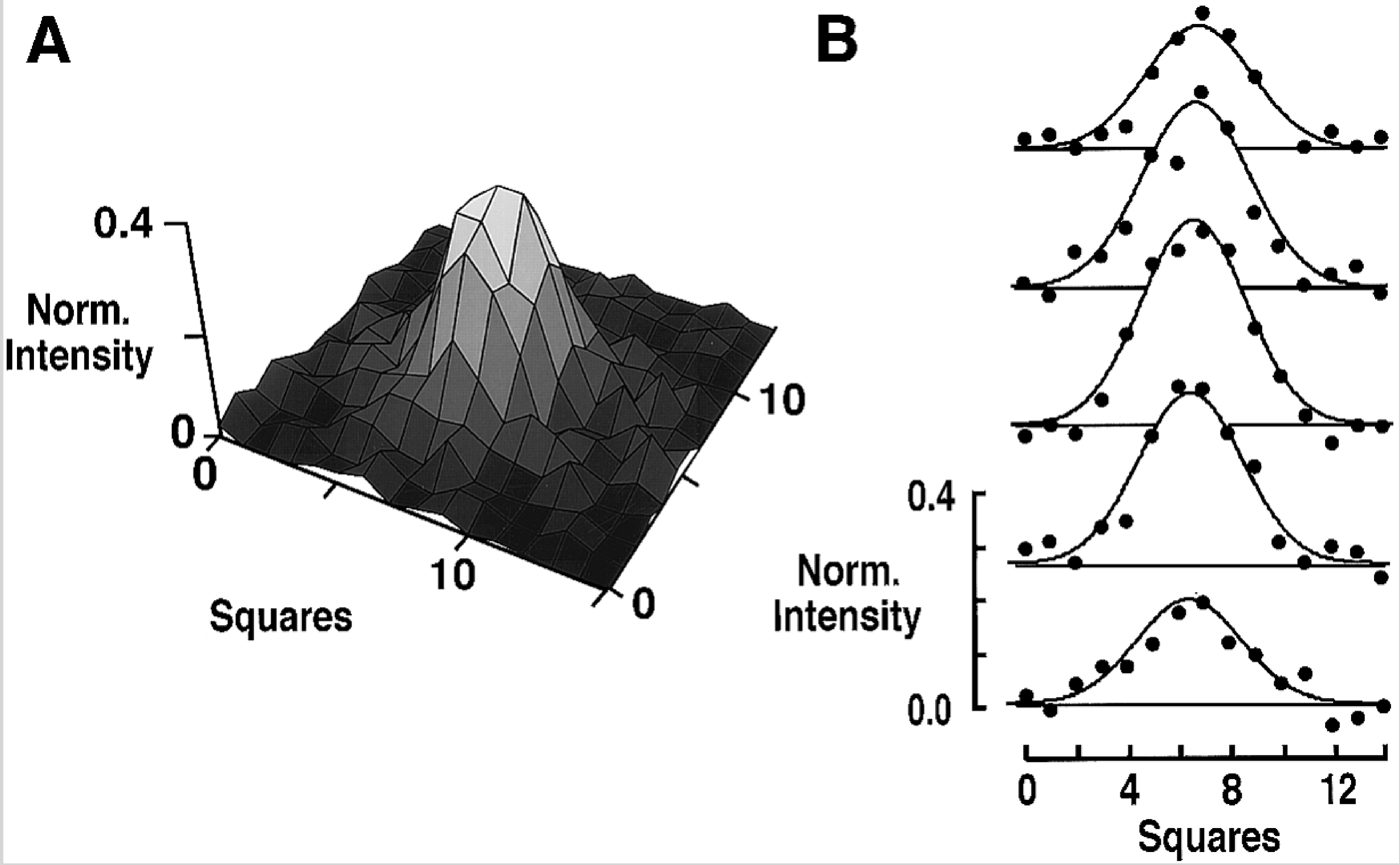

FIG. 4. Gaussian fit to spatial profile of ON BT cell's mean effective stimulus. *A*: mean effective stimulus at its peak 125 ms before spike.

DeVries, S. H., & Baylor, D. A. (1997). Mosaic Arrangement of Ganglion Cell Receptive Fields in Rabbit Retina. *Journal of Neurophysiology, 78*(4), 2048-2060.

Receptive fields of parasol RGCs

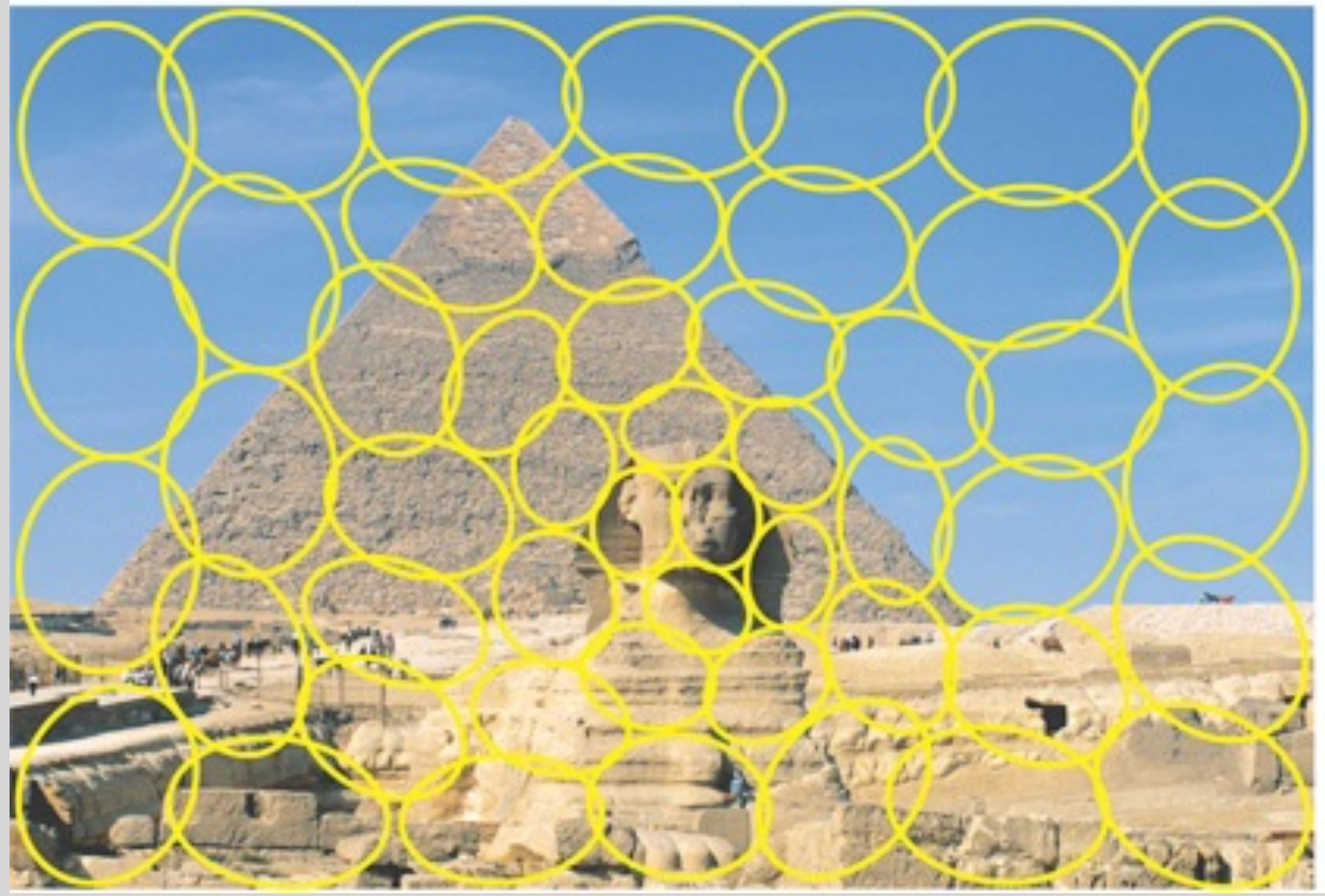

Receptive fields of midget RGCs

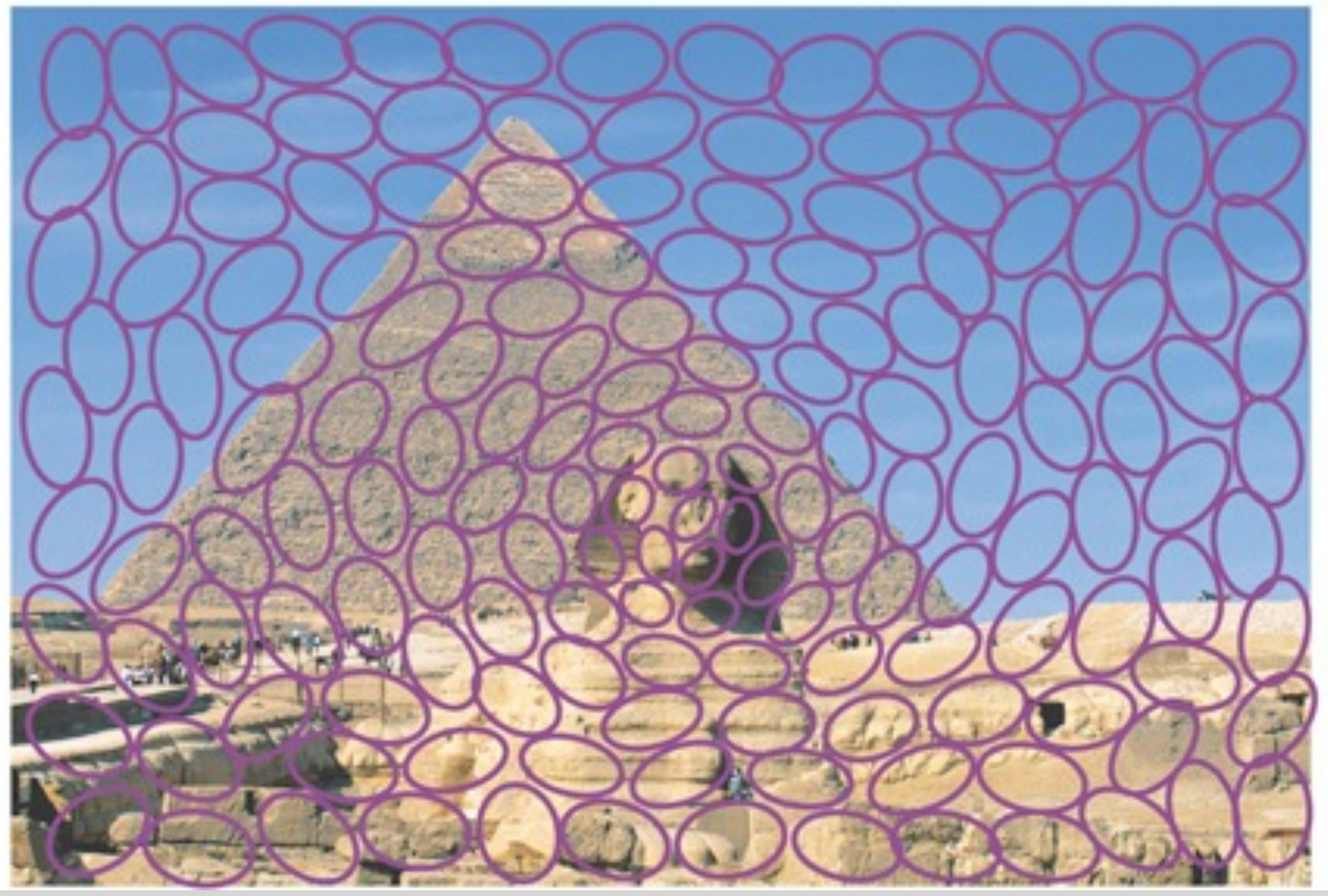

Receptive fields of parasol and midget RGCs

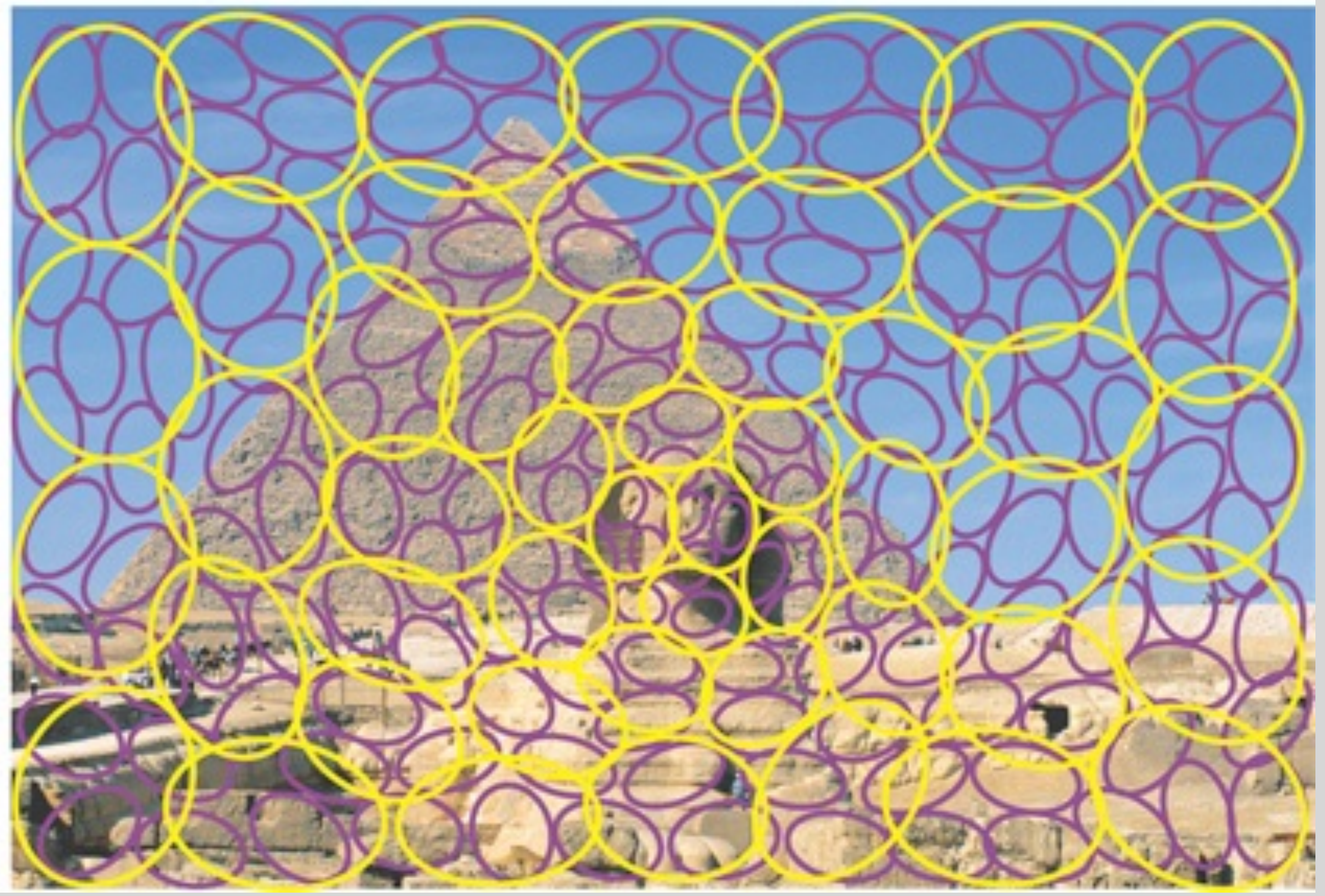

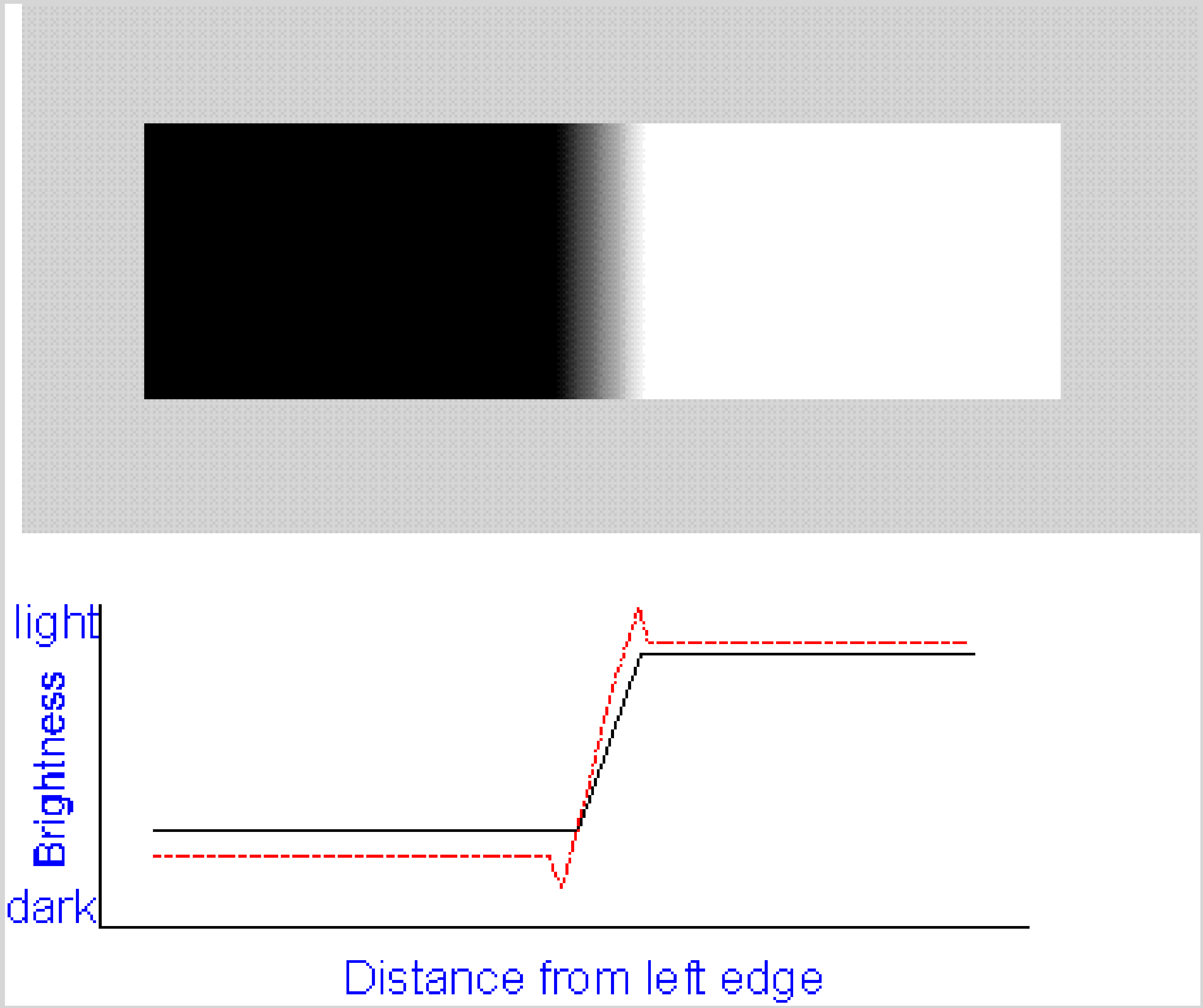
light
Brightness
dark
Distance from left edge

Hermann Grid

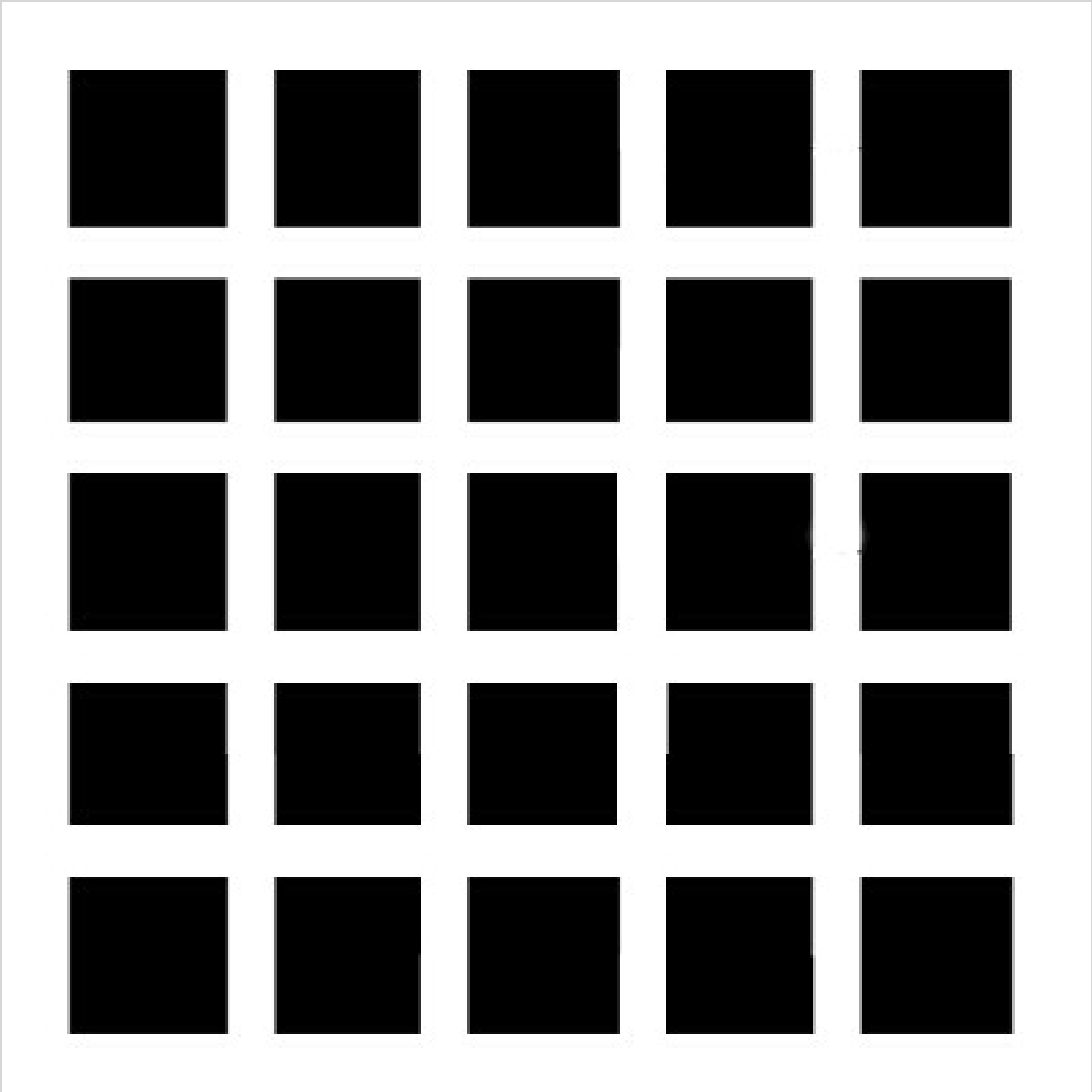

Hermann, L. (1870). Eine Erscheinung simultanen Contrastes. *Pflügers Archiv für die gesamte Physiologie des Menschen und der Tiere, 3*, 13-15.

Hermann Grid

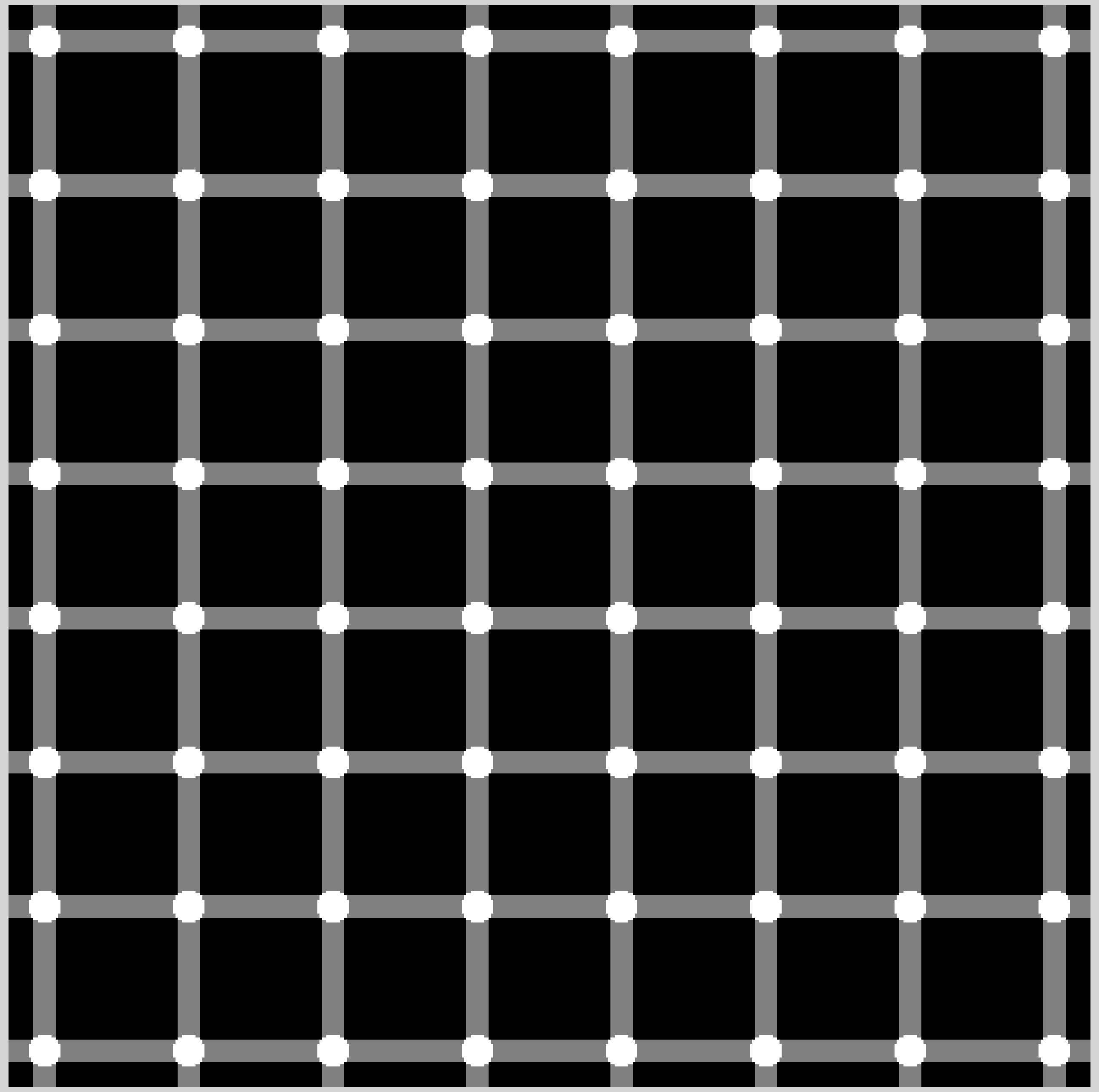

Hermann, L. (1870). Eine Erscheinung simultanen Contrastes. *Pflügers Archiv für die gesamte Physiologie des Menschen und der Tiere, 3*, 13-15.

Enhanced Hermann Grid

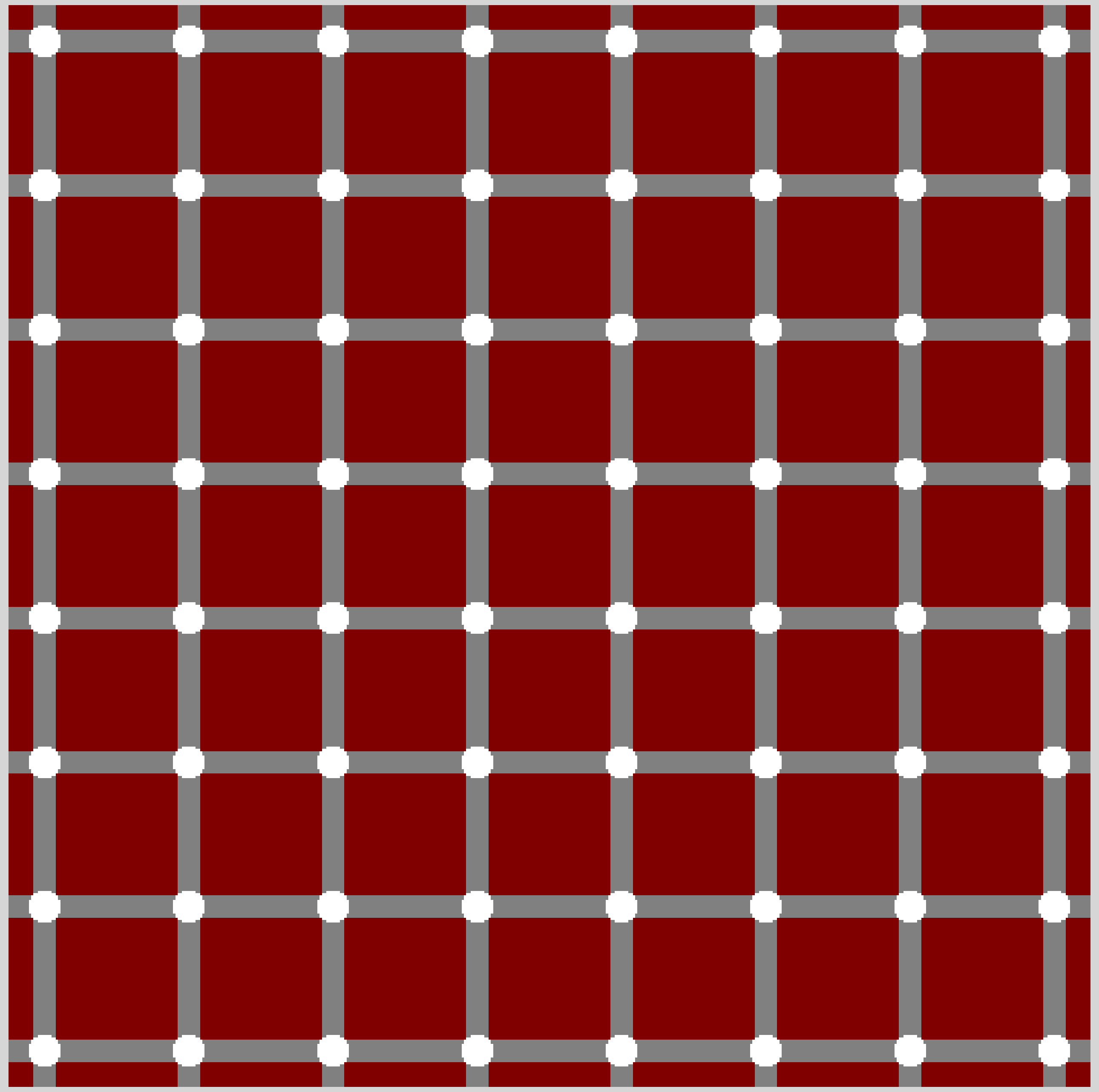

Hermann, L. (1870). Eine Erscheinung simultanen Contrastes. *Pflügers Archiv für die gesamte Physiologie des Menschen und der Tiere, 3*, 13-15.

Perceptive Fields

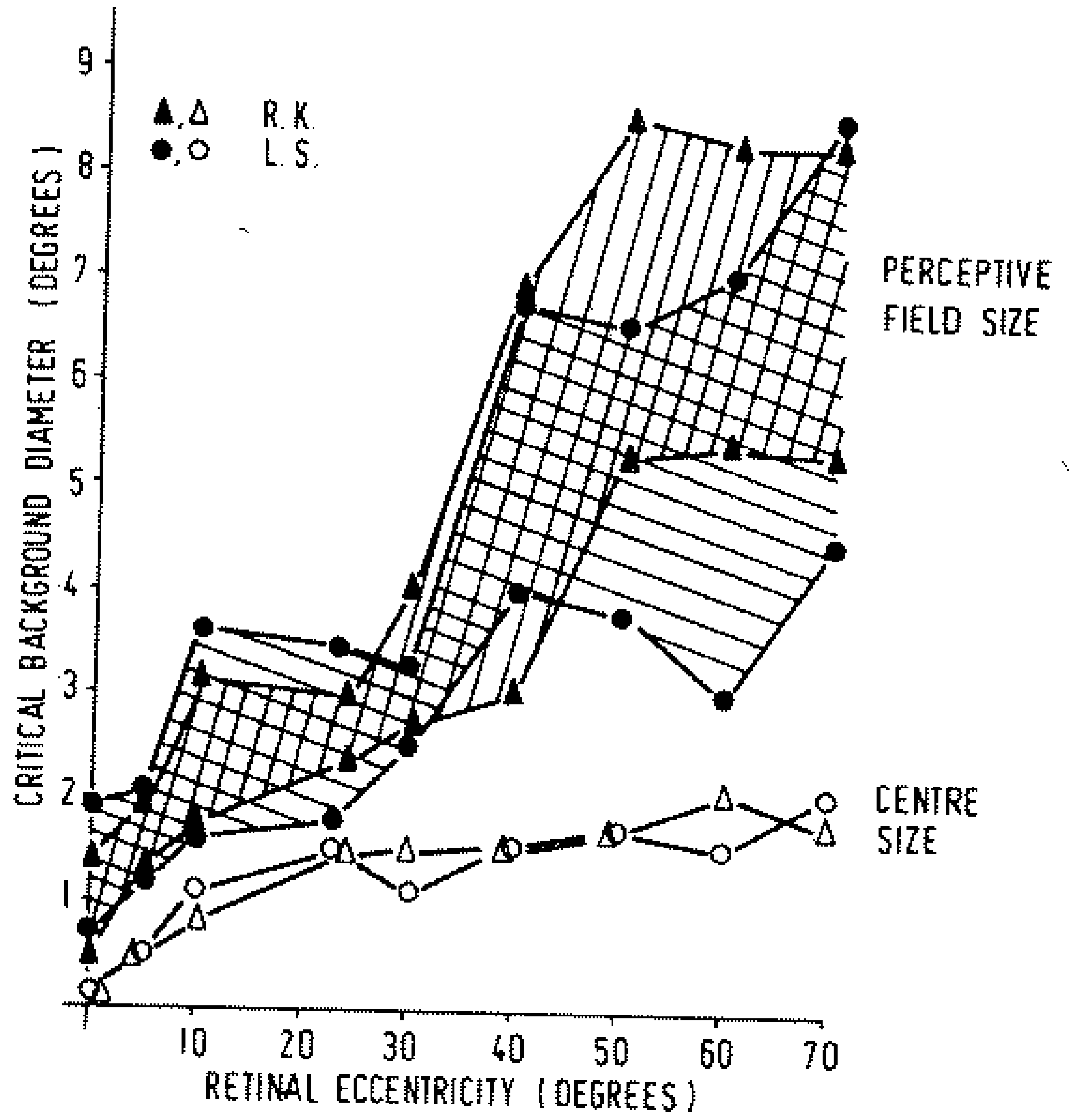

Fig. 2. Centre size (lower curves) and total perceptive field size (upper curves) as a function of eccentricity for both subjects. Values were derived from the curves shown in Fig. 1. Total perceptive field size, given as the range between the two arrows in Fig. 1, increases much more rapidly than centre size. There appears to be a region between 10 and 30° where the total field size remains relatively constant.

Ransom-Hogg, A., & Spillmann, L. (1980). Perceptive field size in fovea and periphery of the light- and dark-adapted retina. *Vision Research, 20*(3), 221–228.

Perceptive Fields

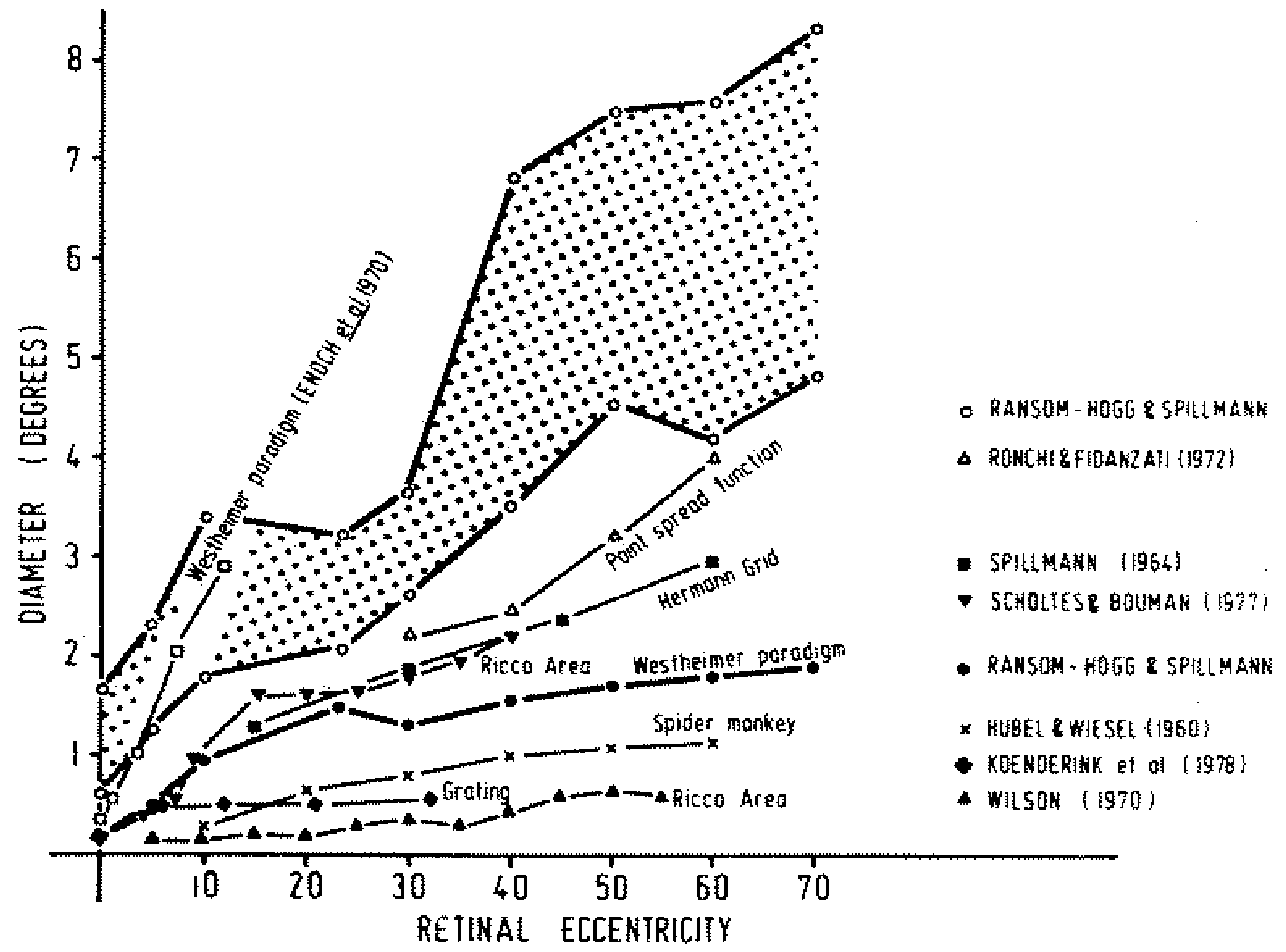

Fig. 7. Perceptive field and perceptive field centre sizes from Fig. 2 are replotted (bold lines). Estimates by other authors of centre (solid symbols) and fields (open symbols) are given for comparison. Curves are labelled with the procedure, and authors are shown next to their respective symbols. For details see text. Neurophysiological estimates of the size of the centres of retinal ganglion cells in the spider monkey (×) are included.

Ransom-Hogg, A., & Spillmann, L. (1980). Perceptive field size in fovea and periphery of the light- and dark-adapted retina. *Vision Research, 20*(3), 221–228.

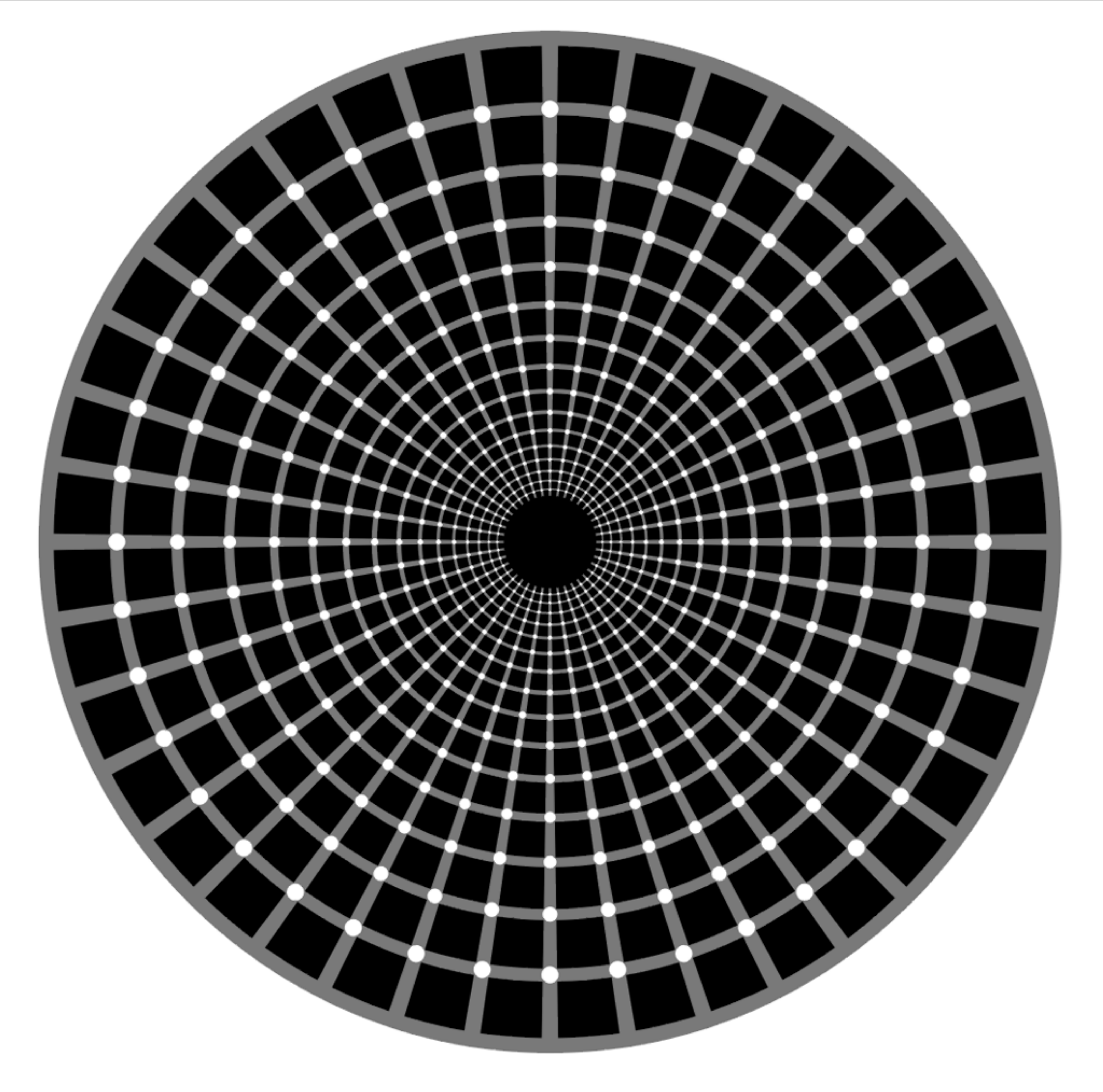

Akiyoshi Kitaoka

Nice Theory, but…

Schiller, P. H., & Carvey, C. E. (2005). The Hermann grid illusion revisited. *Perception, 34*(11), 1375-1397.

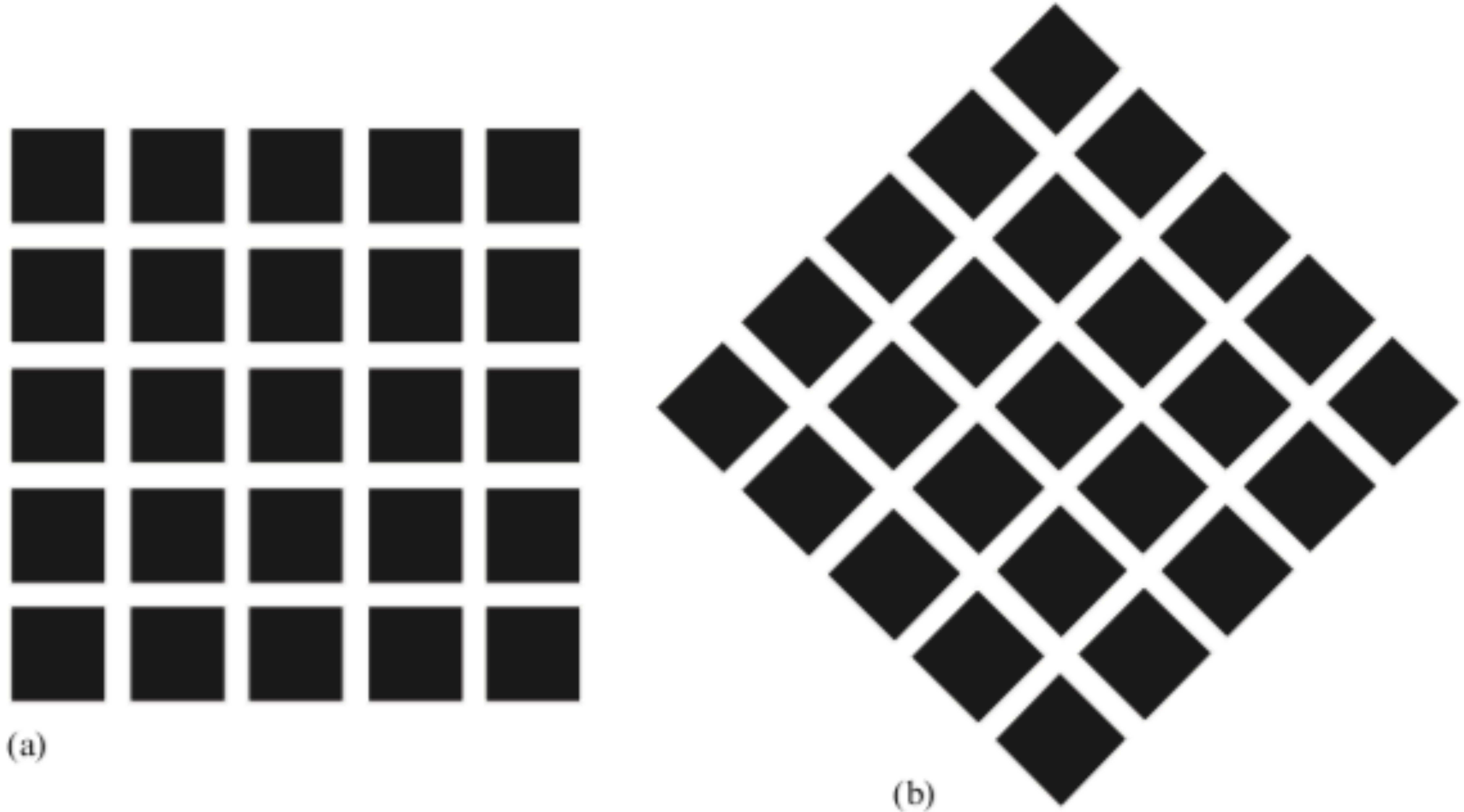

Figure 3. (a) Classic Hermann grid. (b) The illusory effect is reduced when the grid is rotated by 45°.

Schiller, P. H., & Carvey, C. E. (2005). The Hermann grid illusion revisited. *Perception, 34*(11), 1375-1397.

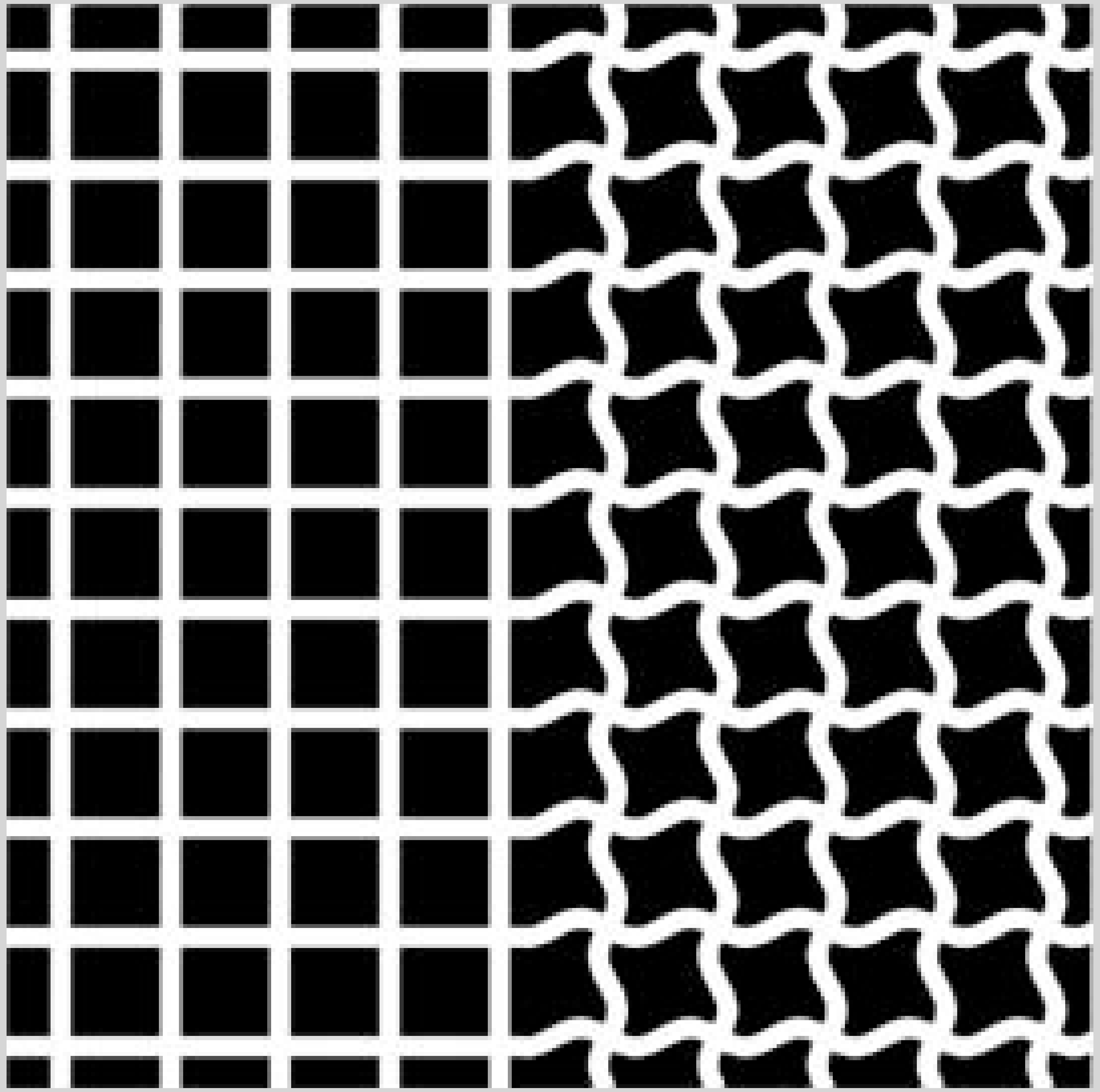

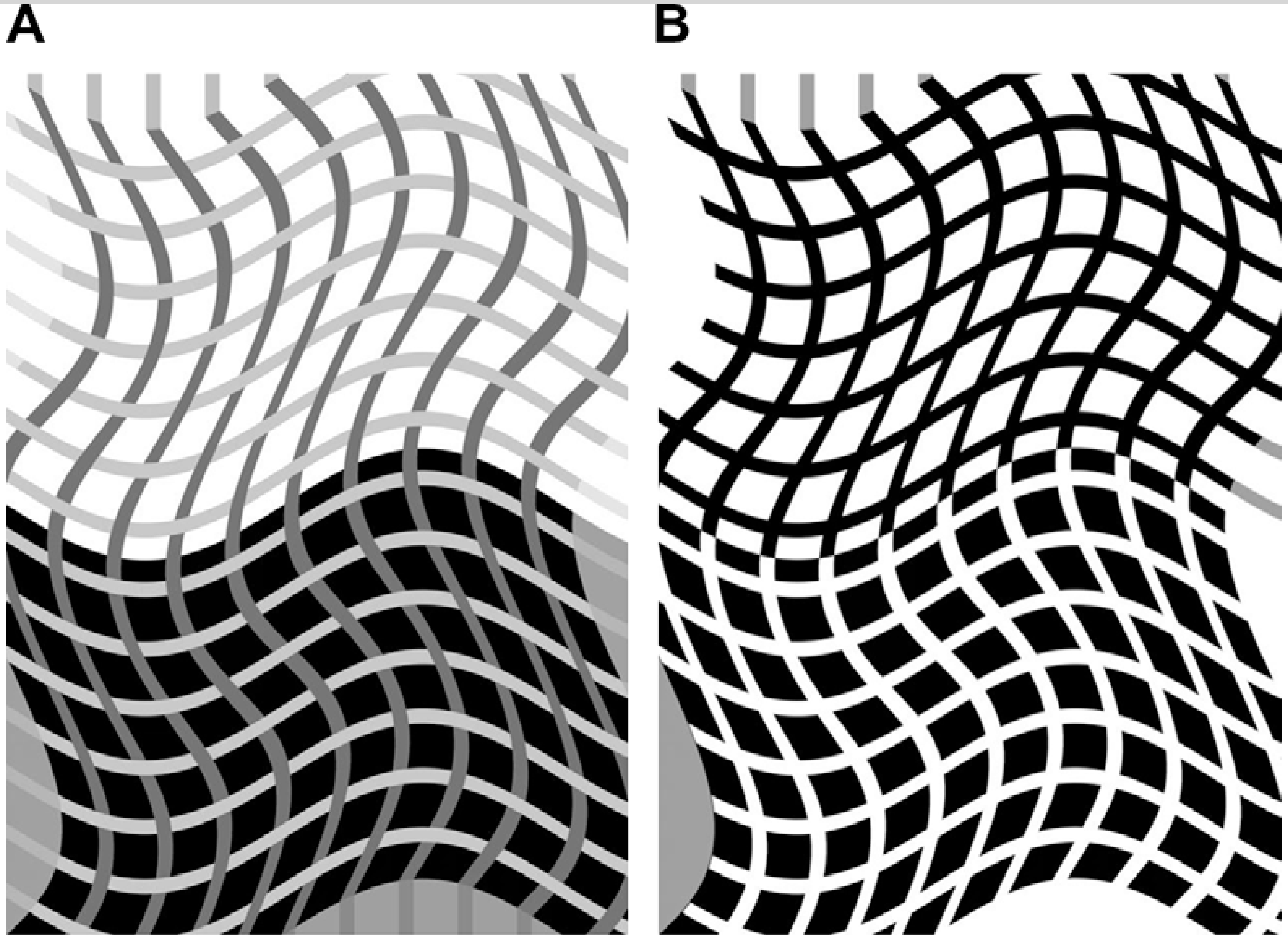

Fig. 9. Patterns made up of wavy bars. (A) Weaves and (B) Hermann grid. The spots for the weaves are barely affected by the wavy pattern, but the spots for the Hermann grid are nearly absent (see also Geier et al., 2004, 2008).

Hamburger, K., & Shapiro, A. G. (2009). Spillmann's weaves are more resilient than Hermann's grid. *Vision Research, 49*(16), 2121-2130. doi: http://dx.doi.org/10.1016/j.visres.2009.06.002

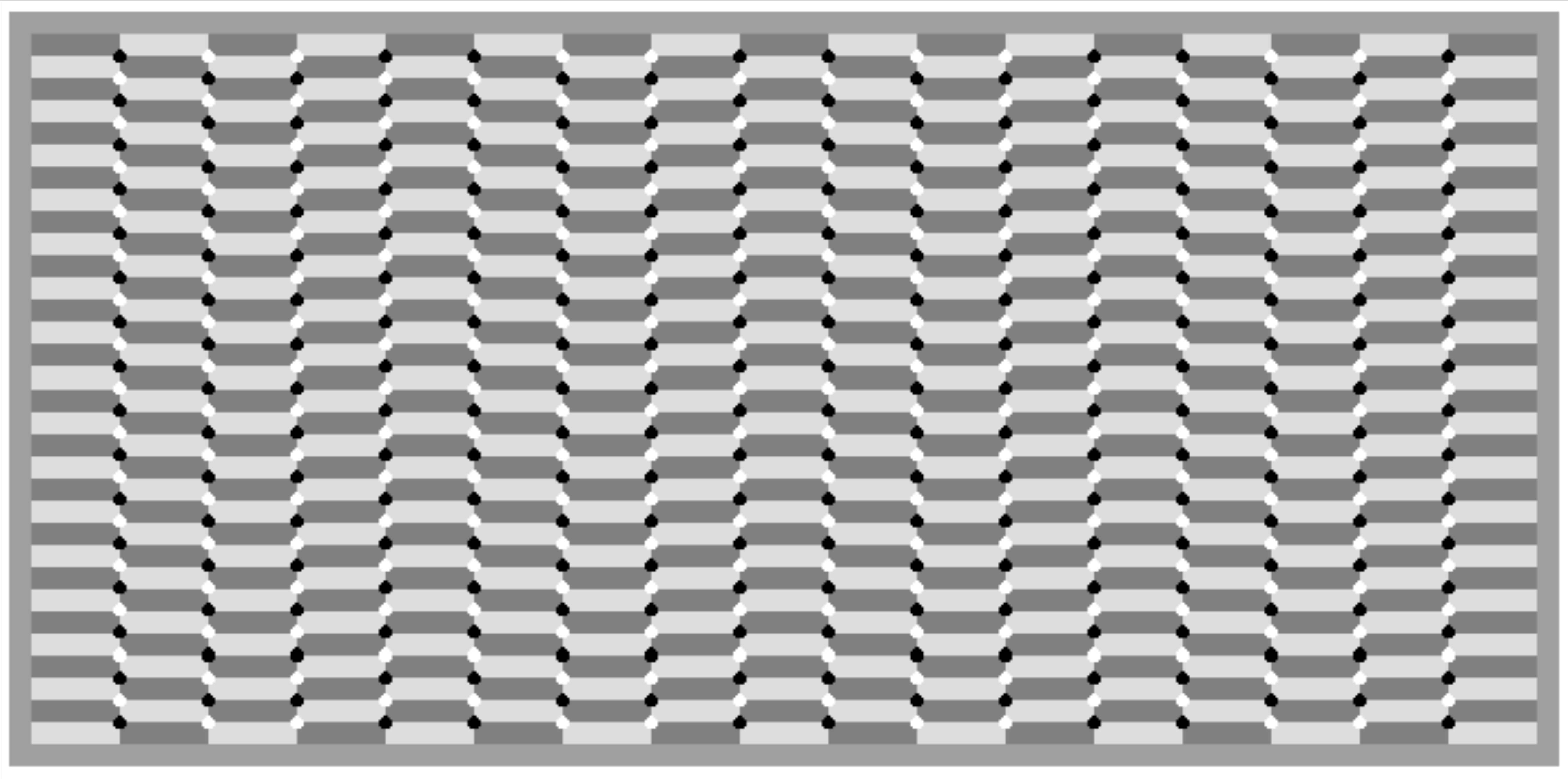

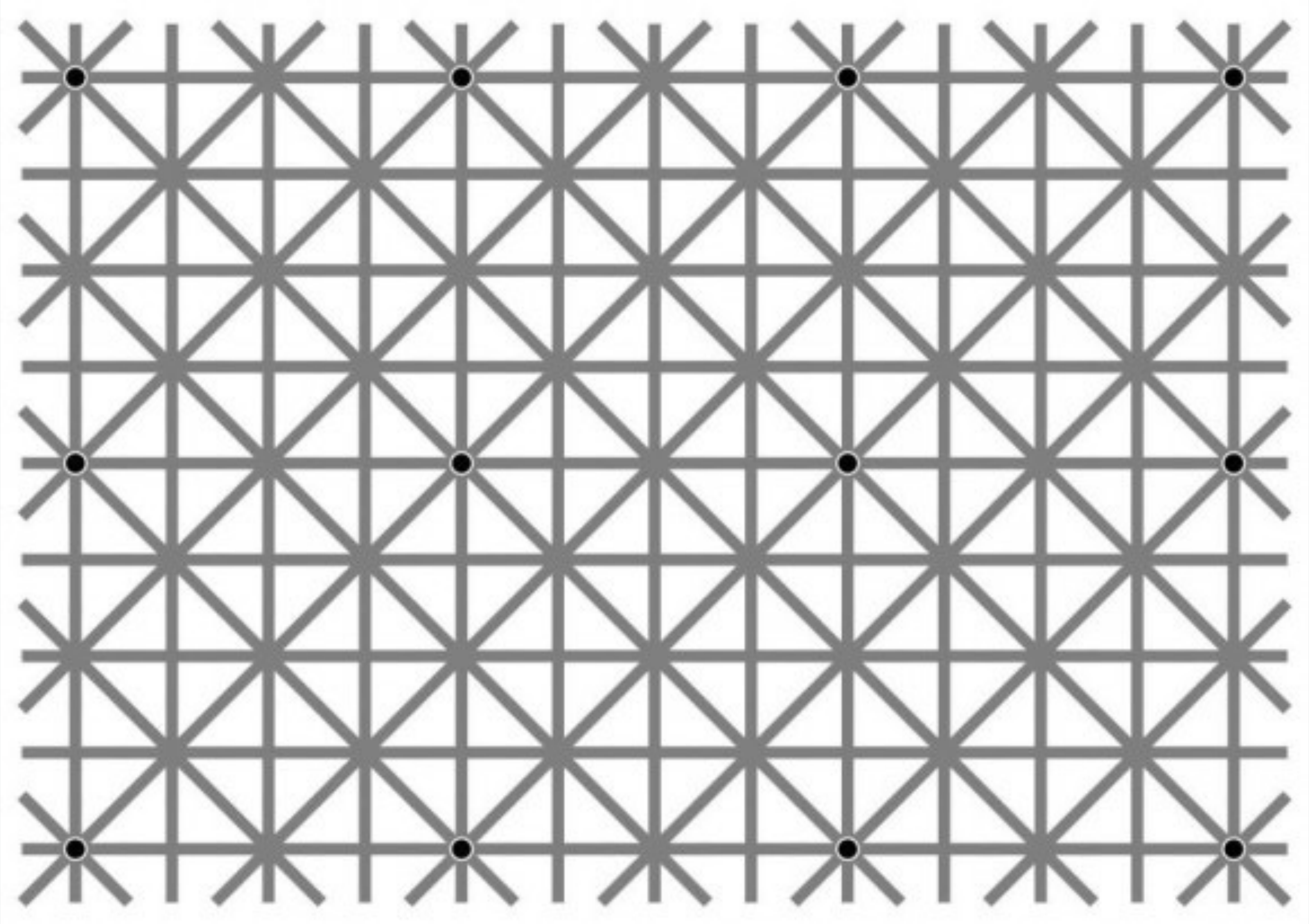

Ninio, J., & Stevens, K. A. (2000). Variations on the Hermann Grid: An Extinction Illusion. *Perception, 29*(10), 1209-1217. doi: 10.1068/p2985

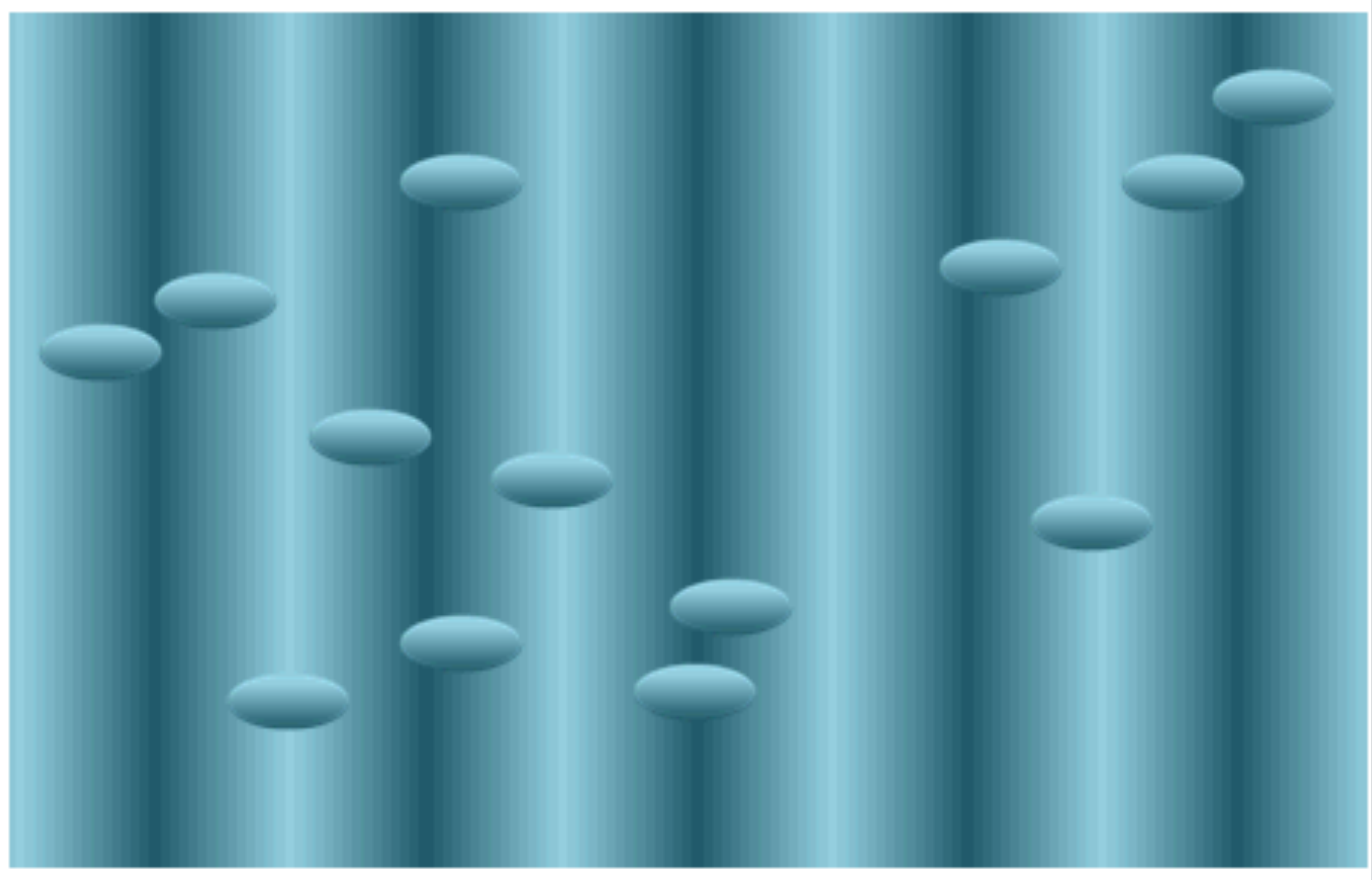

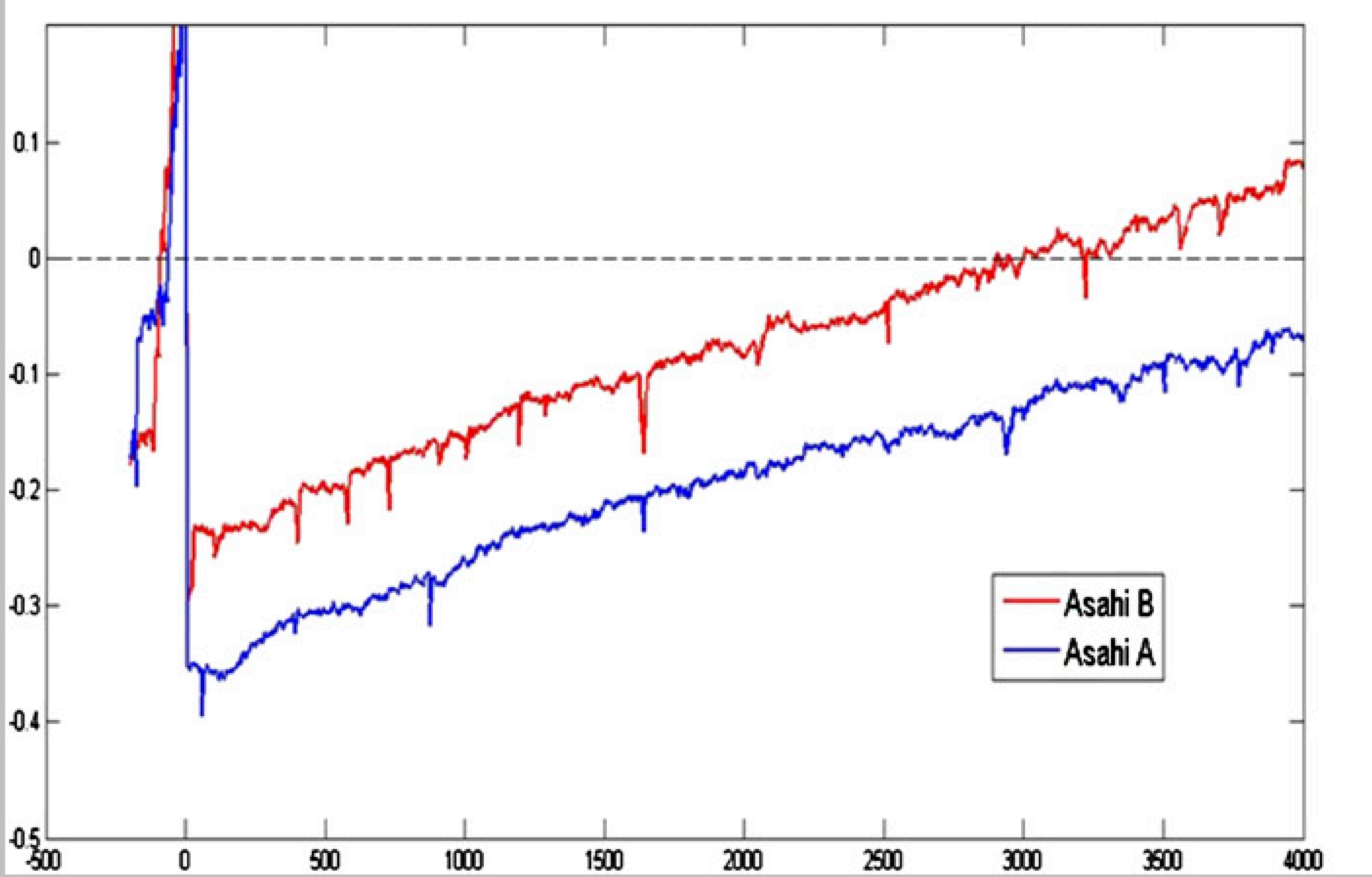
0.1
0
-0.1
-0.2
-0.3
-0.4
-0.5
-500
0
500
1000
1500
2000
2500
3000
3500
4000
Asahi B
Asahi A

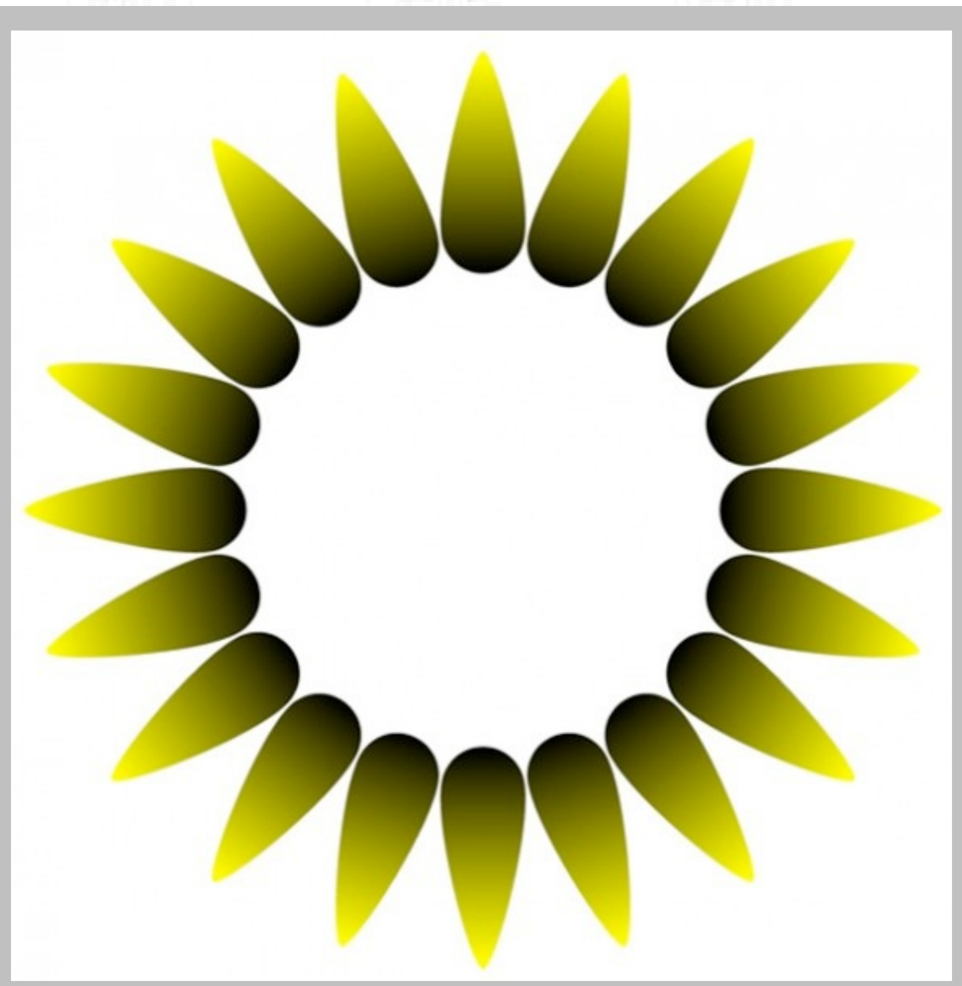

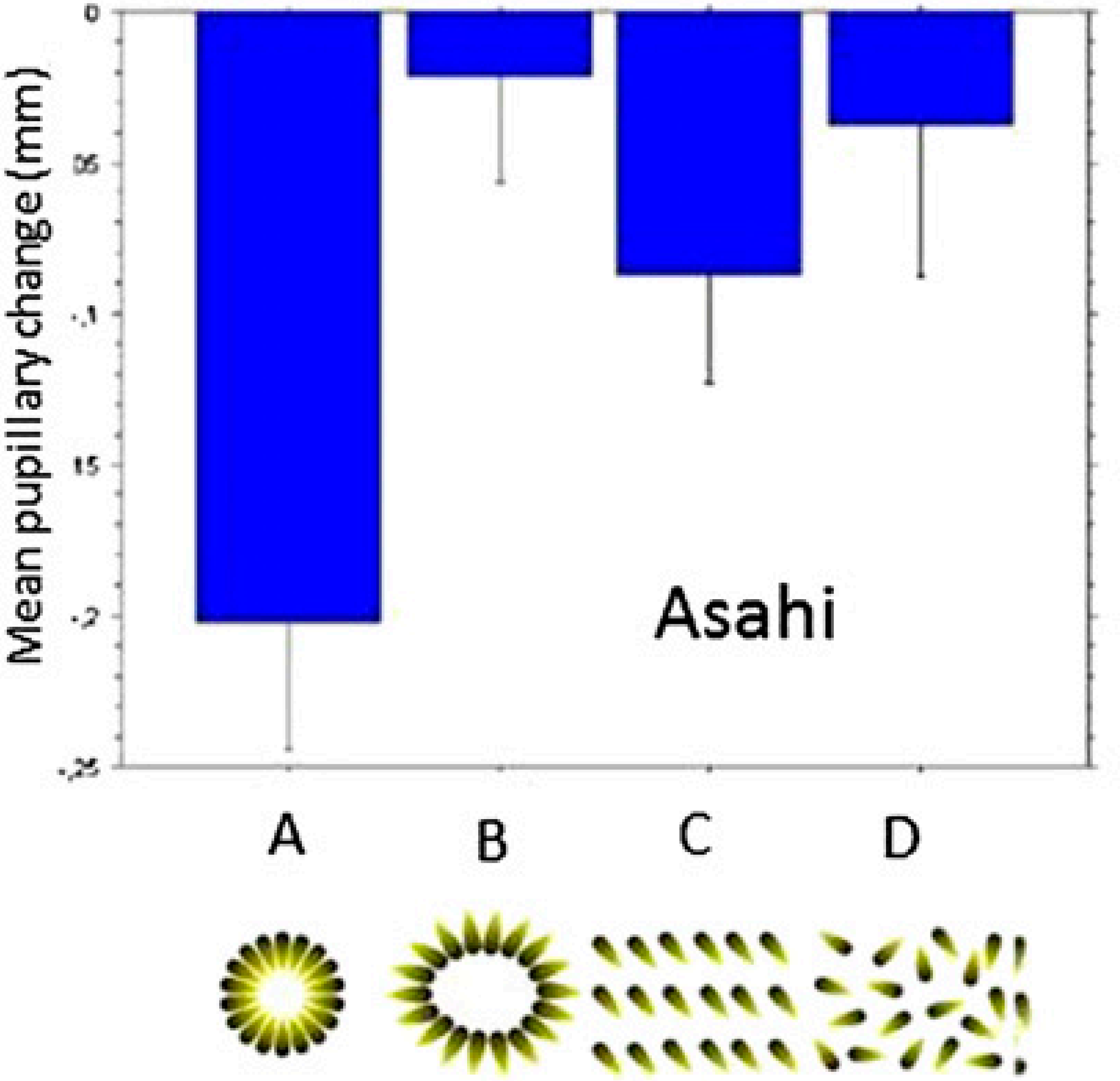
Mean pupillary change (mm)
0
-.05
-.1
-.15
-.2
-.25
Asahi
A
B
C
D

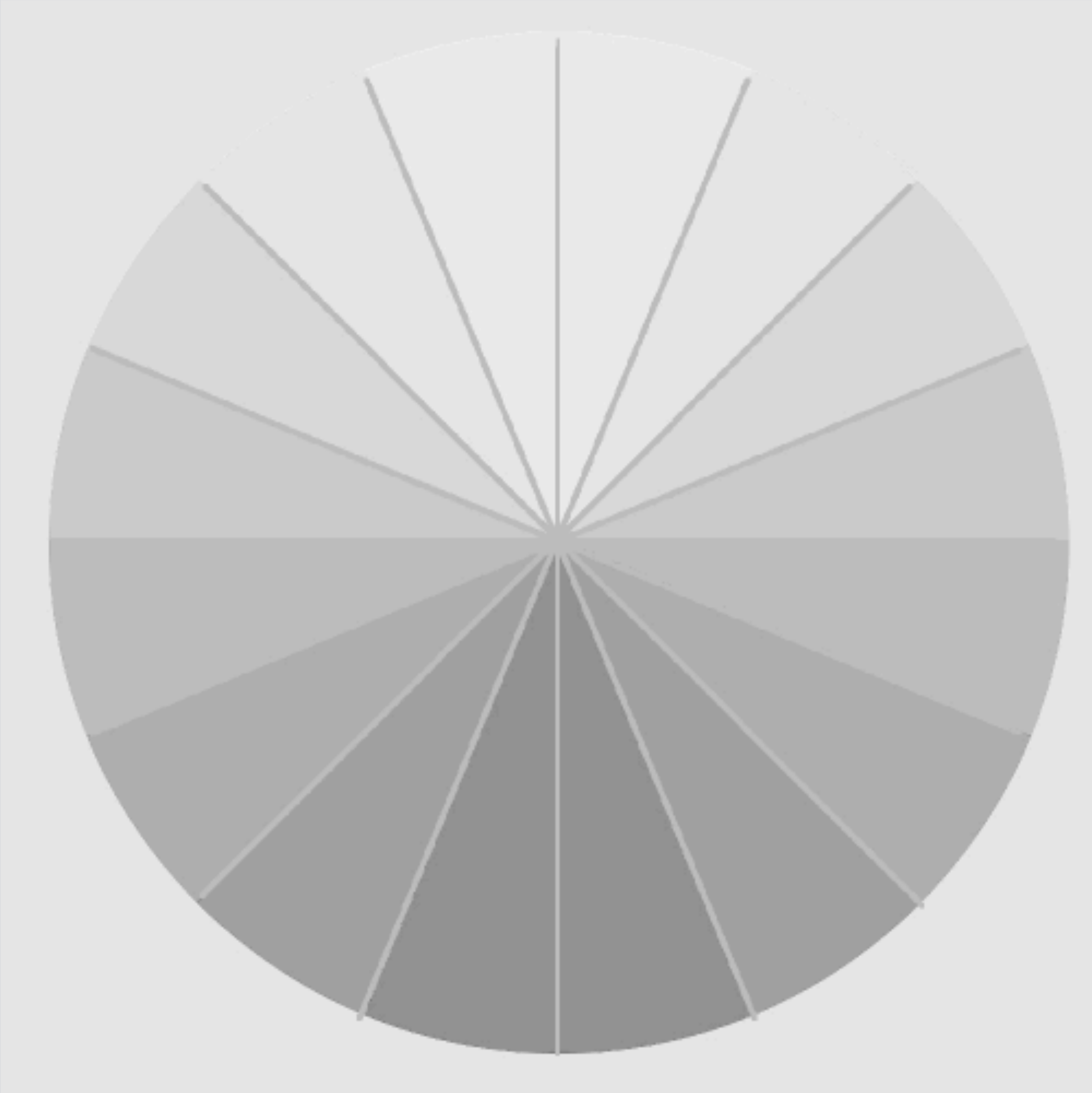

Anstis, S., & Rogers, B. (2011). Illusory rotation of a spoked wheel. *2*(7), 720-723.

The Perpetual Diamond

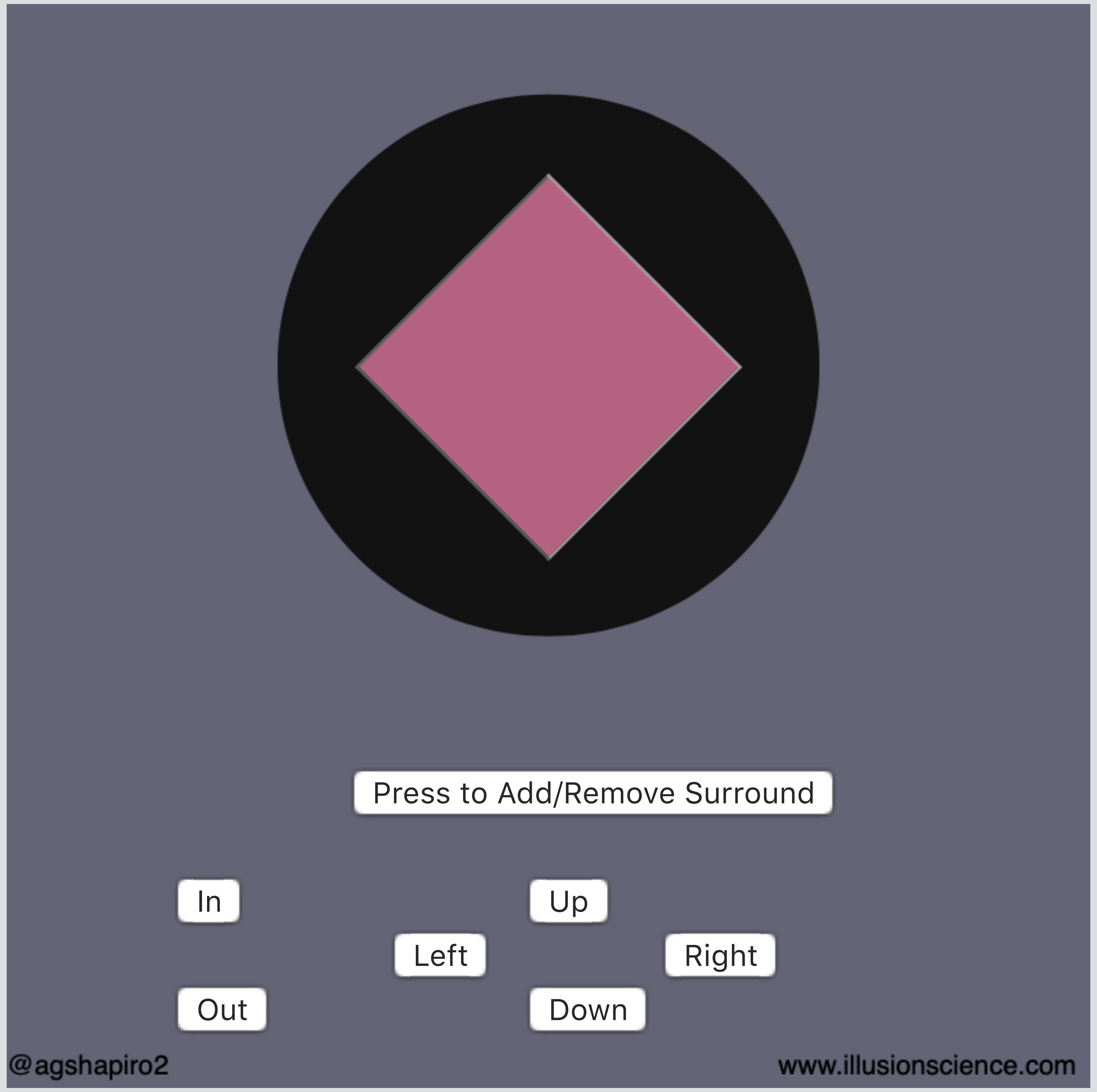

http://illusionscience.com/the-perpetual-diamond/

Flynn, O. J., & Shapiro, A. G. (2018). The Perpetual Diamond: Contrast Reversals Along Thin Edges Create the Appearance of Motion in Objects. *i-Perception, 9*(6), 2041669518815708. doi:10.1177/2041669518815708

The Perpetual Diamond

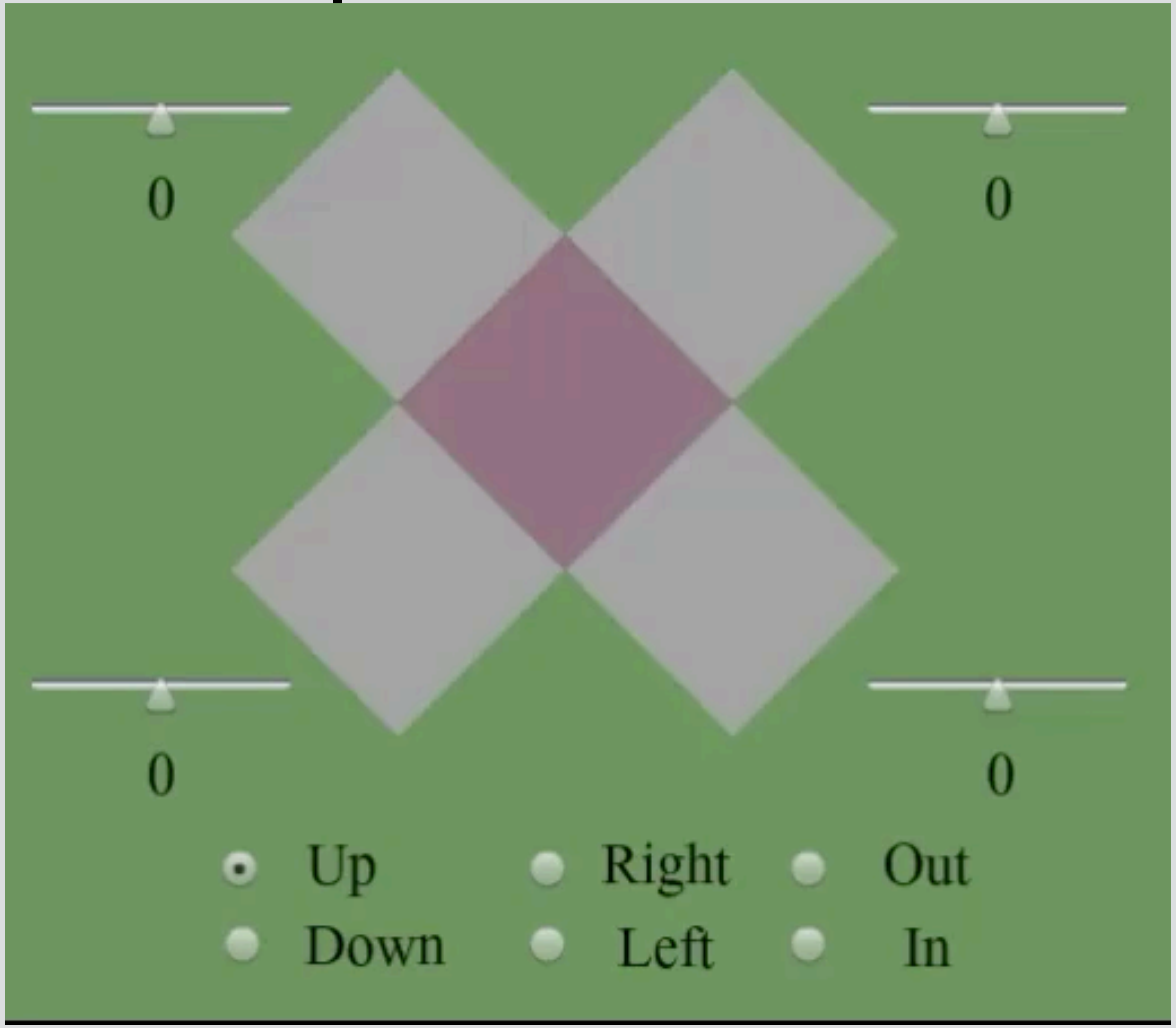

Flynn, O. J., & Shapiro, A. G. (2018). The Perpetual Diamond: Contrast Reversals Along Thin Edges Create the Appearance of Motion in Objects. *i-Perception, 9*(6), 2041669518815708. doi:10.1177/2041669518815708

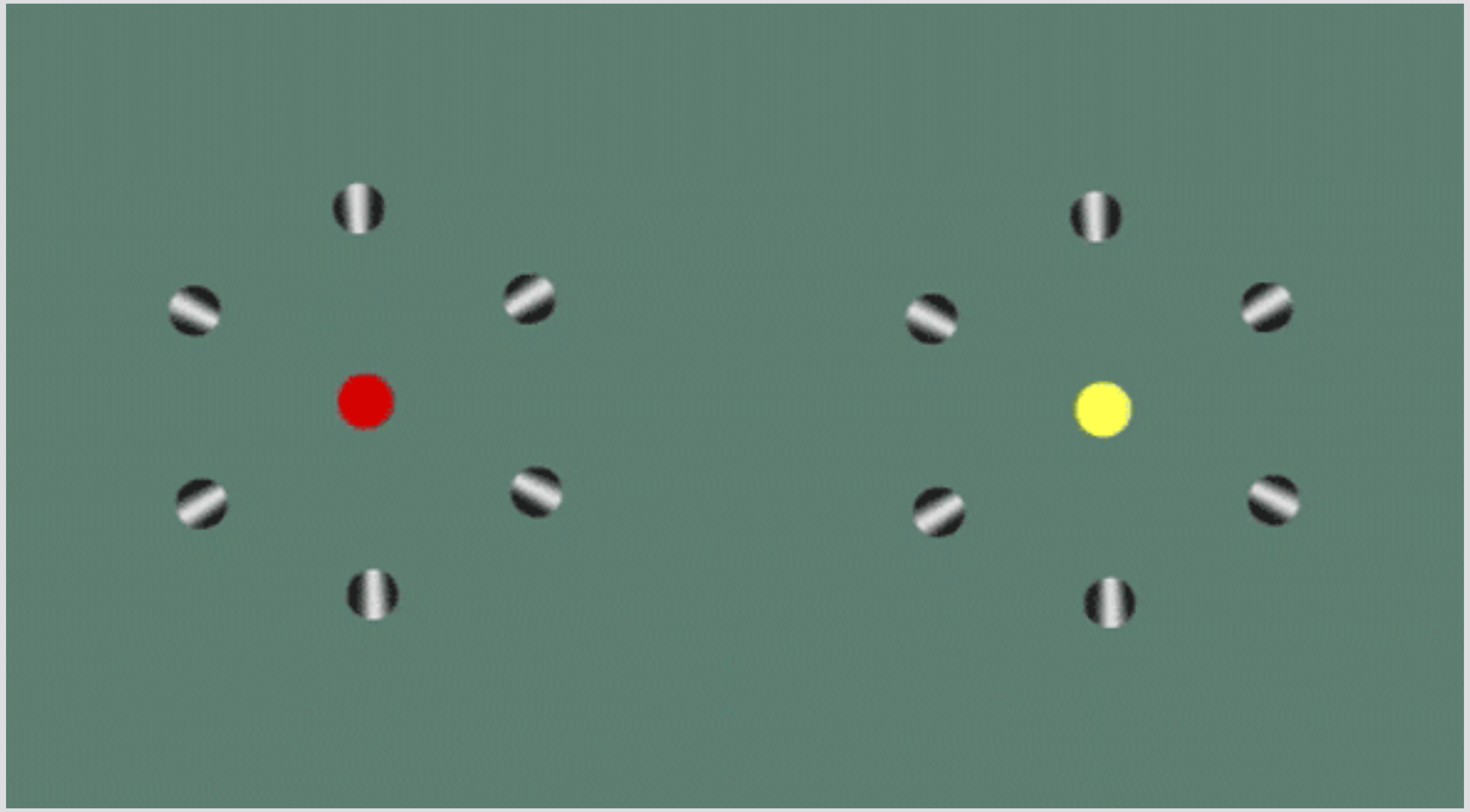

We Don’t See the Stimulus

- We see the result of neural/perceptual processes

The Visual Brain

Andreas Vesalius (1514-1564)

De humani corporis fabrica libri septem (1543)

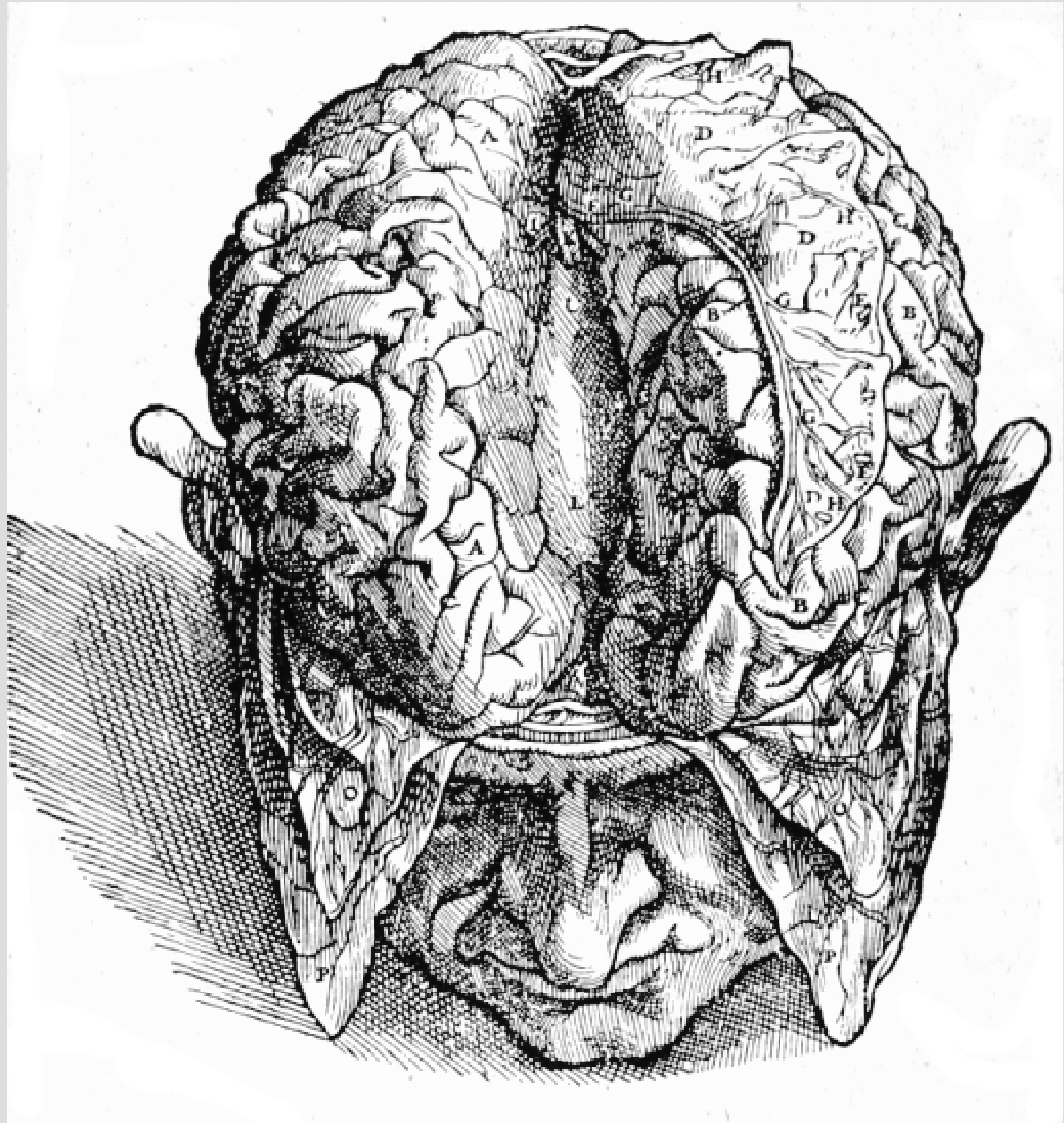

Localization of Function

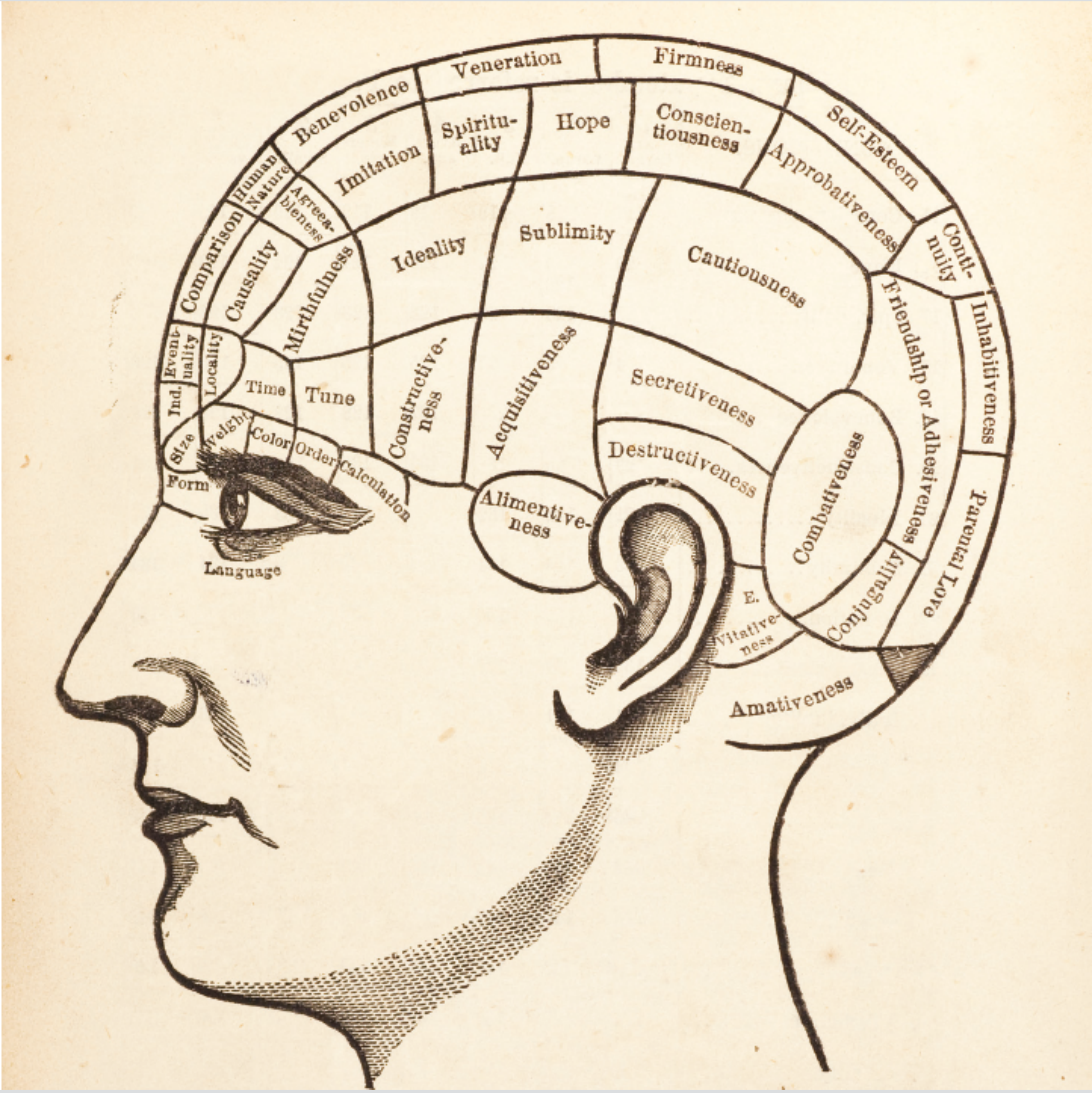

René Descartes (1595-1650)

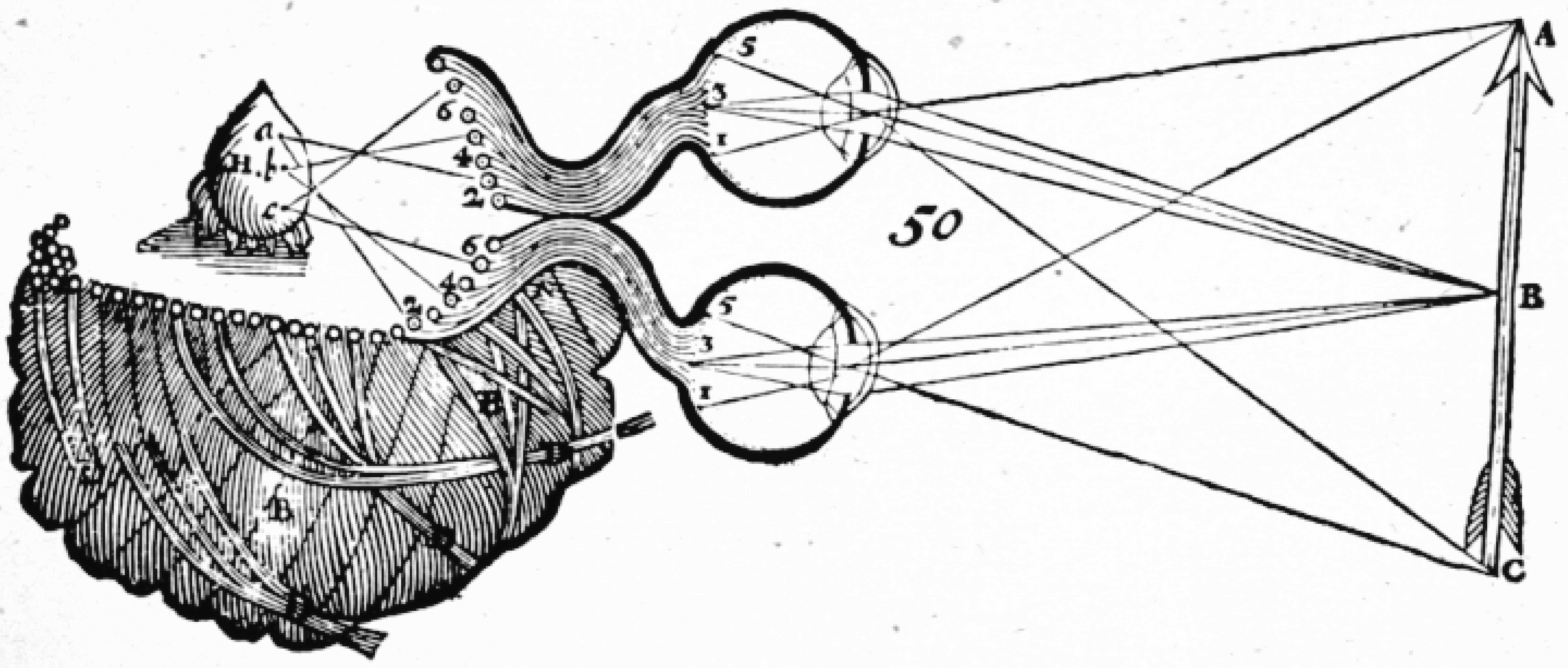

FIGURE 1 Descartes' diagram of the formation of images on the retinae of the eyes and the paths of transmission in the visual nervous system.

Visual Pathways, circa 1967

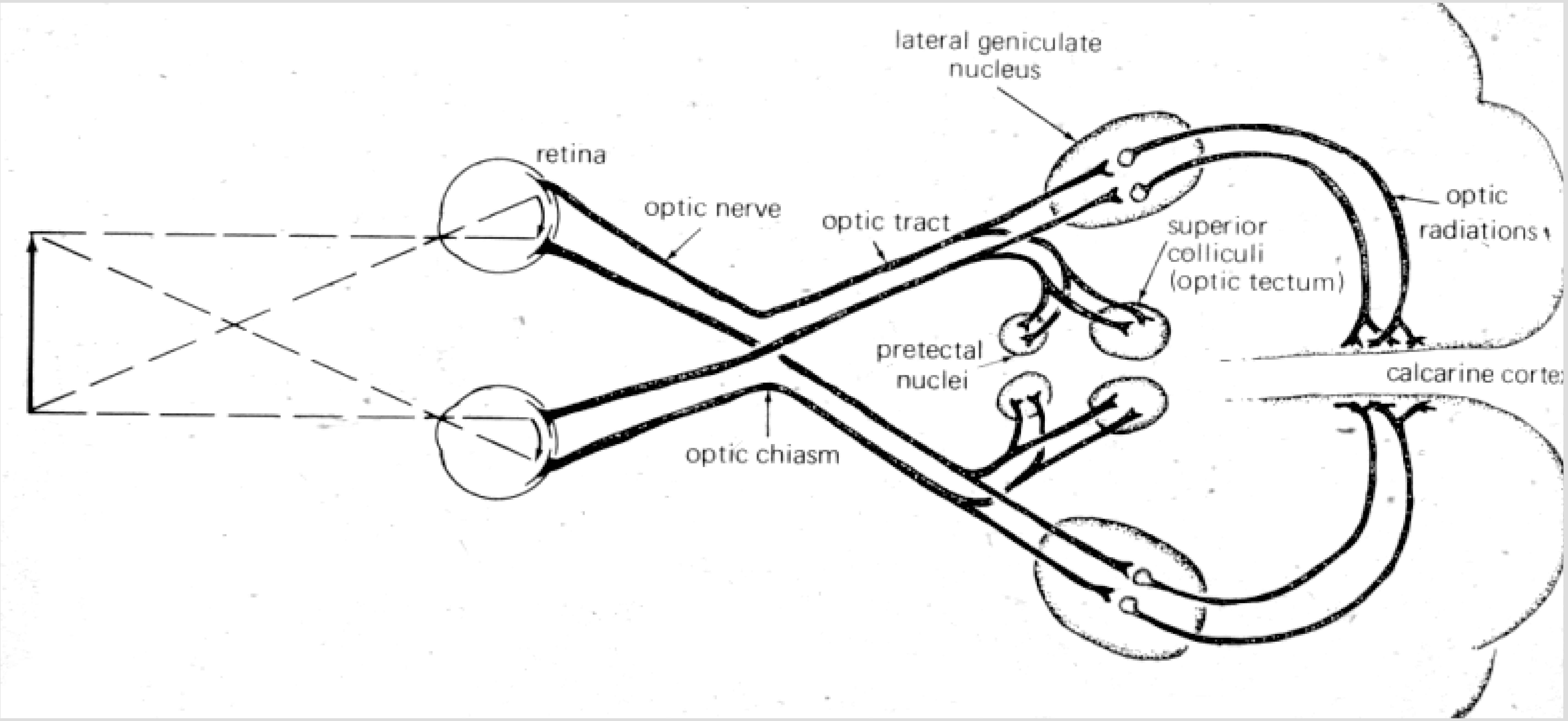

Visual Pathways, circa 1974

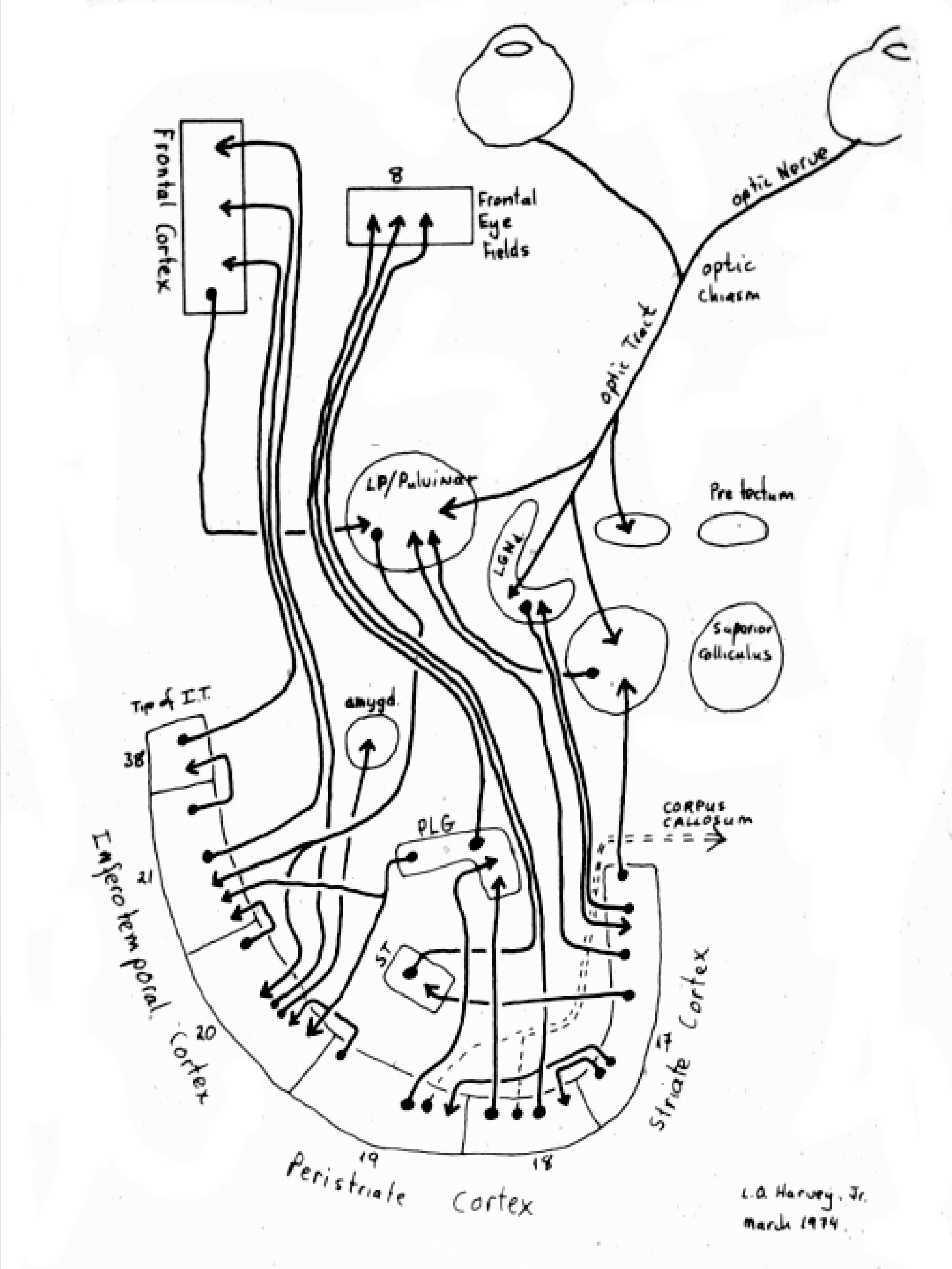

Visual Pathways, circa 1991

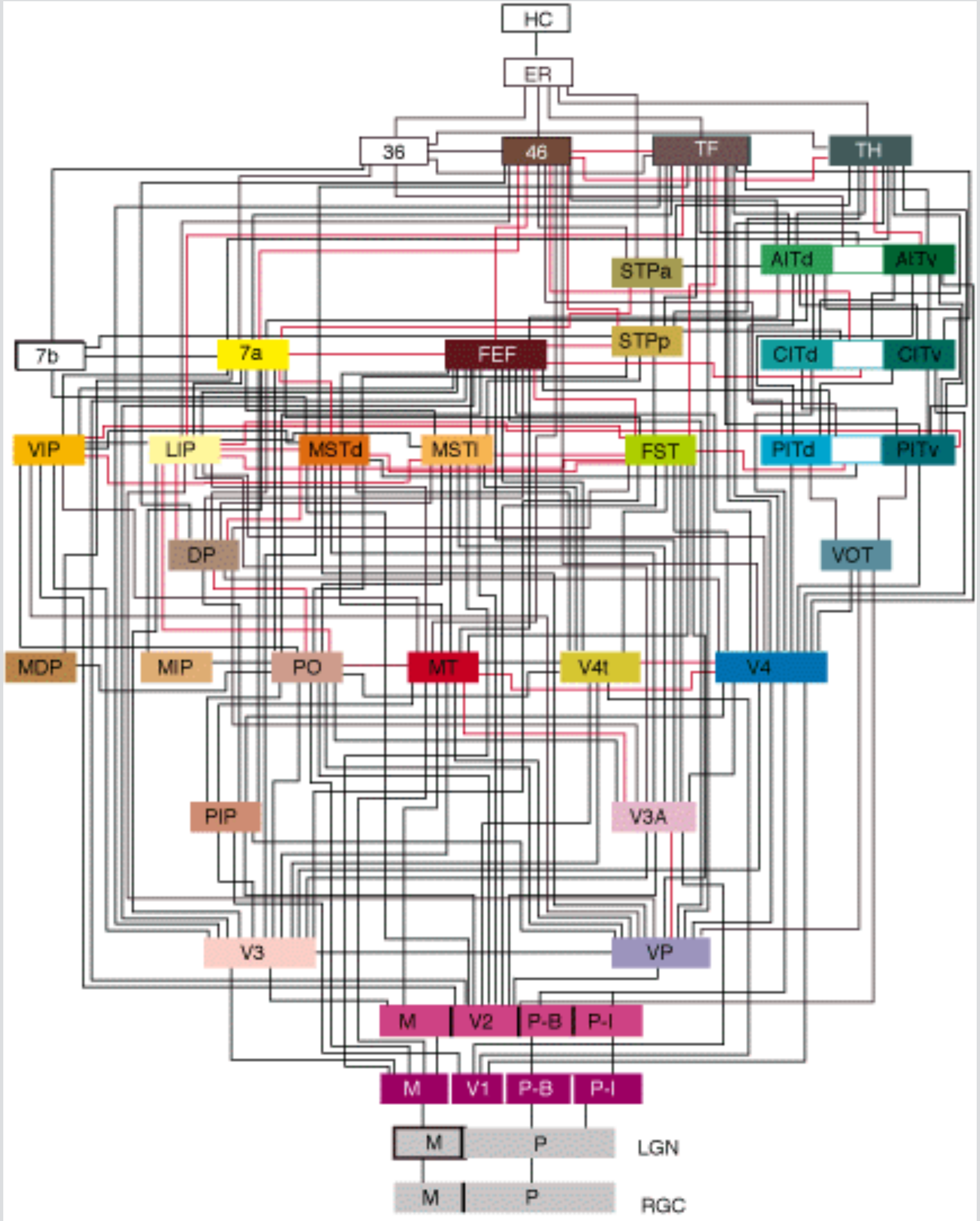

Felleman, D. J., & Van Essen, D. C. (1991). Distributed Hierarchical Processing in the Primate Cerebral Cortex. *Cerebral Cortex, 1*(1), 1-47. doi: 10.1093/cercor/1.1.1

Brain Networks, circa 2016
Lots of fluctuating activity in the normal brain

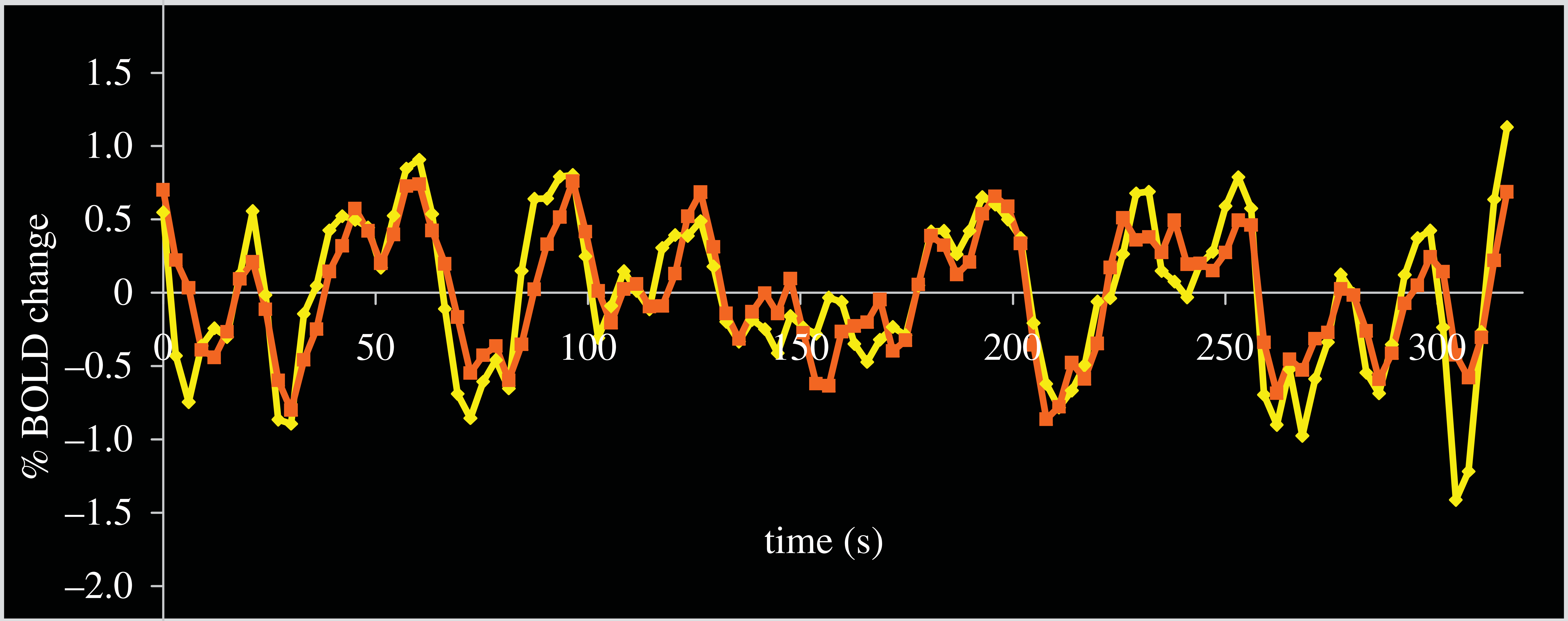

Raichle, M. E. (2015). The restless brain: how intrinsic activity organizes brain function. *Philosophical Transactions of the Royal Society of London B: Biological Sciences, 370*(1668).

Brain Networks, circa 2016
Default Mode Network (DMN)
Activity "At Rest"

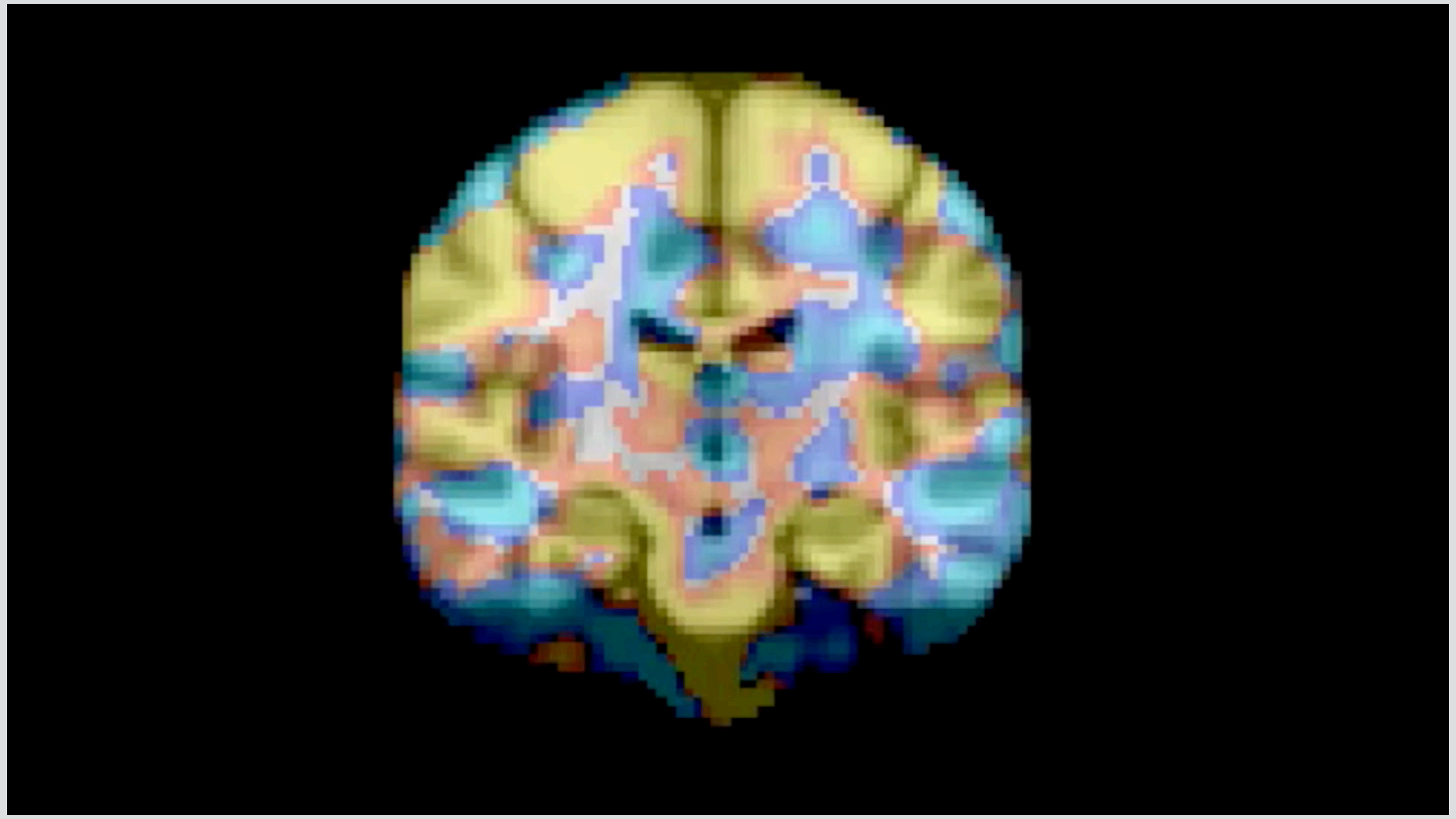

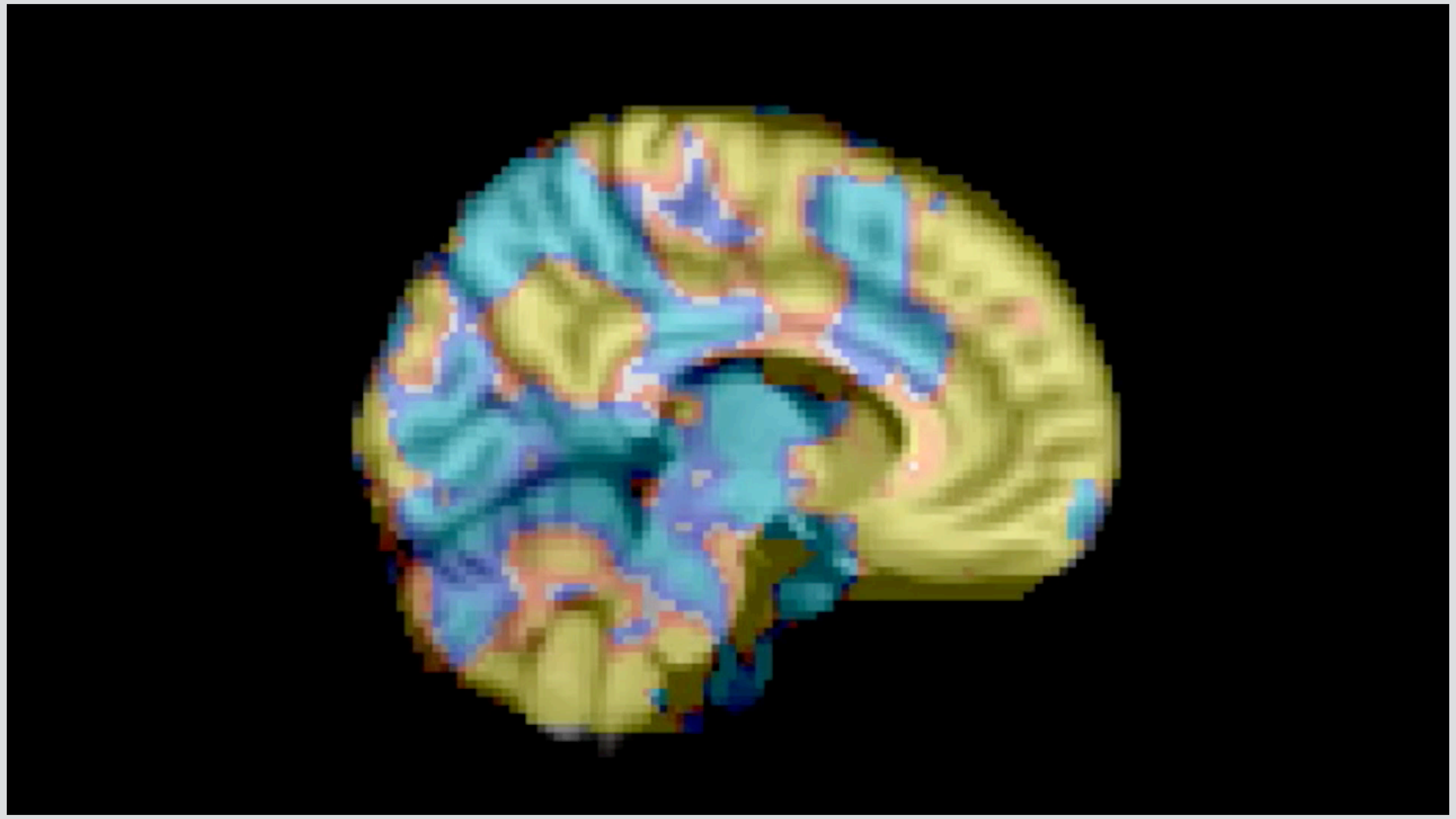

Videos created by Andrew E. Reineberg
Department of Psychology and Neuroscience
University of Colorado Boulder

Brain Networks, circa 2016
Default Mode Network (DMN)
Activity "At Rest"

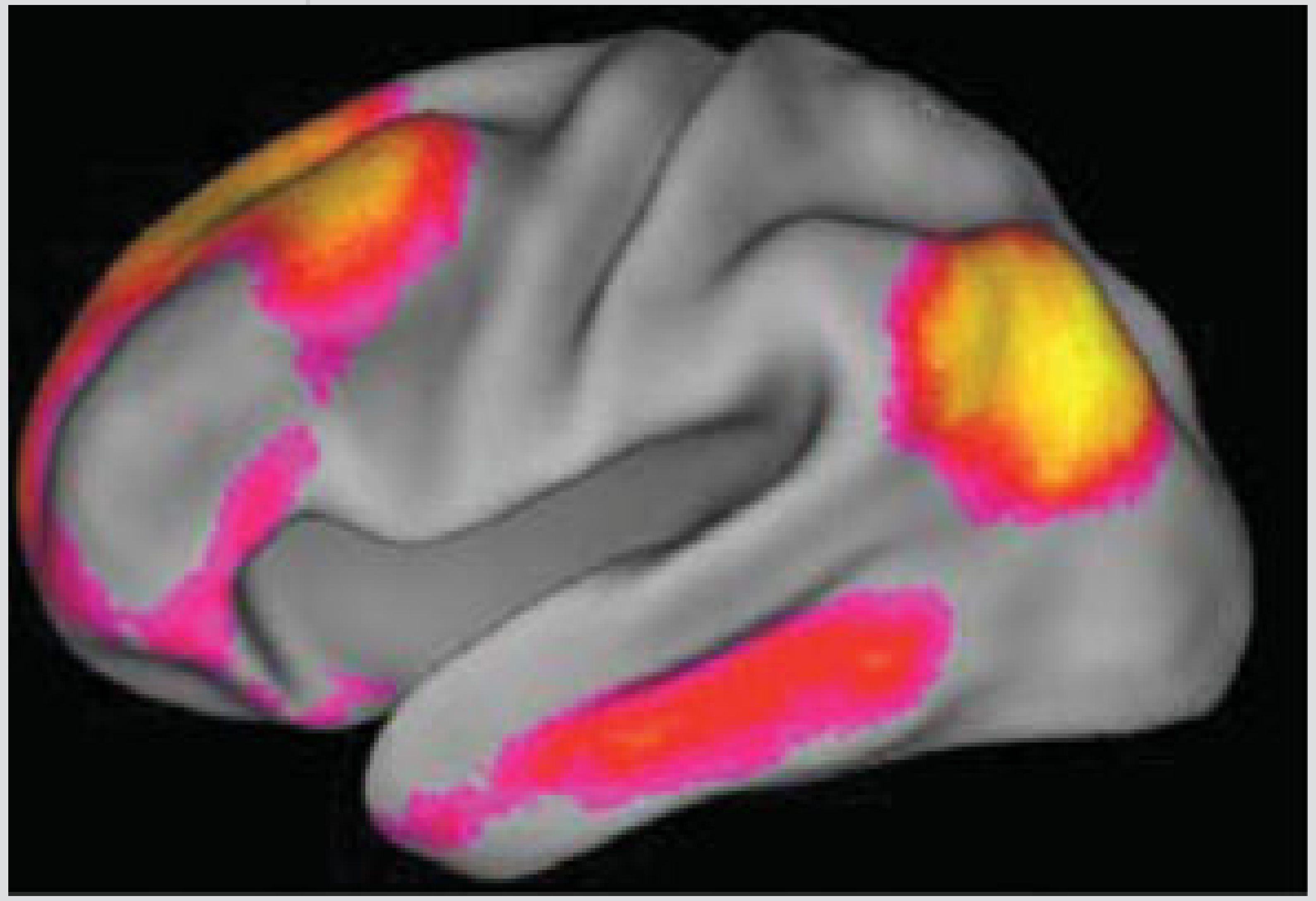

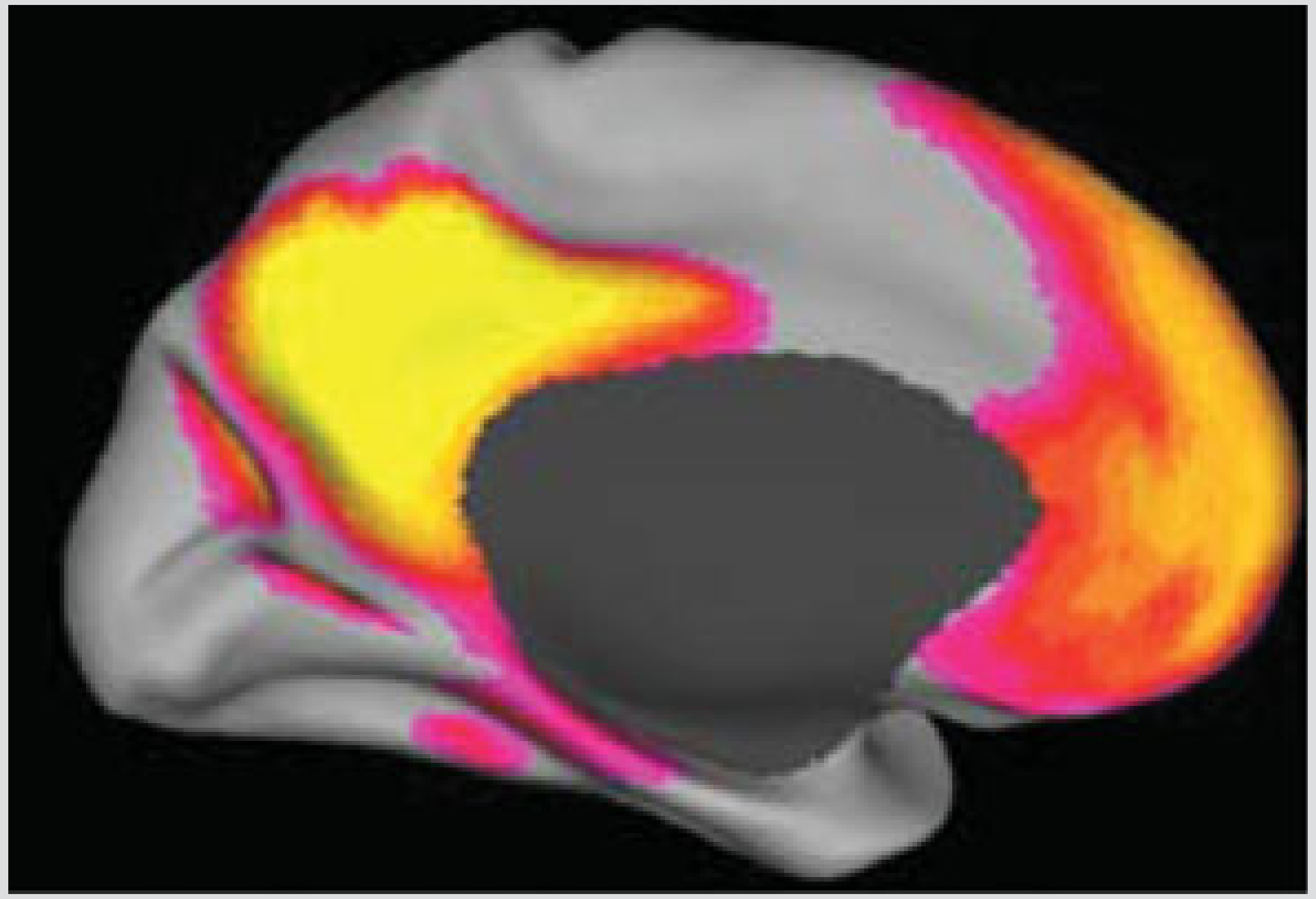

Raichle, M. E. (2015). The restless brain: how intrinsic activity organizes brain function. *Philosophical Transactions of the Royal Society of London B: Biological Sciences, 370*(1668).

Brain Networks, circa 2016
Default Mode Network (DMN)
Activity is Suppressed when Doing Tasks

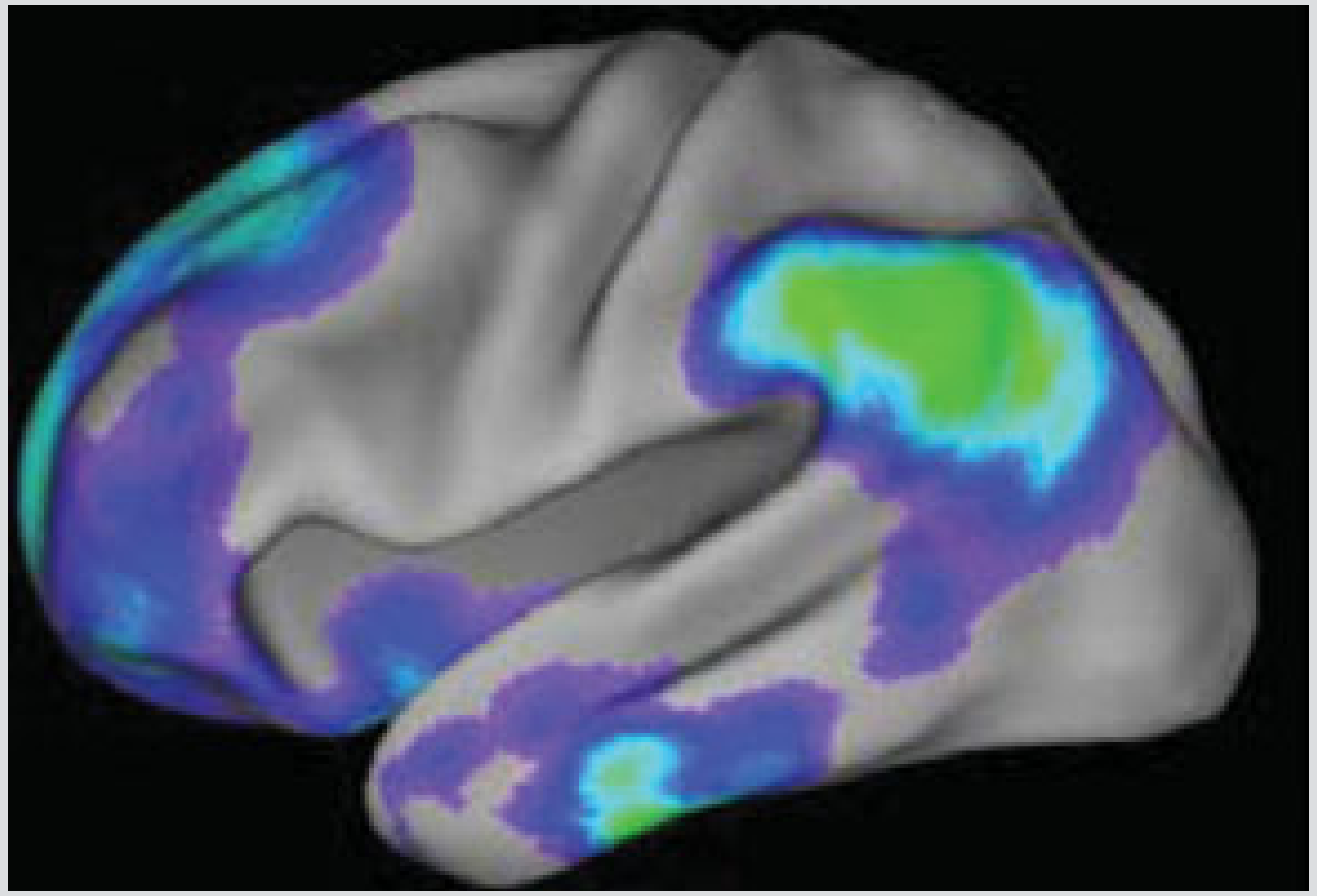

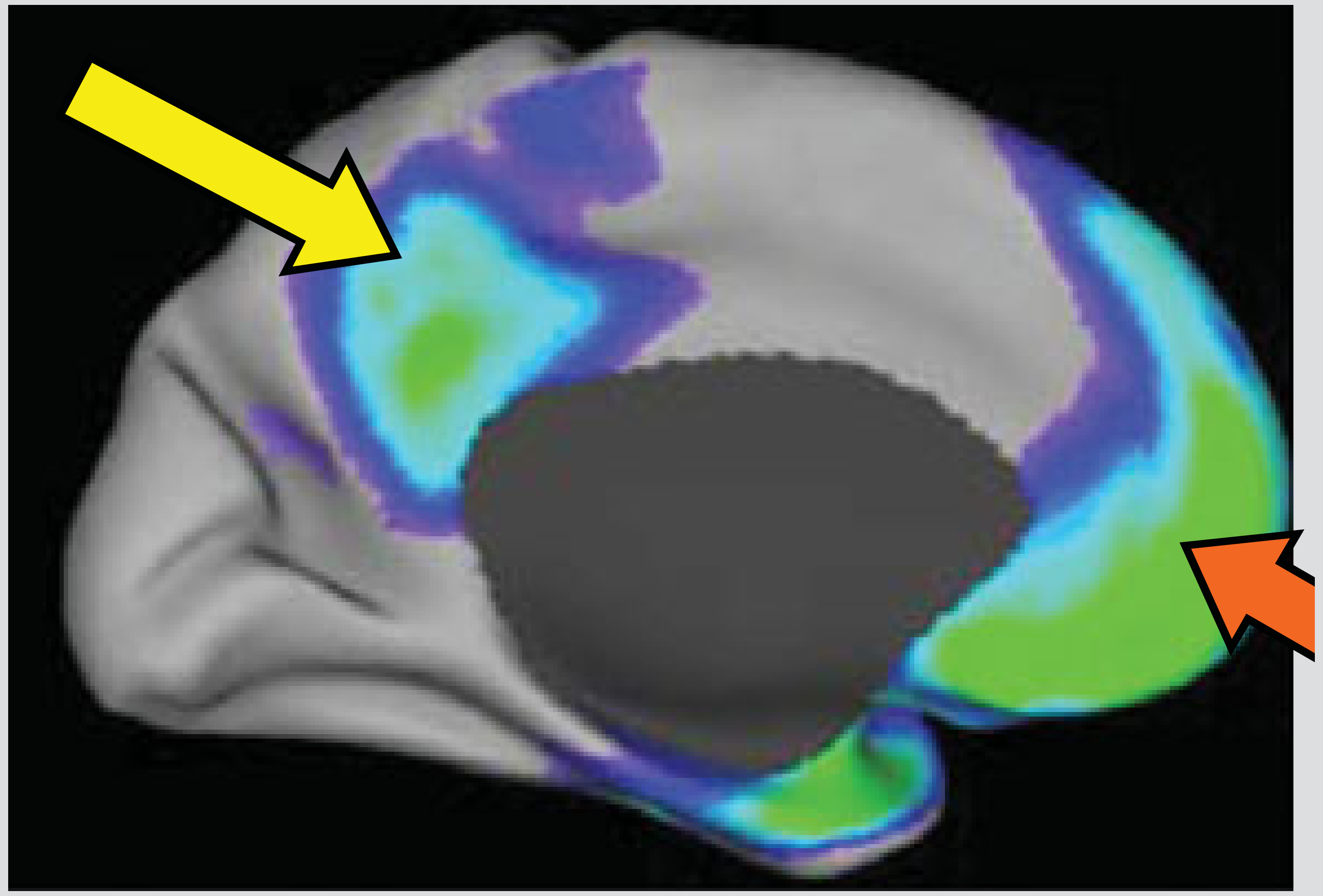

Raichle, M. E. (2015). The restless brain: how intrinsic activity organizes brain function. *Philosophical Transactions of the Royal Society of London B: Biological Sciences, 370*(1668).

Brain Networks, circa 2016
Multiple Networks

(*d*)

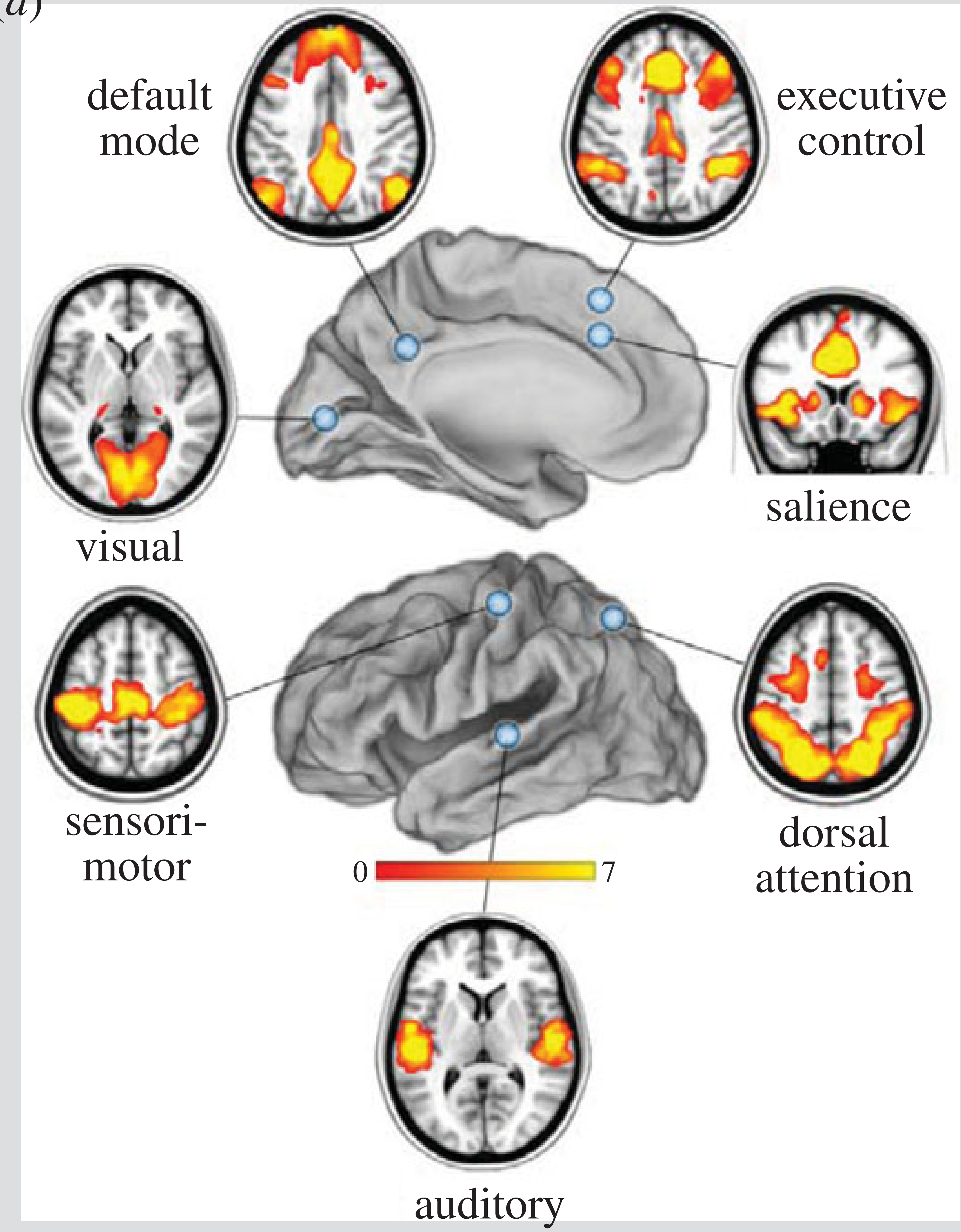

Raichle, M. E. (2015). The restless brain: how intrinsic activity organizes brain function. *Philosophical Transactions of the Royal Society of London B: Biological Sciences, 370*(1668).

Neural Organization

- Component Dominant
  - Modules
- Interaction Dominant
  - Emergent Properties

Interaction Organization

Huth, A. G., de Heer, W. A., Griffiths, T. L., Theunissen, F. E., & Gallant, J. L. (2016). Natural speech reveals the semantic maps that tile human cerebral cortex. *Nature, 532*(7600), 453-458.

http://gallantlab.org/huth2016/

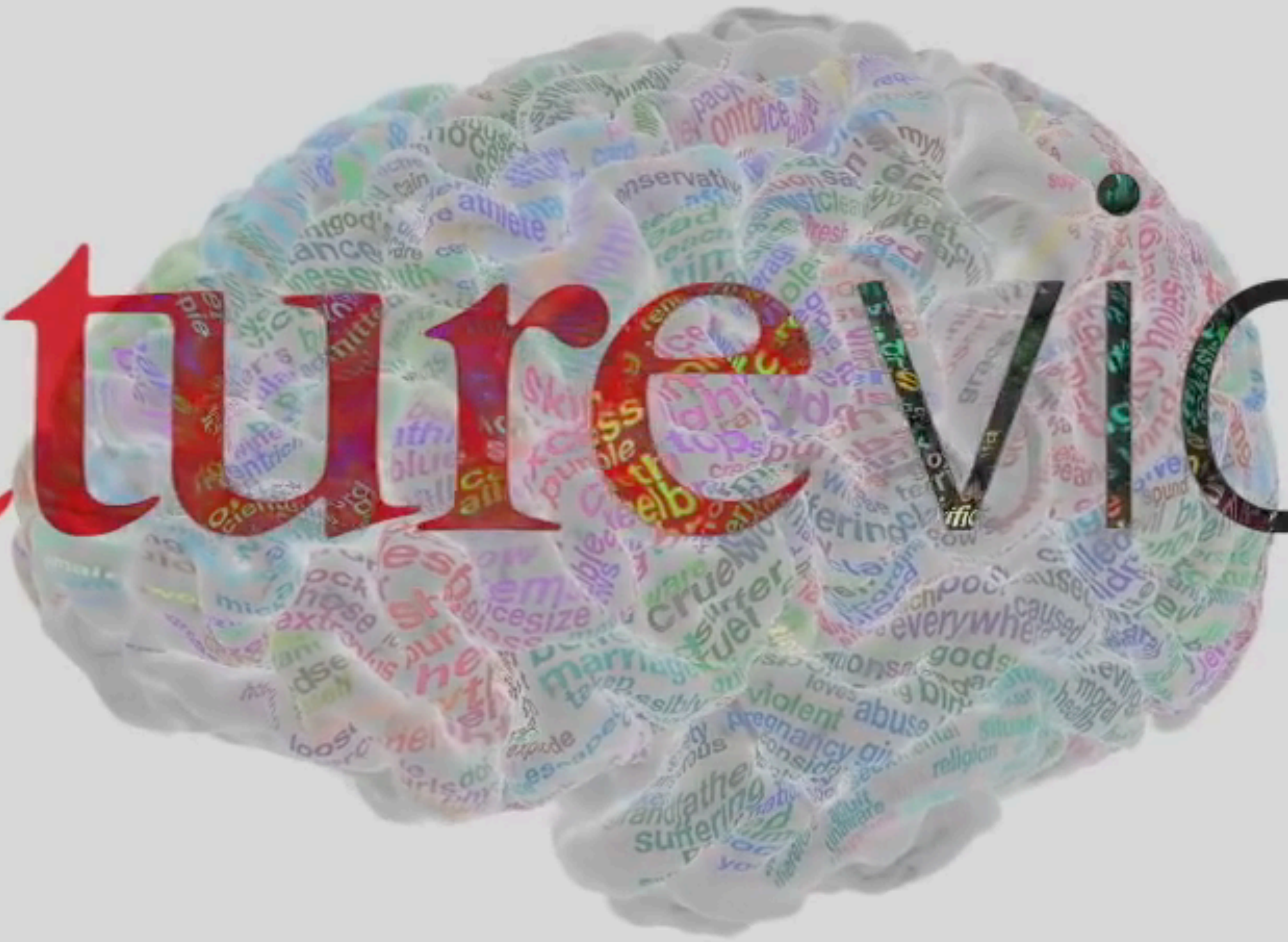
nature video

Retinotopic Mapping

- Retina to LGN to Cortex
- Nonlinear
- Cortical Magnification Factor: M = mmCortex / mmRetina
- M = Around 11-13 in Fovea

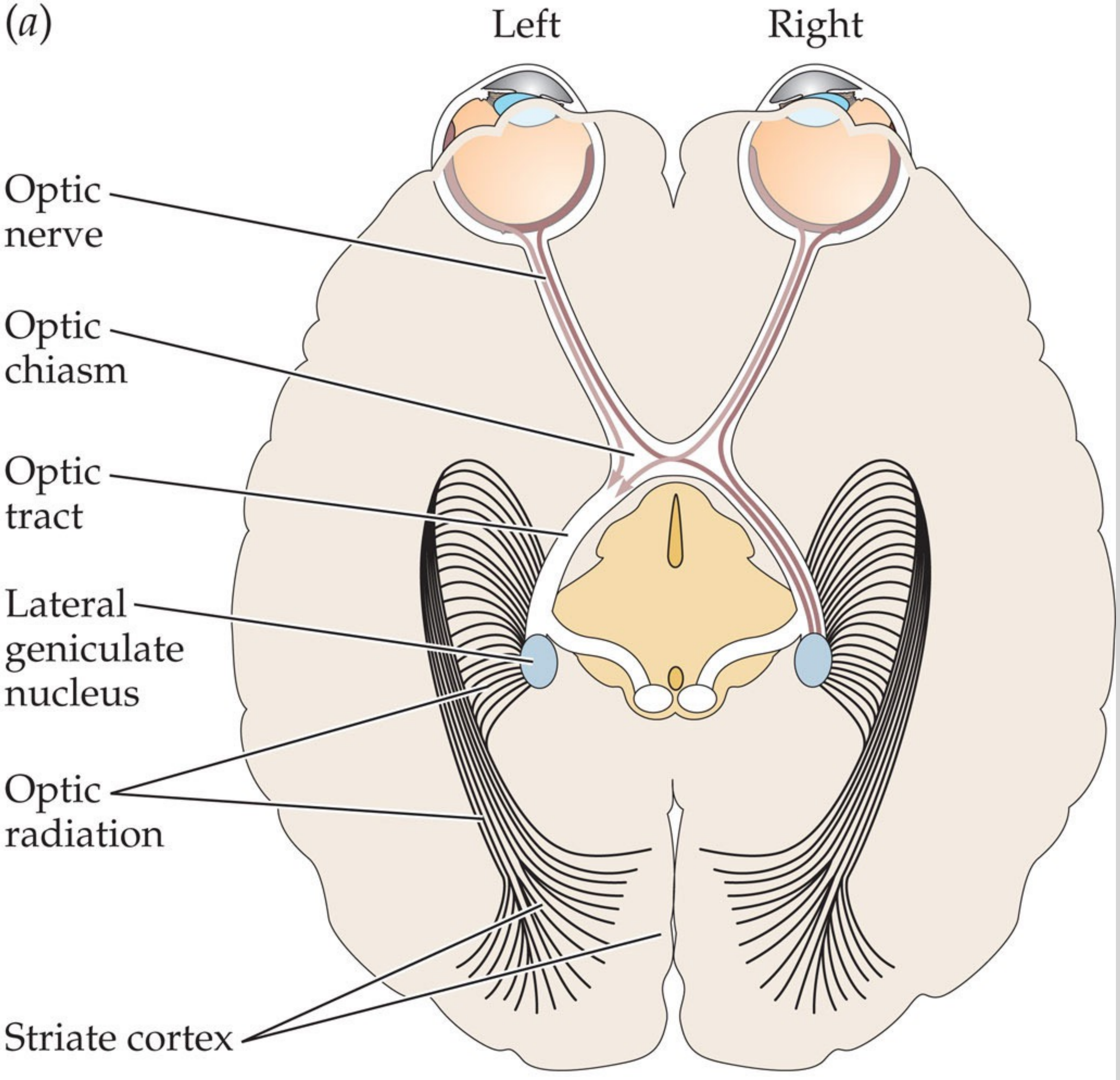

SENSATION & PERCEPTION 4e, **Figure 3.1 (Part 1)**

Lateral Geniculate Nucleus

- Parvocellular
- Magnocellular
- Koniocellular

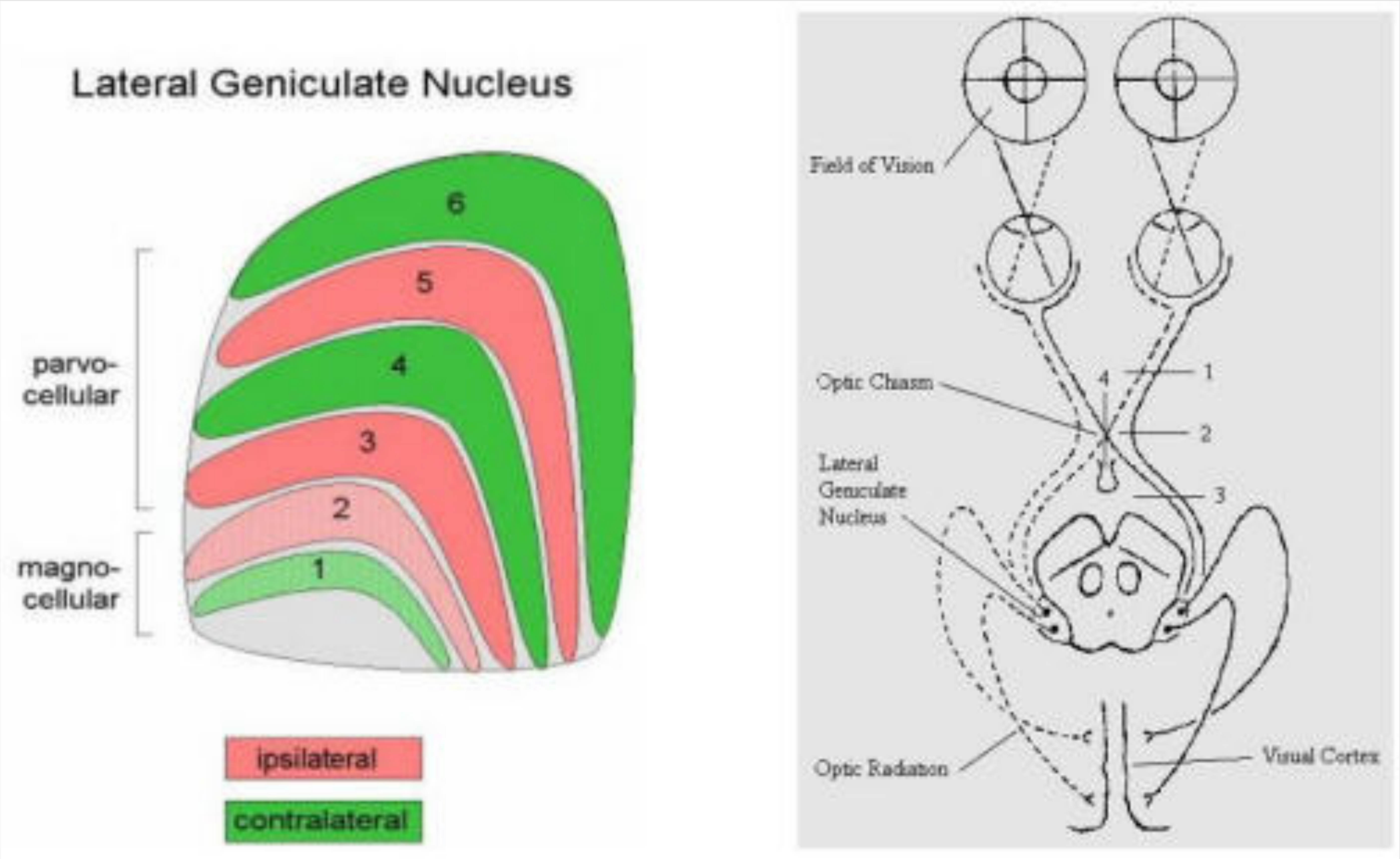

Lateral Geniculate Nucleus

- Parvocellular
  - high spatial resolution
  - color vision
- Magnocellular
  - low spatial resolution
  - high temporal res.
- Koniocellular
  - high spatial resolution
  - color vision

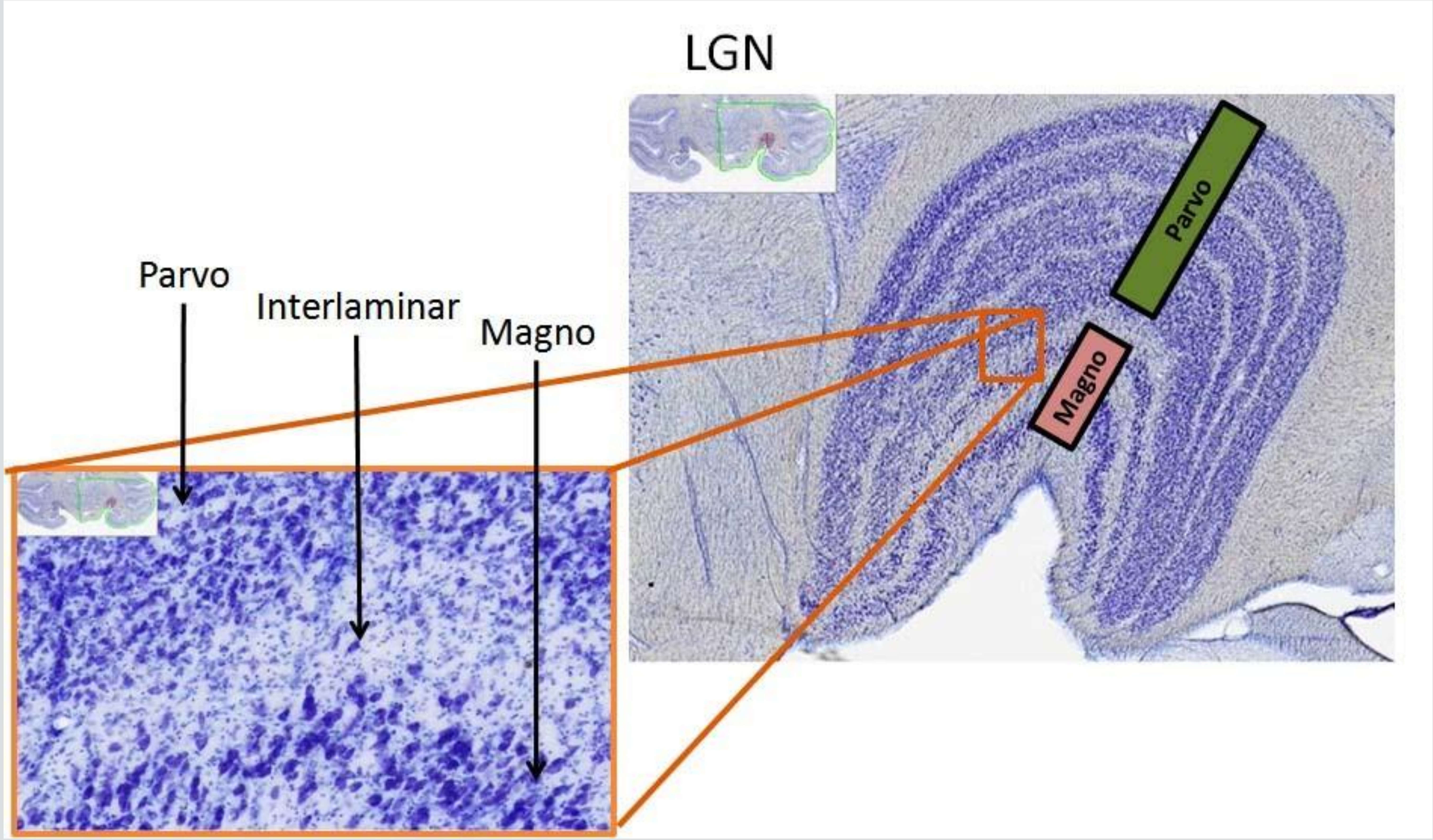

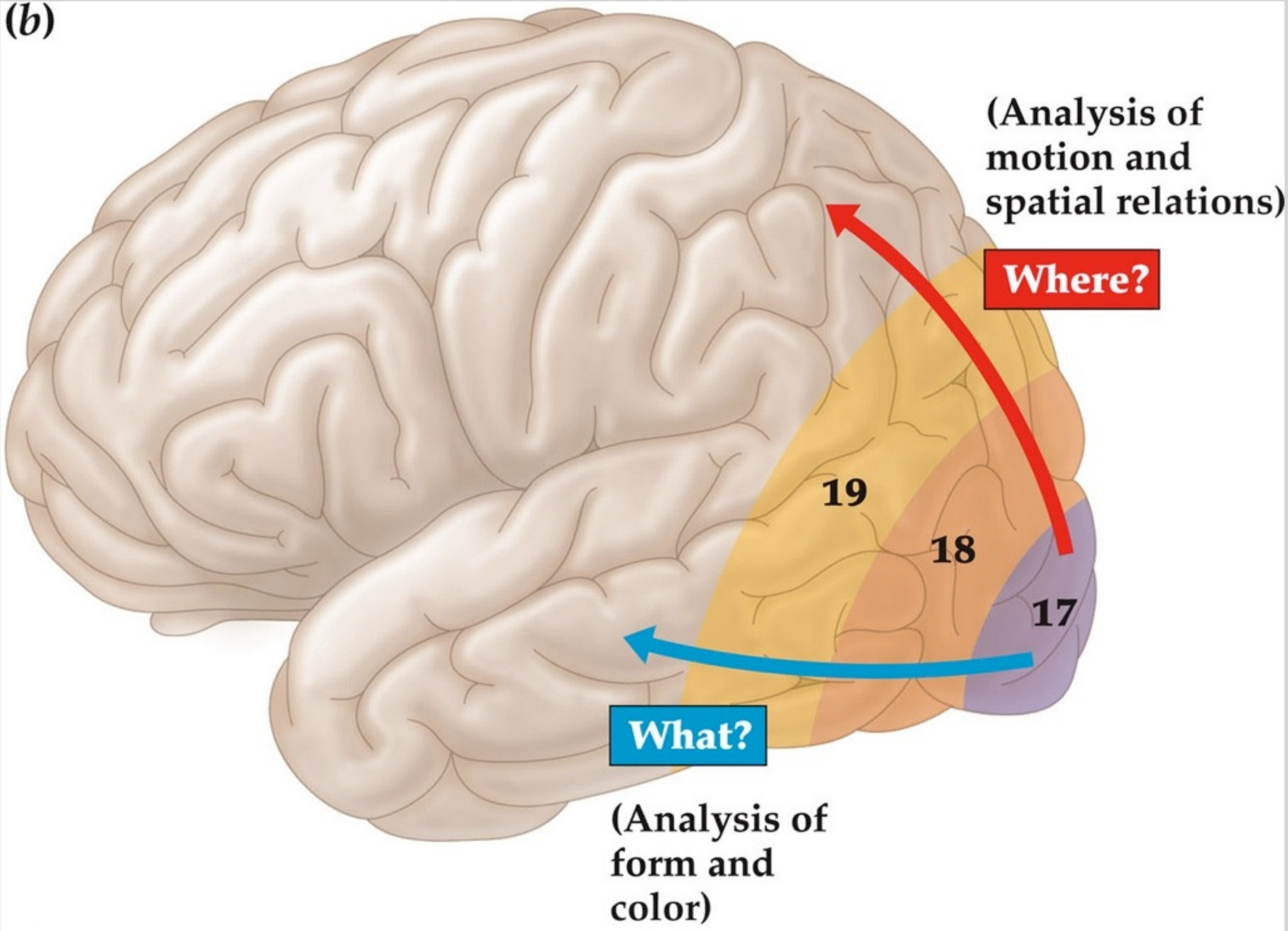

SENSATION & PERCEPTION 3e, Figure 3.1 (Part 2)

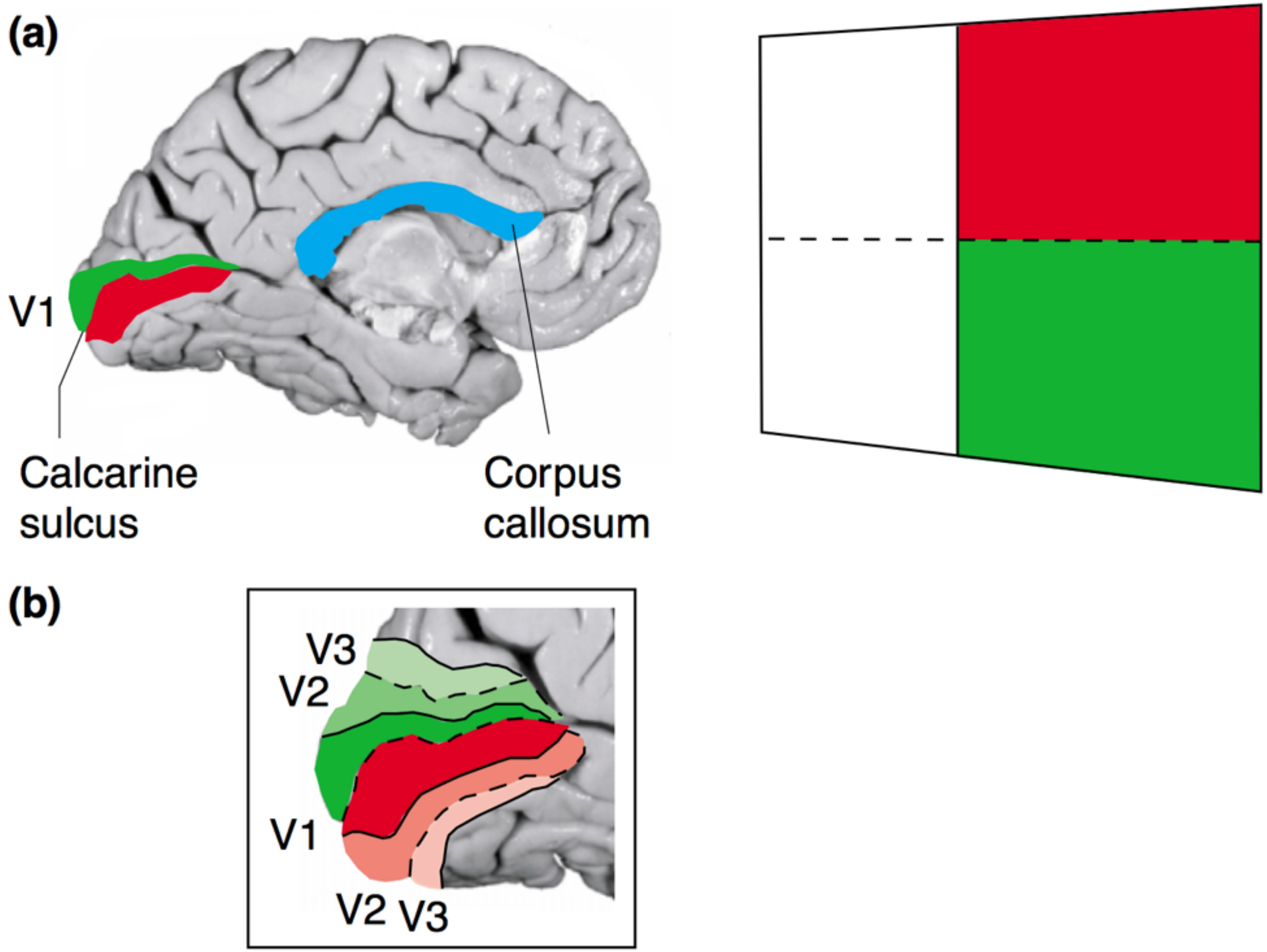
(a)
V1
Calcarine sulcus
Corpus callosum
(b)
V3
V2
V1
V2
V3

Topographical Mapping

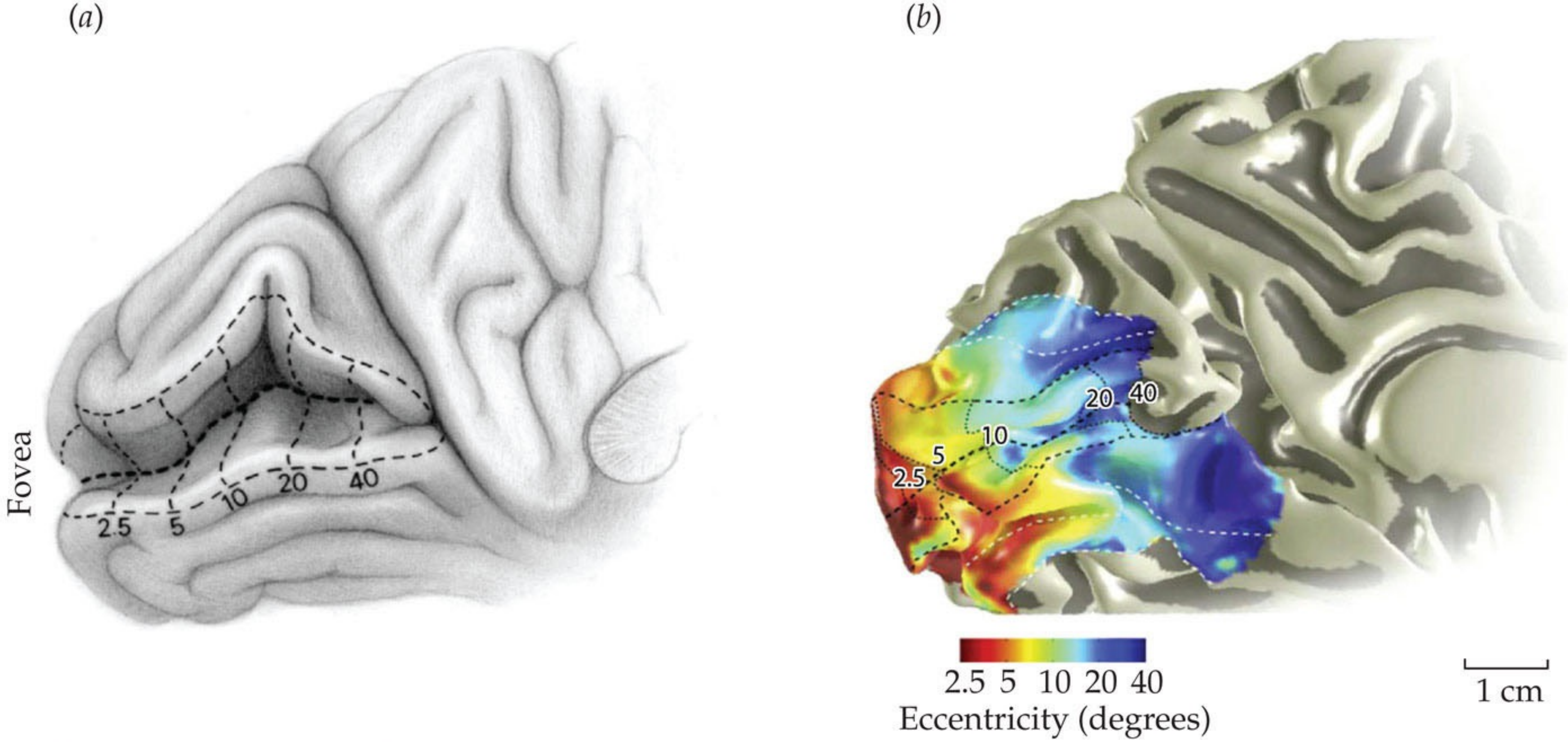

***SENSATION & PERCEPTION 4e*, Figure 3.17**

Functional Significance

- Selective Damage
- Complex Logarithmic Mapping
- Orientation vs Spatial Frequency

Binocular Visual Field

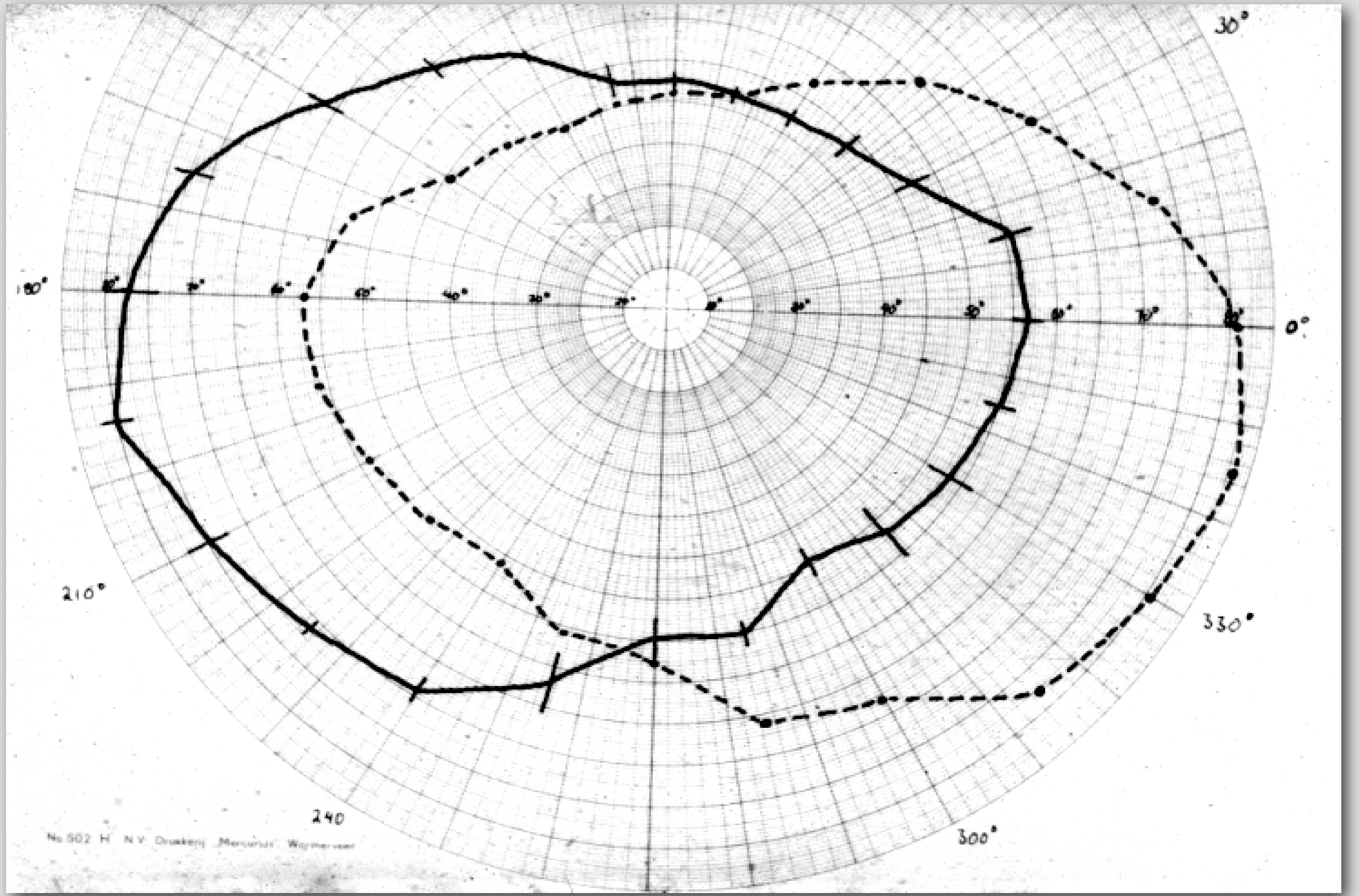

Scotomata

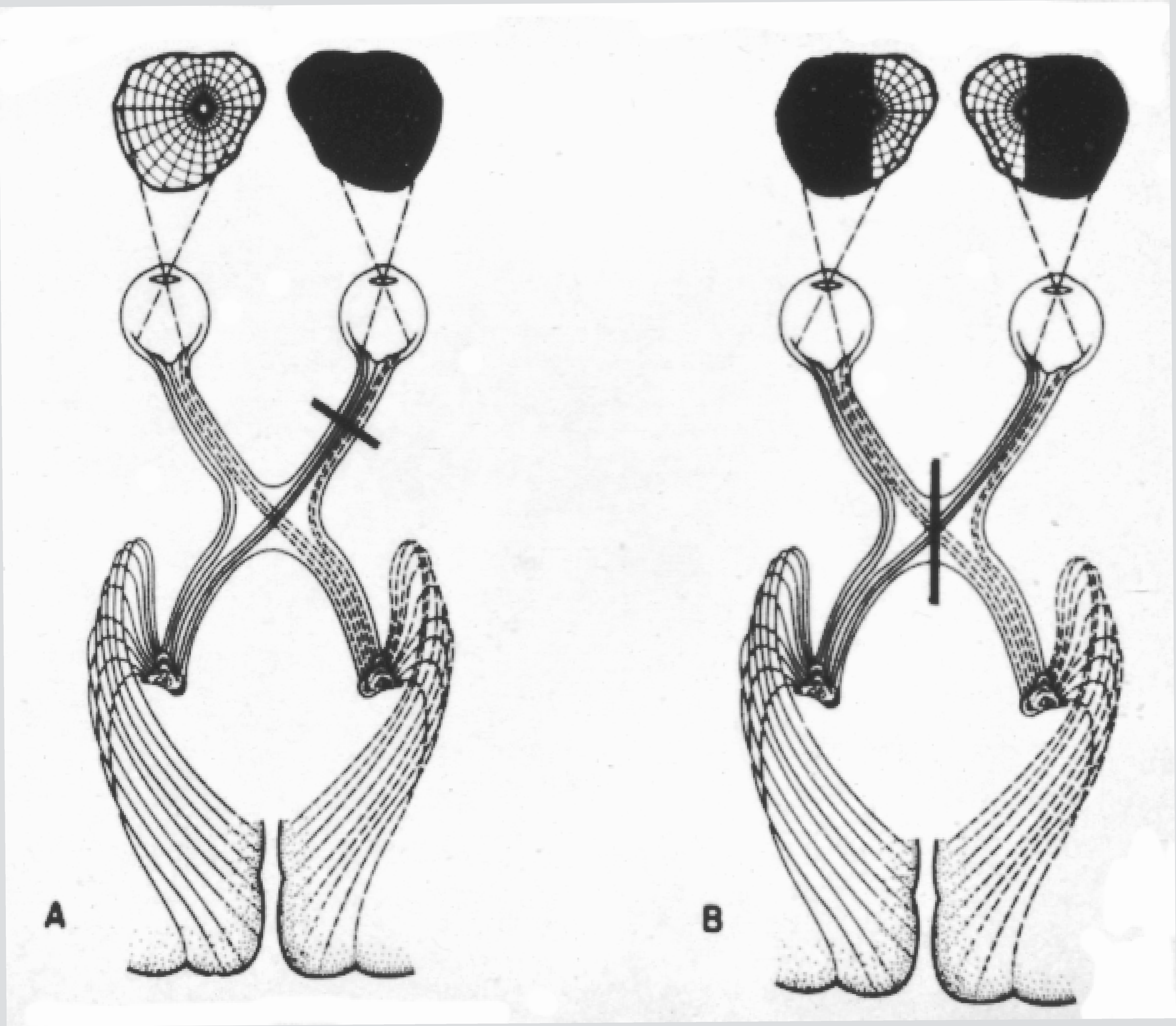

Scotomata

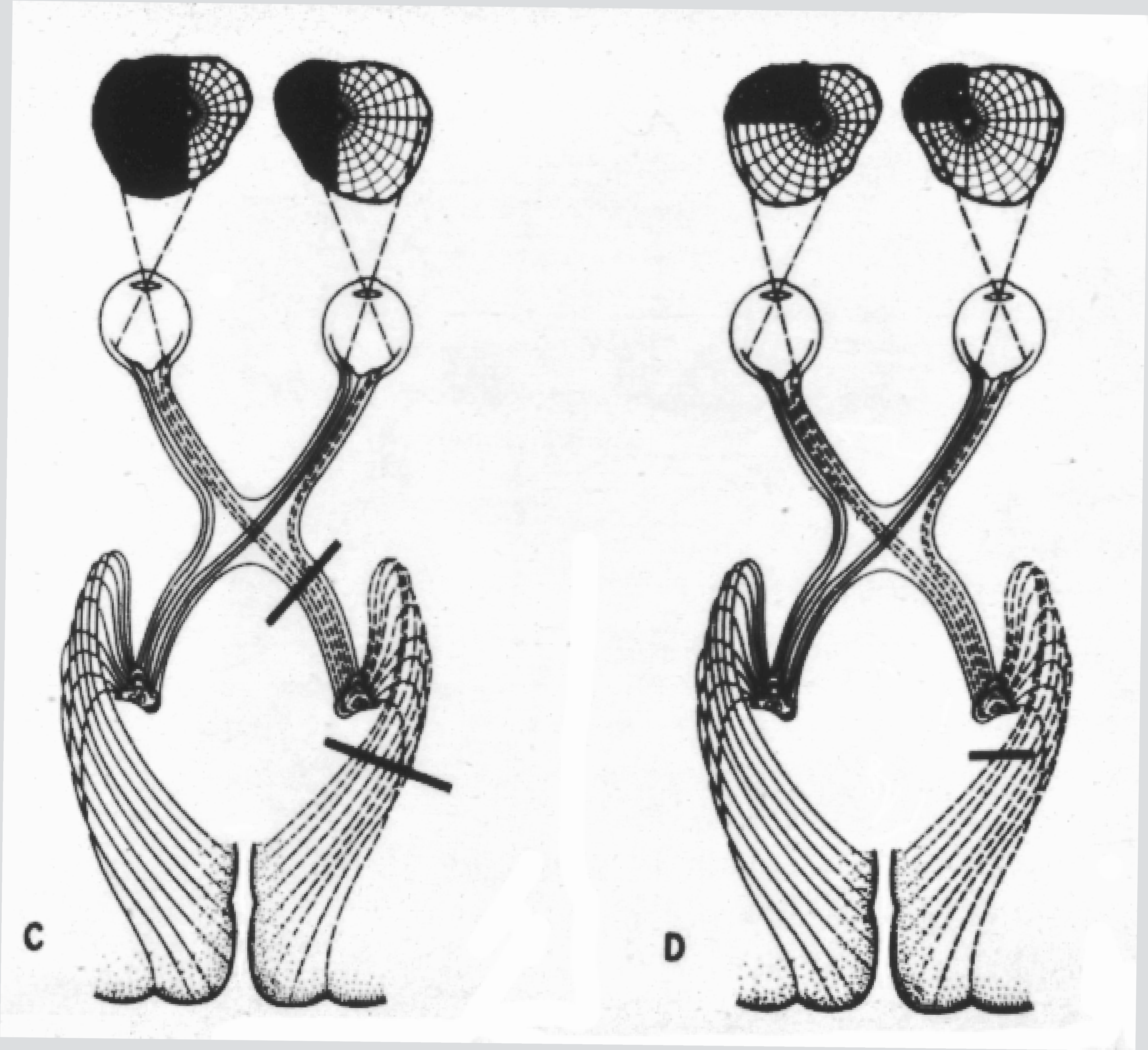

Visual Field Scotoma: A-178

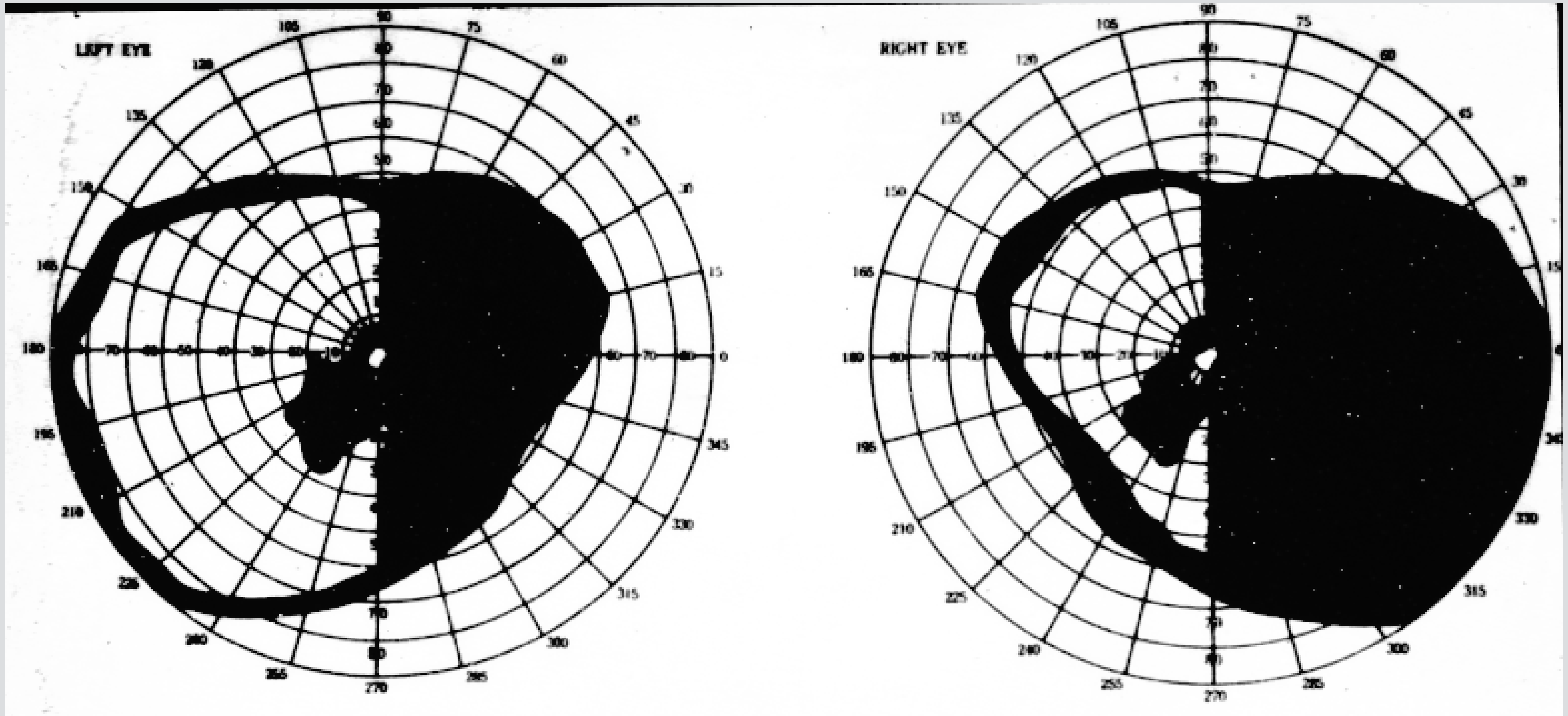

Figure 19a. Case A-178. Right homonymous hemianopia, with irregular defect extending into homonymous left lower quadrants, and arc-shaped defect surrounding the central part of the field. These field defects resulted from a rifle bullet which entered the left midparietal region and traversed the posterior brain substance, making its exit in the right occipital region, 1 cm. to the right of the occipital protuberance.

Visual Field Scotoma: A-178

Visual Field Scotoma: A-178

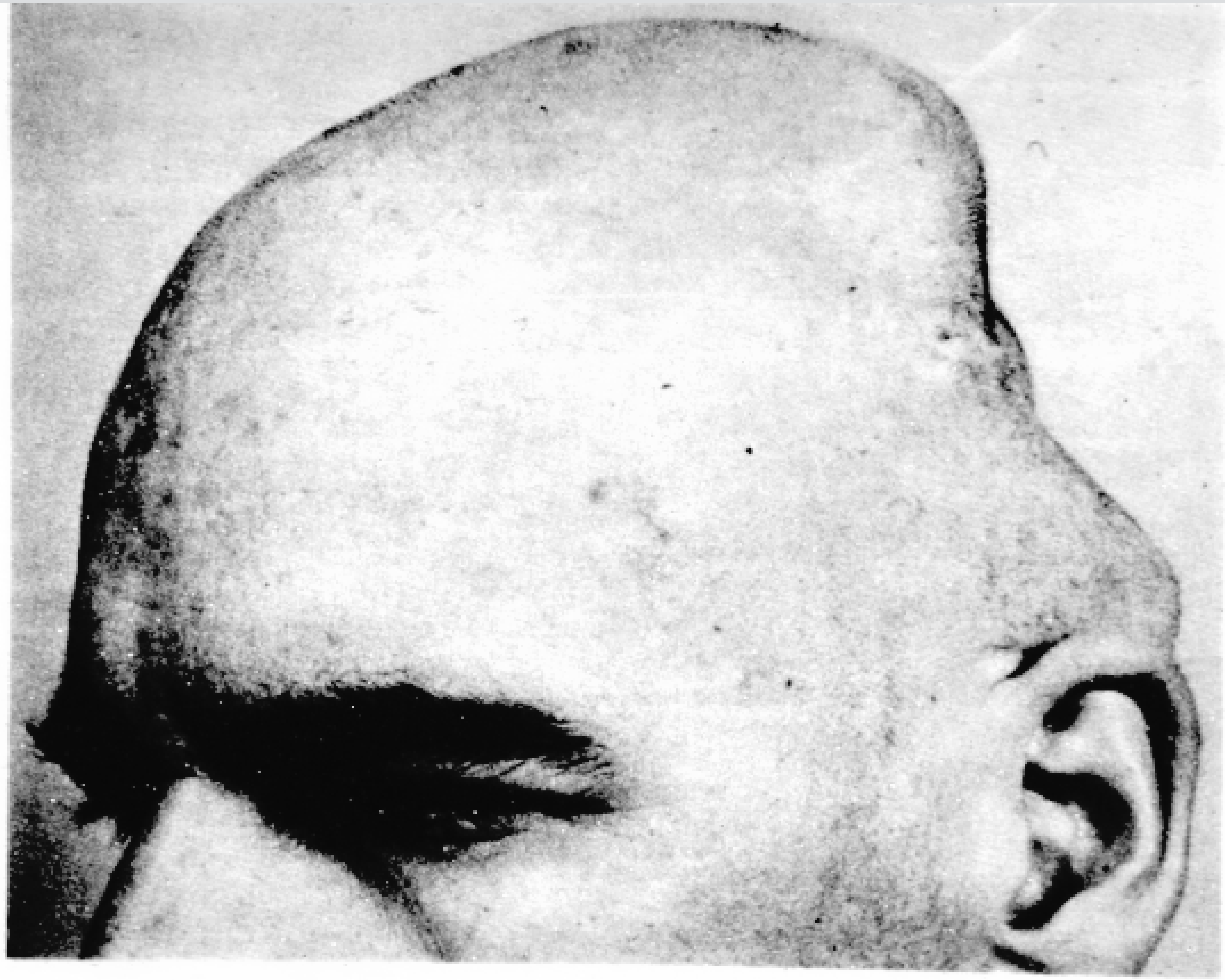

Figures 19b–d. Appearance of the head (case A-178), following surgical removal of fragments from the left midparietal region and the right and left occipital areas.

Visual Field Scotoma: A-67

Homonymous Hemianopia: A-67

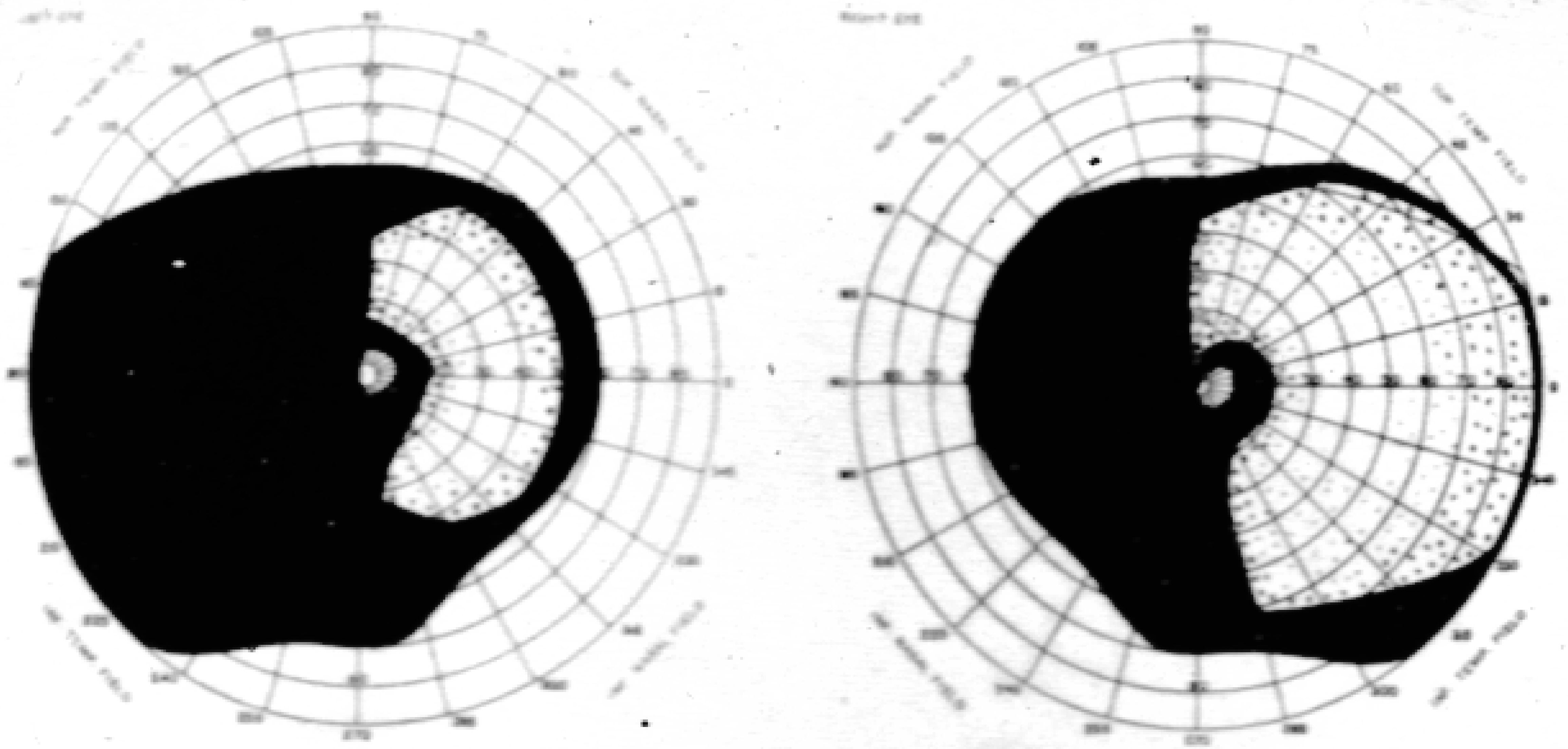

Figure 16a. Case A-67. Left homonymous hemianopia combined with arc-shaped defect forming a half-ring surrounding the right homonymous half of the macular region. This patient was injured by a rifle bullet penetrating the occiput. In the right half-field outside the crescent, fluctuation of targets was marked and stationary targets disappeared within 2–3 sec. Fusion thresholds for flickering light were markedly reduced in the foveal region (i.e., within the arc), and even more so in the right peripheral fields. Apparent movement was reported by this patient when one stationary target was placed inside and another outside the arc-shaped scotoma, and the two targets were illuminated in alternation (see text, pp. 84–86). Snellen acuity: OS 20/100, OD 20/70.

Foveal Sparing: A-29

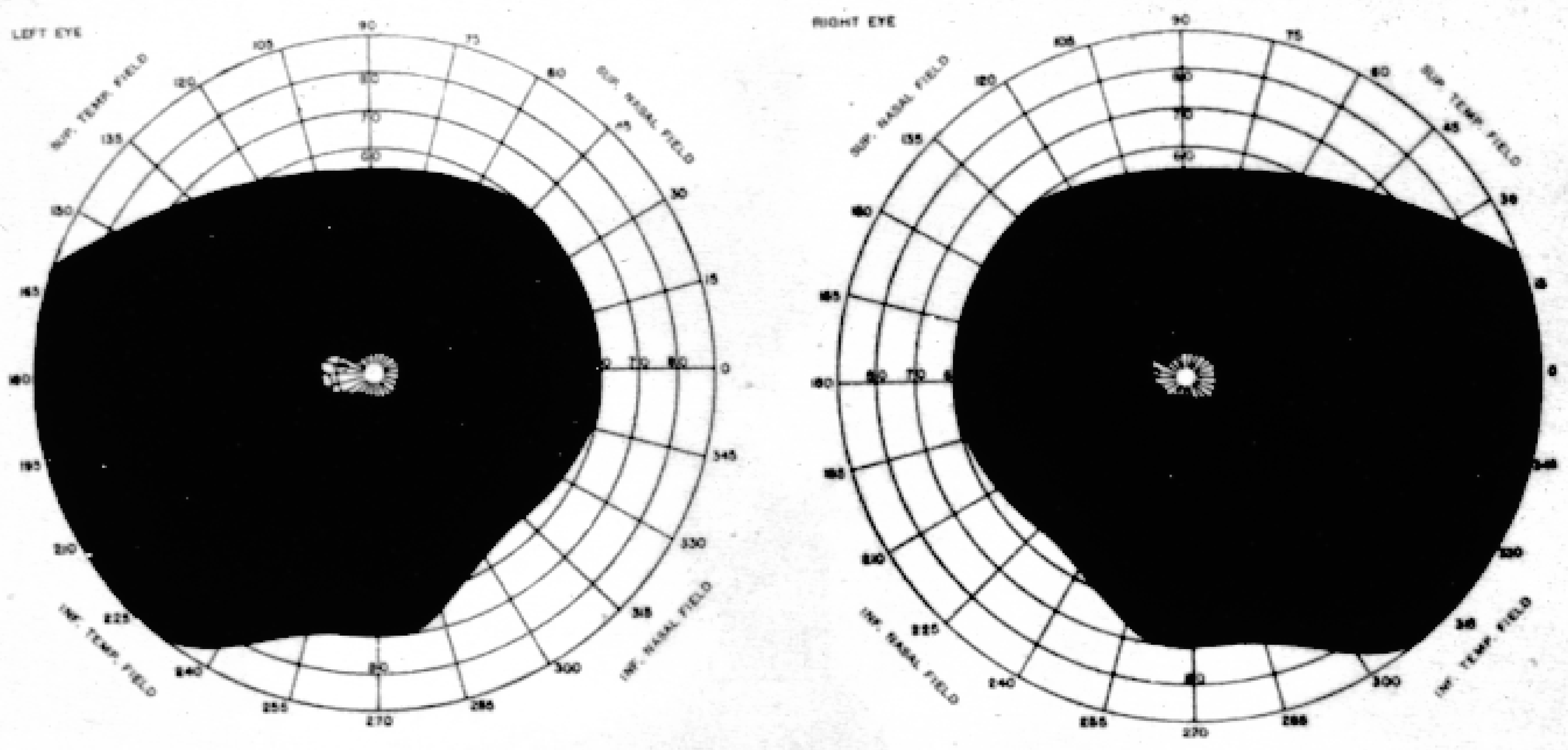

Figure 13a. Case A-29. Extreme instance of concentric contraction, resulting in bilateral hemianopia with irregular macular sparing (peephole vision). Areas in black were blind for hand motion on the perimeter. This unusual type of field defect was the result of a through-and-through bullet wound of the head entering 1 cm. above the pinna of the left ear and making its exit in the right occipital region about 2 cm. above the protuberance and 3 cm. lateral to it.

Hemidecussation of the Retina

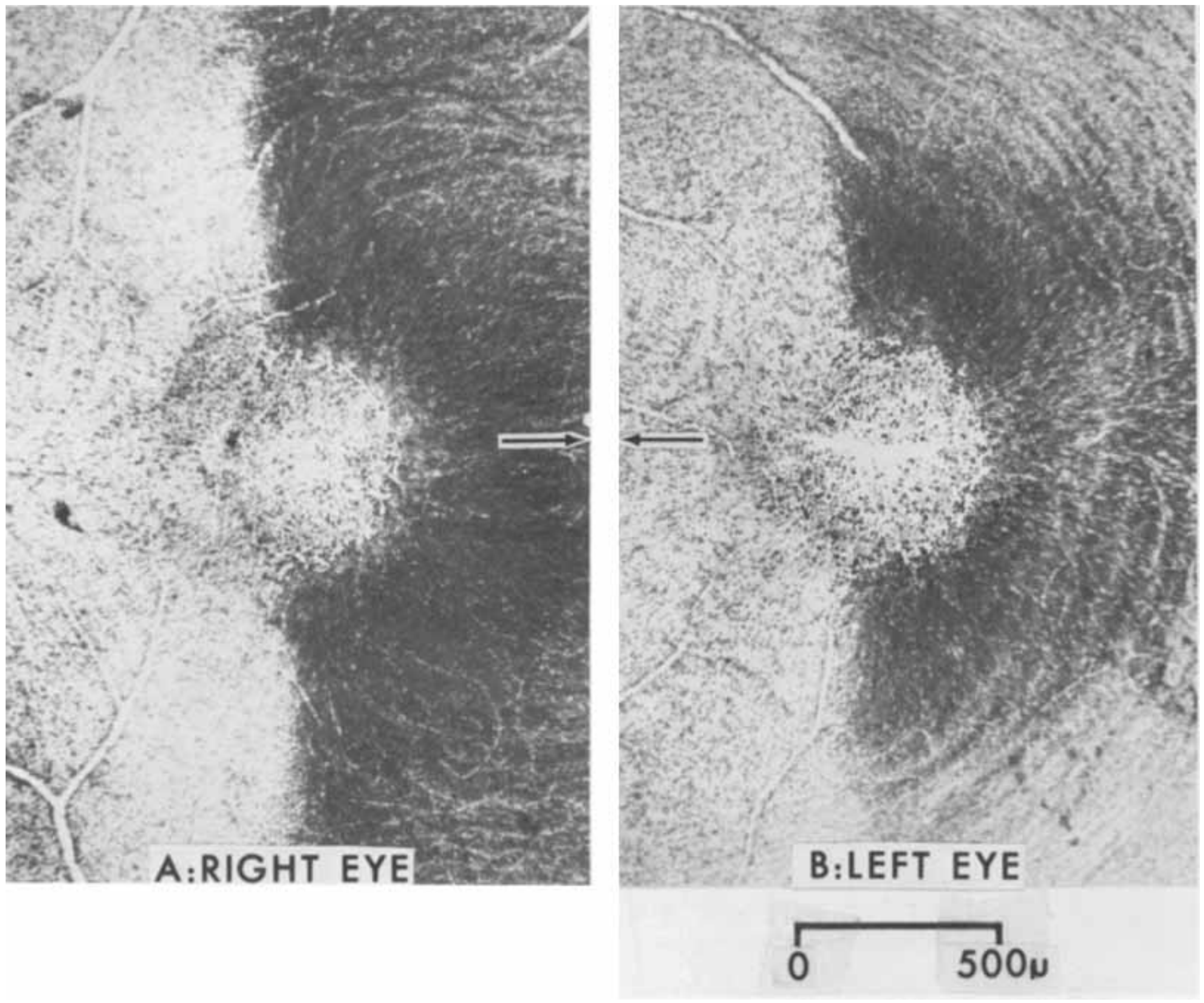

Figs. 4A,B Foveal regions of the retinas of figure 3A,B respectively, at higher magnification. In each retina the arrow points to the optic disc.

Stone, J., Leicester, J., & Sherman, S. M. (1973). The naso-temporal division of the monkey's retina. *Journal of Comparative Neurology, 150*(3), 333-348. doi:10.1002/cne.901500306

Hemidecussation of the Retina

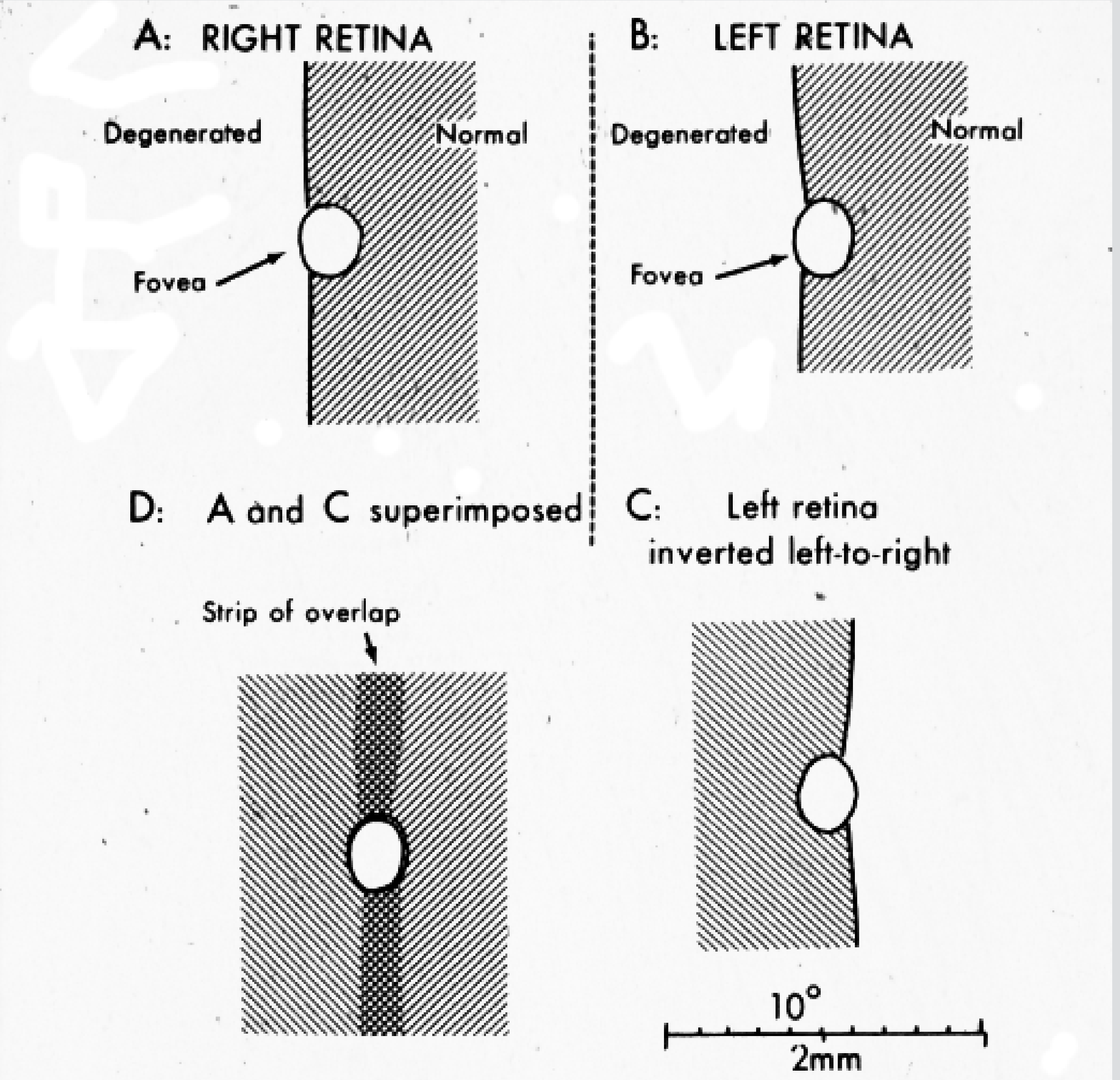

Fig. 8 A: Schematic drawing of the foveal region of the right retina in figure 3A. The outline of the foveola is drawn in and the areas lacking and containing ganglion cells are open and hatched, respectively. The border between these two areas is marked as a line. B: Analogous drawing for the left retina of the same animal. C: The drawing in B reversed left-to-right. D: A and C superimposed. The outlines of the foveolae are matched as closely as possible and the lines are made as close to parallel as possible. This figure gives an estimate of the strip of overlap, marked here with double hatching.

Stone, J., Leicester, J., & Sherman, S. M. (1973). The naso-temporal division of the monkey's retina. *Journal of Comparative Neurology, 150*(3), 333-348. doi:10.1002/cne.901500306

Measuring Left & Right RT

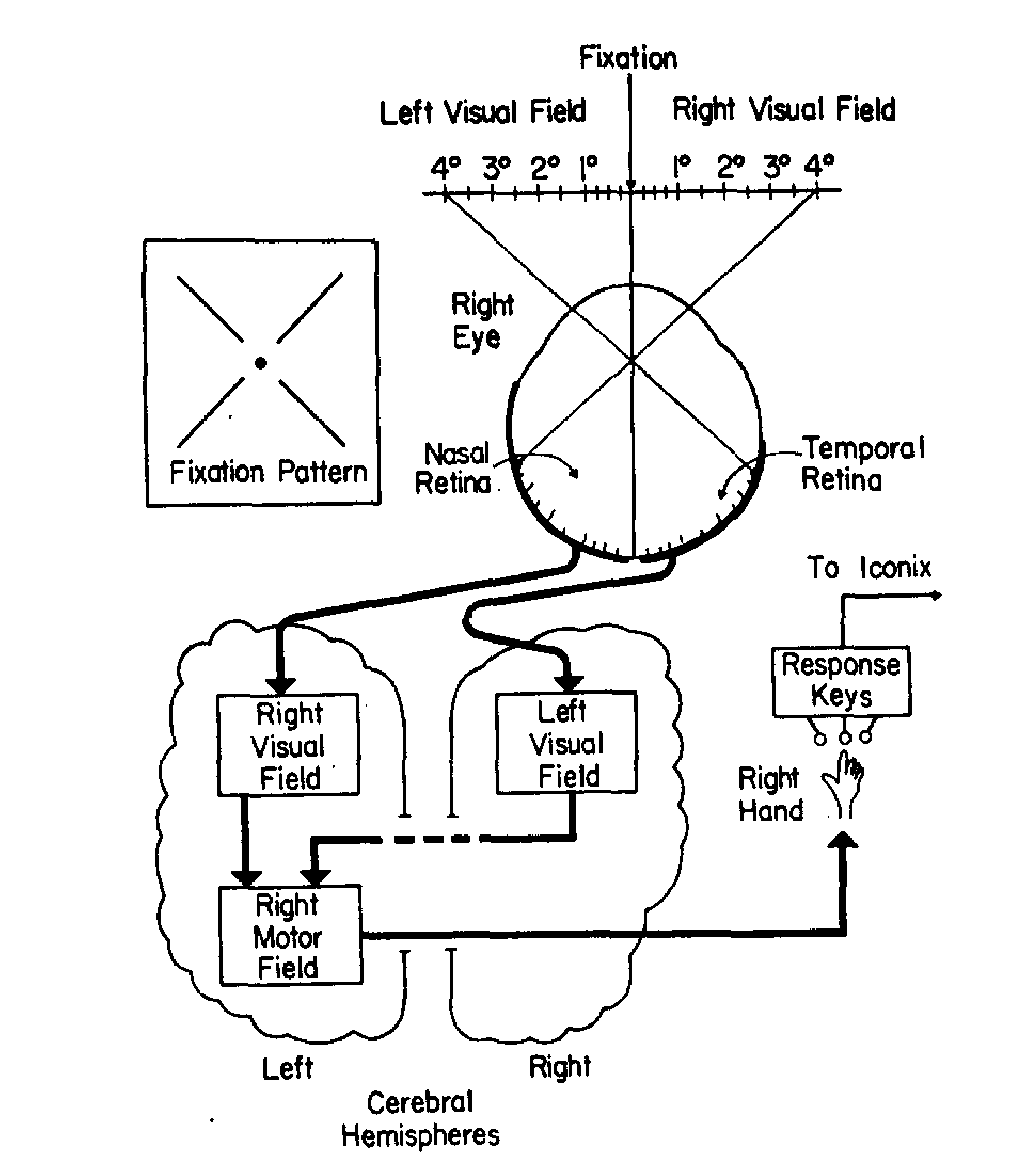

Harvey, L. O., Jr. (1978). Single representation of the visual midline in humans. *Neuropsychologia, 16*(5), 601610.

Left and Right RT

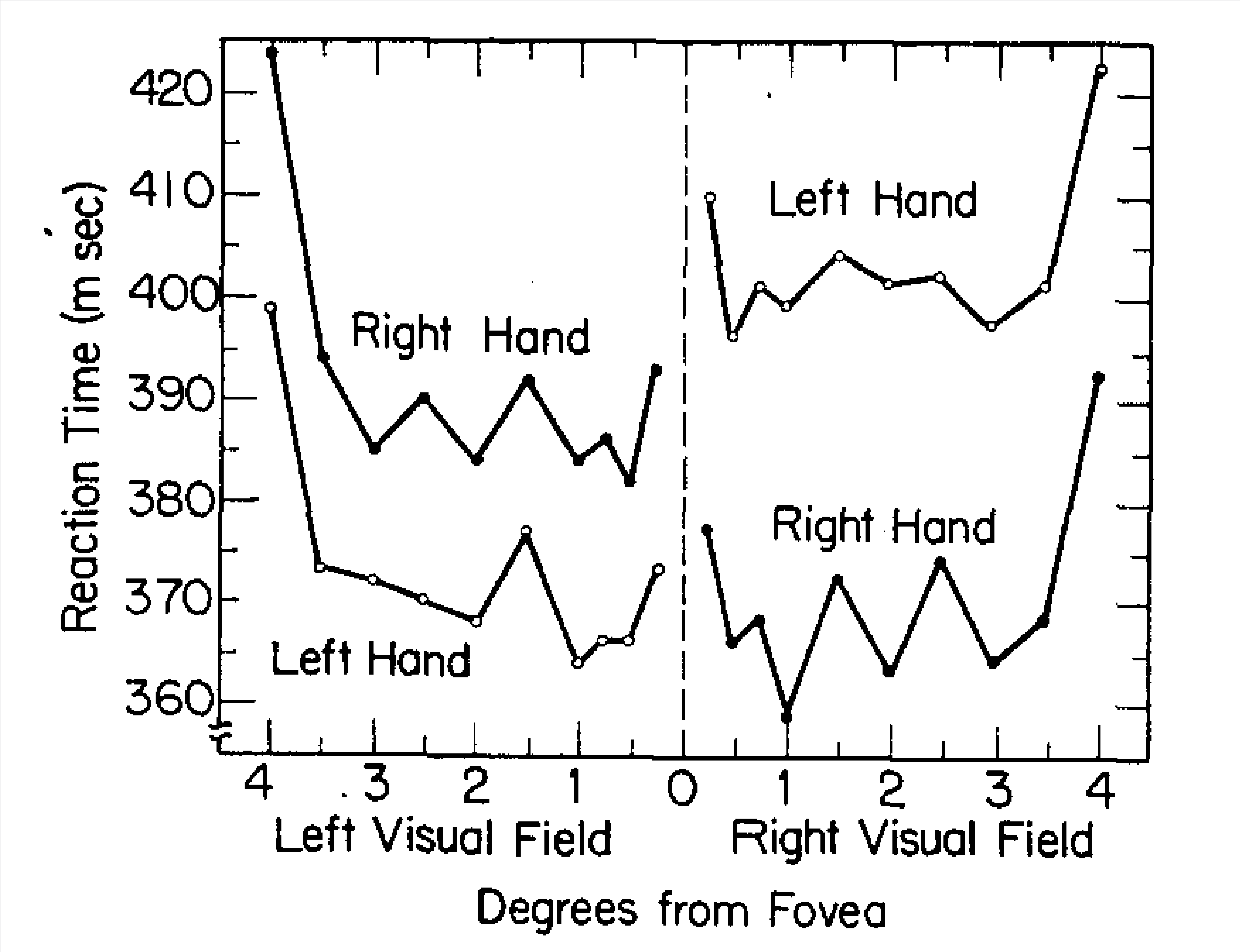

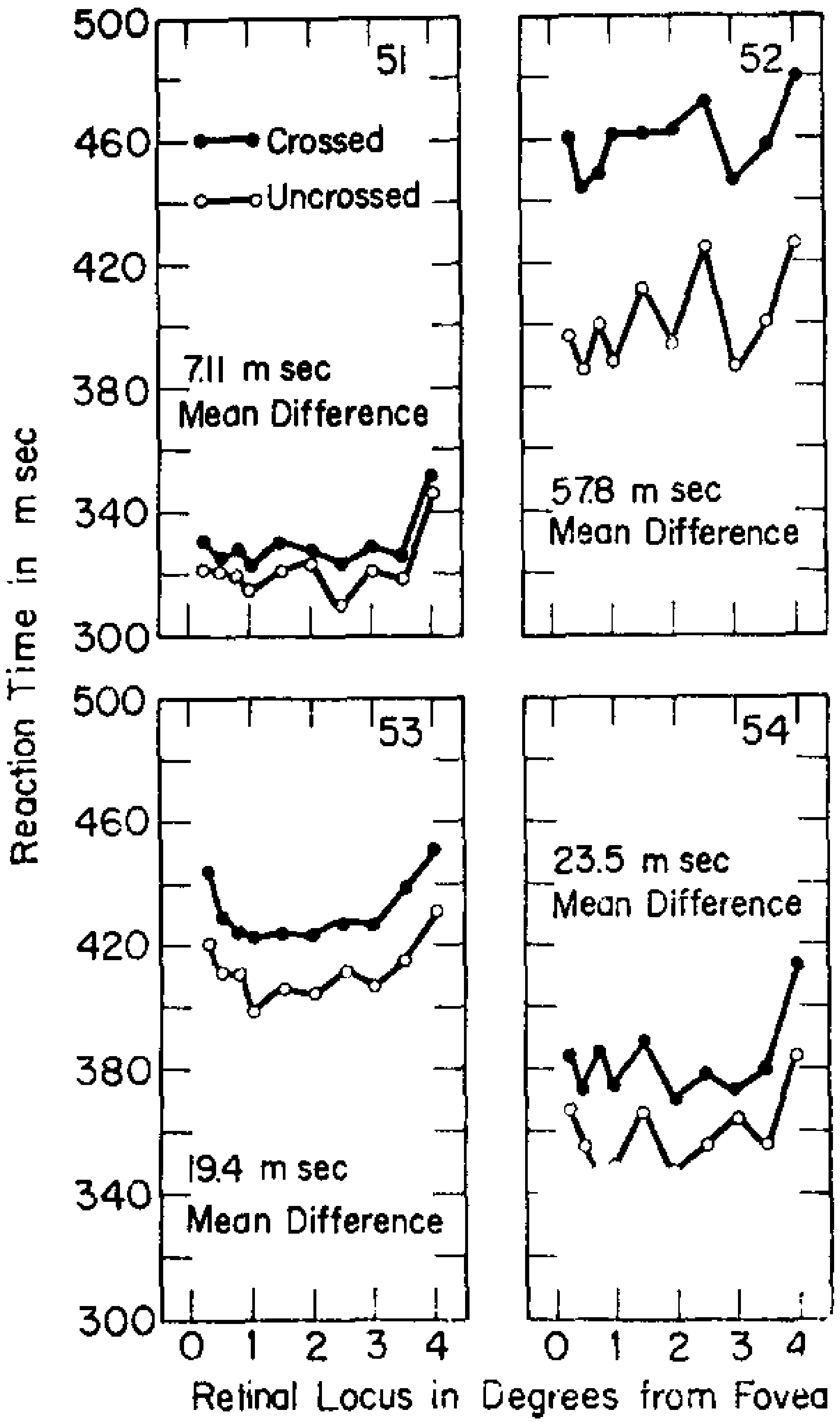

Reaction Time in m sec
500
460
420
380
340
300
51
Crossed
Uncrossed
7.11 m sec
Mean Difference
52
57.8 m sec
Mean Difference
53
19.4 m sec
Mean Difference
54
23.5 m sec
Mean Difference
0 1 2 3 4
Retinal Locus in Degrees from Fovea

Crossed and Uncrossed RT

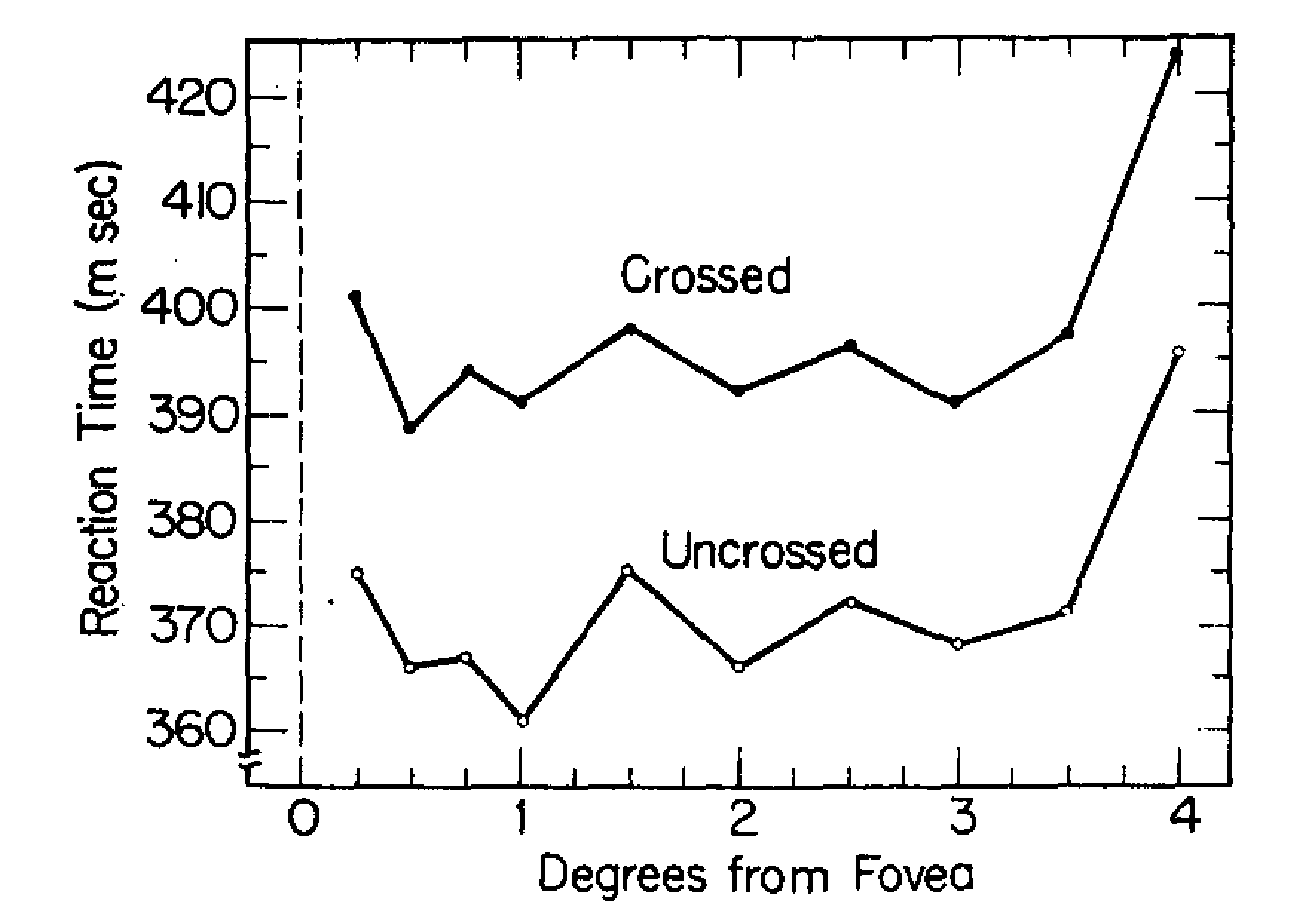

Occular Dominance Stripes

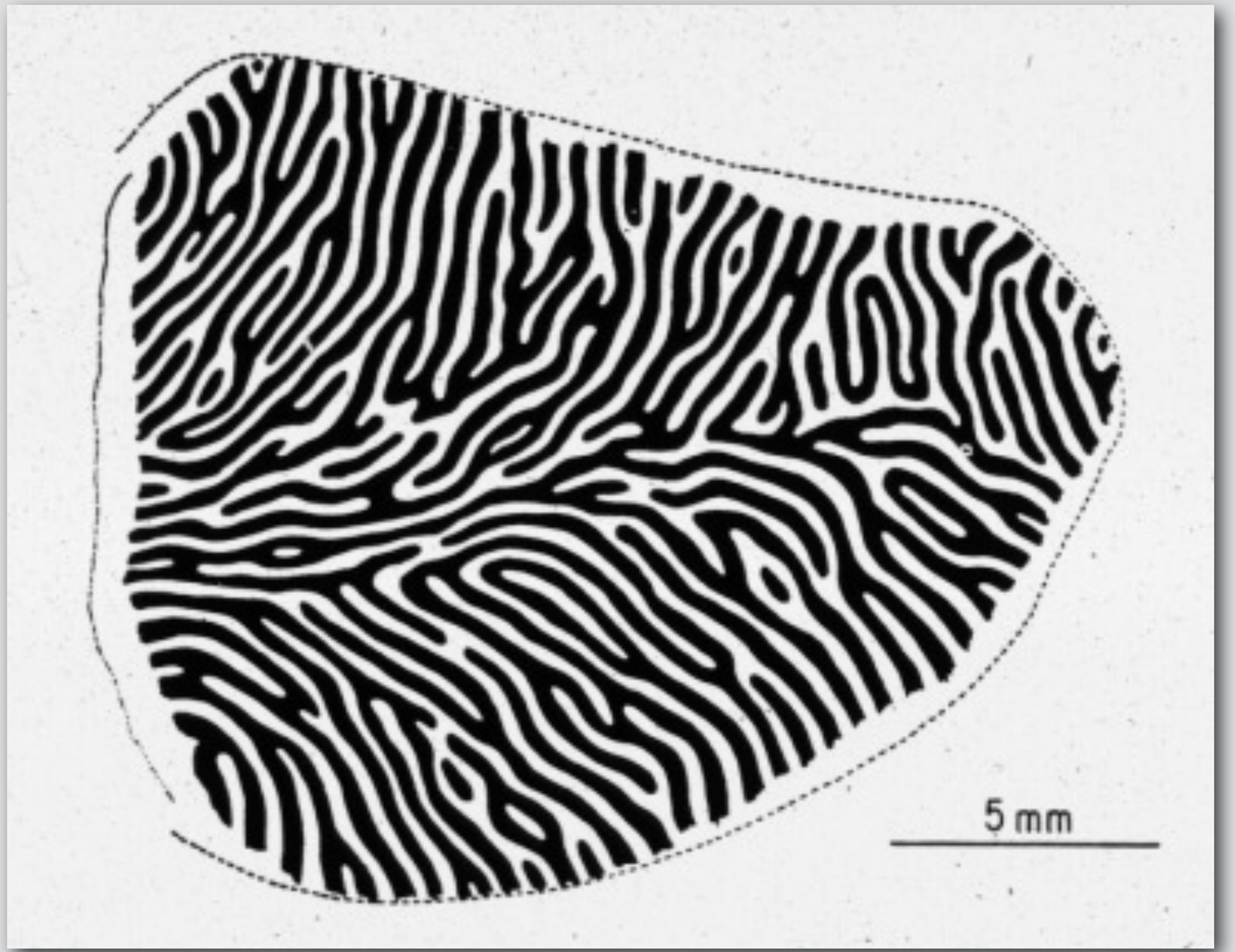

Nonlinear Mapping

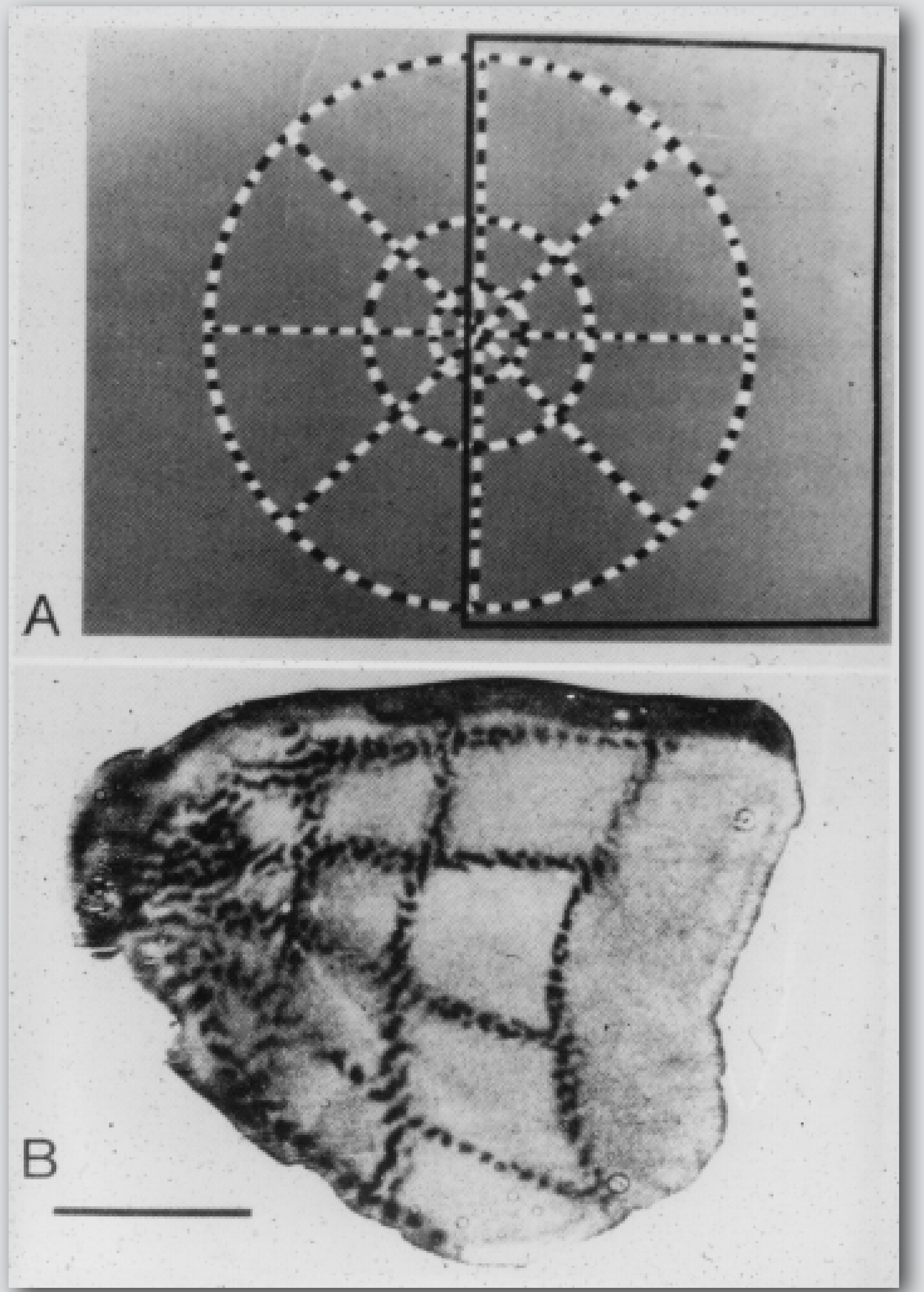

Blobs and Stripes

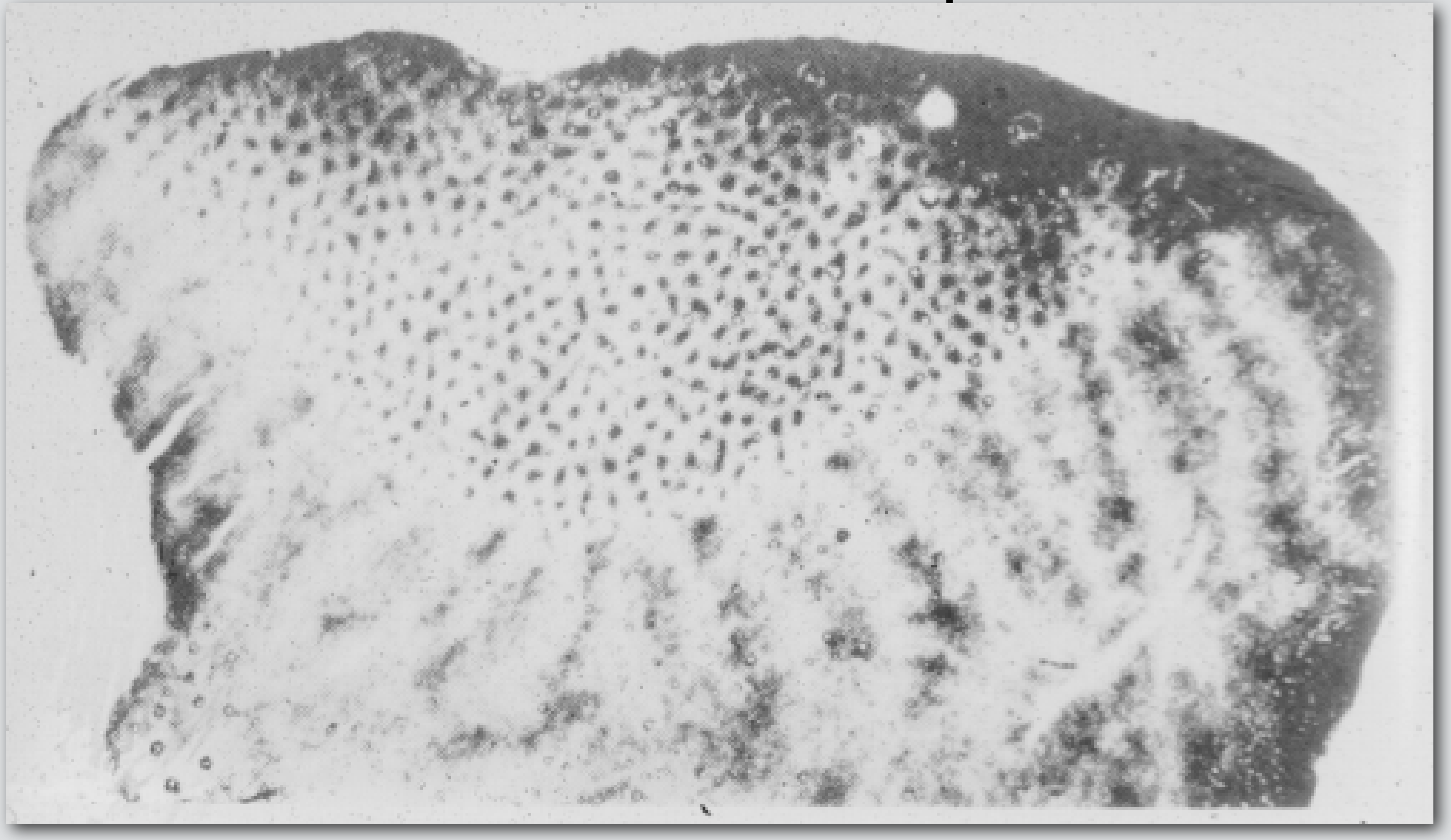

Orientation Tuning in Cortex

David Hubel and Torsten Wiesel

Orientation Tuning in Area 17

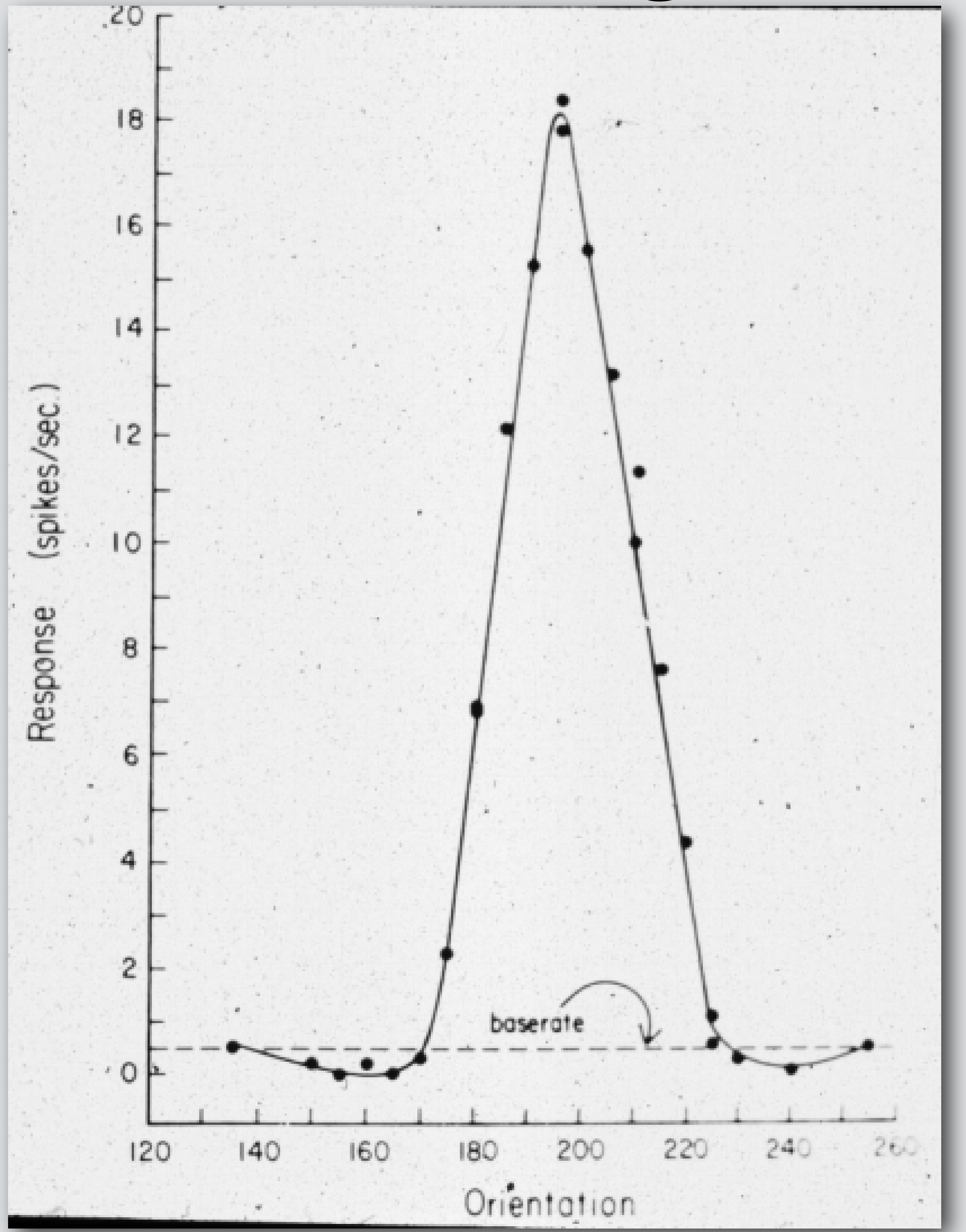

Sequence Regularity

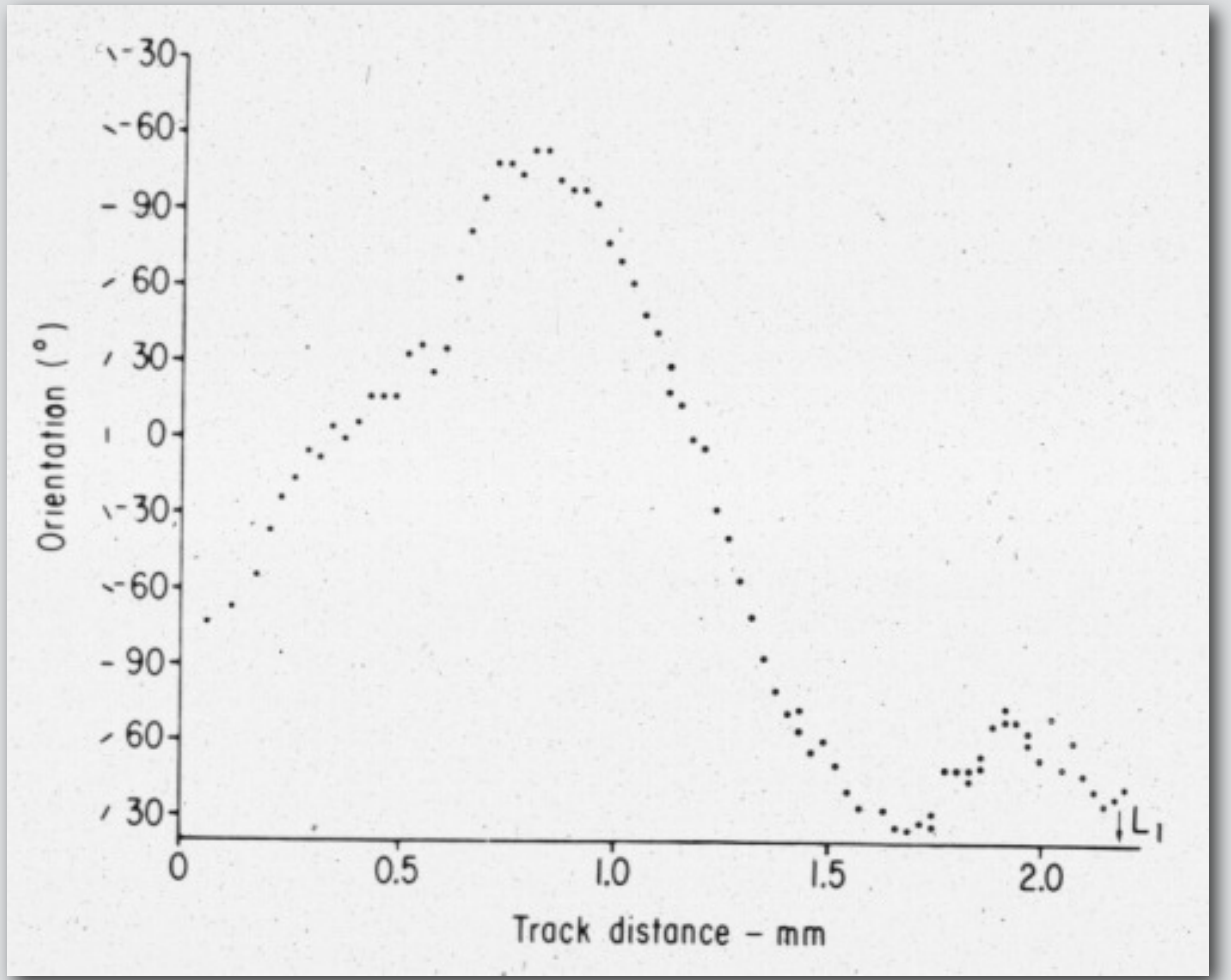

Receptive Fields in Cortex

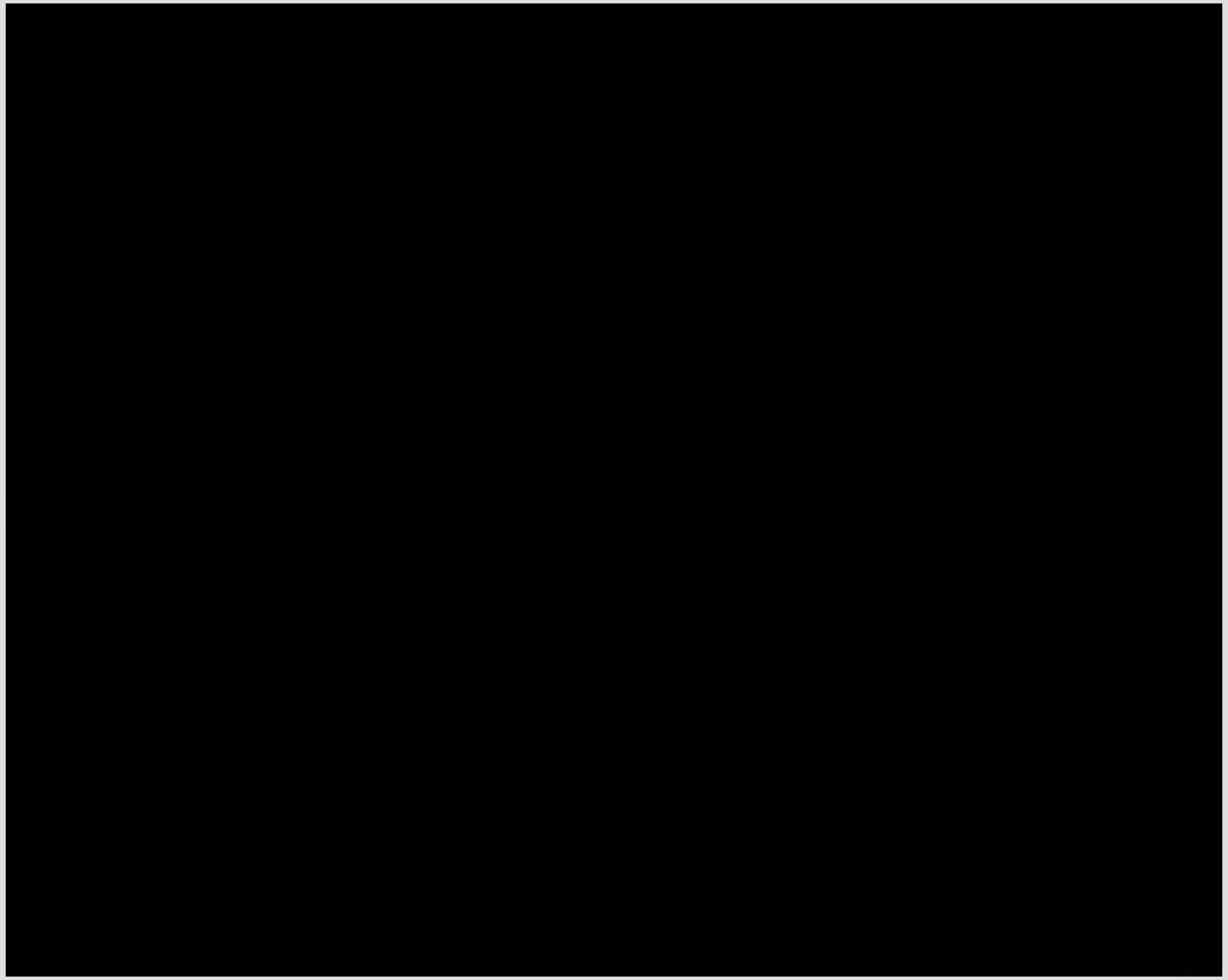

Colin Blakemore

12 Minutes

Effect of Experience

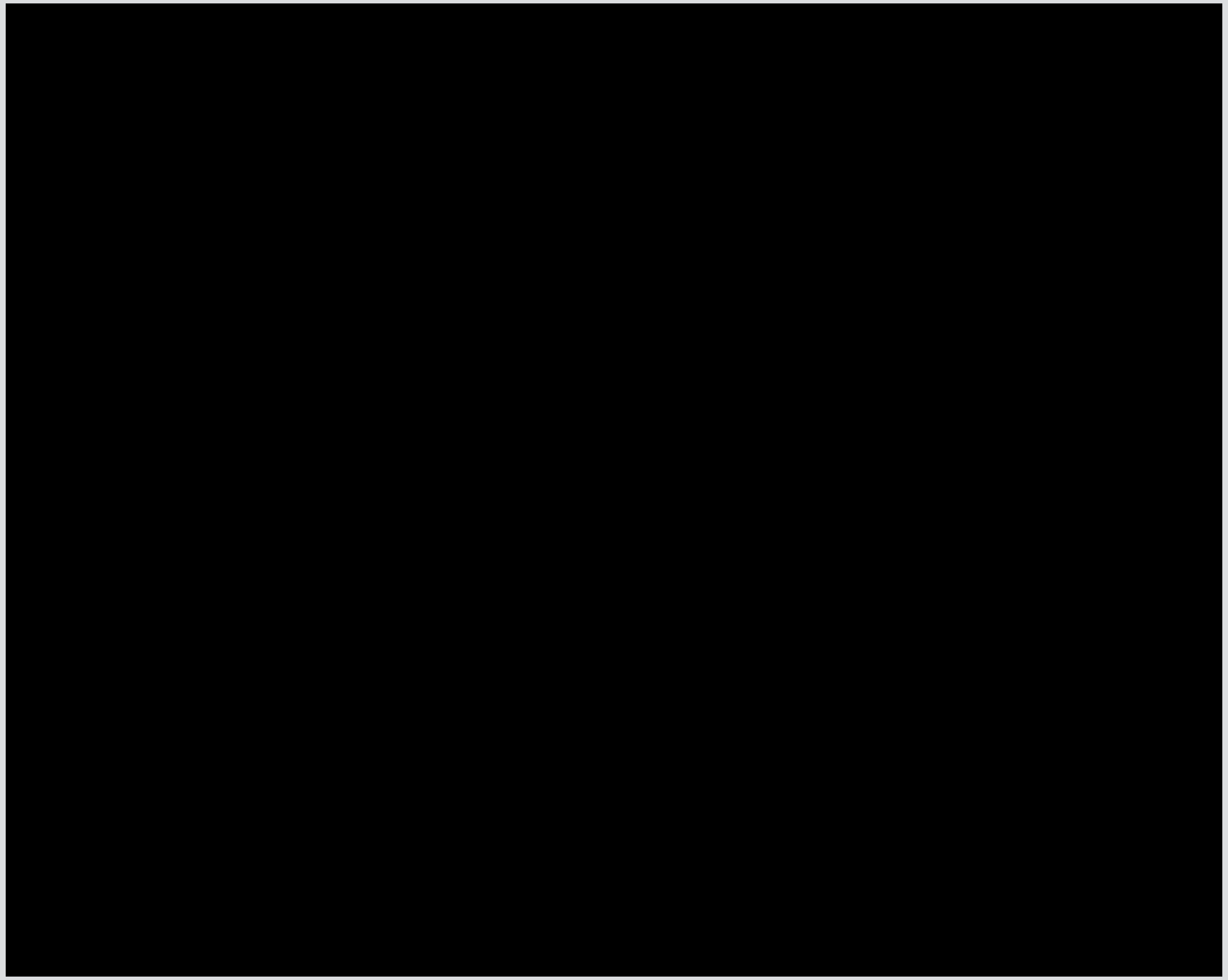

Colin Blakemore

9 Minutes

Retina–Cortical Mapping

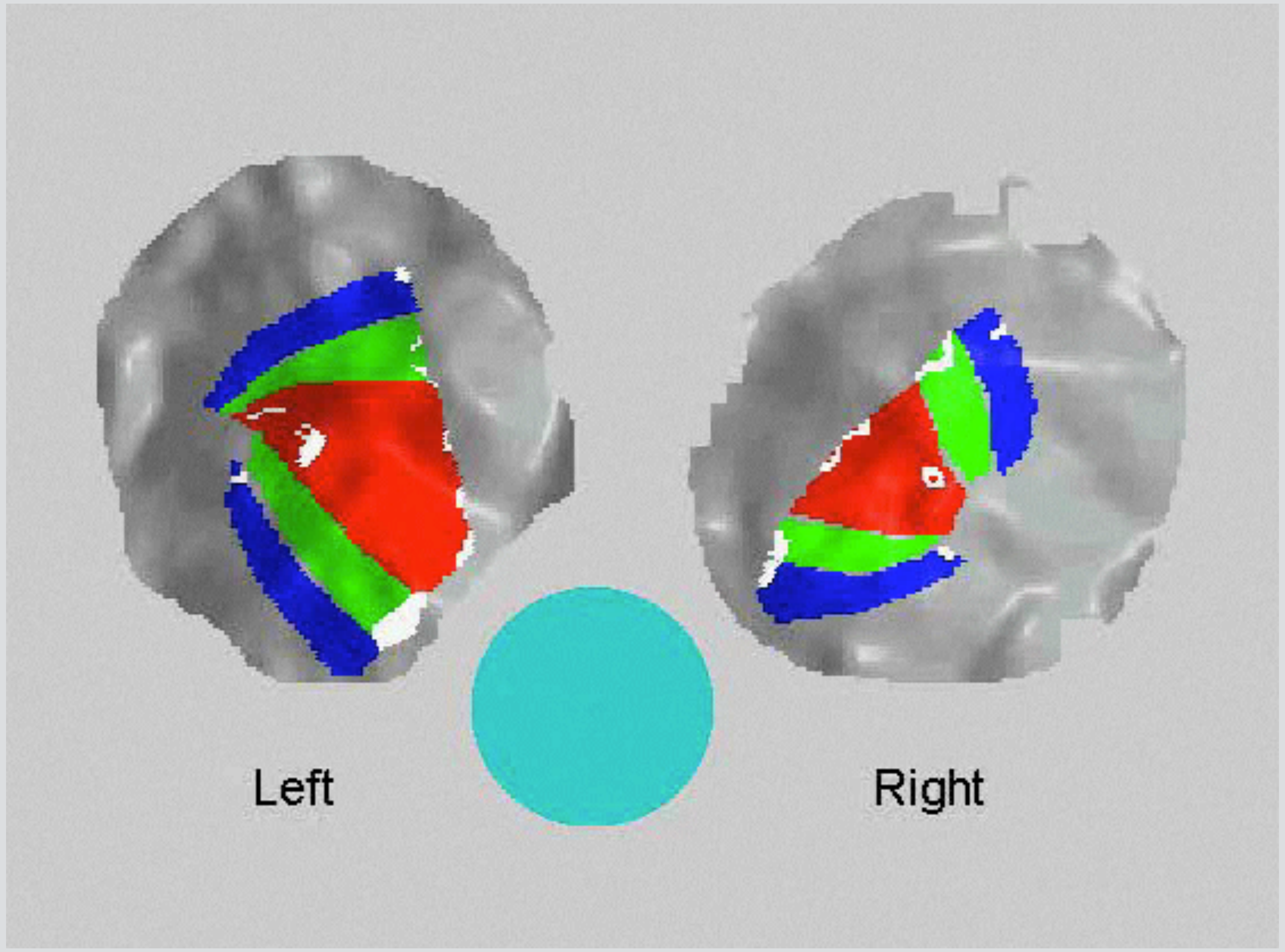

Retina–Cortical Mapping

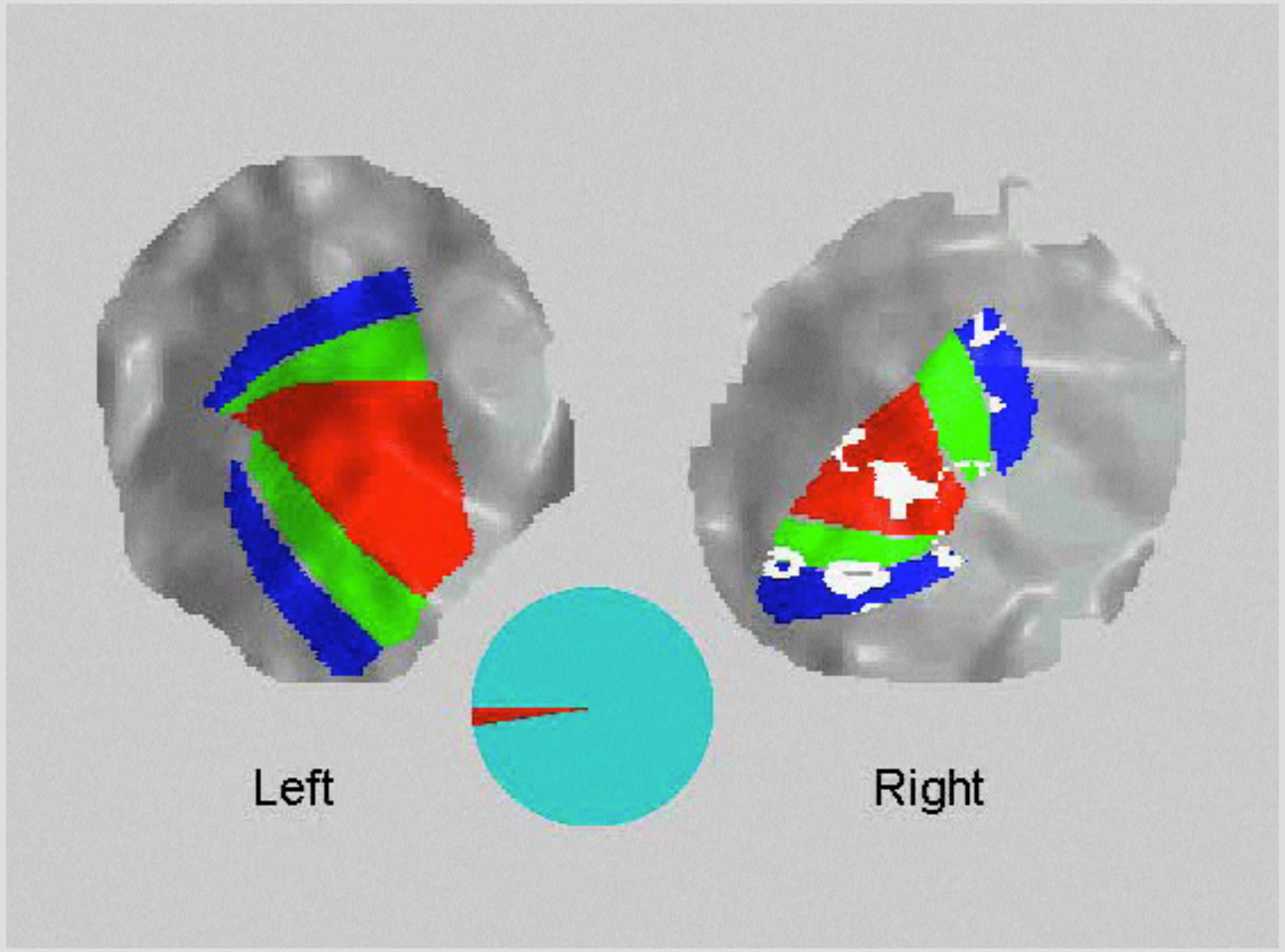

Retina–Cortical Mapping

Visual Field

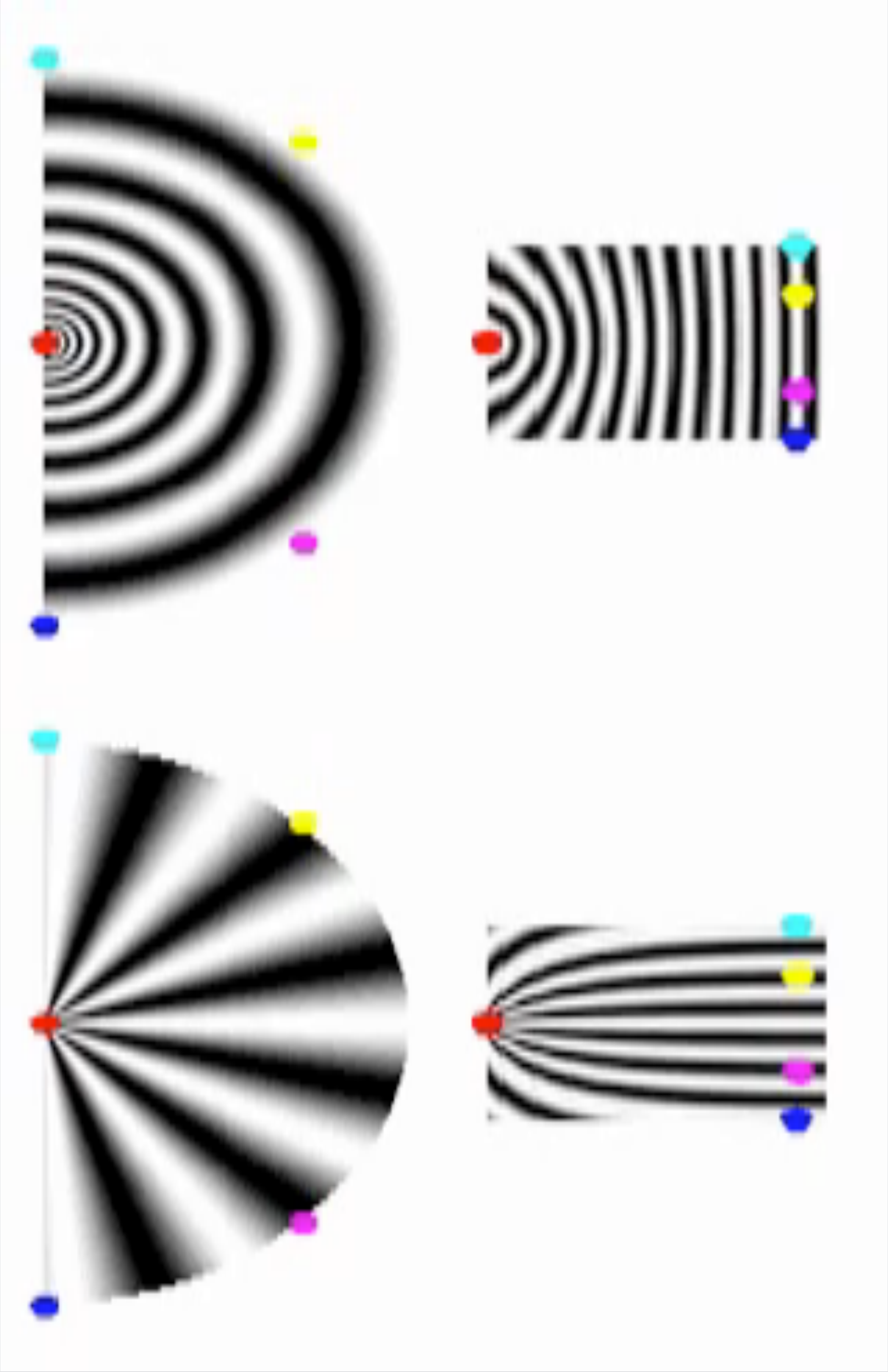

Visual Cortex

Retina–Cortical Mapping

Visual Field

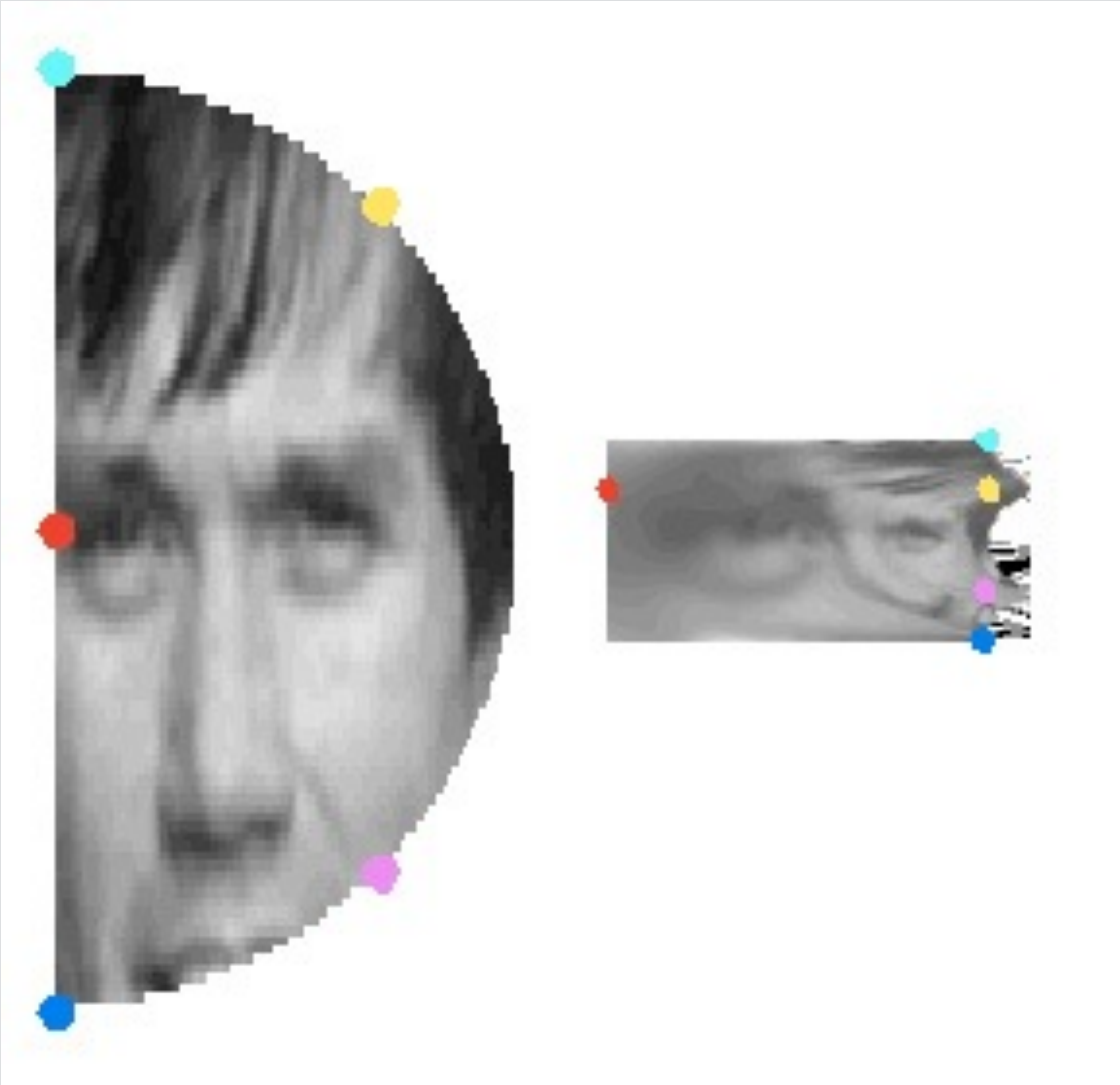

Visual Cortex

Mapping of Movement

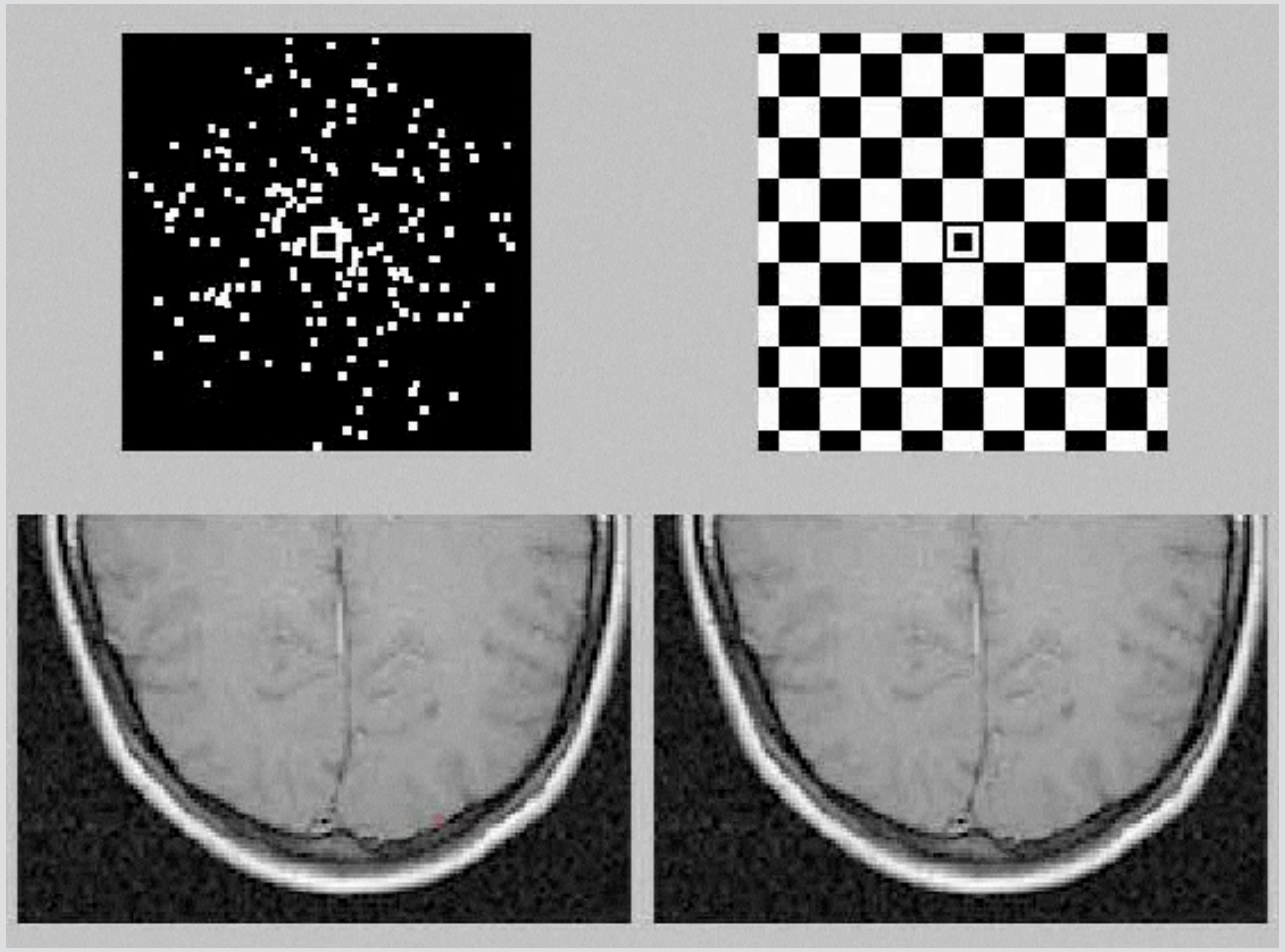

Shifts of Attention

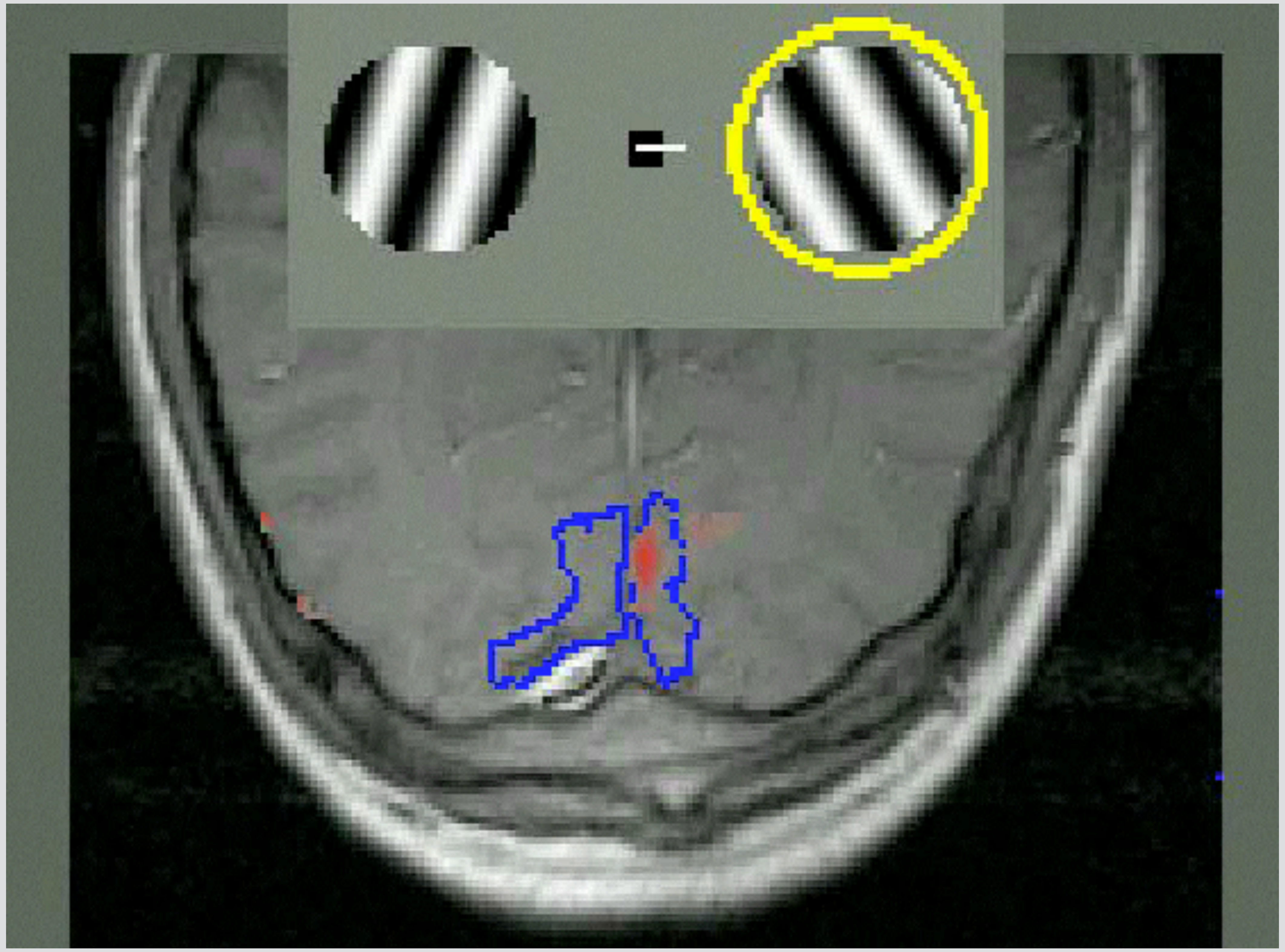

Lauritzen, T. Z., D'Esposito, M., Heeger, D. J., & Silver, M. A. (2009). Top–down flow of visual spatial attention signals from parietal to occipital cortex. *Journal of Vision, 9*(13). doi: 10.1167/9.13.18

Shifts of Attention

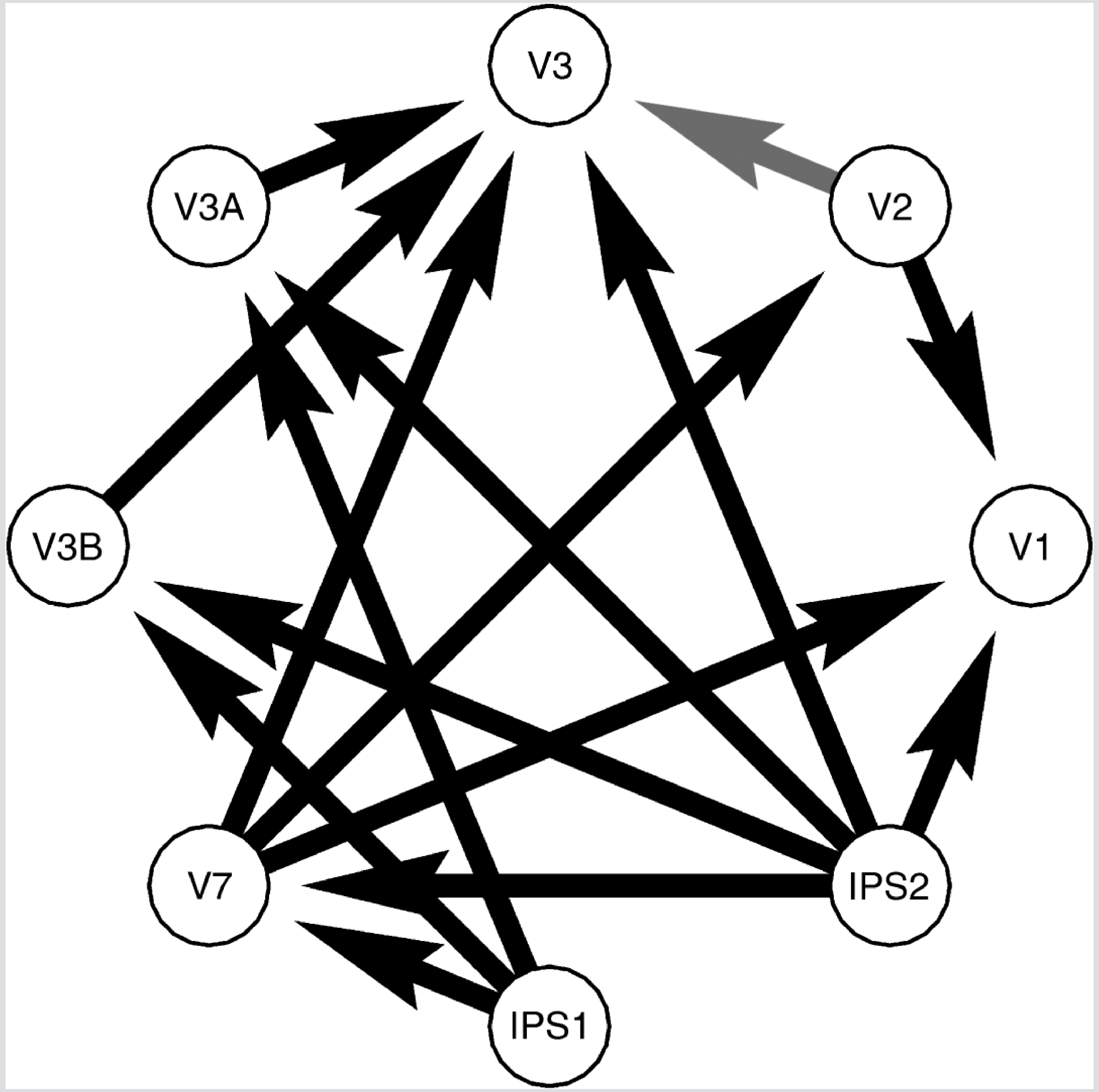

Figure 5. Temporal differences in attention-related activity for pairs of cortical areas. Arrows indicate significant differences in functional connectivity between attention and fixation. Black arrows represent top–down flow of attention signals, and the gray arrow indicates a bottom–up relationship between V2 and V3.

Lauritzen, T. Z., D'Esposito, M., Heeger, D. J., & Silver, M. A. (2009). Top–down flow of visual spatial attention signals from parietal to occipital cortex. *Journal of Vision, 9*(13). doi: 10.1167/9.13.18

Break

Spatial Vision and the Contrast Sensitivity Function

Spatial Vision

- Detecting Contrast
- Detecting Orientation

Fourier Transform

Transform space or time into frequency

What is a Transform?

- A rule or set of rules for turning one set of numbers into another set of numbers
- Many transforms are reversible
- Some transforms are not reversible

N	log N
1	0
2	0.301
3	0.4771
4	0.6021
5	0.699
6	0.7782
7	0.8451
8	0.9031

Why Transform?

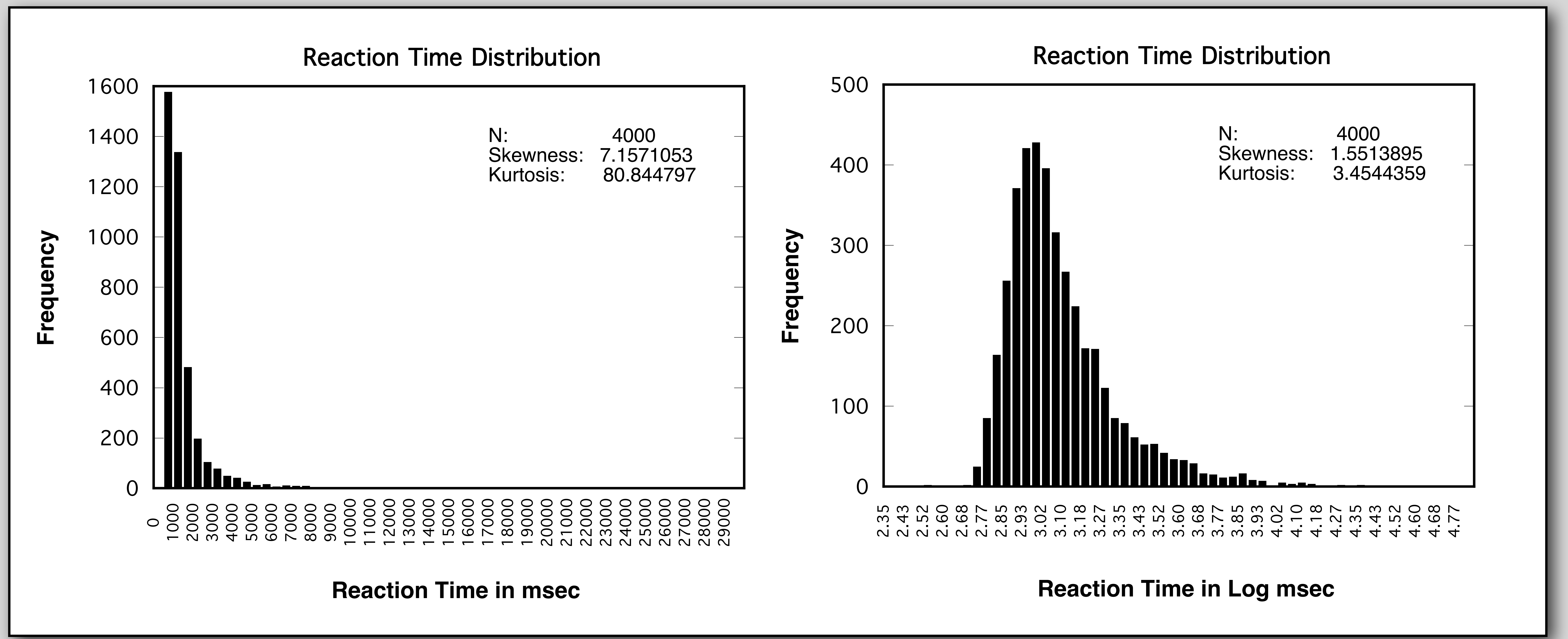

To meet the assumptions of psychological models.

Jean Baptiste Joseph Fourier

- Born:
  - 21 March 1768, Auxerre, France
- Died:
  - 16 May 1830, Paris, France

The Fourier Transform

On the Propagation of Heat in Solid Bodies (1807)

t	h(t)
0	0
1	1.75
2	0.15
3	-0.14
4	0.23
5	-1.5
6	-0.82
7	1.65

$$H(f) = \sum_{t=0}^{N-1} h(t) \cdot B(f,t)$$

f	H(f)
0	1.33, 0.00i
1	3.33,-2.01i
2	0.90,1.26i
3	-3.80,-0.07i
4	-2.19,0.00i
-3	-3.80,0.07i
-2	0.90,-1.26i
-1	3.33,2.01i

The Fourier Transform

- B(f,t) is called a basis function
- For the Fourier transform
  - Basis function is a complex exponential function

$$H(f) = \sum_{t=0}^{N-1} h(t) \cdot B(f,t)$$

$$t = time$$

$$f = frequency$$

$$Basis\,Function = e^{-i \cdot 2\pi \cdot t \cdot f}$$

$$i = \sqrt{-1}$$

Leonhard Euler

- Born:
  - 15 April 1707, Basel, Switzerland
- Died:
  - 18 Sept 1783, St. Petersburg, Russia

Leonhard Euler (1707–1783)

Worked out the relationship between
exponential functions and trigonometric functions

$$e^{ix} = \cos(x) + i\sin(x)$$

Leonhard Euler (1707–1783)

The most beautiful equation in the world:

$$e^{i\pi} = -1$$

Leonhard Euler (1707–1783)

The most beautiful equation in the world:

$$e^{i\pi} = -1$$

$$e \quad (\textit{irrational and transcendental})$$

$$\pi \quad (\textit{irrational and transcendental})$$

$$i \quad (\textit{imaginary number})$$

Leonhard Euler (1707–1783)

The most beautiful equation in the world:

$$e^{i\pi} = -1$$

$$e \quad \left(\textit{irrational and transcendental}\right)$$

$$\pi \quad \left(\textit{irrational and transcendental}\right)$$

$$i \quad \left(\textit{imaginary number}\right)$$

$$e^{ix} = \cos(x) + i\sin(x)$$

$$e^{i\pi} = \cos(\pi) + i\sin(\pi)$$

Leonhard Euler (1707–1783)

The most beautiful equation in the world:

$$\cos(\pi) = -1$$

$$\sin(\pi) = 0$$

$$e^{i\pi} = \cos(\pi) + i\sin(\pi)$$

$$e^{i\pi} = -1 + i \cdot 0$$

$$e^{i\pi} = -1$$

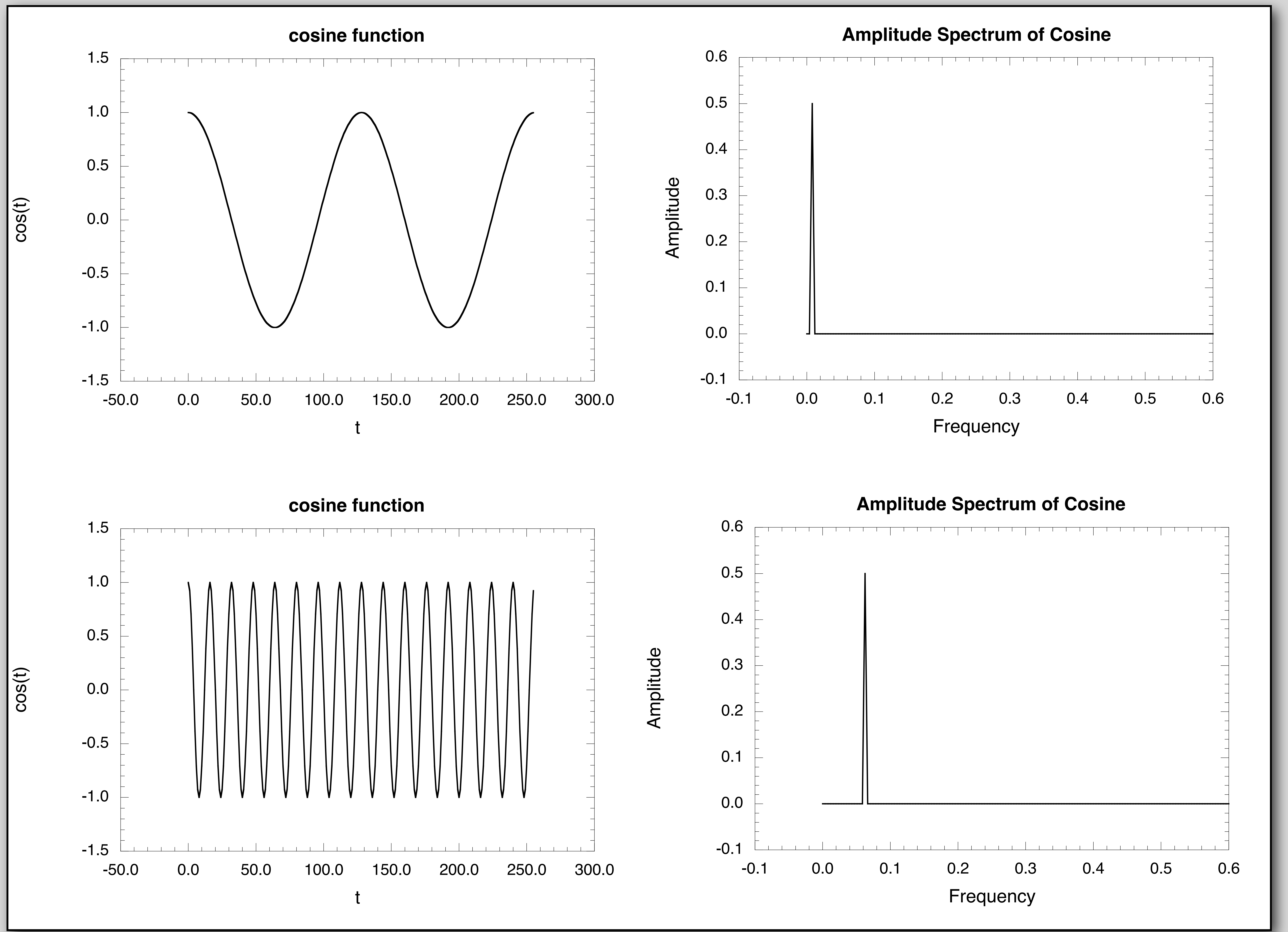
cosine function
cos(t)
t
Amplitude Spectrum of Cosine
Amplitude
Frequency
cosine function
cos(t)
t
Amplitude Spectrum of Cosine
Amplitude
Frequency

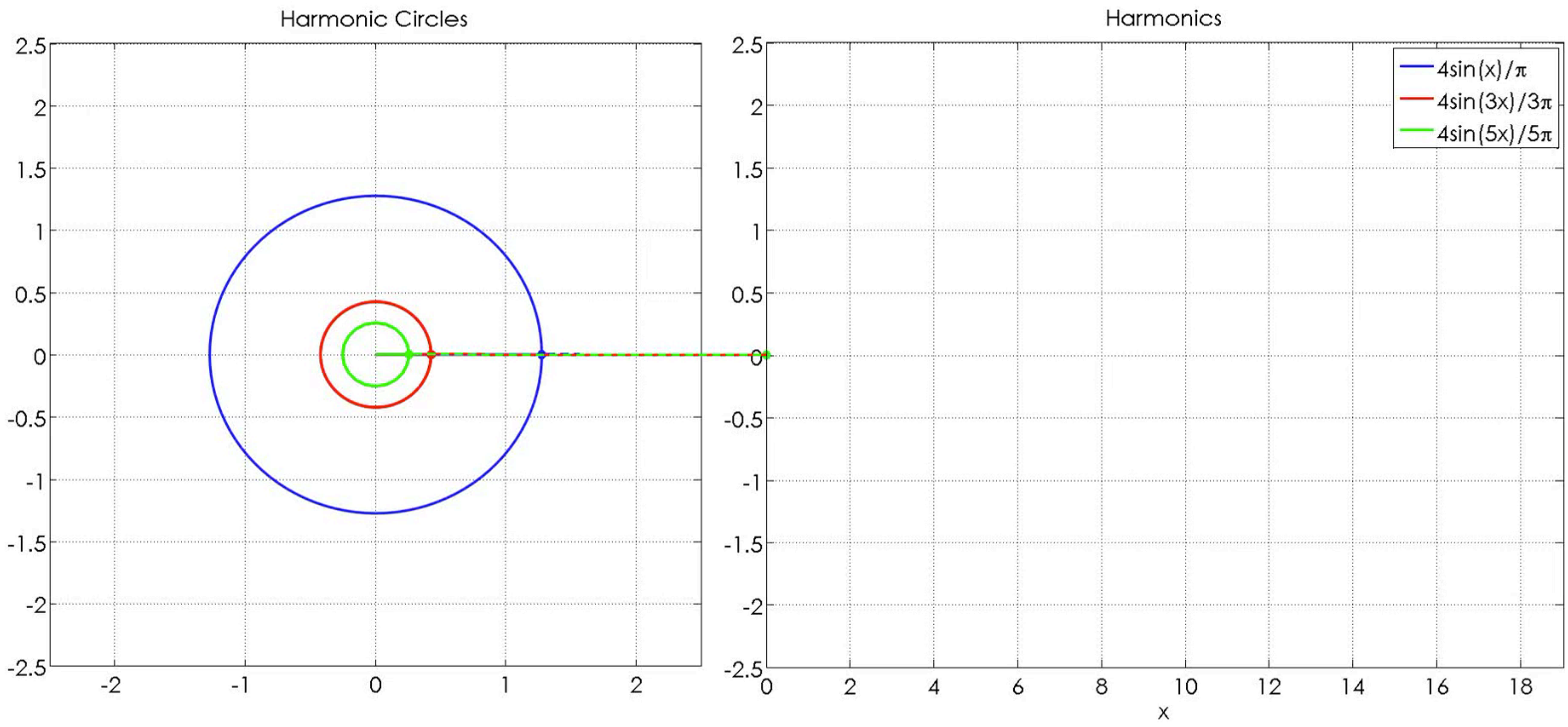

Harmonic Circles
Harmonics
4sin(x)/π
4sin(3x)/3π
4sin(5x)/5π
2.5
2
1.5
1
0.5
0
-0.5
-1
-1.5
-2
-2.5
-2
-1
0
1
2
0
2
4
6
8
10
12
14
16
18
x

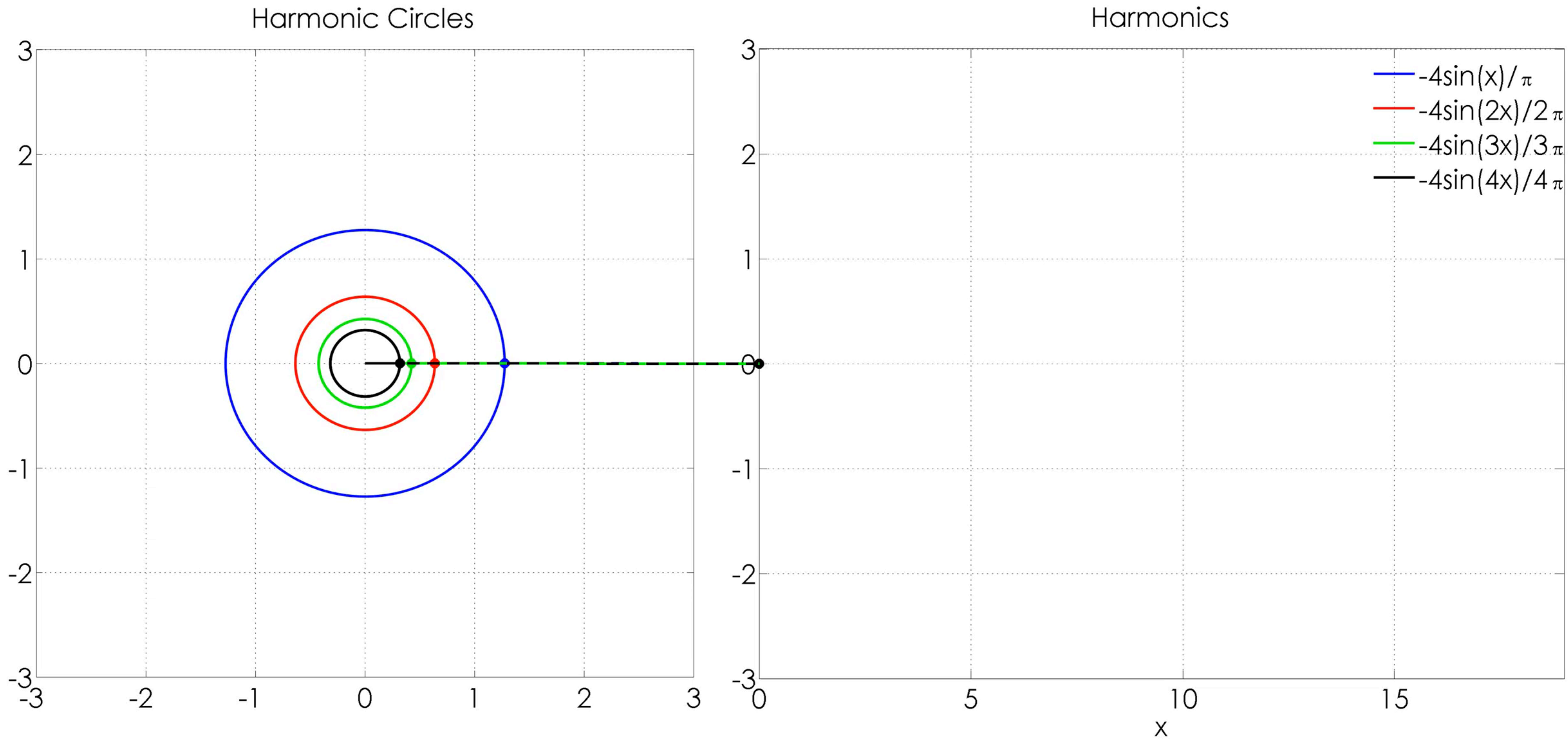

Harmonic Circles
Harmonics
-4sin(x)/π
-4sin(2x)/2π
-4sin(3x)/3π
-4sin(4x)/4π
x

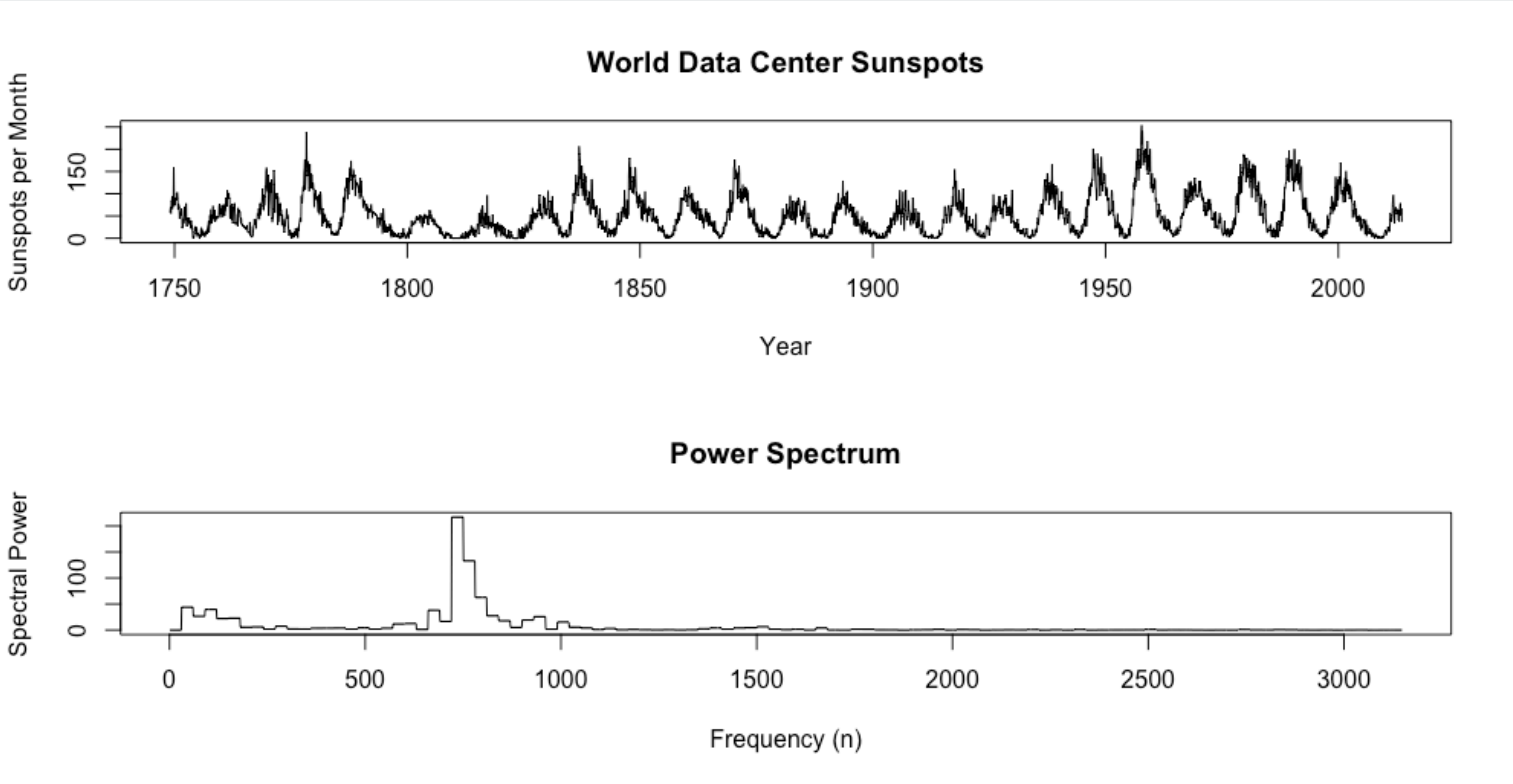
World Data Center Sunspots
Sunspots per Month
0
150
1750
1800
1850
1900
1950
2000
Year
Power Spectrum
Spectral Power
0
100
0
500
1000
1500
2000
2500
3000
Frequency (n)

Spatial Frequencies: Gabor Patches

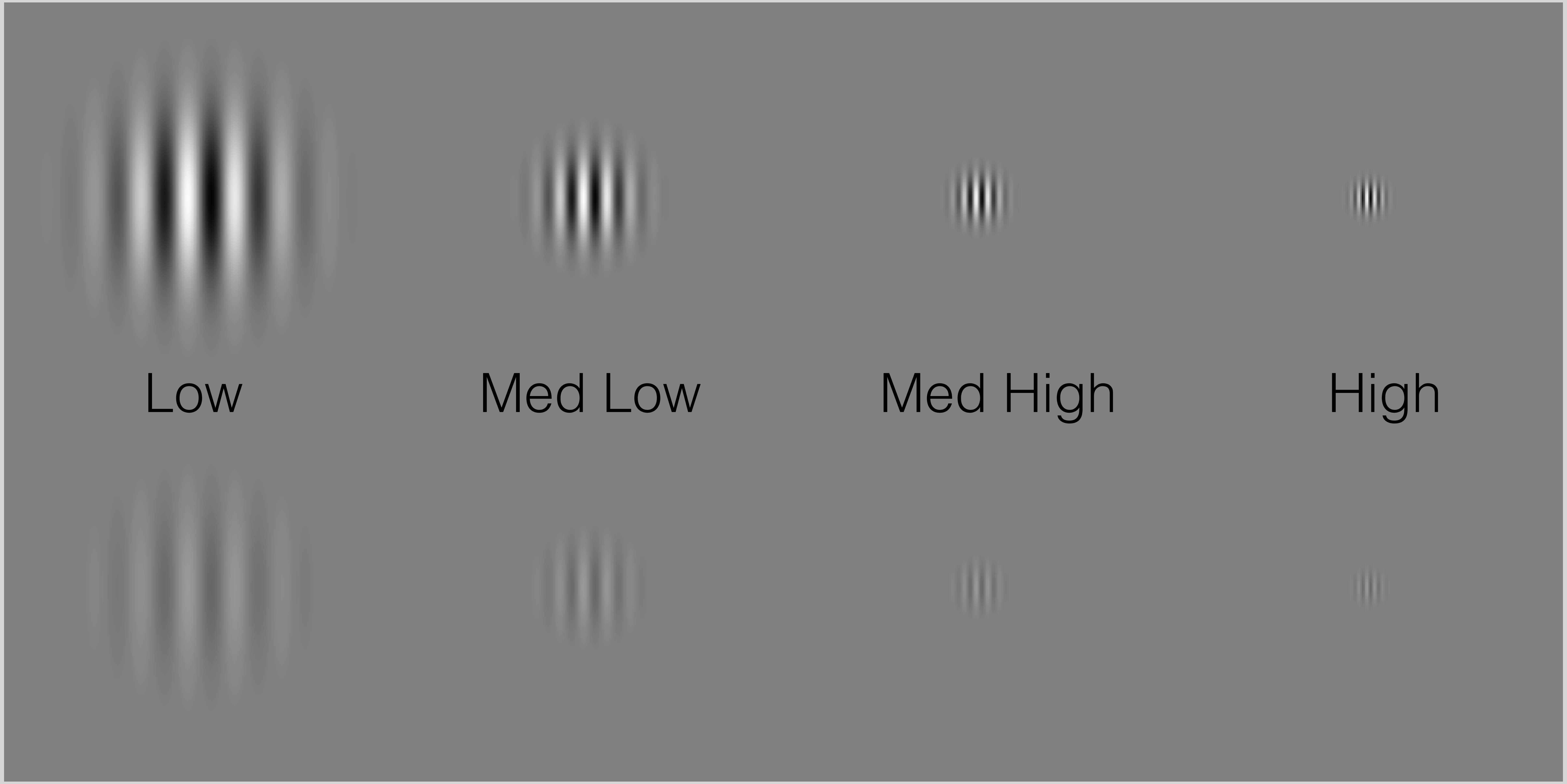

Visual Angle

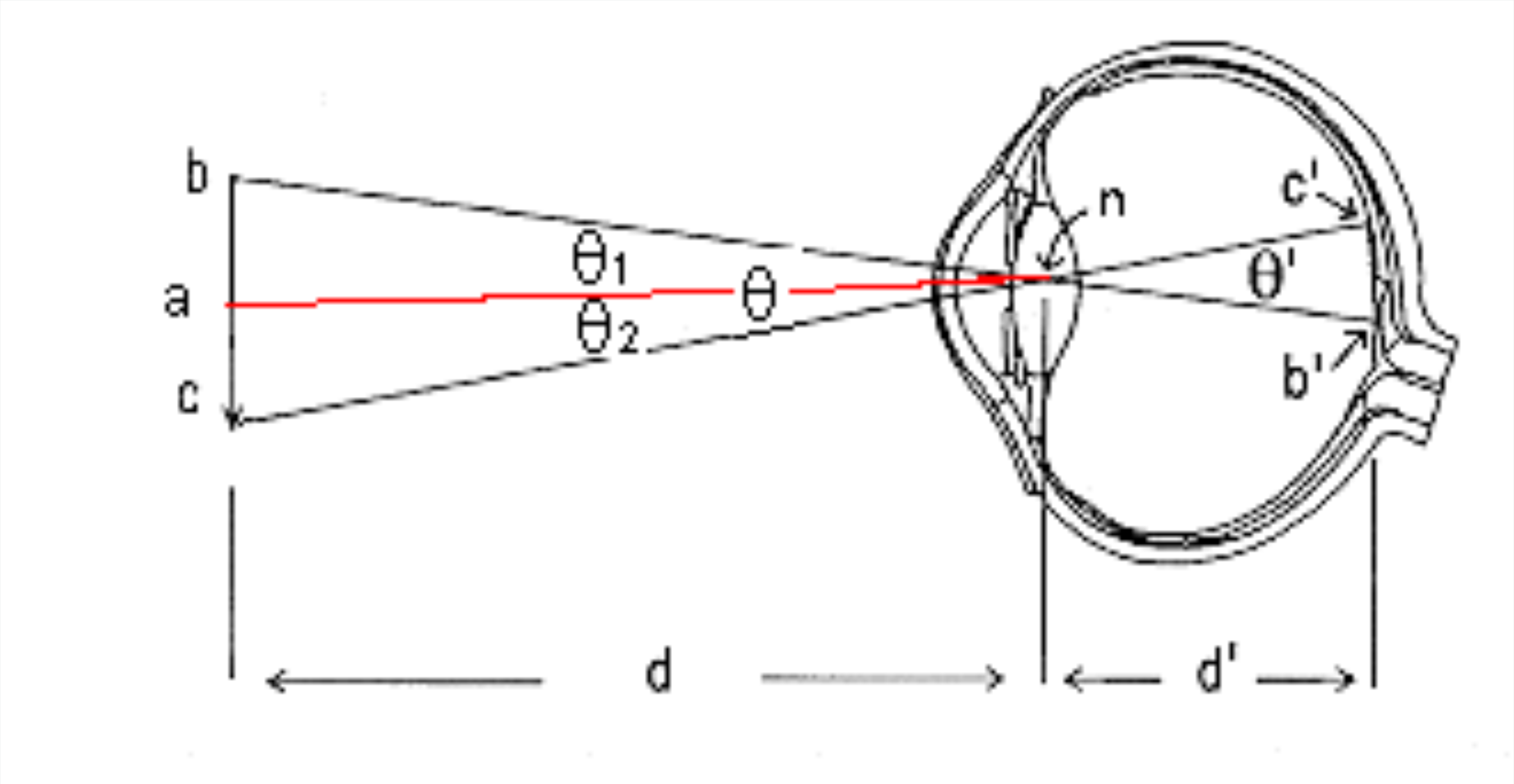

Visual Angle

Visual Angle…

- The angle subtended at the nodal point of the eye by the physical dimensions of an object in the visual field.

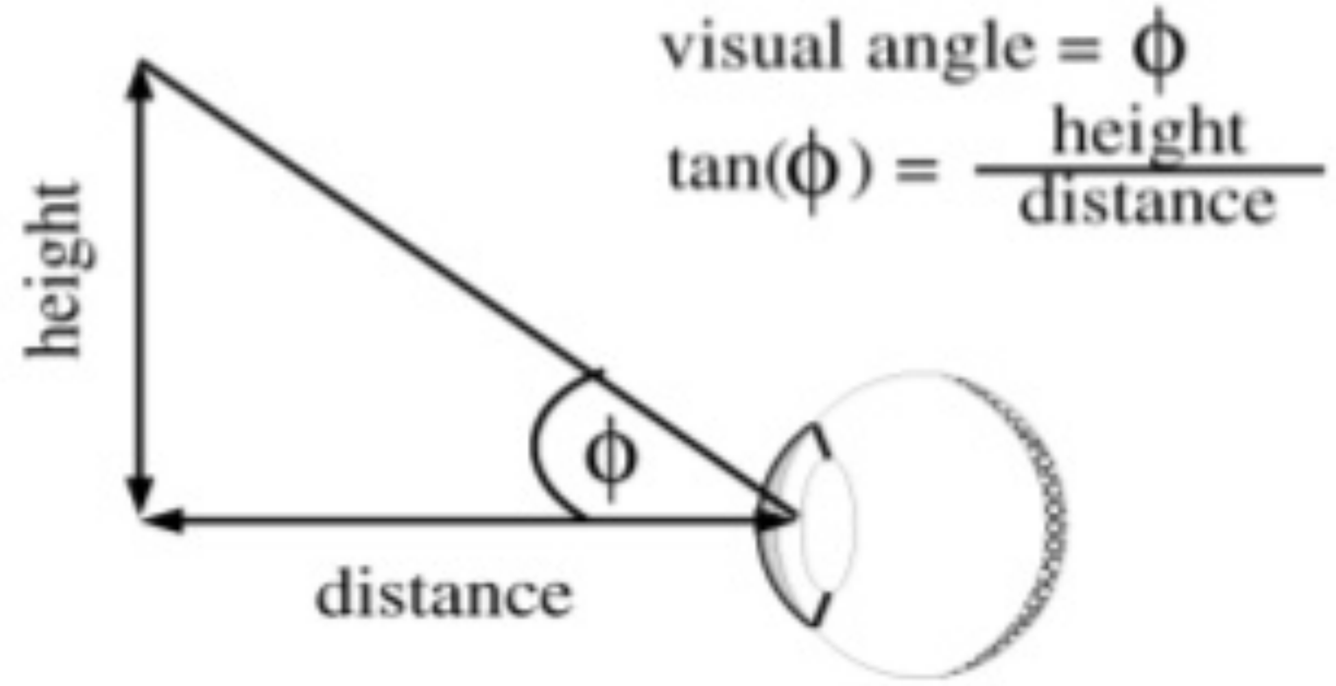

Cycles per Degree

- Distance of pattern from the observer in inches = d
- Resolution of computer screen in pixels/inch = r
- Number of pixels per degree = 180 / pi * d * r
- Number of sine cycles in ppd is the number of cycles per degree

Contrast Sensitivity

- The visual system is not equally sensitive to all spatial frequencies.
- Less sensitive to both low and high spatial frequencies

Contrast Sensitivity Function

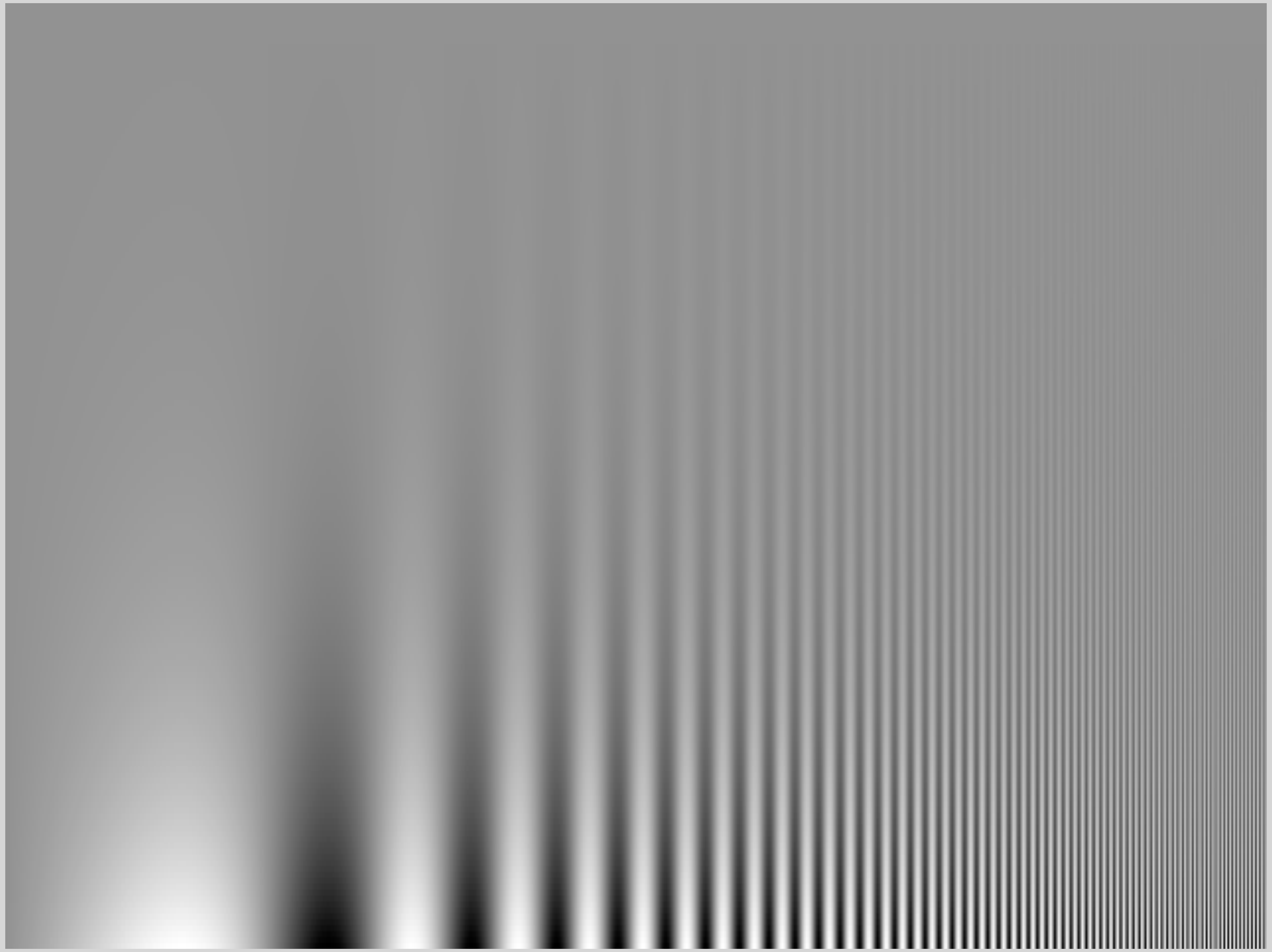

Adaptation Paradigm

Spatial frequency mechanisms

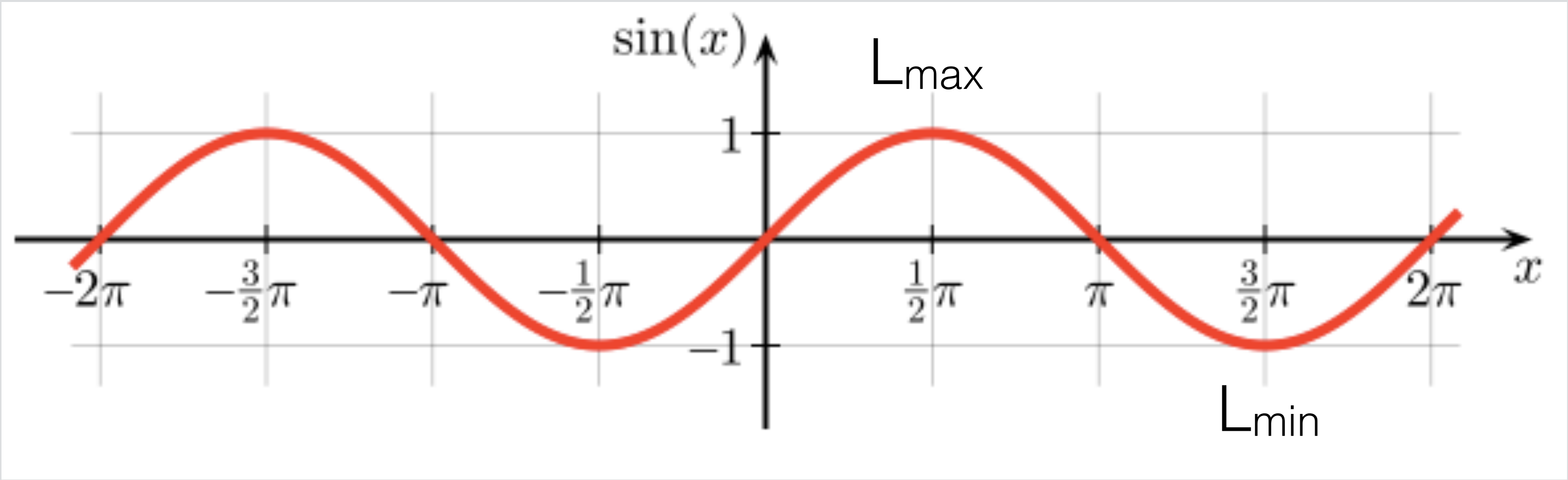

$$Contrast = \frac{(L_{\max} - L_{\min})}{(L_{\max} + L_{\min})}$$

Contrast varies between 0 and 1

$$Threshold\ Contrast = C_t$$

$$Contrast\ Sensitivity = \frac{1}{C_t}$$

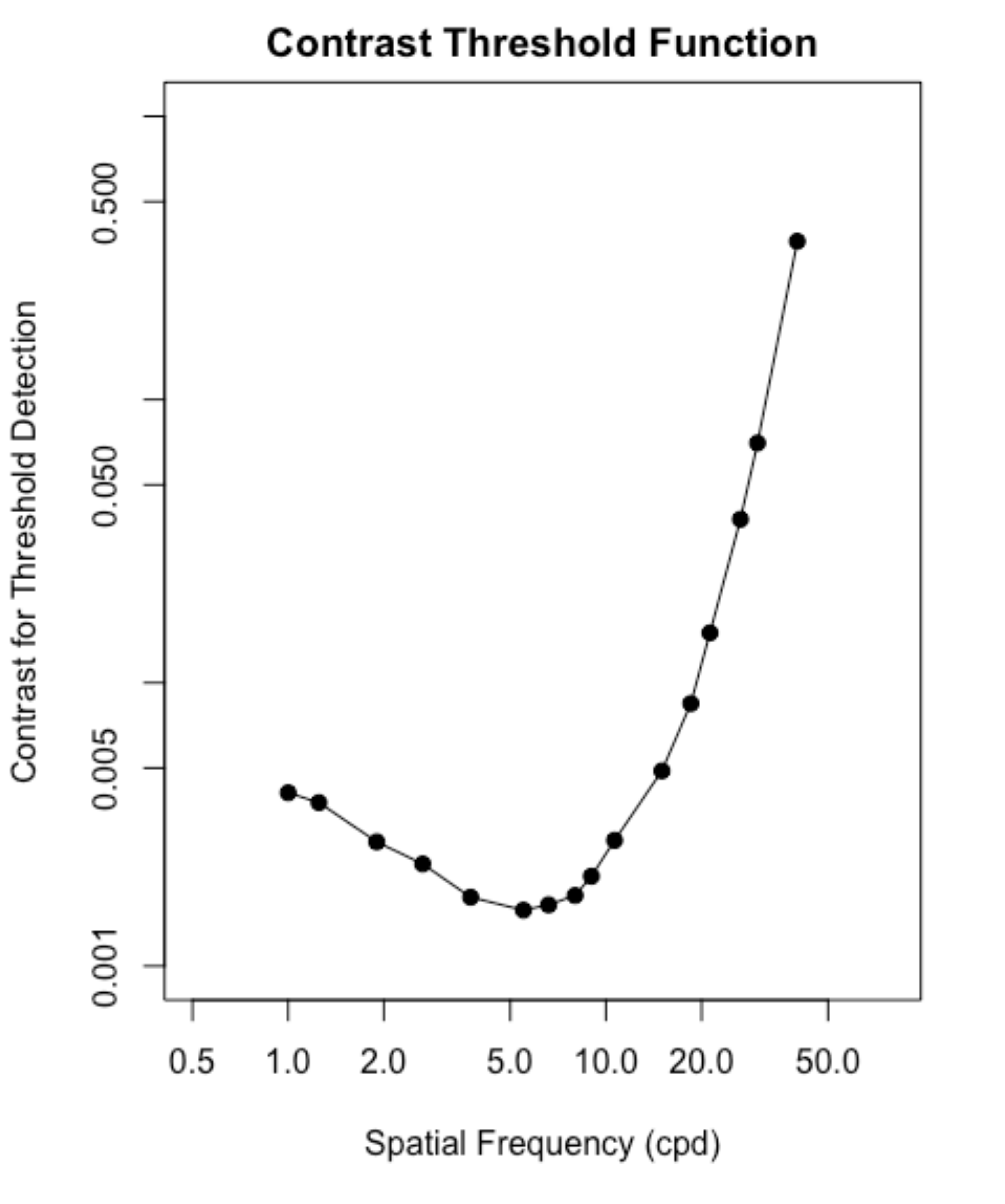

Contrast Threshold Function
Contrast for Threshold Detection
0.001
0.005
0.050
0.500
0.5
1.0
2.0
5.0
10.0
20.0
50.0
Spatial Frequency (cpd)

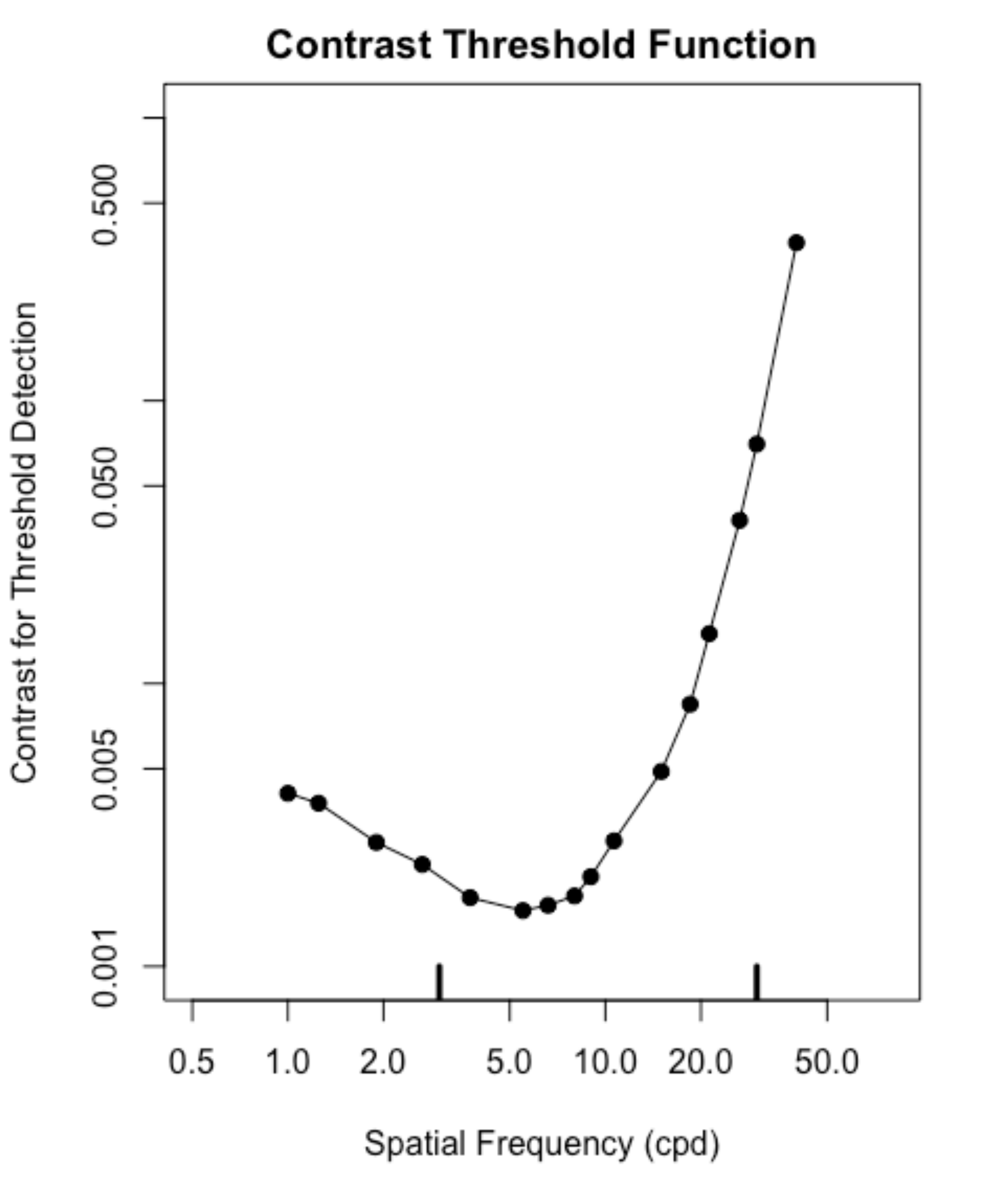

Contrast Threshold Function
Contrast for Threshold Detection
0.500
0.050
0.005
0.001
0.5
1.0
2.0
5.0
10.0
20.0
50.0
Spatial Frequency (cpd)

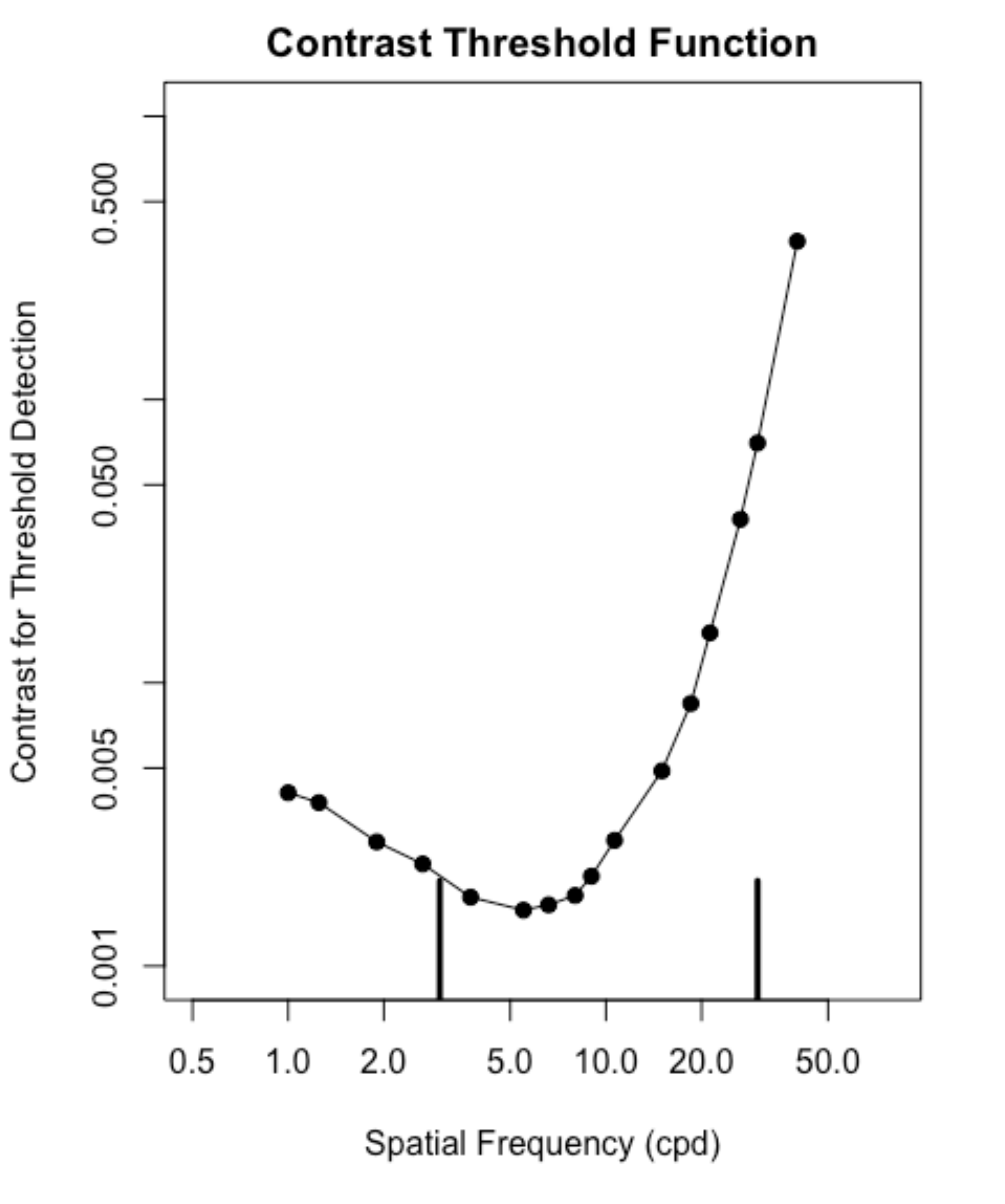

Contrast Threshold Function
Contrast for Threshold Detection
0.500
0.050
0.005
0.001
0.5
1.0
2.0
5.0
10.0
20.0
50.0
Spatial Frequency (cpd)

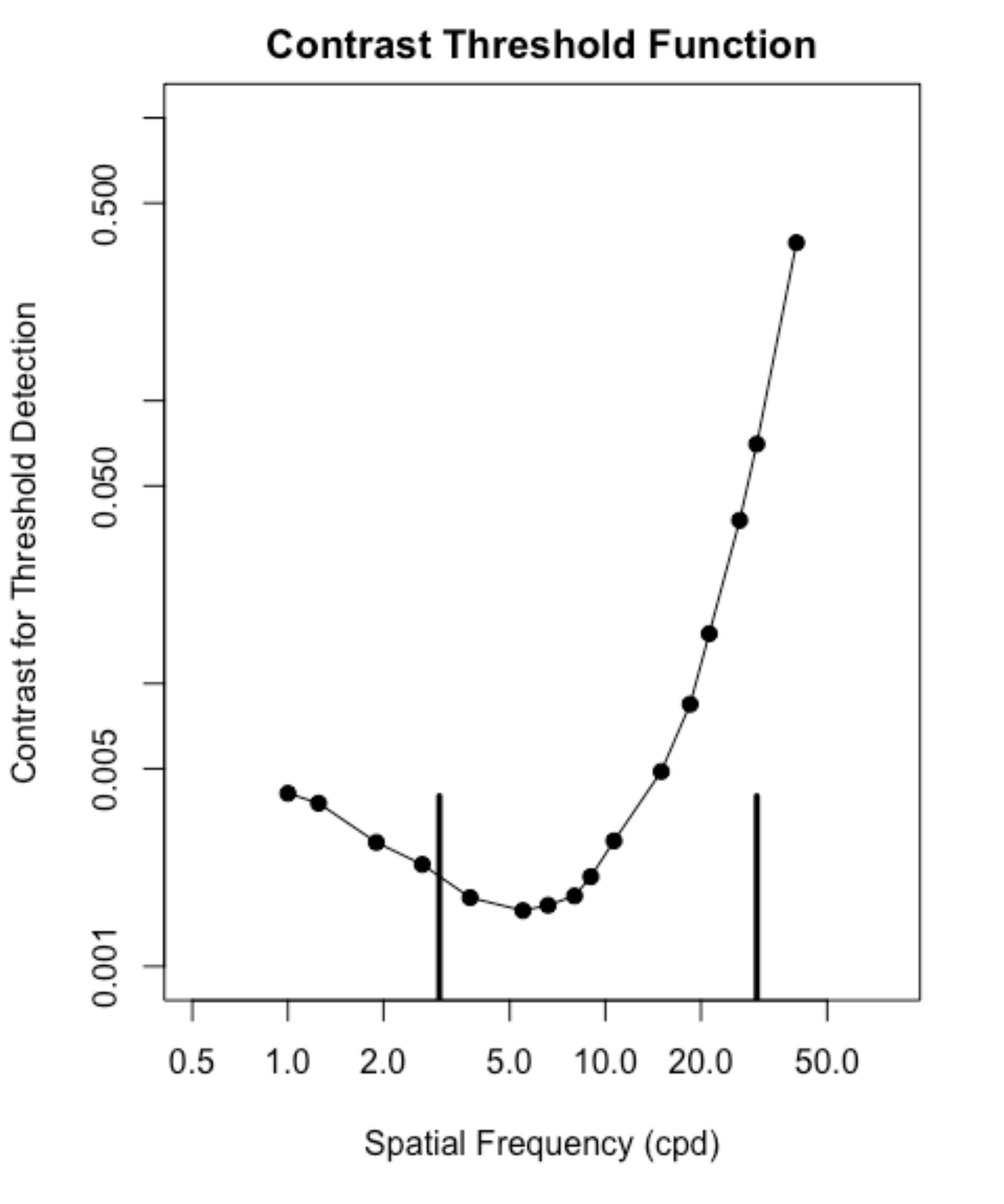
Contrast Threshold Function
Contrast for Threshold Detection
0.500
0.050
0.005
0.001
0.5
1.0
2.0
5.0
10.0
20.0
50.0
Spatial Frequency (cpd)

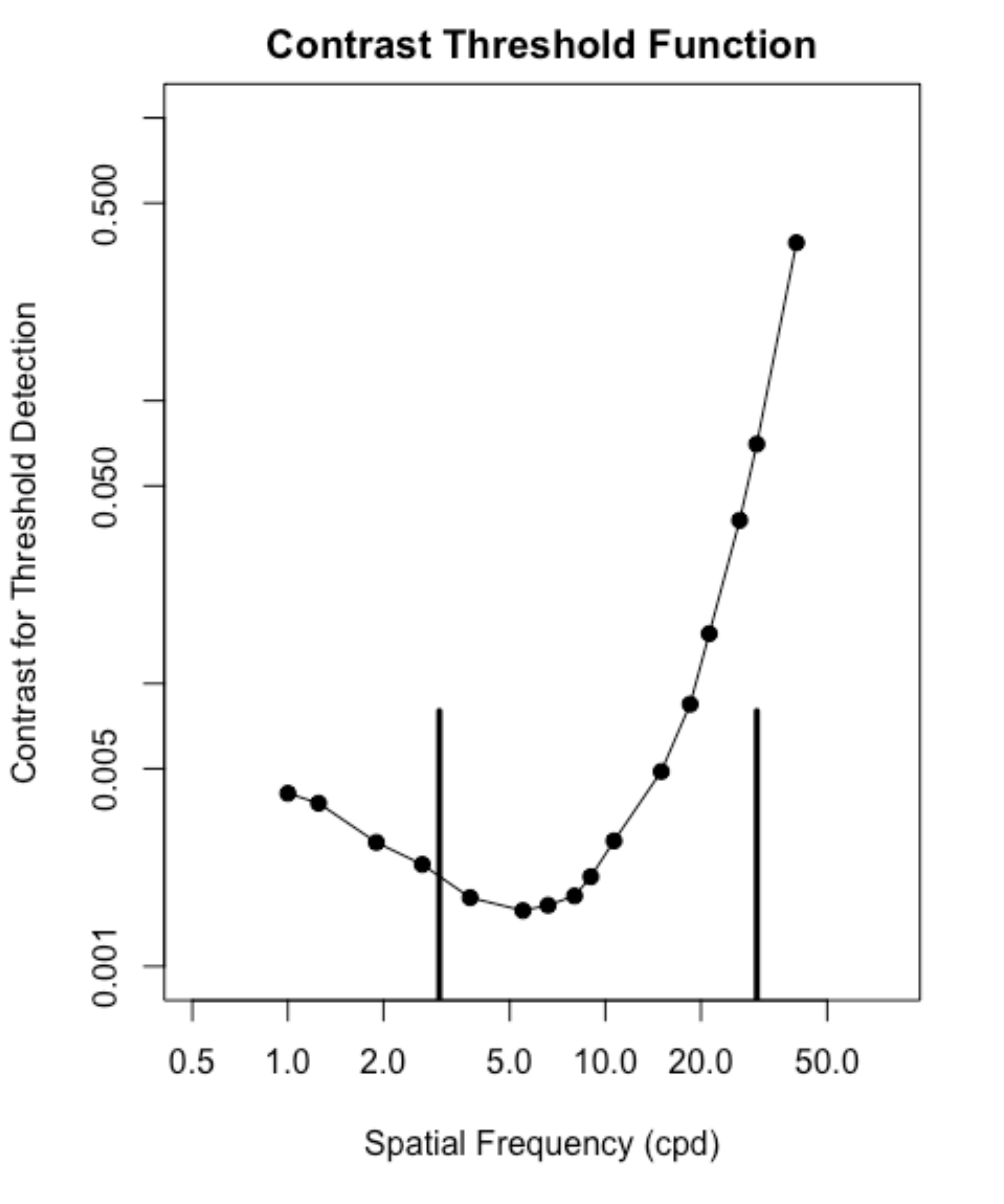
Contrast Threshold Function
Contrast for Threshold Detection
0.500
0.050
0.005
0.001
0.5
1.0
2.0
5.0
10.0
20.0
50.0
Spatial Frequency (cpd)

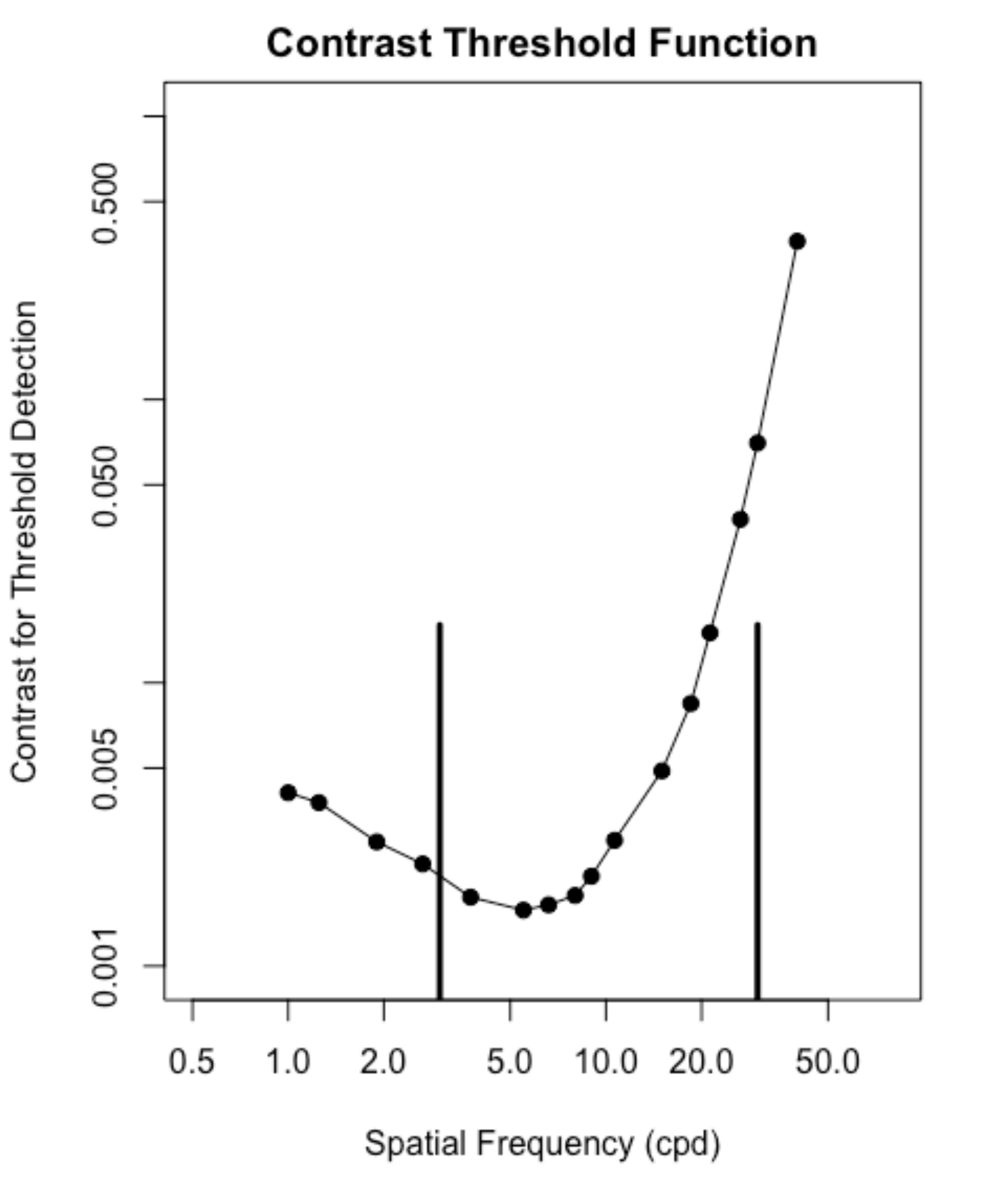

Contrast Threshold Function
Contrast for Threshold Detection
0.001
0.005
0.050
0.500
0.5
1.0
2.0
5.0
10.0
20.0
50.0
Spatial Frequency (cpd)

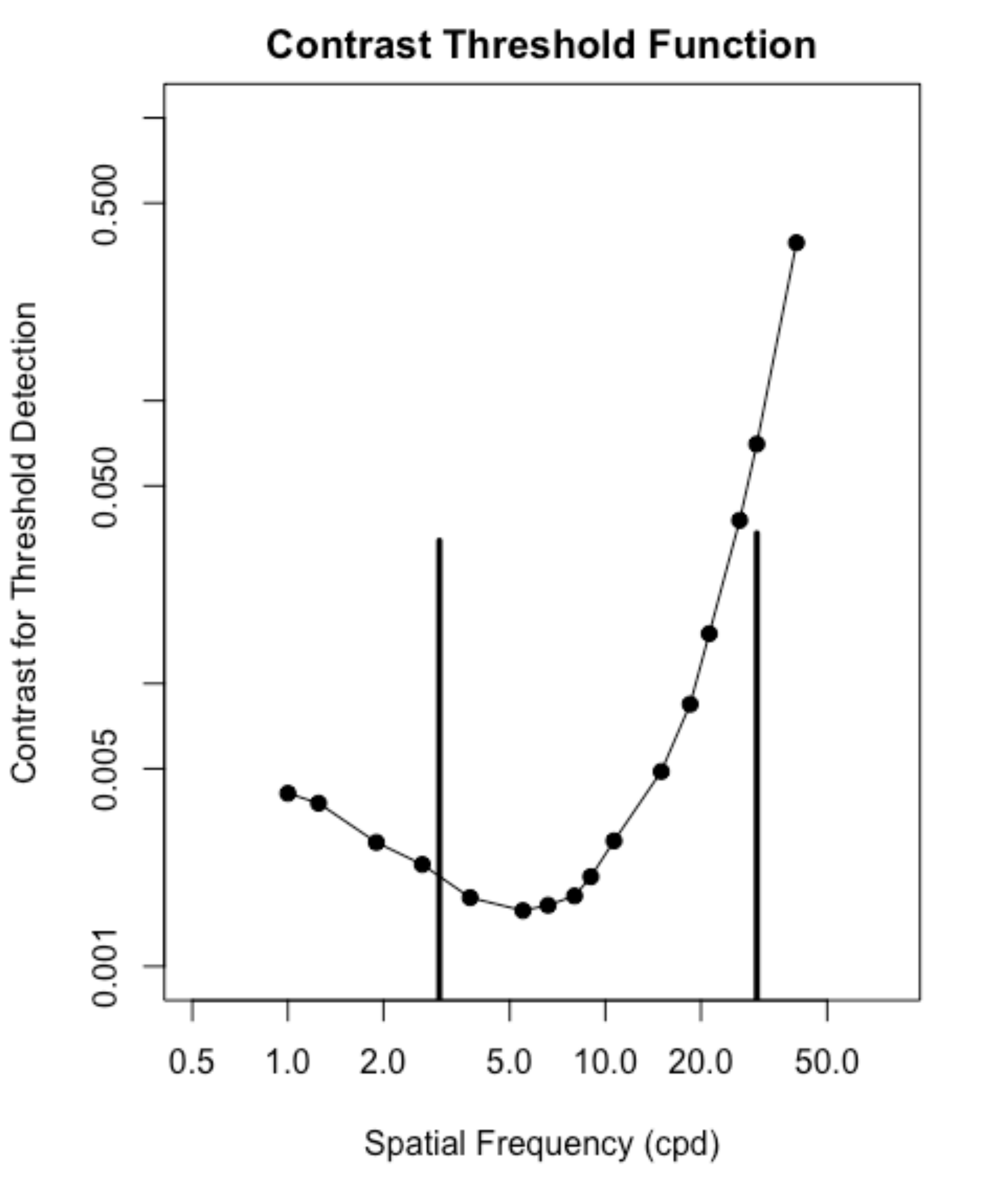
Contrast Threshold Function
Contrast for Threshold Detection
0.001
0.005
0.050
0.500
0.5
1.0
2.0
5.0
10.0
20.0
50.0
Spatial Frequency (cpd)

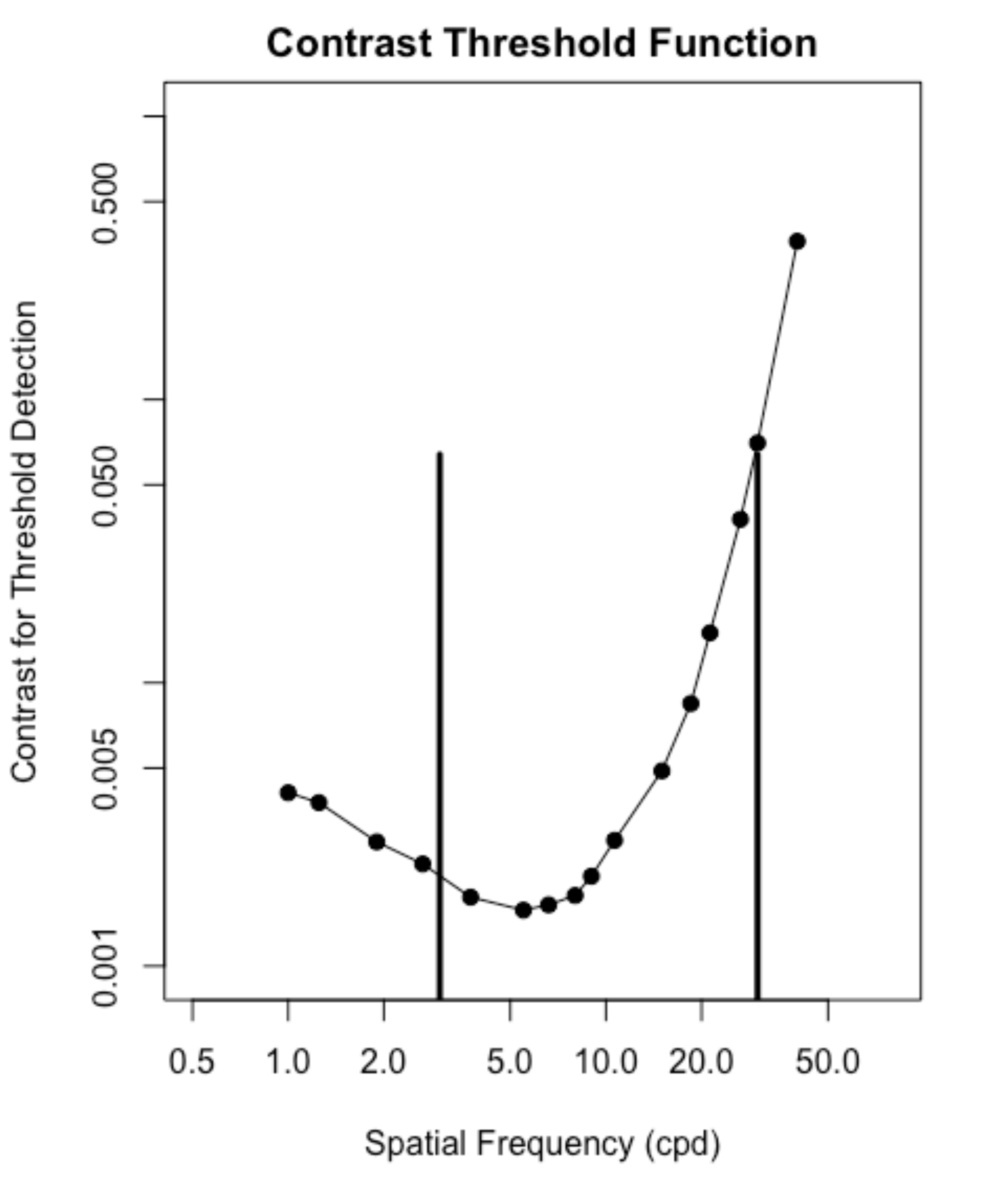

Contrast Threshold Function
Contrast for Threshold Detection
0.500
0.050
0.005
0.001
0.5
1.0
2.0
5.0
10.0
20.0
50.0
Spatial Frequency (cpd)

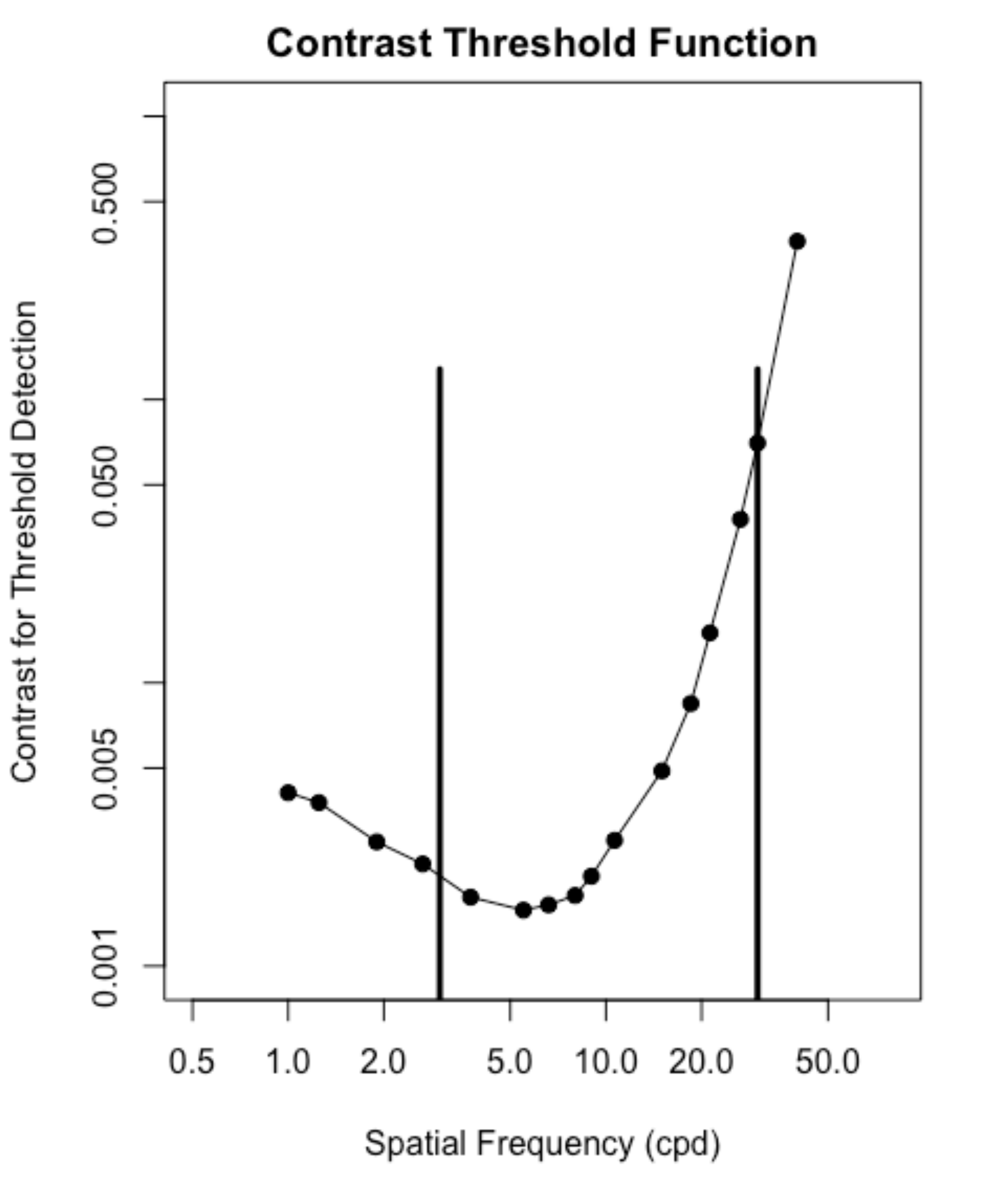
Contrast Threshold Function
Contrast for Threshold Detection
0.500
0.050
0.005
0.001
0.5
1.0
2.0
5.0
10.0
20.0
50.0
Spatial Frequency (cpd)

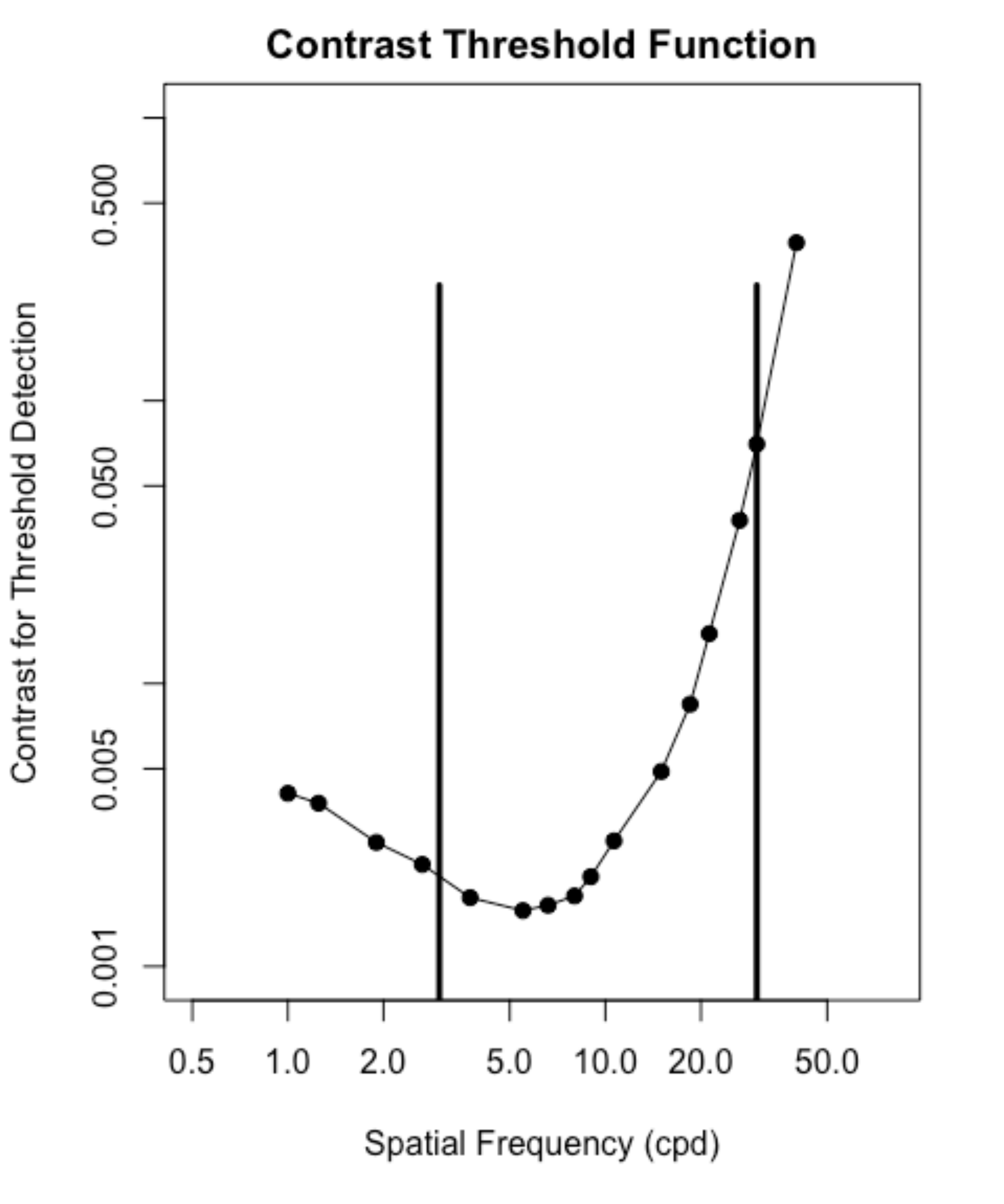
Contrast Threshold Function
Contrast for Threshold Detection
0.500
0.050
0.005
0.001
0.5
1.0
2.0
5.0
10.0
20.0
50.0
Spatial Frequency (cpd)

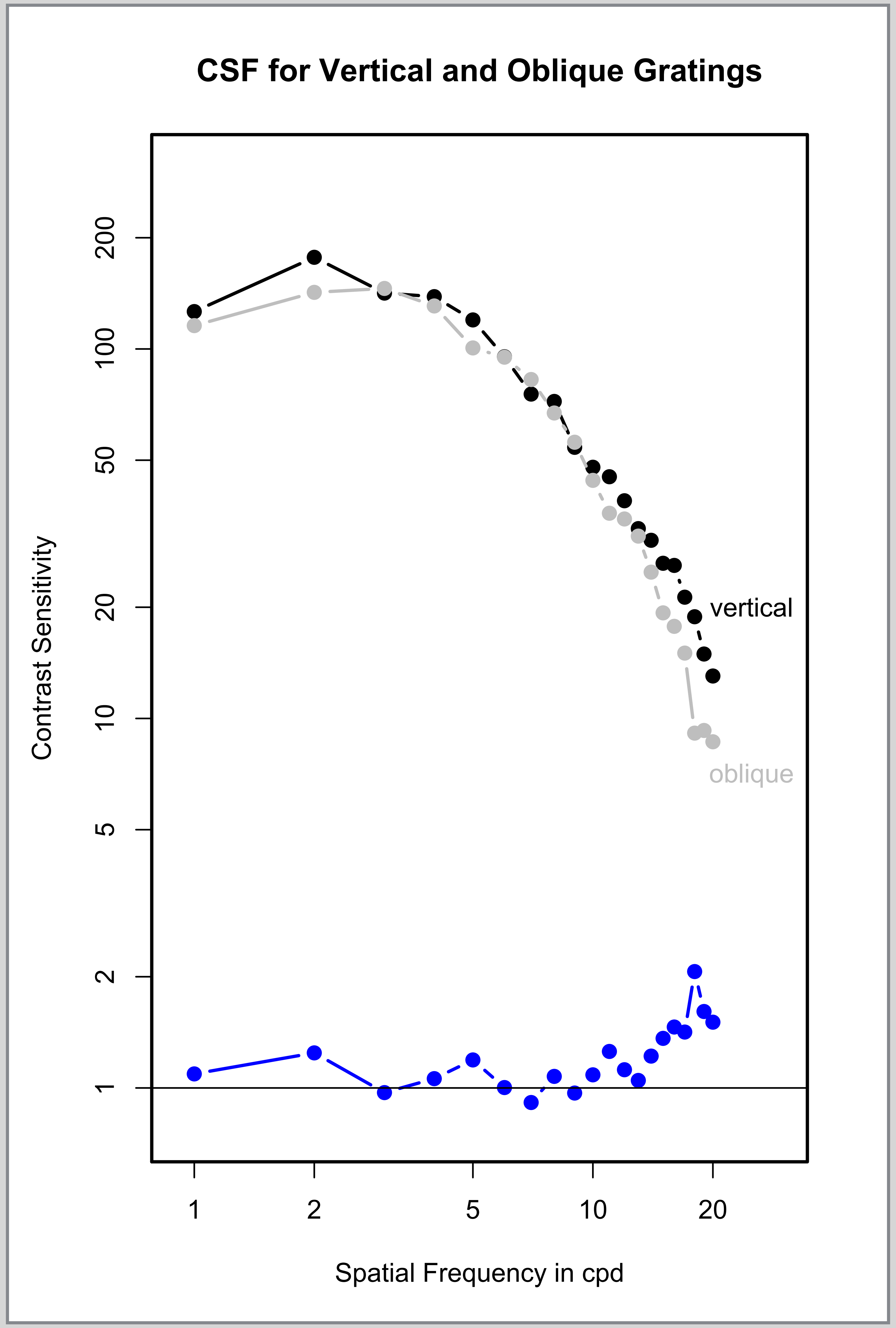

CSF for Vertical and Oblique Gratings
Contrast Sensitivity
200
100
50
20
10
5
2
1
vertical
oblique
1
2
5
10
20
Spatial Frequency in cpd

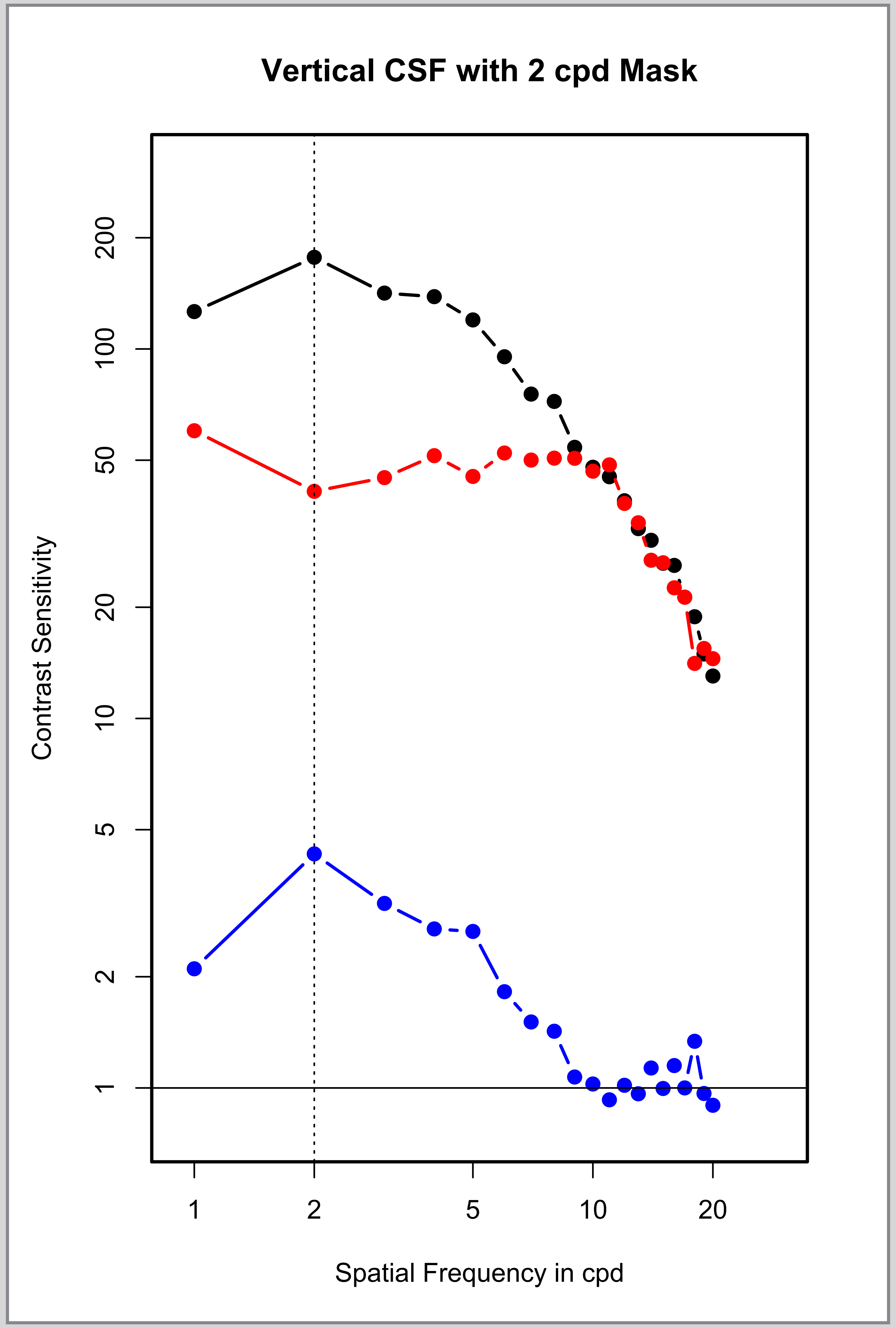

Vertical CSF with 2 cpd Mask
Contrast Sensitivity
200
100
50
20
10
5
2
1
1
2
5
10
20
Spatial Frequency in cpd

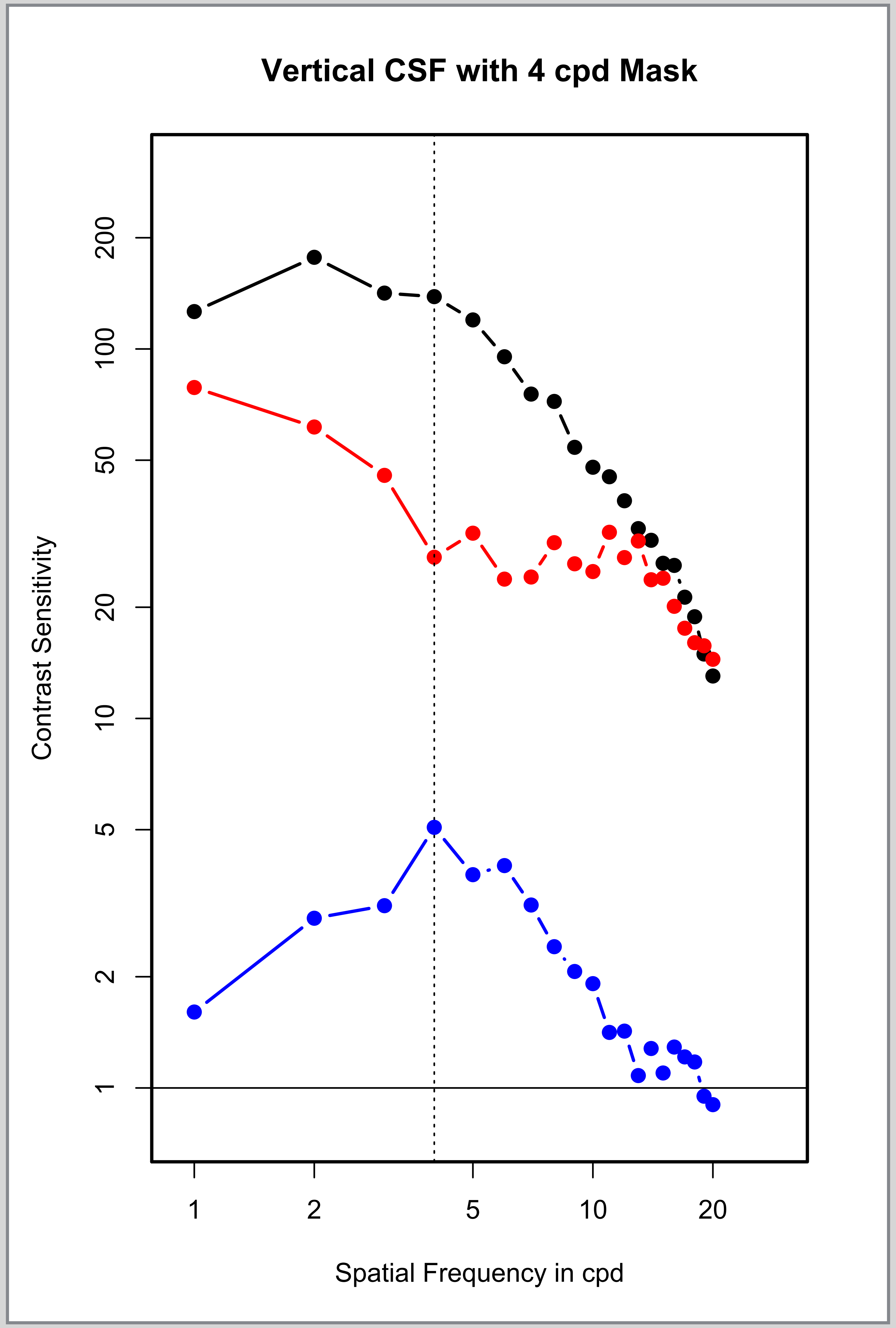

Vertical CSF with 4 cpd Mask
Contrast Sensitivity
200
100
50
20
10
5
2
1
1
2
5
10
20
Spatial Frequency in cpd

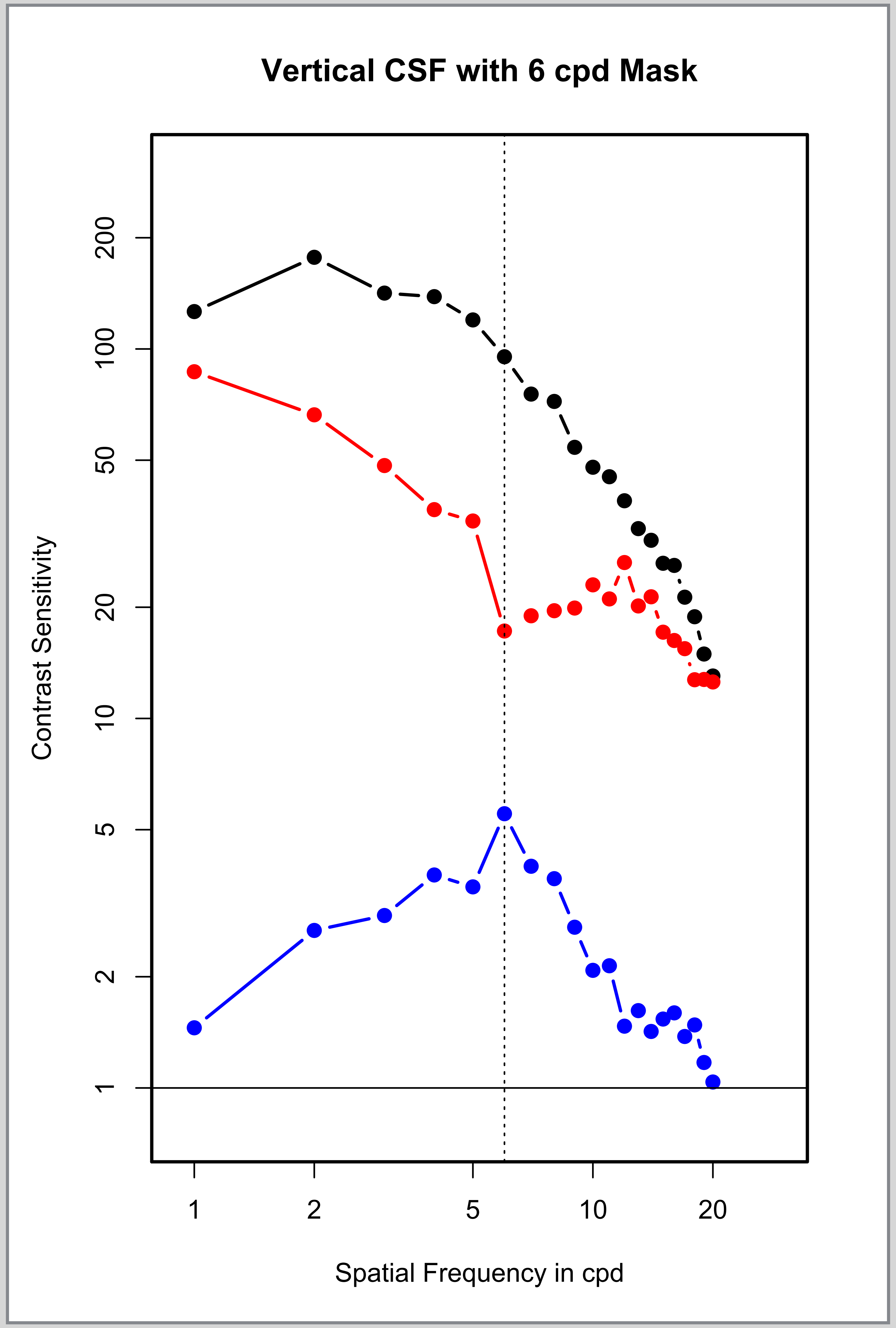
Vertical CSF with 6 cpd Mask
Contrast Sensitivity
200
100
50
20
10
5
2
1
1
2
5
10
20
Spatial Frequency in cpd

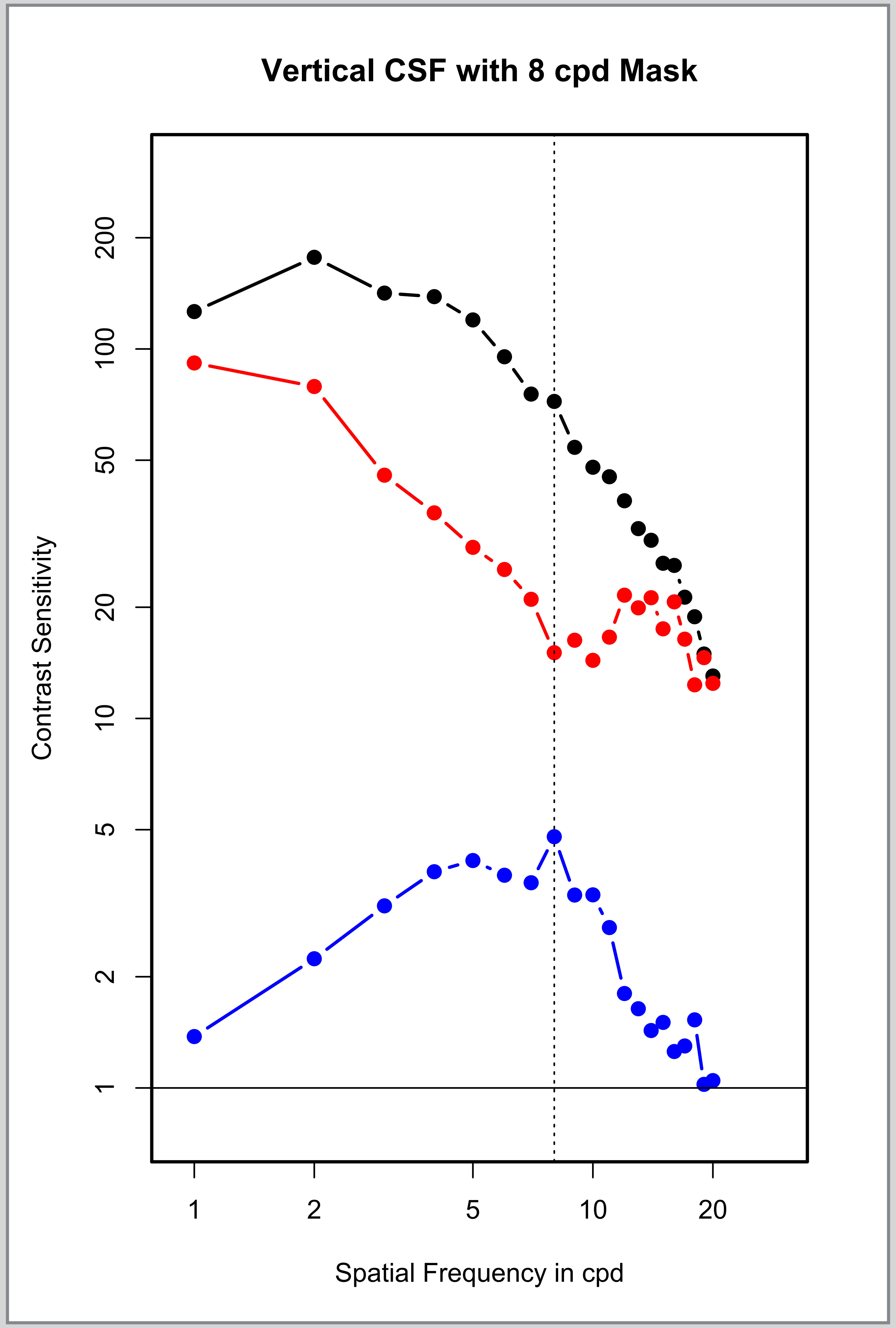

Vertical CSF with 8 cpd Mask
Contrast Sensitivity
200
100
50
20
10
5
2
1
1
2
5
10
20
Spatial Frequency in cpd

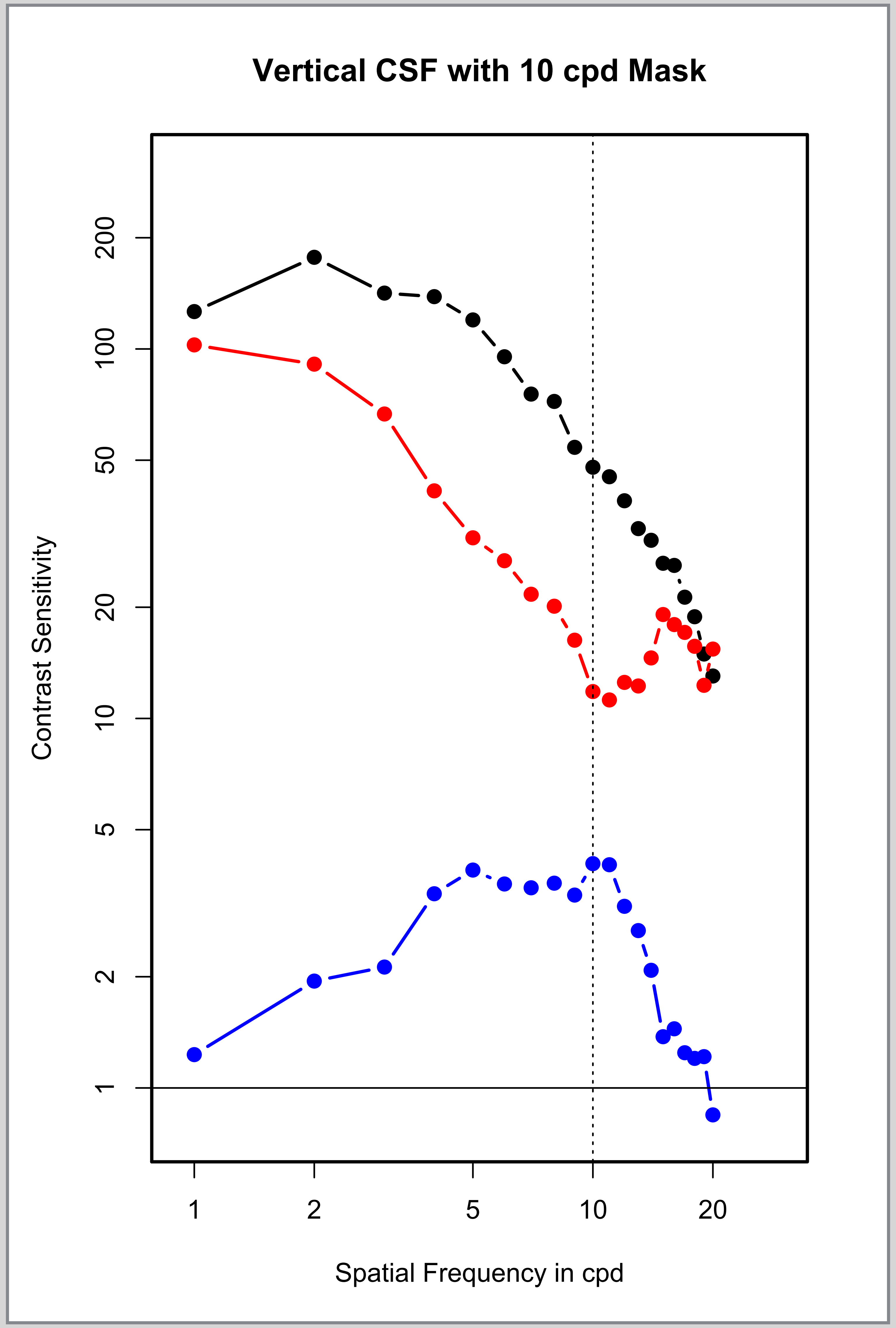

Vertical CSF with 10 cpd Mask
Contrast Sensitivity
200
100
50
20
10
5
2
1
1
2
5
10
20
Spatial Frequency in cpd

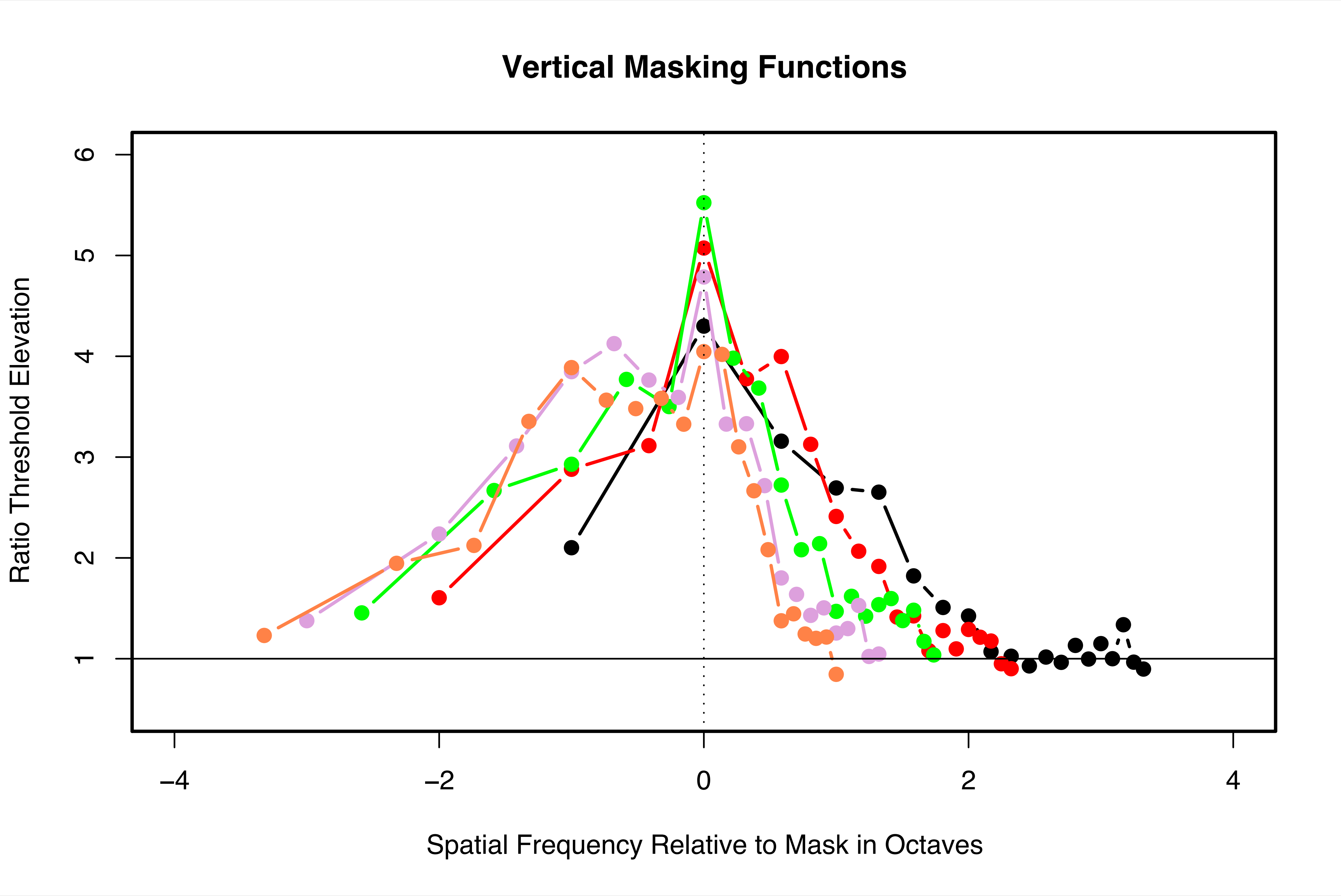
Vertical Masking Functions
Ratio Threshold Elevation
1
2
3
4
5
6
−4
−2
0
2
4
Spatial Frequency Relative to Mask in Octaves

CSFs of Various Animals

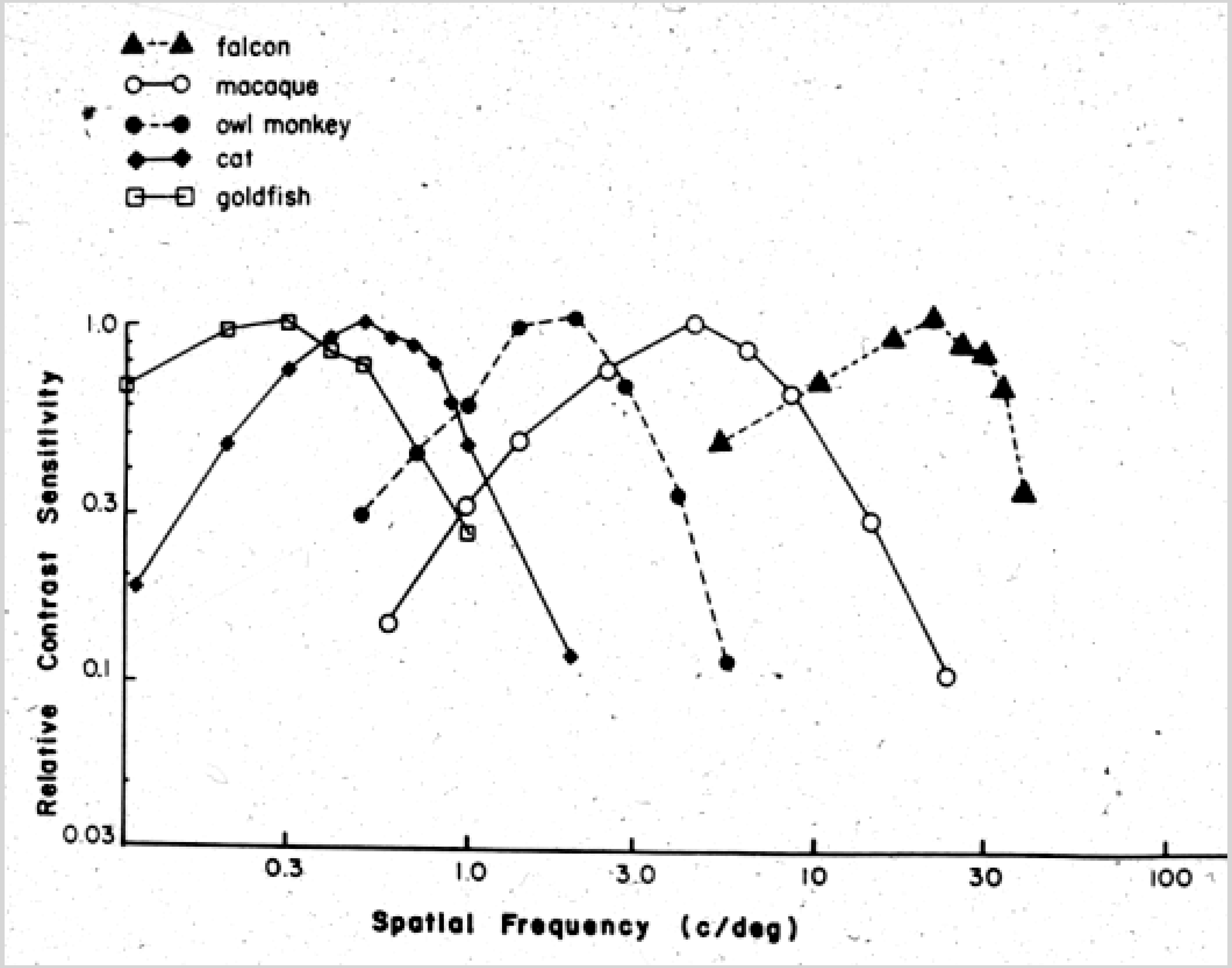

de Valois, R. L., & de Valois, K. K. (1988). *Spatial vison.* New York: Oxford University Press.

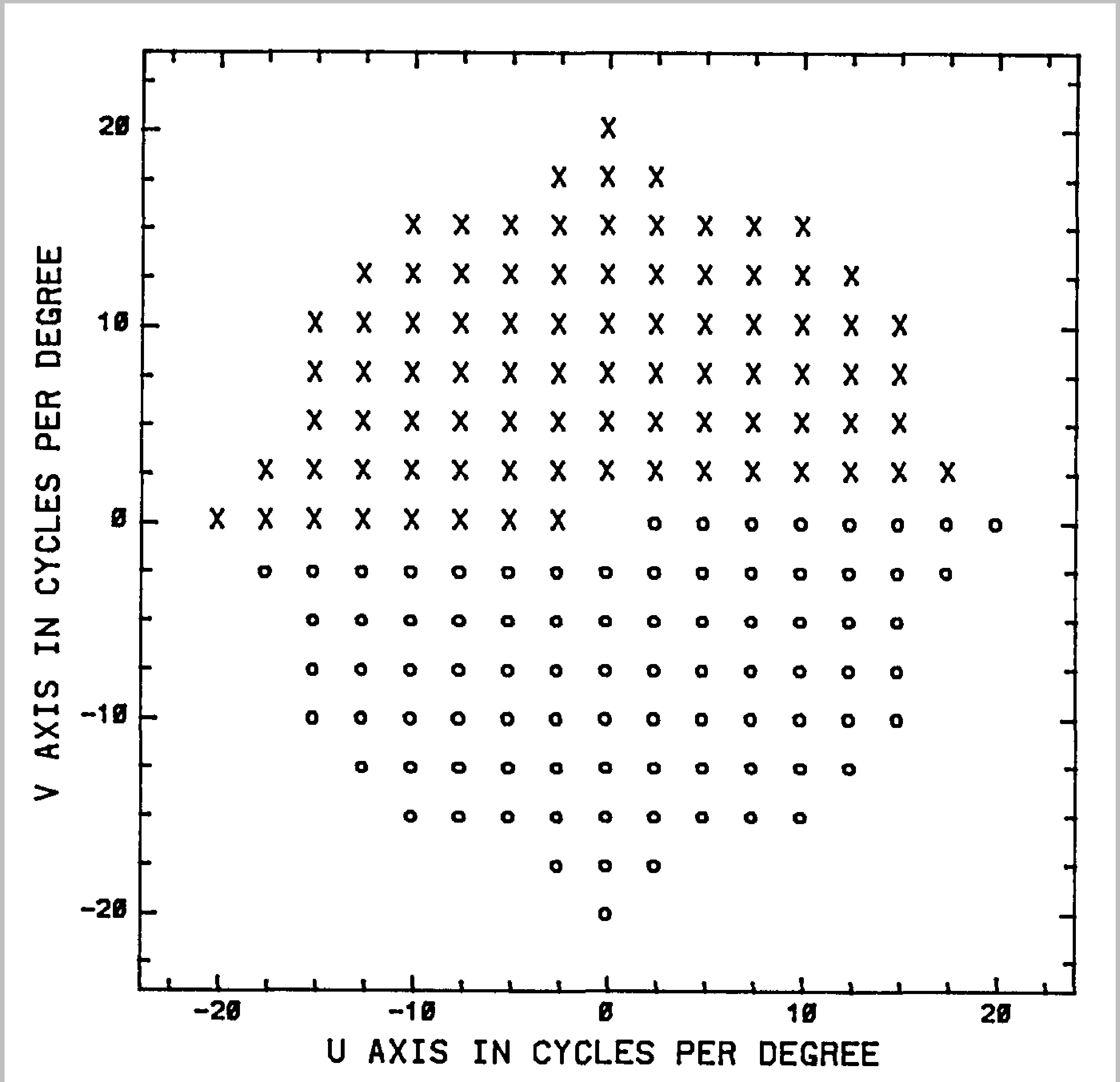

Harvey, L. O., Jr., & Doan, V. V. (1990). Visual masking at different polar angles in the two-dimensional Fourier plane. *Journal of the Optical Society of America A, 7*(1), 116127.

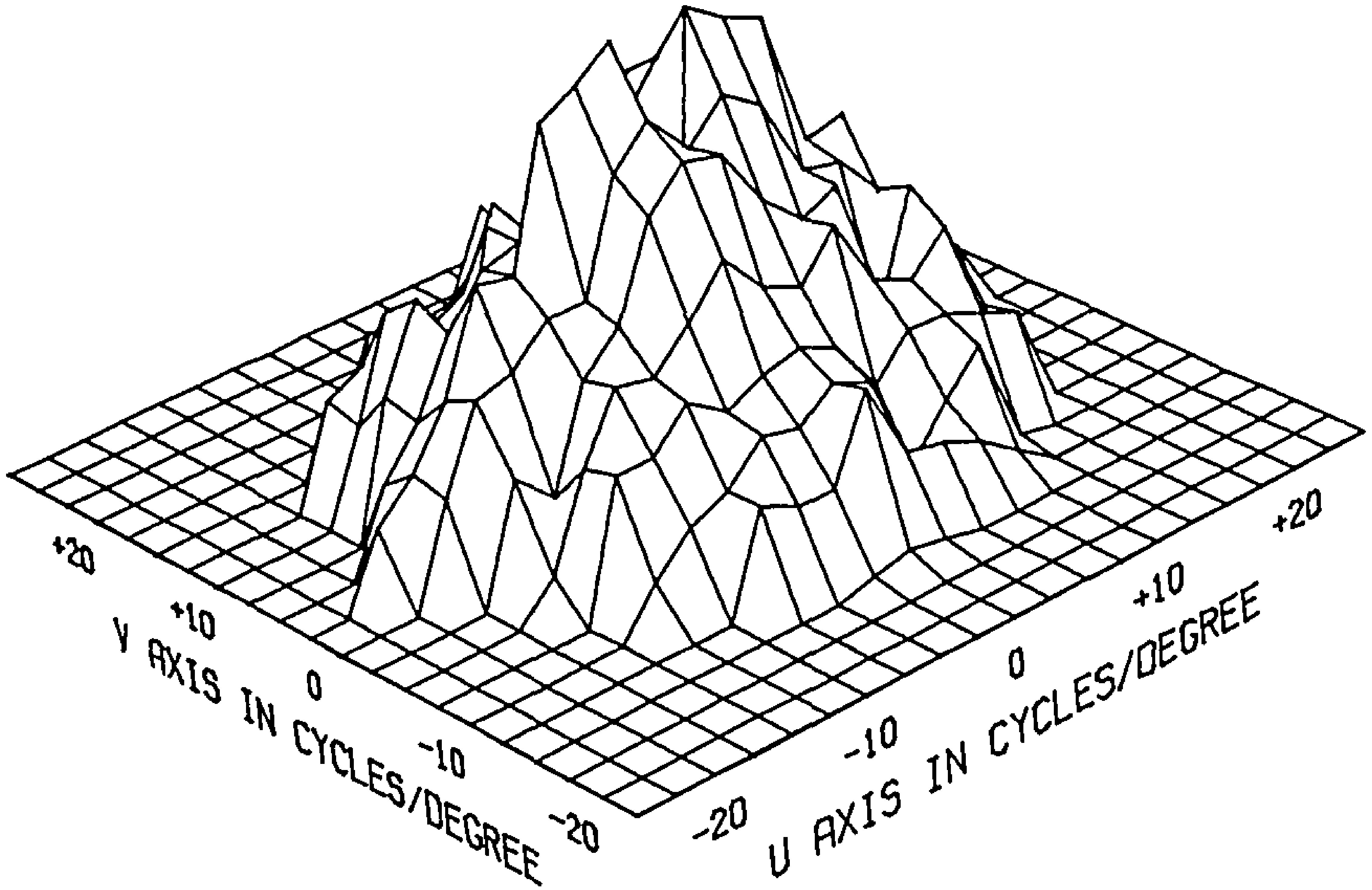

Fig. 2. Log contrast sensitivity as a function of horizontal (u) and vertical (v) spatial-frequency coordinates in cycles per degree of visual angle, with sinusoidal test gratings for observer VVD. The height of the surface represents contrast sensitivity: the reciprocal of the grating contrast required to achieve 75.5% correct on a 3AFC detection task.

Harvey, L. O., Jr., & Doan, V. V. (1990). Visual masking at different polar angles in the two-dimensional Fourier plane. *Journal of the Optical Society of America A, 7*(1), 116127.

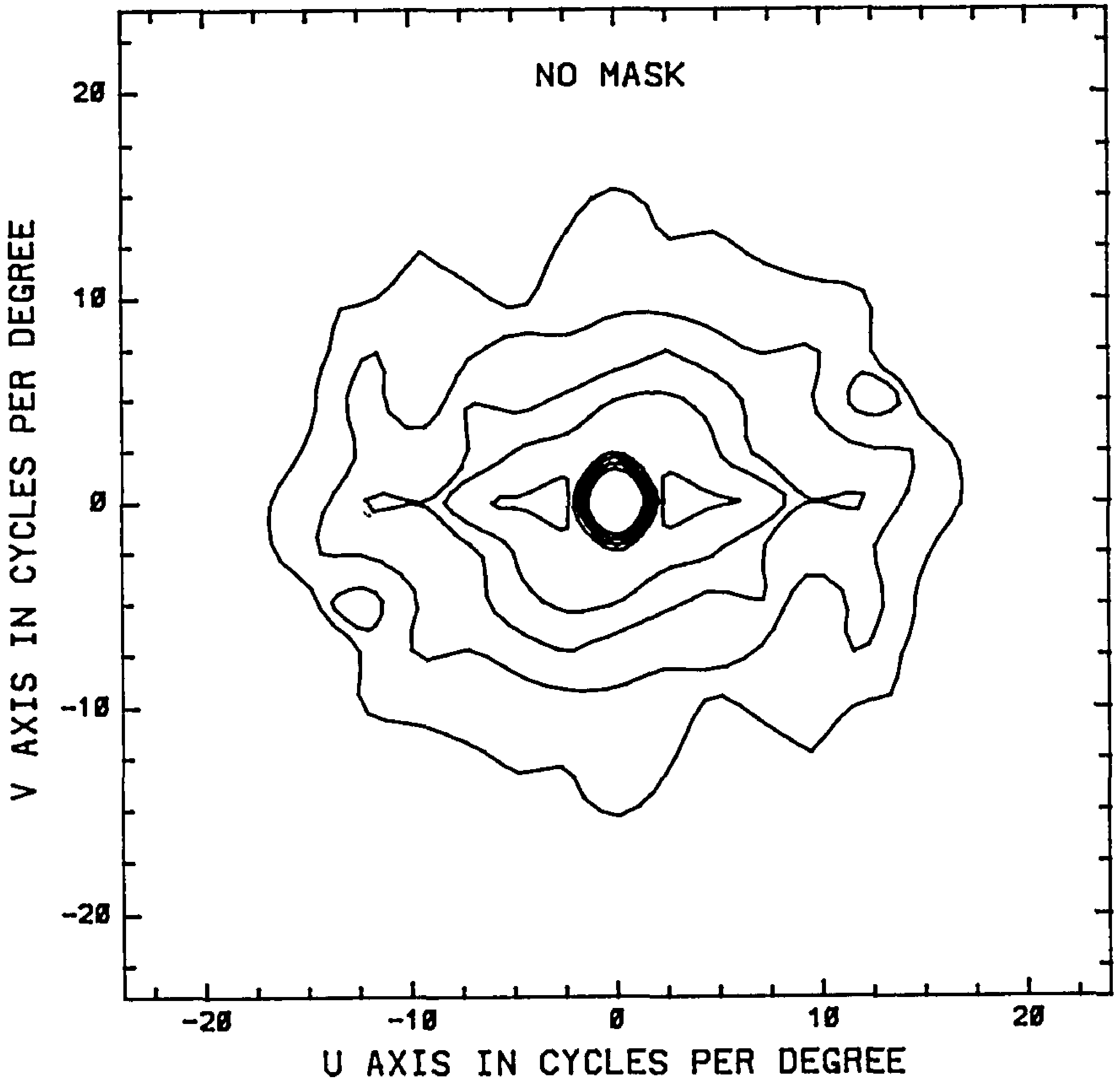

Fig. 3. Isosensitivity contours of VVD's unmasked 2-D contrast sensitivity function plotted in the (u, v) spatial-frequency plane. The outer contour represents a sensitivity of 20, and each contour is an increment of 0.2 log unit in sensitivity.

Harvey, L. O., Jr., & Doan, V. V. (1990). Visual masking at different polar angles in the two-dimensional Fourier plane. *Journal of the Optical Society of America A, 7*(1), 116127.

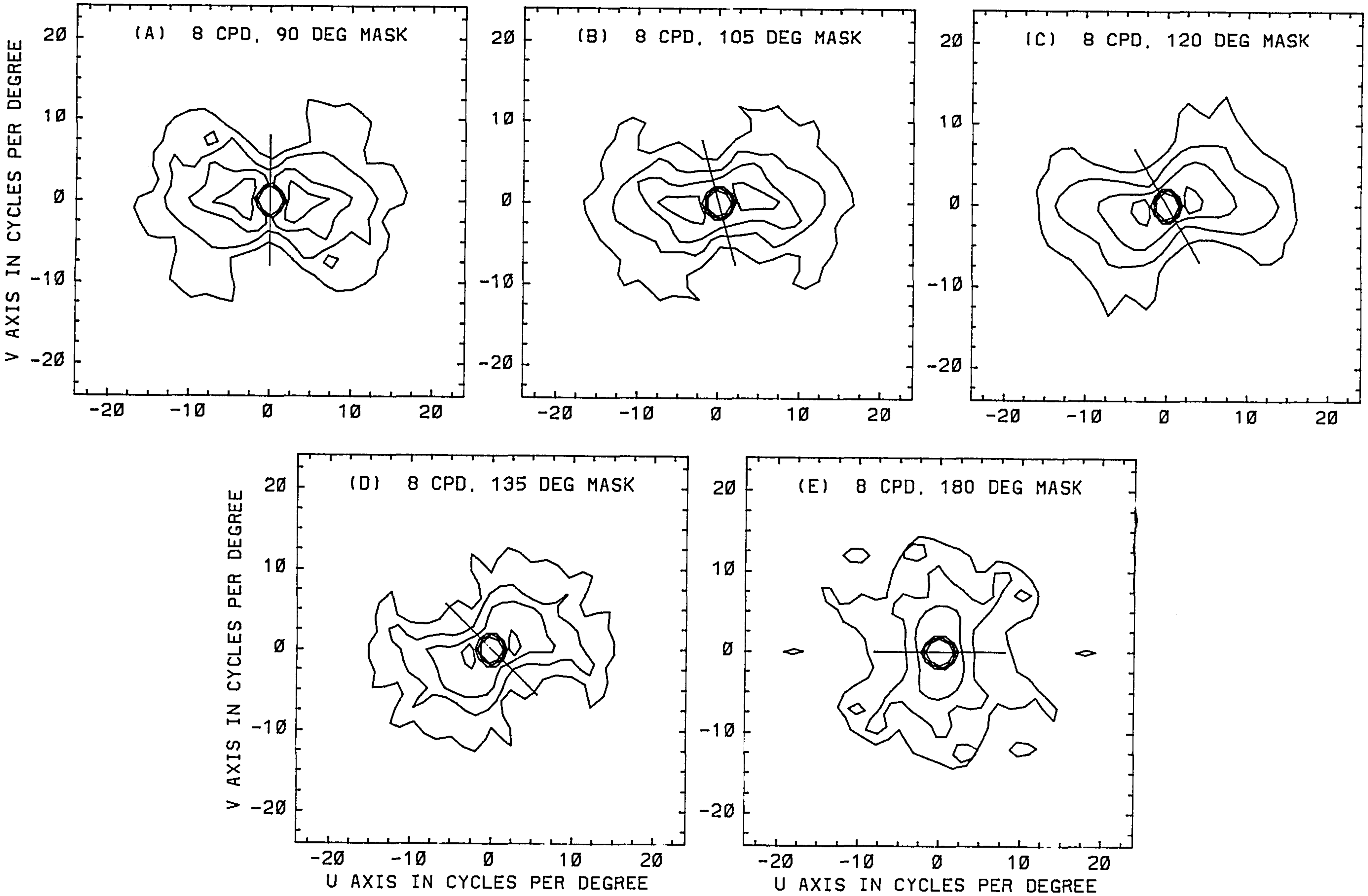

Fig. 4. Isosensitivity contours measured in the presence of an 8-cpd mask, at 0.31 contrast for observer VVD. The ends of the straight line mark the spatial-frequency locus of the mask. Note that the contours are distorted in the region of the mask compared with Fig. 3. Masks were at polar angles of (A) 90.0, (B) 105.0, (C) 120.0, (D) 135.0, and (E) 180.0 deg.

Harvey, L. O., Jr., & Doan, V. V. (1990). Visual masking at different polar angles in the two-dimensional Fourier plane. *Journal of the Optical Society of America A, 7*(1), 116127.

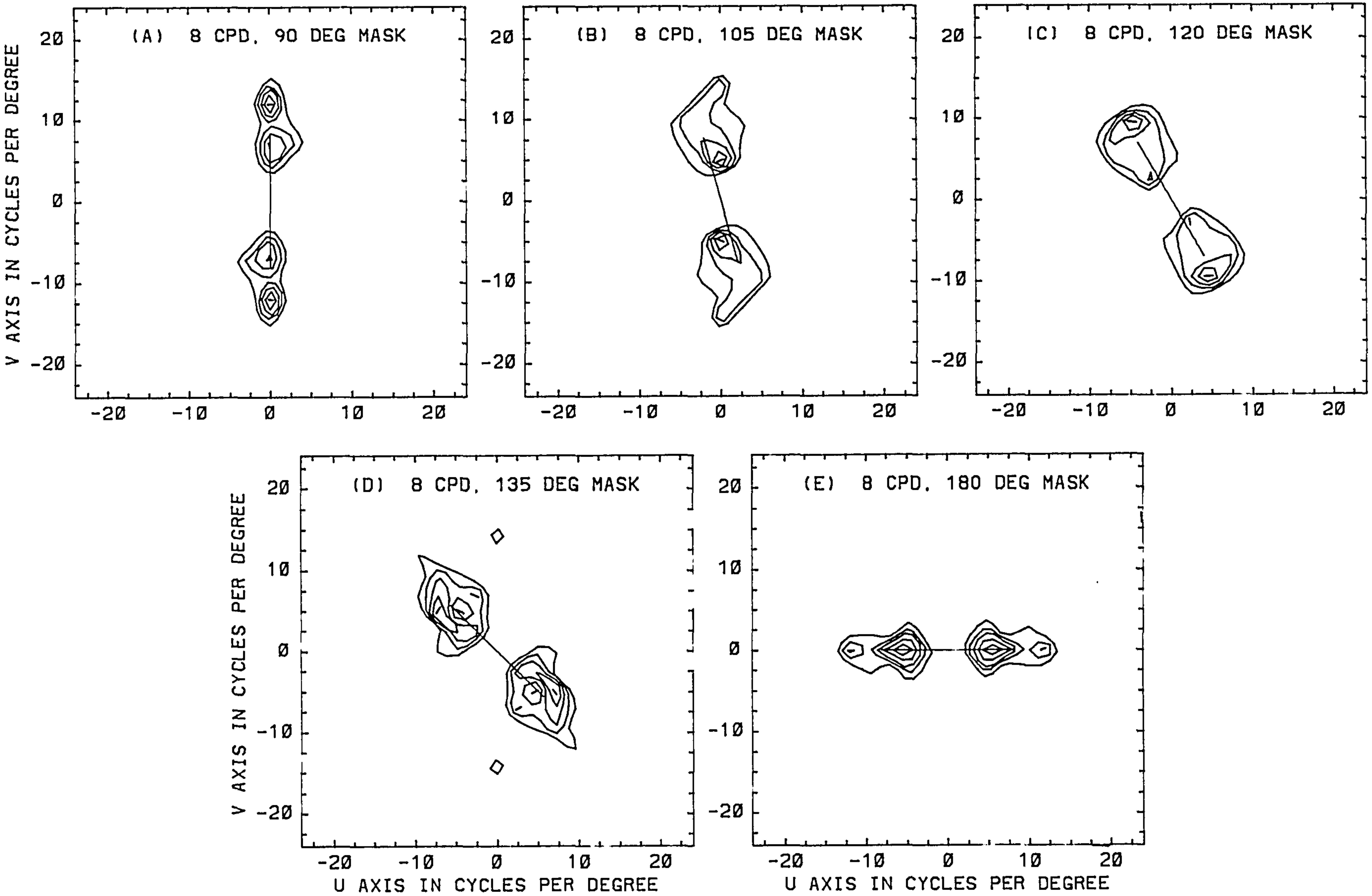

Fig. 5. Proportional threshold elevation contours in horizontal (u) and vertical (v) spatial-frequency space in the presence of an 8-cpd, 0.31-contrast masking grating. The outer contour represents the locus of points where the threshold elevation decreases to $1/e$ of its maximum; the second contour is the 1/2 locus.

Harvey, L. O., Jr., & Doan, V. V. (1990). Visual masking at different polar angles in the two-dimensional Fourier plane. *Journal of the Optical Society of America A, 7*(1), 116127.

Frequency
Domain

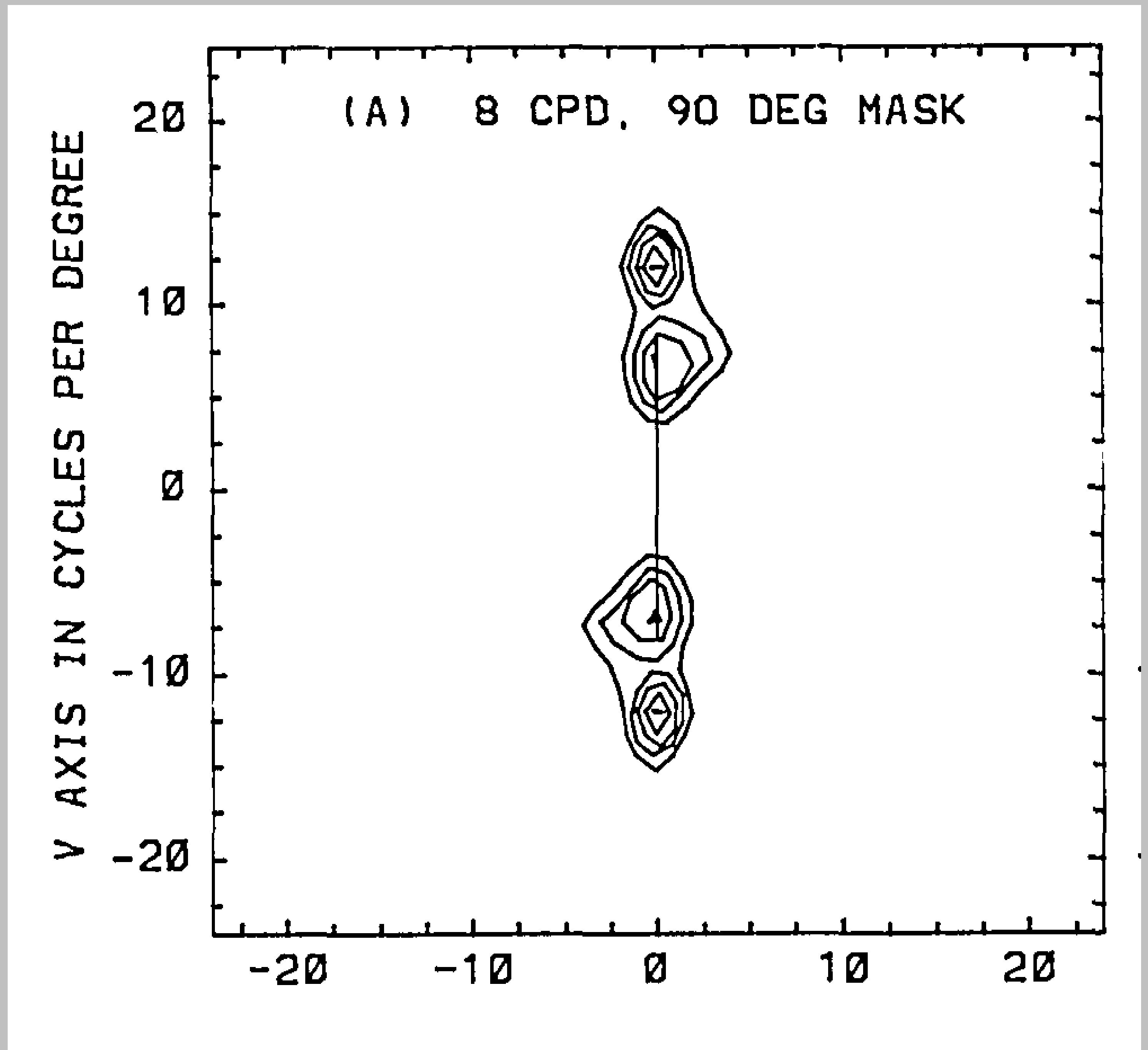

Space
Domain

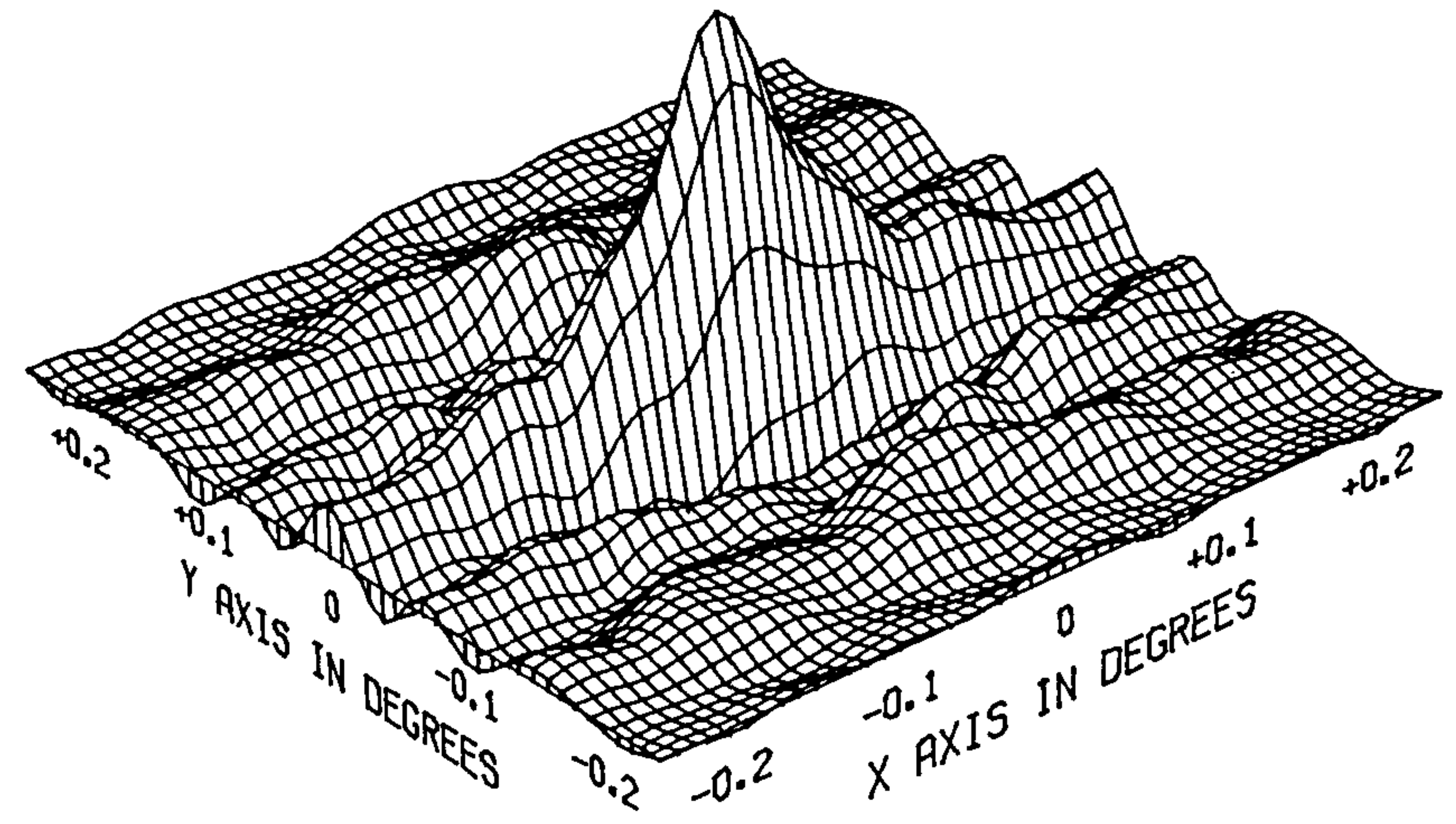

Fig. 10. Even kernel of the inverse Fourier transform of the proportion threshold elevation surface produced by the 8-cpd, 90-deg mask. The coordinate system is in degrees of visual angle, and the origin is in the center of the plane.

Harvey, L. O., Jr., & Doan, V. V. (1990). Visual masking at different polar angles in the two-dimensional Fourier plane. *Journal of the Optical Society of America A, 7*(1), 116127.

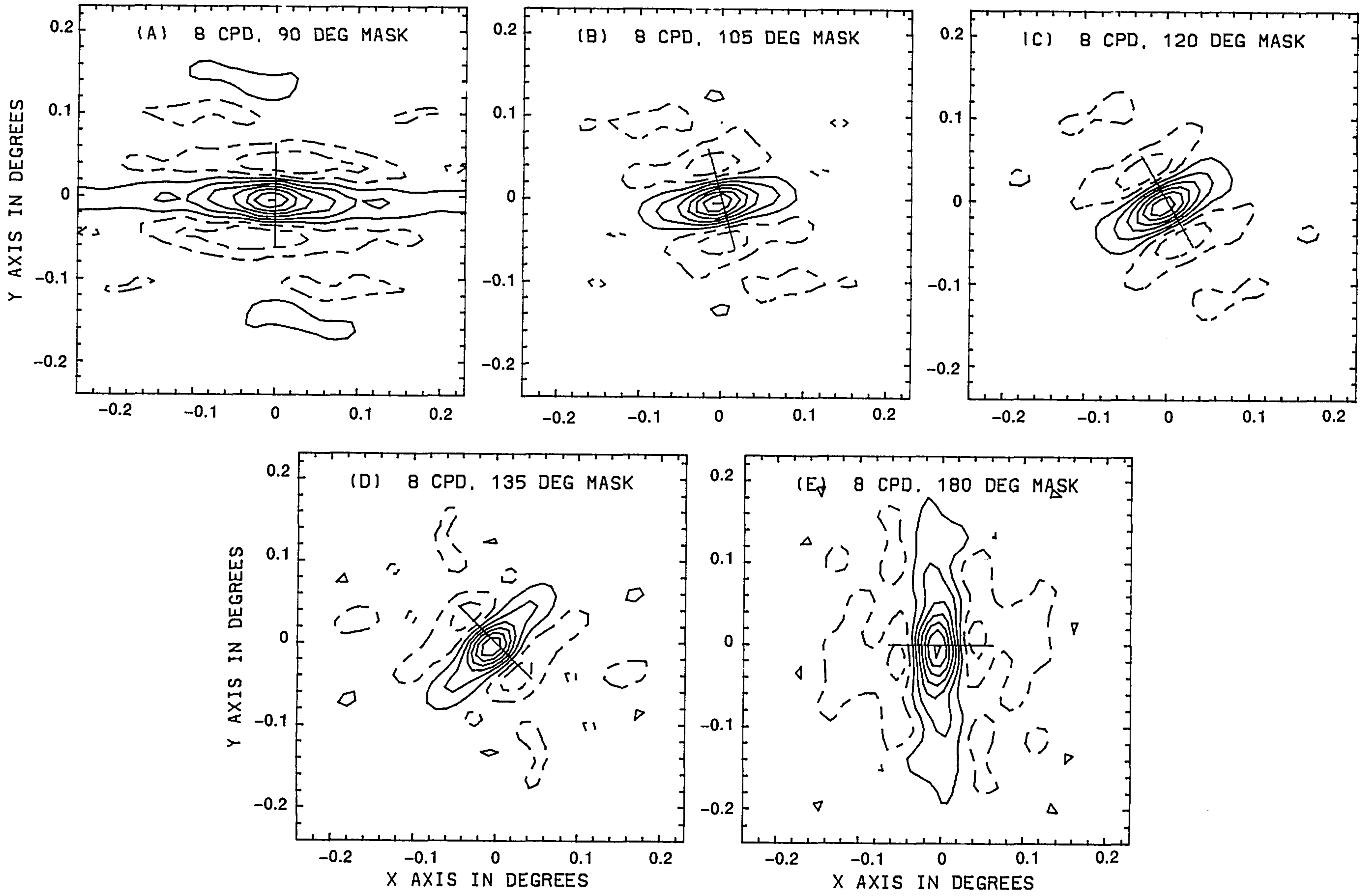

Fig. 11. Contour plots of the even kernel of the inverse Fourier transform of the proportional threshold elevation surfaces produced by an 8-cpd mask of 0.31 contrast. The solid contours show regions of excitation; the dashed contours show regions of inhibition. The short straight line represents the spatial period and orientation of the mask.

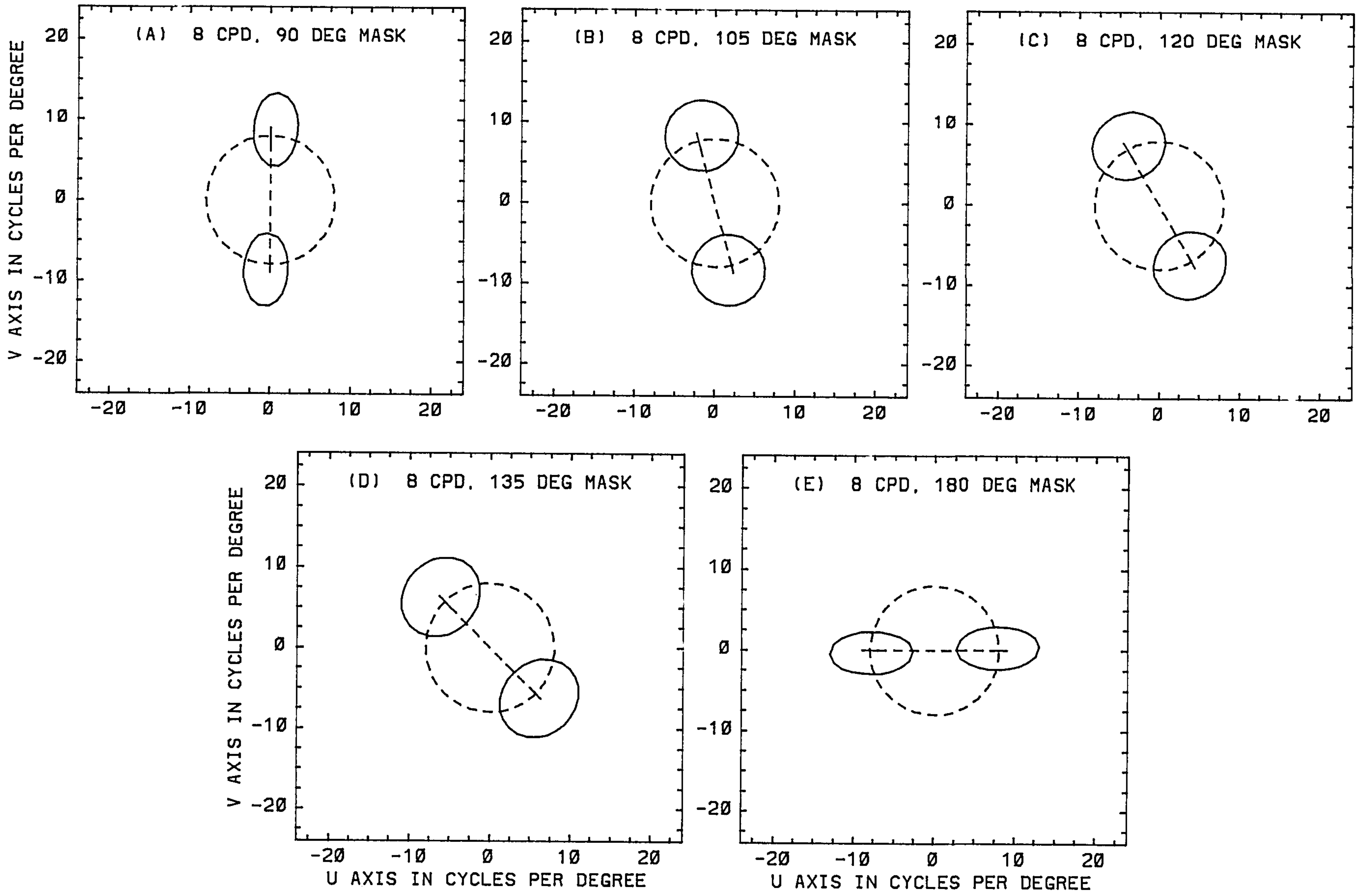

Fig. 12. Half-amplitude contours of the Gaussian envelope of the five Gabor functions fitted to each set of threshold elevation data. The dashed circle marks the 8-cpd locus. The orientation of each line marks the polar orientation of the mask.

Dennis Gabor (1900-1979)

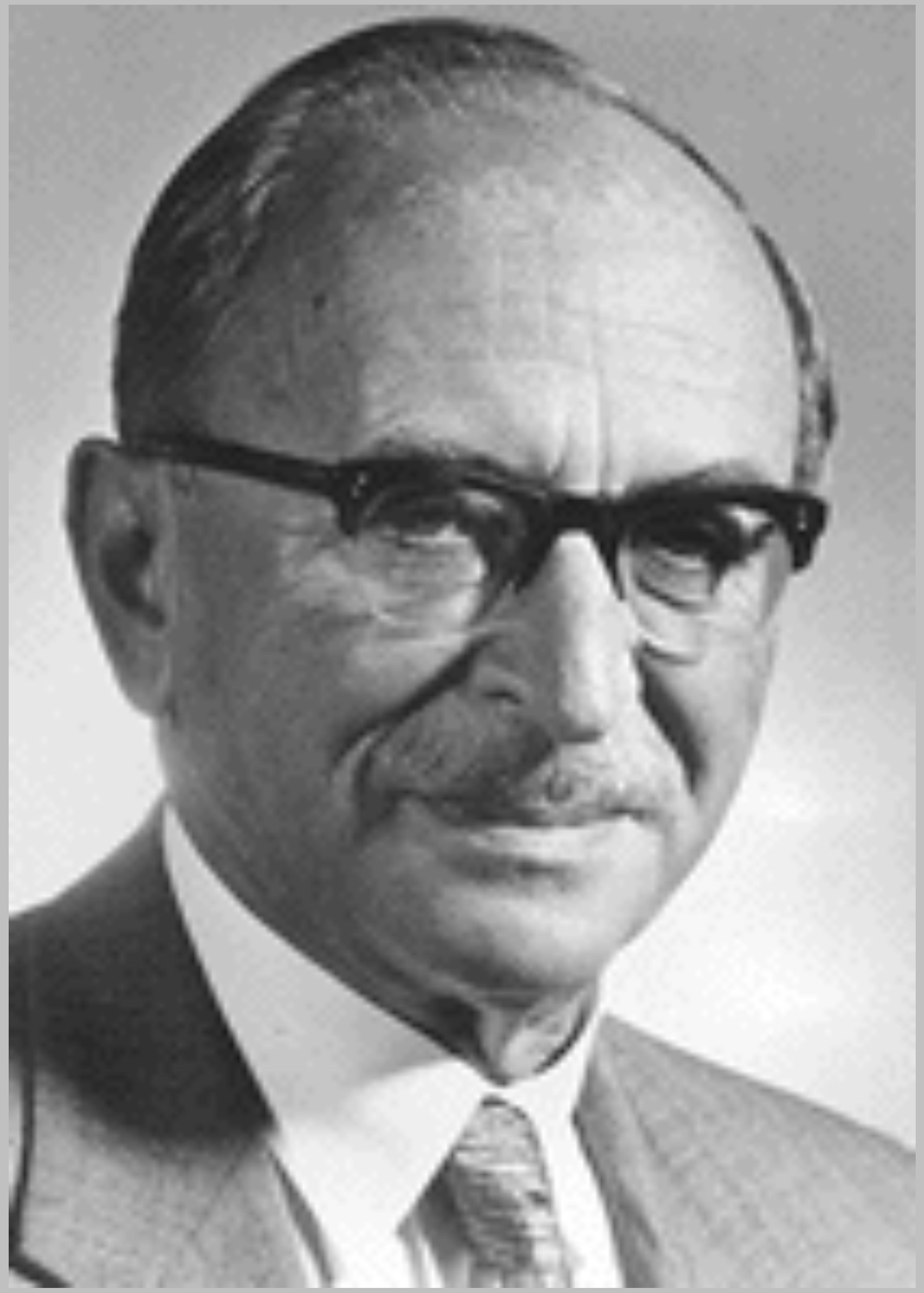

Gabor Function

$$G(x, y) = c \exp[-\pi(x_\phi{}^2 a^2 + y_\phi{}^2 b^2)] \times \exp\{-2\pi i[u_0(x - x_0) + v_0(y - y_0)]\}, \quad (3a)$$

where

$$x_\phi = [(x - x_0)\cos(\phi)] + [(y - y_0)\sin(\phi)],$$

$$y_\phi = -[(x - x_0)\sin(\phi)] + [(y - y_0)\cos(\phi)],$$

and where x and y are the coordinates of spatial position in degrees of visual angle. The form of the Gabor function in the frequency domain is

$$G(u, v) = c \exp\{-\pi[u_\phi{}^2/a^2 + v_\phi{}^2/b^2]\} \times \exp\{-2\pi i[x_0(u - u_0) + y_0(v - v_0)]\}, \quad (3b)$$

where

$$u_\phi = [(u - u_0)\cos(\phi)] + [(v - v_0)\sin(\phi)],$$

$$v_\phi = -[(u - u_0)\sin(\phi)] + [(v - v_0)\cos(\phi)],$$

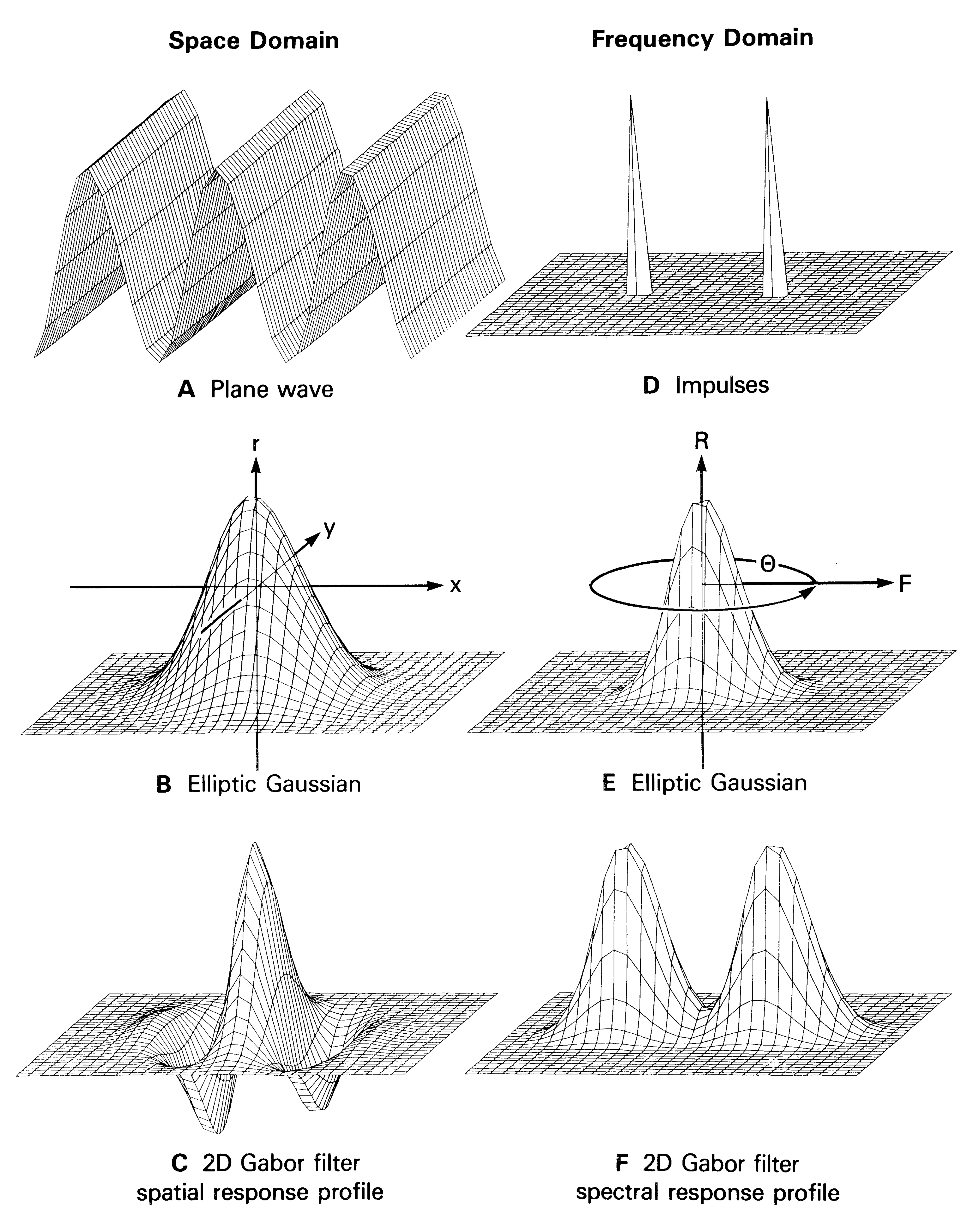

Jones, J. P., & Palmer, L. A. (1987). An evaluation of the two-dimensional Gabor filter model of simple receptive fields in cat striate cortex. *Journal of Neurophysiology, 58*(6), 1233-1258.

Spatial Frequencies: Gabor Patches

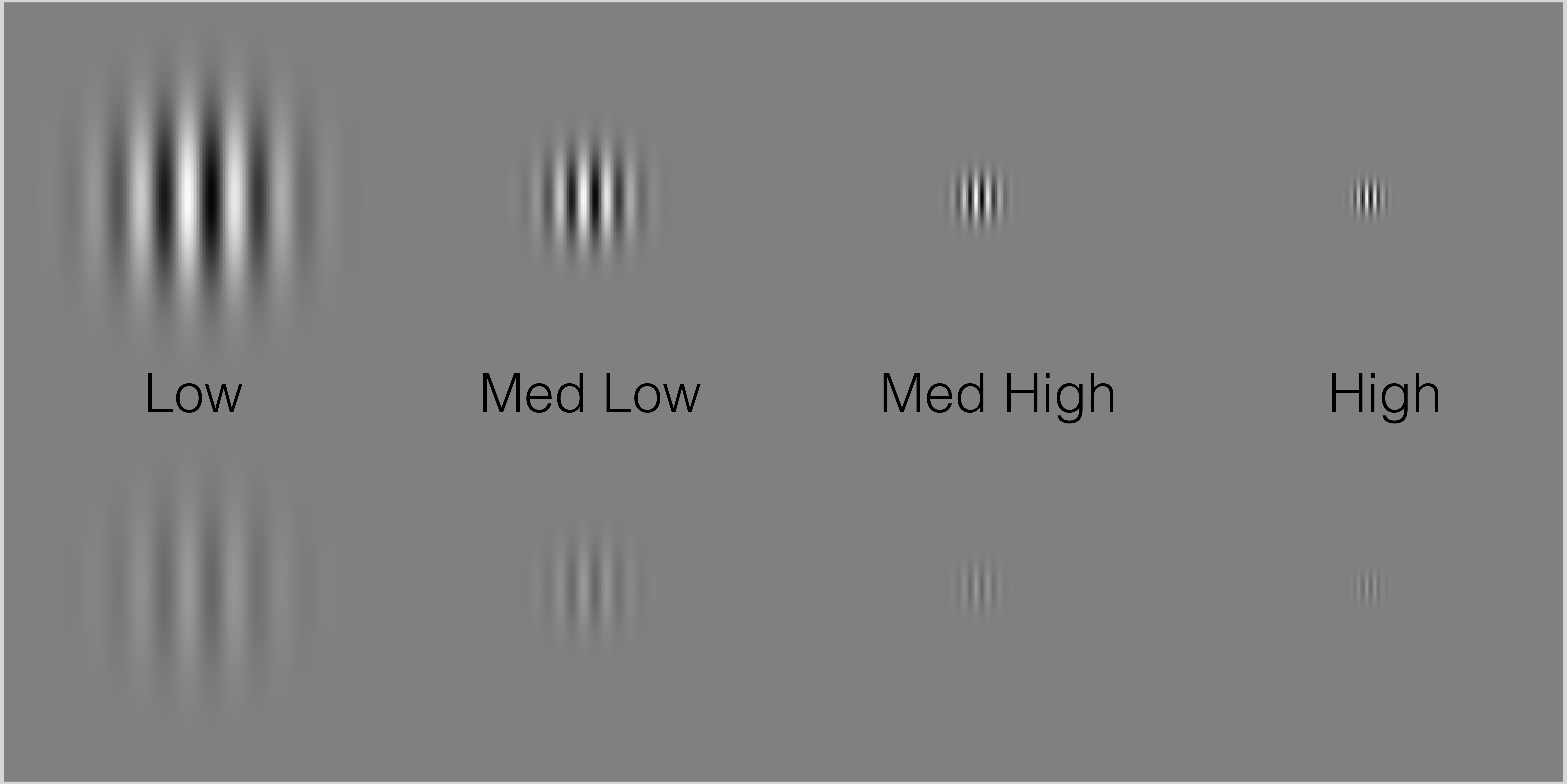

Gabor Function

Cat

Marcelja, S. (1980). Mathematical description of the responses of simple cortical cells. *Journal of the Optical Society of America*, *70*(11), 1297–1300.

Monkey

Daugman, J. G. (1980). Two-dimensional spectral analysis of cortical receptive field profiles. *Vision Research, 20*(10), 847856.

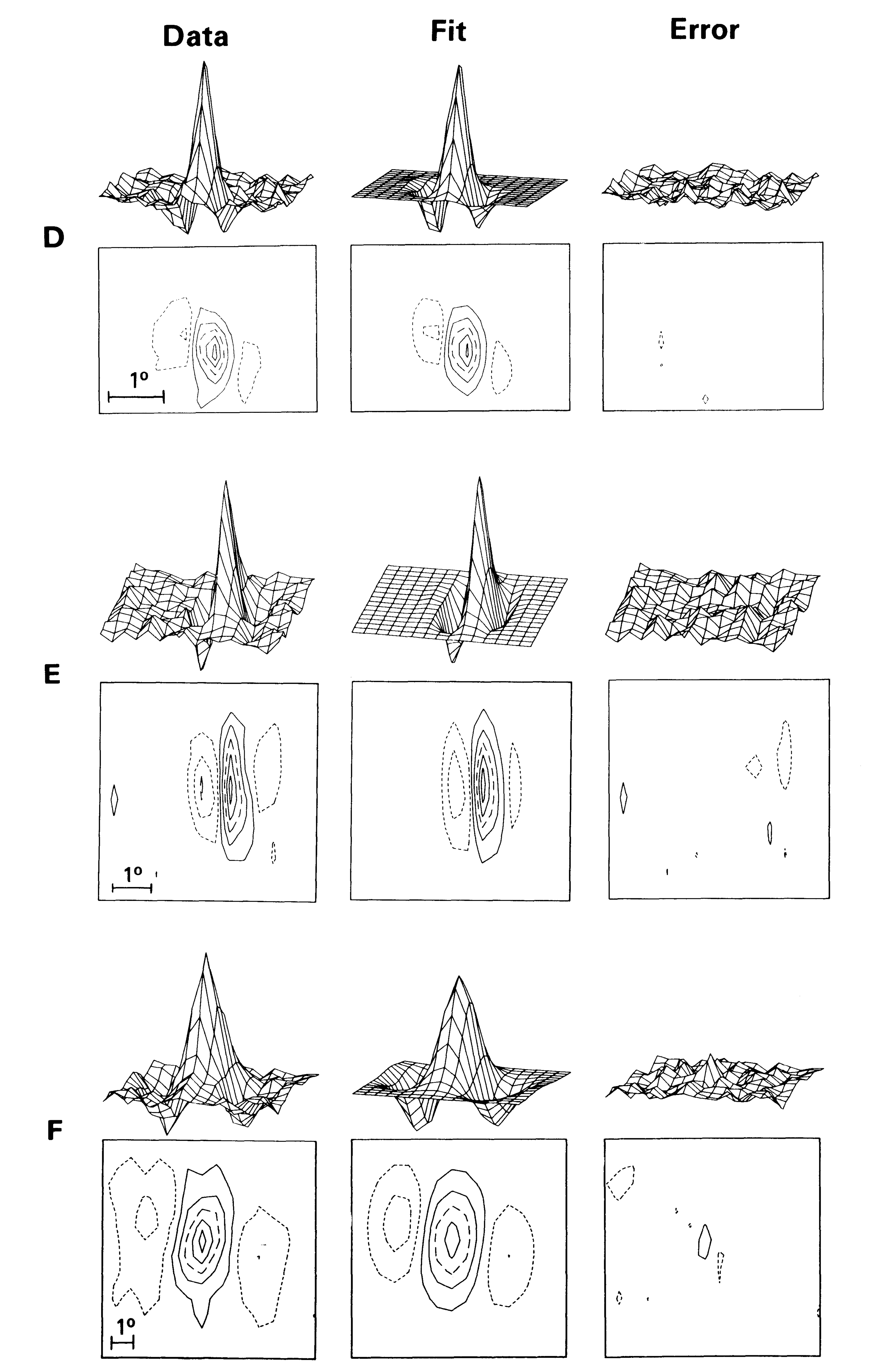

Jones, J. P., & Palmer, L. A. (1987). An evaluation of the two-dimensional Gabor filter model of simple receptive fields in cat striate cortex. *Journal of Neurophysiology, 58*(6), 1233-1258.

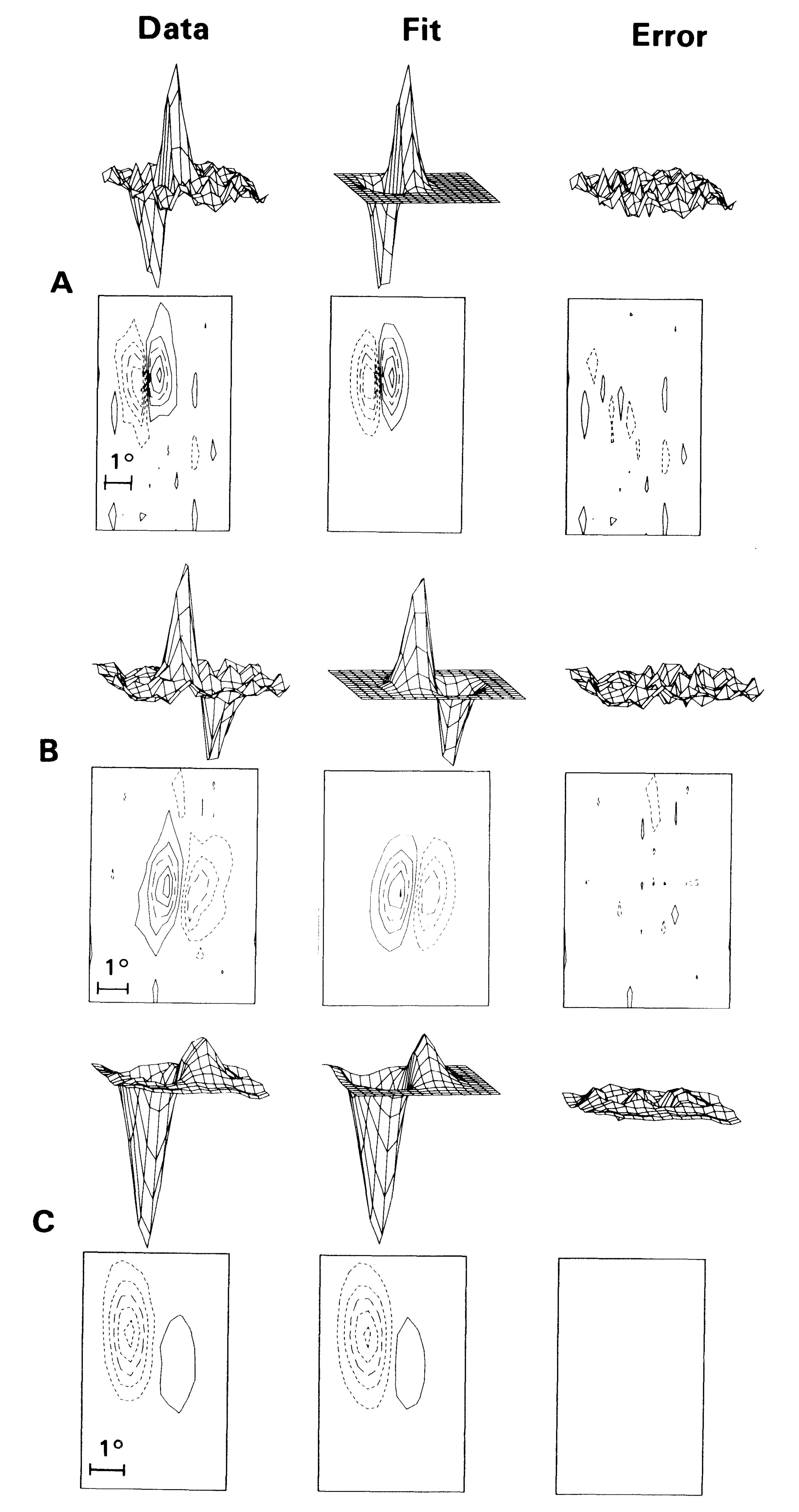

Jones, J. P., & Palmer, L. A. (1987). An evaluation of the two-dimensional Gabor filter model of simple receptive fields in cat striate cortex. *Journal of Neurophysiology, 58*(6), 1233-1258.

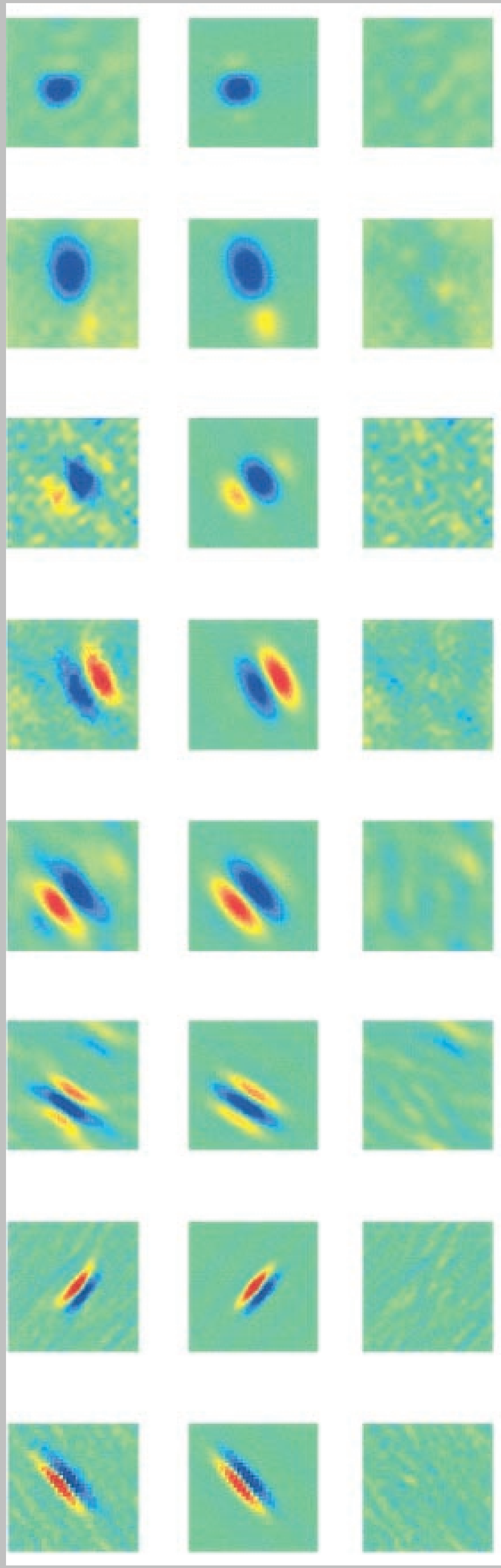

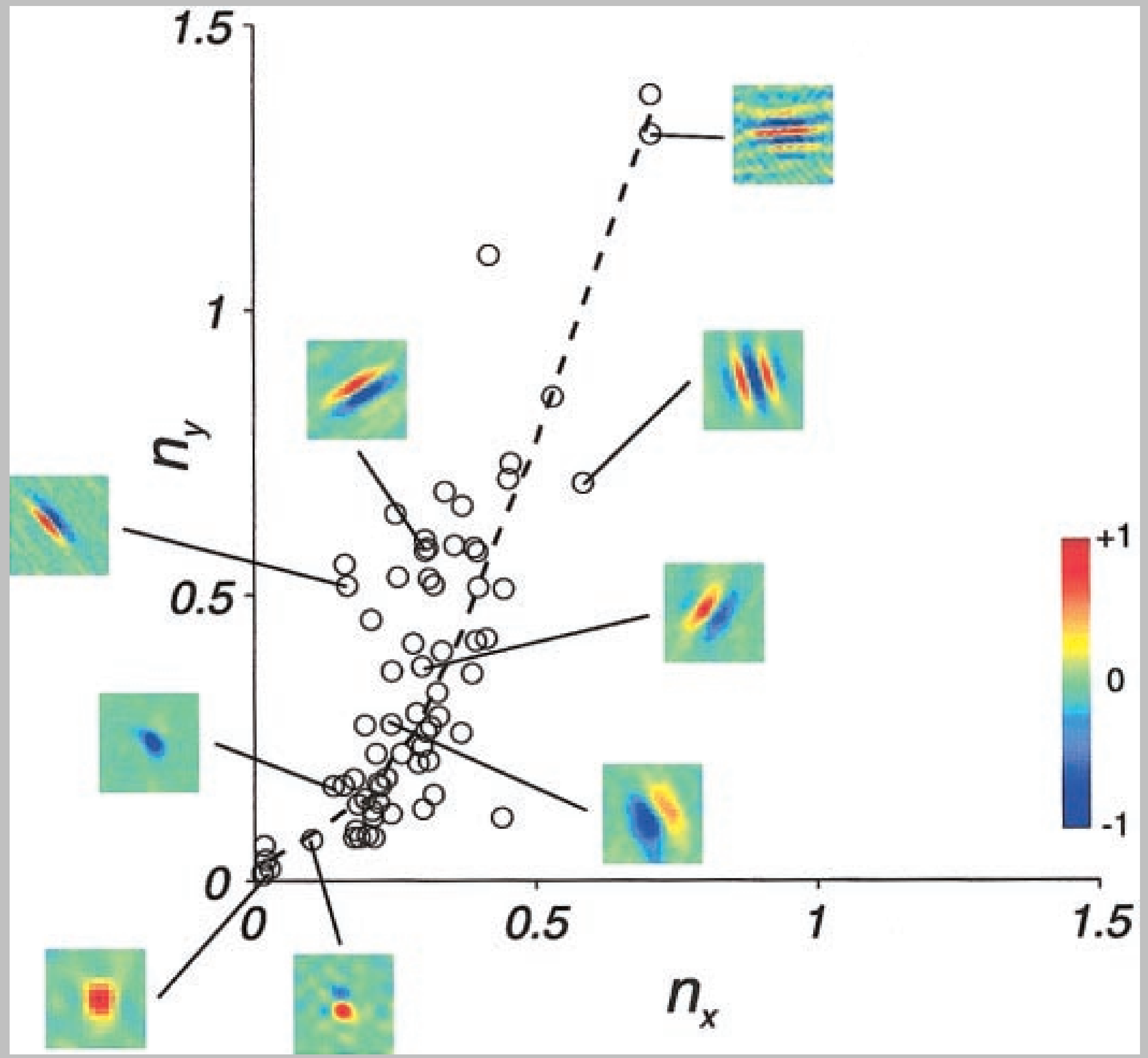

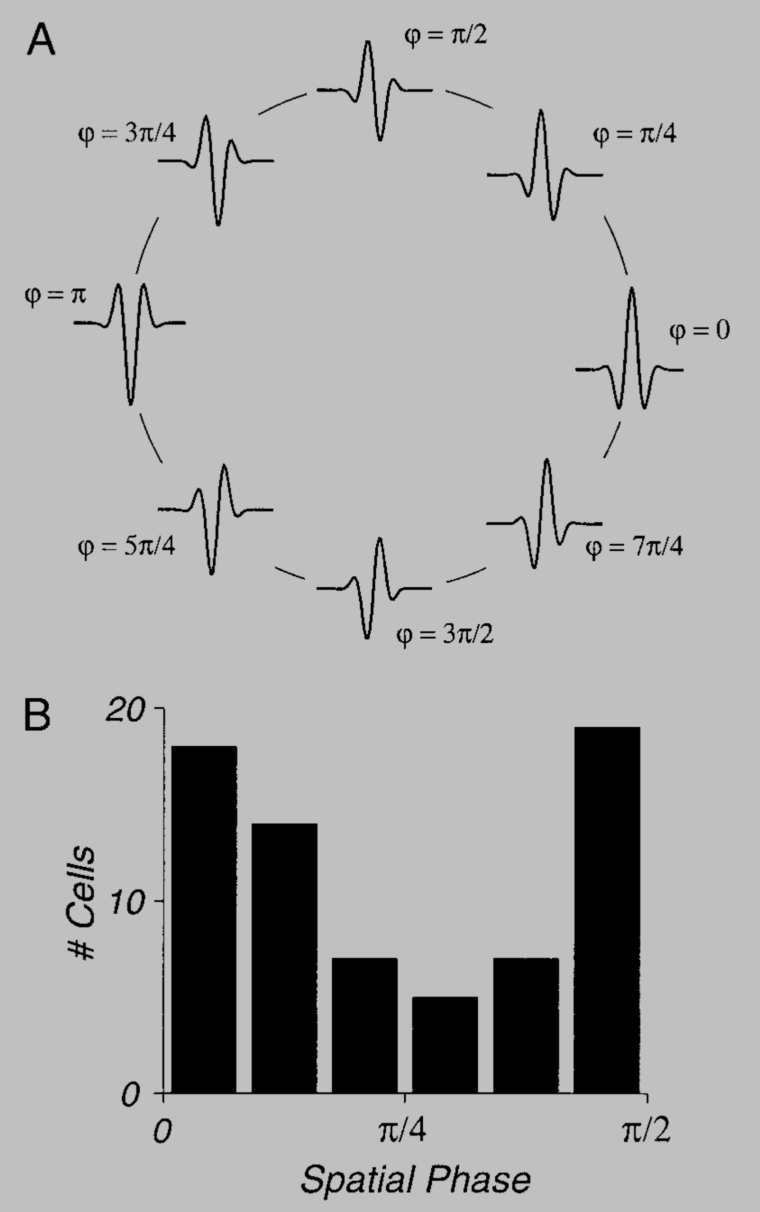

Ringach, D. L. (2002). Spatial Structure and Symmetry of Simple-Cell Receptive Fields in Macaque Primary Visual Cortex. *Journal of Neurophysiology, 88*(1), 455-463.

Visual Information

- Visual stimuli have spatial frequency content (Fourier Analysis).
- High spatial frequencies
  - Sharp borders and fine detail
- Low spatial frequencies
  - Gradual changes and large features

Spatial Frequencies

- Small Receptive Fields detect high spatial frequencies
- Large receptive fields detect low spatial frequencies
- The eye and the brain are extremely adept at performing some tasks using only very low spatial frequencies.

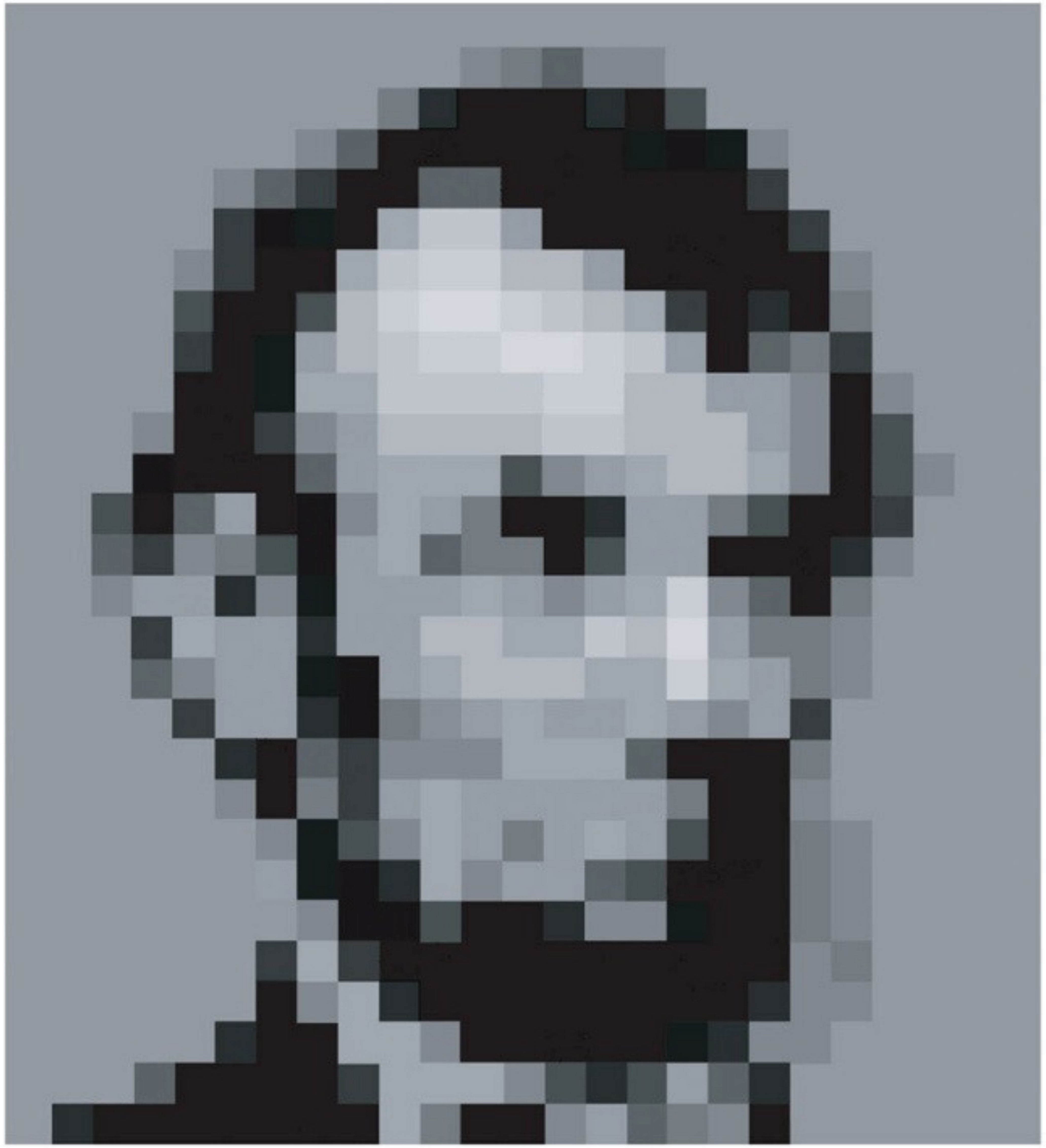

SENSATION AND PERCEPTION, **Figure 3.30**

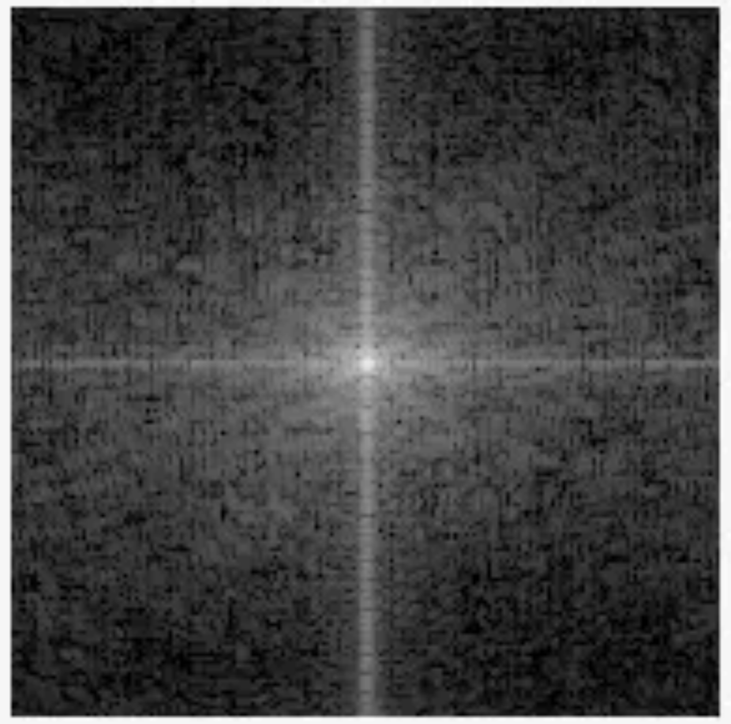

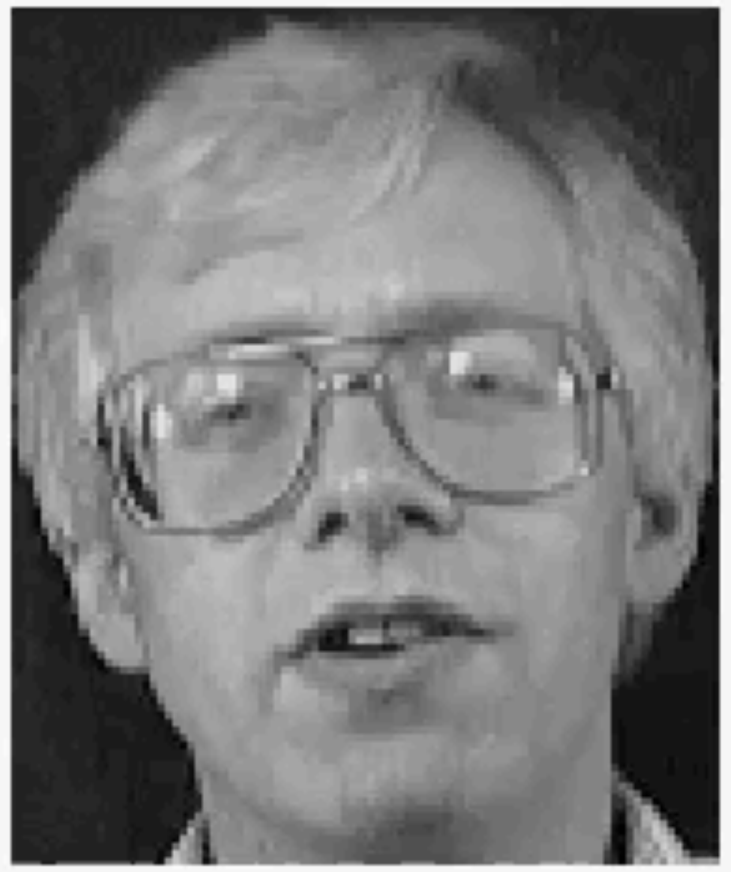

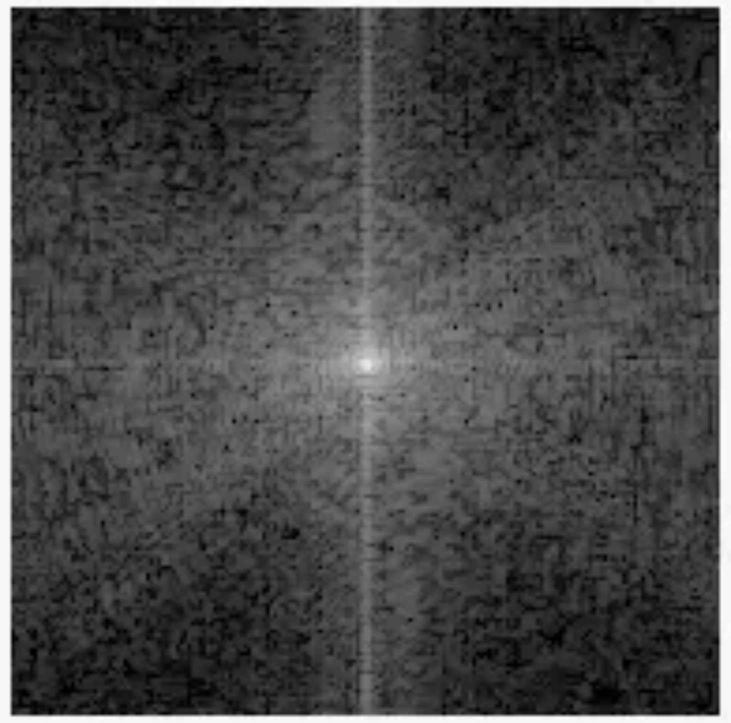

Spatial Frequency Bands

Spatial Frequency Bands

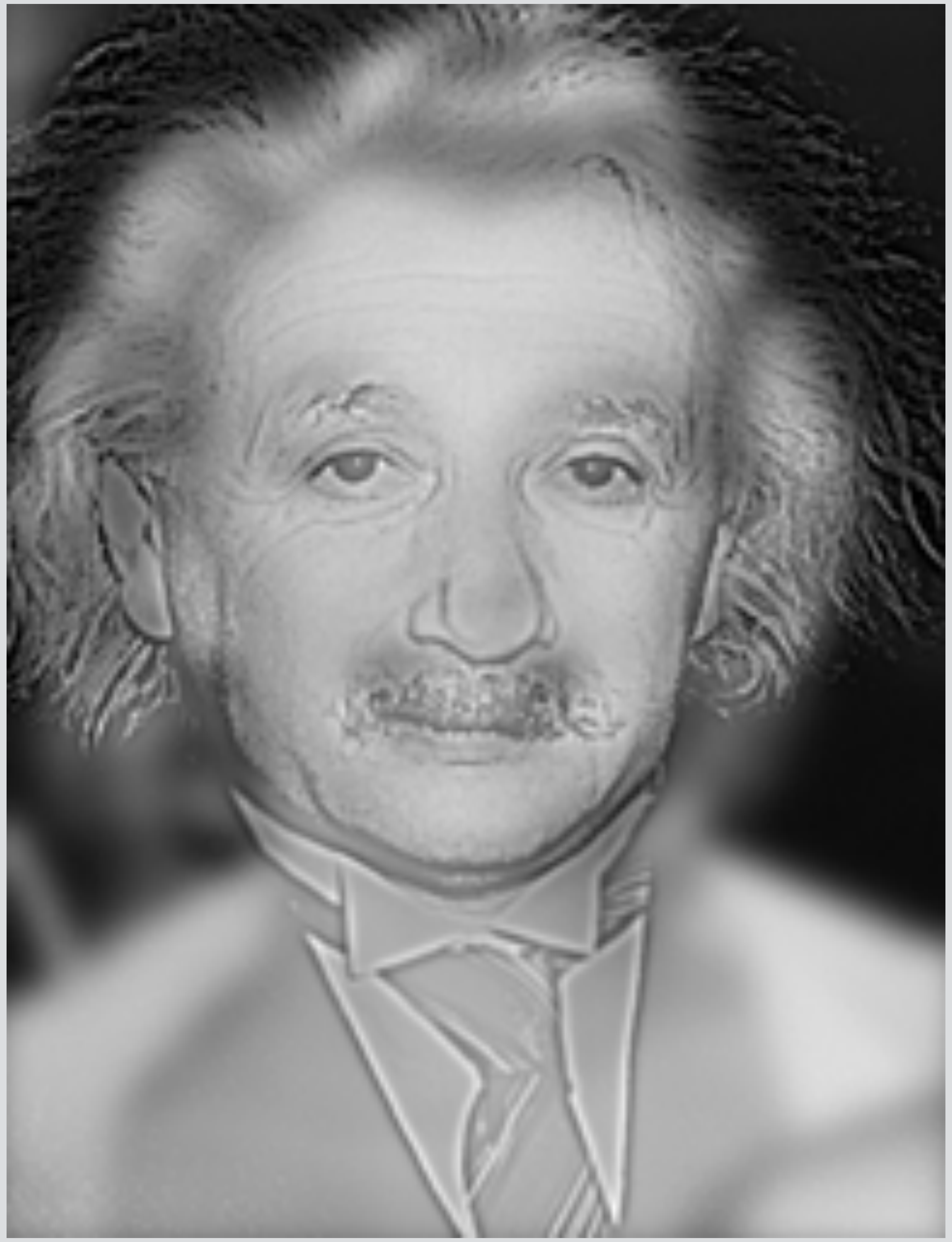

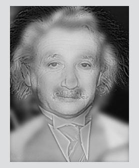

Schyns, P. G., & Oliva, A. (1999). Dr. Angry and mr. Smile: When categorization flexibly modifies the perception of faces in rapid visual presentations. *Cognition, 69*(3), 243-265. Retrieved from http://elsevier.com

Schyns, P. G., & Oliva, A. (1999). Dr. Angry and mr. Smile: When categorization flexibly modifies the perception of faces in rapid visual presentations. *Cognition, 69*(3), 243-265. Retrieved from http://elsevier.com

Effect of Adaptation Level on Contrast Sensitivity

- Two main effects of lowering adaptation level
  - Lower sensitivity
  - Loss of high spatial frequencies

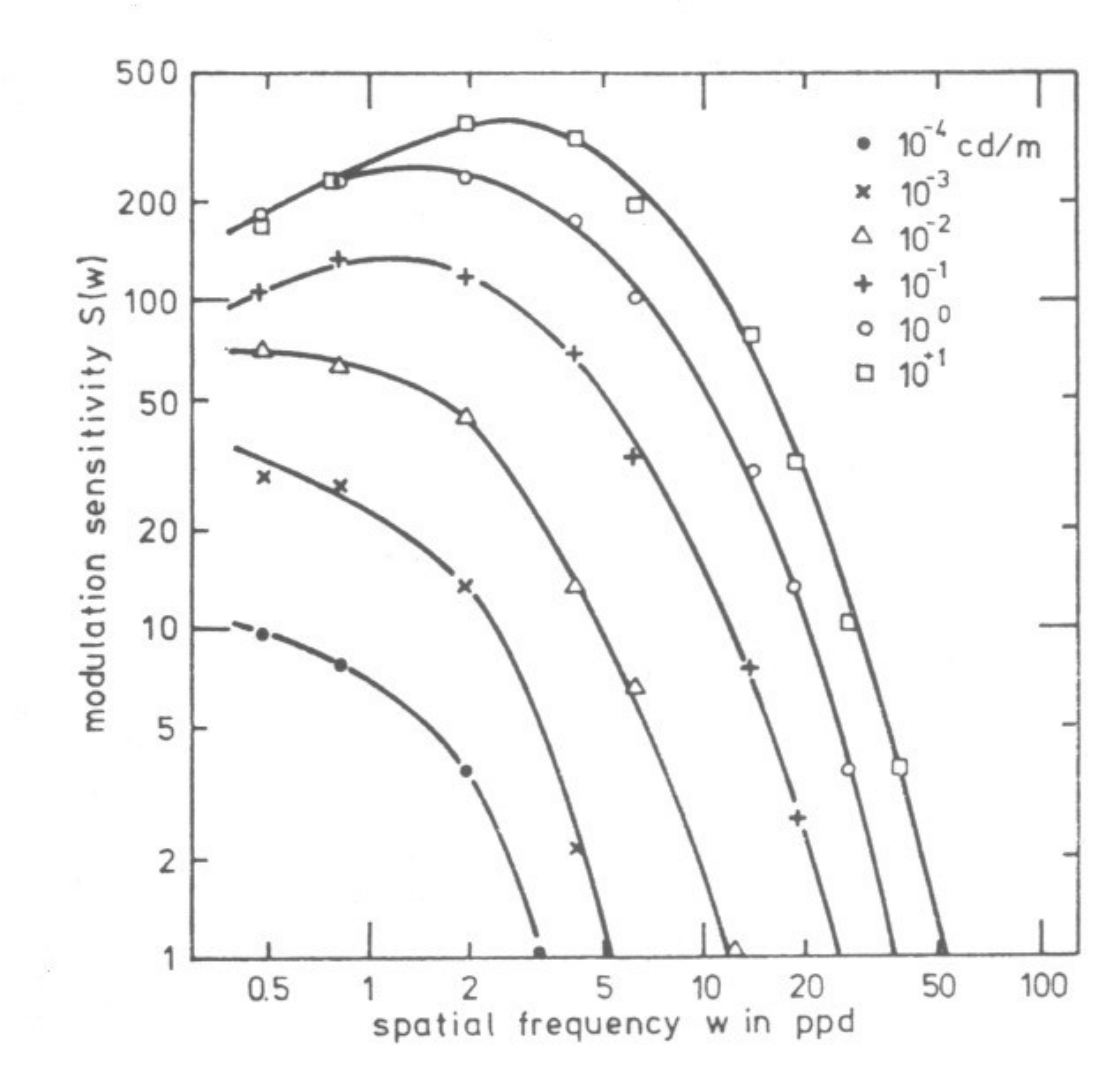

van Meeteren, A., & Vos, J. J. (1972). Resolution and contrast sensitivity at low luminances. *Vision Research, 12*(5), 825–826.

A Typical Scene

Pedestrian Crosswalk

Spatial Frequency Filtering with Contrast Scaling

- Here is what happens when you filter the spatial frequencies and adjust the contrast of the image to be proportional to the loss of absolute contrast sensitivity of the human visual system at the lower levels of light adaptation.

Frequency Filtering with Contrast Scaling

300 td

30 td

3 td

0.3 td

Frequency Filtering with Contrast Scaling

300 td

30 td

3 td

0.3 td

Conclusions

- The retinal image can be described by its spatial frequency content
- The visual system can be described by its sensitivity to various spatial frequencies
- We can approximate vision at low levels by filtering out frequencies that we can’t see at low levels
- The quality of our vision changes at low levels of light

Break

Face Recognition

Analysis & Dynamic Interaction

- Sensory input is broken into separate streams of information
  - Lines & edges
  - angles & orientation,
  - size & scale
  - color
  - movement
- Over 50% of cortex has visual responses
- Reality is constructed from these component parts using goals, expectations, biases, rewards.

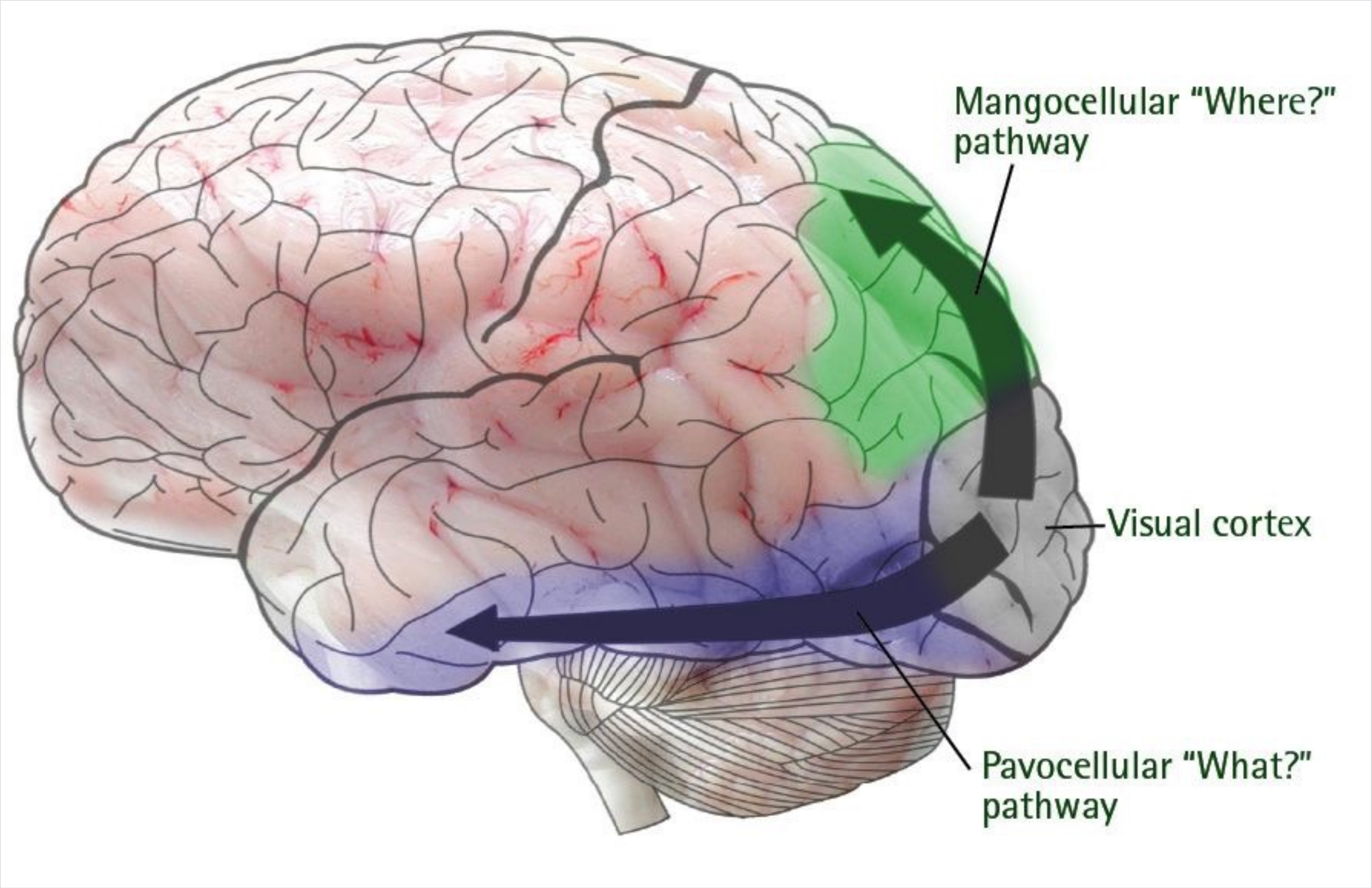

Lines and Contours
Angles and Orientations

“Pop Out”–Ann Treisman

- Curvature
- Tilt
- Color
- Line Ends
- Movement

- Closed Areas
- Contrast
- Brightness

Texture Segregation
Jacob Beck and Bela Julesz

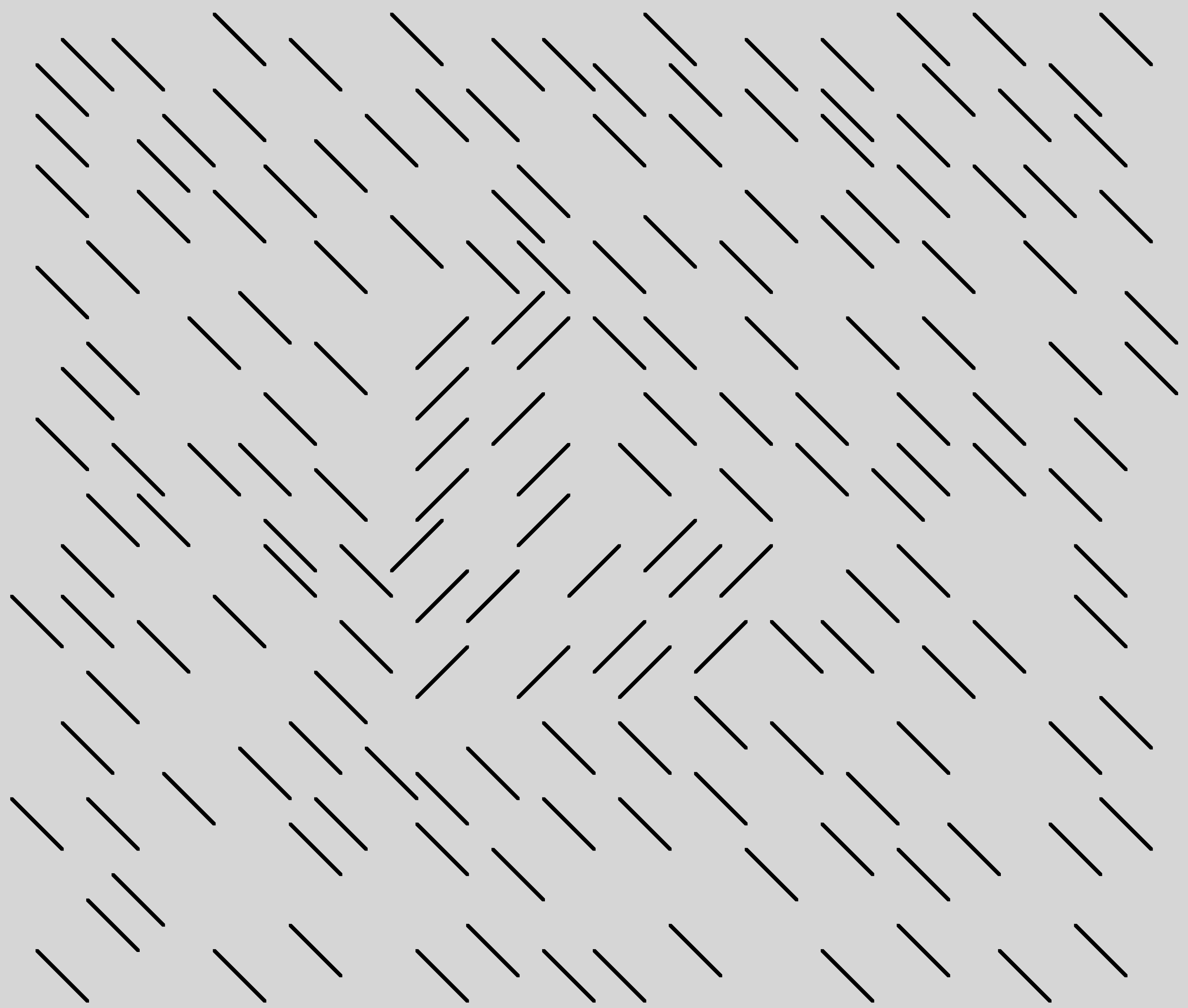

Texture Segregation
Jacob Beck and Bela Julesz

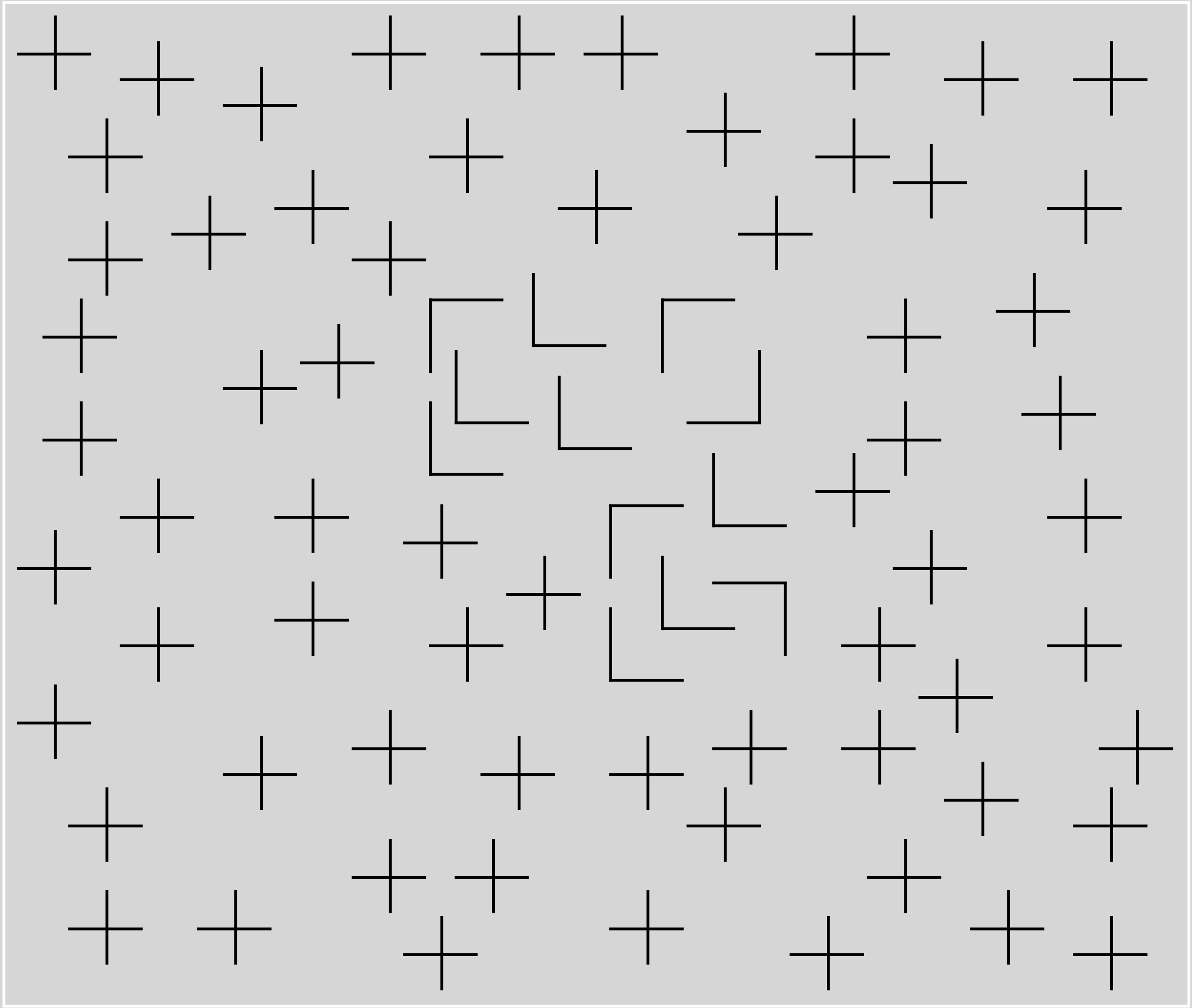

Texture Segregation
Jacob Beck and Bela Julesz

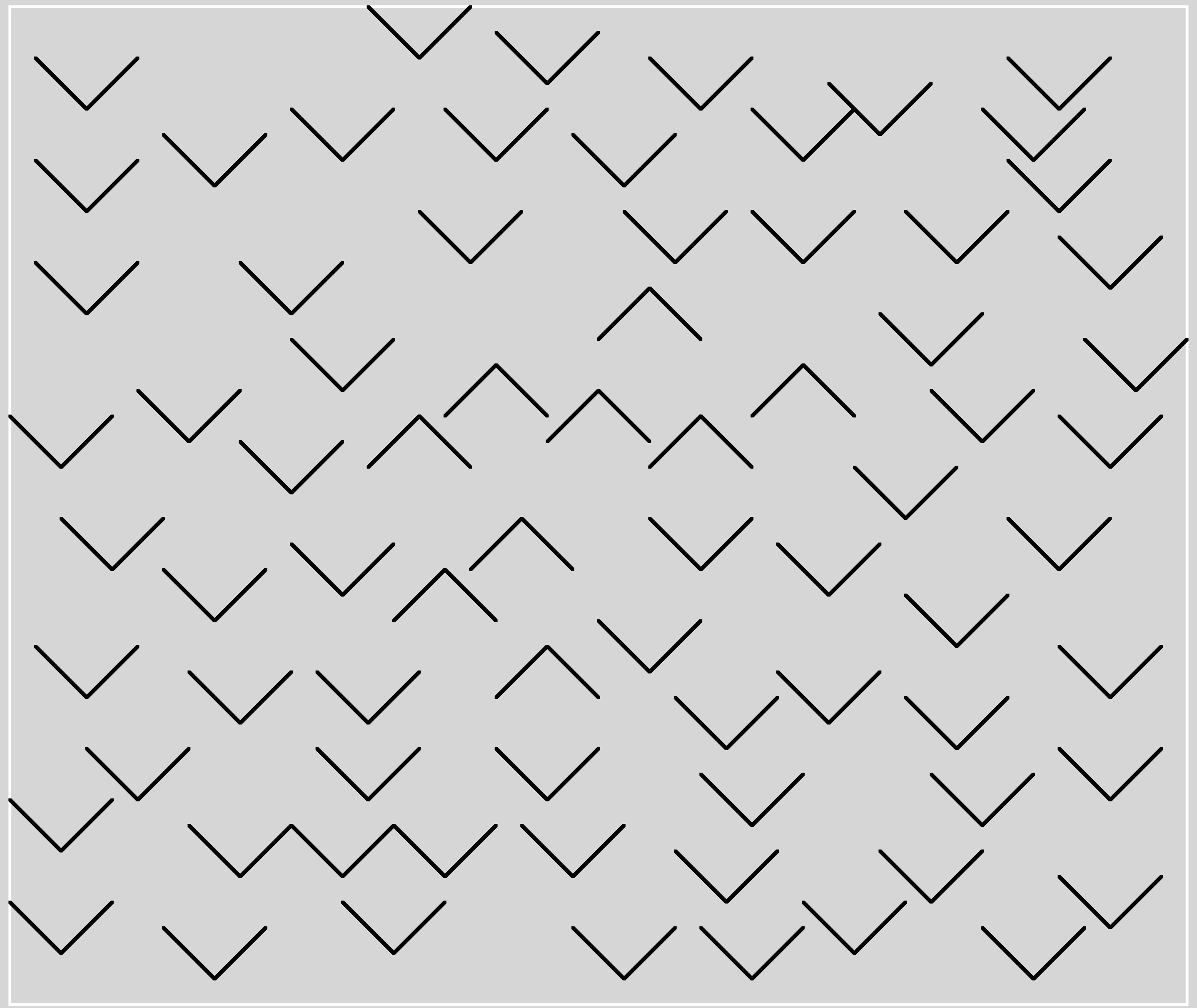

Texture Segregation
Jacob Beck and Bela Julesz

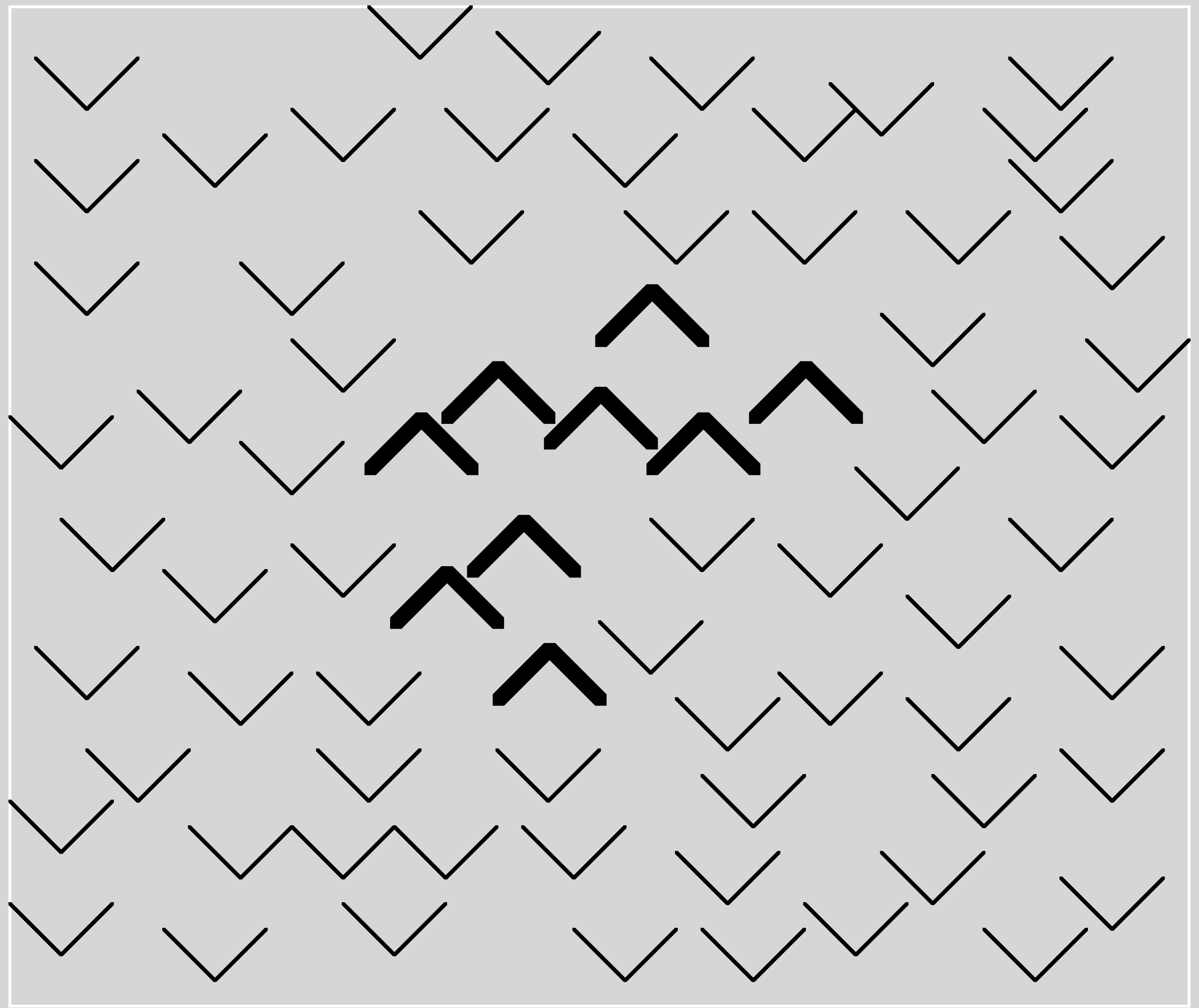

What we perceive does not correspond to physical properties

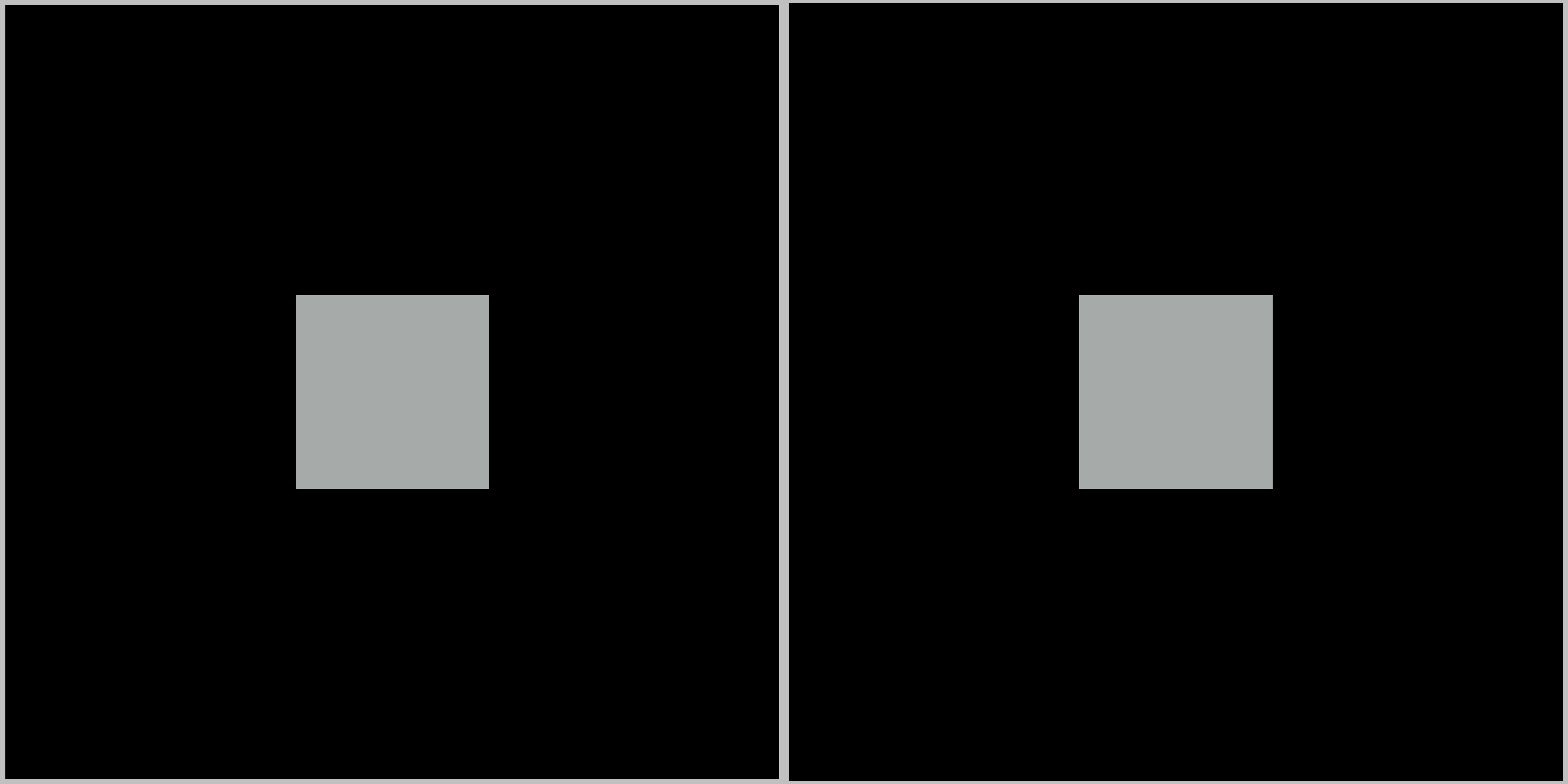

volunteer

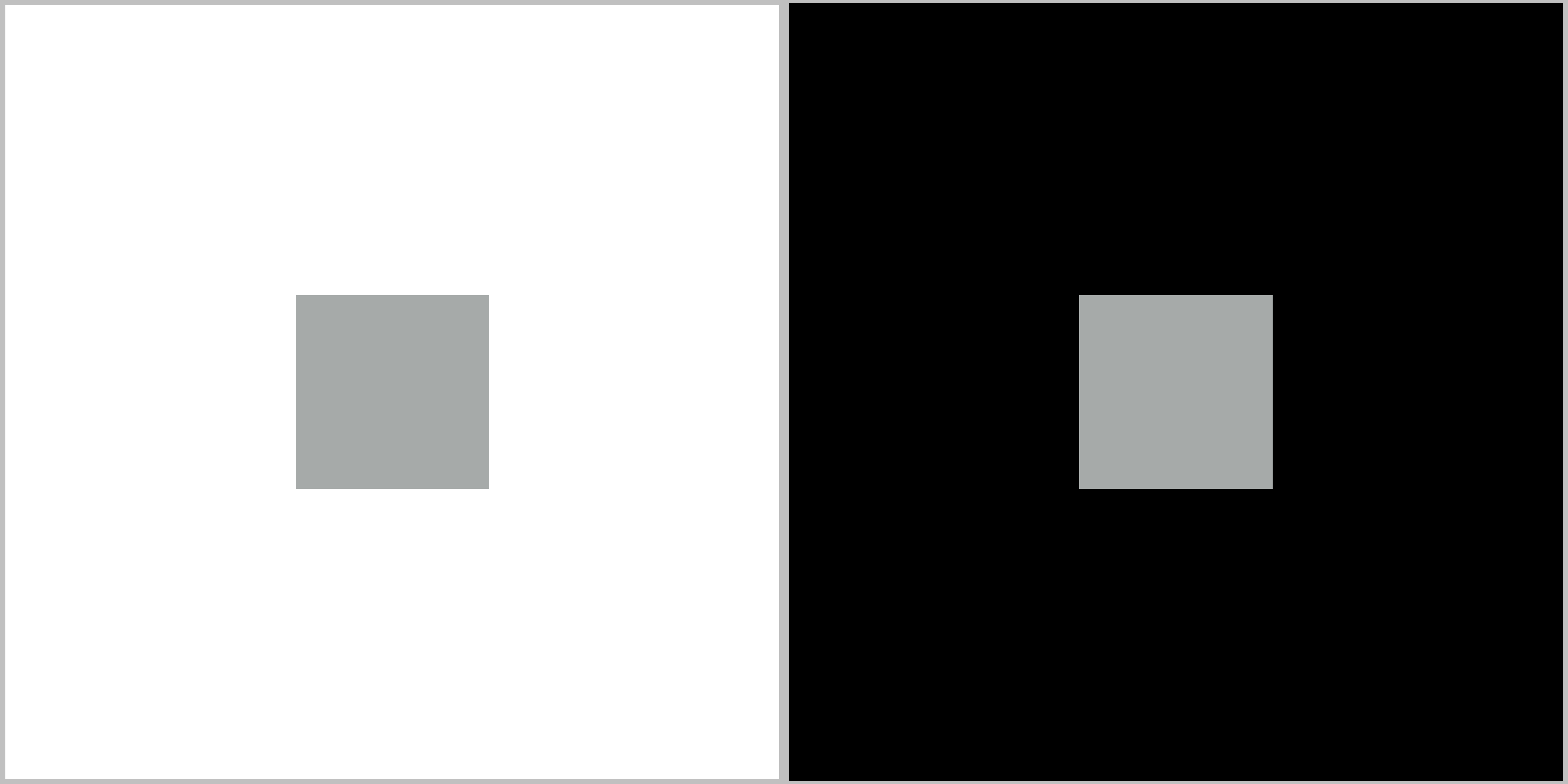

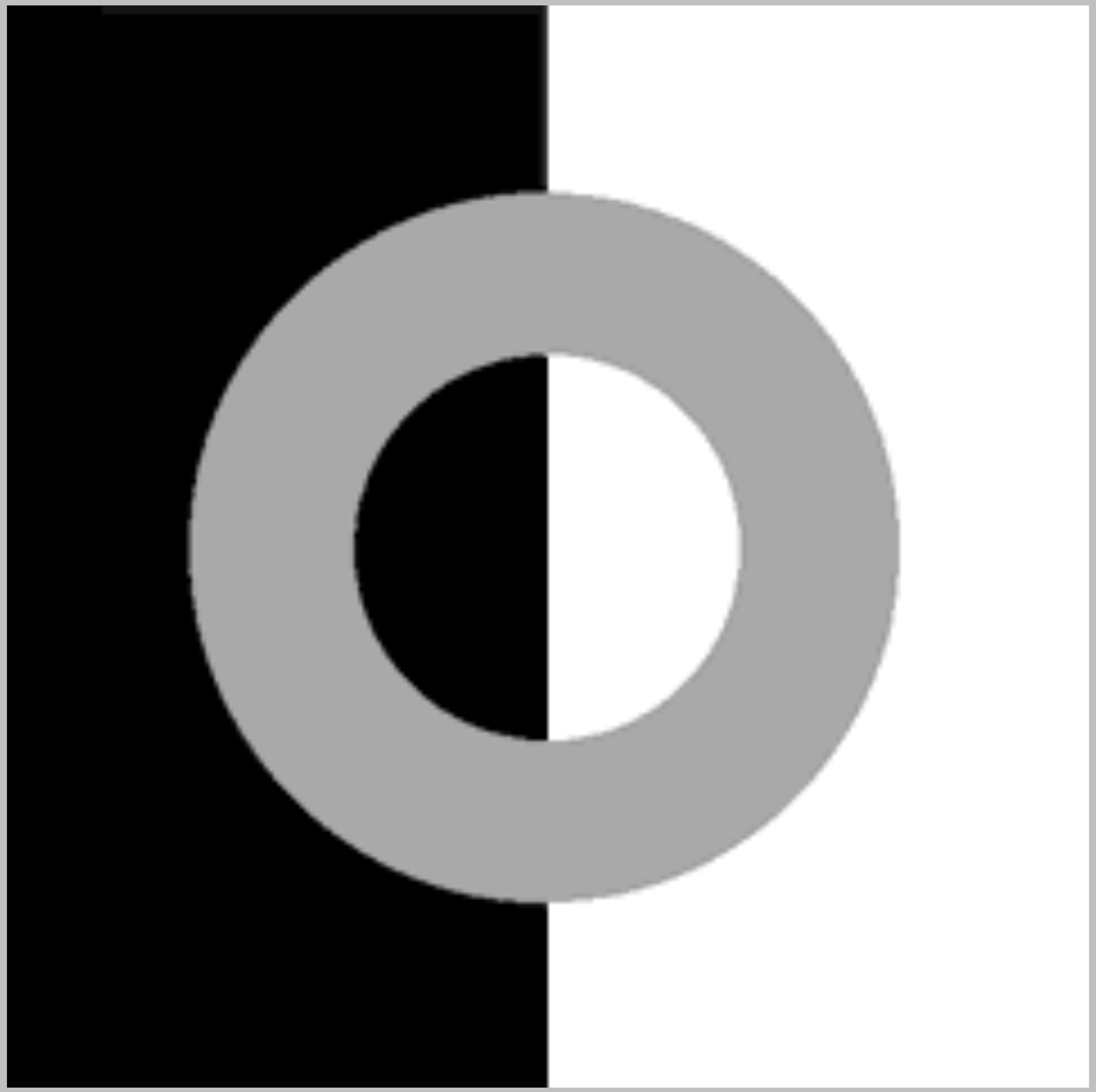

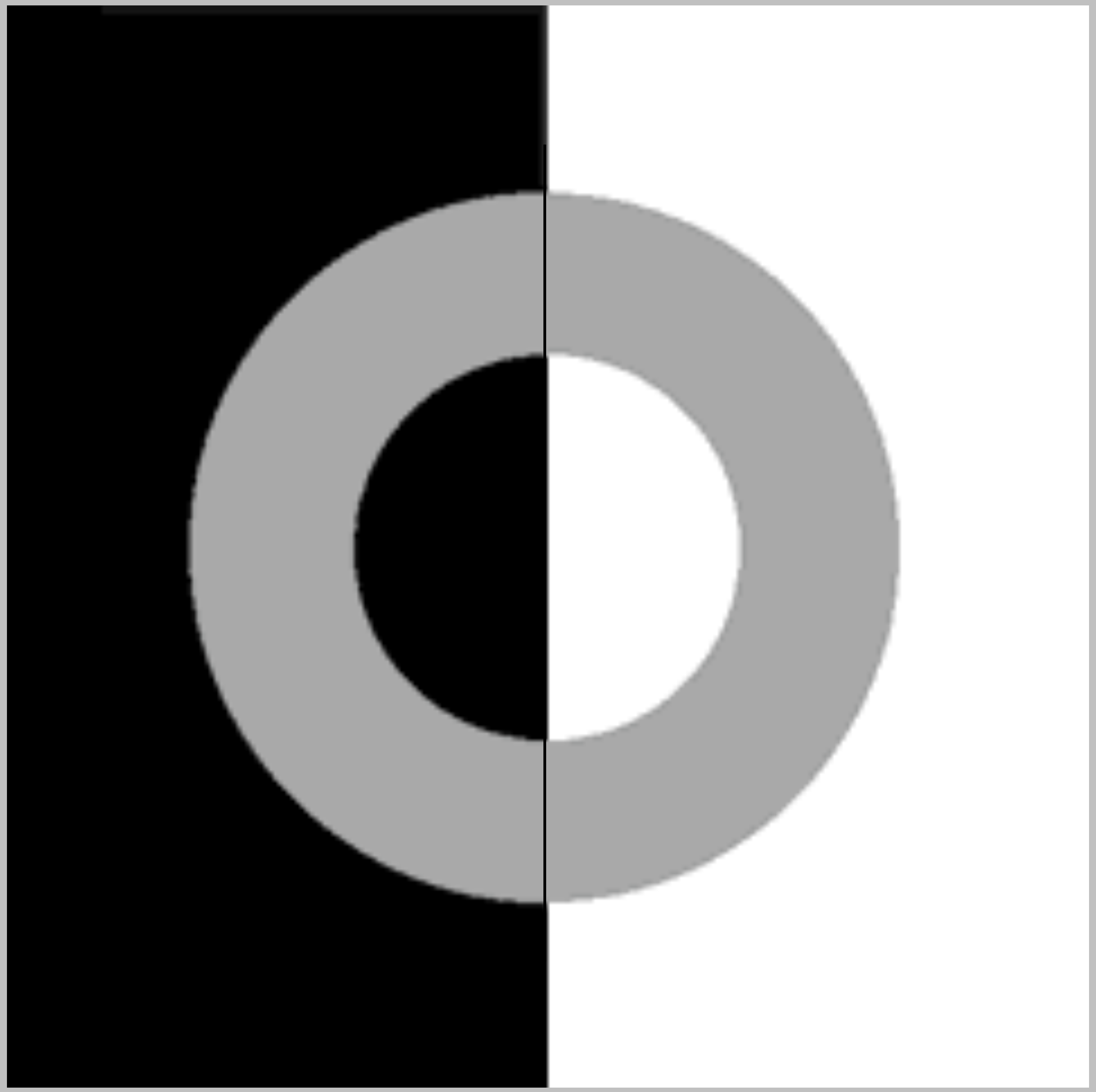

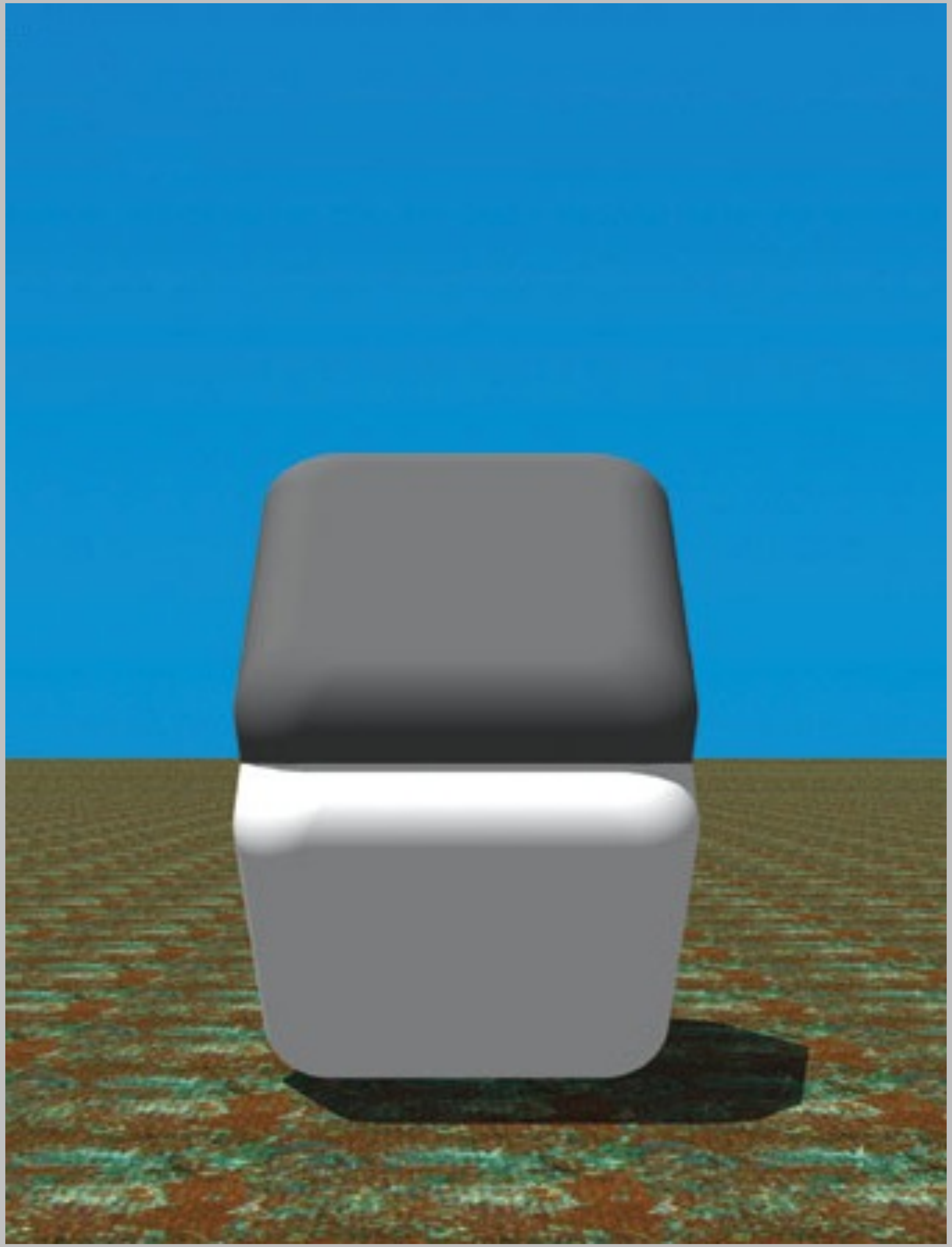

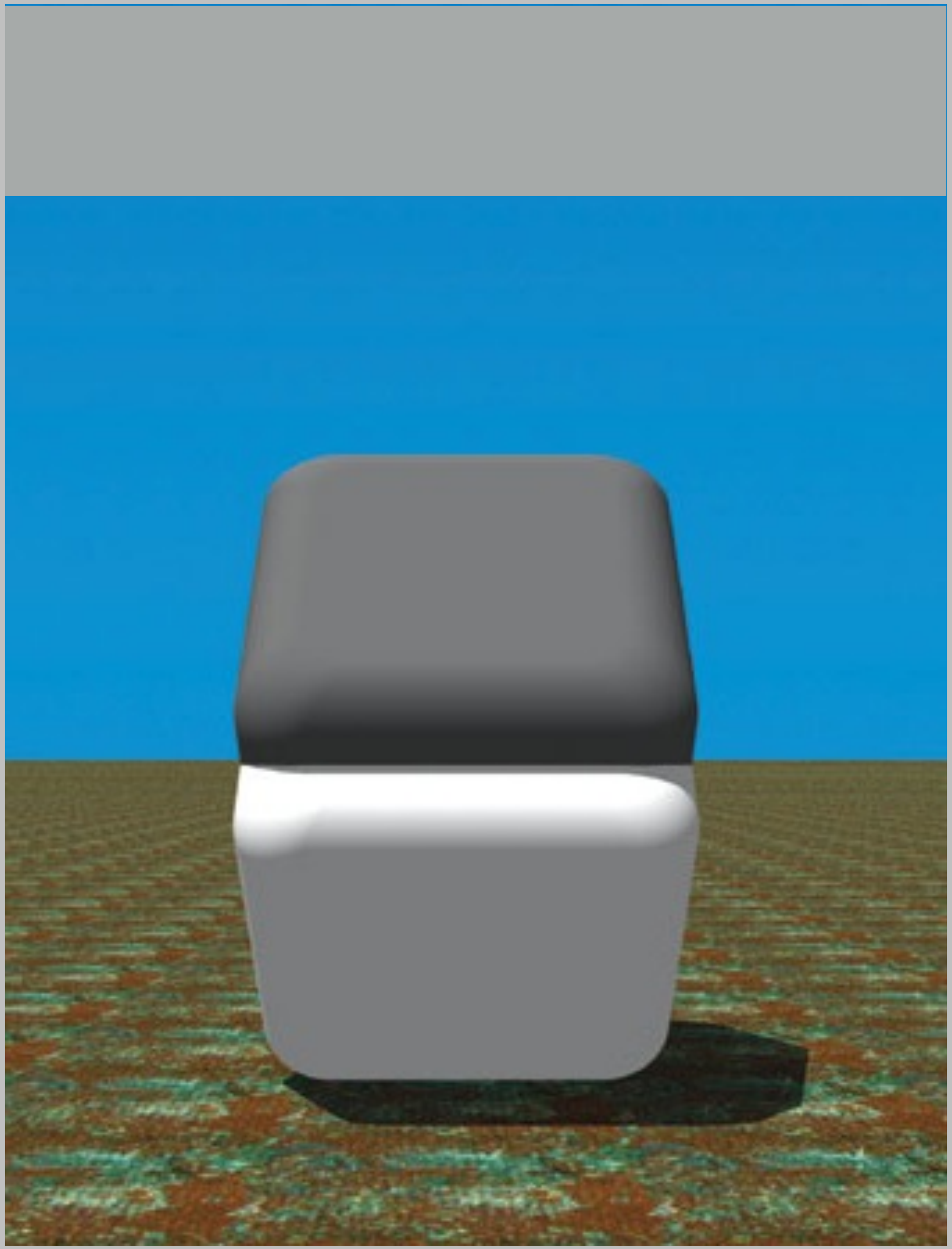

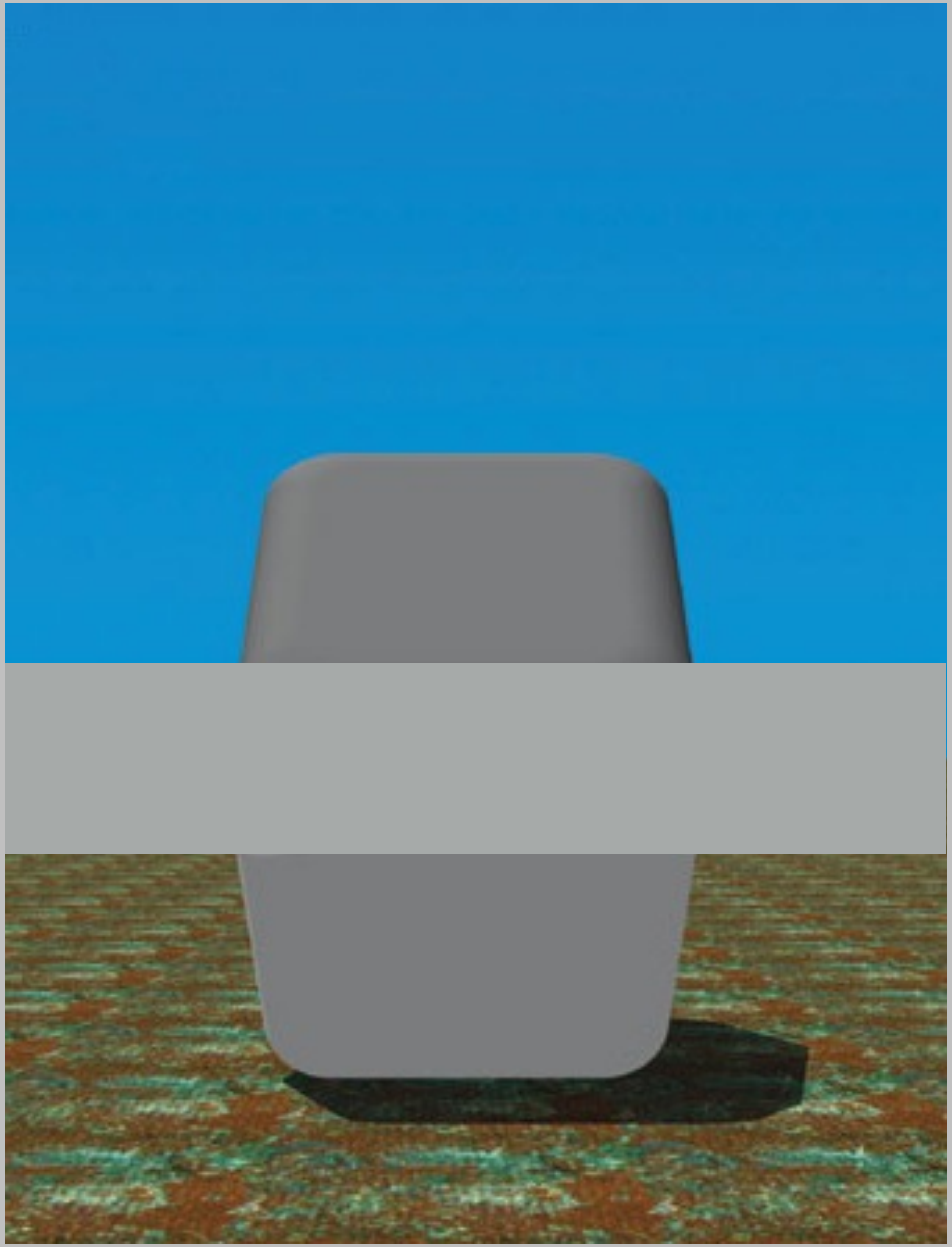

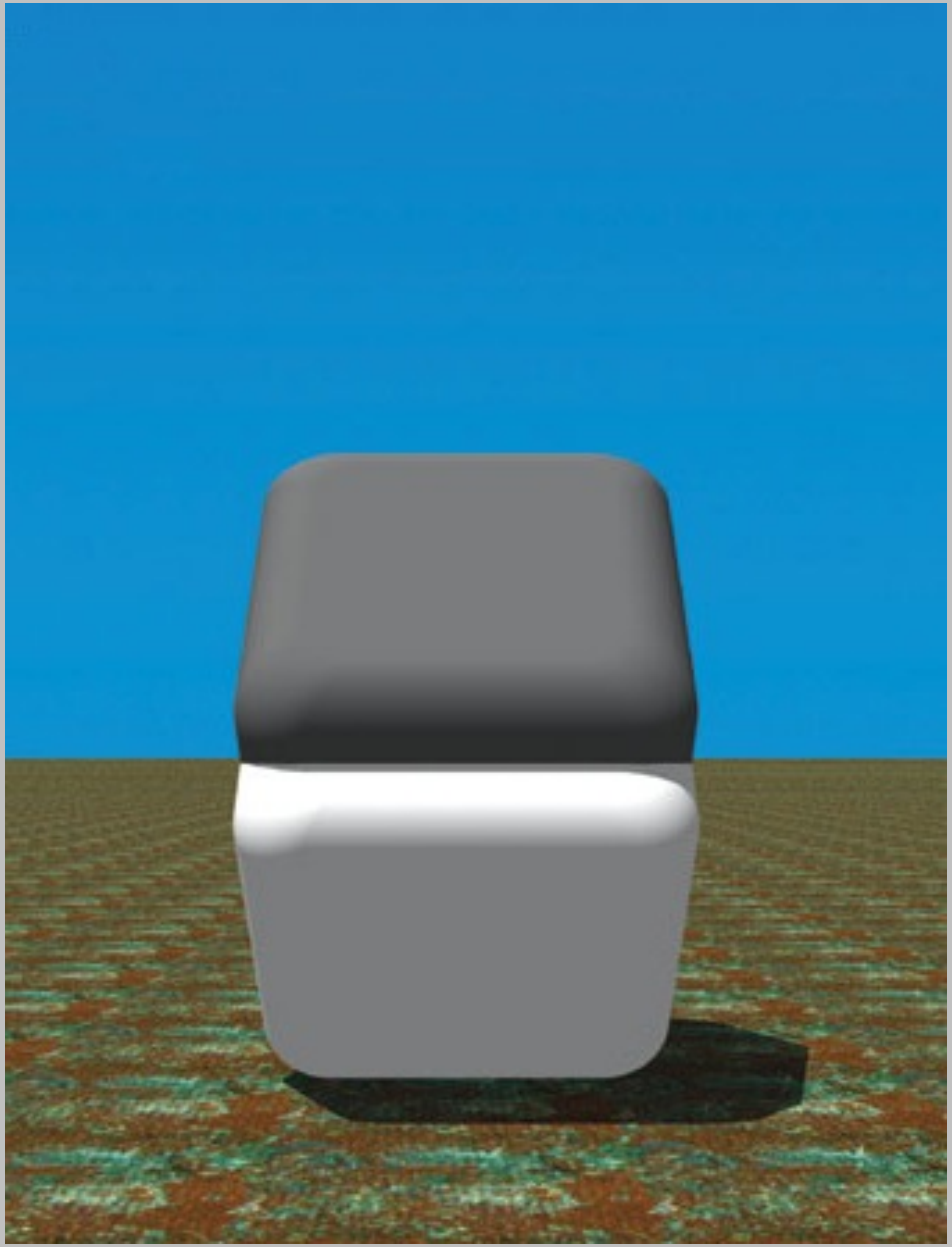

Asahi Figure

Akiyoshi Kitaoka 2005

volunteer

Asahi Figure

Akiyoshi Kitaoka 2005

Modeling Vision

Ganglion Cell Receptive Field

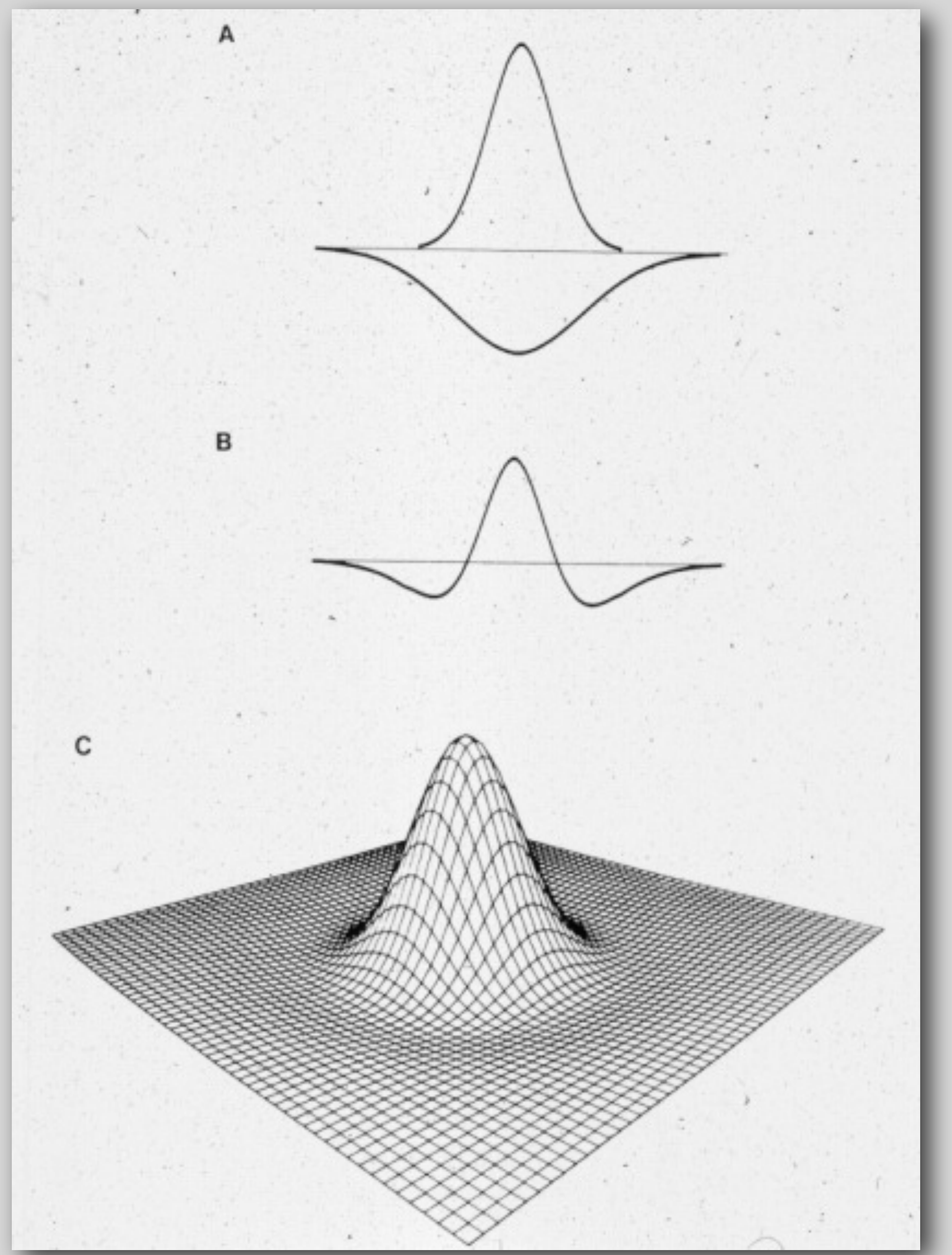

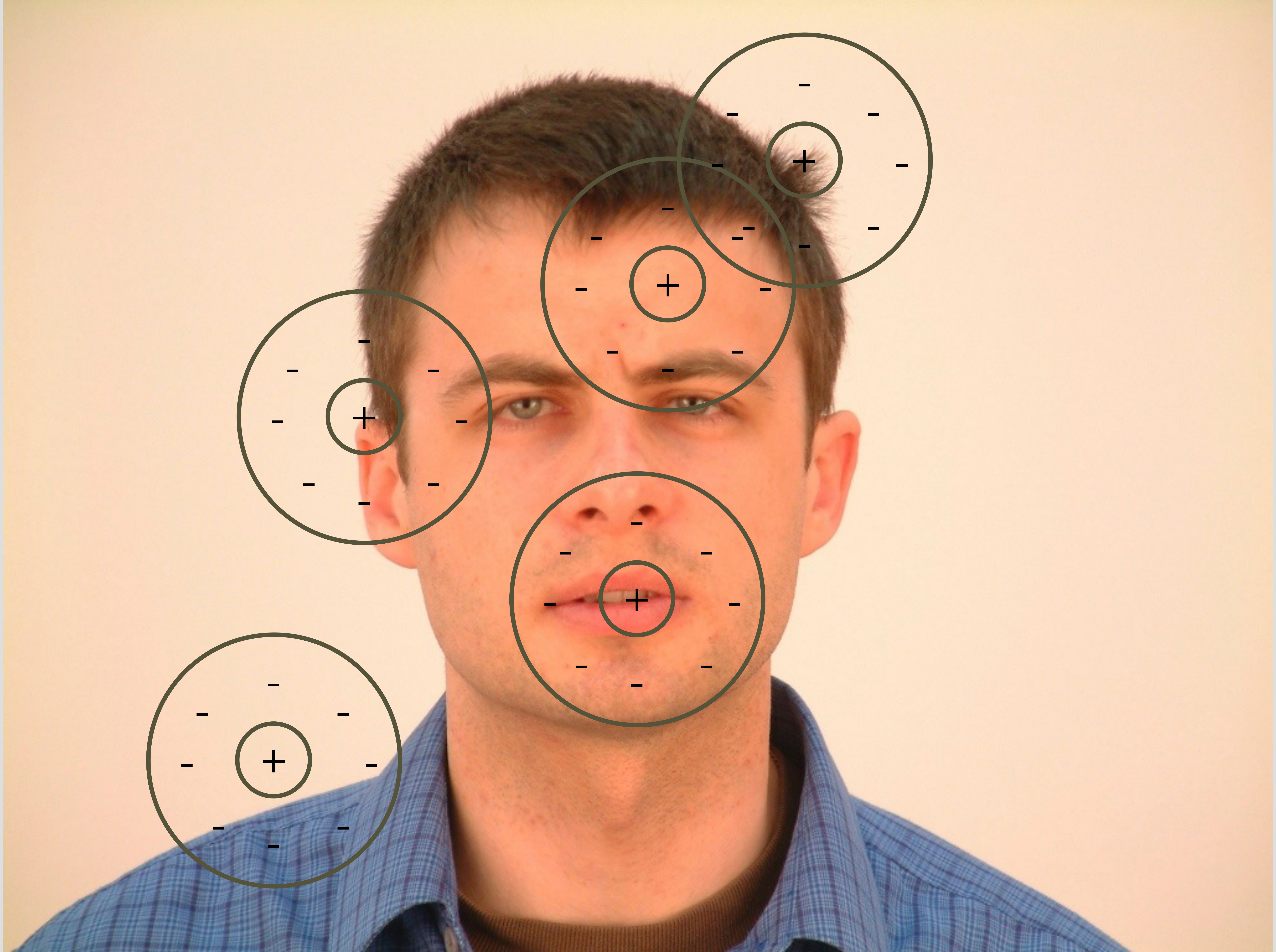

Cortical Cell Receptive Fields

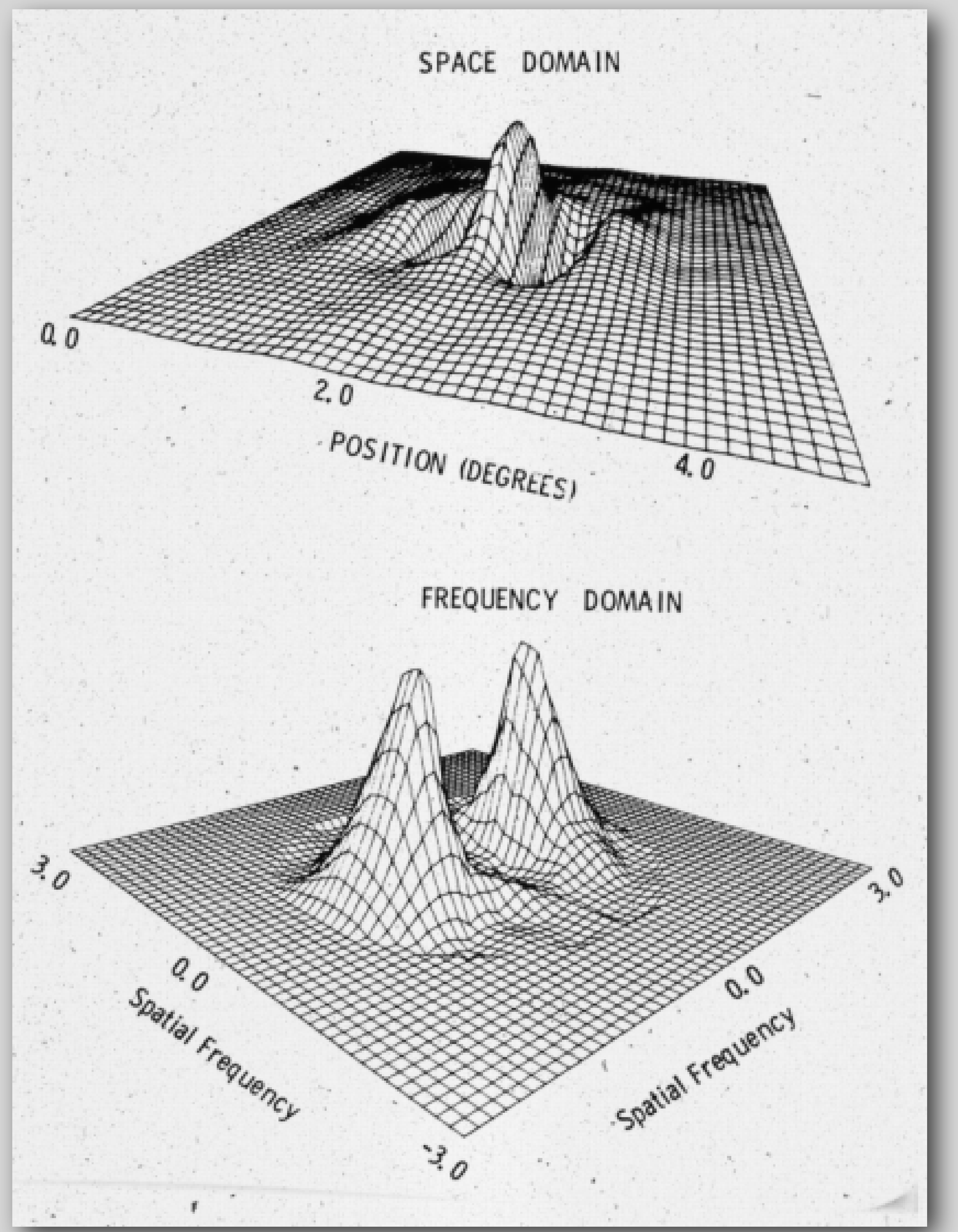

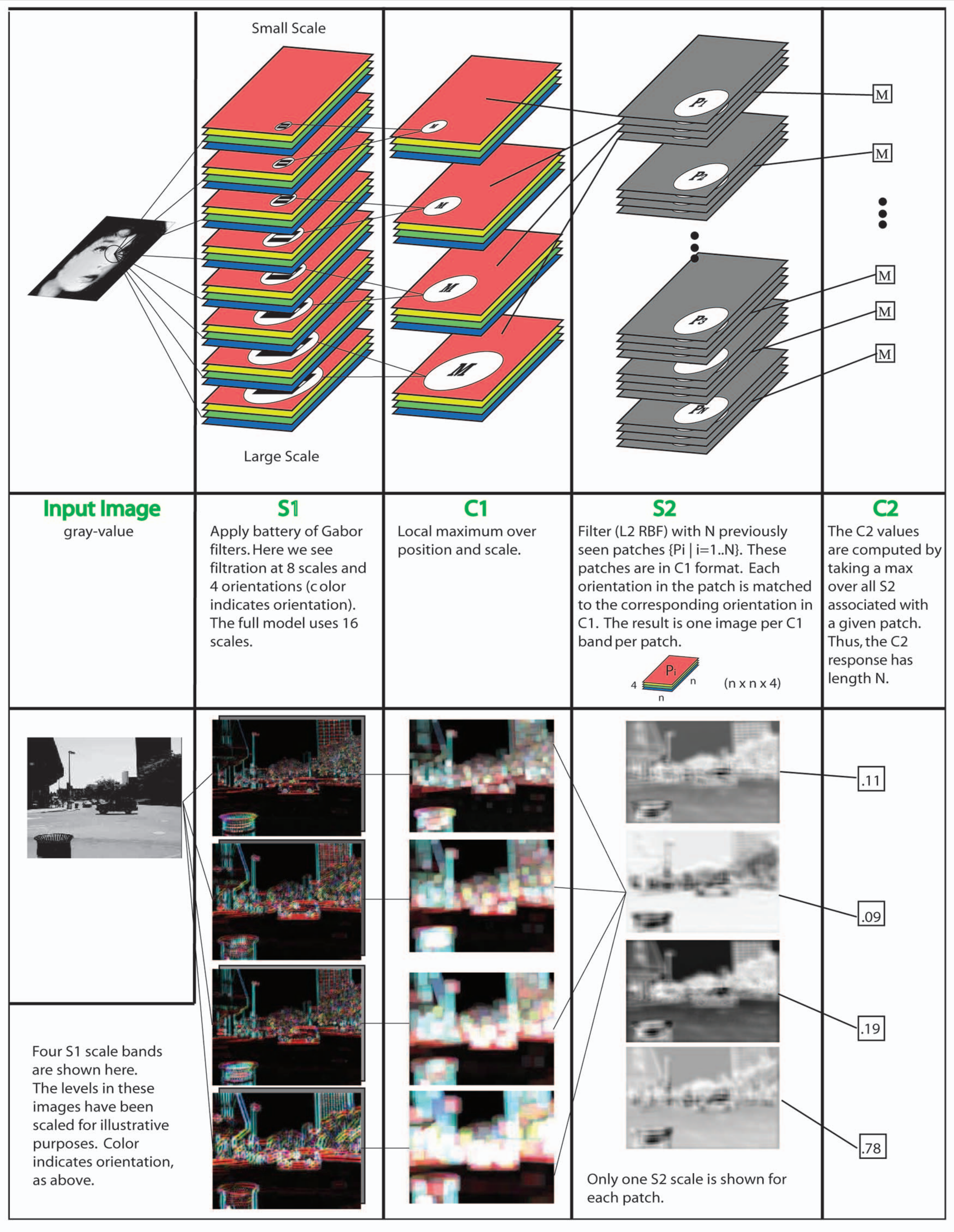

Serre, T., Wolf, L., Bileschi, S., Riesenhuber, M., & Poggio, T. (2007). Robust object recognition with cortex-like mechanisms. *IEEE transactions on pattern analysis and machine intelligence, 29*(3), 411–426.

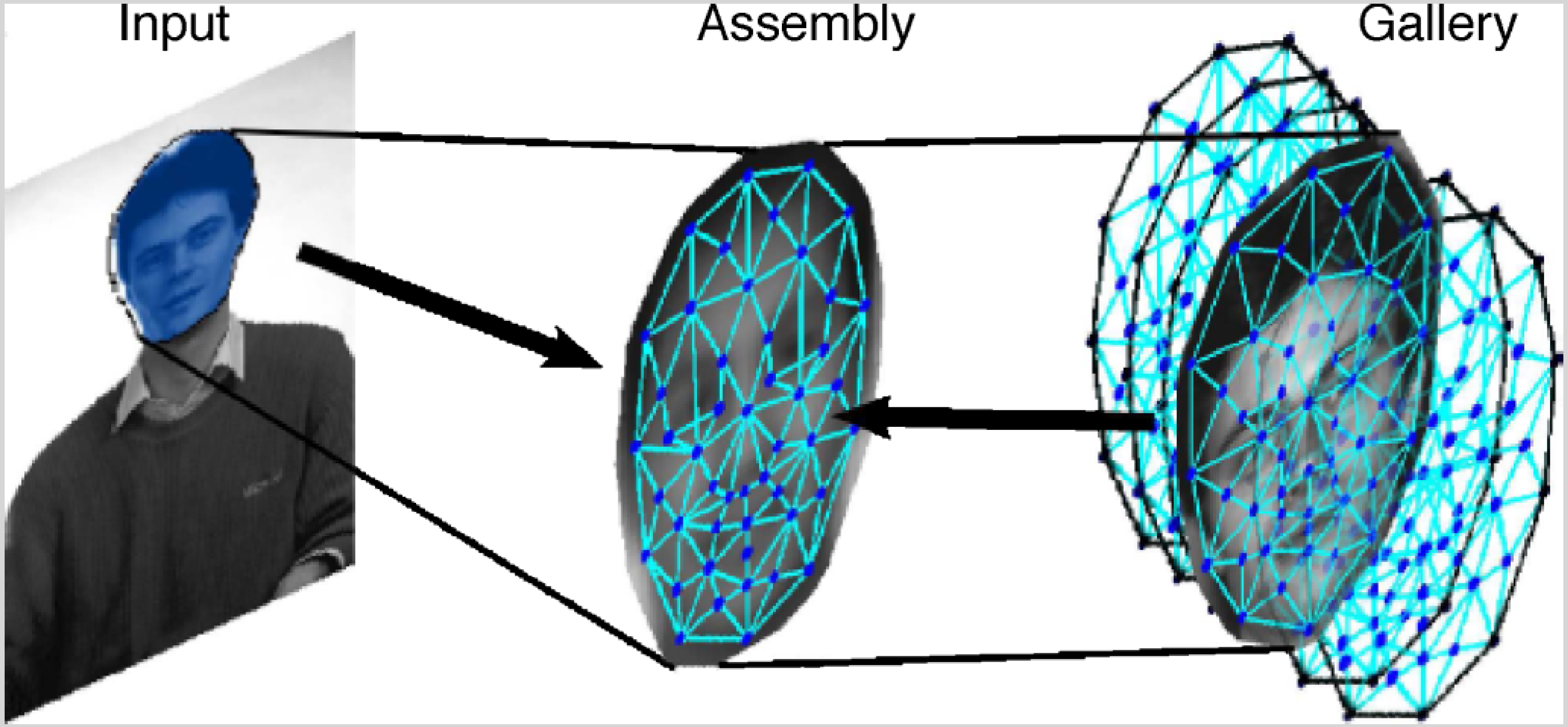

Wolfrum, P., Wolff, C., Lücke, J., & von der Malsburg, C. (2008). A recurrent dynamic model for correspondence-based face recognition. *Journal of Vision, 8*(7), 1–18. doi: 10.1167/8.7.34

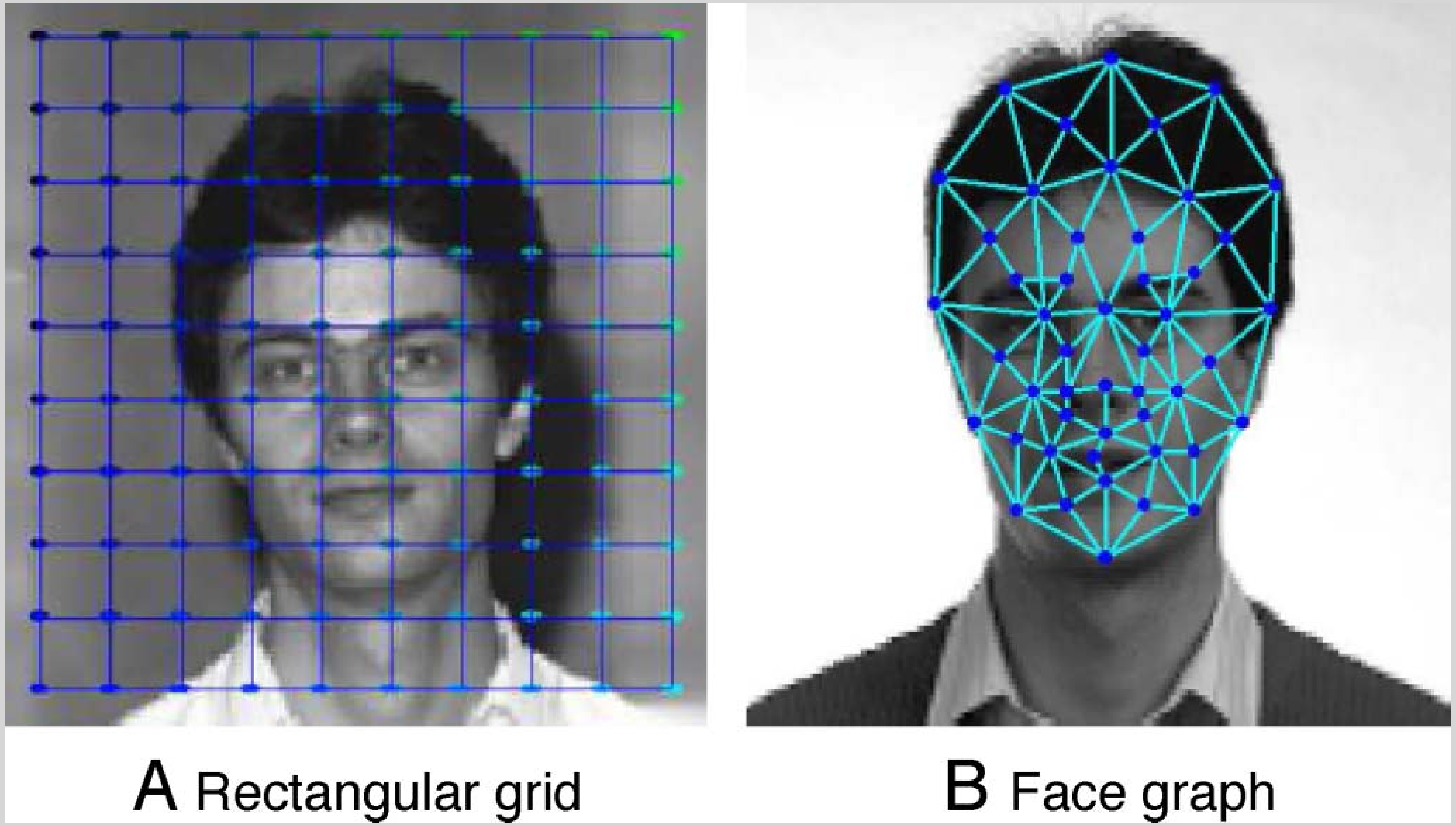

Wolfrum, P., Wolff, C., Lücke, J., & von der Malsburg, C. (2008). A recurrent dynamic model for correspondence-based face recognition. *Journal of Vision, 8*(7), 1–18. doi: 10.1167/8.7.34

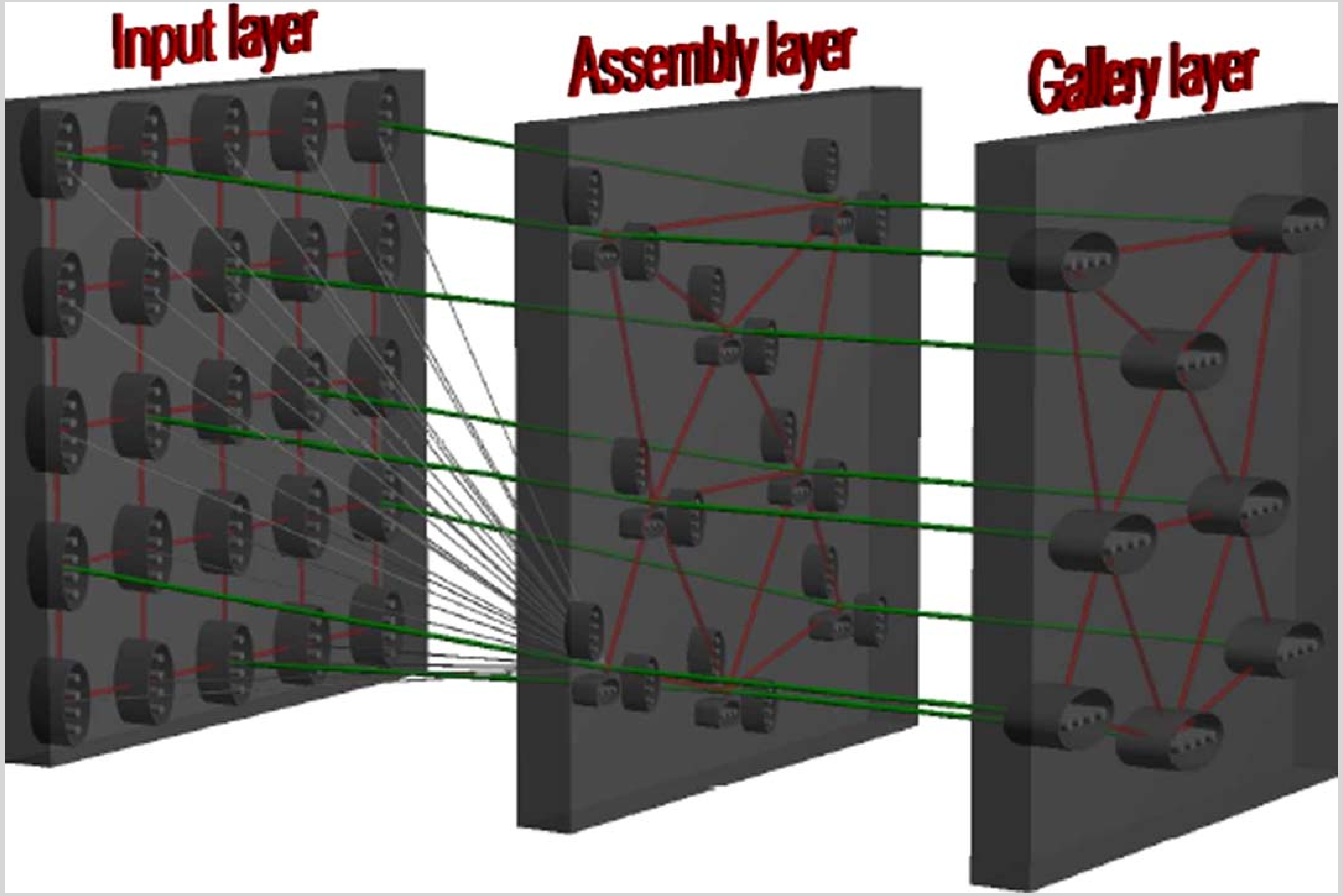

Wolfrum, P., Wolff, C., Lücke, J., & von der Malsburg, C. (2008). A recurrent dynamic model for correspondence-based face recognition. *Journal of Vision, 8*(7), 1–18. doi: 10.1167/8.7.34

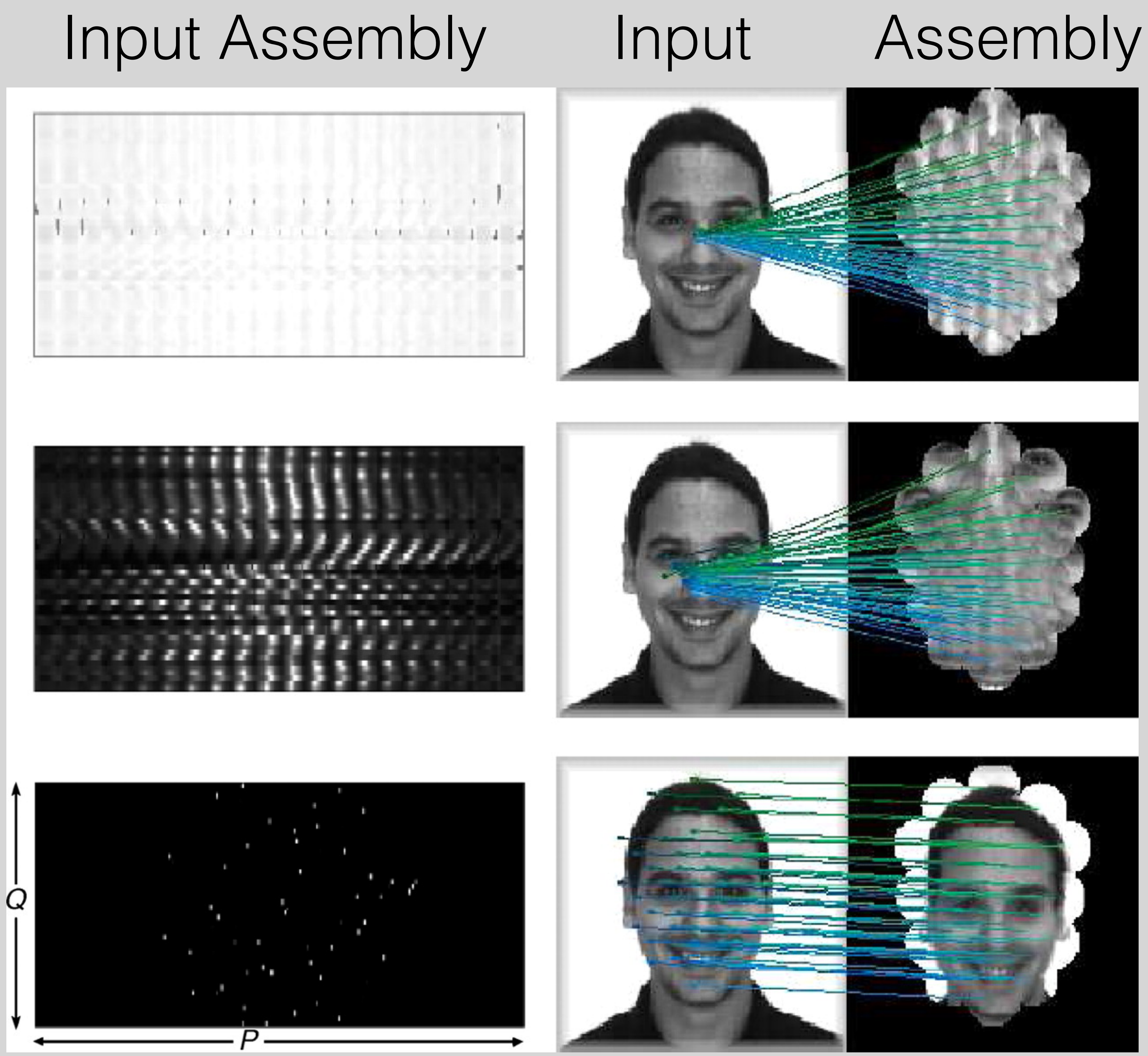

Wolfrum, P., Wolff, C., Lücke, J., & von der Malsburg, C. (2008). A recurrent dynamic model for correspondence-based face recognition. *Journal of Vision, 8*(7), 1–18. doi: 10.1167/8.7.34

Gallery Assembly

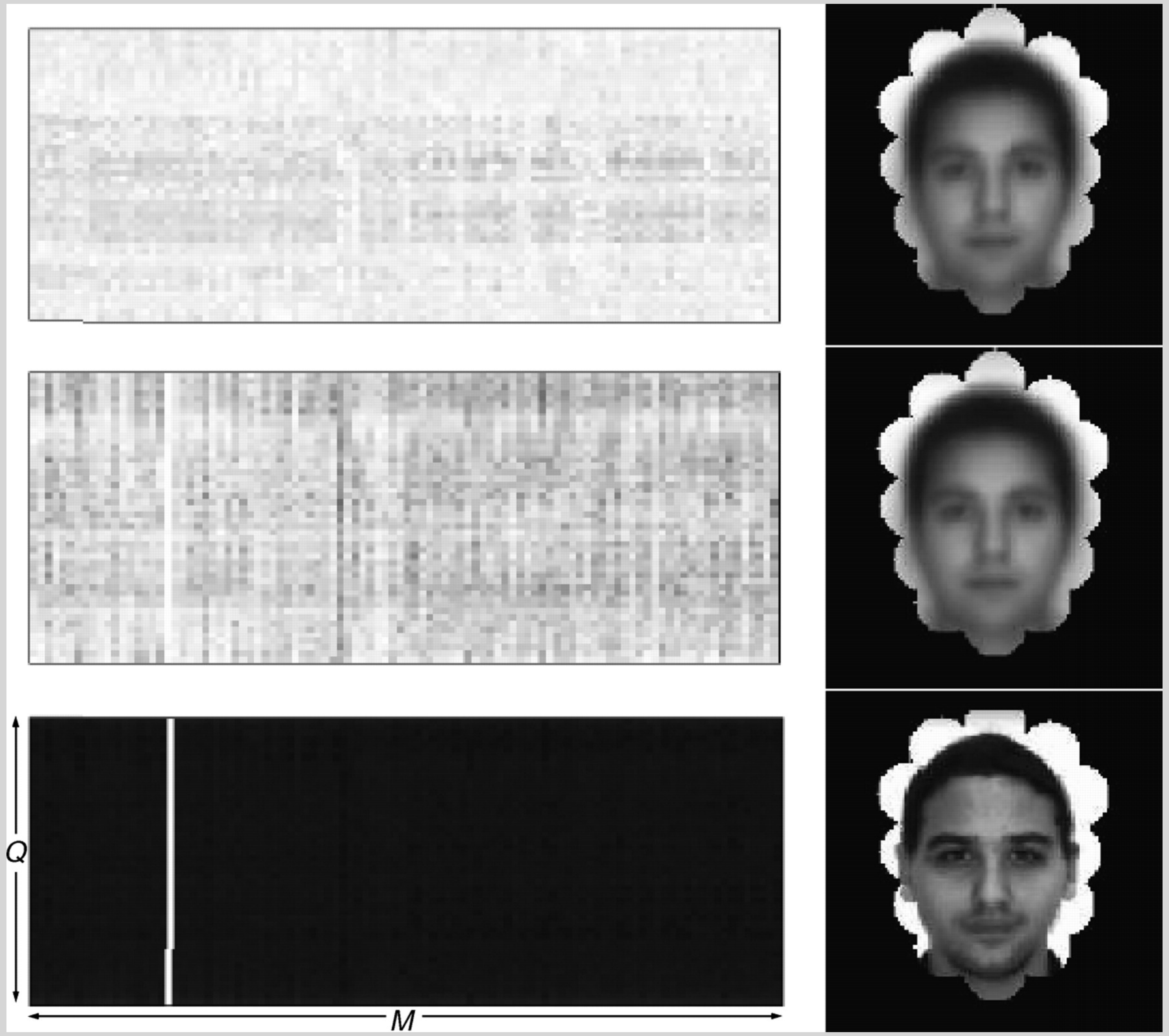

Wolfrum, P., Wolff, C., Lücke, J., & von der Malsburg, C. (2008). A recurrent dynamic model for correspondence-based face recognition. *Journal of Vision, 8*(7), 1–18. doi: 10.1167/8.7.34

Alfred Yarbus, 1967

Eye Scan Patterns

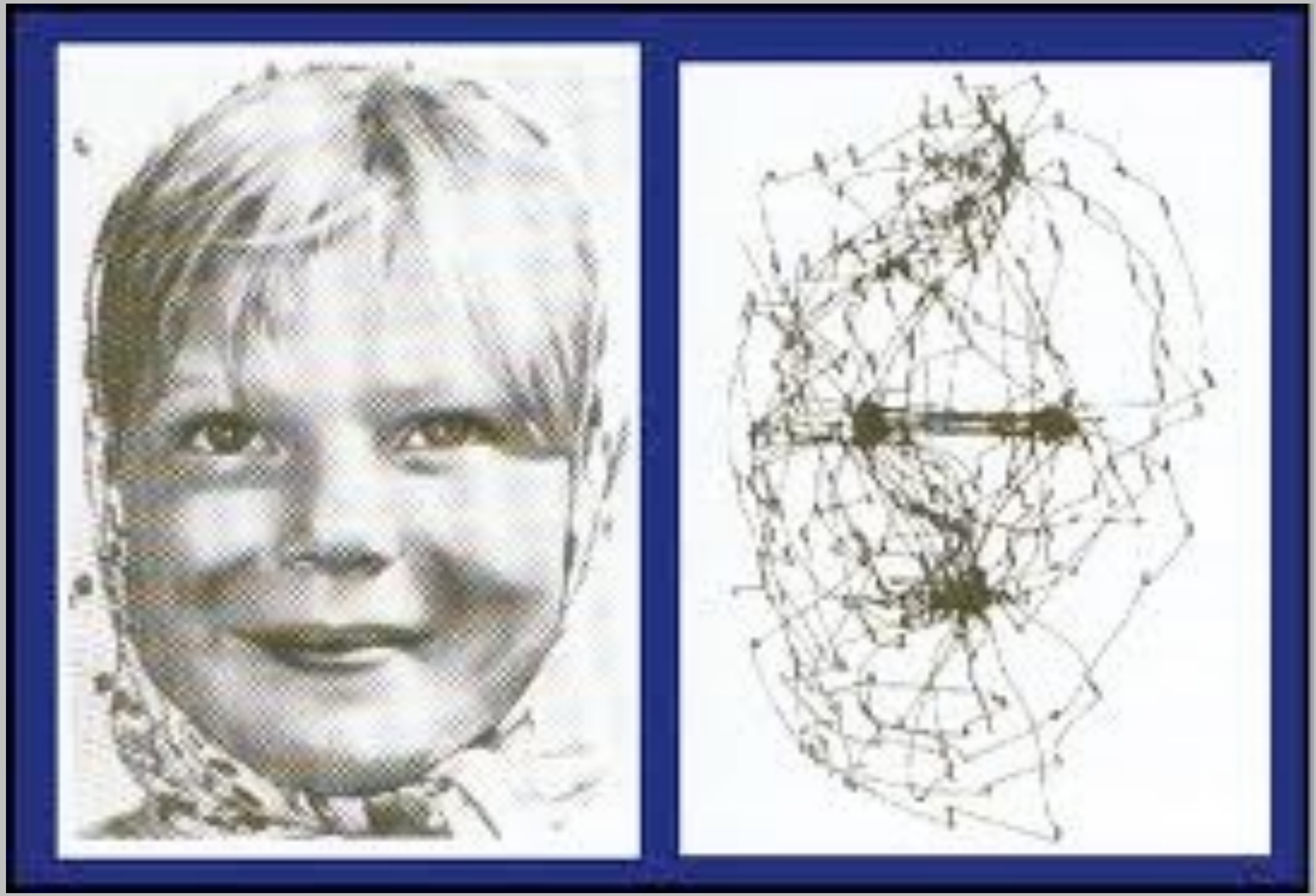

Yarbus, A. L. (1967). *Eye movements and vision* (B. Haigh, Trans.). New York: Plenum Press.

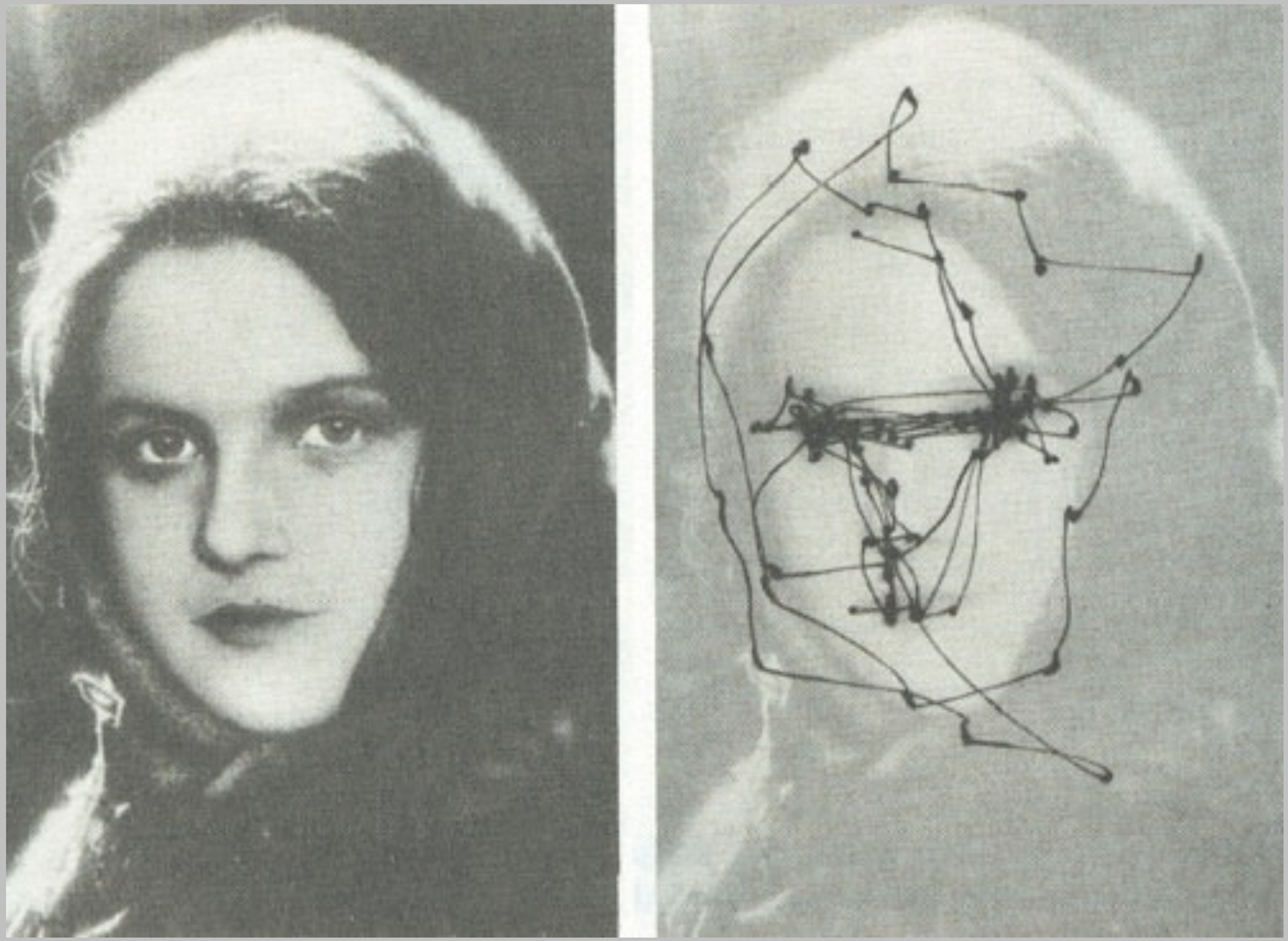

Yarbus, A. L. (1967). *Eye movements and vision* (B. Haigh, Trans.). New York: Plenum Press.

An Unexpected Visitor by Ilya Repin in 1884

Yarbus, A. L. (1967). *Eye movements and vision* (B. Haigh, Trans.). New York: Plenum Press.

Sasha Archibald (http://www.datadeluge.com/2012_10_01_archive.html)

Free Examination

An Unexpected Visitor by Ilya Repin in 1884

Sasha Archibald (http://www.datadeluge.com/2012_10_01_archive.html)

Yarbus, A. L. (1967). *Eye movements and vision* (B. Haigh, Trans.). New York: Plenum Press.

Material Circumstances

An Unexpected Visitor by Ilya Repin in 1884

Sasha Archibald (http://www.datadeluge.com/2012_10_01_archive.html)

Yarbus, A. L. (1967). *Eye movements and vision* (B. Haigh, Trans.). New York: Plenum Press.

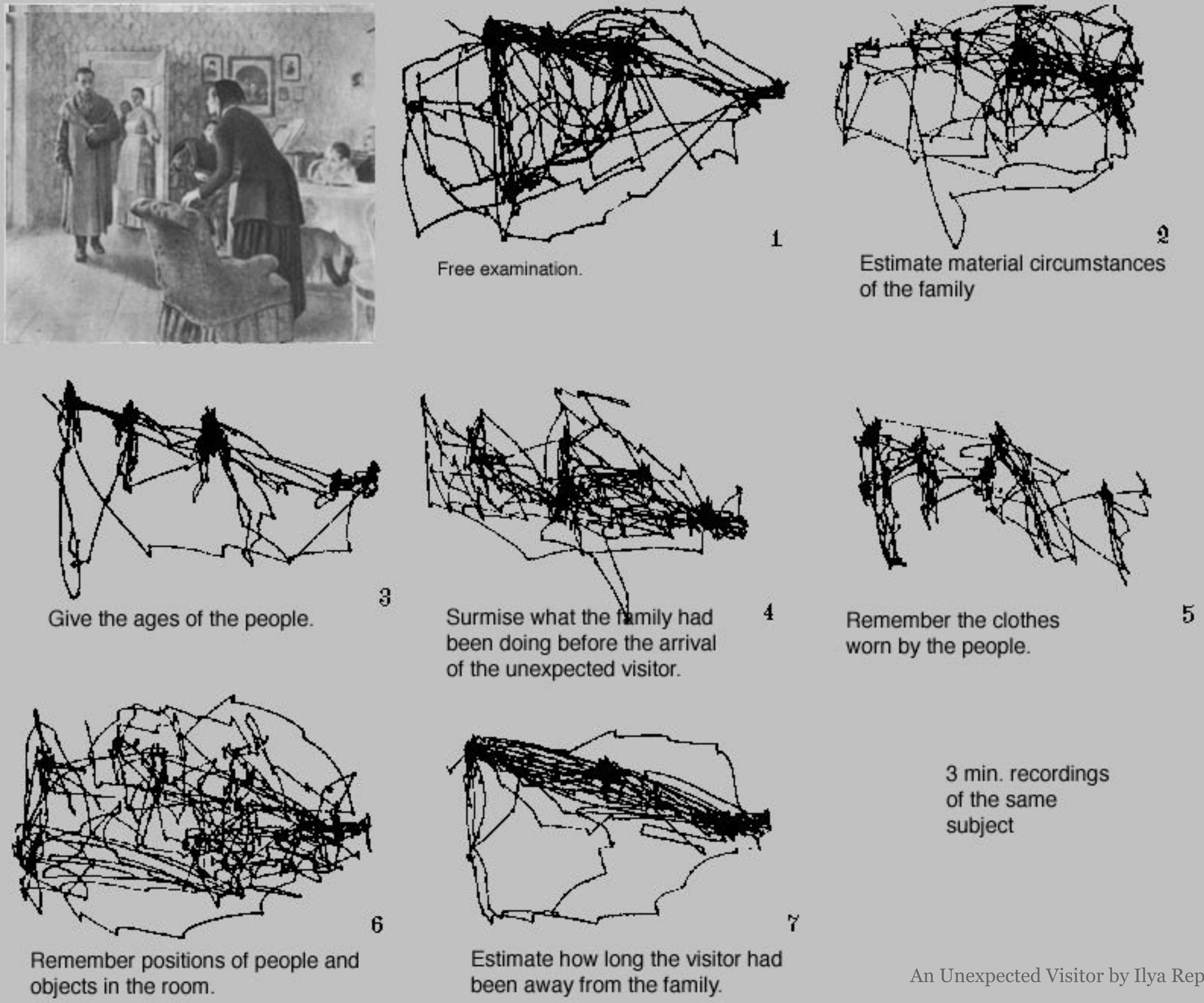

An Unexpected Visitor by Ilya Repin in 1884

Yarbus, A. L. (1967). *Eye movements and vision* (B. Haigh, Trans.). New York: Plenum Press.

Robert Yin, 1969

Inversion Affects Faces

96% 91% 85% 90%

Mean Percent Correct

82% 86% 84% 86

Yin, R. K. (1969). Looking at upside-down faces. *Journal of Experimental Psychology, 81*(1), 141–145.

Peter Thompson (1980)

Feature Inversion Effect (“Thatcher Illusion”)

Figure 2.

Figure 1.

Thompson, P. G. (1980). Margaret Thatcher: A new illusion. *Perception, 9*(4), 483–484.

Figure 1.

Figure 2.

Thompson, P. G. (1980). Margaret Thatcher: A new illusion. *Perception, 9*(4), 483–484.

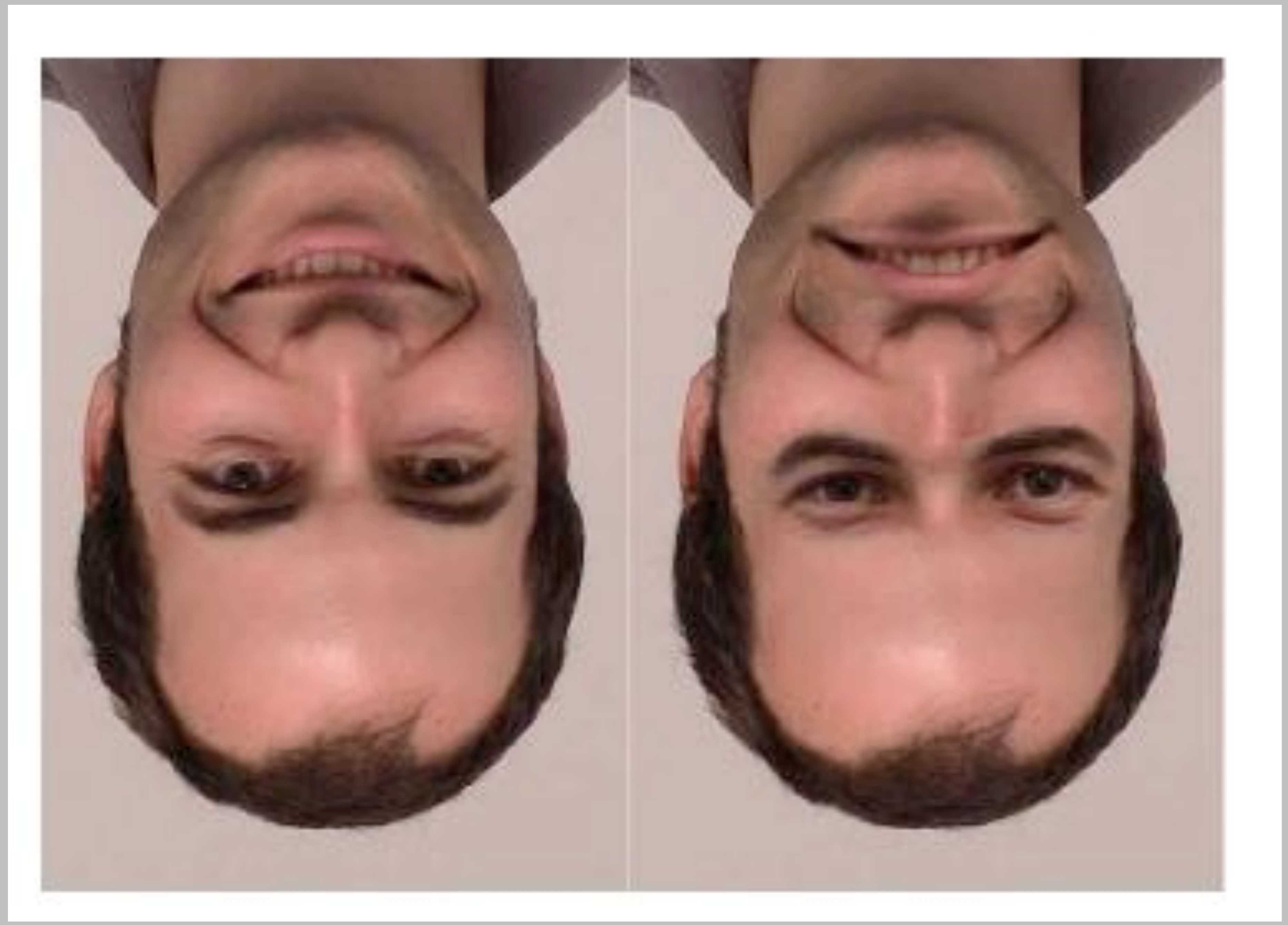

Carbon, C.-C., Schweinberger, S. R., Kaufmann, J. M., & Leder, H. (2005). The Thatcher illusion seen by the brain: An event-related brain potentials study. *Cognitive Brain Research, 24*(3), 544-555. doi: 10.1016/j.cogbrainres.2005.03.008

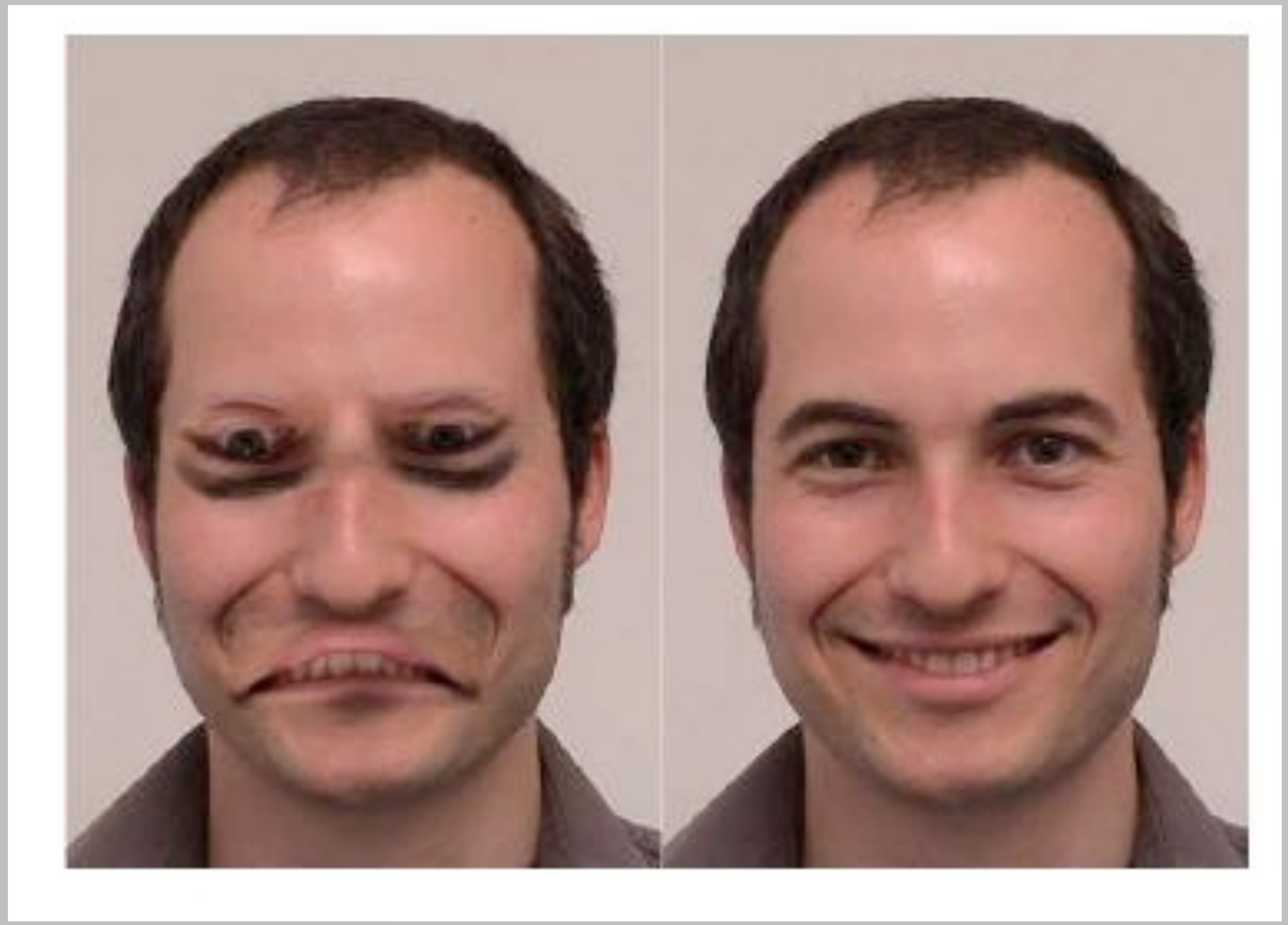

Carbon, C.-C., Schweinberger, S. R., Kaufmann, J. M., & Leder, H. (2005). The Thatcher illusion seen by the brain: An event-related brain potentials study. *Cognitive Brain Research, 24*(3), 544-555. doi: 10.1016/j.cogbrainres.2005.03.008

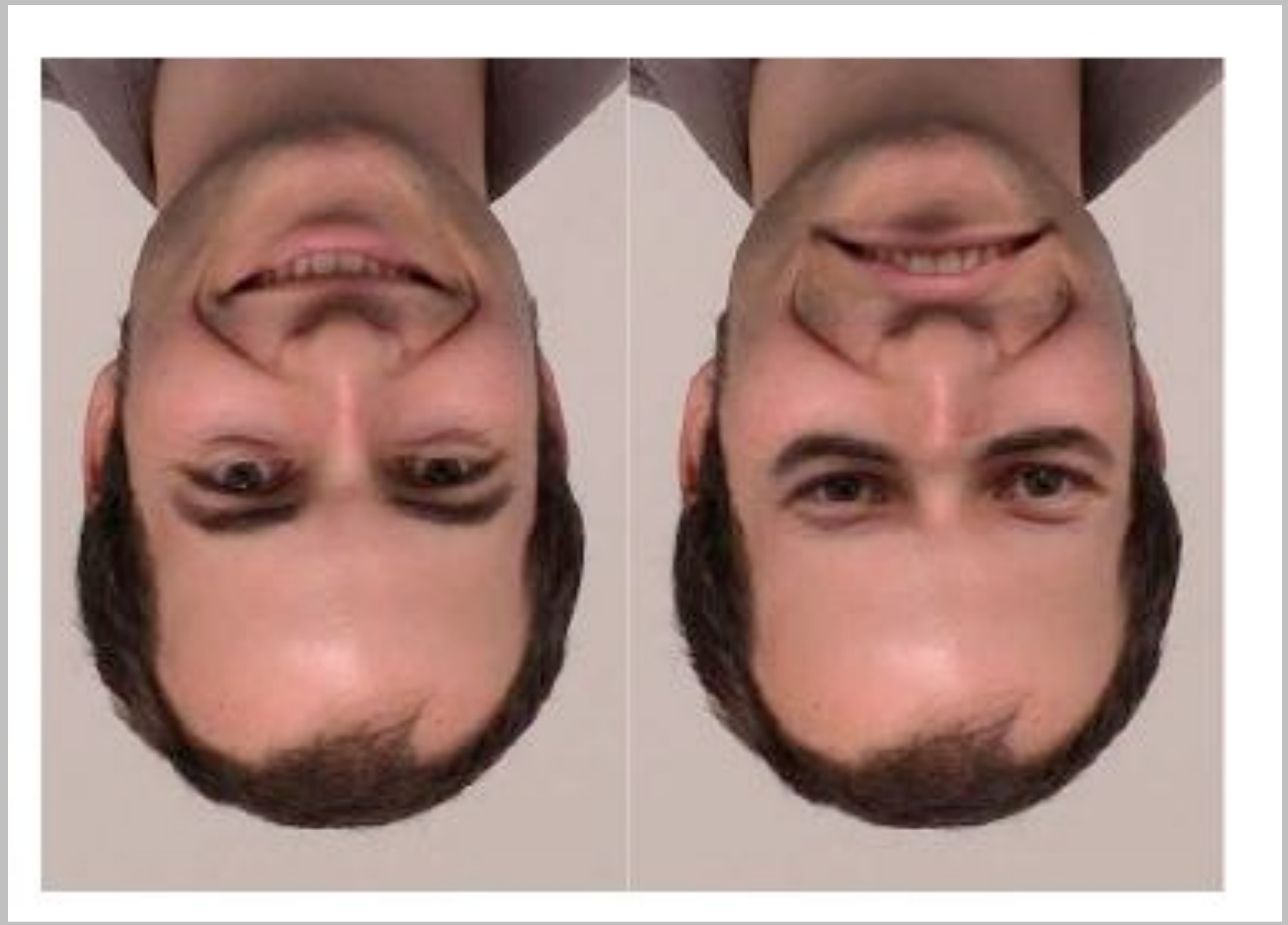

Carbon, C.-C., Schweinberger, S. R., Kaufmann, J. M., & Leder, H. (2005). The Thatcher illusion seen by the brain: An event-related brain potentials study. *Cognitive Brain Research, 24*(3), 544-555. doi: 10.1016/j.cogbrainres.2005.03.008

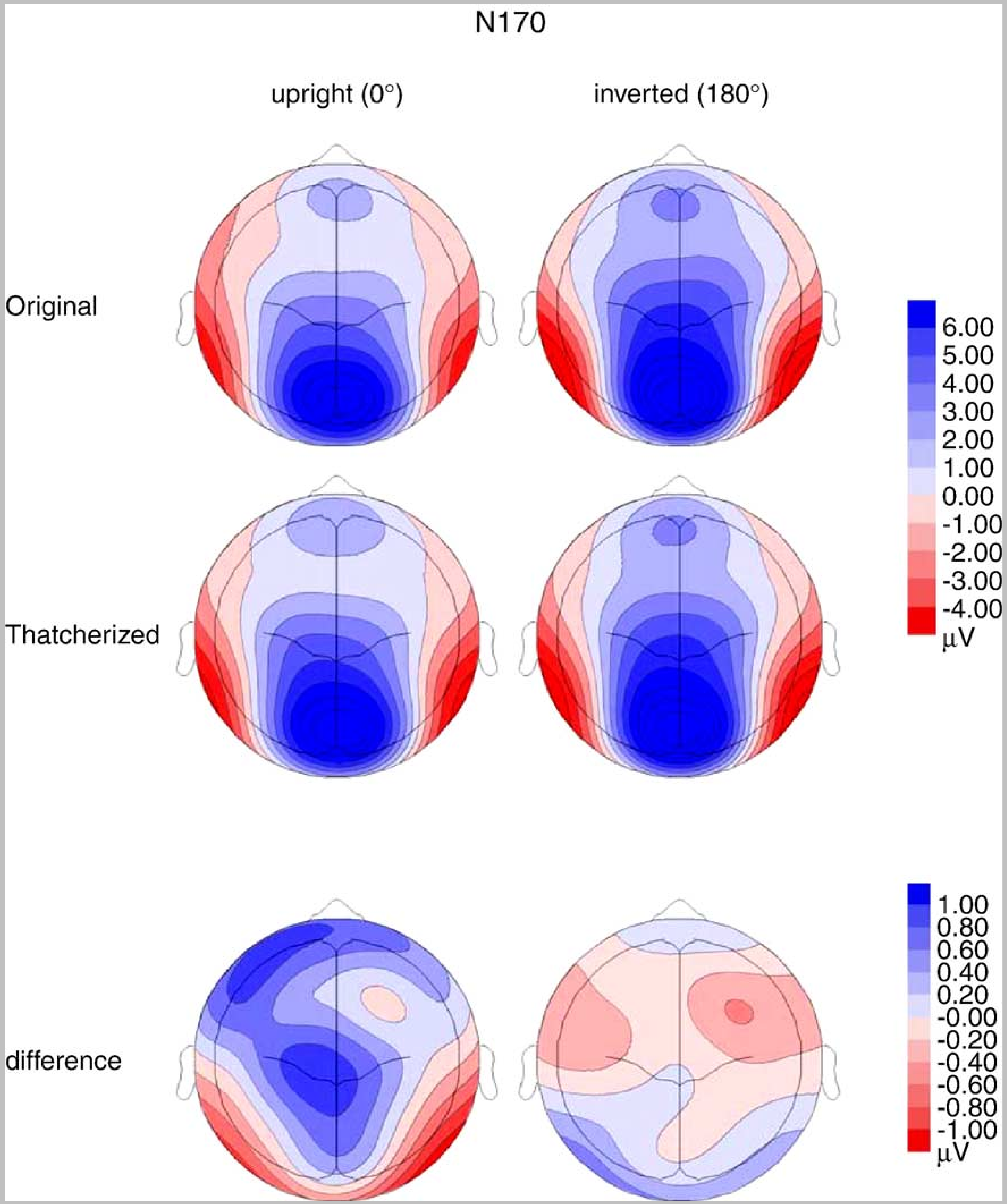

Carbon, C.-C., Schweinberger, S. R., Kaufmann, J. M., & Leder, H. (2005). The Thatcher illusion seen by the brain: An event-related brain potentials study. *Cognitive Brain Research, 24*(3), 544-555. doi: 10.1016/j.cogbrainres.2005.03.008

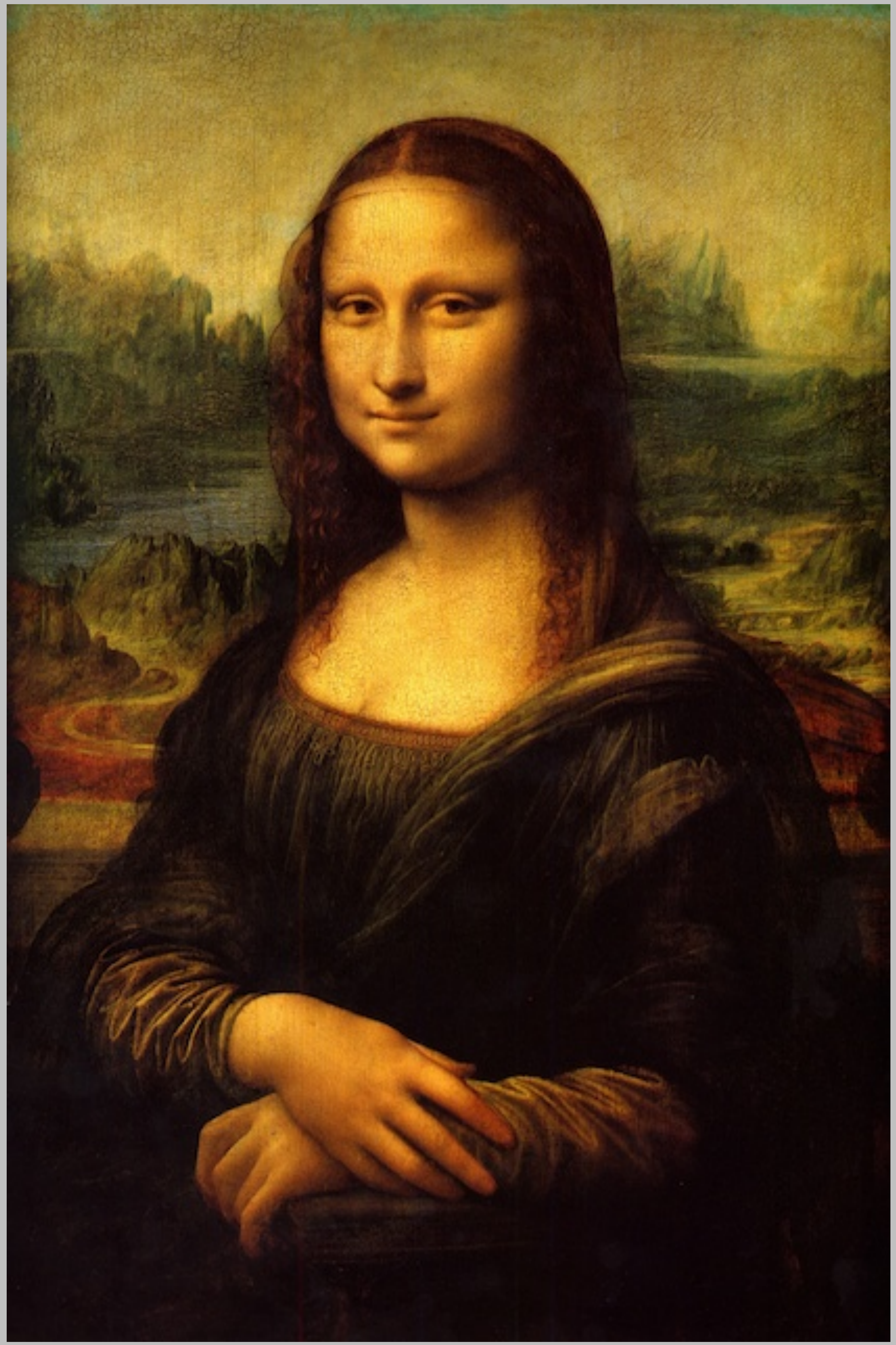

Nancy Kanwisher, 1997

Fusiform Facial Area

Face

Fusiform Face Area

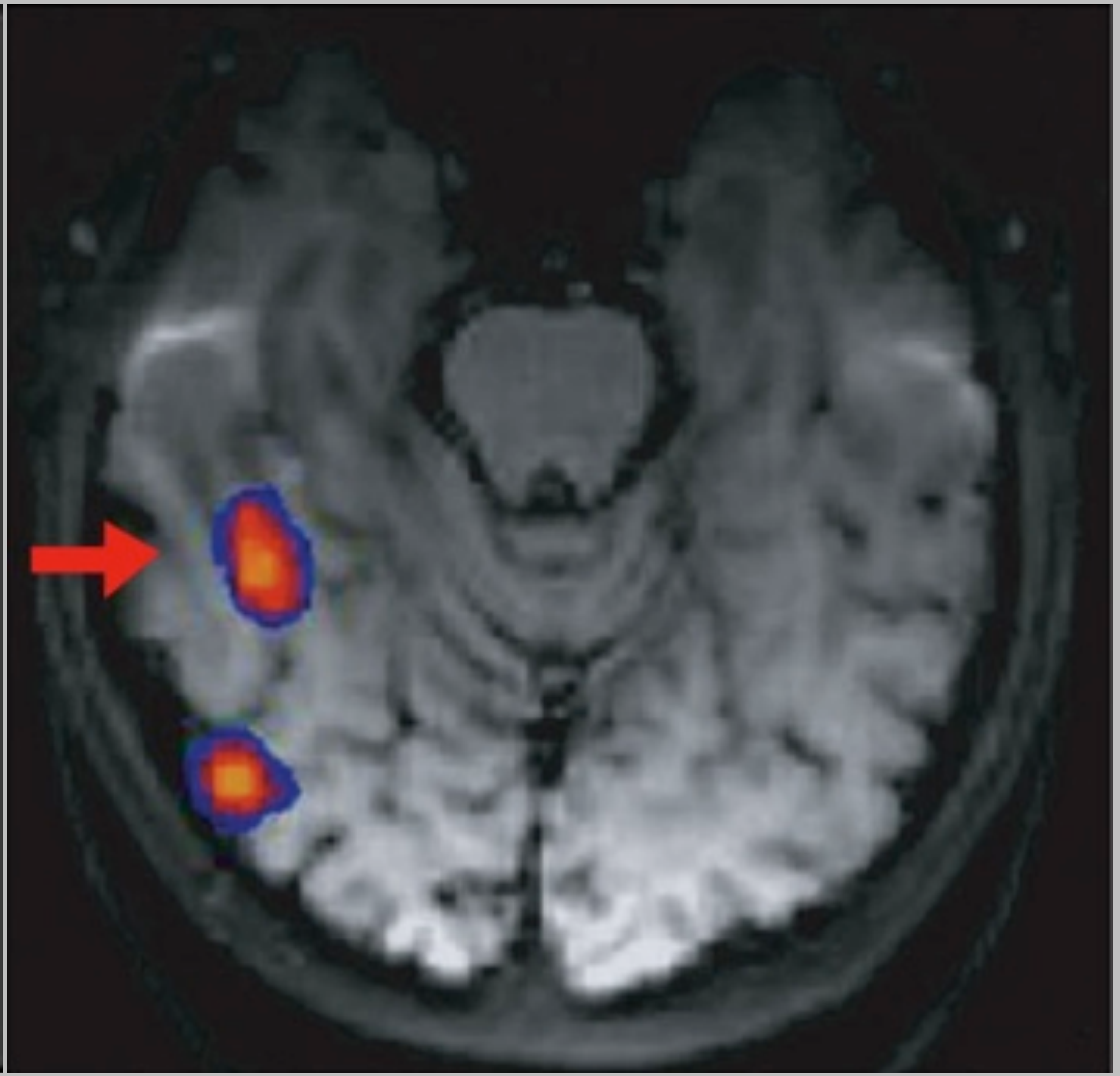

Downing, P., Liu, J., & Kanwisher, N. (2001). Testing cognitive models of visual attention with fMRI and MEG. *Neuropsychologia, 39*(12), 1329-1342. doi: 10.1016/S0028-3932(01)00121-X

House

Parahippocampal Place Area

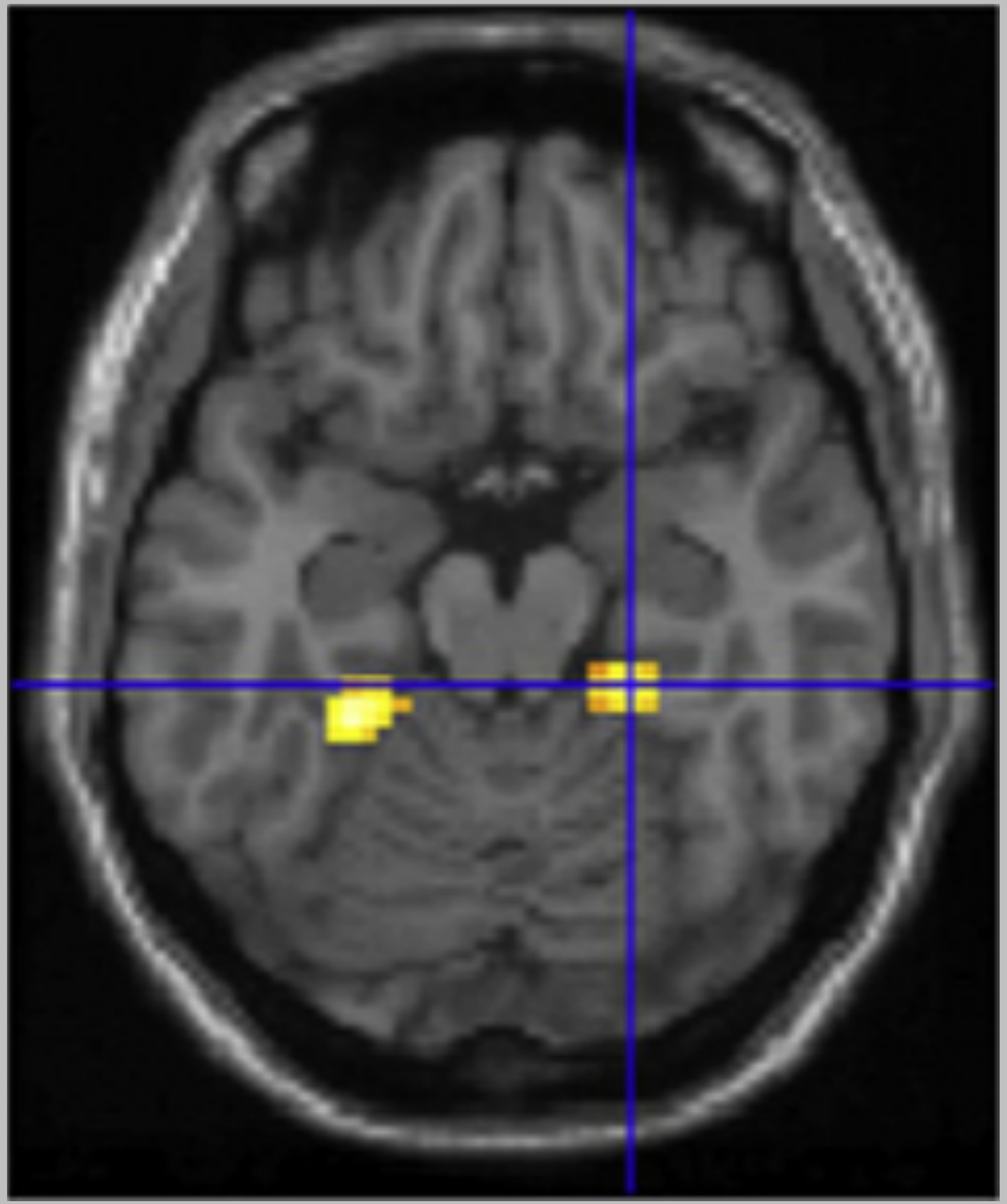

Downing, P., Liu, J., & Kanwisher, N. (2001). Testing cognitive models of visual attention with fMRI and MEG. *Neuropsychologia, 39*(12), 1329-1342. doi: 10.1016/S0028-3932(01)00121-X

Downing, P., Liu, J., & Kanwisher, N. (2001). Testing cognitive models of visual attention with fMRI and MEG. *Neuropsychologia, 39*(12), 1329-1342. doi: 10.1016/S0028-3932(01)00121-X

Face

FFA

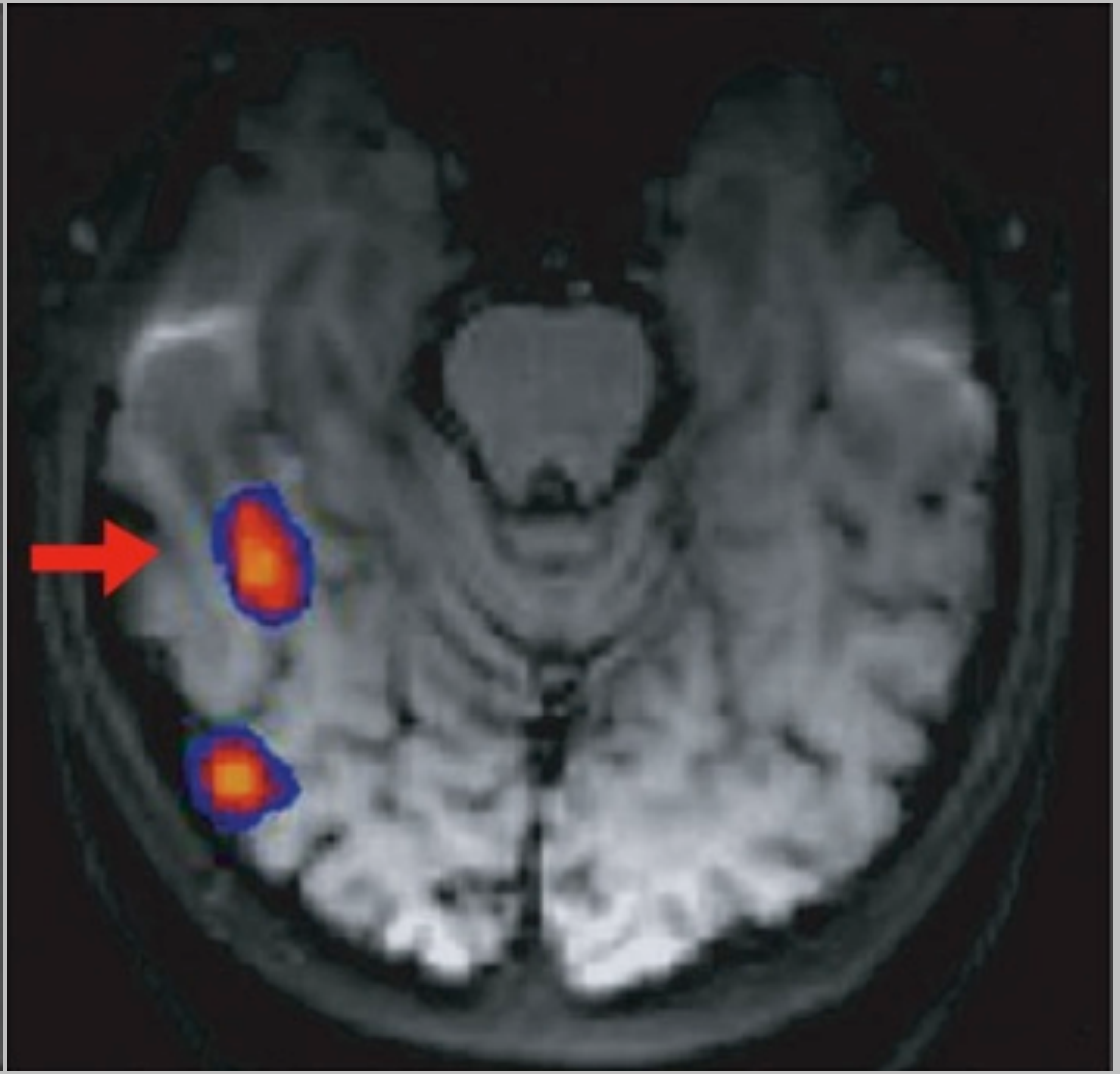

Downing, P., Liu, J., & Kanwisher, N. (2001). Testing cognitive models of visual attention with fMRI and MEG. *Neuropsychologia, 39*(12), 1329-1342. doi: 10.1016/S0028-3932(01)00121-X

House

PPA

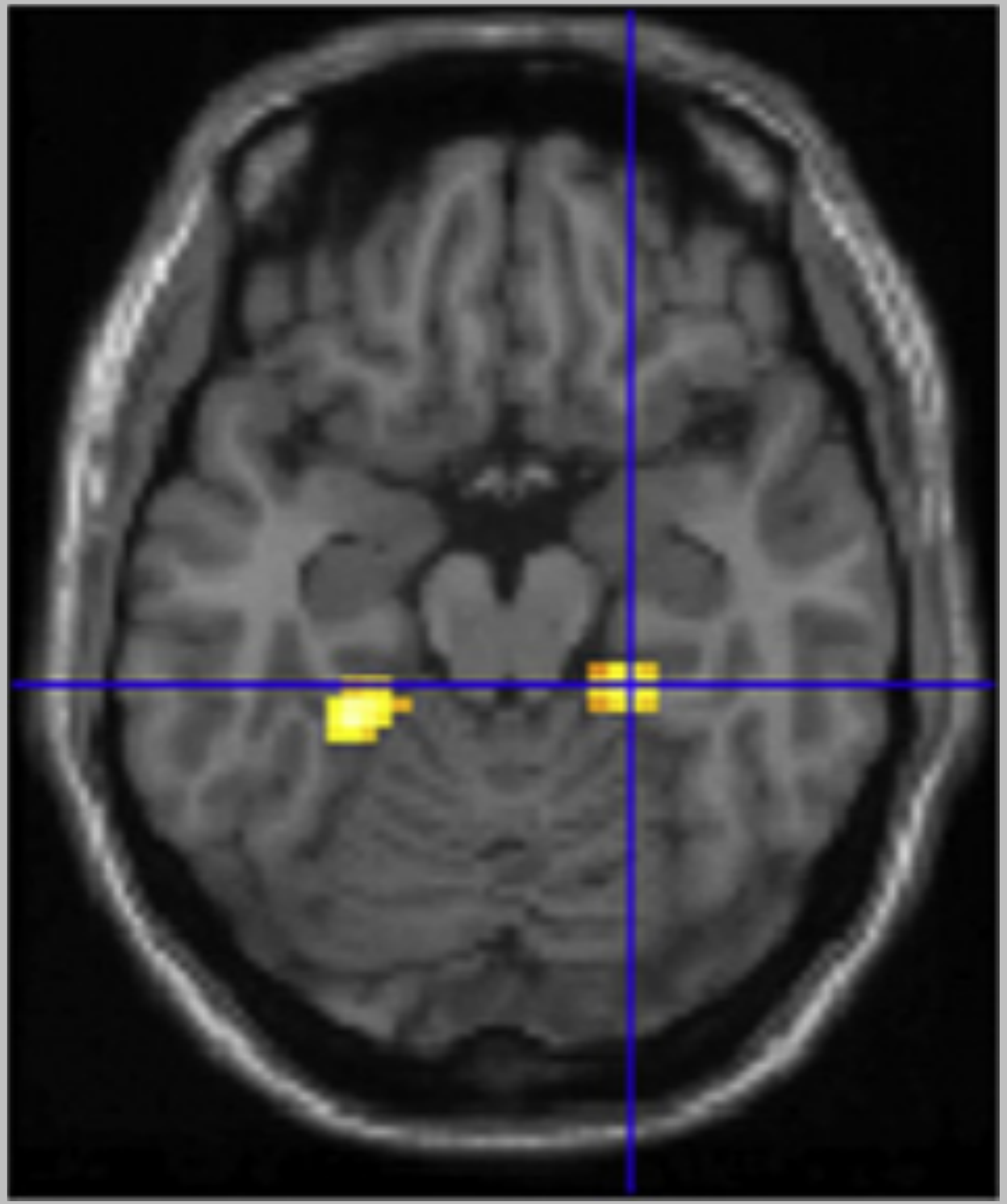

Downing, P., Liu, J., & Kanwisher, N. (2001). Testing cognitive models of visual attention with fMRI and MEG. *Neuropsychologia, 39*(12), 1329-1342. doi: 10.1016/S0028-3932(01)00121-X

Face

FFA

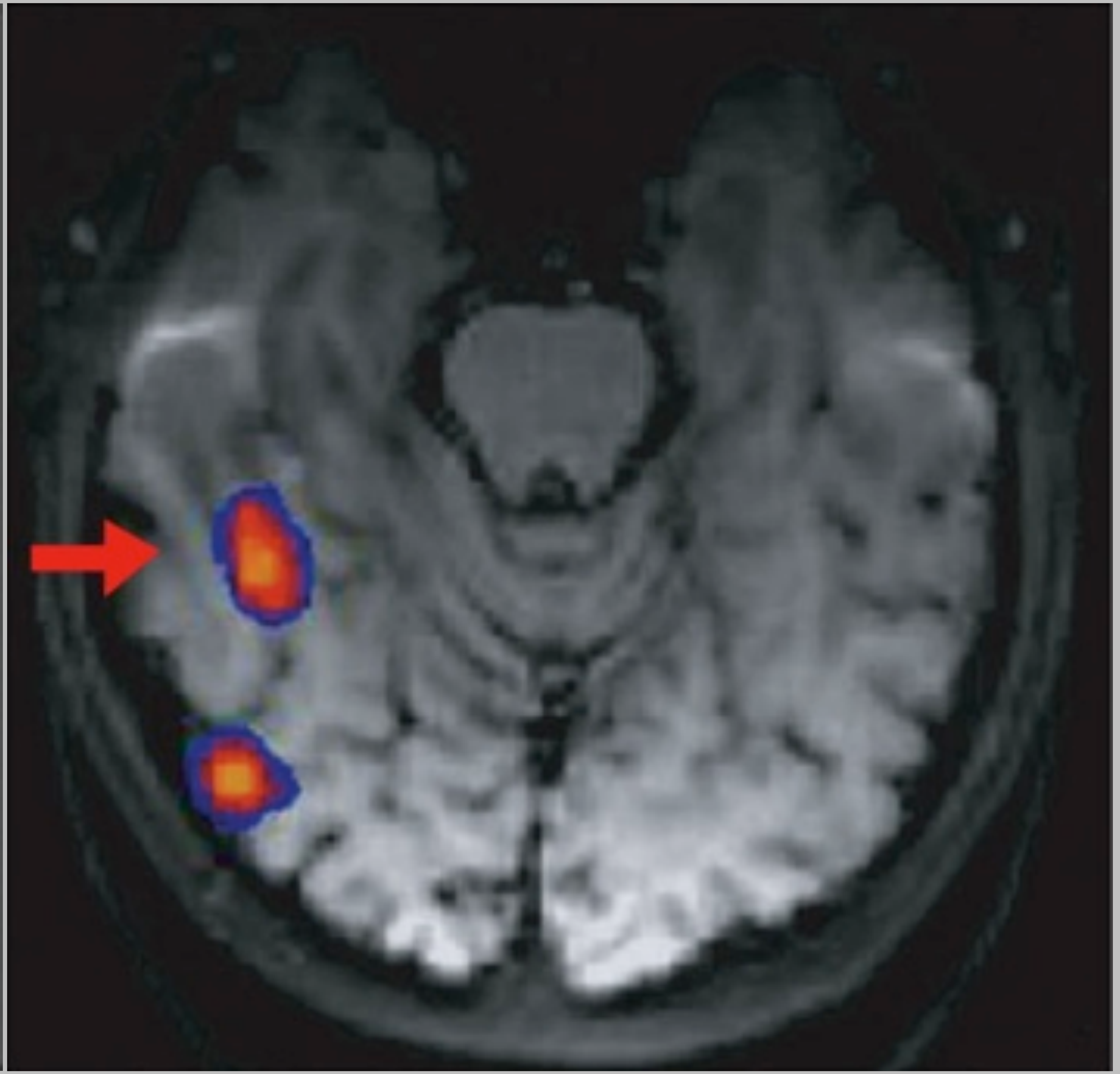

Downing, P., Liu, J., & Kanwisher, N. (2001). Testing cognitive models of visual attention with fMRI and MEG. *Neuropsychologia, 39*(12), 1329-1342. doi: 10.1016/S0028-3932(01)00121-X

House

PPA

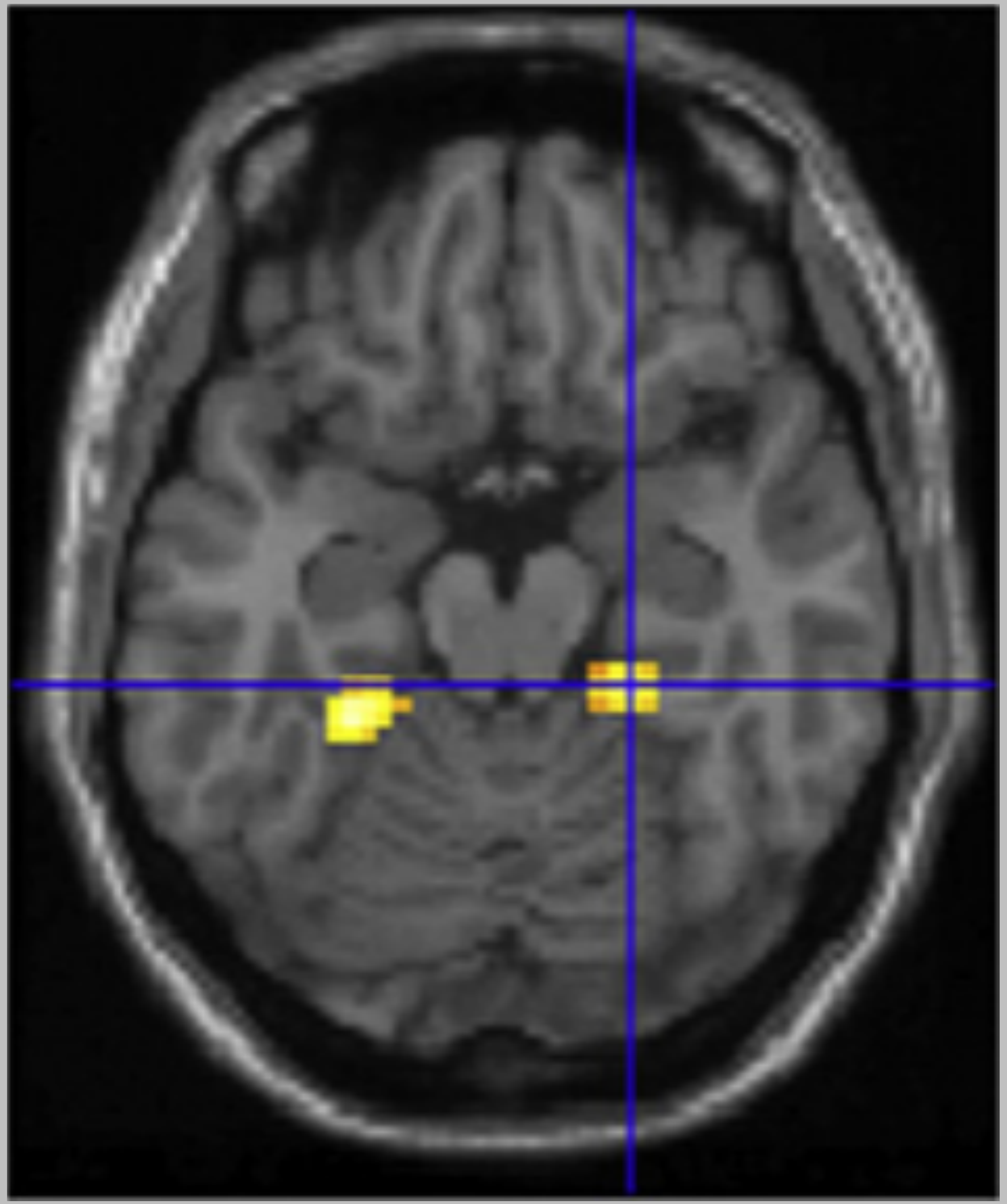

Downing, P., Liu, J., & Kanwisher, N. (2001). Testing cognitive models of visual attention with fMRI and MEG. *Neuropsychologia, 39*(12), 1329-1342. doi: 10.1016/S0028-3932(01)00121-X

Face

FFA

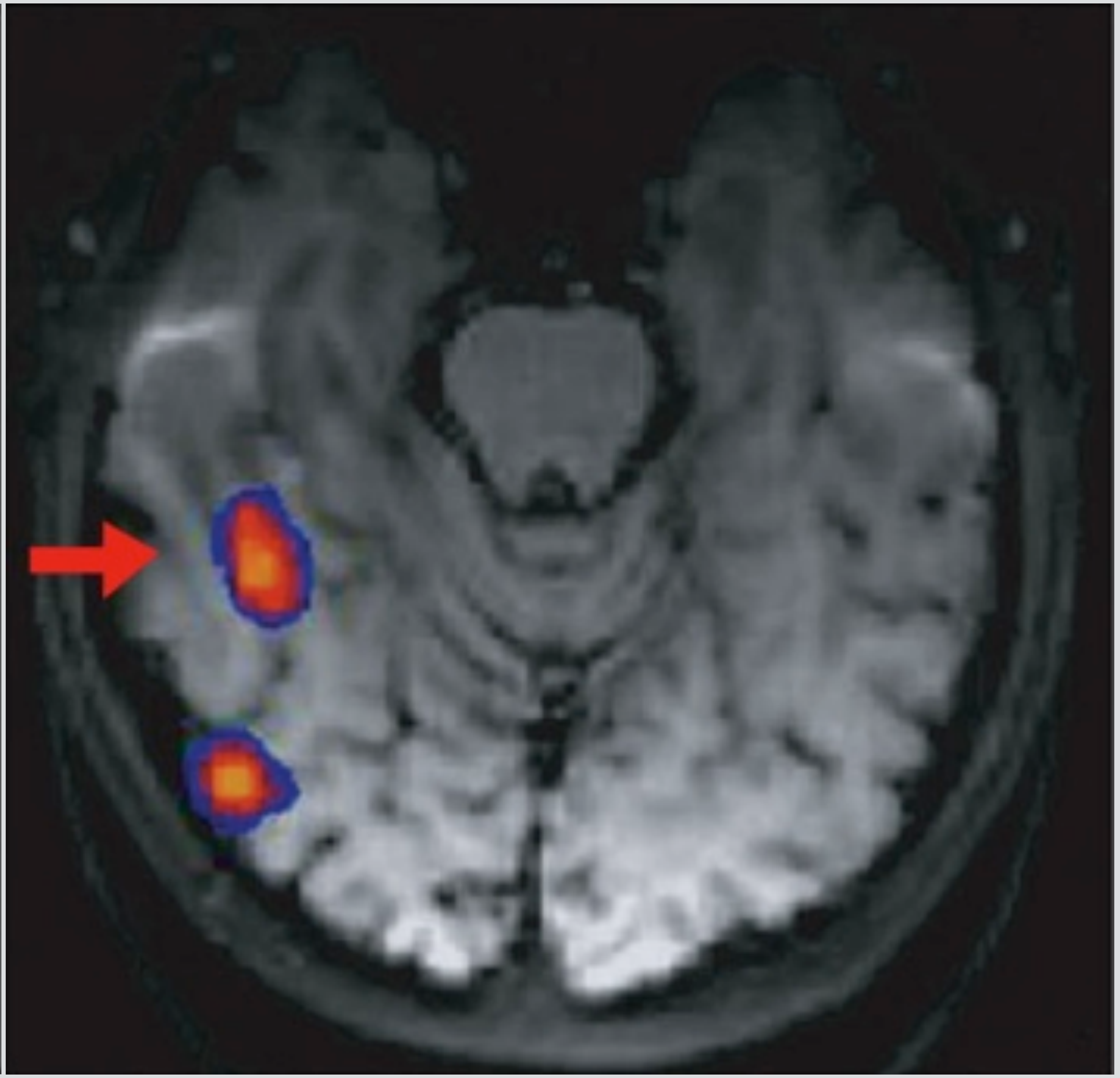

Downing, P., Liu, J., & Kanwisher, N. (2001). Testing cognitive models of visual attention with fMRI and MEG. *Neuropsychologia, 39*(12), 1329-1342. doi: 10.1016/S0028-3932(01)00121-X

House

PPA

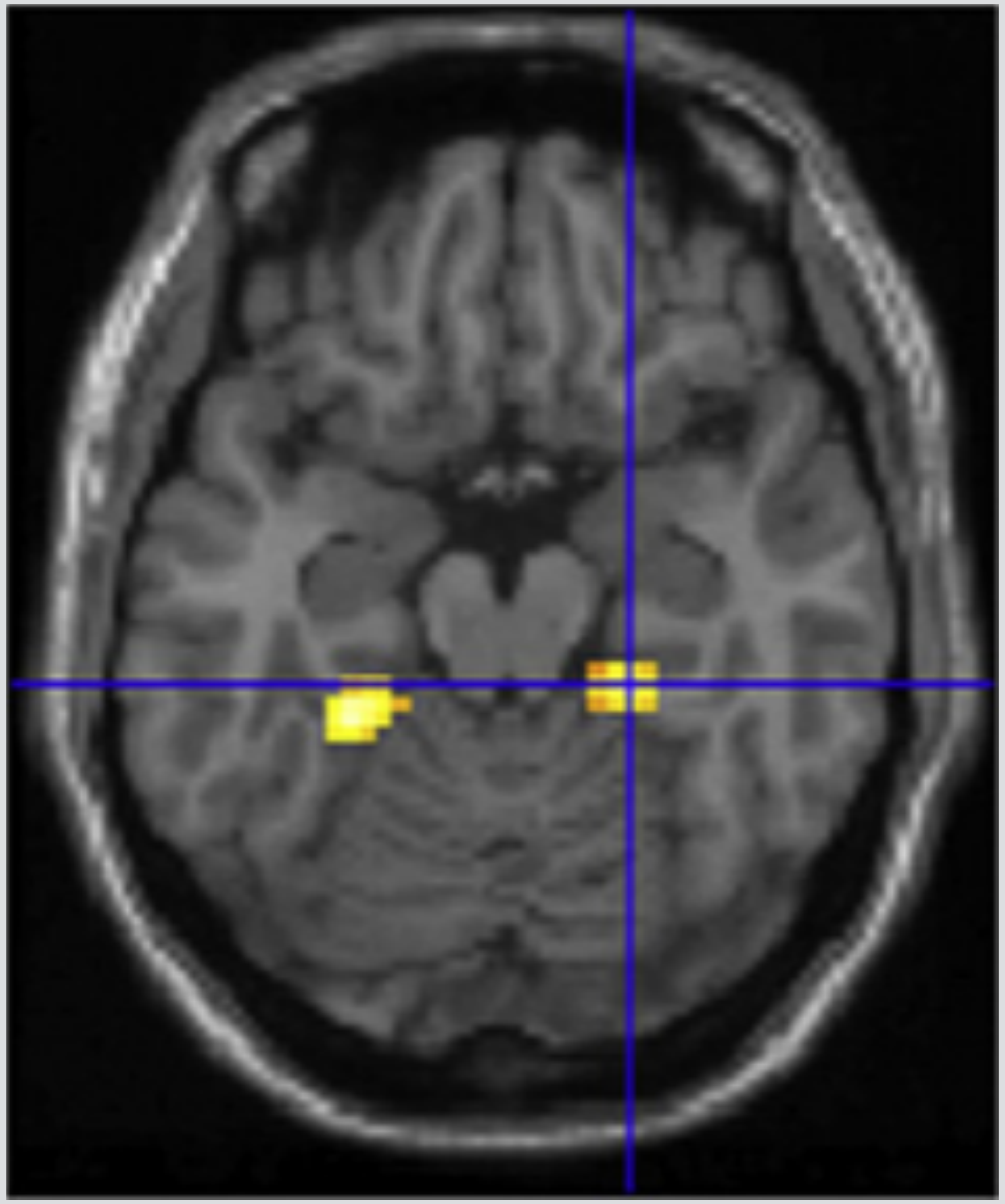

Downing, P., Liu, J., & Kanwisher, N. (2001). Testing cognitive models of visual attention with fMRI and MEG. *Neuropsychologia, 39*(12), 1329-1342. doi: 10.1016/S0028-3932(01)00121-X

Face

FFA

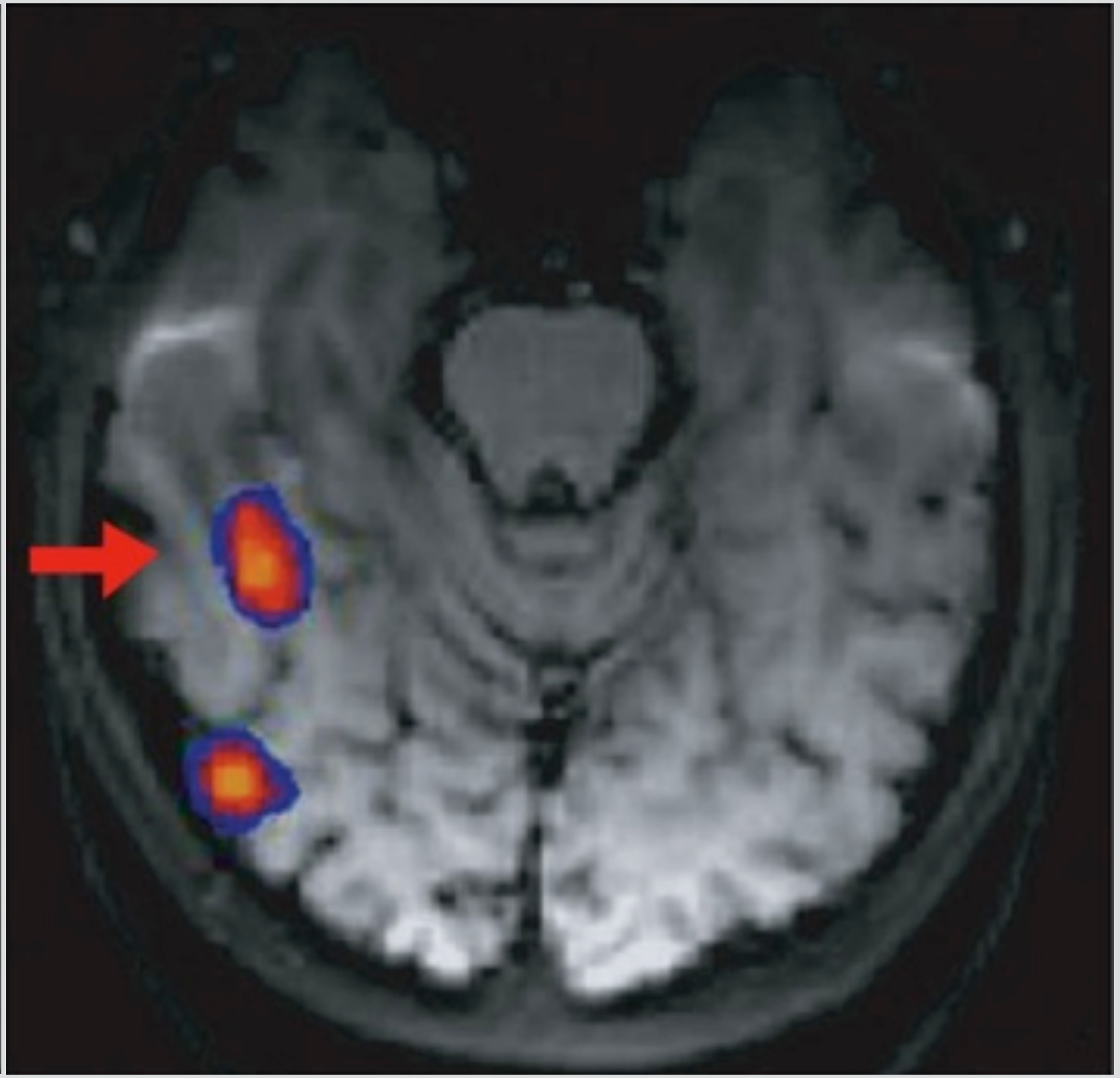

Downing, P., Liu, J., & Kanwisher, N. (2001). Testing cognitive models of visual attention with fMRI and MEG. *Neuropsychologia, 39*(12), 1329-1342. doi: 10.1016/S0028-3932(01)00121-X

House

PPA

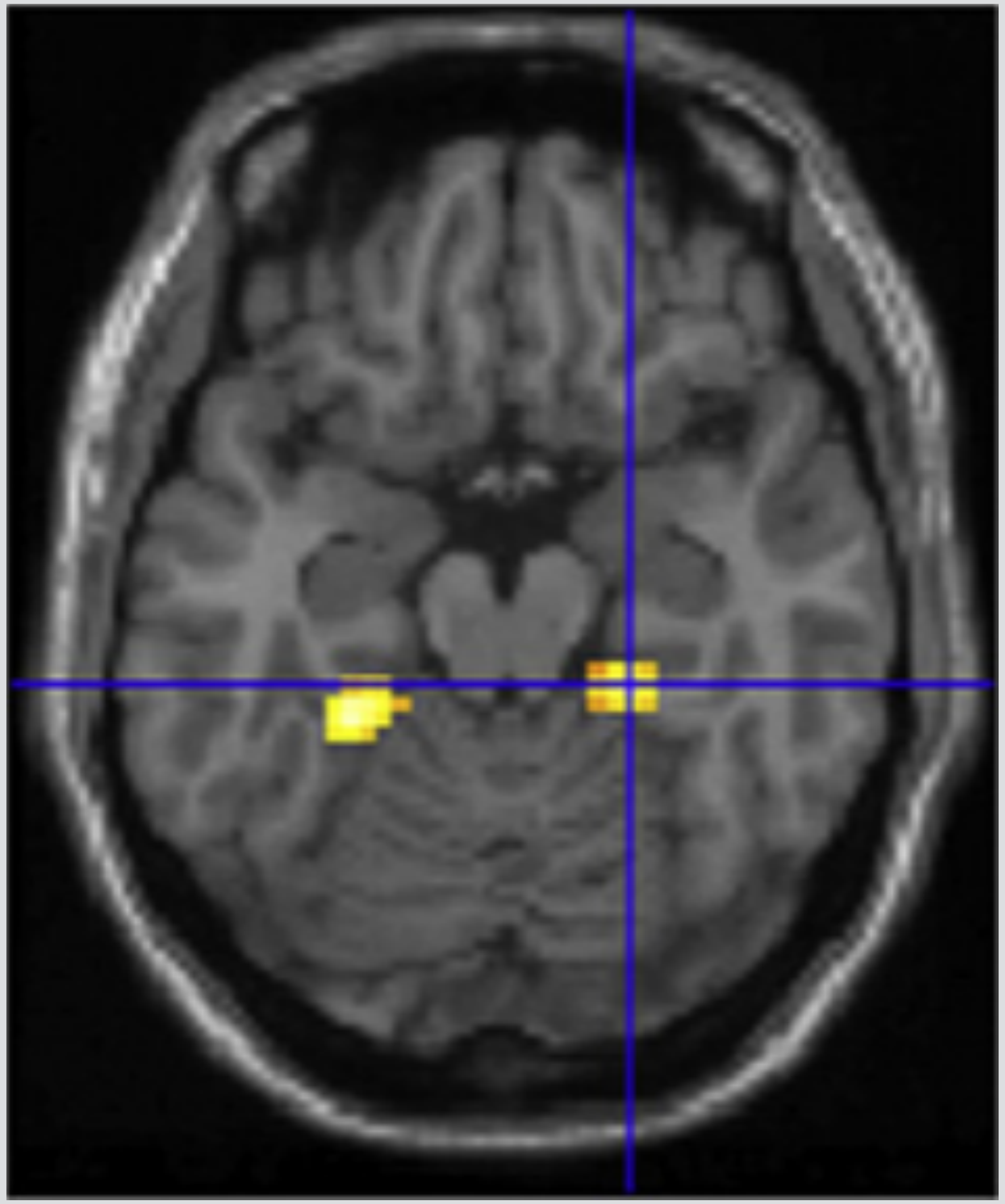

Downing, P., Liu, J., & Kanwisher, N. (2001). Testing cognitive models of visual attention with fMRI and MEG. *Neuropsychologia, 39*(12), 1329-1342. doi: 10.1016/S0028-3932(01)00121-X

Faces and Emotions

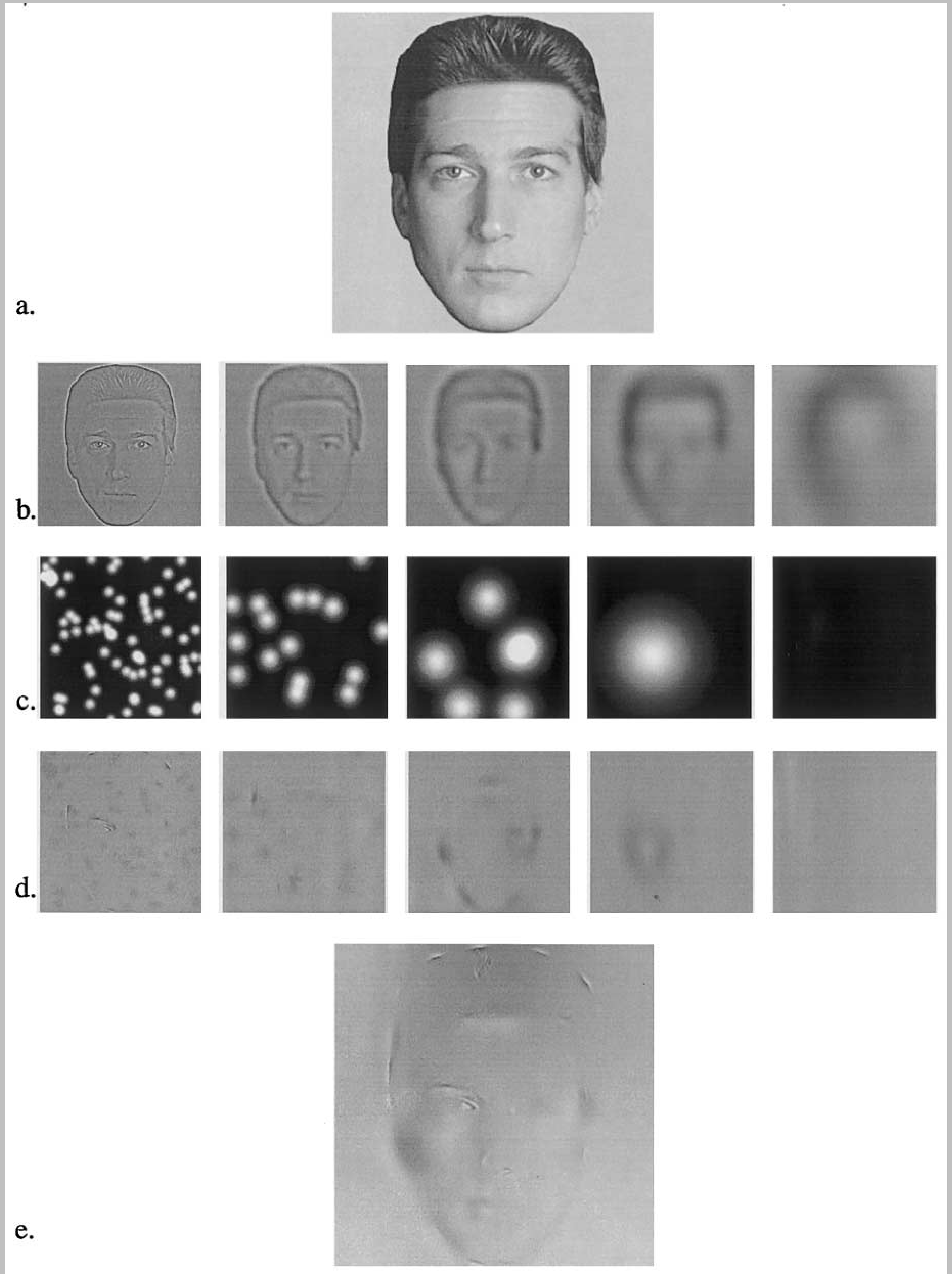

Gosselin, F., & Schyns, P. G. (2001). Bubbles: A technique to reveal the use of information in recognition tasks. *Vision Research, 41*(17), 2261-2271.

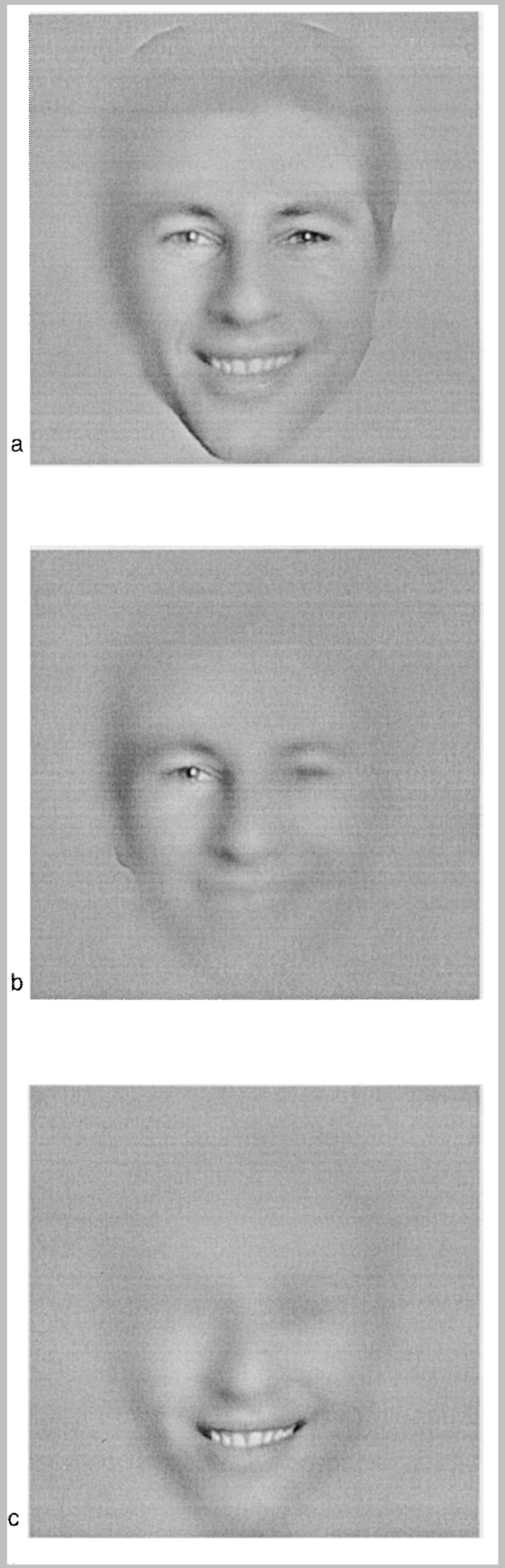

Identify

Gender

Emotion

Schyns, P. G., Bonnar, L., & Gosselin, F. (2002). Show me the features! Understanding recognition from the use of visual information. *Psychological Science, 13*(5), 402-409.

Grandmother Cell?

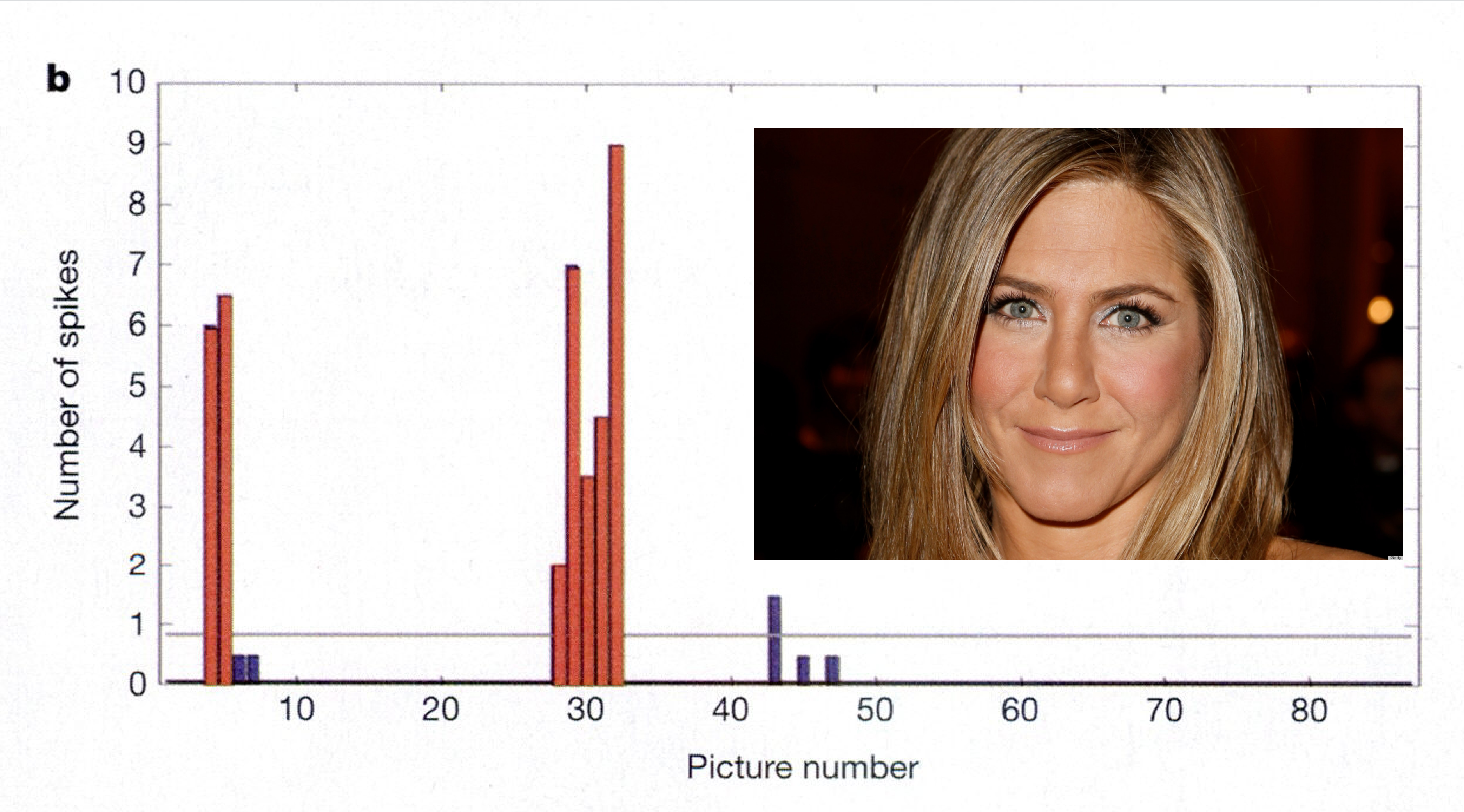

Quian Quiroga, R., Reddy, L., Kreiman, G., Koch, C., & Fried, I. (2005). Invariant visual representation by single neurons in the human brain. *Nature, 435*(7045), 1102-1107.

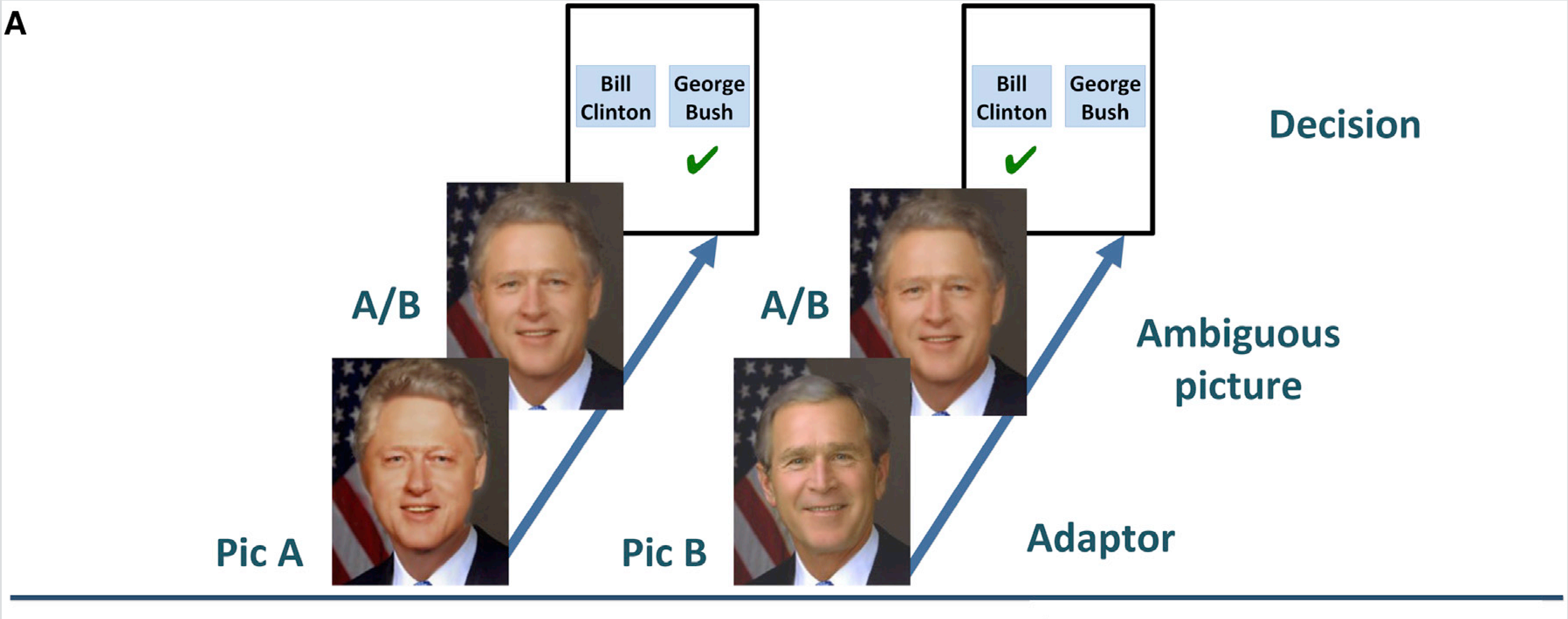

Quian Quiroga, R., Kraskov, A., Mormann, F., Fried, I., & Koch, C. (2014). Single-Cell Responses to Face Adaptation in the Human Medial Temporal Lobe. *Neuron*(0). doi: http://dx.doi.org/10.1016/j.neuron.2014.09.006

Main Points

- Faces are important
- Different Features play different roles
    - Eyes and Mouth are important
- The brain has special areas for faces

Attractors in Space

Giovanelli Illusion

Giovanelli, G. (1966). Stati di tensione e di equilibrio nel campo percettivo. *Revista di Psicologia, 60*(4), 327–335.

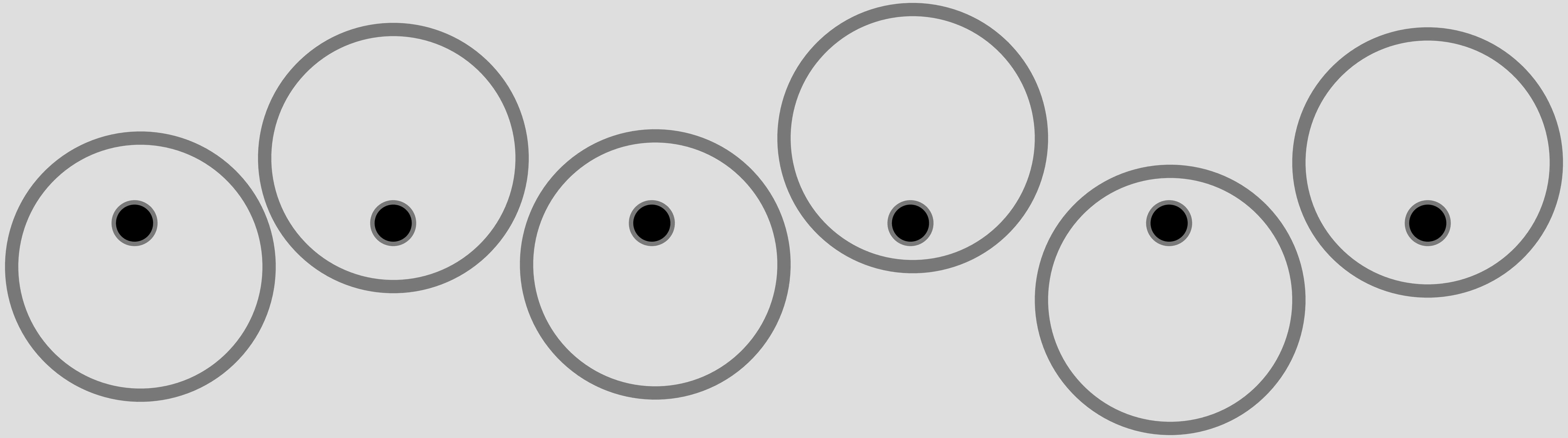

Giovanelli Illusion

Giovanelli, G. (1966). Stati di tensione e di equilibrio nel campo percettivo. *Revista di Psicologia, 60*(4), 327–335.

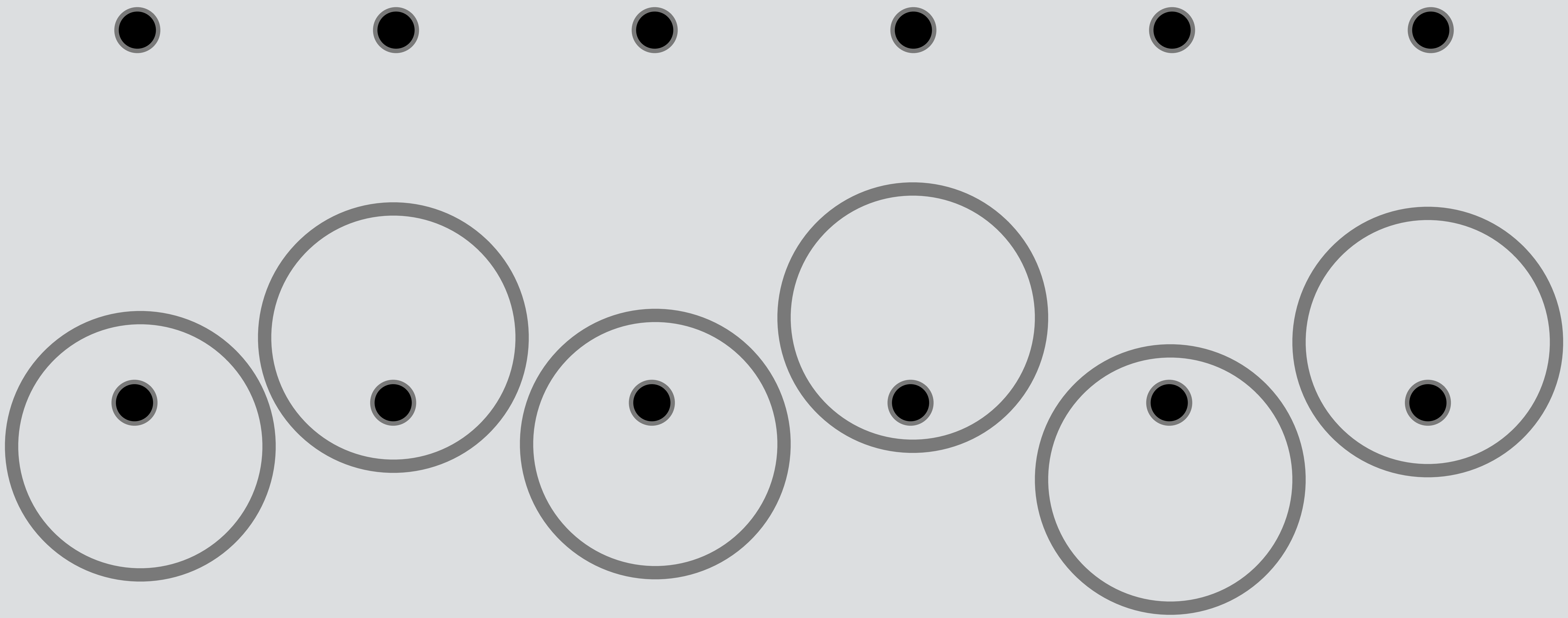

Giovanelli Illusion

Giovanelli, G. (1966). Stati di tensione e di equilibrio nel campo percettivo. *Revista di Psicologia, 60*(4), 327–335.

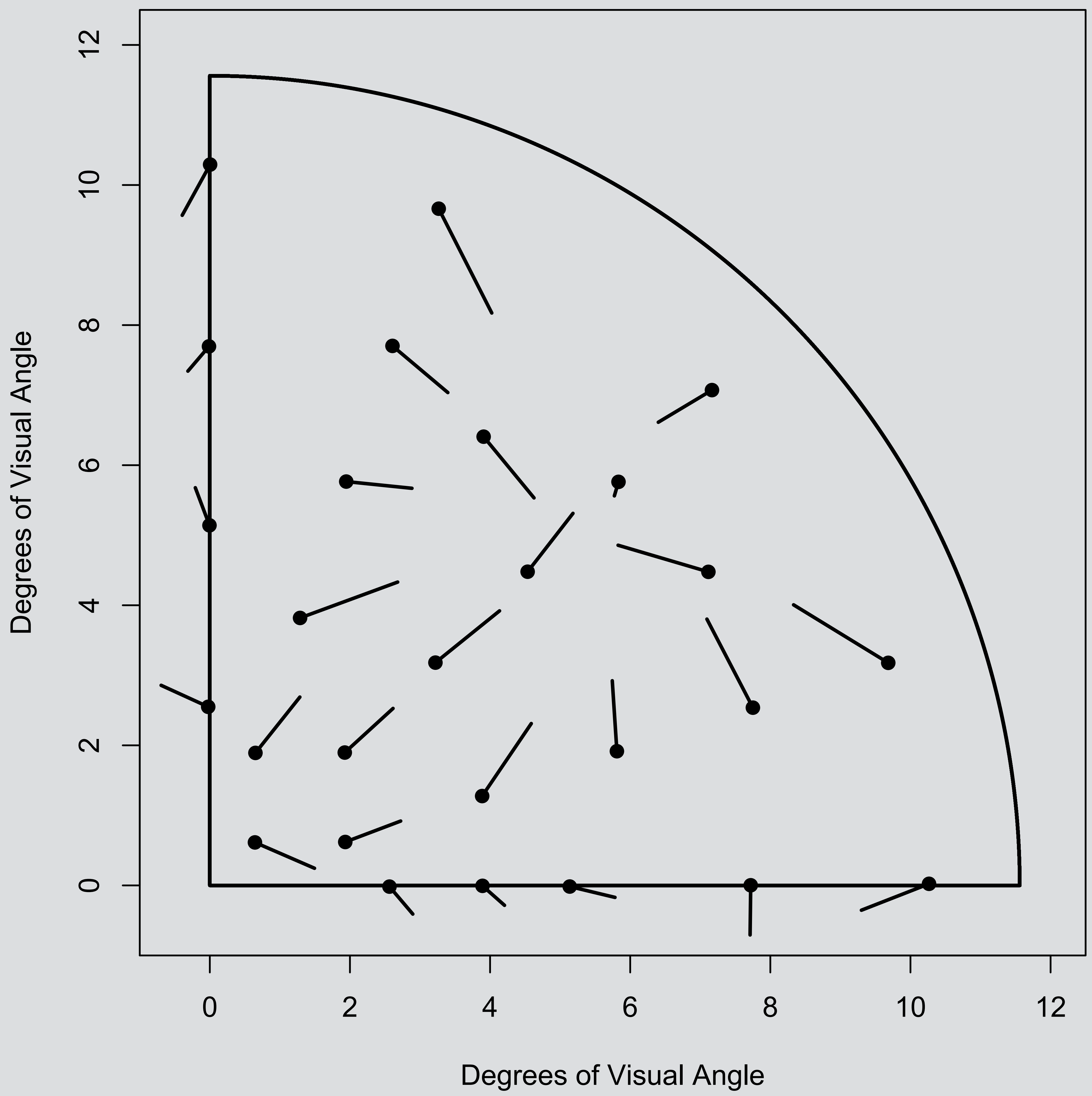

Attneave, F. (1955). Perception of place in a circular field. *American Journal of Psychology, 68*(1), 69–82.

Observed Vector Field

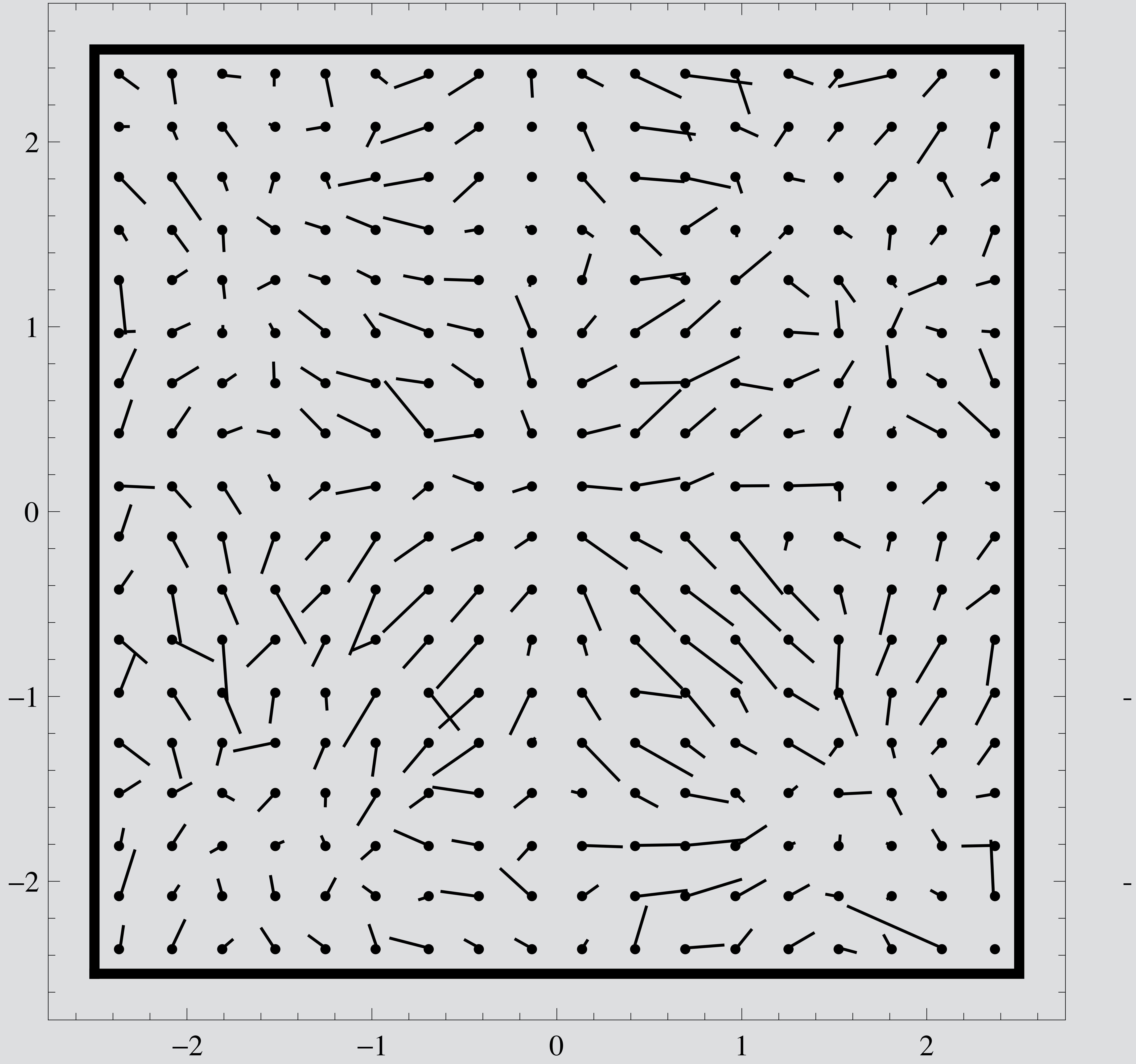

Harvey, L. O., Jr., & Schmidt, E. K. (2014). Self-organizing properties of the visual field: Gestalt forces in action. In A. Geremek, M. W. Greenlee & S. Magnussen (Eds.), *Perception Beyond Gestalt: Progress in vision research* (pp. 67–81). London: Psychology Press: Taylor & Francis Group.

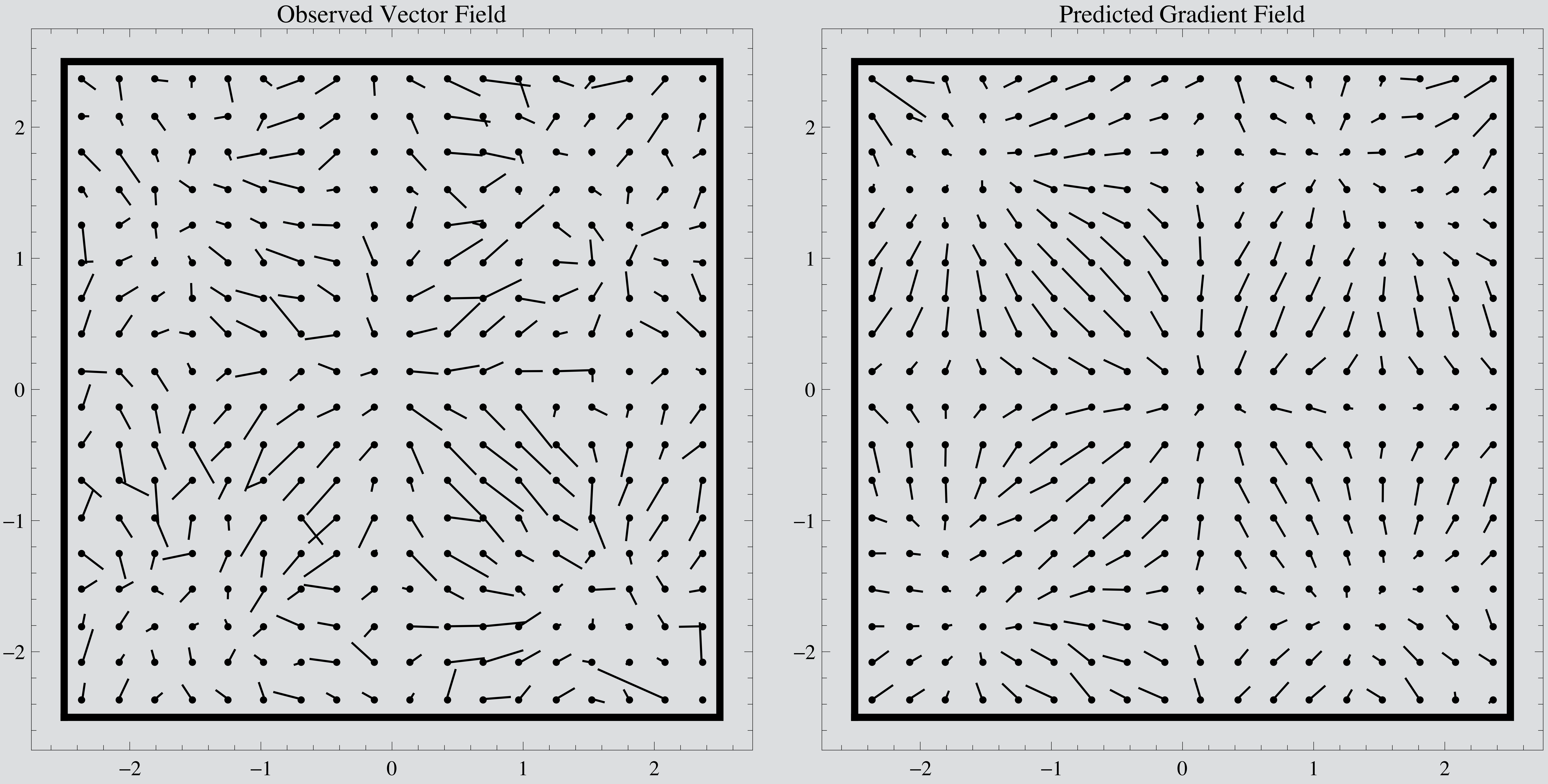

Harvey, L. O., Jr., & Schmidt, E. K. (2014). Self-organizing properties of the visual field: Gestalt forces in action. In A. Geremek, M. W. Greenlee & S. Magnussen (Eds.), *Perception Beyond Gestalt: Progress in vision research* (pp. 67–81). London: Psychology Press: Taylor & Francis Group.

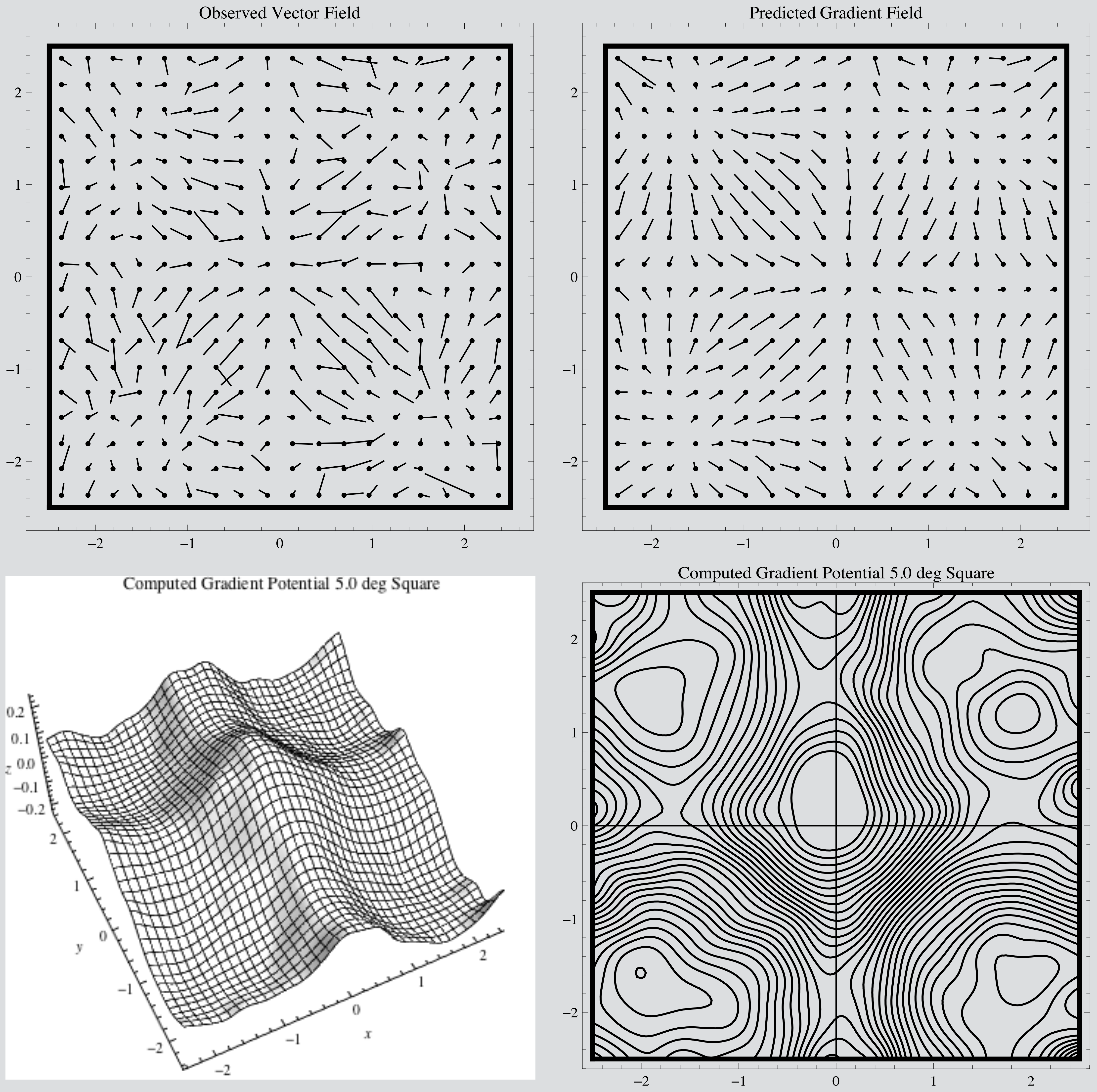

Harvey, L. O., Jr., & Schmidt, E. K. (2014). Self-organizing properties of the visual field: Gestalt forces in action. In A. Geremek, M. W. Greenlee & S. Magnussen (Eds.), *Perception Beyond Gestalt: Progress in vision research* (pp. 67–81). London: Psychology Press: Taylor & Francis Group.

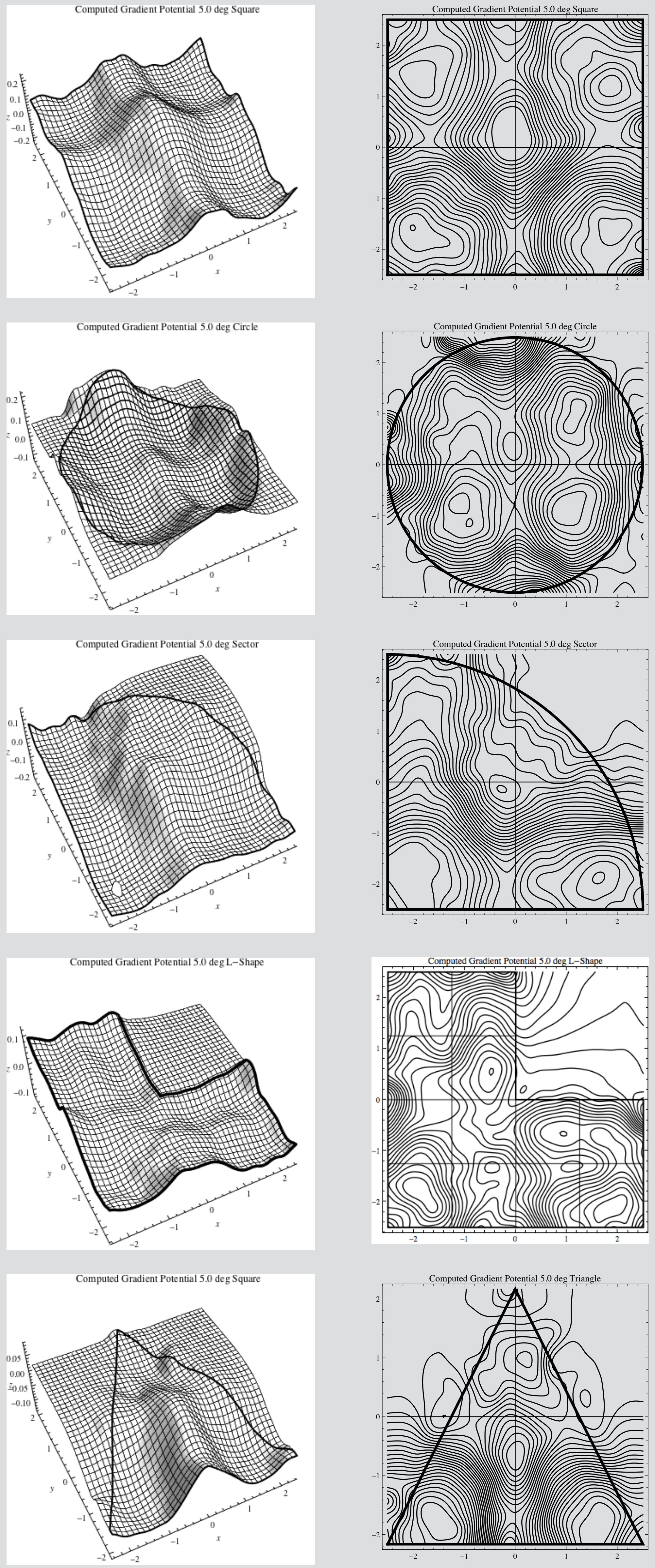

Harvey, L. O., Jr., & Schmidt, E. K. (2014). Self-organizing properties of the visual field: Gestalt forces in action. In A. Geremek, M. W. Greenlee & S. Magnussen (Eds.), *Perception Beyond Gestalt: Progress in vision research* (pp. 67–81). London: Psychology Press: Taylor & Francis Group.

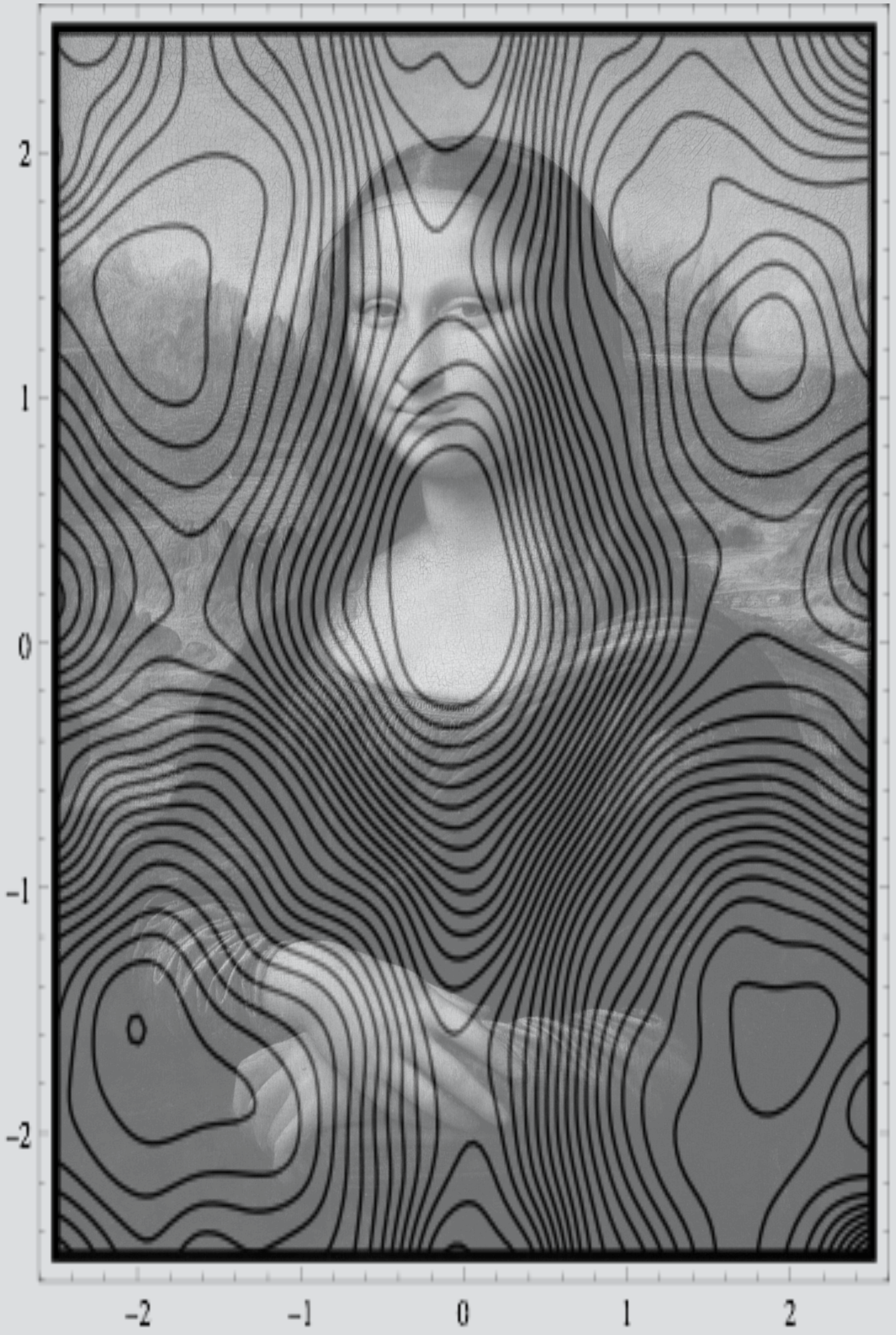

Harvey, L. O., Jr., & Schmidt, E. K. (2014). Self-organizing properties of the visual field: Gestalt forces in action. In A. Geremek, M. W. Greenlee & S. Magnussen (Eds.), *Perception Beyond Gestalt: Progress in vision research* (pp. 67–81). London: Psychology Press: Taylor & Francis Group.

Color Perception

It’s in your mind

Why should we even see color?

- Detection
  - Make objects stand out
  - Make objects “invisible”
- Discrimination
  - Separate objects
- Identification
  - Decide what an object is

Basic Principle

Light has no color!

Benham's Top

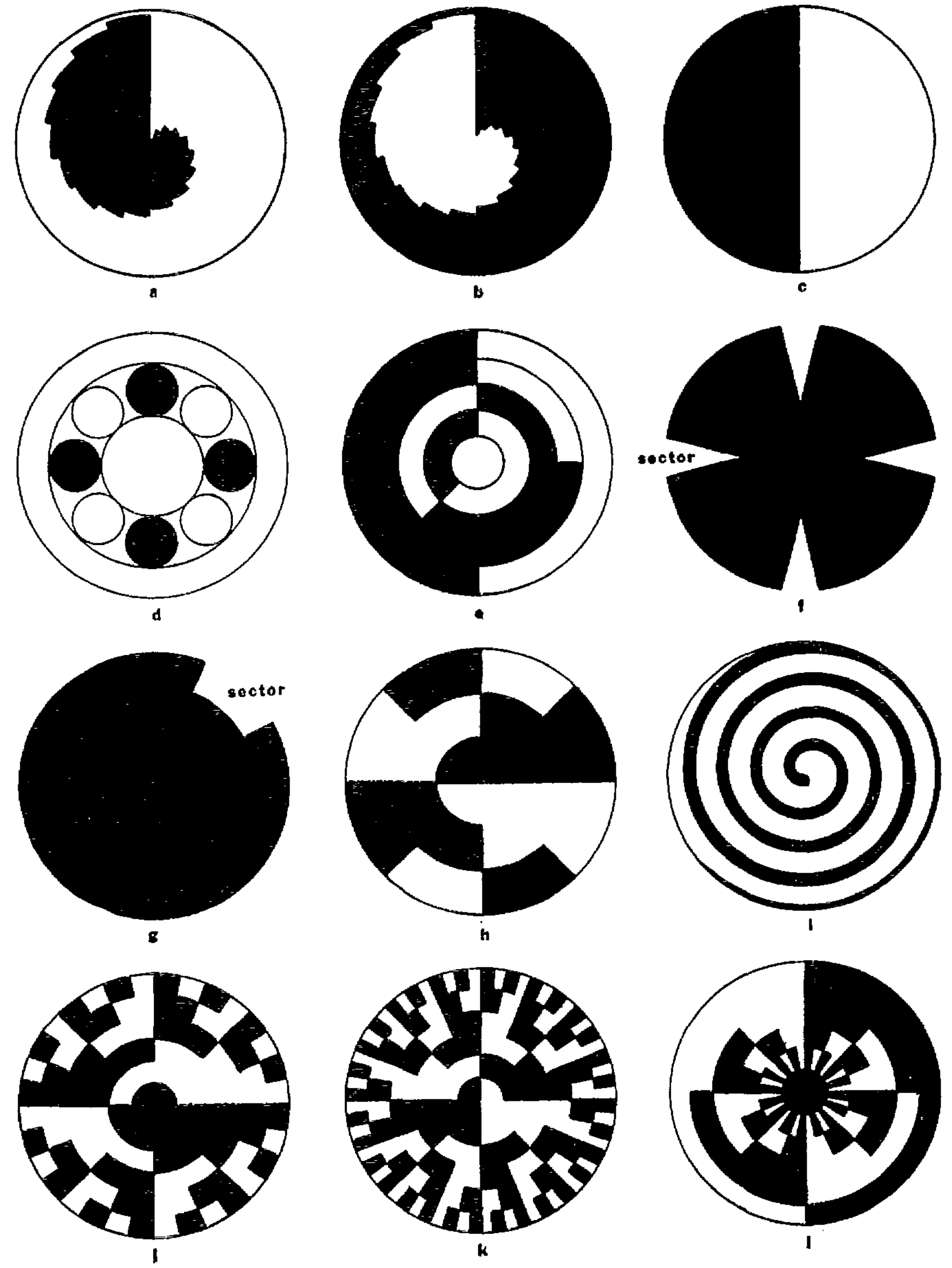

FIG. 1. DISKS FOR THE PRODUCTION OF THE SUBJECTIVE COLORS.
Figs. 1a, 1b, 1c, Fechner; Fig. 1d, Dove; Fig. 1e, John Smith; Figs. 1f, 1g, Rood; Figs. 1h, 1i, Helmholtz; Figs. 1j, 1k, 1l, Brücke.

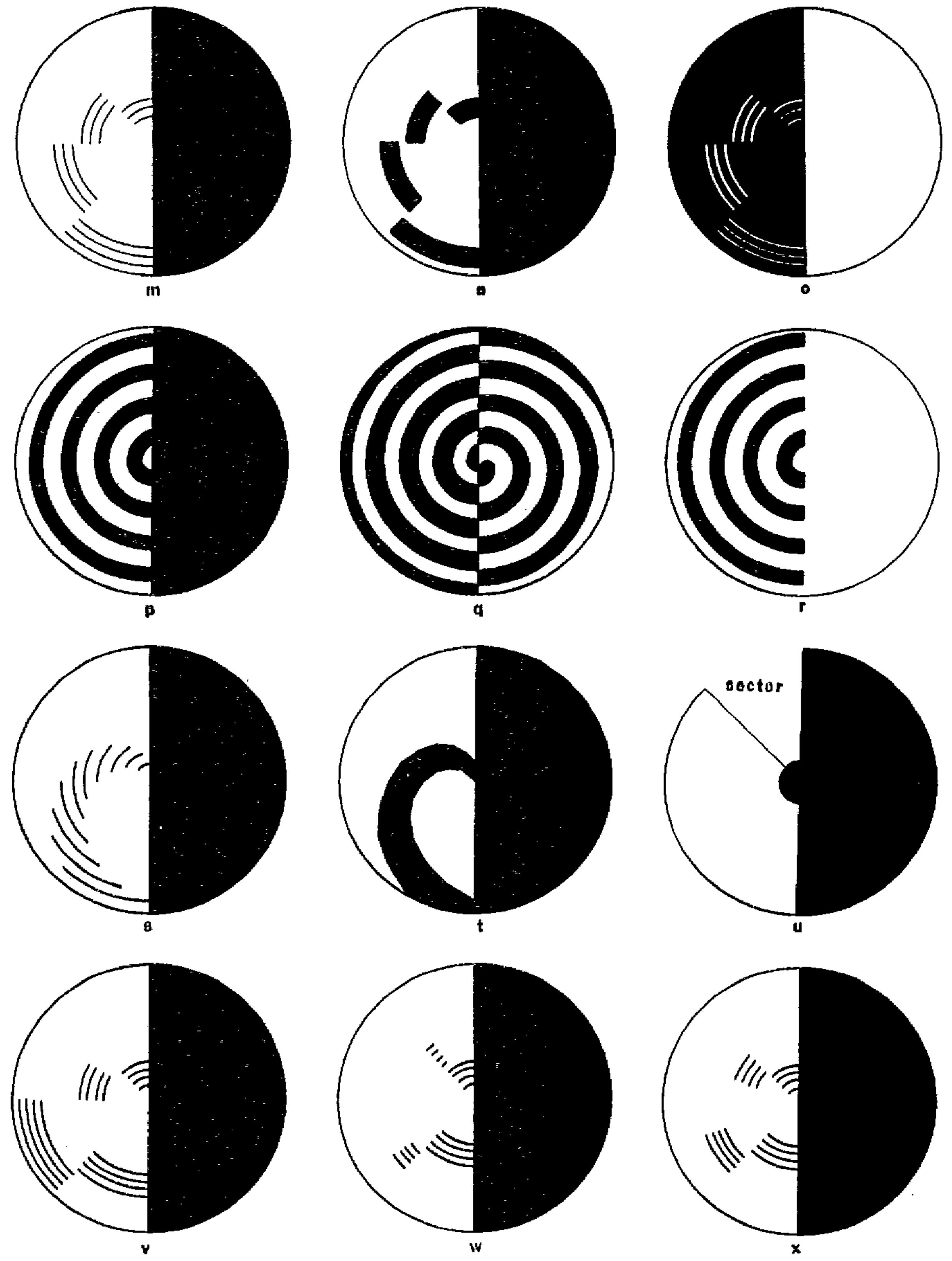

FIG. 1. (CONTINUED). DISKS FOR THE PRODUCTION OF THE SUBJECTIVE COLORS.
Fig. 1m, Benham; Figs. 1n, 1o, Finnegan and Moore; Figs. 1p, 1q, 1r, Hurst; Figs. 1s, 1t, Wolf; Fig. 1u, Bidwell; Figs. 1v, 1w, 1x, Bagley.

Cohen, J., & Gordon, D. A. (1949). The prevost-fechner-benham subjective colors. *Psychological Bulletin, 46*(2), 97-136. doi:http://dx.doi.org/10.1037/h0060841

Benham's Top

Michael Bach
University of Freiburg

http://www.michaelbach.de/ot/col_benham/

Physical Properties of Light

- Intensity
- Dominant Wavelength
- Colormetric Purity

Color Experience has Three Dimensions

- Hue
- Saturation
- Brightness

Where Does Color Come From?

- Three Stages
  - Stage 1 cone mechanisms (color mixing and matching)
  - Stage 2: color-discrimination mechanisms
  - Stage 3: color appearance mechanisms

Three Stages of Color Vision

- Receptor Stage (Color Matching)
  - Three Types of Cones (S, M, L)
  - Need Three Primaries (R, G, B)
- Stage 2 Cone Opponent Processes (Discrimination)
  - Red-Green Opponent Process
  - Yellow-Blue Opponent Process
  - Luminance Process
- Stage 3 Color Opponent Processes (Appearance)
  - Red-Green
  - Yellow-Blue

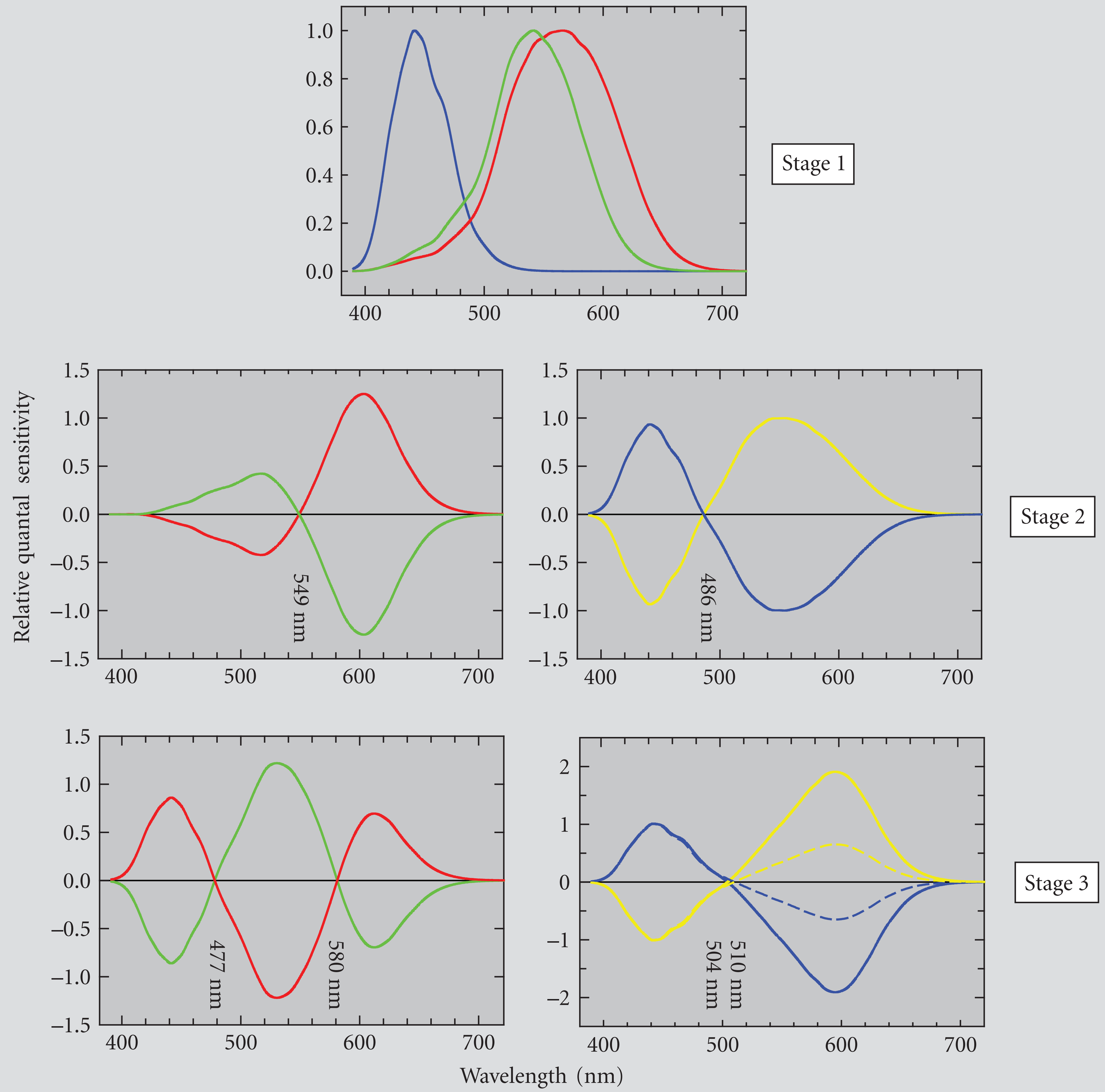

Stockman, A., & Brainard, D. H. (2010). Color Vision Mechanisms. In M. Bass, J. M. Enoch, & V. Lakshminarayanan (Eds.), *The Optical Society of America Handbook of Optics* (3rd ed., Vol. Volume III: Vision and Vision Optics, pp. 11.11–11.104). New York: McGraw-Hill.
Brainard, D. H., & Stockman, A. (2010). Colorimetry. In M. Bass, J. M. Enoch, & V. Lakshminarayanan (Eds.), *The Optical Society of America Handbook of Optics* (3rd ed., Vol. Volume III: Vision and Vision Optics, pp. 10.11–10.56). New York: McGraw-Hill.

Three Stages of Color Vision

- Receptor Stage (Color Matching)
  - Three Types of Cones (S, M, L)
  - Need Three Primaries (R, G, B)
- Stage 2 Cone Opponent Processes (Discrimination)
  - Red-Green Opponent Process
  - Yellow-Blue Opponent Process
  - Luminance Process
- Stage 3 Color Opponent Processes (Appearance)
  - Red-Green
  - Yellow-Blue

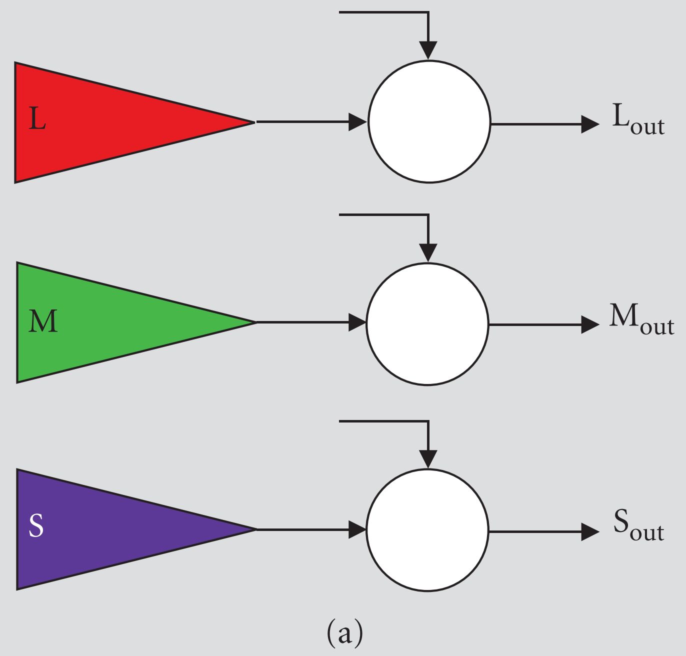

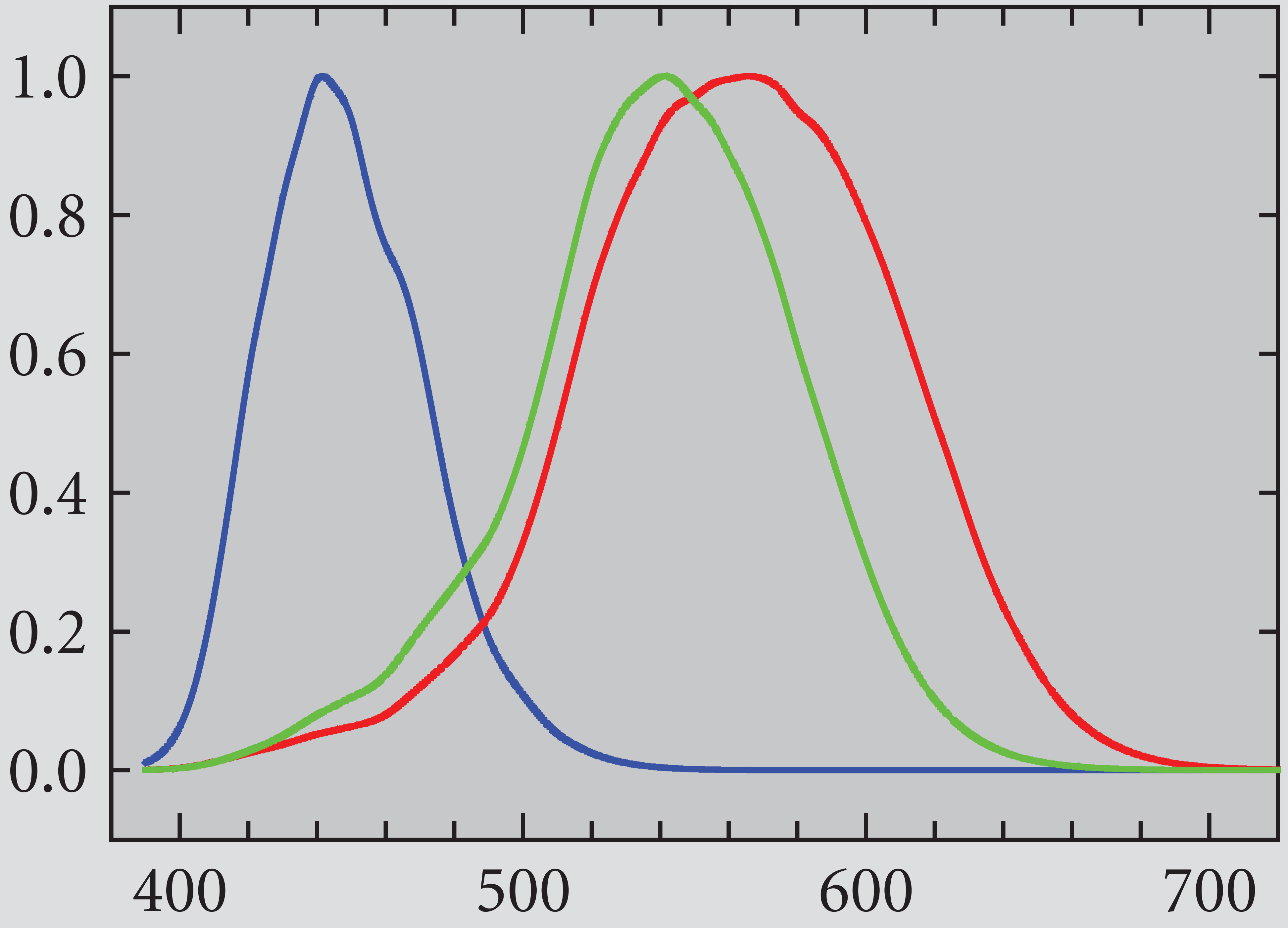

Stage 1

Stockman, A., & Brainard, D. H. (2010). Color Vision Mechanisms. In M. Bass, J. M. Enoch, & V. Lakshminarayanan (Eds.), *The Optical Society of America Handbook of Optics* (3rd ed., Vol. Volume III: Vision and Vision Optics, pp. 11.11–11.104). New York: McGraw-Hill.
Brainard, D. H., & Stockman, A. (2010). Colorimetry. In M. Bass, J. M. Enoch, & V. Lakshminarayanan (Eds.), *The Optical Society of America Handbook of Optics* (3rd ed., Vol. Volume III: Vision and Vision Optics, pp. 10.11–10.56). New York: McGraw-Hill.

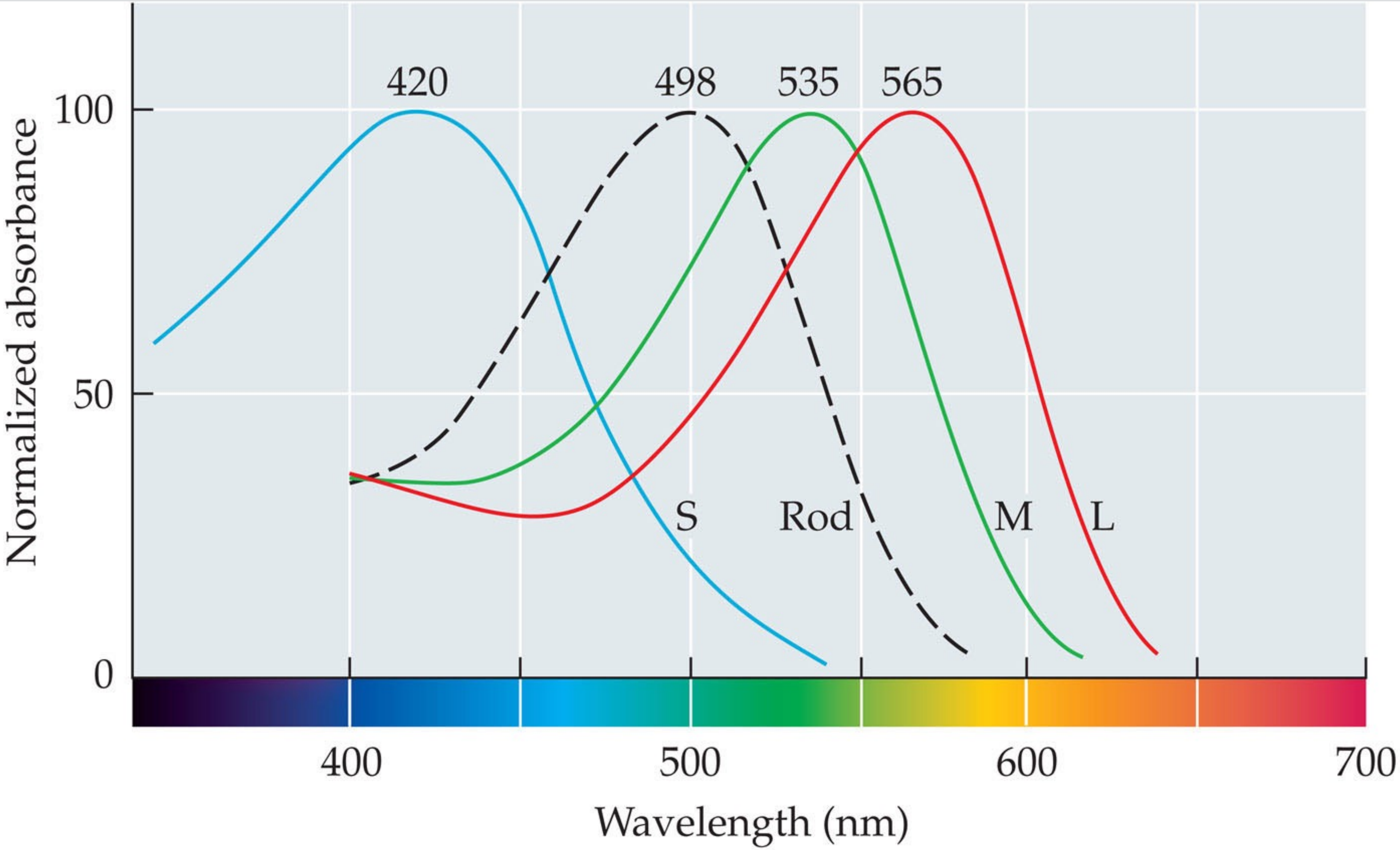

***SENSATION & PERCEPTION 4e,* Figure 5.1**

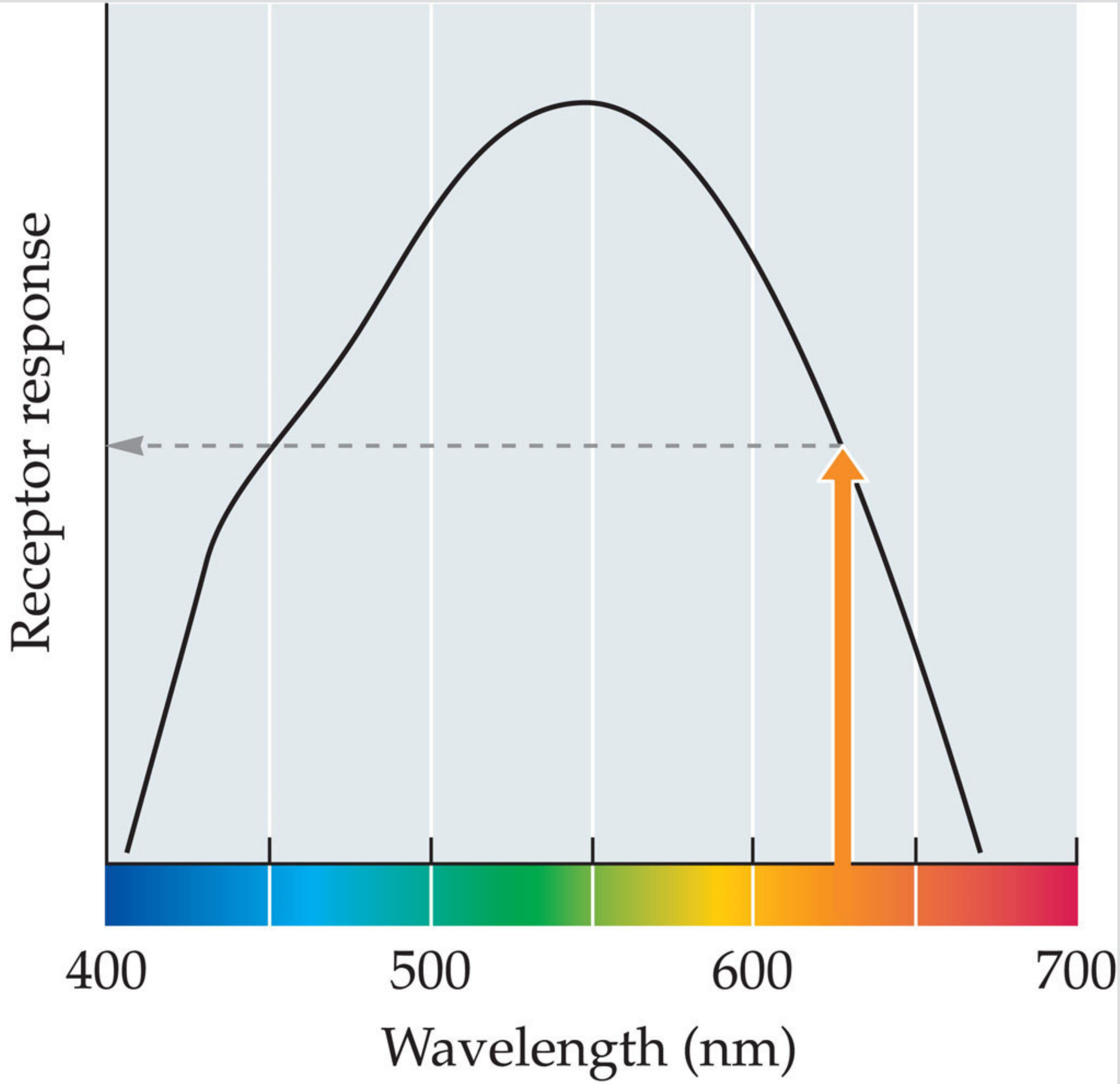

SENSATION & PERCEPTION 4e, Figure 5.2

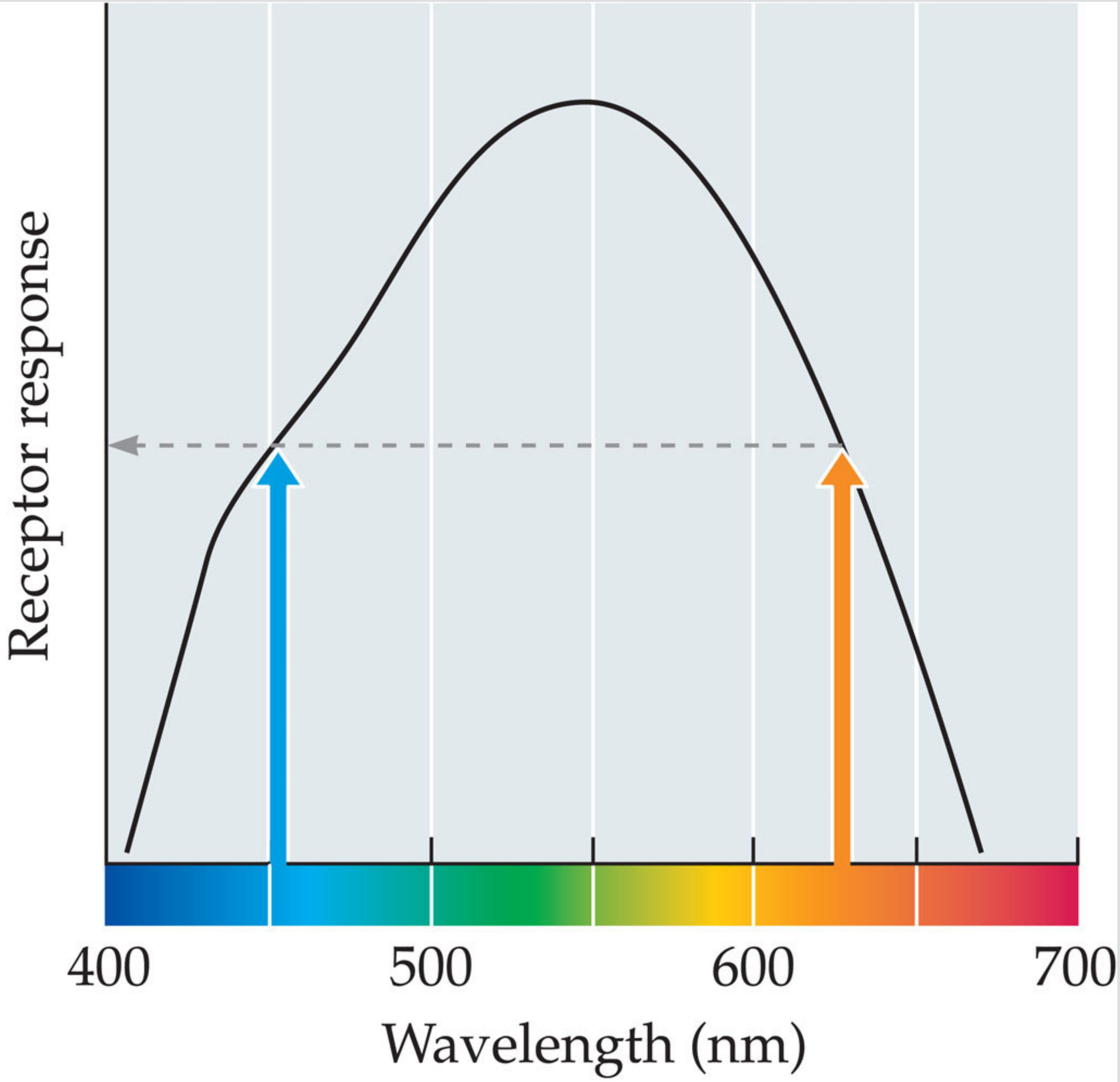

SENSATION & PERCEPTION 4e, **Figure 5.3**

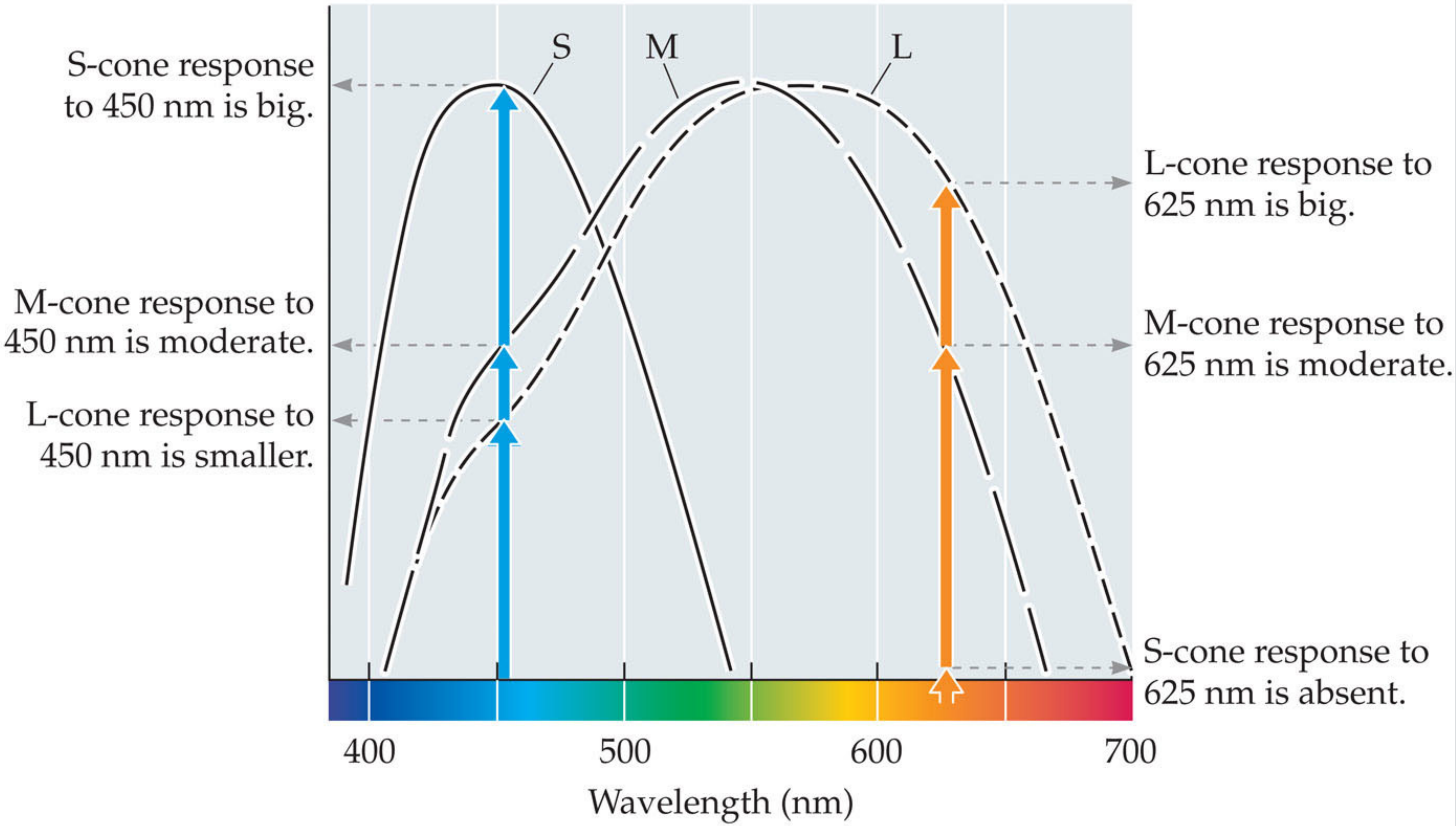

***SENSATION & PERCEPTION 4e,* Figure 5.5**

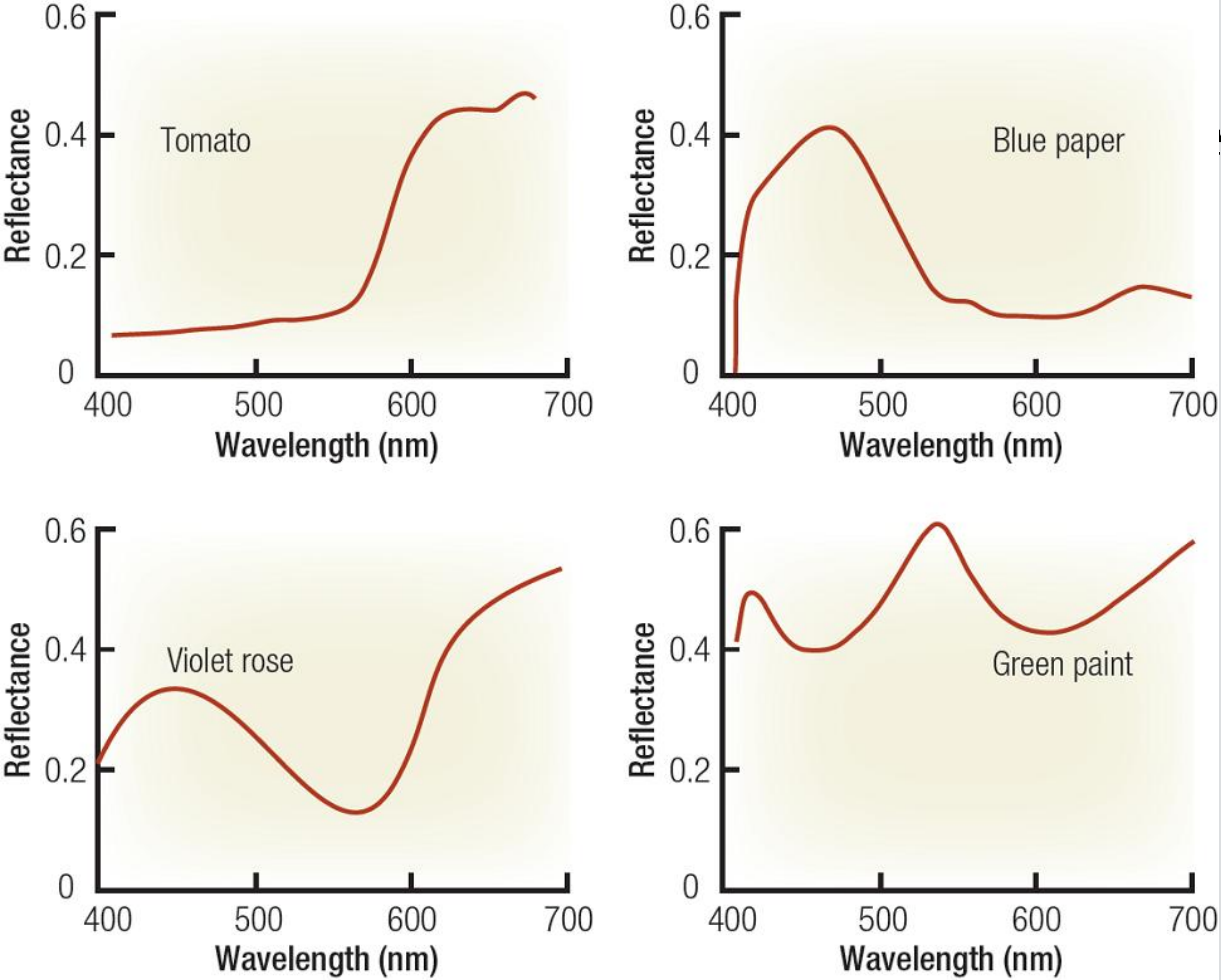
Tomato
Blue paper
Violet rose
Green paint
Reflectance
Wavelength (nm)
0
0.2
0.4
0.6
400
500
600
700

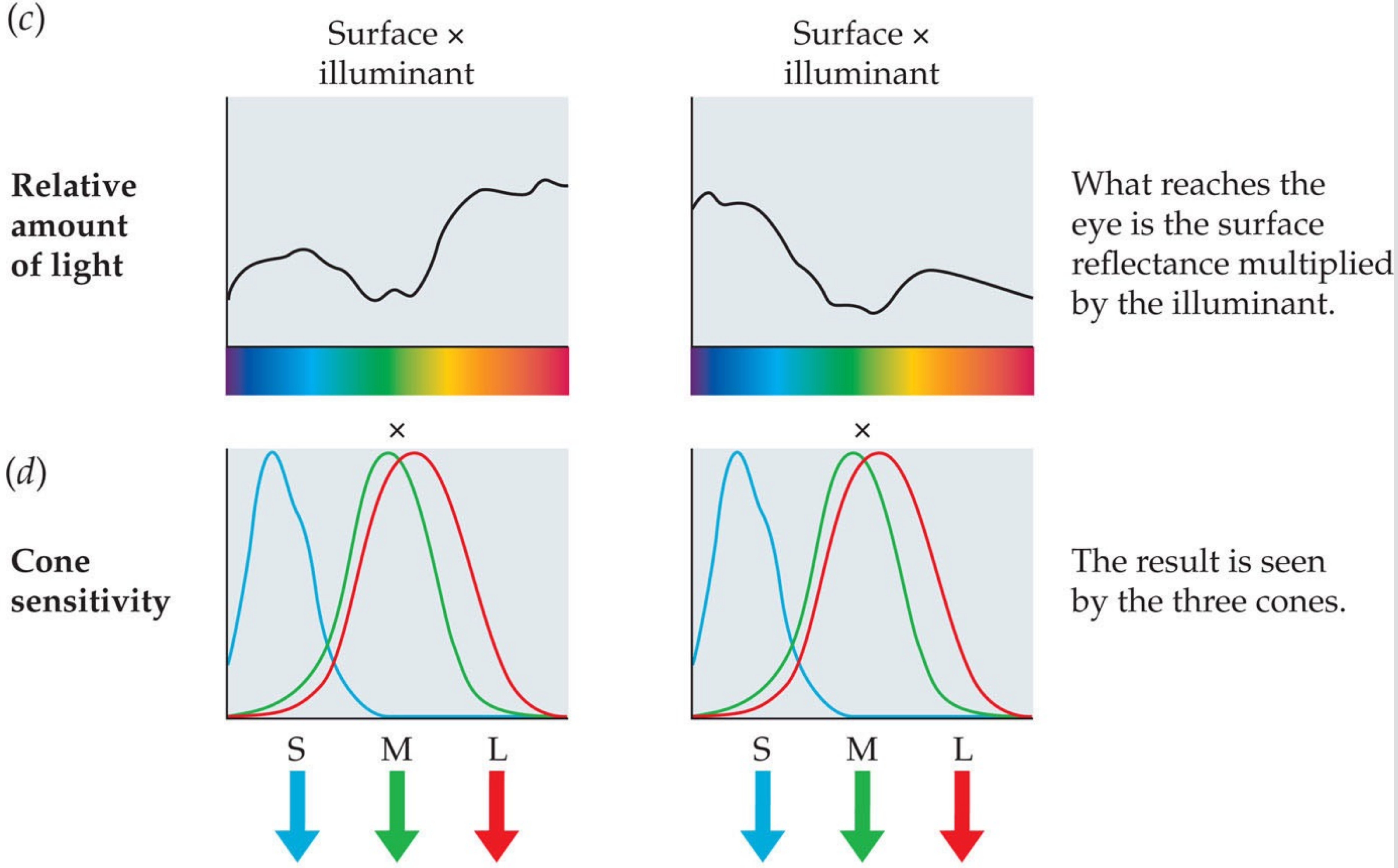

SENSATION & PERCEPTION 4e, Figure 5.23 (Part 2)

Receptor Stage: Color Matching
Tristimulus Values

Tristimulus X, Y, Z

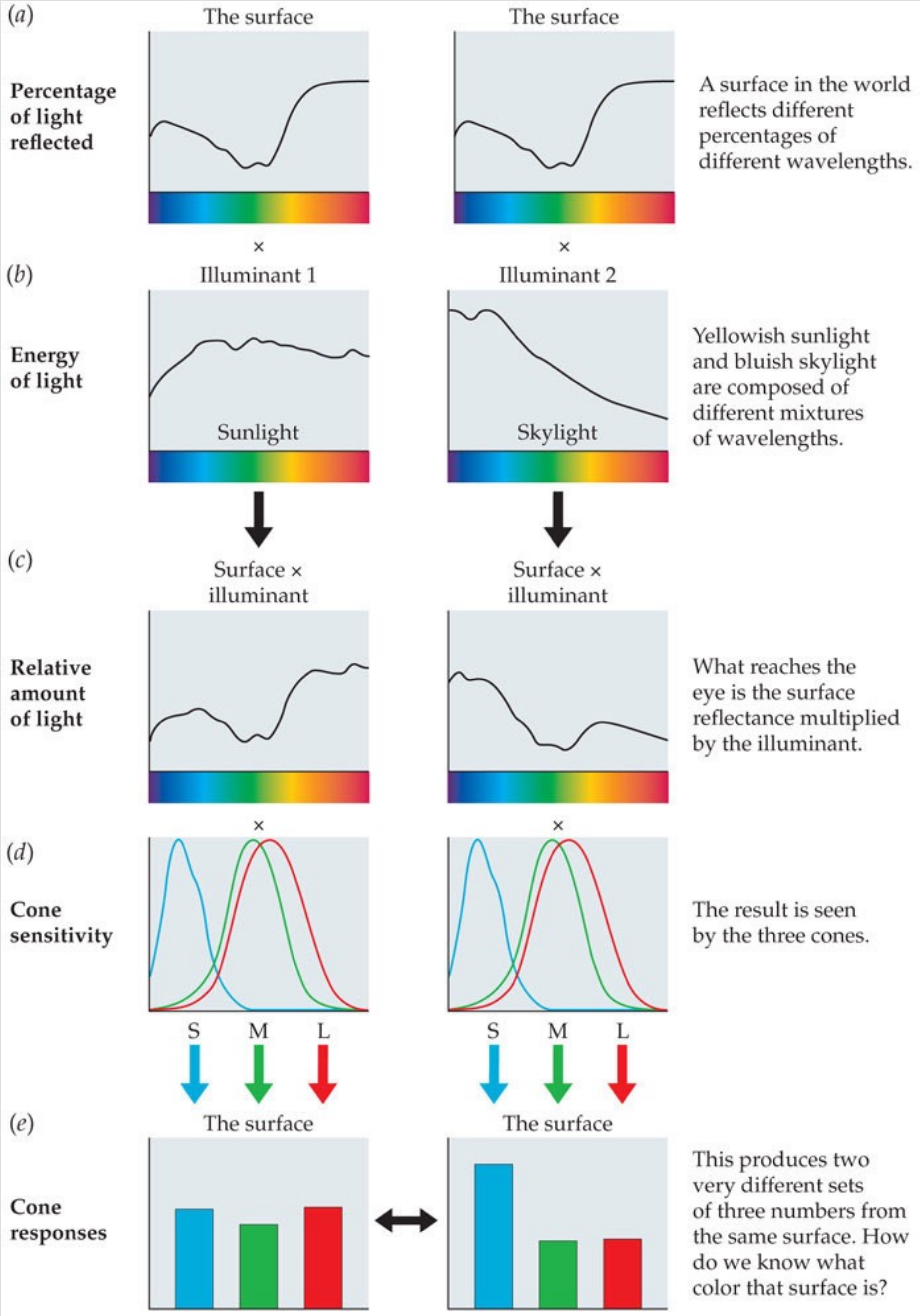

***SENSATION & PERCEPTION 4e*, Figure 5.23**

Color Matching

- Bipartite Field
- Need only 3 primaries to match any color
- Primaries must not be matched by mixture of the other two
- Many possible sets of primaries
- C.I.E. Tristimulus values (X, Y, Z)

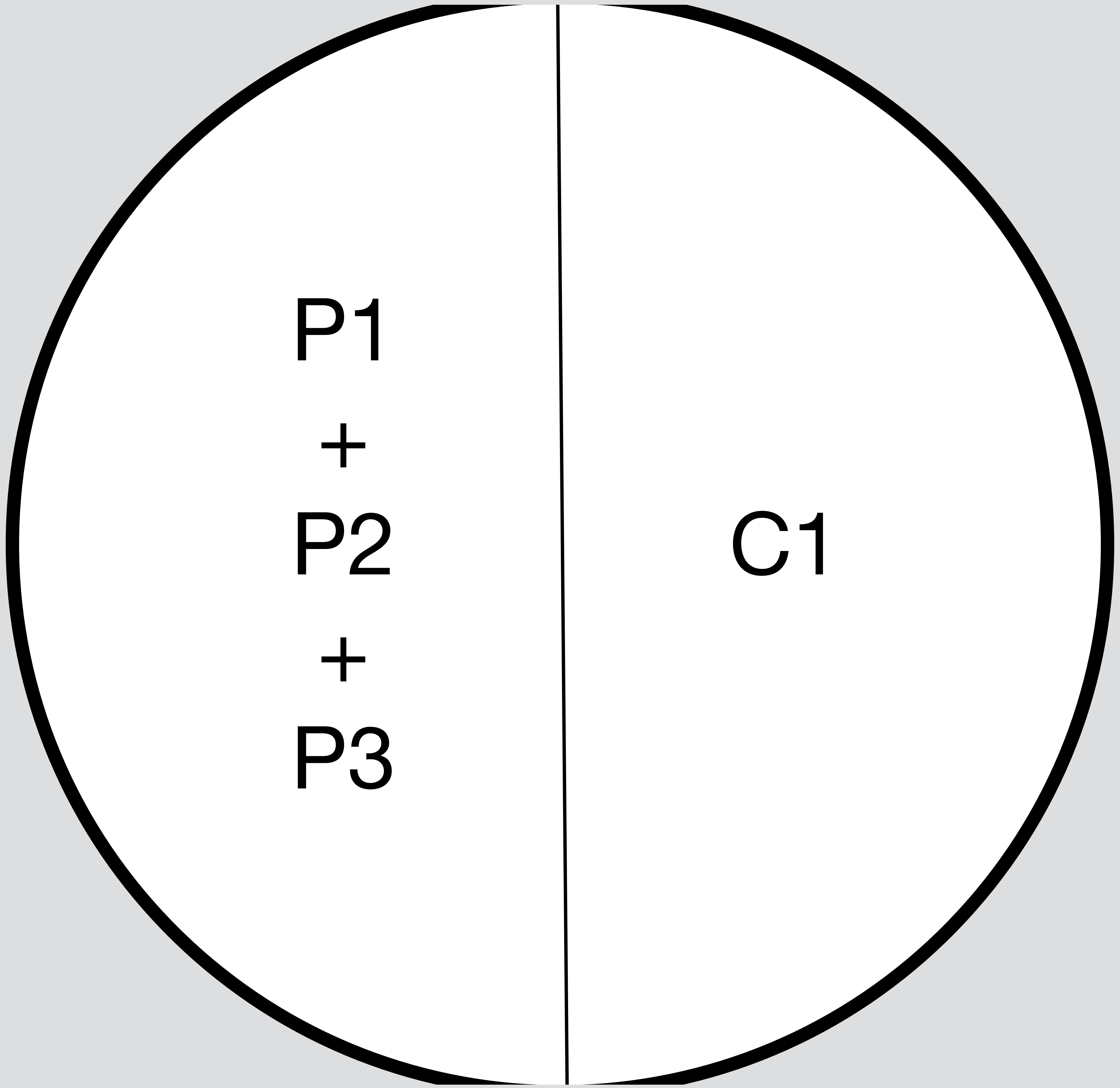

Color matching

Colors are assessed by matching them with reference colors on a small-field bipartite screen

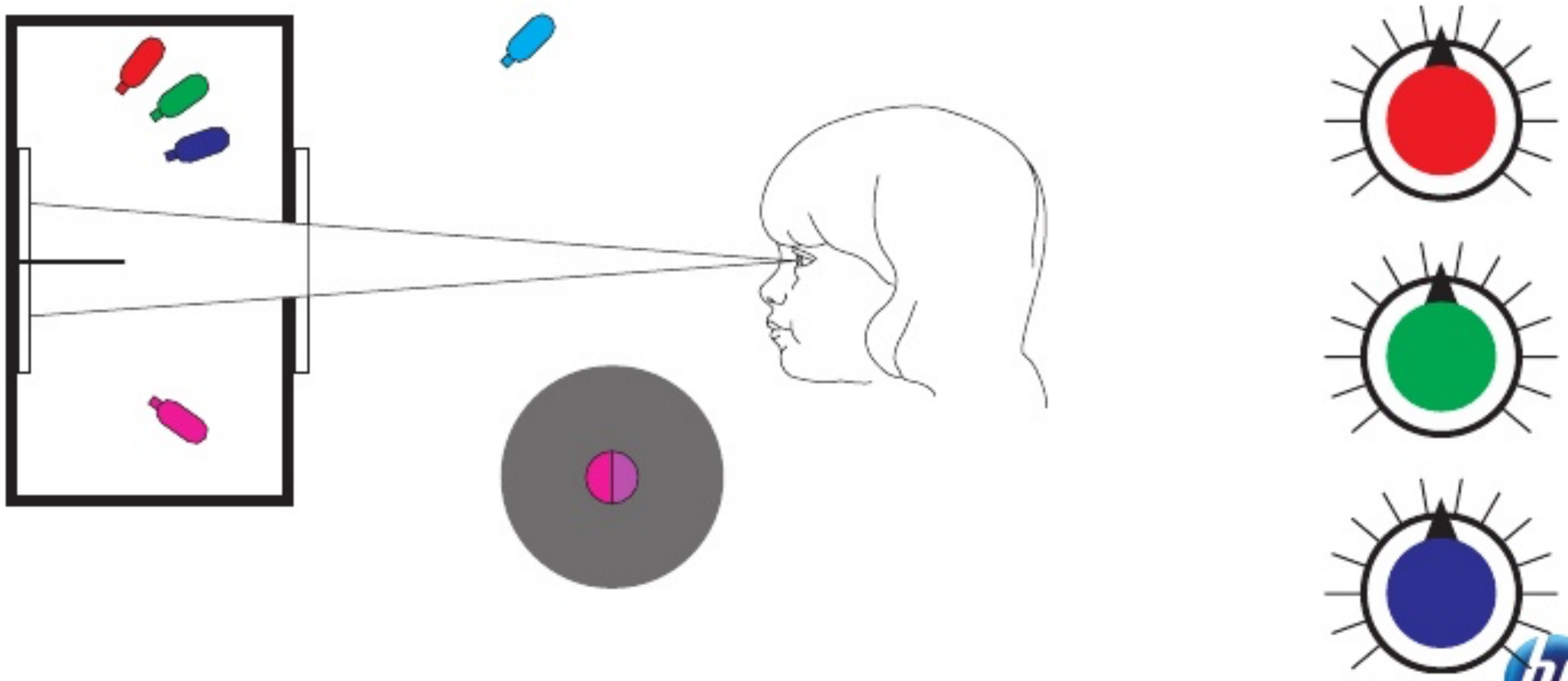

Receptor Stage: Matching

- Three Cone Types: S, M, L
- Two Colors will appear identical when they evoke the same response pattern in the three cone types
- C.I.E. Tristimulus Values: X, Y, Z
- C.I.E. Chromaticity Coordinates: x, y, z

Receptor Stage: Color Matching
Tristimulus Values

$$C_1 \equiv 1X + 2Y + 3Z$$

$$C_2 \equiv 3X + 1Y + 1Z$$

$$C_{1+2} \equiv 4X + 3Y + 4Z$$

Receptor Stage: Color Matching Tristimulus Values

$$C_1 \equiv 0.45\,X + 1.05\,Y + 0.50\,Z$$

$$C_2 \equiv 1.35\,X + 3.15\,Y + 1.50\,Z$$

$$C_{1+2} \equiv 1.80\,X + 4.20\,Y + 2.00\,Z$$

C.I.E. Chromaticity:
Relative amount of X, Y, Z Tristimulus Values

$$x = \frac{X}{X + Y + Z}$$

$$y = \frac{Y}{X + Y + Z}$$

$$z = \frac{Z}{X + Y + Z}$$

Receptor Stage: Color Matching
Chromaticity Coordinates

$$x = \frac{X}{X+Y+Z}$$

$$y = \frac{Y}{X+Y+Z}$$

$$z = \frac{Z}{X+Y+Z}$$

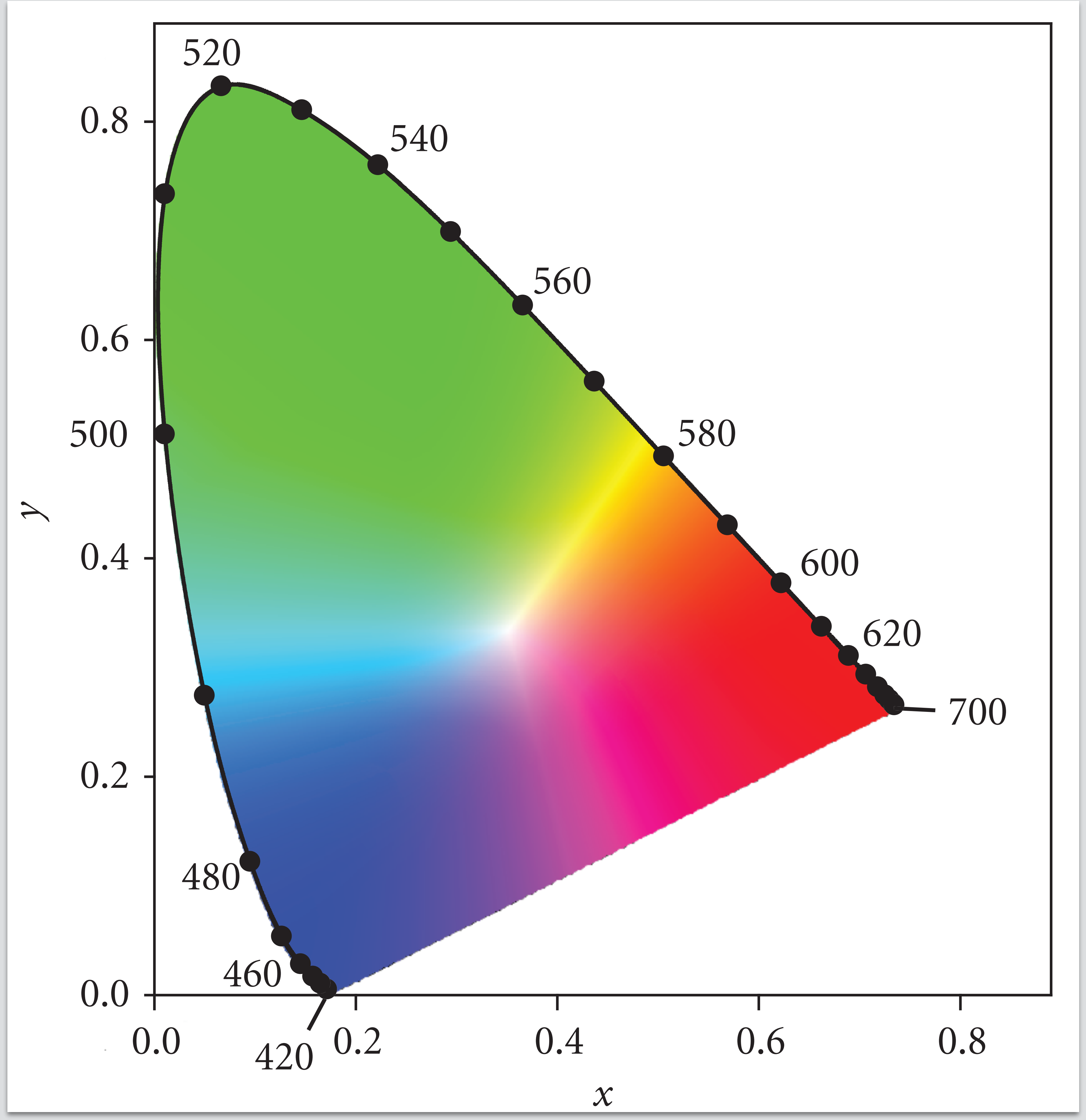

Stockman, A., & Brainard, D. H. (2010). Color Vision Mechanisms. In M. Bass, J. M. Enoch, & V. Lakshminarayanan (Eds.), *The Optical Society of America Handbook of Optics* (3rd ed., Vol. Volume III: Vision and Vision Optics, pp. 11.11–11.104). New York: McGraw-Hill.
Brainard, D. H., & Stockman, A. (2010). Colorimetry. In M. Bass, J. M. Enoch, & V. Lakshminarayanan (Eds.), *The Optical Society of America Handbook of Optics* (3rd ed., Vol. Volume III: Vision and Vision Optics, pp. 10.11–10.56). New York: McGraw-Hill.

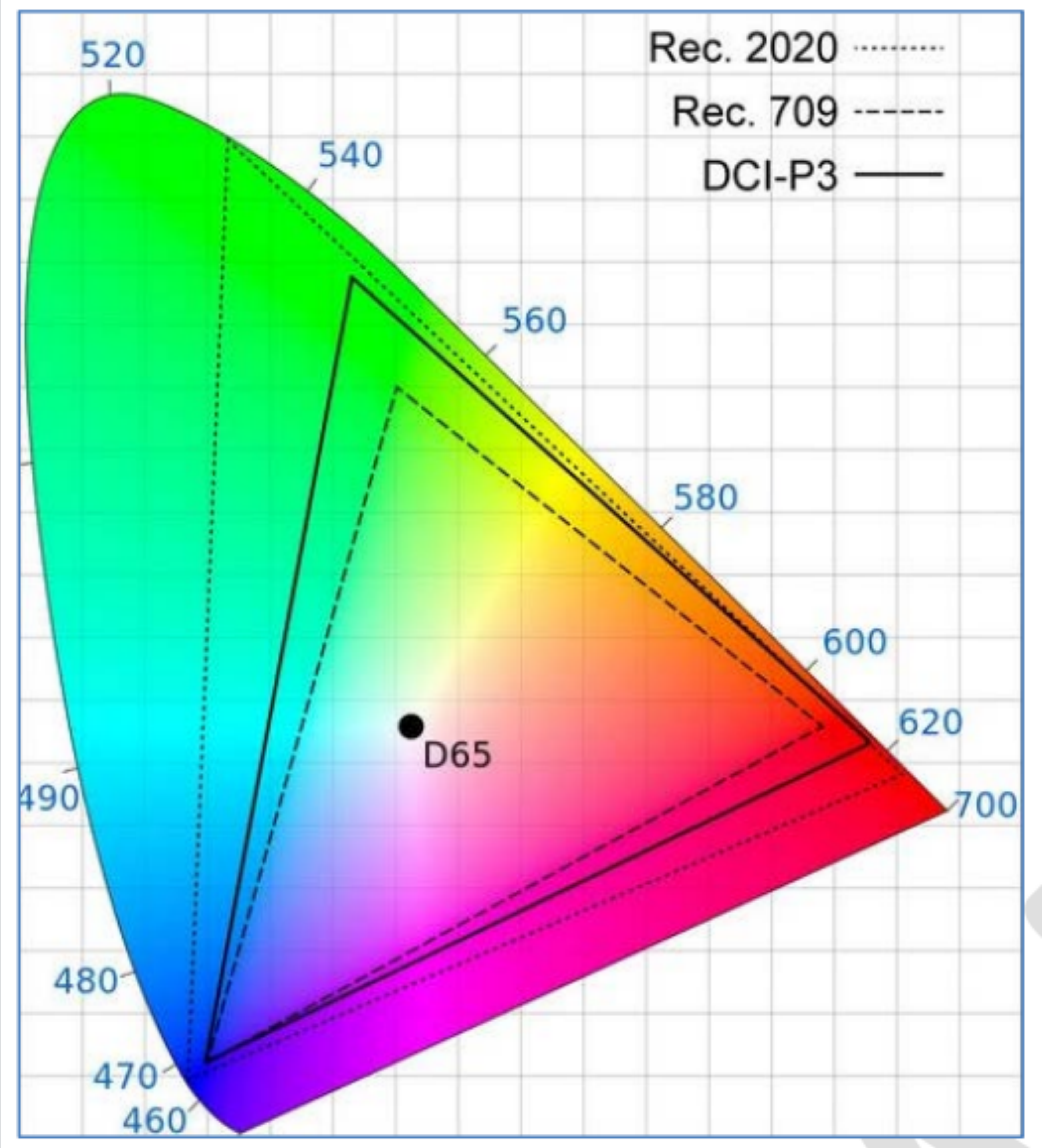
Rec. 2020
Rec. 709
DCI-P3
520
540
560
580
600
620
700
490
480
470
460
D65

Three Stages of Color Vision

- Receptor Stage (Color Matching)
    - Three Types of Cones (S, M, L)
    - Need Three Primaries (R, G, B)
- Stage 2 Cone Opponent Processes (Discrimination)
    - Red-Green Opponent Process
    - Yellow-Blue Opponent Process
    - Luminance Process
- Stage 3 Color Opponent Processes (Appearance)
    - Red-Green
    - Yellow-Blue

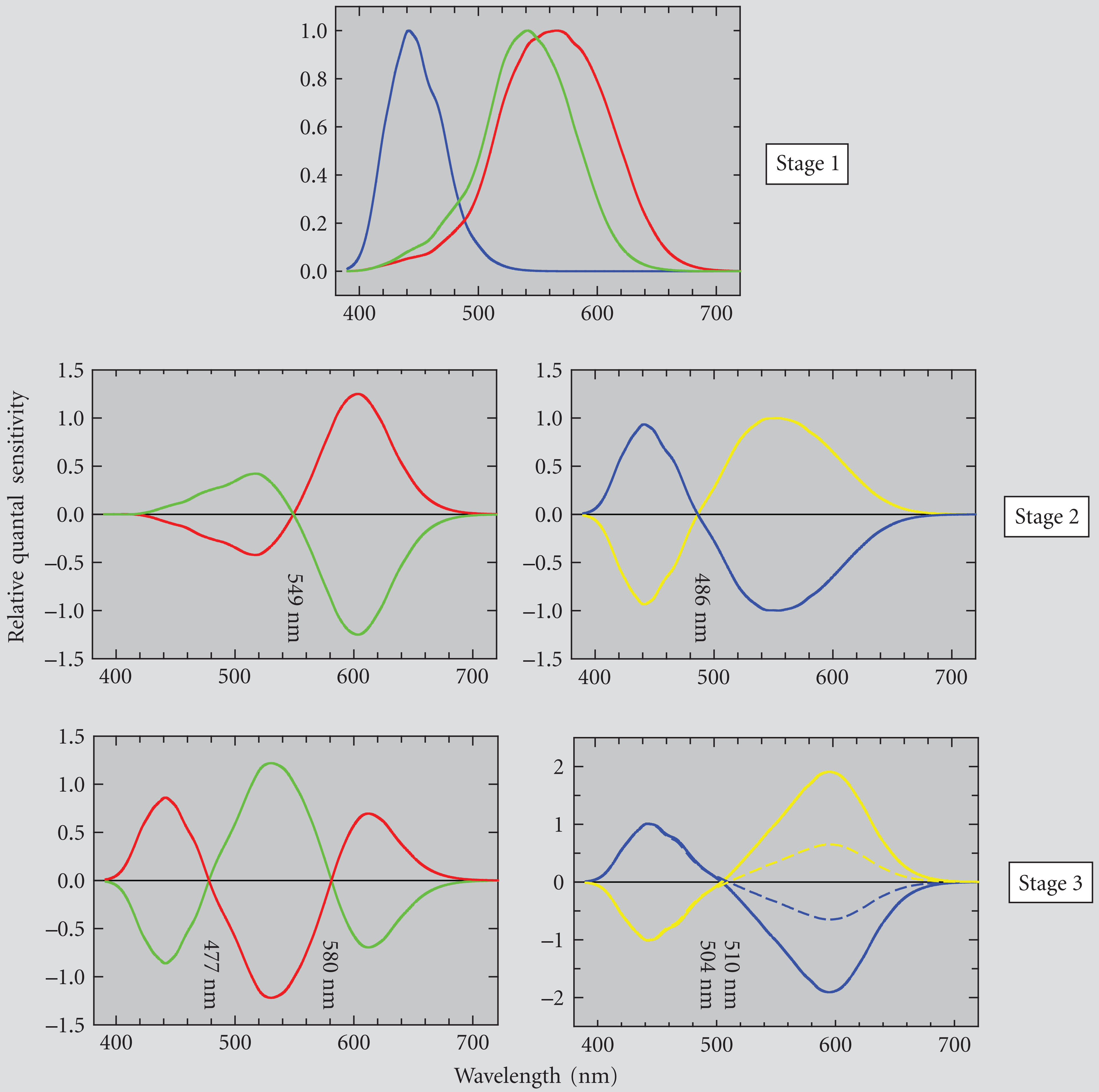

Three Stages of Color Vision

- Receptor Stage (Color Matching)
    - Three Types of Cones (S, M, L)
    - Need Three Primaries (R, G, B)
- Stage 2 Cone Opponent Processes (Discrimination)
    - Red-Green Opponent Process
    - Yellow-Blue Opponent Process
    - Luminance Process
- Stage 3 Color Opponent Processes (Appearance)
    - Red-Green
    - Yellow-Blue

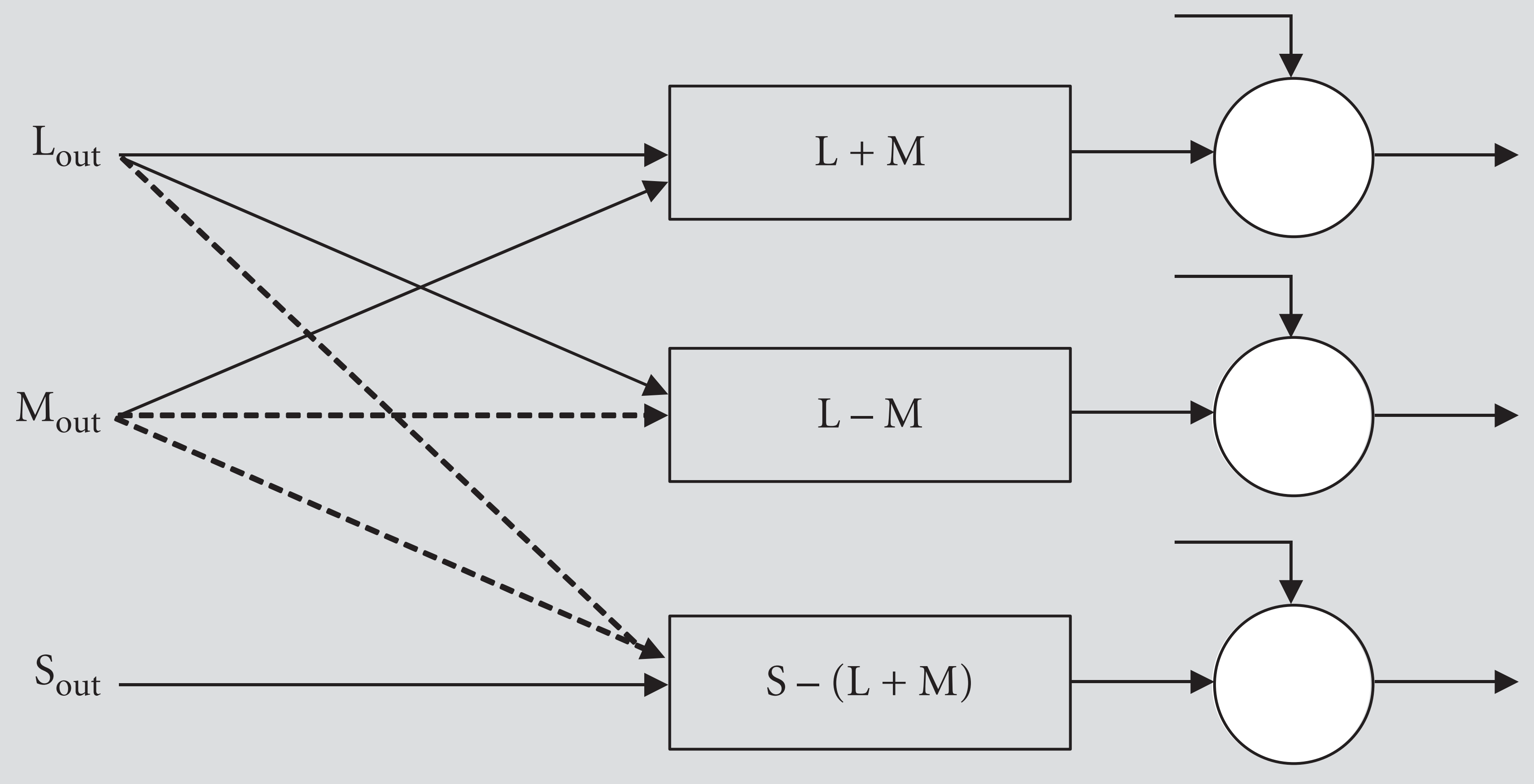

(b)

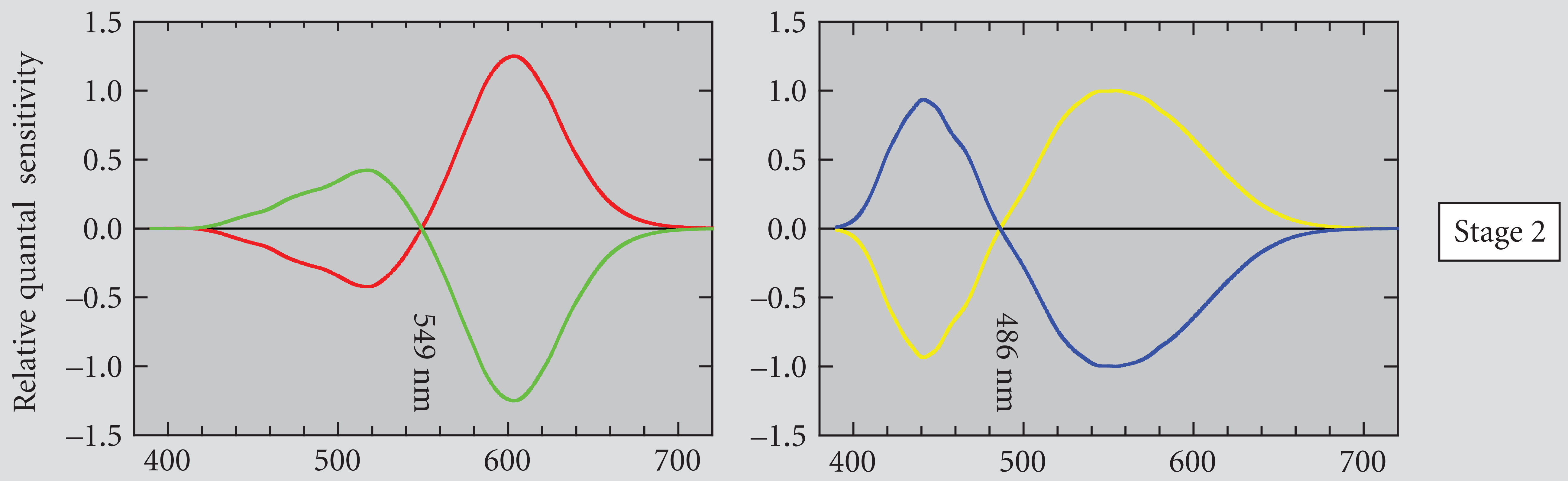

Three Stages of Color Vision

- Receptor Stage (Color Matching)
  - Three Types of Cones (S, M, L)
  - Need Three Primaries (R, G, B)
- Stage 2 Cone Opponent Processes (Discrimination)
  - Red-Green Opponent Process
  - Yellow-Blue Opponent Process
  - Luminance Process
- Stage 3 Color Opponent Processes (Appearance)
  - Red-Green
  - Yellow-Blue

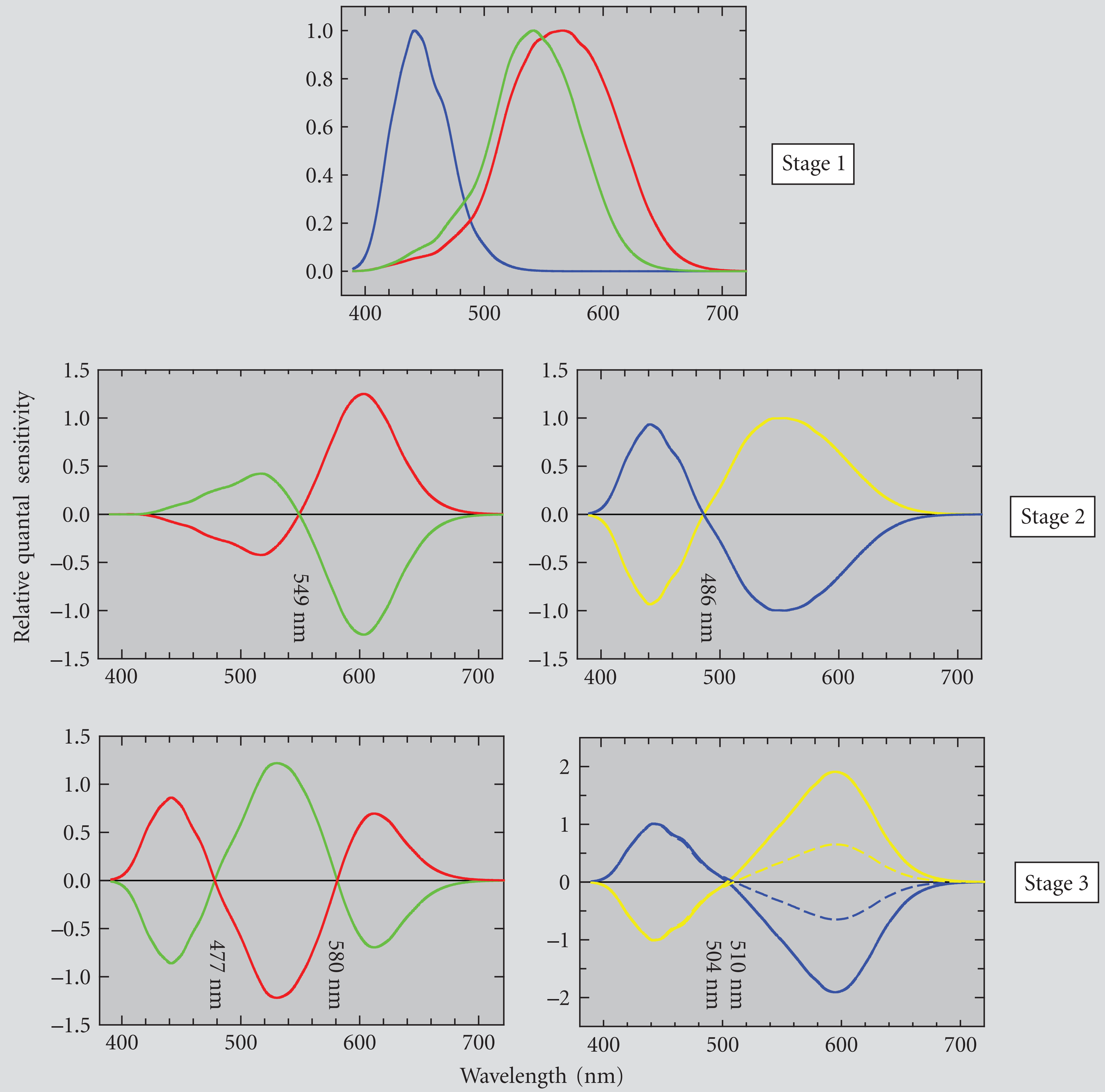

Color Appearance: Naming

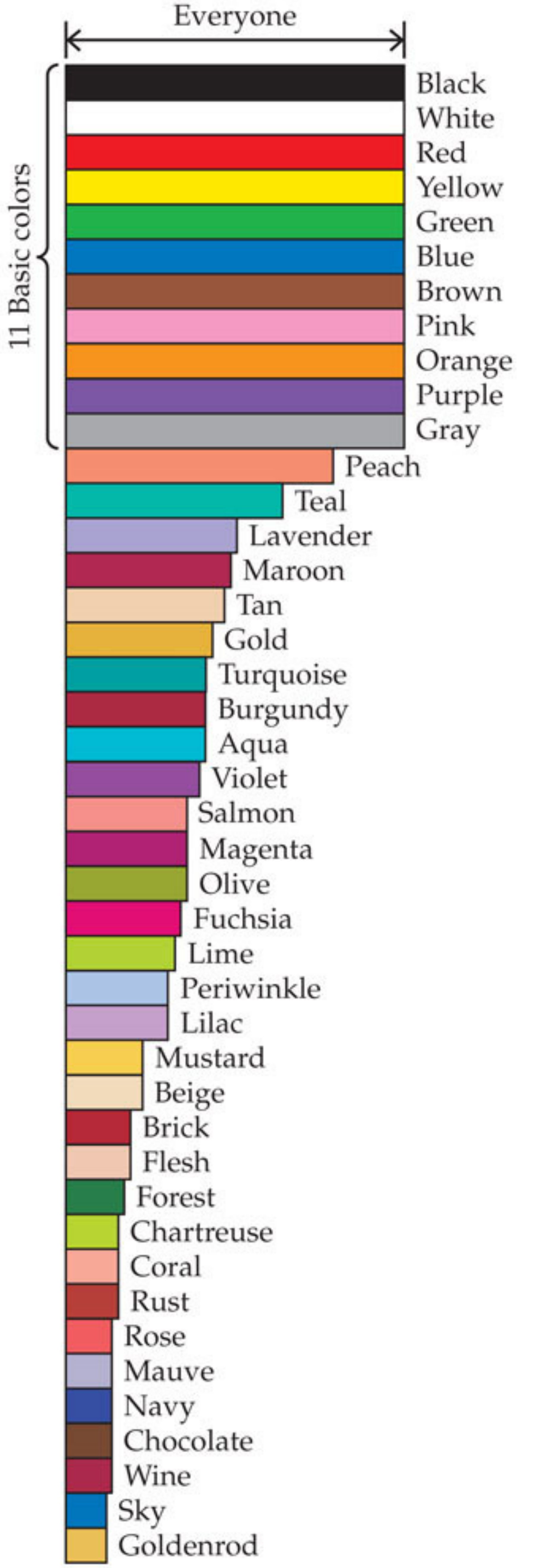

***SENSATION & PERCEPTION 4e,* Figure 5.19**

Cone Response

Cone Opponent Processes

Color Opponent Processes

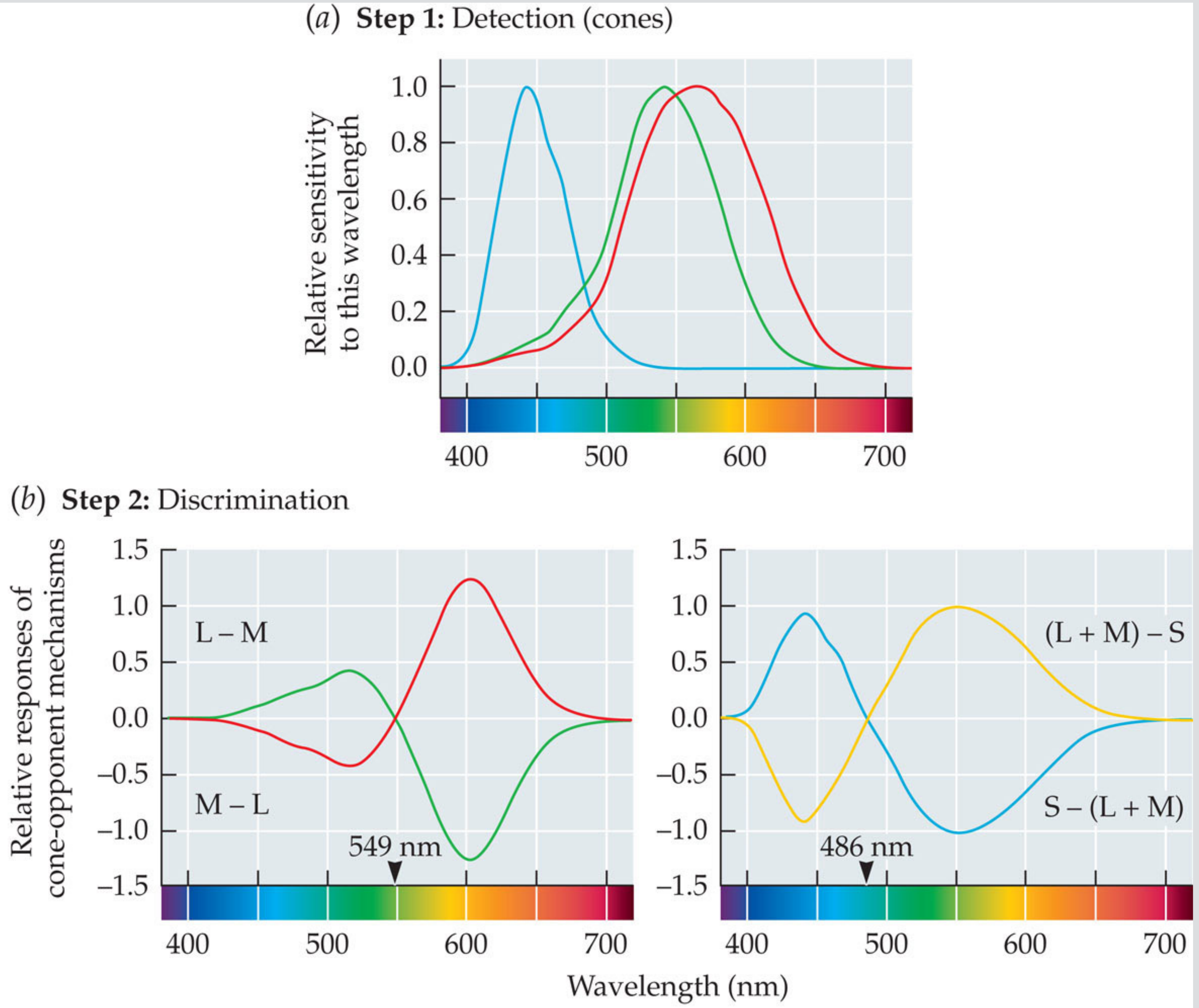

SENSATION & PERCEPTION 4e, Figure 5.17 (Part 1)

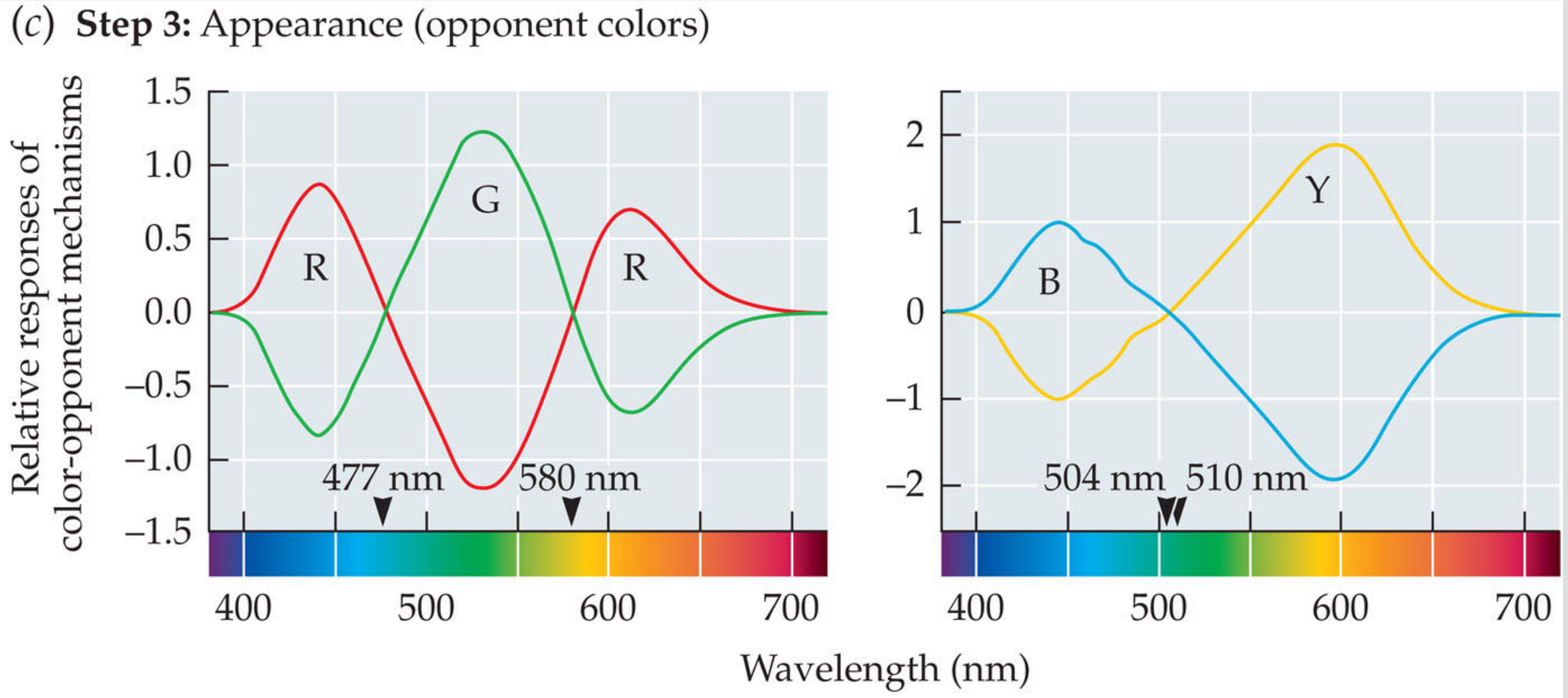

SENSATION & PERCEPTION 4e, Figure 5.17 (Part 2)

(*a*)

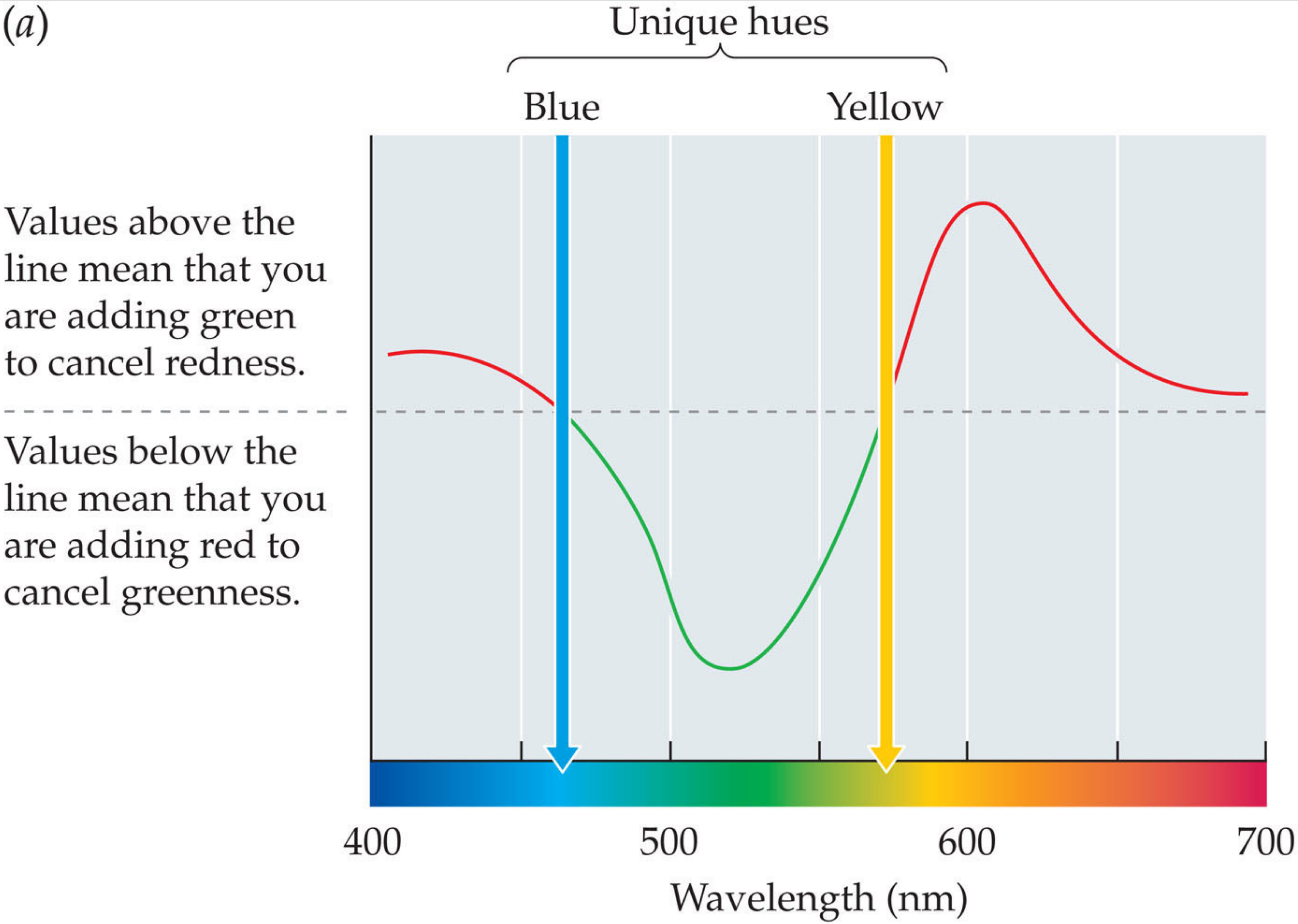

***SENSATION & PERCEPTION 4e,* Figure 5.16 (Part 1)**

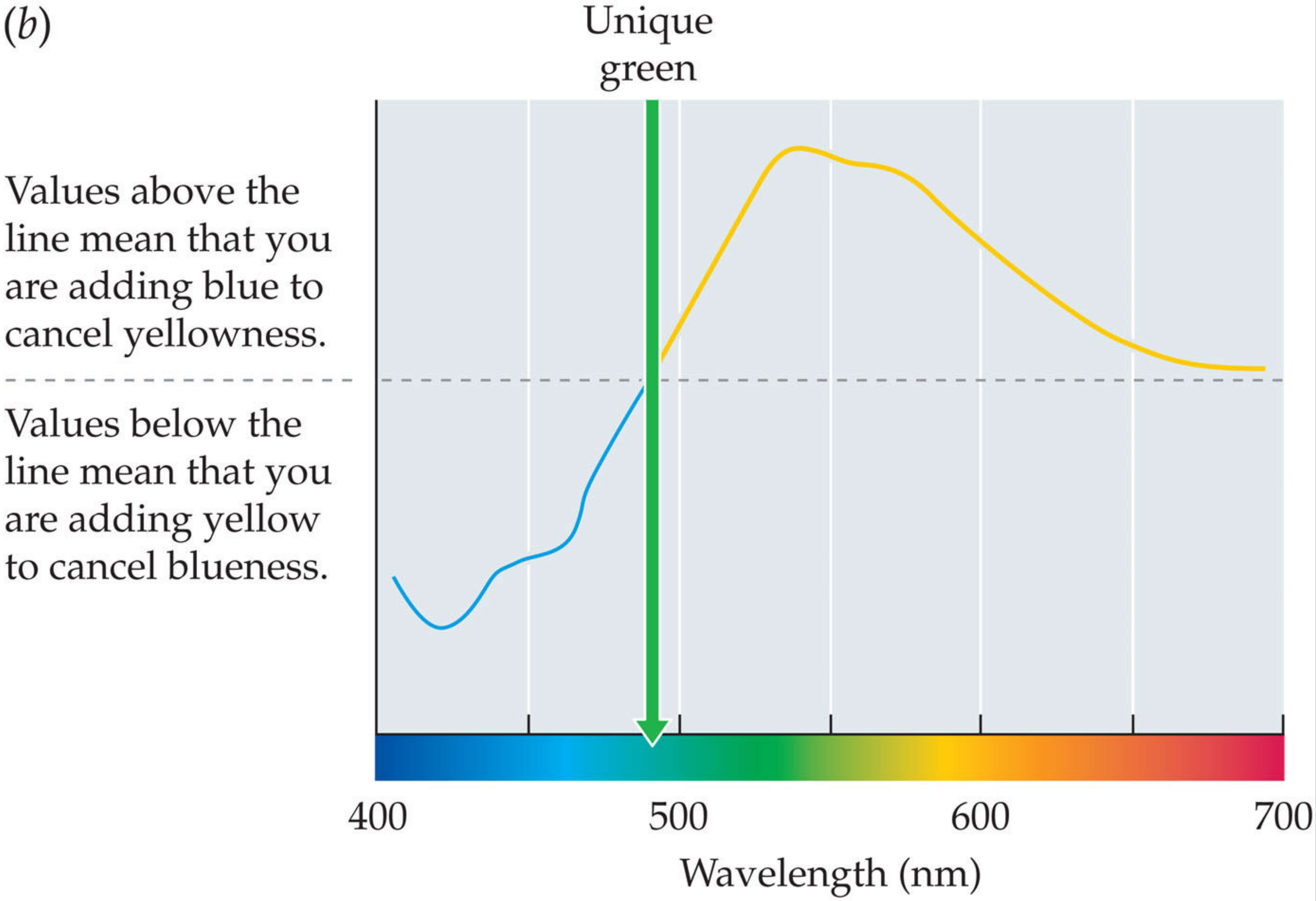

SENSATION & PERCEPTION 4e, **Figure 5.16 (Part 2)**

Opponent Processes: Color Appearance

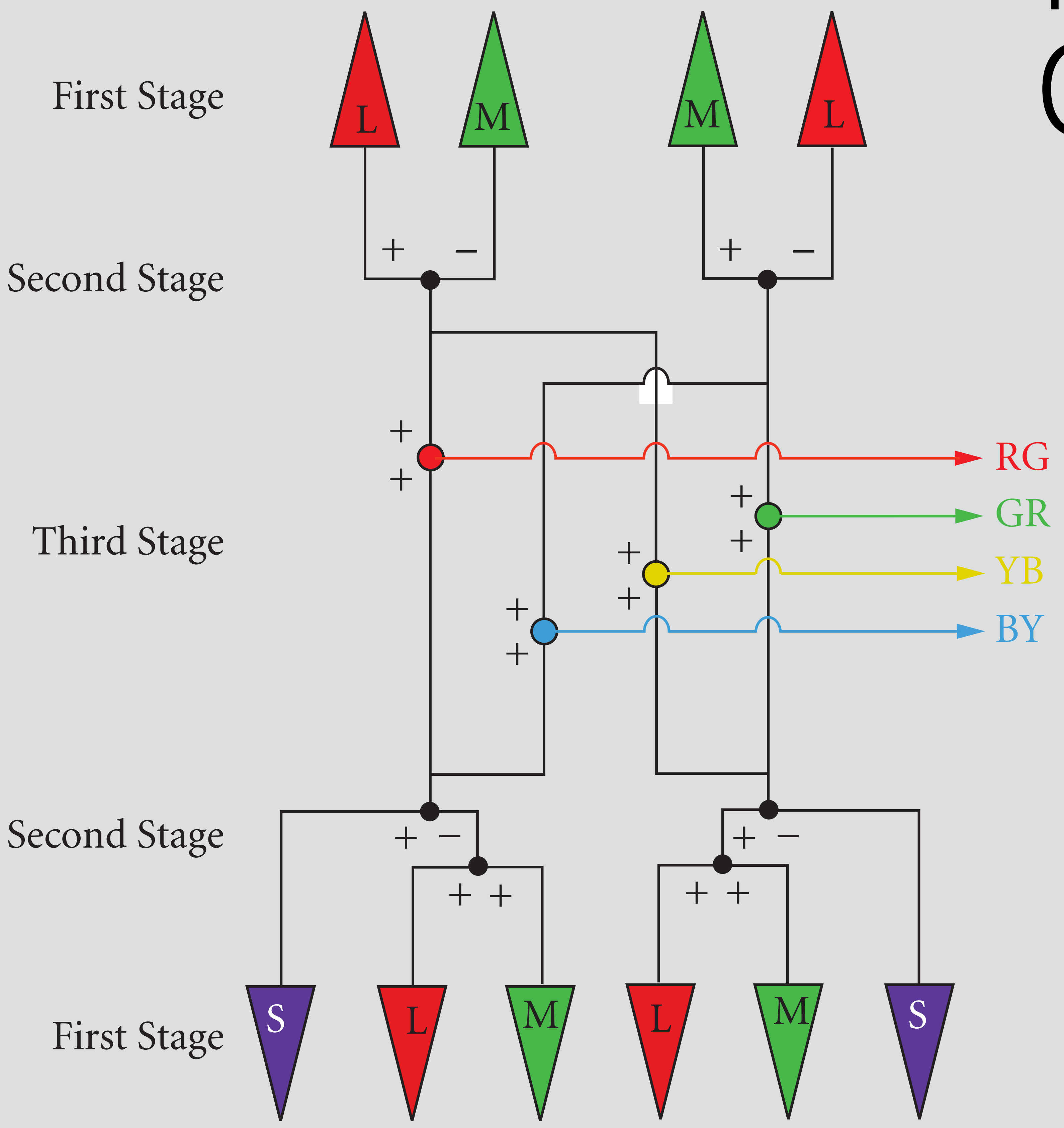

FIGURE 39 Three-stage Müller zone model. *First stage:* L-, M-, and S-cone photoreceptors (top and bottom). *Second stage:* L–M and M–L cone opponency (top) and S–(L+M) and (L+M)–S cone opponency (bottom). *Third stage:* Color opponency (center) is achieved by summing the various cone-opponent second-stage outputs.

$$rg = 1.86L - 2.90M + S$$

$$yb = 3.24L - 2.21M - S$$

Stockman, A., & Brainard, D. H. (2010). Color Vision Mechanisms. In M. Bass, J. M. Enoch, & V. Lakshminarayanan (Eds.), *The Optical Society of America Handbook of Optics* (3rd ed., Vol. Volume III: Vision and Vision Optics, pp. 11.11–11.104). New York: McGraw-Hill.
Brainard, D. H., & Stockman, A. (2010). Colorimetry. In M. Bass, J. M. Enoch, & V. Lakshminarayanan (Eds.), *The Optical Society of America Handbook of Optics* (3rd ed., Vol. Volume III: Vision and Vision Optics, pp. 10.11–10.56). New York: McGraw-Hill.

Opponent Processes

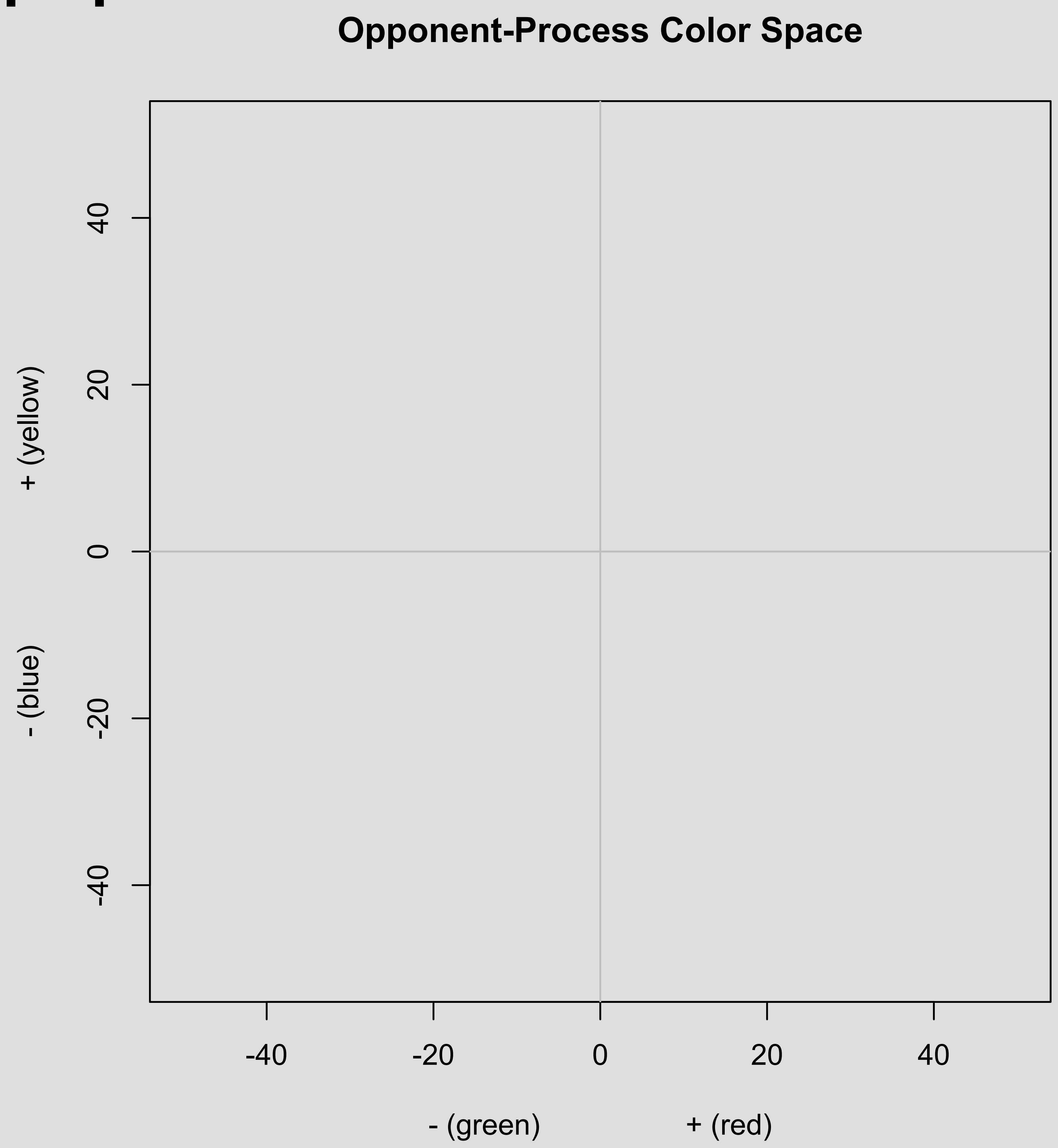

$$rg = 1.86L - 2.90M + S$$

$$yb = 3.24L - 2.21M - S$$

Color Opponent Processes

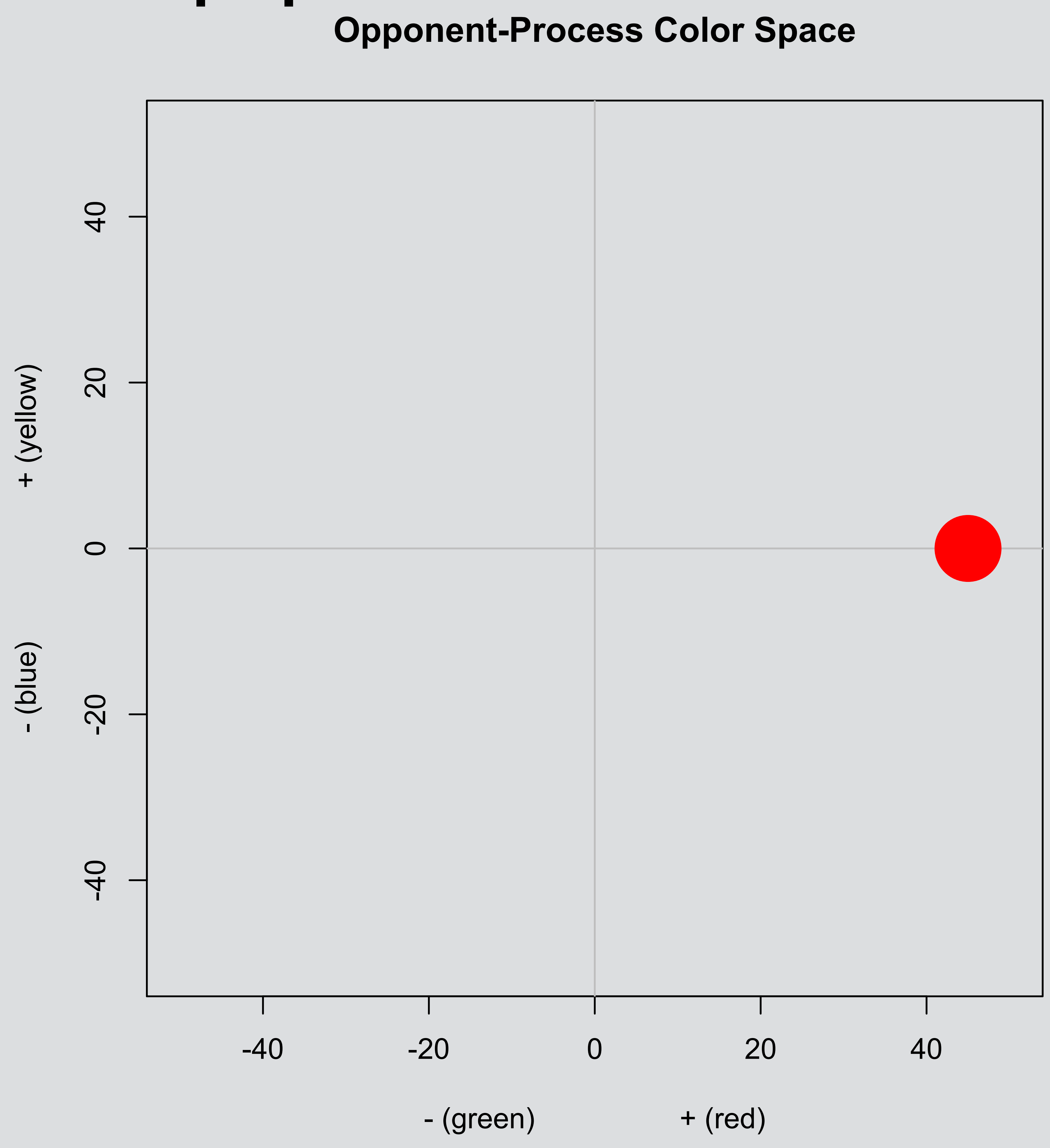

$$rg = 1.86L - 2.90M + S$$
$$yb = 3.24L - 2.21M - S$$

Color Opponent Processes

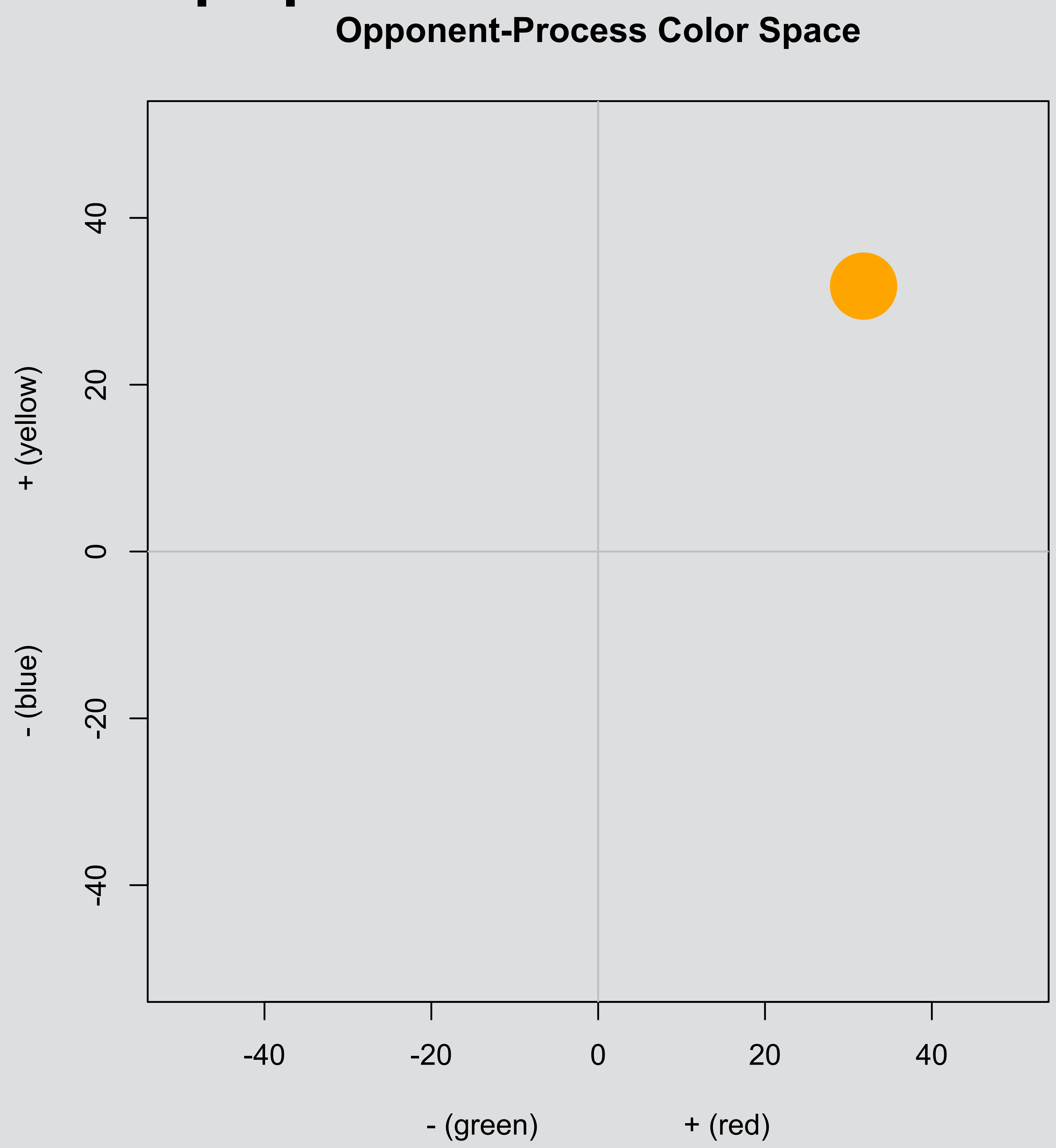

$$rg = 1.86L - 2.90M + S$$
$$yb = 3.24L - 2.21M - S$$

Color Opponent Processes

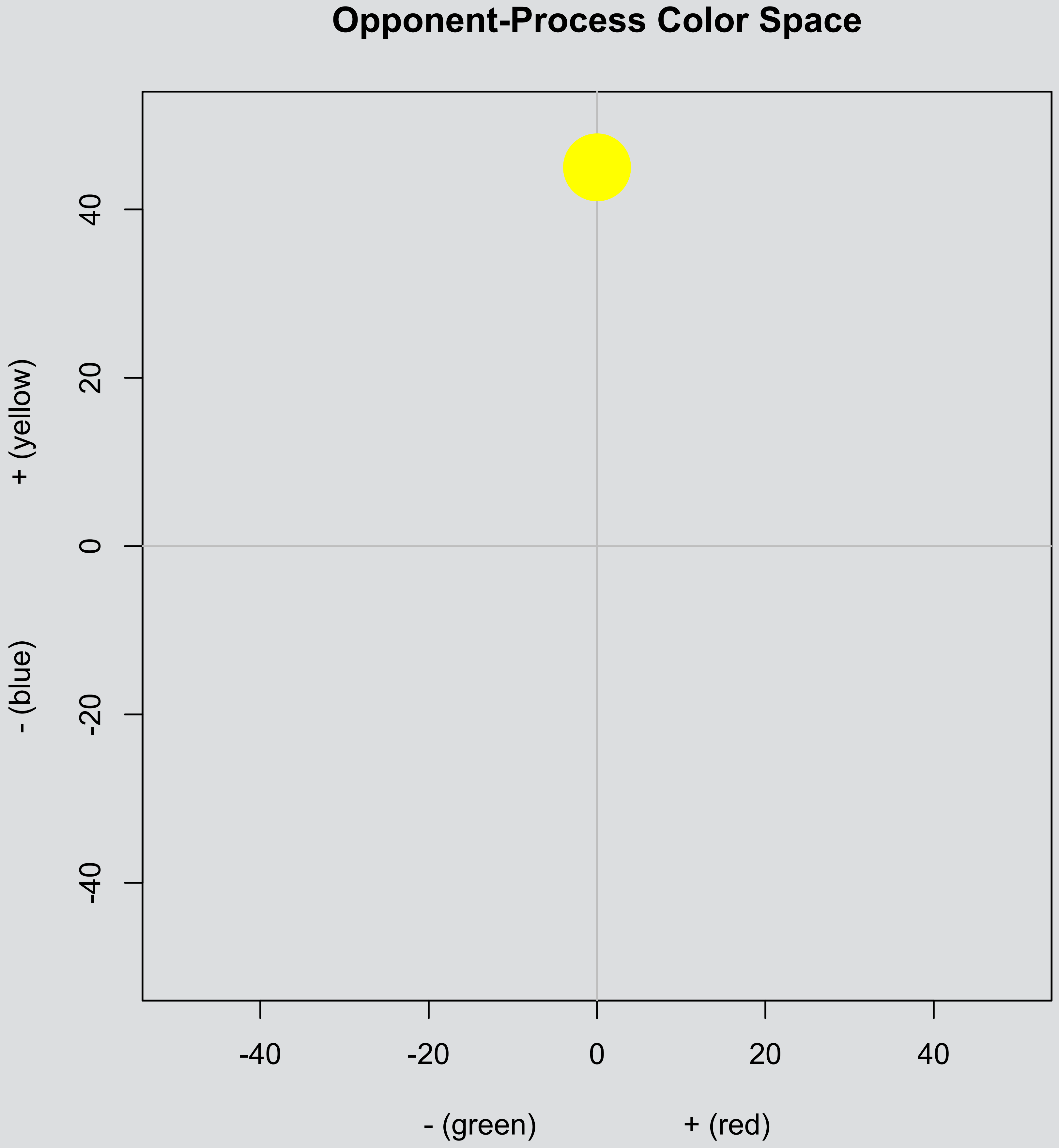

$$rg = 1.86L - 2.90M + S$$
$$yb = 3.24L - 2.21M - S$$

Color Opponent Processes

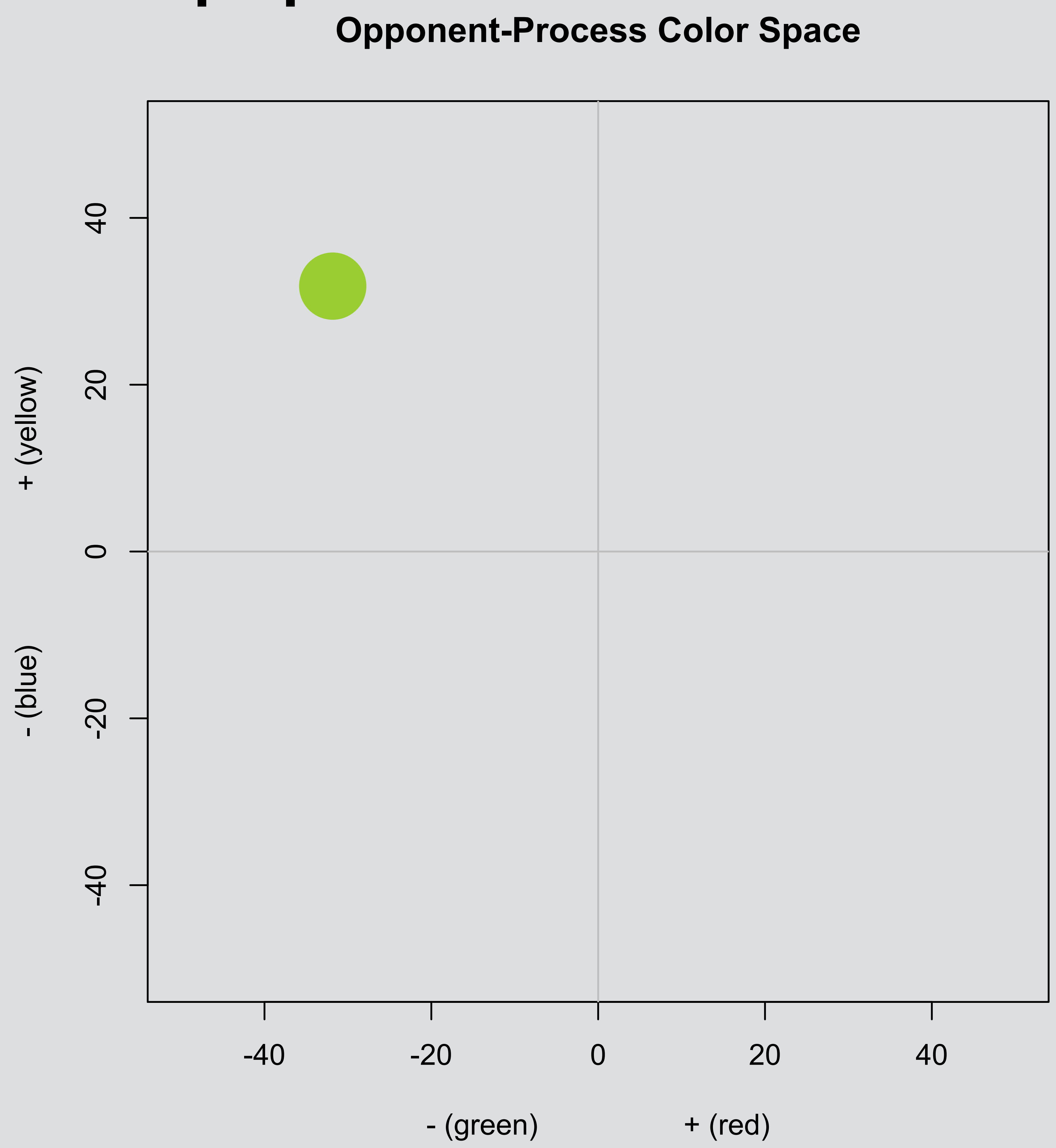

$$rg = 1.86L - 2.90M + S$$

$$yb = 3.24L - 2.21M - S$$

Color Opponent Processes

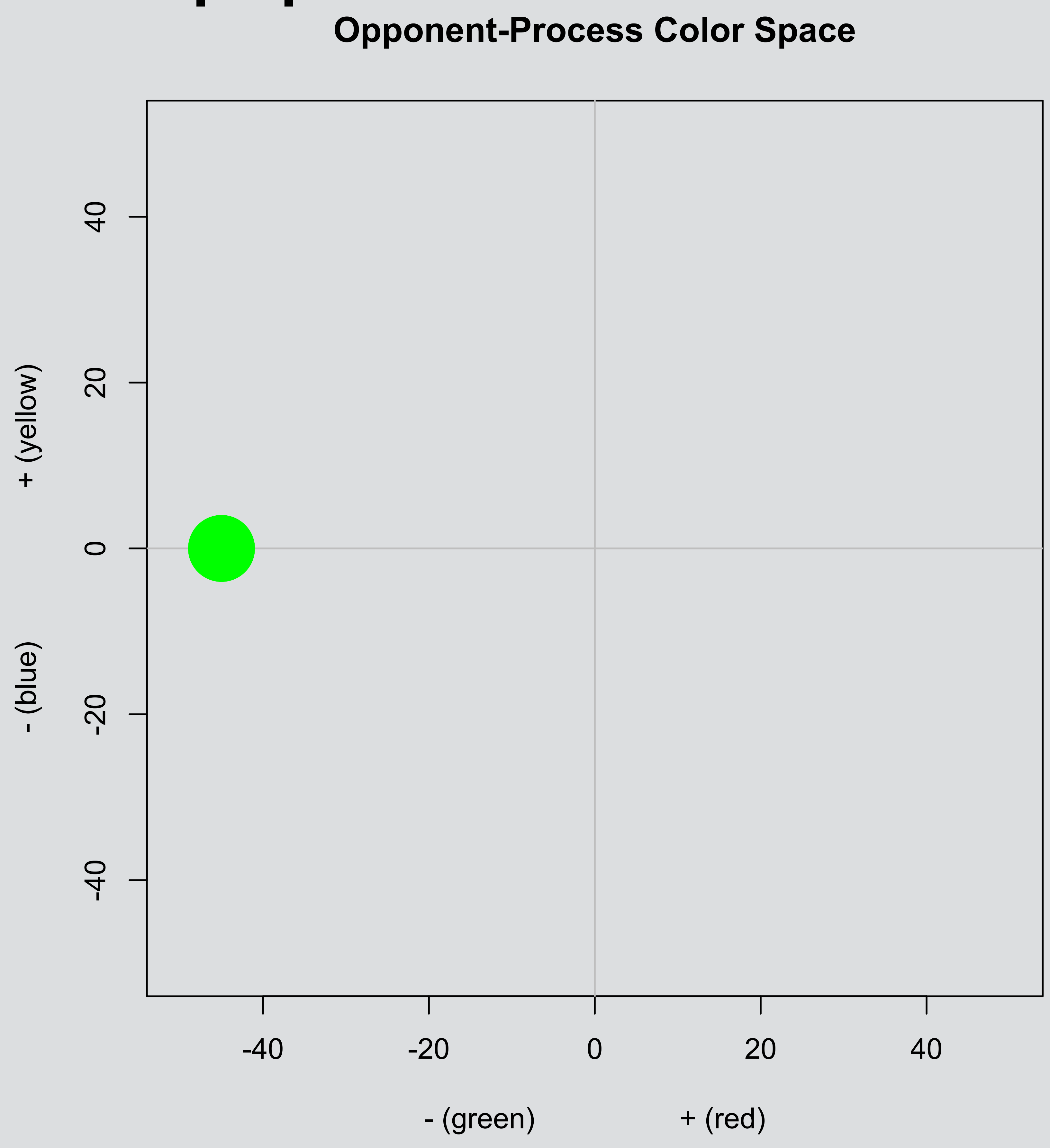

$$rg = 1.86L - 2.90M + S$$
$$yb = 3.24L - 2.21M - S$$

Color Opponent Processes

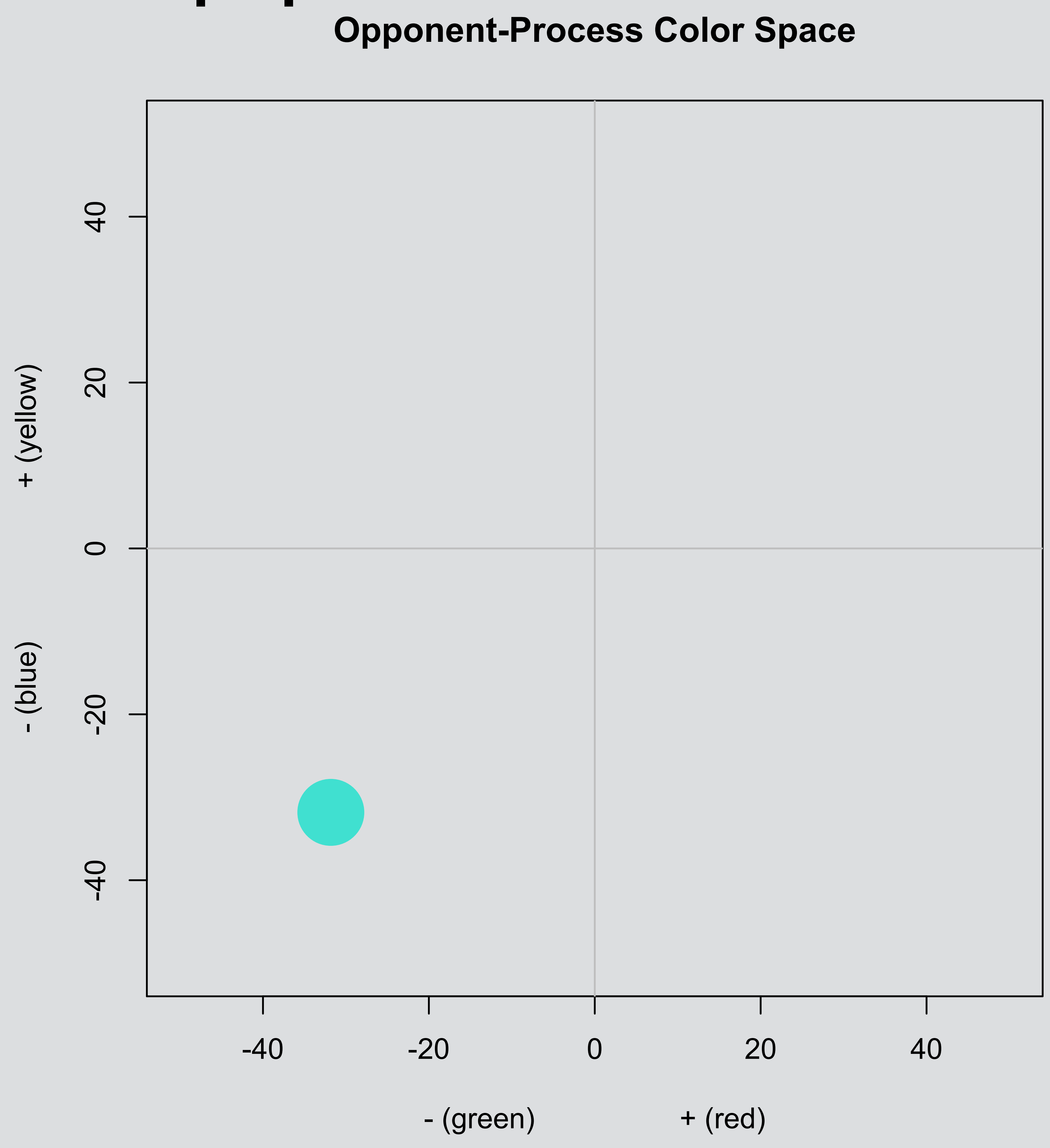

$$rg = 1.86L - 2.90M + S$$

$$yb = 3.24L - 2.21M - S$$

Color Opponent Processes

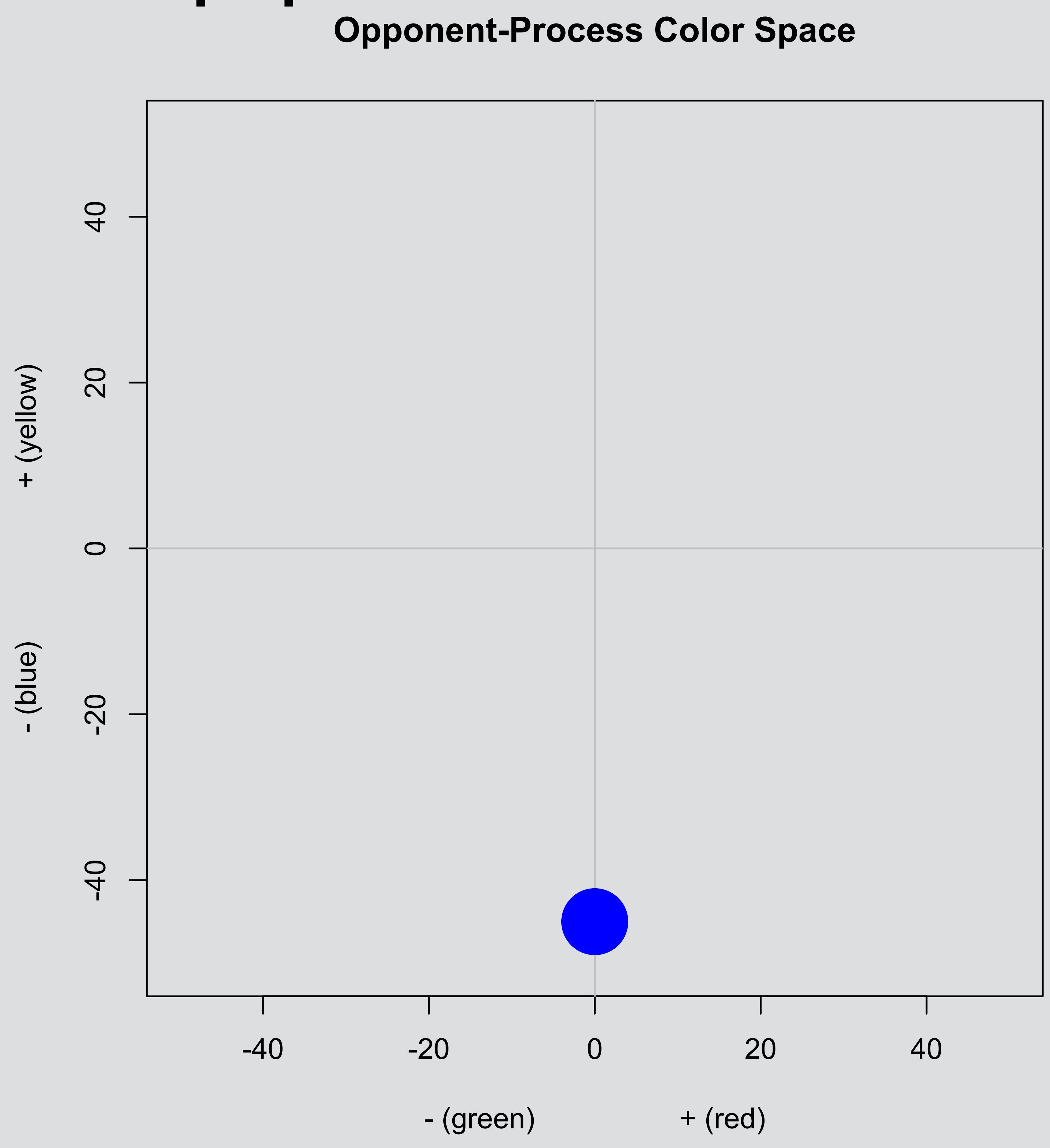

$$rg = 1.86L - 2.90M + S$$

$$yb = 3.24L - 2.21M - S$$

Color Opponent Processes

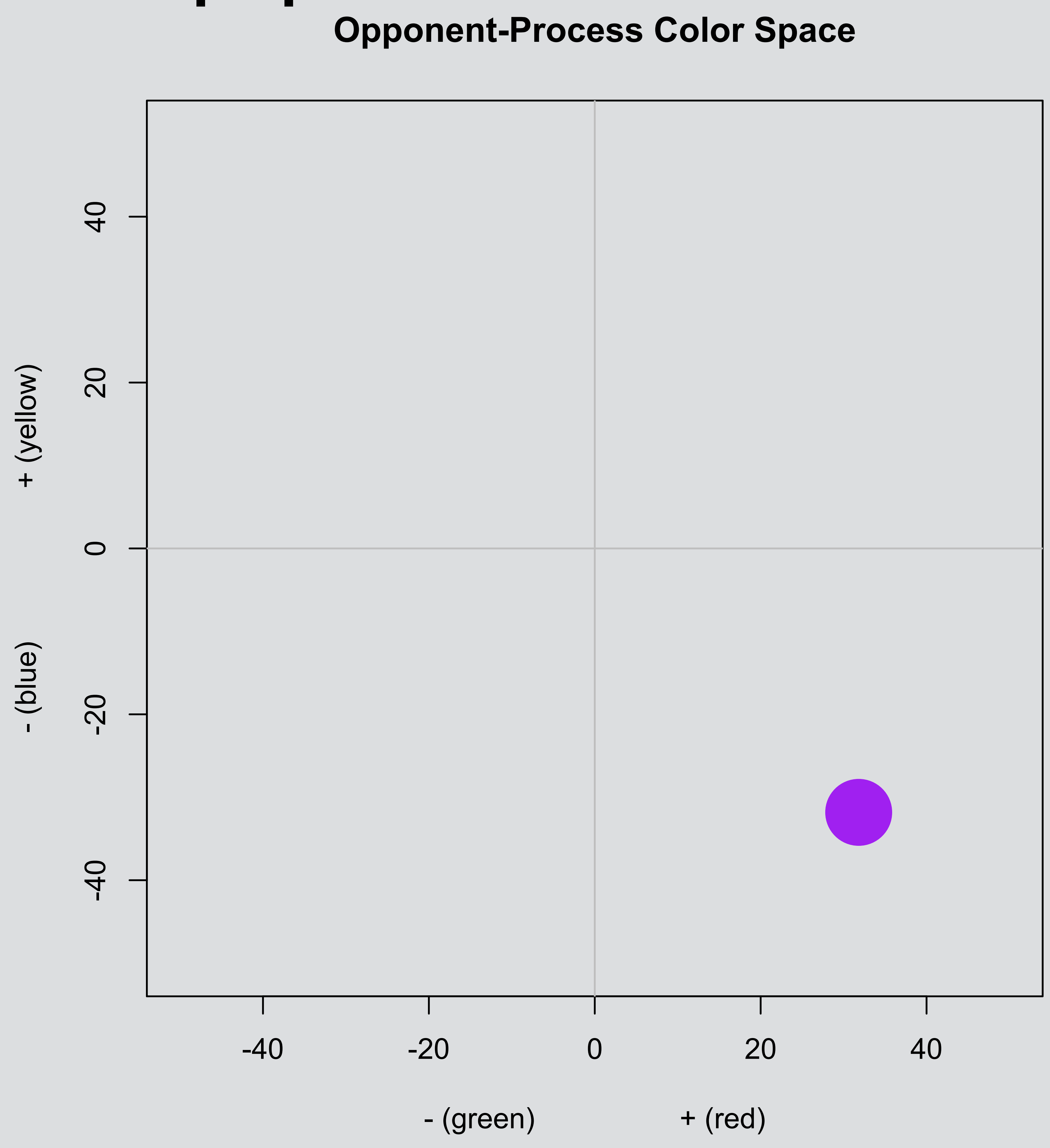

$$rg = 1.86L - 2.90M + S$$

$$yb = 3.24L - 2.21M - S$$

Color Opponent Processes

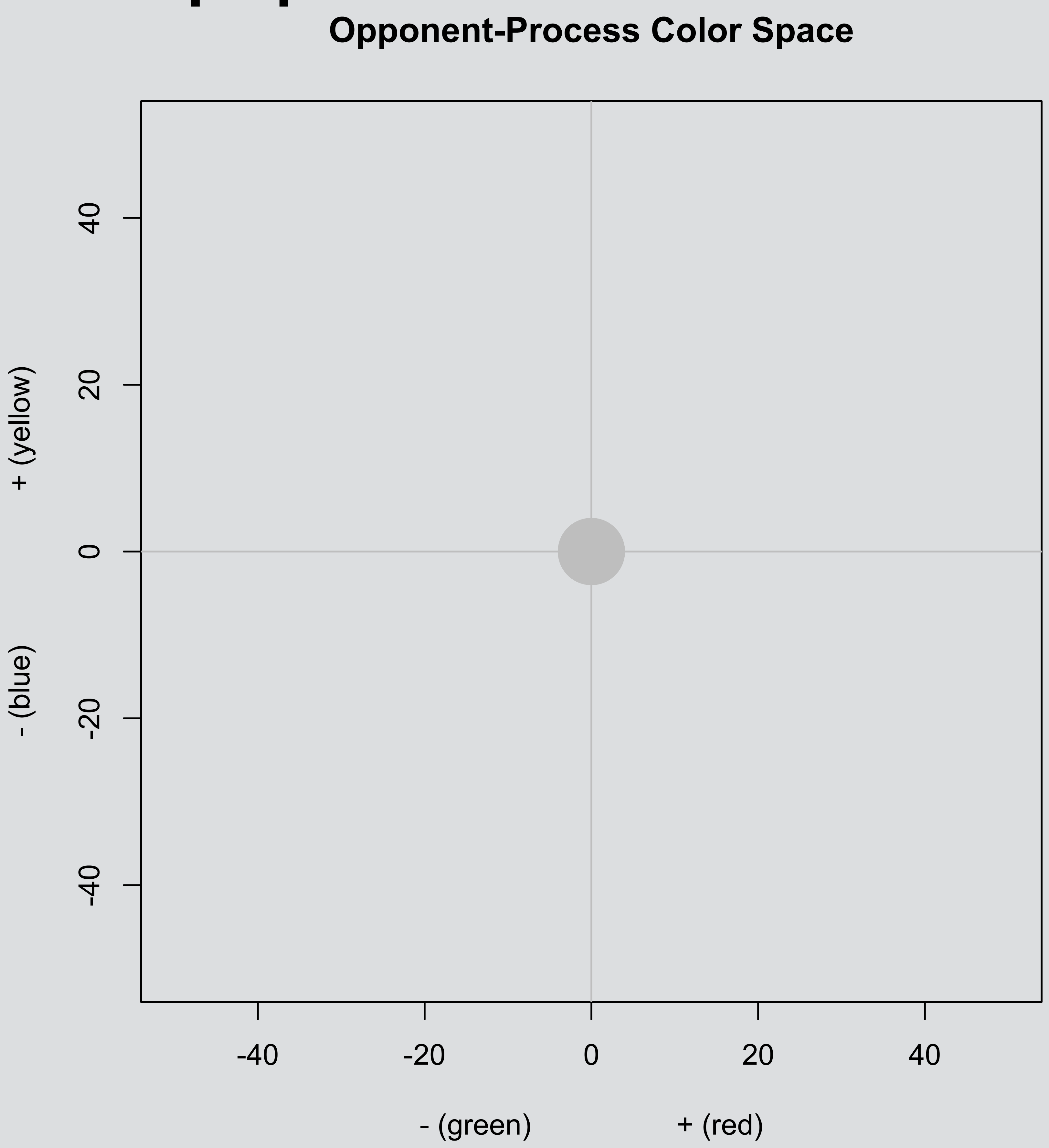

$$rg = 1.86L - 2.90M + S$$

$$yb = 3.24L - 2.21M - S$$

Color Opponent Processes

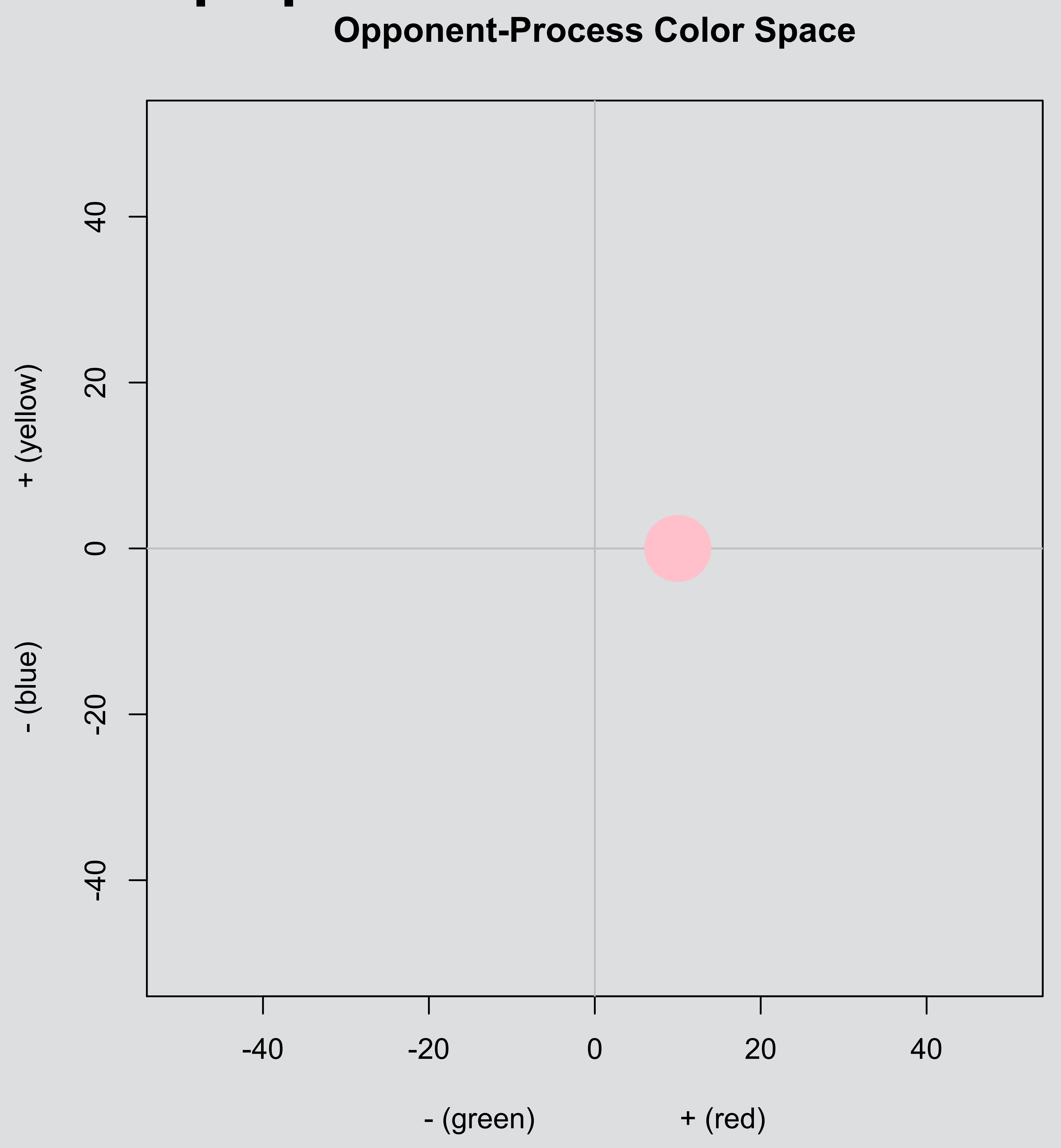

$$rg = 1.86L - 2.90M + S$$

$$yb = 3.24L - 2.21M - S$$

Afterimages

- Afterimages based on complimentary colors.
- Keep looking at the same spot in the center of the picture for 20 seconds.
- Look at a white surface: what do you see?

DARWIN ILLUSION.
ROB JENKINS (UNIVERSITY OF GLASGOW), RICHARD WISEMAN (UNIVERSITY OF HERTFORDSHIRE).

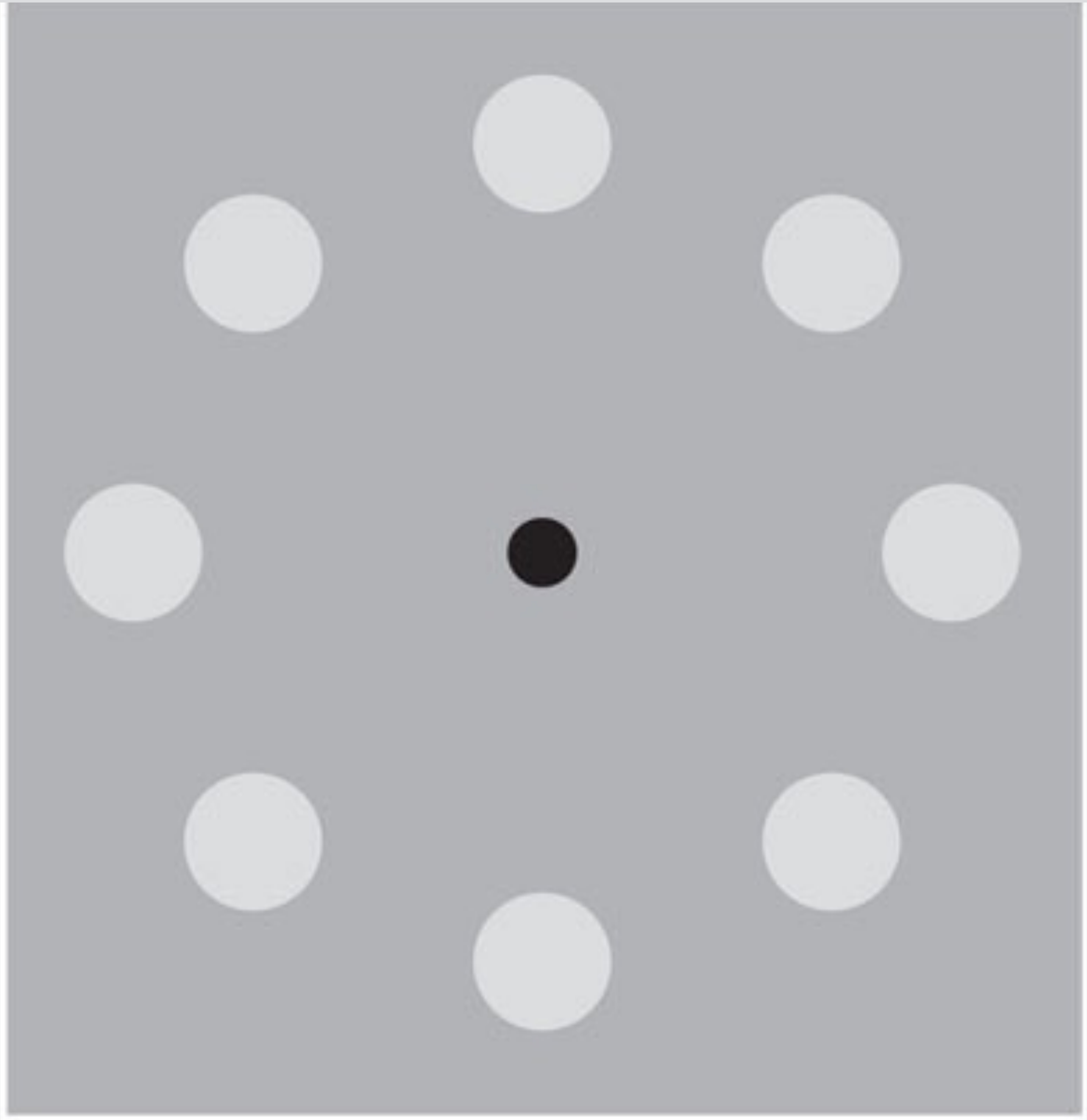

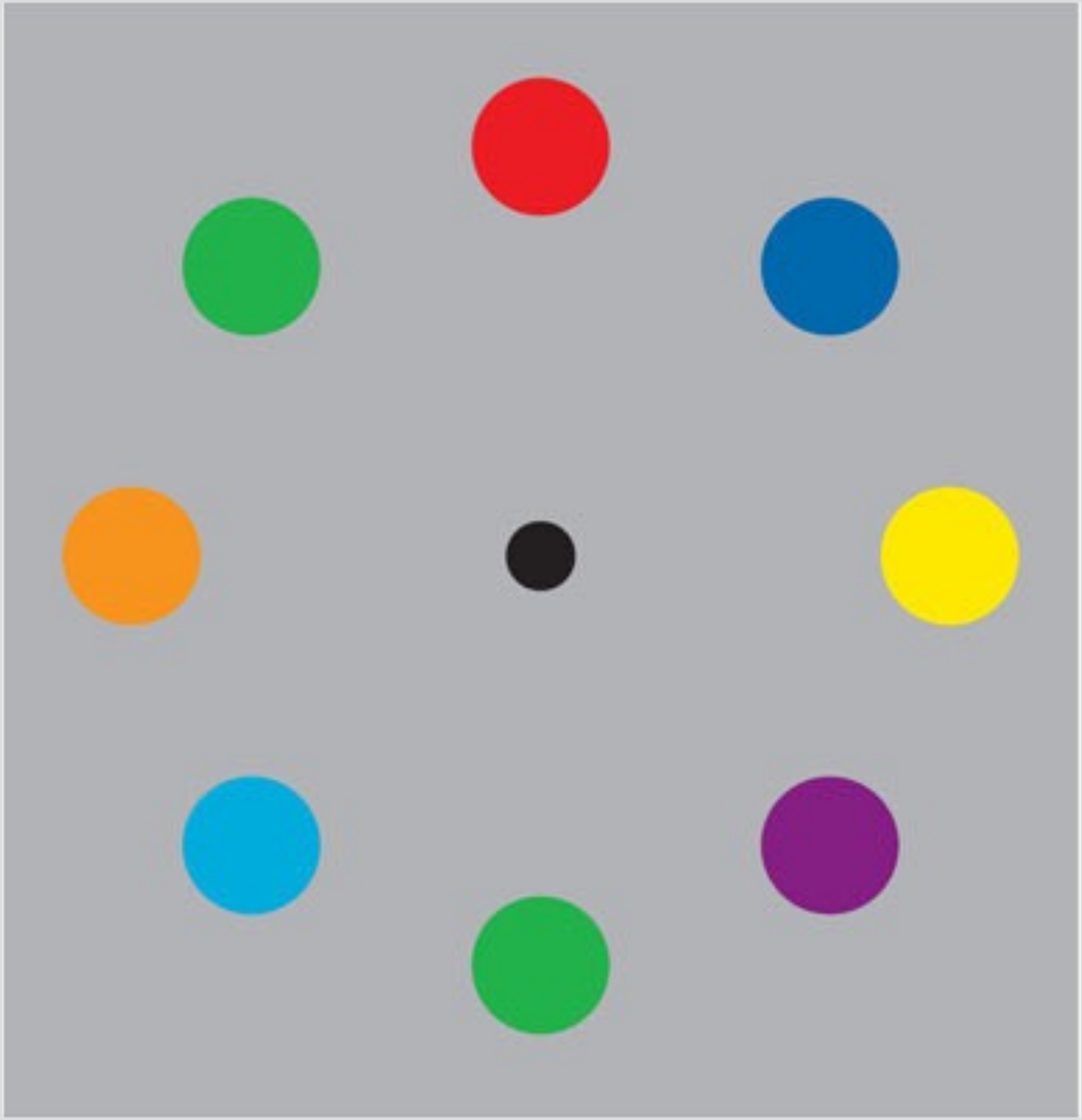

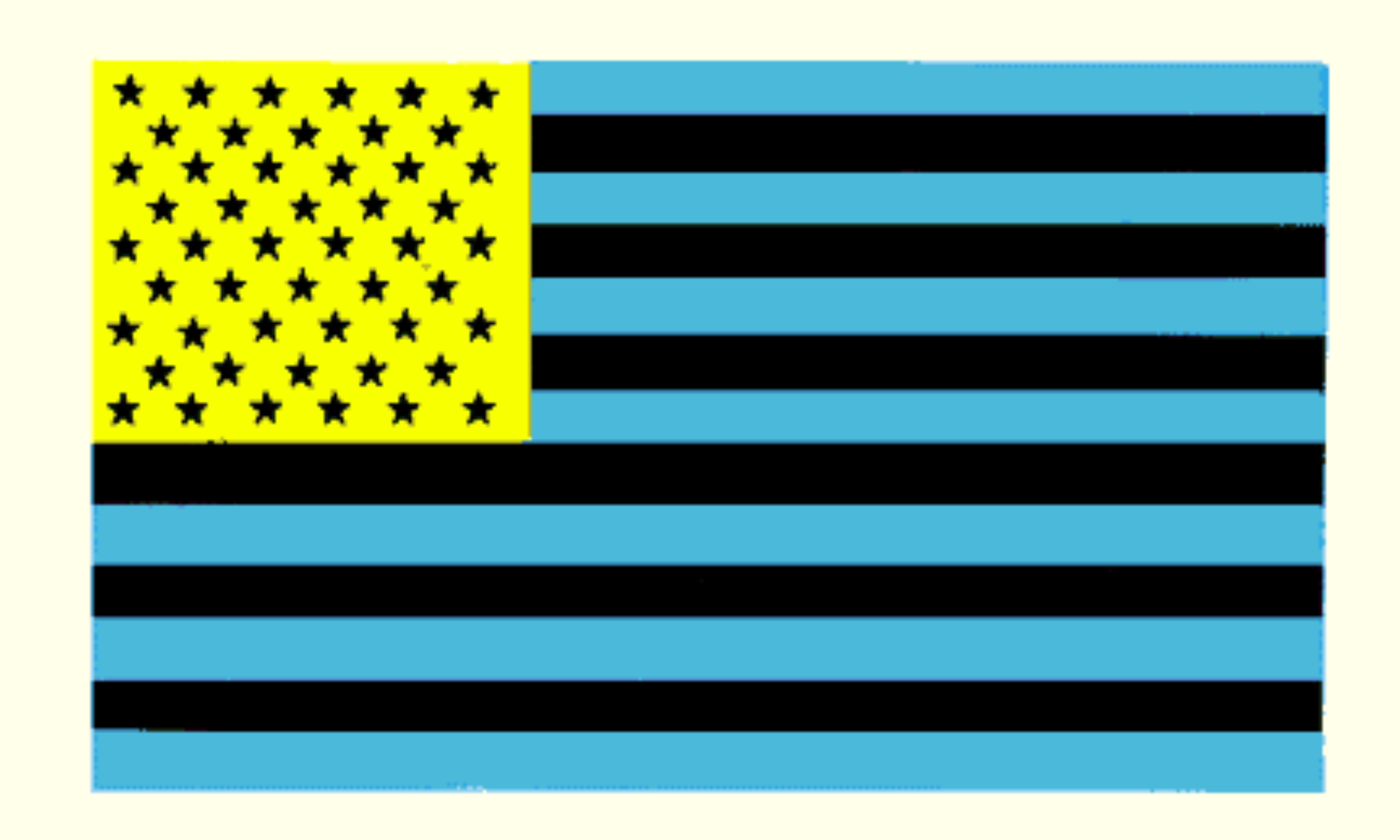

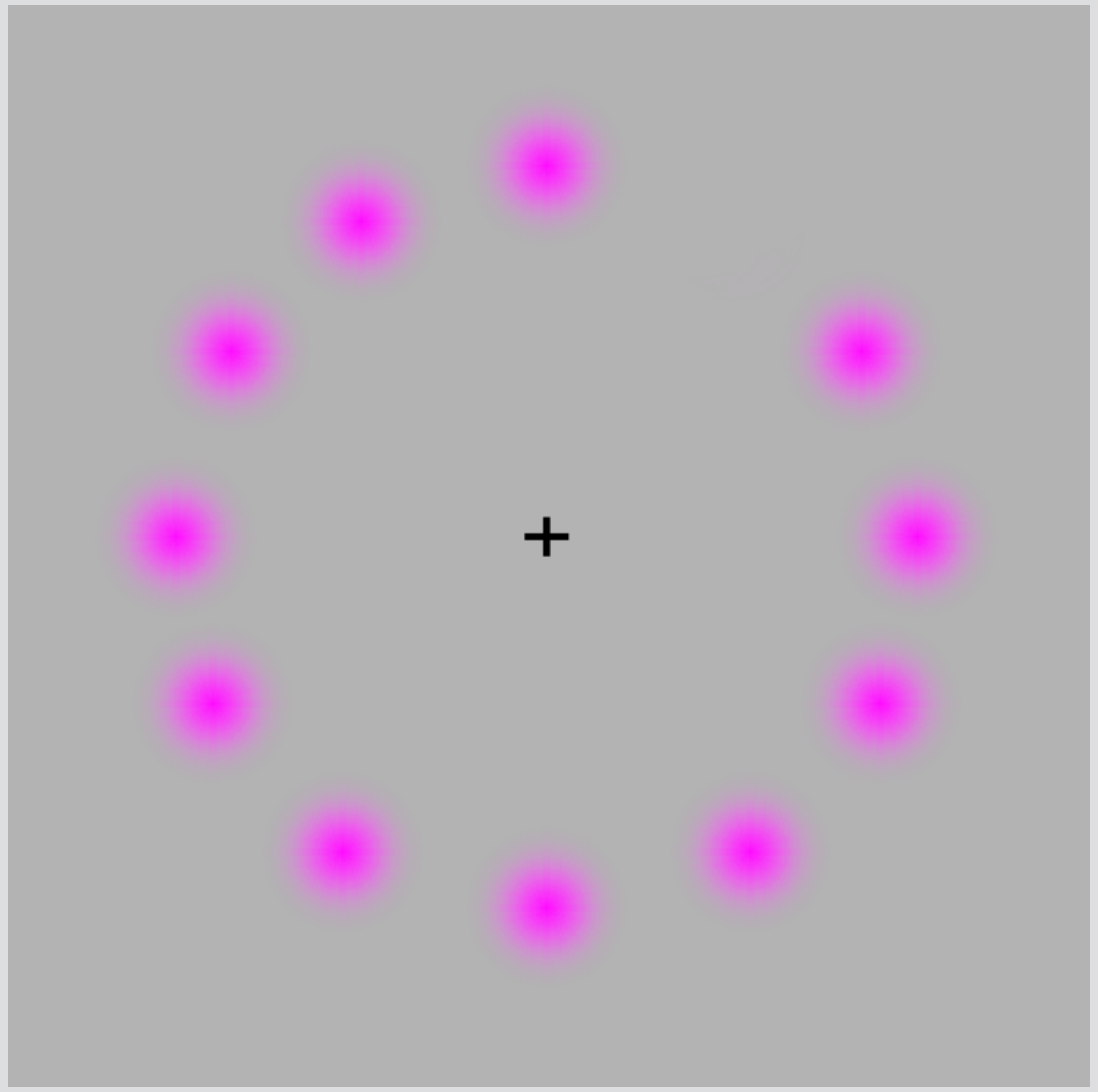

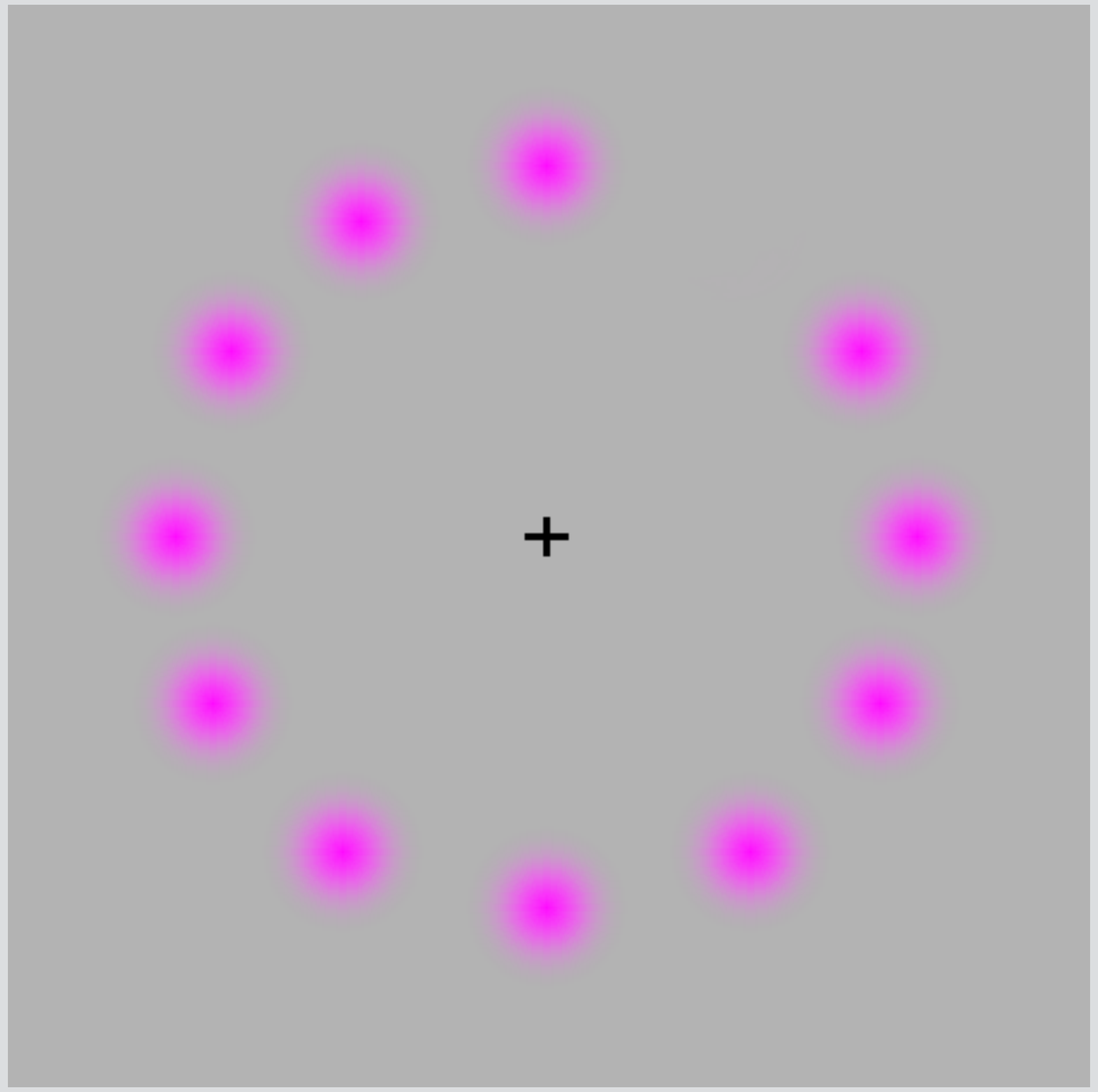

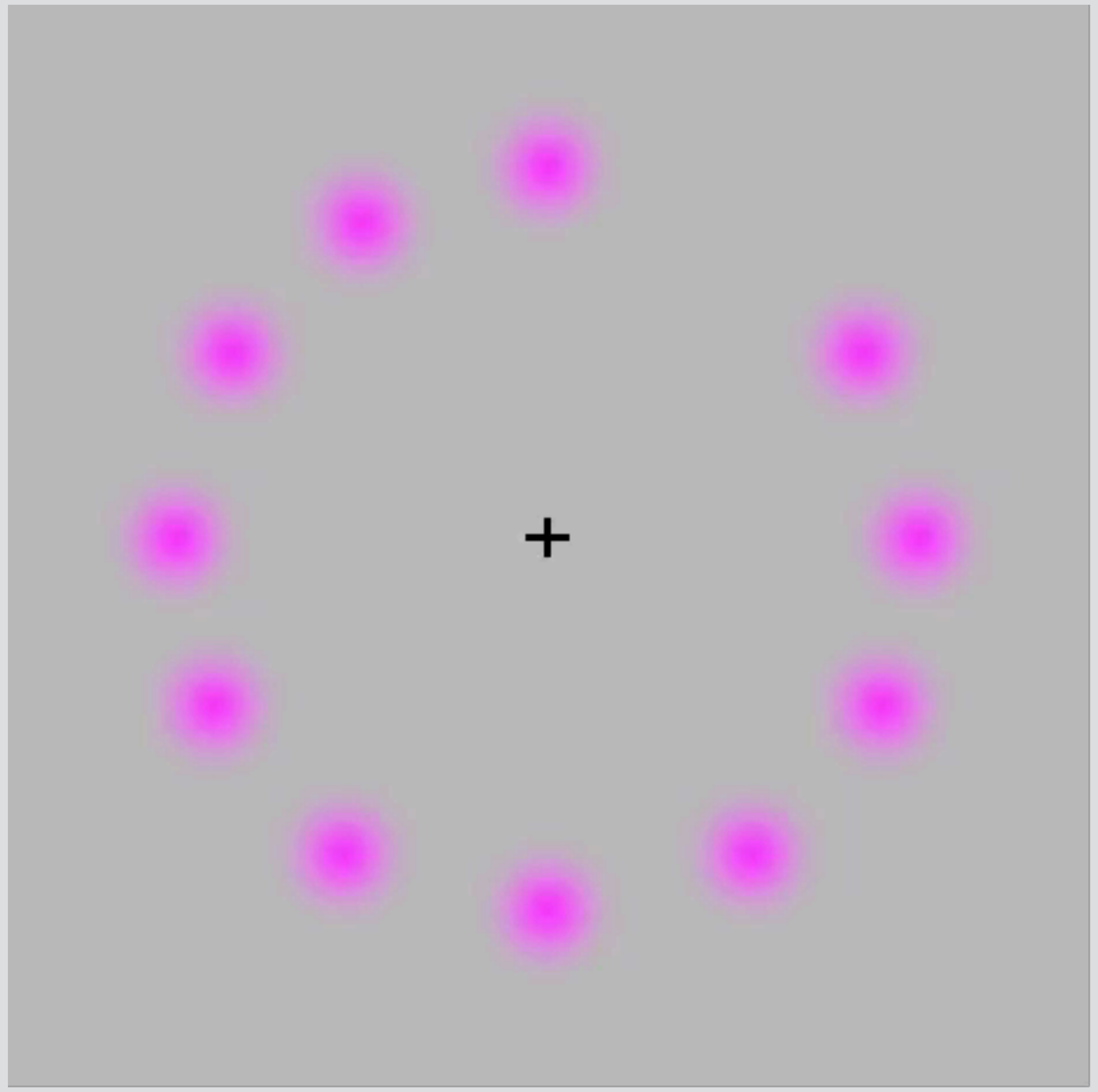

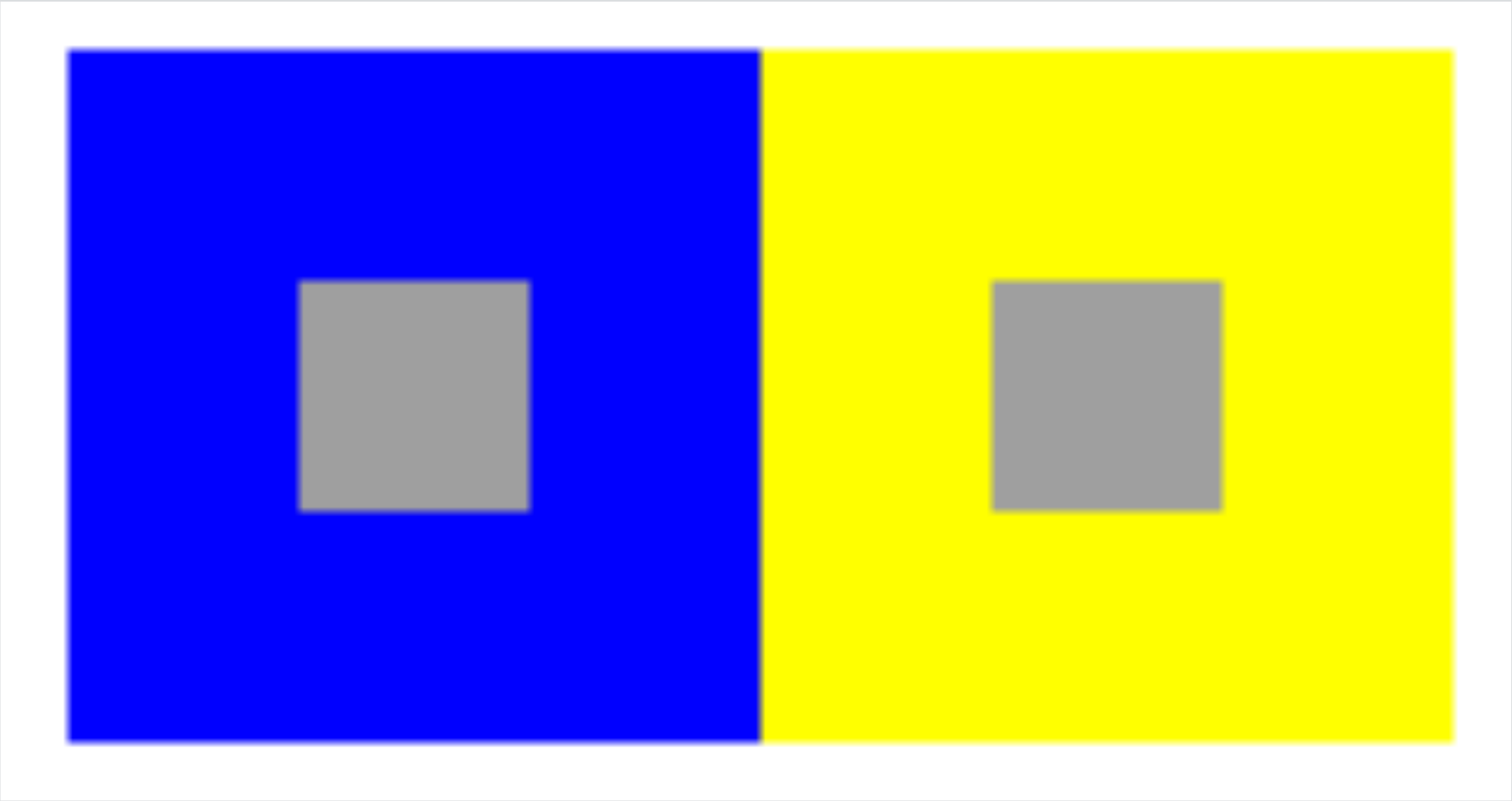

Color Processing

Black and White Stream
Red and Green Stream
Yellow and Blue Stream

John Sadowski

http://www.johnsadowski.com/color_illusion_tutorial.html

McCollough Effect

Celeste McCollough Howard (1927–)

McCollough, C. (1965). Color adaptation of edge-detectors in the human visual system. *Science, 149*, 1115–1116.
McCollough, C. (1965). The conditioning of color perception. *American Journal of Psychology, 78*(3), 362–378.

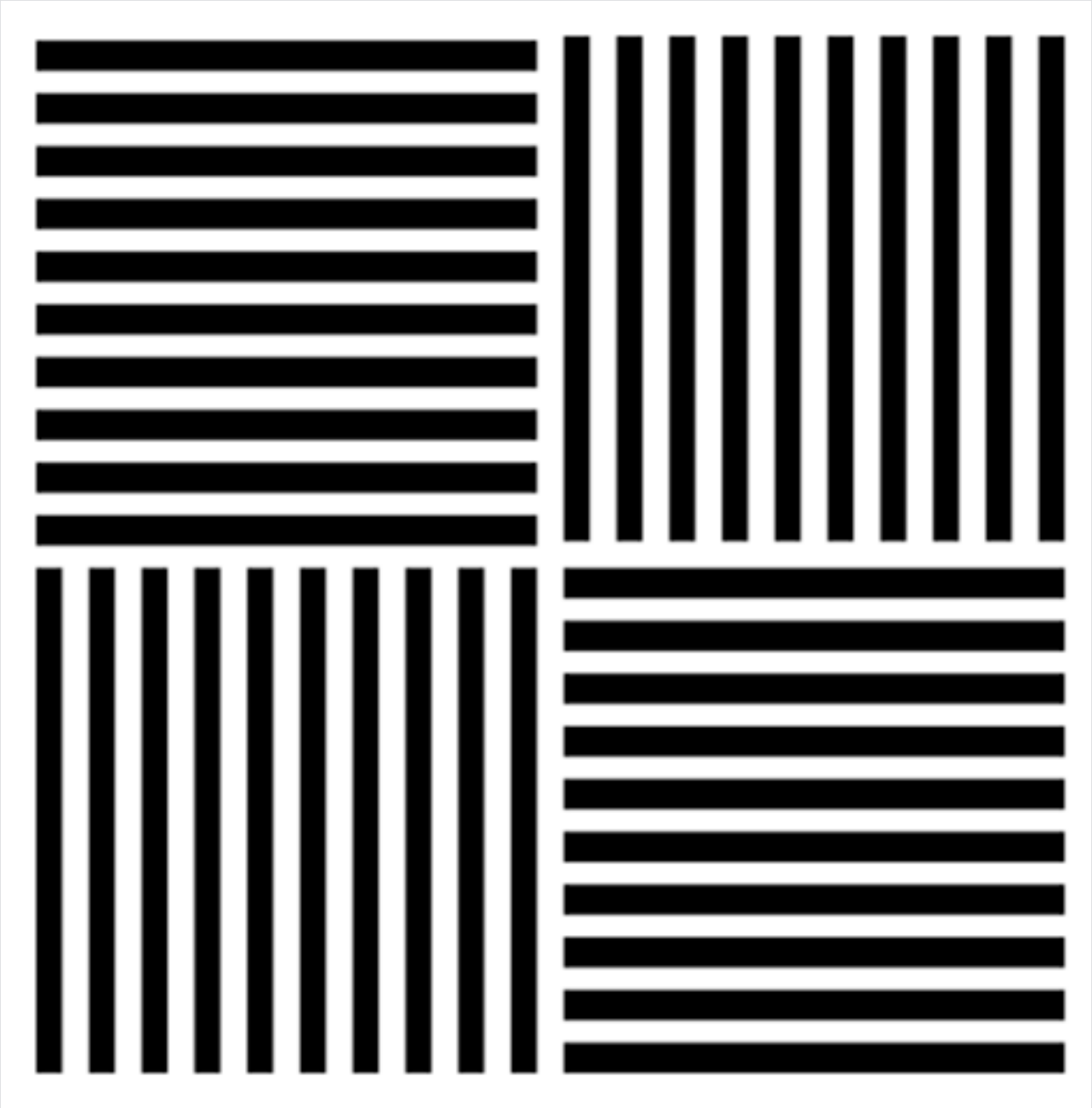

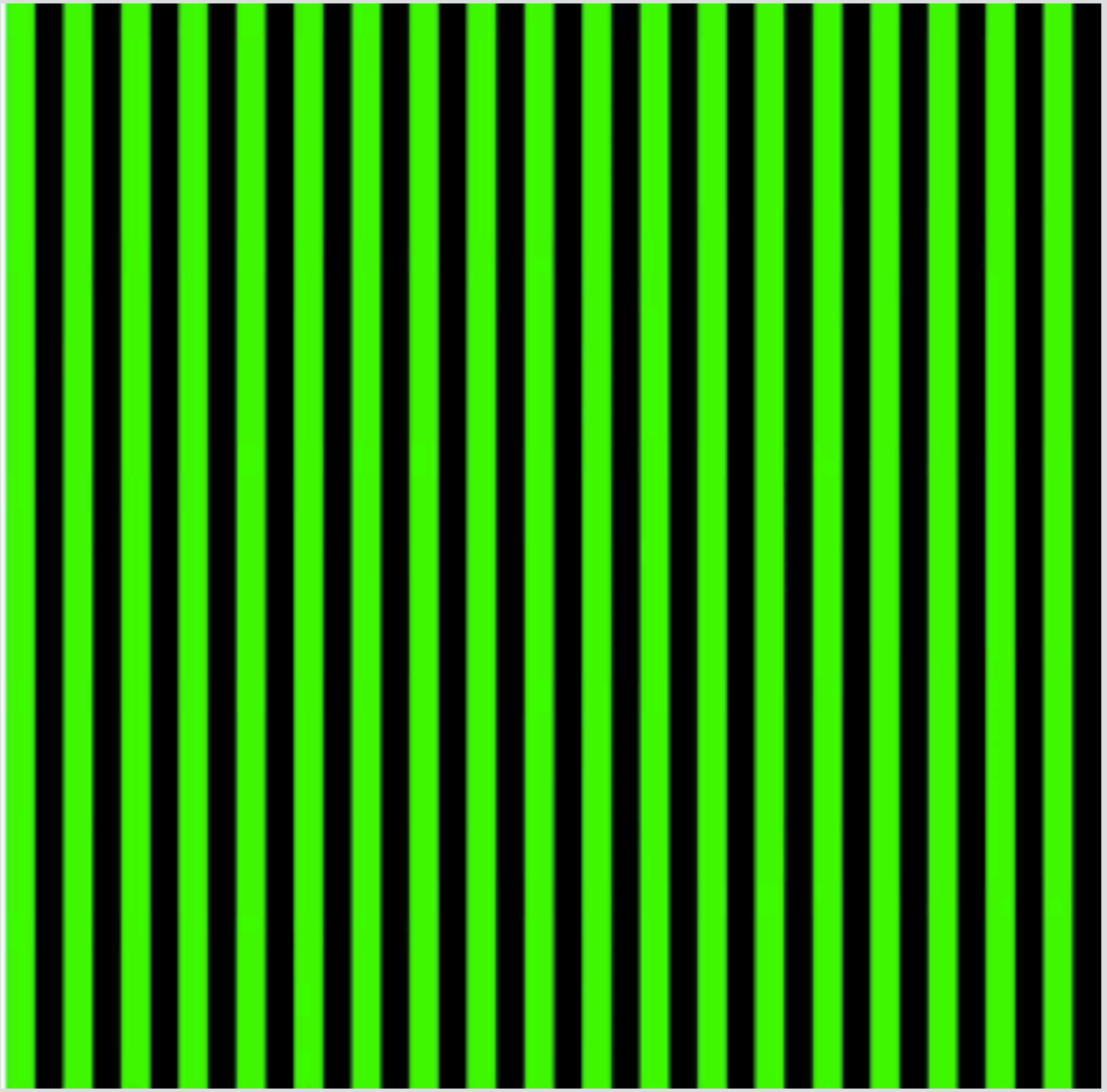

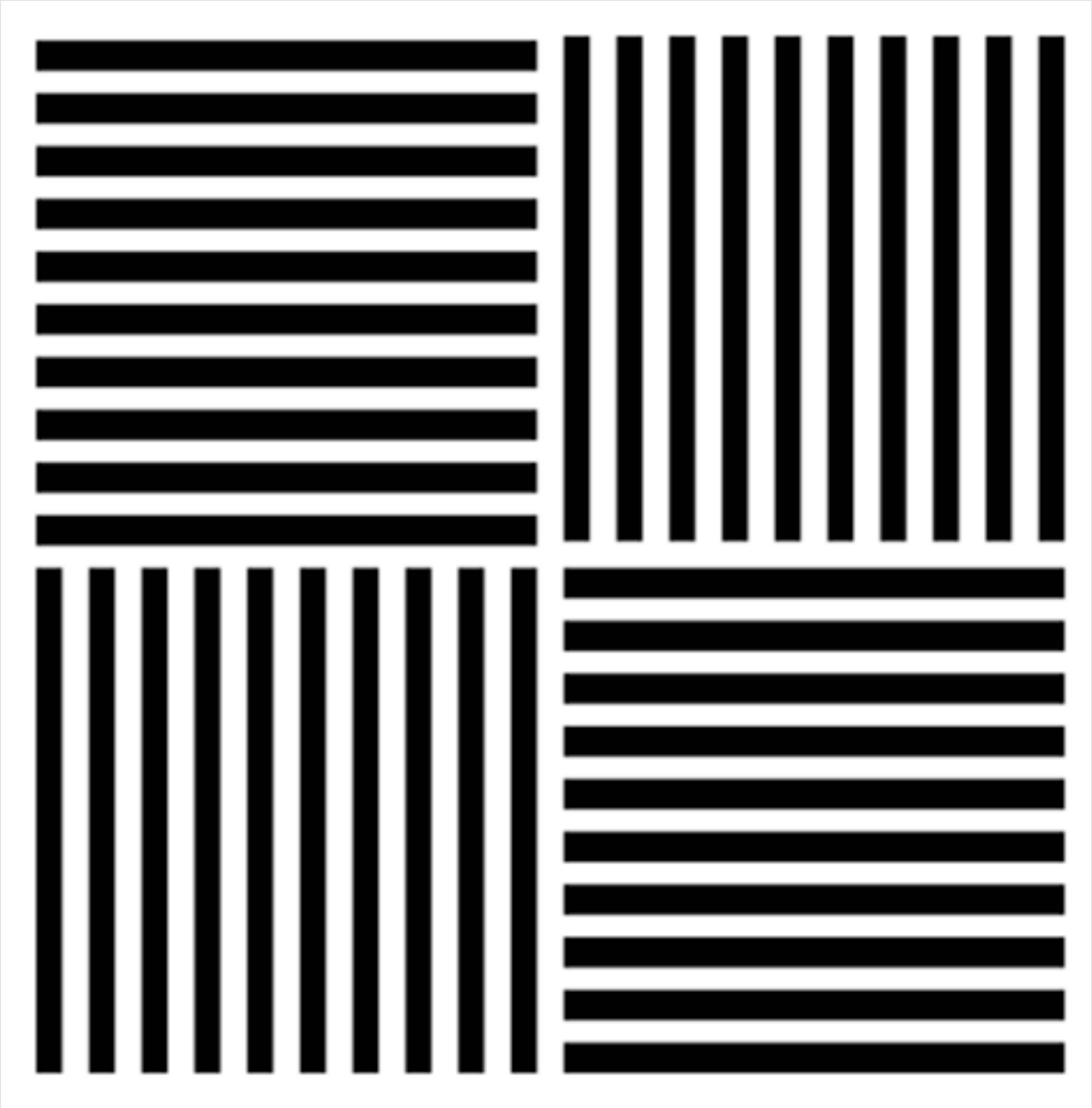

The Color Wheel

- Relative amounts of r/g and y/b contribution
  - Two colors on opposite sides of the wheel
  - Two colors on opposite sides of the color wheel, which when placed next to each other make both appear brighter.

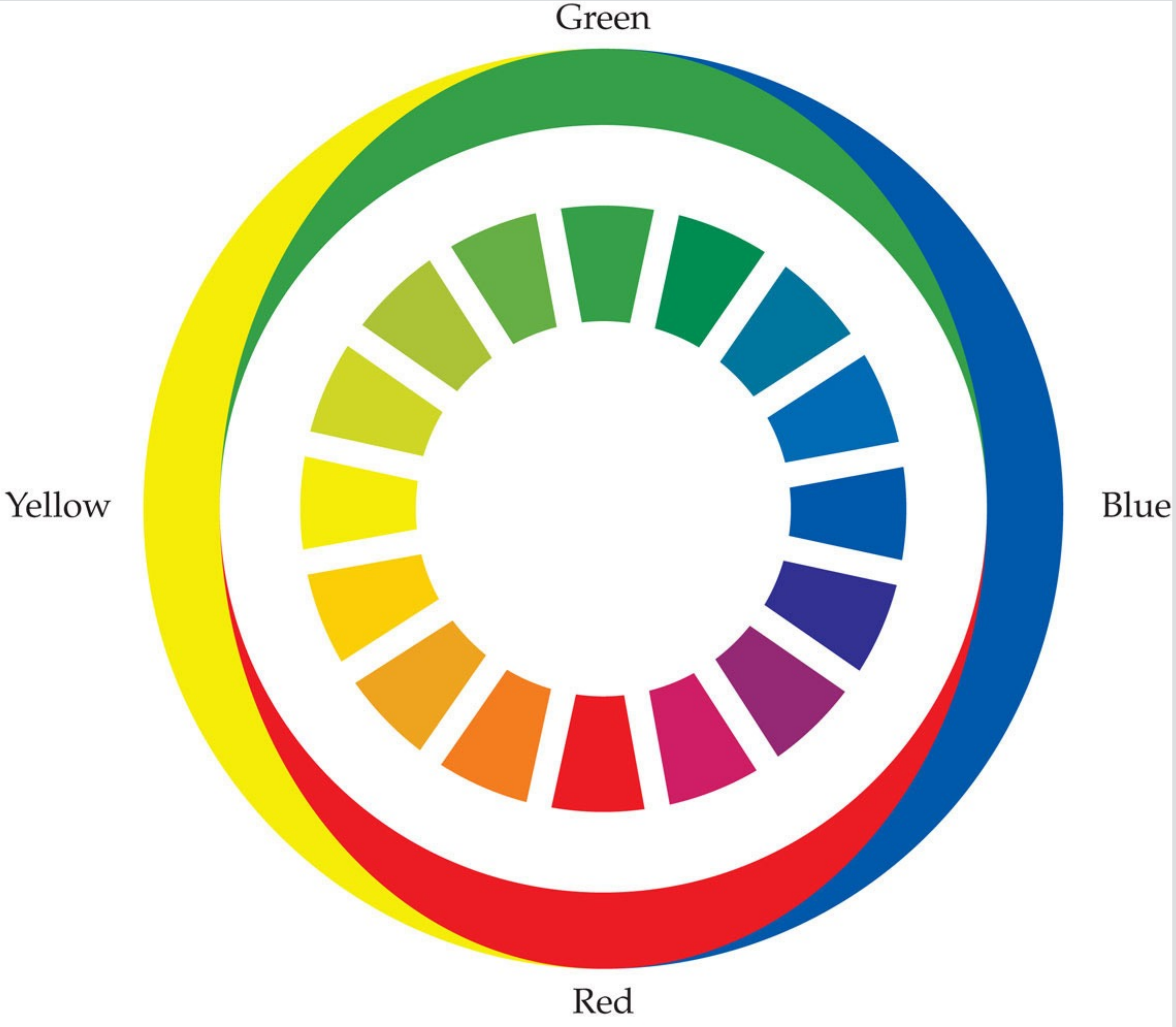

***SENSATION & PERCEPTION 4e*, Figure 5.14**

“Color Blindness”

- Trichromacy: 3 primaries to match all colors
- Dichromacy: 2 primaries to match all colors
- Monocromacy:1 primary to match all colors

Dichromacy

- Protanopia
    - Missing L-cone pigment (X chromosome)
    - Neutral point at 498nm
- Deuteranopia
    - Missing M-cone pigment (X chromosome)
    - Neutral point at 502 nm
- Tritanopia (chromosome 7)
    - No single wavelength neutral point

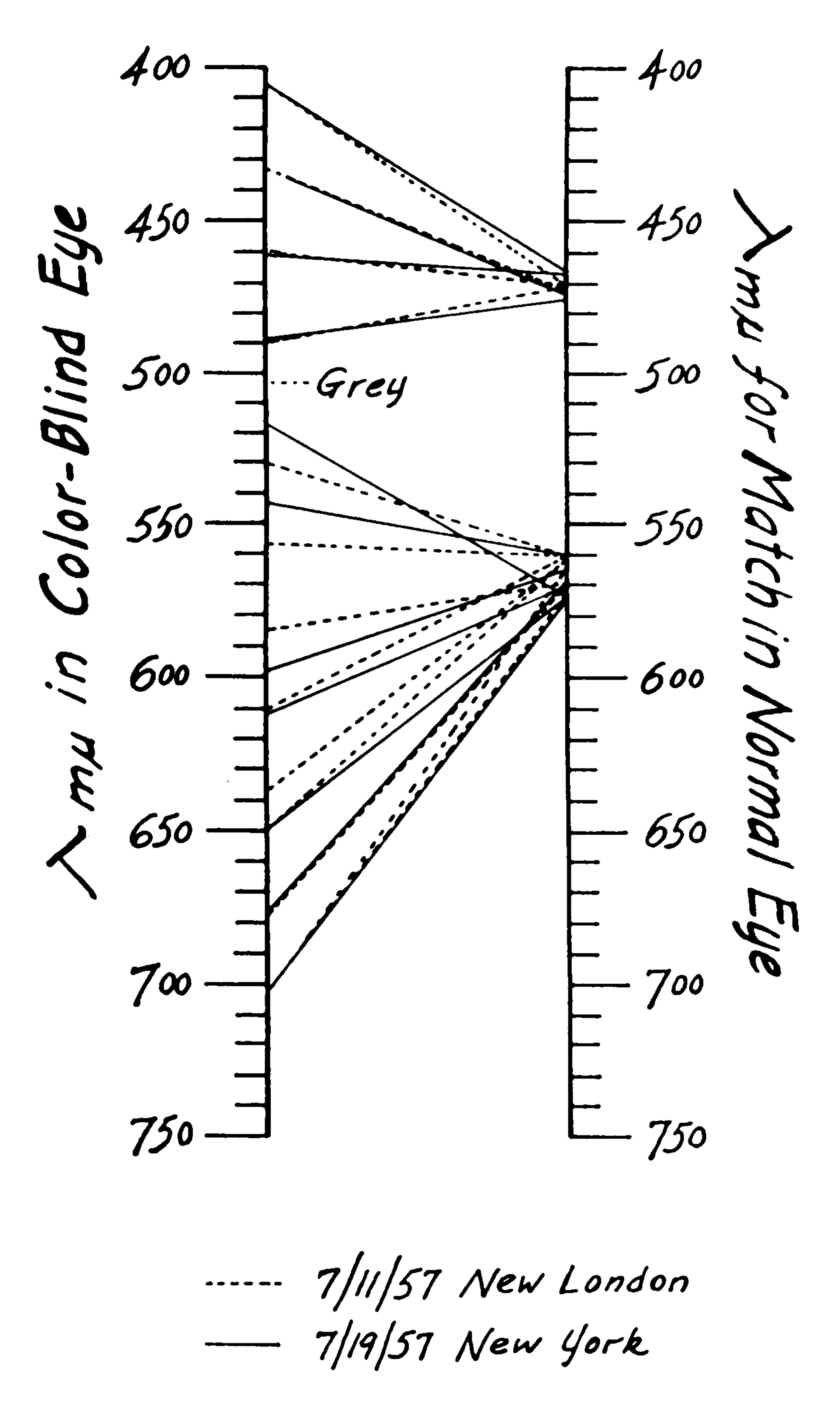

a

Fig. 5. Results of the experiment on binocular color matching. The wavelengths seen by the color-blind eye (left scale) are matched by the indicated wavelengths in the normal eye (right scale).

Graham, C. H., & Hsia, Y. (1958). Color defect and color theory: Studies on normal and color blind persons including a unilaterally dichromatic subject. *Science, 127*(3300), 675682.

a

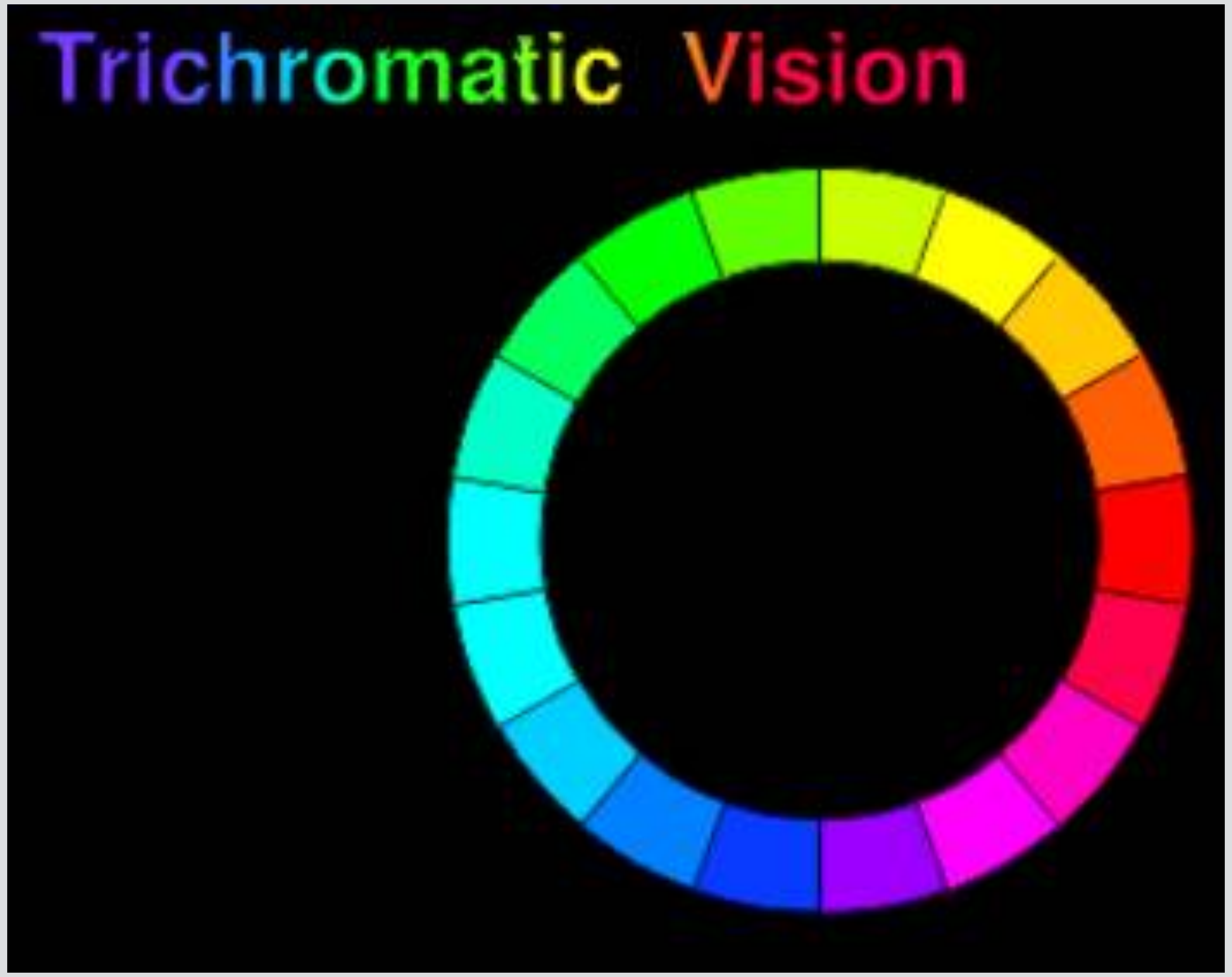

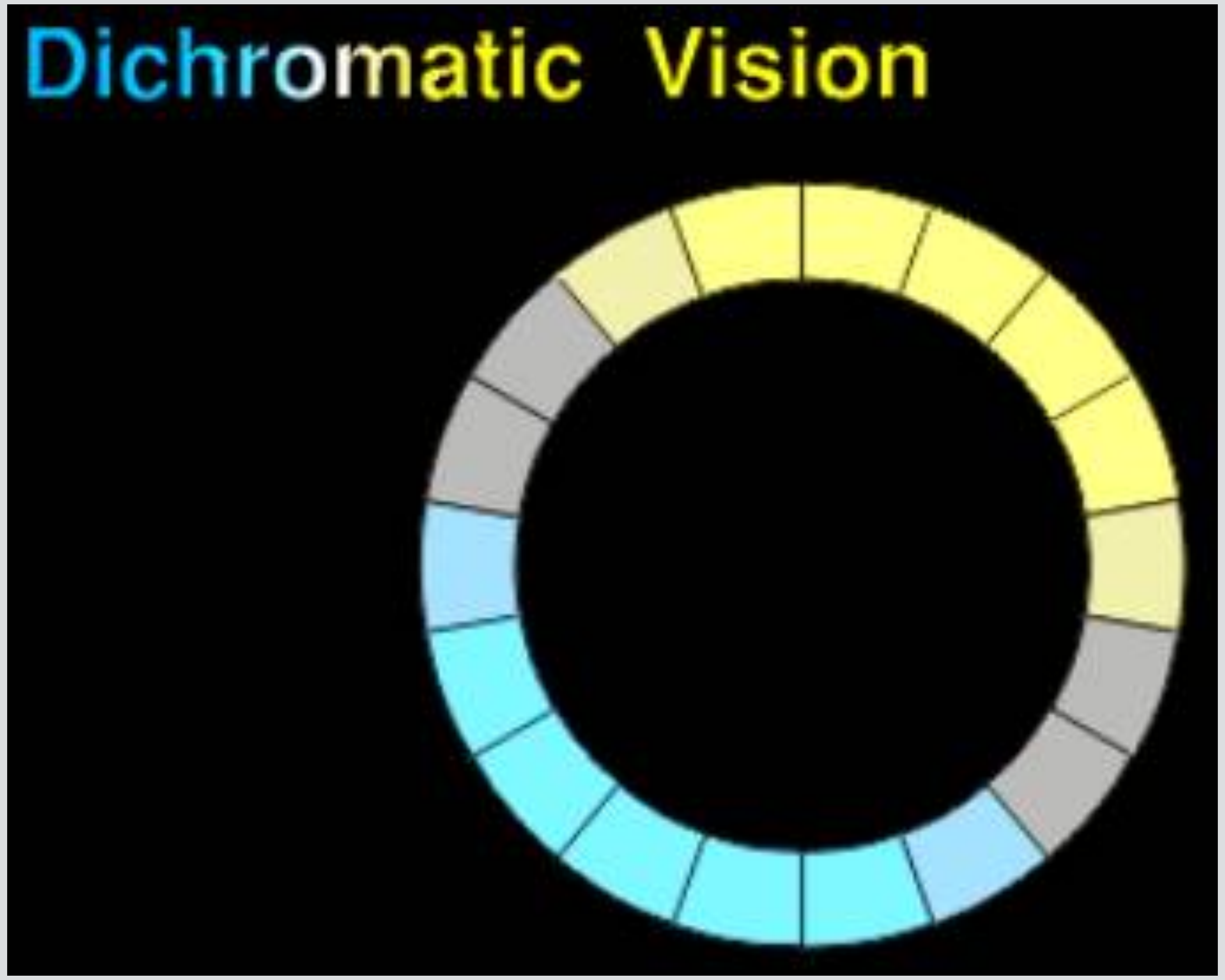

Graham, C. H., & Hsia, Y. (1958). Color defect and color theory: Studies on normal and color blind persons including a unilaterally dichromatic subject. *Science, 127*(3300), 675682.

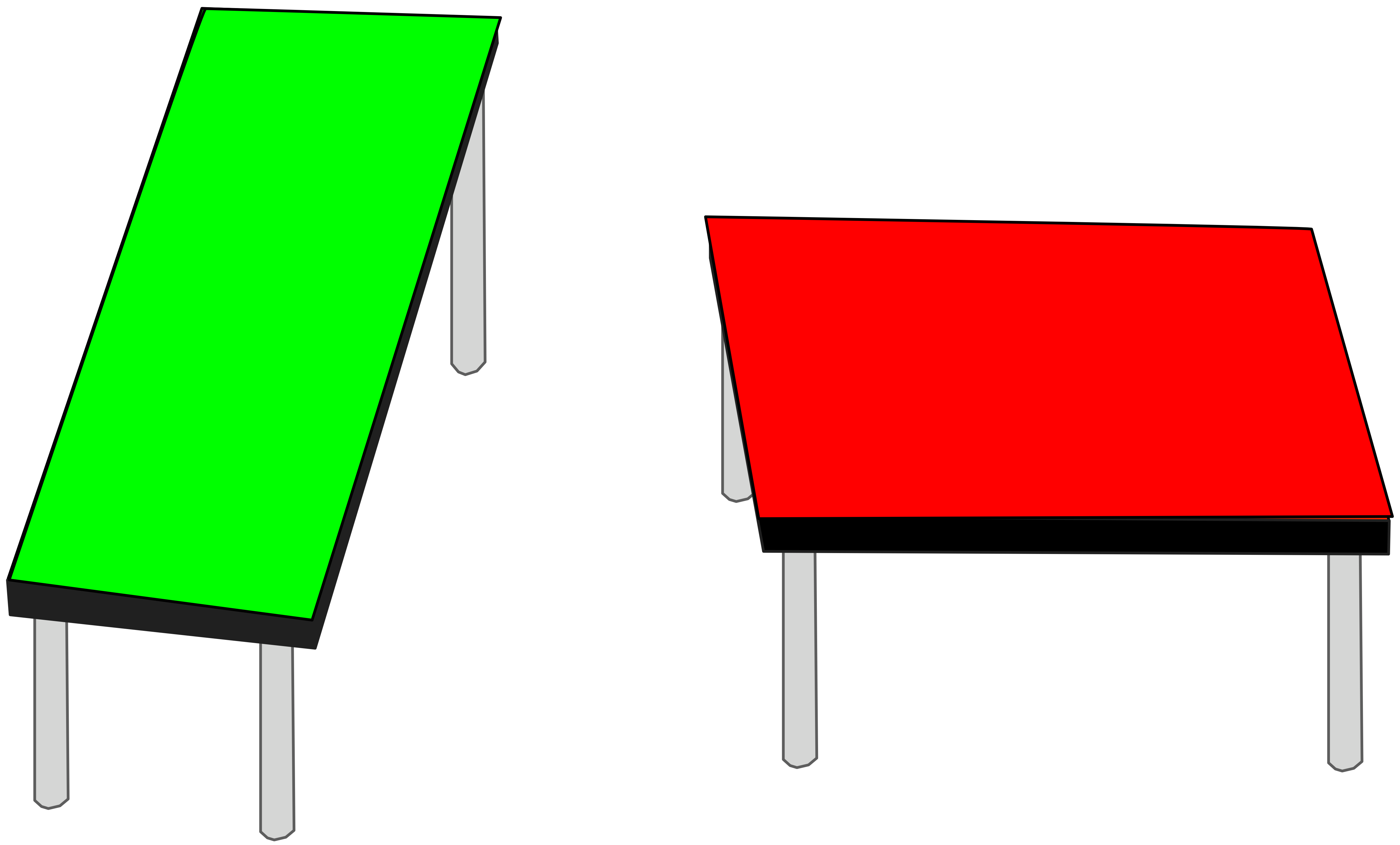

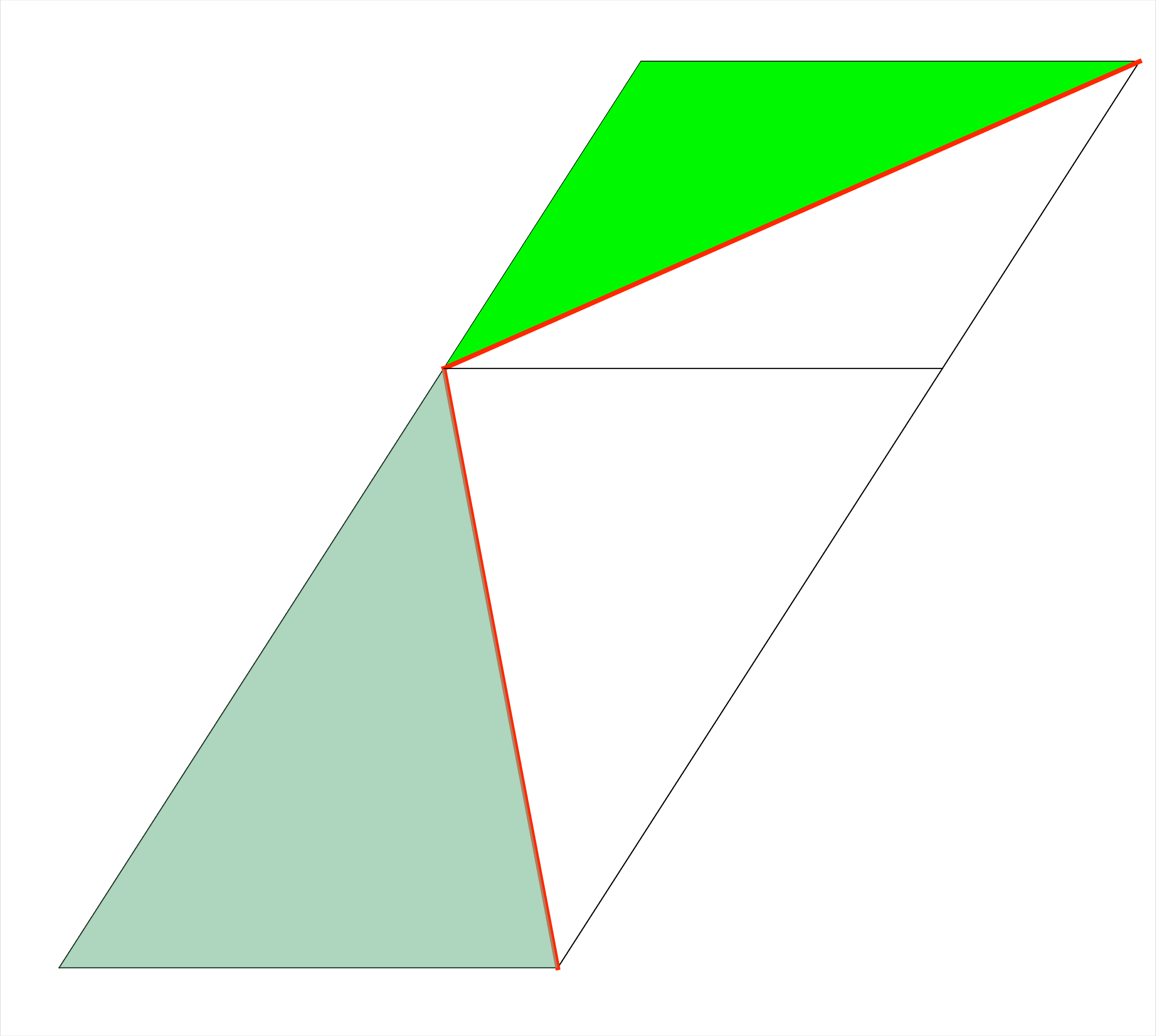

Mathematica
Demo

Conclusions

- Vision invokes all levels of neuroscience
  - Molecular
  - Cellular
  - Systems
  - Behavioral

Conclusions

- Some visual functions are well-understood
  - Neural organization of retina
  - Color Vision (behavioral)
- Many visual functions are not well-understood
  - Color Vision (systems)
  - Object Recognition
  - Conscious Experience

Levels of Understanding

- Molecular
- Cellular
- Systems
- Behavioral
- We want it all!

The End